Monsoon Monograph
(Volume 2)

Editors

Ajit Tyagi
G.C. Asnani
U. S. De
H. R. Hatwar
A. B. Mazumdar

GOVERNMENT OF INDIA
MINISTRY OF EARTH SCIENCES
INDIA METEOROLOGICAL DEPARTMENT

GOVERNMENT OF INDIA
MINISTRY OF EARTH SCIENCES
INDIA METEOROLOGICAL DEPARTMENT

Monsoon Monograph
(Volume 2)

Editors

AVM (Dr.) Ajit Tyagi
Director General

Prof. G. C. Asnani
WMO Professor of Meteorology (Retd.)

Dr. U. S. De
ADGM, India Meteorological Department (Retd.)

Dr. H. R. Hatwar
ADGM, India Meteorological Department (Retd.)

Dr. A. B. Mazumdar
DDGM, India Meteorological Department (Retd.)

INDIA METEOROLOGICAL DEPARTMENT

2012

Monsoon Monograph Volume II

CONTENTS

Preface

Chapter	*Topic*	*Pages No.*
Chapter - 1	Synoptic Systems during Monsoon season - ***P. V. Joseph***	1-34
Chapter - 2	Indian Monsoon variability - ***D. R. Pattanaik***	35-77
Chapter - 3	Tele-connections of Monsoon - ***M. Rajeevan***	78-128
Chapter - 4	Oceans and the Indian monsoon - ***Sulochana Gadgil and P. A. Francis***	129-188
Chapter - 5	Monsoon Simulation - ***R. Krishnan, Ayantika Dey Choudhury, Rajib Chattopadhyay, and M. Mujumdar***	189-232
Chapter- 6	Modeling of forecast sensitivity of the march of the monsoon isochrones from Kerala to New Delhi during the first 25 days. - ***T. N. Krishnamurti, Anu Simo, Aupe Thomas, Akhilesh Mishra, Dev Sikka, Dev Niyogi, Aridam Chakraborty and Li Li***	233-265
Chapter - 7	Predictability of the Indian monsoon in coupled general circulation models - ***V. Krishnamurty and J. Shukla***	266-306
Chapter - 8	Short Range Forecasting of Monsoons - ***S. K. Roy Bhowmick***	307-358
Chapter - 9	Medium Range Forecasting of Monsoons - ***A. K. Bohra and L. Harenduprakash***	359-412
Chapter - 10	Extended Range forecasting of Monsoon - ***U. C. Mohanty, P. Sinha, M. A. Kulkarni, N. Acharya, A. Singh, A. Nair and M. M. N. Rao***	413-467
Chapter - 11	Long Range Forecasting of Monsoon - ***D. S. Pai***	468-504
Chapter - 12	Monsoon Aspects related to Climate change - ***R. H. Kriplani and Ashwini Kulkarni***	505-559

एयर वाईस मार्शल (डॉ) अजित त्यागी
मौसम विज्ञान विभाग के महानिदेशक

Air Vice Marshal (Dr.) Ajit Tyagi
Director General of Meteorology &
Permanent Representative of India with W. M. O.

भारत सरकार
भारत मौसम विज्ञान विभाग
मौसम भवन, लोदी रोड,
नई दिल्ली - 110 003

GOVERNMENT OF INDIA
India Meteorological Department
Mausam Bhavan. Lodhi Road'
New Delhi – 110 003

Preface

Monsoon is traditionally defined as a seasonally reversing wind system accompanied by seasonal changes in atmospheric circulation and precipitation. A semi-annual reversal in the wind direction, a typical characteristic of monsoon, is caused due to differential heating of continents and oceans and the Coriolis force. The term was first used in English in the then British India and neighbouring countries, to refer to the large-scale seasonal winds blowing from the Bay of Bengal and Arabian Sea from southwesterly direction bringing heavy rainfall to the area. The monsoon rainfall is considered to be that which occurs in any region that receives most of its annual rain during a particular season. The English word '*monsoon' has* its origin in the Arabic word *mausim* ("season"). The definition includes major wind systems that change direction seasonally and allows other regions of the world to qualify as monsoon regions

The unique physiographic features of south Asia, with the vast Asian continent spread over equatorial to polar latitudes in the Northern Hemisphere contrasted by the extensive water surface of the Indian Ocean, spread over the equatorial to Antarctic latitudes in the Southern Hemisphere, primarily supports the development of intense thermal centres of action due to differential heating of land and oceans. The resultant pressure patterns and the meridional circulations in summer and winter are further accentuated by the presence of high mountain massifs (Himalayan and Tibetan Plateau) of south Asia, leading to the establishment of the South-West (SW) and the North-East (NE) monsoon, respectively.

The importance of the monsoons for India is manifold. Out of these two, the SW monsoon is more important as it accounts for over 75% of the annual rainfall in most parts of India, outside Tamil Nadu and Jammu and Kashmir. The economy of India is substantially dependent on its agriculture, which, in spite of development of irrigation facilities, is primarily and largely, rain-fed. It is thus dependent on the quantum and distribution of rainfall during the SW monsoon season. As such, the failure of SW monsoon, adversely affects the agricultural production in India and, in turn, the Indian economy. The SW monsoon, which is the main source of rainfall for India, is characterised by a high variability, both on spatial and temporal scales. This variability is a major feature and reason of the dependency of Indian agricultural economy on the SW monsoon rainfall

Due to its great socio-economic importance and its challenge as a complex scientific problem impacting on the global scale, there had been extensive research work on Indian Summer Monsoon in India and abroad, for almost over four centuries. An exhaustive summary of the research work on Indian Summer Monsoon, particularly carried out in India, was documented by Dr. Y. P. Rao, in 1976, in the form of a Meteorological Monograph (No. 1/1976), entitled 'South West Monsoon', which served as a

Tele : 91-11-24611842 Fax : 91-11-24611792
E-mail : dgm.hq@imd.gov.in / dgmmet@gmail.com / ajit.tyagi@gmail.com

principal reference document for research workers and operational weather forecasters for more than past thirty years.

During past few decades, there have been new developments in the understanding of Indian summer monsoon, particularly in the light of availability of extensive data sets, new research methodologies including modelling and field campaigns. Also, the issue of global warming has raised several questions about monsoon circulation and thus, has added a new dimension to it. In view of these developments, India Meteorological Department (IMD), which is the nodal agency for national meteorological services for India, has decided to bring out a comprehensive publication in the form of **'Meteorological Monograph on Monsoons'**.

Considering its wide scope, this publication will be brought out in two volumes. This volume contains the chapters on synoptic systems during monsoon season, monsoon variability on different temporal scales, tele-connections of monsoon, monsoon oceanic aspects, monsoon simulation, predictability of monsoon using coupled general circulation models, forecasting of monsoon in short; medium; extended range and long range time scales, and aspects of monsoon in relation to climate change. The second volume also includes a chapter on modeling of forecast sensitivity of progress of monsoon northward from southern tip of India during the onset and advance process.

The first volume contains chapters on scientific studies on monsoon, monsoons over other south Asian countries and elsewhere in the world, characteristics of Indian monsoon such as climatological aspects, onset; advance and withdrawal, components and semi-permanent systems of monsoon, operational procedures during monsoon as observed by IMD, observational aids used to monitor monsoon, orographic monsoon rainfall, extreme weather events related to monsoon, monsoon and agriculture, and northeast monsoon. The first volume also contains a chapter on Indian summer monsoon experiments.

All the contributors of this publication are eminent and experienced meteorologists from leading organizations in India and abroad of national and international repute. With its wide ranging scope and contents, this publication is intended to serve as a comprehensive reference publication for both, operational meteorologists and meteorological research scientists.

I take this opportunity to thank all the authors from India as well as from outside India including the authors from south Asian countries for their valuable contributions in making the monograph a comprehensive reference publication on monsoon over south Asian countries. I also thank other members of the editorial board viz., Prof. G. C. Asnani, Dr. U. S. De, Dr. H. R. Hatwar and Dr. A. B. Mazumadar for judiciously editing the publication. I also thank Dr. Medha Khole, IMD Pune and Dr. D. R. Pattanaik, IMD New Delhi in coordinating the work and bringing out the publications in time. Also I would like to thank Shri S. B. Gaonkar, and staff members of section of I & D of O/o DDGM (WF); Mr. Yogesh Visale and the staff members of the DTP unit of ADGM (R) Office, Pune for page setting and printing of the document.

New Delhi

Dated

(Ajit Tyagi)

Director General of Meteorology
India Meteorological Department

CHAPTER 1

SYNOPTIC SYSTEMS DURING MONSOON SEASON

P.V. Joseph

Cochin University of Science and Technology

joporathur@gmail.com

1.1. The environment of monsoon synoptic systems

Monsoon Depressions (MD) and Monsoon Lows (ML) form over North Bay of Bengal, north of 18°N and adjoining land areas and move west-north-westwards towards northwest India during the four summer monsoon months of June to September. Another important synoptic system of the Asian summer monsoon is the Mid Tropospheric Cyclone (MTC). It is quasi-stationary and occurs over northeast Arabian Sea and adjoining land areas. MTC is also known to occur over Indo-China. These synoptic scale weather systems are embedded in the large scale monsoon circulation which has significant control on the temporal and spatial distribution of the rainfall associated with them and also on their motion. Fig.1.1 shows the usual locations of these systems enclosed by Box-A. This is the region of the Climatological lower and mid-tropospheric Monsoon Trough (MT). The Climatological locations of the MT over India at sea level and at 4 km (600 hPa) above are shown in Fig.1.2. From the surface to 600 hPa the MT slopes to the south only through a couple of degrees of latitude along longitude 86°E (eastern India) but slopes through about 10 degrees of latitude along longitude 74°E (western India). The slope angle depends both on the horizontal temperature gradient and the horizontal wind shear in the MT zone. The north-south temperature gradient with warm temperatures to the north in monsoon months has large magnitudes on the western parts of India which partly explains the observed slope.

A Low Level Jetstream (LLJ) exists in the monsoon field over peninsular India and neighborhood (Joseph and Raman, 1966). This LLJ is part of a major inter-

hemispheric LLJ with its core near the 850 hPa level (Findlater, 1969). The Climatological LLJ of July as a mean of 40 years (1961-2000) may be seen in Fig.1.3. The LLJ and the associated band of convective clouds during active and break monsoon spells as composites of more than 60 days each are shown in Fig.1.4a,b taken from Joseph and Sijikumar (2004). . During active monsoon spells the LLJ axis with winds of 20 to 30 m/s at 850 hPa pass through peninsular India. In break monsoon spells the LLJ bypasses India and flows south of India. The upper troposphere of the monsoon area has the Tropical Easterly Jetstream (TEJ) with its core in the 150 hPa – 100 hPa layer – Koteswaram (1958). The mean TEJ at 150 hPa of July (representative of the monsoon season) is shown in Fig. 1.5. TEJ is strongest over the peninsular India and the adjoining Arabian Sea. The subtropical westerly jet stream which in non-monsoon months flows south of the Himalayas is seen flowing north of the mountain range in the monsoon season. Box –B in Fig.1.1 is characterized by strong LLJ in the lower troposphere and strong TEJ in the upper troposphere. The large vertical wind shear in this area as seen in Fig.1.6 taken from Keshavamurti and Shankar Rao (1992) is not conducive for the formation of intense synoptic scale low pressure systems like depressions or tropical cyclones. However feeble synoptic scale cyclonic circulations form in this box, in the middle and the lower troposphere in the break monsoon phase as documented by Koteswaram (1950) and Mukherjee and Natarajan (1968). Troughs form off the west coast of India in the low level monsoon westerlies that cause considerable rainfall along and off (sea-ward) the west coast of India particularly to the north of the LLJ axis (Rao, 1976).

Box –A has feebler vertical wind shear than Box-B which supports the formation of MD and MTC there, but not intense tropical cyclones. Sea Surface Temperatures (SST) over the north Indian Ocean (box B and part of A) has a bimodal annual variation (Hasternath and Lamb, 1979). Here SST falls beginning from May and reaches a minimum in August, whereas in the oceans to the east (Pacific) and to the west (Atlantic), SST rises from May and reaches maximum in August. North Bay of Bengal (in box-A) does not show the characteristic strong monsoon cooling of the north Indian Ocean. Here, where monsoon depressions have their genesis, SST remains close to 29°C during the monsoon season.

Box-C is an area that generates the largest number of tropical cyclones (Typhoons), compared to the other ocean basins of the world. SST is very high here during the monsoon season and the Equatorial Trough, a continuation of the monsoon trough passes through this area. Here both TEJ and LLJ are weak and hence the vertical wind shear is feeble. In box-C the frequency of tropical cyclones is high during the monsoon season and maximum in August– Gray (1978). In north Indian ocean, genesis of tropical cyclones is suppressed during the monsoon season, but the frequency of depressions (MD in box-A) is highest in August. The tropical cyclones that form in box-C influence the Asian summer monsoon and its synoptic systems in many ways.

In box – D covering the summer monsoon areas of Africa, the main synoptic systems are Easterly Waves. There are two Jetstreams in this box during June to September, the African Easterly Jetstream (AEJ) with its core near 600 hPa and the Tropical Easterly Jetstream, a continuation of the TEJ of box-B, but much weaker. Fig.1.7 gives the vertical profile of the mean zonal wind of July and August in box-D (Dhonneur,1981). AEJ and TEJ are marked in the figure. Monsoon westerlies are weak and shallow compared to box-B. Easterly waves form in box-D in the region of cyclonic wind shear (vorticity) to the south of AEJ. These easterly waves have the largest amplitude around 650 hPa. Their average wavelength is about 2500 km and they move westward, 6-7 degrees longitude per day. They have cold core below 650 hPa and warm core above. Convective activity and rainfall occur at and ahead of the wave trough (Reed, 1978).

The south Asian summer monsoon area is characterized by large south to north temperature gradient in the whole troposphere with temperature maximum along about latitude 30°N as may be seen in Fig. 1.8 (Rao, 1976). Both MD and MTC are located in areas having large horizontal and vertical wind shears. Thus barotropic and baroclinic instabilities of the basic flow are likely to be important in the formation of these synoptic systems. The monsoon airmass has considerable moisture as may be seen from Fig.1.9. Moisture is in abundance upto mid-tropospheric levels (Ananthakrishnan et al, 1965). Large values of conditional instability (Convective Available Potential Energy – CAPE) is present in the monsoon atmosphere (Srinivasan and Sadasivan, 1975). Thus deep convective heating of the

atmosphere and CISK could be important in relation to these systems. There have been several studies on these instability mechanisms, reviews of which are given by Das (1986).and Keshavamurty and Sankar Rao (1992).

1.2. Monsoon Depression (MD)

The climatological (30 year) average number of monsoon depressions which form during June to September has varied considerably in the climate change scenario. The seasonal frequency of monsoon depressions has decreased over the years from about 12 about 100 years ago to about 4 in recent years (see fig. 1.10). In addition weaker systems called Monsoon Lows (ML) also form during the season. There is wide scatter in the time interval between the formations of successive MDs; it may be as small as 3 days and may even exceed a month. 90% of MDs last 2-5 days; the remaining 10% has life of a week or more. The most frequent spatial distance between two co-existing MDs is 1100-2000 Km. Individual depressions during July and August follow a track which is close to the mean track, which runs in a west to northwest direction. The scatter of the tracks in June and September is larger and many of them re-curve in a northerly or northeasterly direction. More details may be found in Sikka (1977). Tracks of MDs of June to September are given in India Meteorological Department (1979). 850 hPa wind around a typical MD on two days in its life cycle showing its motion and the associated LLJ and the active monsoon conditions prevailing are given in Figs. 1.11a, b. In general MDs which form mostly in the active phase of the monsoon intraseasonal oscillation (the active – break cycle) increases the strength of the monsoon circulation over India during its life duration resulting in a surge in the rainfall activity over India, particularly along its west coast.

The three dimensional structure of MDs has been studied by Krishnamurti et al (1975) and Godbole (1977). A detailed picture is given in the review by Sikka (1977). In a typical MD the circulation is cyclonic upto 1000 Km from the centre in the horizontal (in the lower troposphere) and 9 Km in the vertical. Maximum cyclonic tangential winds (V_θ) are at a height of 0.9 to 1.5 Km at a radial distance of 300 to 400 Km from the surface centre. Anticyclonic V_θ commences at an altitude of about 10 Km and its maximum occurs at a height of 12 Km and at a radial distance of 500

– 600 Km from the surface centre. Inflow (radial wind V_R) occurs from the surface to a height of 5 Km upto radial distance of 900Km , with maximum occurring at 1 – 1.5 Km height at a radial distance of 200-300 Km. Outflow dominates above 6 Km and attains its maximum at a height of 10-11 Km at a radial distance of 400-600 Km from the surface centre. Vertical cross sections through the surface centre of a composite of several MDs in tangential and radial winds are given in fig. 1.12 (taken from Sikka, 1977). V_θ and V_R shown in the figure are values averaged around the center (0 to 360^0) for any radial distance. The central regions of the MD within a radius of about 400 Km from the depression center have large cyclonic vorticity in the lower and middle troposphere. The maximum vorticity is to the south of the surface centre at about 850 hPa. The axis of the MD is not vertical unlike in a tropical cyclone. It tilts to the south from the surface to 500 hPa and to the southeast between 500 and 300 hPa in agreement with its temperature structure. Sea level isobars and 850 hPa wind field of a typical MD are given in Fig.1.13. Unlike in tropical cyclones, there is considerable asymmetry in the wind field around the centre of the MD, with the highest wind speeds occurring generally in the south sector and the lowest speeds in the northwest sector. Tropical cyclones form in an environment of weak winds of the ITCZ, but MD forms when monsoon is in the active phase, in a region with strong westerly and easterly winds around the monsoon trough which slopes south with height. The monsoon westerlies have an embedded LLJ with core winds of 25 – 30 m/s. MD is really a vortex with feeble winds of the order of 10 m/s around its center superposed on the lower tropospheric strong monsoon circulation around the monsoon trough as may be seen in Fig.1.3 (active monsoon). MD has a cold core in the lower troposphere upto about 600 hPa and a warm core above. The thermal amplitude (temperature difference between the cold and warm sectors of the MD at an isobaric level) is large in the lower troposphere. The aircraft measurements made during the FGGE Monsoon Experiment (MONEX-1979) in the field of a monsoon depression (Joseph and Chakraborty, 1980) showed that the thermal amplitude is about 8^0C at 850 and 6^0C at 700 hPa. The southwest sector was the coldest and the northwest sector the warmest (see Fig.1.14)

The 24 hour accumulated rainfall associated with a depression is marked in the surface level isobar chart of Fig.1.13. Rainfall is highly asymmetric with respect to the surface centre of the MD. Large 24 hour rainfalls are mostly confined to the

southwest sector of a westward moving MD, within a radius of about 400 Km from the centre– Pisharoty and Asnani (1957) and Venkataraman et al (1974). In this sector typical rainfall amounts are 10-20 cms per day. Isolated falls of 30 cms per day occur in this area. Rainfall in the southwest sector of a MD has considerable diurnal variation, the heaviest falls occurring in the early morning hours 0230 to 0830 hours Indian Standard Time. Rainfall associated with a depression is caused by both deep convective clouds and also by stratiform clouds (Rao, 1976). Houze and Churchil (1987) found in the field of MD mesoscale areas with intense convective clouds, but large areas had rain with predominantly stratiform clouds. Stano et al (2002) studied the hydrometeor structure of monsoon depressions of 1999 using TRMM radar observations and found preponderance of stratiform rain in the depression field. Computations have shown that maximum upward air motion in the MD existed at about 800 hPa agreeing closely with the area of large rainfall. The computed level of non-divergence is found to be very low, around 800 hPa – Rao and Rajamani (1970), Krishnamurti (1968) and Das et al (1971).

Three factors are important in causing upward motion and rainfall in the south-west sector of a MD.

(a) Boundary layer frictional effects cause rising motion in areas of cyclonic vorticity which is maximum in the south sector of the MD, within a radial distance of 400 Km from the surface centre of the MD (see Figs. 1.12 and 1.13)

(b) Warm air advection in the lower troposphere from the warm northwest to the cold southwest sector of the MD within a radial distance of 400 Km from the surface center of the MD contributes to the upward motion and rainfall (see Fig. 1.14)

(c) Vorticity advection in the lower troposphere contributes to upward motion in the southwest sector and descending motion in the southeast sector as cyclonic vorticity is maximum south of the depression centre in the lowest few kilometers upto a radial distance of about 400 Kms where tangential wind has maximum strength (see Figs. 1.12 and 1.13).

There are many synoptic conditions preceding the formation of MD – see Sikka (1977). Some of the important ones among them are the following:

(1) Movement of the Monsoon Trough at sea level to a position passing through the North Bay of Bengal.

(2) Negative pressure tendency in an area of synoptic system size over the head Bay of Bengal. This fall in pressure is found to occur in association with westward moving negative isallobaric areas in 87 percent of the cases in a ten year period studied by Saha, Shukla and Sanders (1981). Only in 23 percent of the cases they found that such movements were associated with typhoons or named tropical storms in western Pacific Ocean, in general agreement with earlier studies.

(3) Strengthening of the monsoon current over peninsular India and the central Bay of Bengal (LLJ) to over 20 m/s (Active monsoon as in Fig.1.4a). This increases the cyclonic shear vorticity in the lowest 3-4 Km of the atmosphere in North Bay of Bengal, the usual place of MD genesis.

(4) Increased divergence in the upper troposphere over North Bay of Bengal – Koteswaram and George (1958).

(5) Formation of a cyclonic circulation in the middle troposphere and its descent to sea level

(6) Persistence of a bright cloud mass, about 500 Km in diameter over North Bay of Bengal and increased rainfall there. MD centre forms near the northern edge of such a cloud mass (possibly CISK mechanism is operating).

(7) The vertical wind shear over North Bay of Bengal decreases appreciably prior to the formation of a MD – Raman et al (1981).

The basic movement of a monsoon depression is to the west-northwest. However in June and September many MDs recurve to the north under the influence of the upper tropospheric westerlies. After crossing the central parts of India MDs generally weaken or die. Occasionally MDs take a more westerly course and reach Gujarat, Rajasthan and even Pakistan. When a MD recurved to the north and north-east, the associated heavy rainfall is not in the south-west sector, but in the MDs forward sector. MDs embedded in the strong lower tropospheric monsoon westerlies (LLJ) move westwards. The cause of this westward movement against the monsoon current has not been well understood and needs study. Goswami (1987) has

however suggested a mechanism for the zone of maximum rainfall in the western sector of a MD and proposed a feedback mechanism for the observed westward movement of the MD.

1.3. Mid Tropospheric Cyclone (MTC)

The name MTC is given to those synoptic systems found over south Asia during the summer monsoon months whose cyclonic vorticity has a maximum between 700 and 500 hPa, with much smaller values at the surface. In contrast MDs have large cyclonic vorticity from the surface to 500 hPa with maximum around 850 hPa. MTCs move slowly westwards or remain quasi-stationary for several days, unlike MDs which move 300 – 500 Kms per day. MTCs occur over north-east Arabian sea and adjoining land areas and occasionally also over Indo-China.- Krishnamurti and Hawkins (1970). See also Fig.1.1. Carr (1977) has given a review of the knowledge till then about MTCs.

An MTC over north-east Arabian sea has been studied by Miller and Keshavamurthy (1968). Its large scale features remained quasi-stationary from 2 to 10 July 1963. They made composites using data of this period. Fig.1.15 a, b, c gives the streamline analysis of the wind field close to the surface (low level), and at 700 and 600 hPa respectively and Fig.1.15 d gives the isotherms at 700 hPa for the composited MTC of 2 to 10 July 1963. At low levels there is no closed circulation. Only a weak trough is seen. There is a cyclonic vortex from 700 to 500 hPa and it is maximum developed at 600 hPa where winds of 20 m/s were seen in meso-scale bands about 300 – 400 kms to the west and south of the MTC center. Above 300 hPa winds were easterlies with maximum speeds 20 to 40 m/s between 150 and 100 hPa. The horizontal size scale of the MTC (radius of the vortex is about 600 km) is about half that of the MD. The vertical scale of the MTC is about 6 km. In the MTC convergence is maximum between 600 and 500 hPa. The maximum cyclonic vorticity is at about 600 hPa. Vorticity is anticyclonic above 300 hPa. The MTC studied was cold cored below 500 hPa and warm cored above.

Convection (rainfall) was found to be most intense away from the center in the western and southern quadrants, where convective cloud tops reached heights of 15

kms. Rainfall of 5 to 10 cms per day occurred there with isolated rainfall reaching 30 cms per day. Along the west coast of India there was a rainfall maximum 200-300 kms south of the MTC center. Vorticity advection and warm air advection in the lower troposphere are the main factors causing vertical motion that produced this rainfall. MDs had an additional factor, namely the strong cyclonic vorticity in the frictional boundary layer which is absent in MTCs. Some of the important differences between MDs and MTCs are brought out in the schematic diagram (Fig.1.16).

Miller and Keshavamurthy (1968) have computed divergence, vorticity and vertical motion from the streamline analysis of their composite MTC at several levels. Increase in cyclonic vorticity with height upto 500 hPa and slope of the line of maximum cyclonic vorticity towards the south and west are seen. .Maximum convergence is at 500 hPa and the computed level of non-divergence is close to 300 hPa. Vertical velocity (ascent) near the center of the MTC was found to be maximum at about 300 hPa. They found a large area of heavy cumulonimbus (cb) clouds to the west and south-west of the MTC center. All the heavy rain has not been due to cumulonimbus clouds. The heavy rain in the southern portions of the MTC, particularly along the coast, is due to stratiform clouds with embedded large cumulus.

Carr (1977) made a survey of the daily satellite photographs of the 10 year period 1967 to 1976 in conjunction with the annual reports on the south west monsoon published in the then Indian Journal of Meteorology and Geophysics (now called Mausam) and found the following.

(i) MTCs are not as frequent as MDs and may form one to four times in a monsoon season. They are more common in the first half of the monsoon season

(ii) The life duration of most MTCs is 3 to 7 days. A few have lived more than a week, like the MTC of July 1963 studied by Miller and Keshavamurthy (1968).

(iii) All MTCs do not develop in situ over the north-eastern Arabian Sea. A few originated as MDs over the Bay of Bengal, moved westwards and became MTCs when they reached the western part of India. The climatological mean monsoon trough at 600 hPa with its associated cyclonic vorticity passes

through the mean MTC center location (see Fig. 1.2). Intensification of this vorticity can lead to MTC formation

Krishnamurti and Hawkins (1970) performed a diagnostic study of an MTC which formed over Indo-China in July 1966. This MTC had a weak surface low and an intense 500 hPa vortex. There was east-north-easterly flow above 300 hPa. The MTC axis sloped to the west. It moved slowly westwards during its life time. This MTC had a weak cold anomaly below 600 hPa and a warm core above. Upward motion was found west of the MTC and subsidence to the east.

1.4. Monsoon Lows

Monsoon Lows (ML) less intense than monsoon depressions form frequently during the monsoon season in the Bay of Bengal, the Arabian Sea and over land in the monsoon trough region. According to the criteria followed by IMD a low pressure area is called a ML if the wind speed within the associated cyclonic circulation is less than 17 knots. When the wind speed is 17 knots or more it becomes a depression or a more intense system like a cyclonic storm. These criteria are used when the system is over the sea. Over land different criteria are used. If a low pressure area has two or more closed isobars at 2 hPa intervals, it is called a depression; with only one closed isobar it is a low.

MD and ML are the main components of monsoon Low Pressure Systems (LPS). LPS includes also systems of higher intensity than depression. Like cyclonic storm. Sikka (1980) studied the LPS which formed over India in July and August during 5 good monsoon (excess rainfall) years and 5 bad monsoon (deficient rainfall) years and found that there was no difference between good and bad years in respect of the number of MD, similar to the findings of Dhar et al (1980, 1981) and also in the number of MD days, but there was notable difference in the number of LPS days. The most important feature of good monsoon years was the greater frequency of cyclogenesis (LPS days) which kept the monsoon trough in the normal position with higher cyclonic vorticity in the monsoon trough zone that resulted in increased rainfall in the monsoon over India.

Mooley and Shukla (1987) made an exhaustive study of the frequency of LPS and LPS days during the monsoon seasons of the 96 years (1888 to 1983). They found that both ML and MD are very similar in their structural characteristics and produced copious rainfall during the monsoon season. Rainfall associated with ML was less intense but covered a relatively larger area compared to MD. The total rainfall associated with a ML was found to be almost on par with that with a MD.

Their main findings are the following:

(1) The mean number of LPS days in the monsoon season (June to September) I is 56.6 with a standard deviation of 11.7

(2) About 70.5% of the LPS have life duration of 5 days or less, 28% have life 6 to 10 days and only 1.5% survive more than 10 days

(3) The mean sea level pressure anomaly of a LPS is -5.7 hPa with a standard deviation of 3.6 hPa.

(4) The preferred area of dissipation of LPS is between 22N and 26N latitudes and 88E.and 92E longitudes in years of deficit monsoon rainfall

(5) The number of LPS days in a monsoon season is positively correlated (at 5% level of significance) to the monsoon rainfall of India as a whole. The relation with central India rainfall is significant at 1% level. Similarly the extent of westward movement of LPS is positively correlated to the monsoon rainfall of India at 1% level of significance, LPS moving more westwards over India in good rainfall years.

Sikka (2006) extended the work of Mooley and Shukla (1987).The procedure followed was the same. The morning (0300UT) sea level synoptic pressure analysis, published in the Indian Daily Weather Report (IDWR) for the months of June to September of the 20 year period 1984 to 2003 formed the basic data. Combining the two studies Sikka (2006) analysed the long time series of LPS data for the period 1888 to 2003. Table 1.1 shows the number of LPS, LPS days and mean life of the LPS in each of the 11 decades 1891 – 2000. The number of LPS, LPS days and the mean life span of LPS are all higher in the three decades beginning in 1971. In recent years several authors have studied LPS, references to which are given in Sikka (2006)

Table-1.1: Decadal number of LPS, LPS days and their mean life duration

Decade	Number of LPS	LPS days	Mean LPS life (days)
1891-1900	133	621	4.7
1901-1910	126	549	4.4
1911-1920	114	449	3.9
1921-1930	134	573	4.3
1931-1940	117	492	4.2
1941-1950	139	554	4.0
1951-1960	122	501	4.1
1961-1970	125	542	4.3
1971-180	143	707	5.0
1981-1990	139	712	5.1
1991-2000	131	684	5.2

Another class of monsoon lows form over the Bay of Bengal when the monsoon is weak or in a break monsoon phase. Koteswaram (1950) found that these lows (cyclonic circulations) occur at levels above 850 hPa in the latitude belt 10N to 15N and move west-north-westwards across the Bay of Bengal strengthening the monsoon current south of this latitude belt and causing the initiation of the following active monsoon spell. Some of these upper air lows have associated monsoon lows at the sea level. Mukherjee and Natarajan (1968) studied such systems during July and August of 20 years (1946-1965). Nine such low latitude monsoon lows occurred during that period. All these cases were during break monsoon phase. These systems caused heavy rainfall in Tamil Nadu as they moved westwards.

1.5. Off-shore Troughs and vortices

Wave troughs develop in the low level monsoon westerlies just off the west coast of peninsular India anywhere from north Kerala to south Gujarat when the monsoon is in the active phase. These have been called off – shore Troughs. The development of the trough is seen as a weakening of the normal pressure gradient at the sea level and weak southerly / southwesterly surface winds along parts of the

coast instead of the normal westerly winds 24 hour pressure changes and pressure departures from normal also indicate the presence of the off-shore trough. These troughs form more often near coastal Karnataka and slowly shift about 2 degrees of latitude per day northwards, though they may also appear and disappear in situ over any area. Upper winds are affected only in the lowest one kilometer of the atmosphere. Cyclonic vorticity may be present above I km also but in the form of shear vorticity – Rao (1976). It is found that nearly half the number of monsoon situations producing copious rainfall in Konkan and three quarters of such occasions in coastal Karnataka are in association with off-shore troughs.

George (1956) found that at times shallow and small (meso-scale) vortices form in these off-shore troughs which cause heavy rainfall in small areas along the west coast of peninsular India away from the Western Ghats (Sahyadri Mountains). These have been called off-shore vortices. They have a diameter less than 150 km and vertical extent less than 1.5 km. from sea level. Off-shore vortices move south to north along the coast. George (1956) identified these vortices and assessed their motion from the variation of the direction of surface winds at the coastal observatories. Mukherjee et al (1978) found that the off-shore troughs off the Maharastra-Goa coast are most prominent in July. He studied the vortices embedded in these found that (a) they form just south of Goa, mostly in the first half of July and move northwards at a speed of about 100 Km per day and (b) Heavy rainfall associated with them is more along the coast and less over the slopes of the Western Ghats. Mukherjee et al (1984) studied an off-shore vortex using the MONEX-1979 research aircraft dropwindsonde data.. The vortex was on the meso-scale and was shallow.

Arabian sea Monsoon Experiment (ARMEX-I) was conducted during June to August of 2002 to understand the formation and meteorology of off-shore troughs and the embedded meso-scale vortices. Madan et al (2005) finds that the three heavy rainfall events along the west coast of India (rainfall exceeding 12 cms per day) that occurred on 14-16 June, 20-22 June and 07-10 August were associated with off-shore trough and or off-shore vortices. They found that off-shore troughs are associated with strong (active) monsoon conditions and the location of formation of off-shore vortex had been on the cyclonic shear side of the low level jetstream.

1.6. Tropical Cyclones of West Pacific Ocean and Monsoon

Tropical west Pacific Ocean north of the equator generates on average 26 out of the 79 tropical cyclones produced by the global oceans in a year – Gray (1978). About 60% of these occur during the four months June to September. When India gets its monsoon rains. Many of these reach typhoon and super typhoon intensities. Krishnamurti et al (1977) and Saha et al (1981) find that a large percentage of monsoon depressions and lows forming over North Bay of Bengal were associated with remnants of tropical cyclones of west Pacific moving westwards. Raman (1955) associated breaks in Indian monsoon with north moving west Pacific tropical cyclones. The monsoon rainfall of India and the number of tropical cyclone days in west Pacific showed a negative correlation in a study by Rajeevan (1993). He also found that tropical cyclone genesis over the west Pacific Ocean is enhanced during weak phase of the Indian monsoon and suppressed during the strong phase on the intra-seasonal time scale. On the inter-annual time scale using data of 56 years (1948-2003) Kumar and Krishnan (2005) find that cyclogenesis over west Pacific is 1.33 times higher in weak monsoon years compared to strong monsoon years. Their finding on the direction of movement of tropical cyclones of west Pacific is given in section 1.7. Joseph (1990) showed the existence of an out of phase relation between convection in the Indian ocean and cyclogenesis in west Pacific ocean on the 30-50 day time scale during April to July, studying the large scale changes occurring in the atmosphere over these ocean basins in association with monsoon onset over Kerala**.**

1.7 Influence of Mid-latitude Westerlies

During the monsoon season mid-latitude westerlies and the sub-tropical westerly jetrstream move to north of India (north of latitude 30N) as may be seen in fig. 1.5. Still systems in the westerlies exercise considerable influence on monsoon synoptic systems and rainfall. During the monsoon season Western Disturbances and troughs in upper tropospheric westerlies regularly move from west to east across Indian longitudes. These westerly troughs affect the monsoon in four different ways – Rao (1976).

(1) Triggering and intensifying lower tropospheric lows
(2) Enhancing rainfall in pre-existing synoptic weather systems
(3) Causing recurvature of monsoon depressions and lows and
(4) Leading to onset of break monsoon conditions

Ramaswamy (1962) studied the synoptic situation over India and neighbourhood during a period of 8 days in which normal monsoon conditions were followed by a break monsoon conditions. He found that during the break a trough in the mid-latitude westerlies (Rossby Wave) with a jet embedded in it increased considerably in its amplitude and destroyed the Tibetan High at 500 hPa level. Protruding into India and Pakistan the large amplitude trough contributed to the occurrence of heavy rainfall along and near the foot hills of the Himalayas, a characteristic of break monsoon condition. Consequent to these developments the sub-tropical westerly Jetstream, which had moved to the north of the Himalayas at the time of monsoon onset over India, re-entered the Indian sub-continent during the break monsoon period. This study supplemented by the examination of 700 hPa charts of the northern hemisphere of 10 years suggested that active monsoon over India is associated with 'high index circulation' in mid-latitudes over Asia and neighbourhood while weak or break monsoon is associated with 'low index circulation' over the same region

In the years of large scale droughts in the Indian southwest monsoon rains during the decade 1965 to 1974, sub-tropical westerlies of the upper troposphere protruded southwards into areas immediately west of India during the monsoon season (Joseph, 1978), this feature persisting right from the previous winter.. Joseph et al (1981) and using a longer data set Parthasarathy et al (1991) showed that the monthly mean meridional wind anomaly over India in the upper troposphere is strong southerly in May preceding drought monsoon years and has high and statistically significant correlation with the subsequent monsoon rainfall; of India.

Studying years with severe drought monsoons in India, Raman and Rao (1981) found that in these years there were long monsoon breaks and these breaks were associated with 'blocking highs' one each over west Asia and east Asia and a deep trough in between protruding to India. Joseph and Srinivasan (1999)

identified large amplitude circum-global stationary Rossby Wave trains with wavelength in the range 50-60 degree longitude (wave number 6 or 7) in May by analyzing 200 hPa wind anomalies. The spatial phase of these waves differed by about 20 degrees of longitude between drought and excess rainfall Indian monsoons. In drought Indian monsoon years these Rossby Waves have a trough protruding equatorwards into northwest India as found by Joseph (1978). Joseph and Srinivasan (1999) named this wave train Asia Pacific Wave (APW). They hypothesised that the APW was forced in the sub-tropical westerlies and jetstream by the upper tropospheric divergent areas associated with the monsoon (and pre-monsoon) heat sources that has east-west shift between years associated with the tropospheric biennial oscillation. Other explanations have been given to the excitation of these Rossby wave trains by Krishnan and Majumdar (1999), Ding and Wang (2007) and Krishnan and Kumar (2009). The phase of the APW has persistence from May into the monsoon season – Sathiyamoorthi et al (2002) and Ding and Wang (2005). The composite APW of June to September at 200 hPa of five extreme drought (DRY) monsoons (1965, 1972, 1979, 1982 and 1987) and five extreme excess (WET) monsoons (1961, 1970, 1975, 1983, 1988) of the three decades 1960s, 1970s and 1980s are shown if figs.1.17 a ,b. The APW trough in 200 hPa wind anomaly intrudes into northwest India in the drought composite(fig.1.17a) The wave trough further to the east is associated with the preferred northward motion of west Pacific typhoons observed in drought Indian monsoon years by Kumar and Krishnan (2005). Fig. 1.17b shows the 200 hPa wind anomaly `which is favourable for tropical cyclones of west Pacific to move westwards to the Indian Ocean to trigger monsoon depressions and monsoon lows in the WET monsoon composite.

1.8. Intra-seasonal and long period variations

Lower tropospheric wind field and convection of the monsoon area of south Asia have two prominent intra-seasonal oscillations with periods around 40 days and 15 days – Sikka and Gadgil (1980), Krishnamurti and Subramanyam (1982), Krishnamurti and Bhalme (1976) and Krishnamurti and Ardanuy (1980). The phase of the 40-day mode moves from south to north over India and that of the 15-day mode from east to west. Fig.1.18 from an analysis by Yasunari (1981) shows the

phase lag relations of the 850 hPa geopotential heights filtered for these two intra-seasonal oscillations, with reference point being Nagpur in central India. Active – Break cycle of the monsoon is a manifestation of the 40-day mode – Goswami (2004).

The low level jetstream over south Asia has two semi-permanent locations (see Fig. 1.4 a, b) one corresponding to the active phase and the other to the break phase of the monsoon, as shown by Joseph and Sijikumar (2004). There is strong air-sea interaction over the Indian and west Pacific oceans in the active – break cycle as seen from the study of Joseph and Sabin (2008) and the papers referred therein. Monsoon depressions are associated with the active phase of the monsoon when the LLJ passes through peninsular India and there is considerable shear vorticity associated with it over North Bay of Bengal which is the main genesis area for MD. Joseph and Sabin (2008) has shown that active monsoon conditions are triggered when the Sea surface Temperature (SST) over north Bay of Bengal attain high values (maxima) in the 40-day mode. Large shear vorticity in the low levels and high SST are favourable for the genesis of MD and ML. Using the genesis and track data of the LPS of the 40 years 1954 to 1993, Goswamy et al (2003) showed that the genesis of LPS is nearly 3.5 times more during active monsoon when compared to break monsoon in the Intraseasonal oscillation. They also showed that LPS are spatially clustered along the monsoon trough region during the active phase of the monsoon – see figs. 1.19 a, b from Goswamy et al (2003).

We have very reliable data on monsoon depressions (as they form close to coast and move over land with a dense network of observatories) since 1891 from IMD sources. Analysis of this long data series has shown that MD frequency of the season June to September had a prominent 39 – year oscillation superposed on a decreasing linear trend (see 1.10). Harmonic analysis was performed on the trend removed monsoon depression frequency of 116 years (1891-2007) which showed that the third harmonic (period 39 years) has the highest amplitude. The third harmonic of the MD frequency and the third harmonic of the annual frequency of tropical cyclones of Arabian Sea and the Bay of Bengal of the same 116 years are shown in Fig.1.20 for comparison. Both of them have the same amplitude and their phases differ only by a couple of years. We have to do research to find the causes

for the 39-year oscillation in MD and cyclones and the long term decreasing trend (climate change) in monsoon depression frequency.

References

Ananthakrishnan, R., Selvam, M. M. and Chellappa, R., 1965, “Seasonal variation of precipitable water vapour in the atmosphere”, Ind.Jour.Met and Geophys., 16, 371-385.

Carr, F. H., 1977, “Mid-tropospheric cyclones of the summer monsoon” ,PAGEOPH, 115, 1383-1412.

Das, P. K., Datta, R. K., and Chabra, B. M., 1971, “Diagnostic study of vertical motion vis-à-vis large scale cloud systems”, Indian Journal of Meteorology and Geophysics, 22, 331-336

Das, P. K.,1986 , “Monsoons”, Fifth IMO Lecture, World Met Organization, 155 pp.

Dhar, O. N., Rakhecha, P. R., Mandal, B. N., 1980, “Is the number of cyclonic disturbances traversing India during a monsoon season related to the rainfall of that season?”, Mausam, 31, 119-124

Dhar, O. N., Rakhecha, P. R., Mandal, B. N., 1981, “Influence of tropical disturbances on monthly rainfall of India”, Monthly Weather Review,109, 188-190

Dhonneur, G., 1981, “'The cloud clusters – the main component of the Sahalian Meteorology”, Int.Conf.on early results of FGGE and large scale aspects of its Monsoon Experiments, Tallahassee, U.S.A., WMO Geneva, Session 8, 11-15.

Ding, Q., Wang, B., 2005, “Circumglobal teleconnection in the northern hemisphere summer”, Journal of Climate, 18, 3483-3505.

Ding, Q., Wang, B., 2007, “Intraseasonal teleconnection between the summer Eurasian wave train and the Indian monsoon”, Journal of Climate, 20, 3751-3767.

Findlater, J, 1969, “A major low level air current near the Indian ocean during the northern summer”, Quarterly Journal of Royal Meteorological Society, 95, 362-380.

George, P. A. 1856, “Effect of off-shore vortices on rainfall along the west coast of India”, Indian Journal of Meteorology and Geophysics, 7, 225-240.

Godbole, R. V., 1977, “the composite structure of the monsoon depression”, Tellus, 29, 25-40.

Goswami, B. N. 1987, “A mechanism for the west-north-west movement of monsoon depressions”, Nature, 326, 376-378

Goswami, B. N., Ajaya Mohan, R. S., Xavier, P. K., Sengupta, D., 2003, "Clustering of synoptic activity by Indian summer monsoon intra-seasonal oscillation" , Geophysical Research Letters, 30, 1431, doi:10.1029/2002GL016,734.

Goswami, B. N., 2005, "Intra-seasonal variability in the tropical ocean – atmosphere", Lau K.M and Duane Waliser (Eds.), Chapter-2, Praxis Publishing

Gray, W. M., 1978, "Hurricanes: Their formation, structure and likely role in the tropical circulation, Meteorology of Tropical Oceans, D.B.Shaw, (Ed.), Royal Meteorological Society, 155-218.

Hastenrath, S. and Lamb, P. J., 1979, "Climate atlas of the Indian Ocean, Part -I - Surface climate and atmospheric circulation", The University of Wisconsin Press, USA, 93 pp.

Houze, R. A. and Churchill, D. N., 1987, "Mesoscale organization and cloud microphysics in a Bay of Bengal depression", Journal of the Atmospheric Sciences, 44, 1845-1867

India Meteorological Department, 1979, "Tracks of storms and depressions in the Bay of Bengal and the Arabian Sea 1877-1970", India Meteorological Department, 194 pp.

Joseph, P. V. and Raman, P. L., 1966, "Existence of low level westerly jet stream over peninsular India during July", Ind.Jour.Met and Geophys., 17, 407-410.

Joseph, P. V., 1978, " Sub-tropical westerlies in relation to large scale failure of Indian monsoon", Indian Journal of Meteorology Hydrology and Geophysics, 29,: 412-418

Joseph, P. V. and Chakravorthy, K. K., 1980, "Lower tropospheric temperature structure of the monsoon depression", 11-14 August 1979', Results of Summer MONEX field phase research (Part B), FGGE Operations Report, 9, 257-265.

Joseph, P. V., Mukhopadhyaya, R. K., Dixit, W. V., Vaidya D. V., 1981, "Meridional wind index for long range forecasting of Indian summer monsoon rainfall", Mausam, 32, 31-34

Joseph, P. V., 1990, "Monsoon variability in relation to equatorial trough activity over Indian and west Pacific oceans, Mausam, 41, 291-296

Joseph, P. V., Srinivasan J., 1999, "Rossby waves in May and the Indian summer monsoon rainfall", Tellus, 51A, 854-864

Joseph, P. V. and Sijikumar, S., 2004, "Intraseasonal variability of the low level jetstream of the Asian summer monsoon", Journal of Climatology, 17, 1449-1458.

Joseph, P. V., Sabin, T. P., 2008, “An Ocean-Atmosphere Interaction Mechanism for the Active - Break Cycle of the Asian Summer Monsoon”, Climate Dynamics, 30, 553-566

Keshavamurty, R. N., Sankar, Rao, M., 1992, “The Physics of Monsoons”, Allied Publishers Ltd., 199 pages

Koteswaram, P., 1950, “Upper level lows in low latitudes in the Indian area during south-west monsoon season and breaks in the monsoon”, Ind. Jour. Met and Geophys., 1, 162-164

Koteswaram, P., 1958, “The easterly jet stream in the tropics”, Tellus, 10, 43-57.

Koteswaram, P., and George, C. A., 1958, “On the formation of monsoon depressions in the Bay of Bengal”, Ind.Jour.Met and Geophys., 9, 9-22.

Krishnamurti, T. N., 1968, “A diagno0stic balanced model for studies of weather systems of low and high latitudes”, Monthly Weather Review, 96, 197-207.

Krishnamurthi, T. N., Hawkins, R. S., 1970, “Mid tropospheric cyclones of the south-west monsoon”, J.Appl.Meteor., 9, 442-458.

Krishnamurthi, T. N. Kanamitsu, M., Godbole, R., Chang, C. B., Carr, F., and Chow, J. H., 1975 , “Study of a monsoon depression (I). Synoptic structure”, Jour.Met.Soc., Japan, 53, 227-240.

Krishnamurti, T. N., Bhalme H. N., 1976, “Oscillations of a monsoon system, Part-I: Observational aspects”, Journal of Atmospheric Science,33, 1937-1954

Krishnamurti, T. N., Molinari, J., Pan, H. L., Wong, V., 1977, “Downstream amplification and formation of monsoon disturbances, ,Monthly Weather Review, 105, 1281-1297.

Krishnamurti, T. N., Ardanuy, P., 1980, “The 10-20 day westward propagation mode and breaks in the monsoon”, Tellus, 32, 15-26.

Krishnamurti, T. N., Subrahmanyam, D., 1982, “The 30-50 day mode at 850 hPa during MONEX”, Journal of Atmospheric Science, 39, 2088-2095.

Krishnan, R., Majumdar, M., 1999, “Remotely and regionally forced pre-monsoon signals over northern India and neighbourhood”, Quarterly Journal of Royal Meteorological Society, 125, 55-78.

Krishnan, R., Kumar, V., 2009, “Internal feedbacks from monsoon – midlatitude interactions during droughts in the India summer monsoon, Journal of the Atmospheric Sciences, 66, 553-577.

Kumar, V., Krishnan, R., 2005, “On the association between the Indian summer monsoon and the tropical cyclone activity over northwest Pacific”, Current Science, 88, 602-612

Madan, O. P., Mohanty, U. C., Iyengar, G., Shivhare, R. P., Rao, A. P., Sam, N. V., Bhatla, R., 2005, “Off-shore trough and very heavy rainfall events along the west coast of India during ARMEX-2002, Mausam, 56, 37-48.

Miller, F. R. and Keshavamurty, R. N., 1968, “Structure of an Arabian Sea summer monsoon system”, I.I.O.E. Met. Monograph, No.1, East-West Center Press, Honolulu, 94 pp.

Mooley, D. A. , Shukla, J., 1987, “Characteristics of the westward moving summer monsoon low pressure systems over the Indian region and their relationship with the monsoon rainfall”, Dept. of Meteorology, University of Maryland, College Park MD, USA

Mukherjee, A. K. and Natarajan, G., 1968, “Westward moving sea level low pressure systems in the south Bay of Bengal during south-west monsoon'”, Ind.Jour.Met and Geophys., 19, 286-288.

Mukherjee, A. K., Rao M. K., Shah, K. C., 1978, “Vortices embedded in the trough of low pressure off Maharashtra – Goa coasts during the month of July”, Indian Journal of Meteorology, Hydrology and Geophysics, 29, 61-65.

Mukherjee, A. K., De, U. S., SinhaRay, K. C., 1984, “The dynamics of an off-shore vortex in east Arabian sea and the associated rainfall, Mausam, 35, 233-234.

Parthasarathy, B., Rupa Kumar, K., Deshpande, V. R., 1991, “Indian summer monsoon rainfall and 200-mbar meridional wind index: application for long range prediction”, International Journal of Climatology, 11, 165-176

Pisharoty, P. R. and Asnani, G. C., 1957, “Rainfall around monsoon depressions over India”, Ind.Jour.Met and Geophys., 8, 15-20.

Rajeevan, M., 1993, “Inter-relationship between NW Pacific typhoon activity and Indian summer monsoon on inter-annual and intra-seasonal time scales”, ,Mausam, 44, 109-111.

Raman, C. R. V., 1955, “ Breaks in the Indian southwest monsoon and typhoons in southwest Pacific”, Current Science, 24, 219-220

Raman, C. R. V., Rao, Y. P., Subramanian, S. K. and Jose, A., Maliekal, 1981, “Tropospheric wind shear oscillations as a characteristic of the south-west monsoon atmosphere”, Mon.Wea.Rev., 109, 224-229.

Raman, C. R. V., Rao Y. P., 1981, “Blocking highs over Asia and monsoon droughts over India”, Nature, 289,271-273.

Ramaswamy, C. , 1962, “ Breaks in the Indian summer monsoon as a phenomenon of interaction between the easterly and the sub-tropical westerly Jetstreams”, Tellus, 14, 337-349.

Rao, K., V. and Rajamani, S., 1970, “Diagnostic study of a monsoon depression by geostrophic baroclinic model”, Indian Journal of Meteorology and Geophysics, 21, 187-194.

Rao, Y. P., 1976, “Southwest Monsoon”, Meteorological Monograph, Synoptic Meteorology, 1/76, India Meteorological Department, Delhi, India. 140 pp.

Reed, R. J. 1978., “The structure and behavior of easterly waves over West Africa and the Atlantic in Meteorology over the Tropical Oceans”, Editor D.B. Shaw, Royal Meteorological Society, Brecknell, U.K., 278 pp.

Saha, K. R., Sanders, F., Shukla, J., 1981, “Westward propagating predecessors of monsoon depressions”, Mon.Wea.Rev,. 109, 330-343.

Sathiyamoorthy, V., Mohankumar, K. and Joseph P. V., 2002, “Interannual variability of total ozone and its relation with Asia Pacific wave”, Tellus, 54B, :269-277

Sikka, D. R., 1977, “Some aspects of the life history, structure and movement of monsoon depressions”, PAGEOPH, 115, 1501-1529.

Sikka, D. R., 1980, “Some aspects of the large scale fluctuations of summer monsoon rainfall over India in relation to fluctuations in the planetary and regional scale circulation parameters”, Proceedings of Indian Academy of Sciences (Earth and Planetary Sciences), 89, 179-195.

Sikka, D. R., Gadgil, S., 1980, “On the maximum cloud zone and the ITCZ over Indian longitudes during the southwest monsoon”, Monthly Weather Review, 108, 1840-1853

Sikka, D. R., 2006, “ A study on the monsoon Low Pressure Systems over the Indian region and their relationship with drought and excess monsoon seasonal rainfall”, COLA Technical Report, Center for Ocean, Land, Atmosphere studies, 4041 Powder Mill Road, Calverton, MD, USA

Srinivasan, V. and Sadasivan, V., 1975, “Thermodynamic structure of the atmosphere over India during south-west monsoon season”, Indian Jour.Met.Hydr.and Geophys., 26, 169-180.

Stano, G., Krishnamurti, T. N., Vijaya kumar, T. S. V., and Chakraborty, A., 2002, “ Hydrometeor structure of a composite monsoon depression using the TRMM radar”, Tellus, 54A, 370-381

Venkataraman, K. S., Choudhury , A., and Banerjee, A . K., 1974, “A study of hourly rainfall distribution around monsoon depression centre in central India”, Ind.Jour.Met and Geophys., 25, 239-244.

Yasunari, T., 1981, “Structure of an Indian summer monsoon system with around 40 day period”, Journal of the Meteorological Society of Japan, 59, 336-354

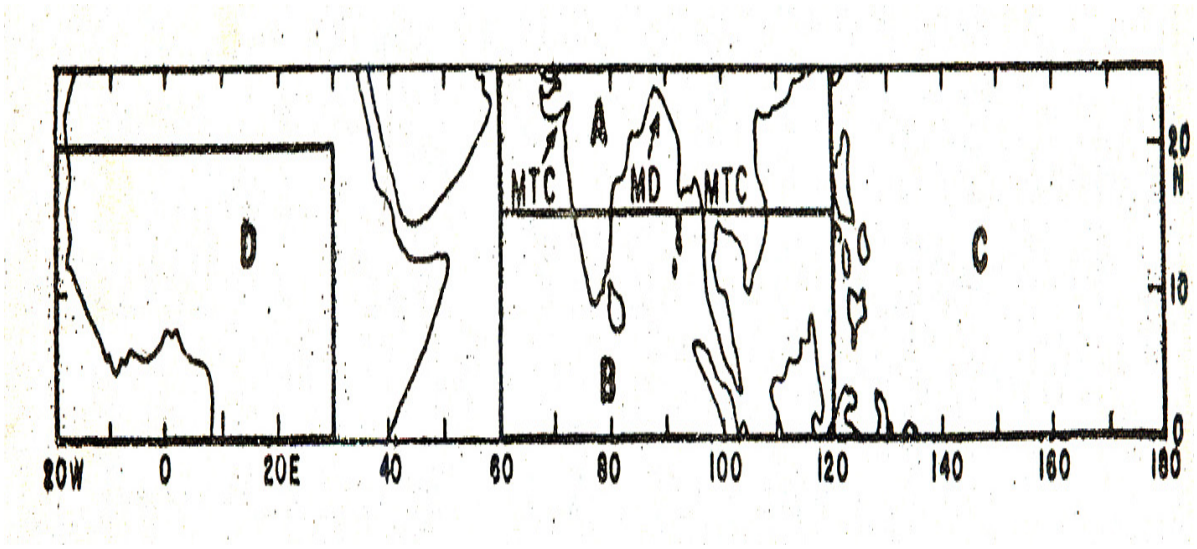

Fig.1.1 : The large-scale monsoon circulation has different characteristics in the 4 broad areas marked A, B, C and D as described in the text. Synoptic systems MD and MTC develop in area-A

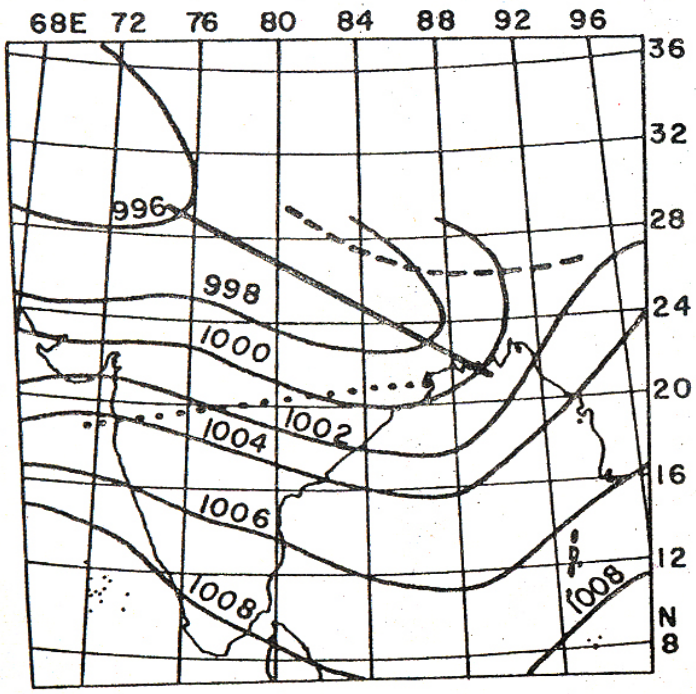

Fig.1.2 : The climatological locations of the Monsoon Trough over India at sea level (thick unbroken line) and at 4 Km asl (line of dots) are marked along with the mean surface isobars

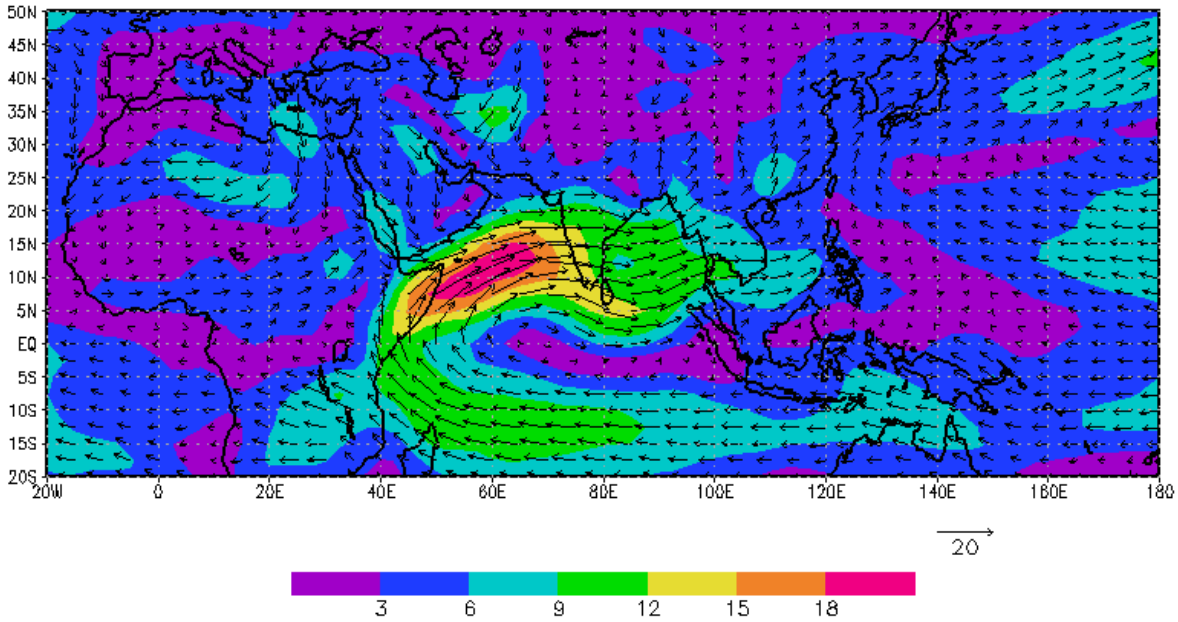

Fig.1.3 : The climatological Low Level Jetstream (LLJ) as mean wind of 40 years (1961-2000) at 850 hPa level (NCEP reanalysis data)

In Active Monsoon- Low Level Jetstream passes through India

From Joseph P.V. and Sijikumar S. (2004)

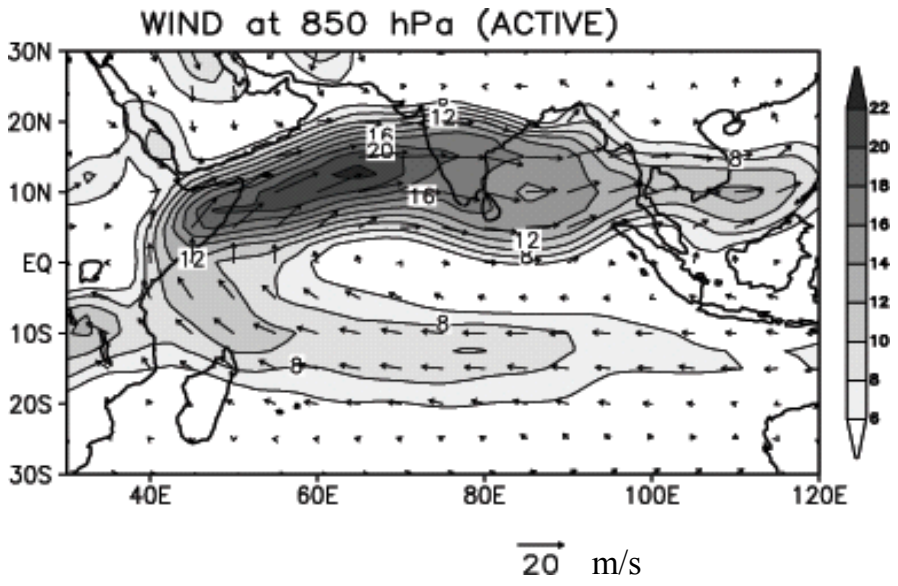

Fig. 1.4 a

In Break Monsoon - Low Level Jetstream bypasses India

From Joseph P.V. and Sijikumar S. (2004)

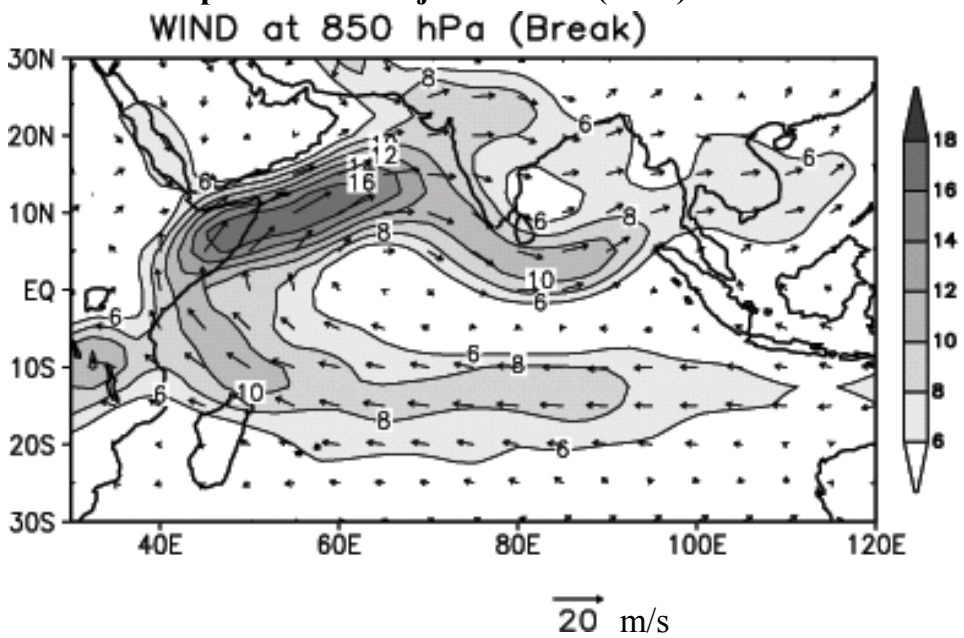

Fig. 1.4 b

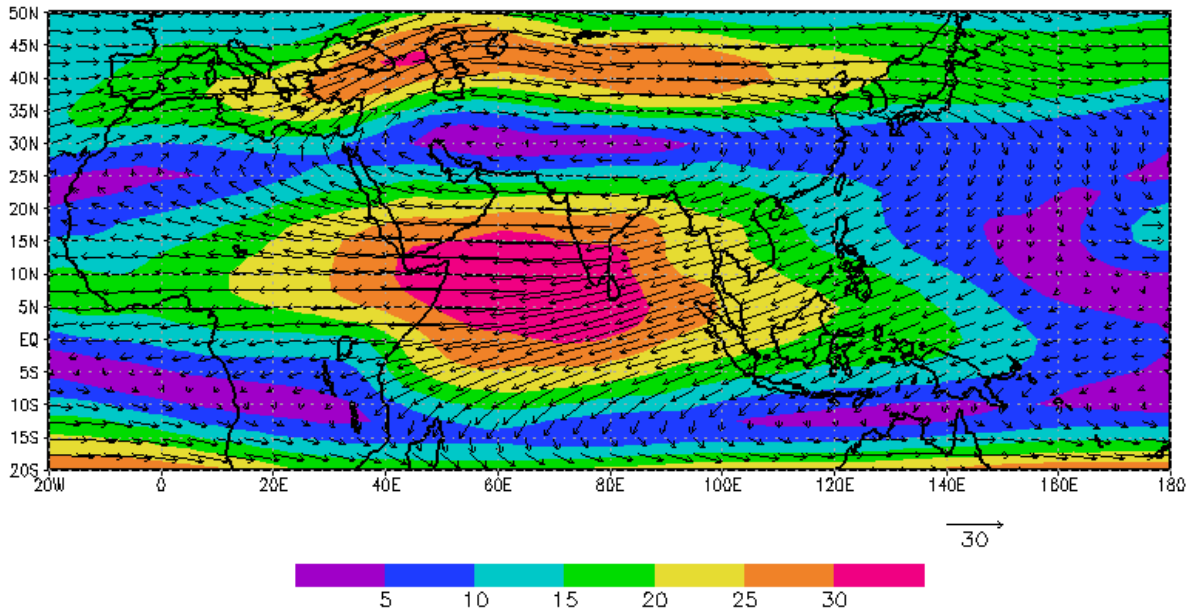

Fig.1.5 : The climatological Tropical Easterly Jetstream (TEJ) as mean wind of 40 years (1961-2000) at 150 hPa level (NCEP data)

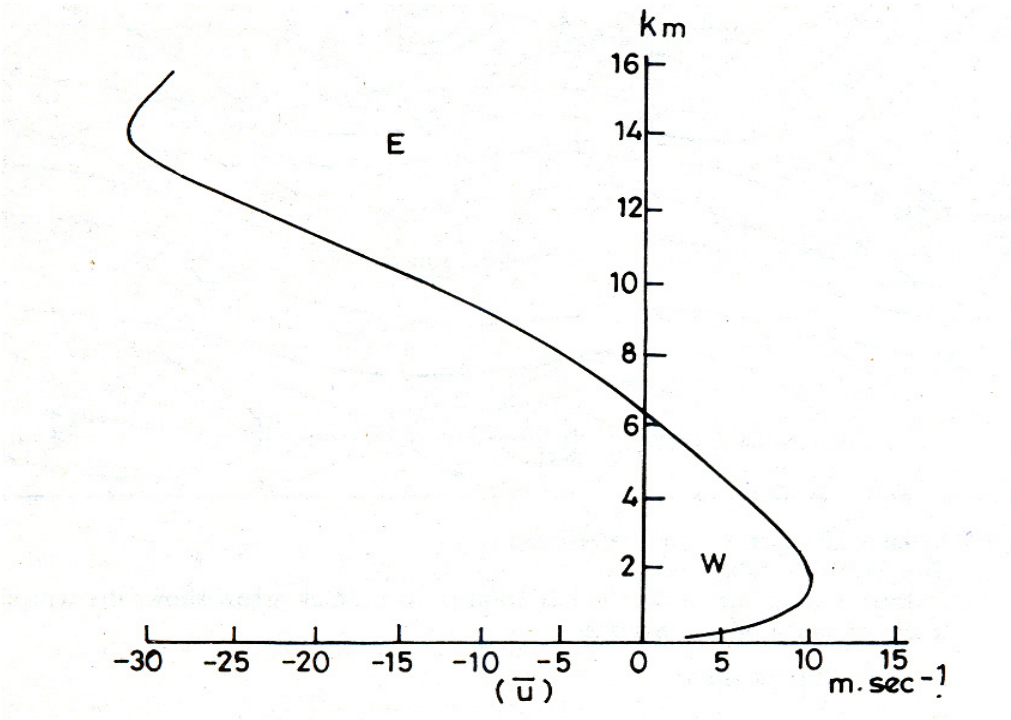

Fig. 1.6 : Vertical profile of mean zonal wind at Trivandrum (8.5N, 76.9E) in box-B for july and August (from Keshavamurti and Shankar Rao, 1992)

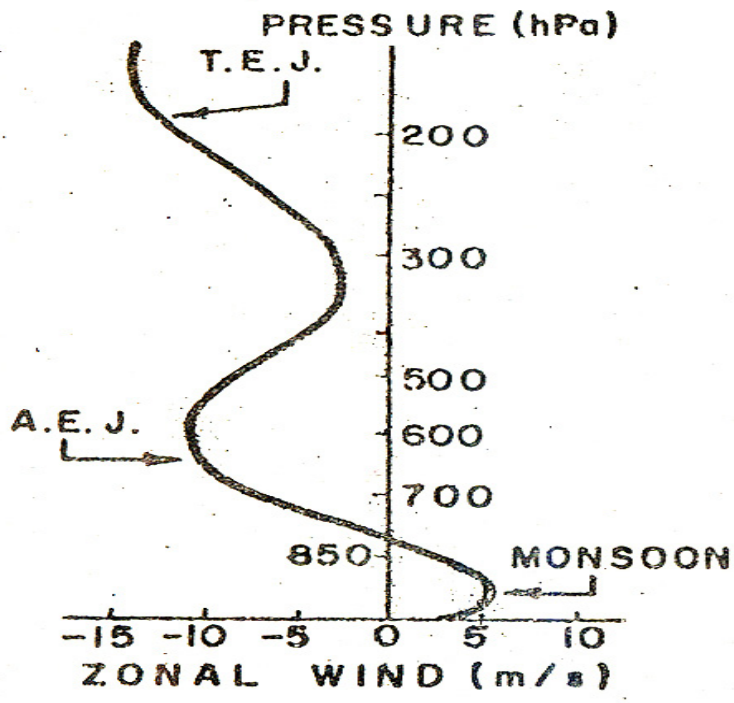

Fig.1.7 : Vertical profile of means zonal wind of July and August of box-D. (from Dhonneur, 1981)

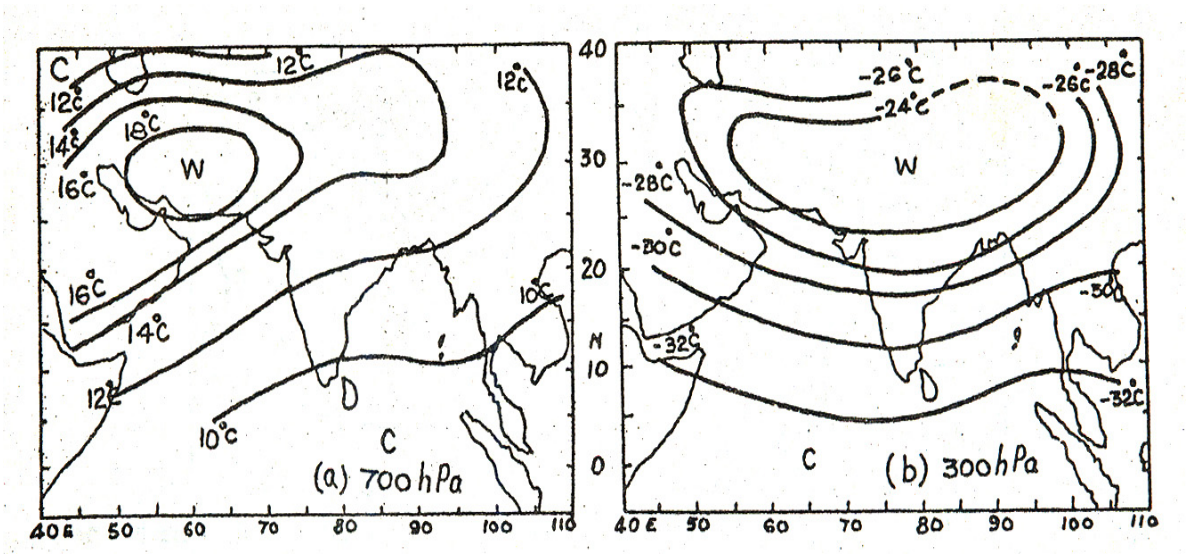

Fig. 1.8 : Climatological mean upper air temperature (a) 700 hPa and (b) 300hPa (from Rao, 1976).

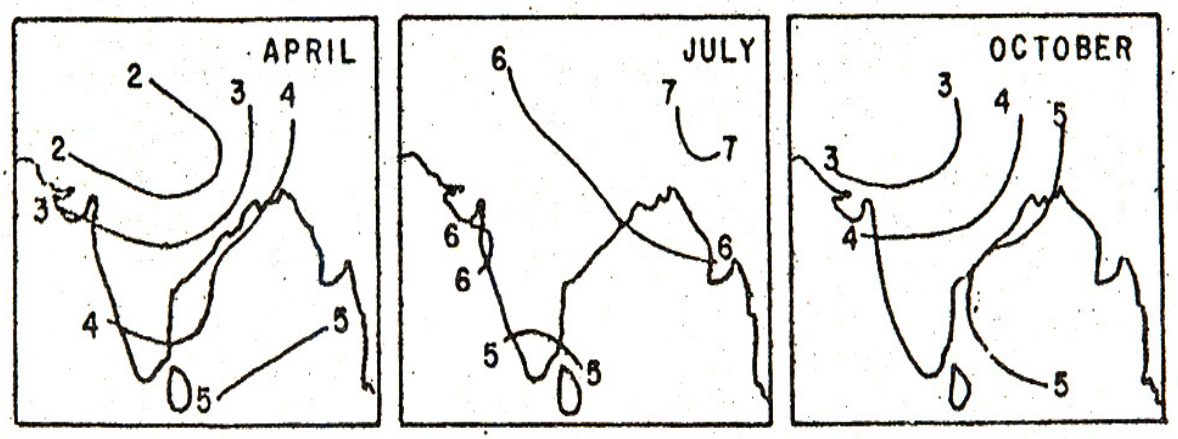

Fig.1.9 : Climatological Precipitable Water Vapour in the atmosphere (in grams per sq cm) during April, July and October (from Ananthakrishnan et al, 1965)

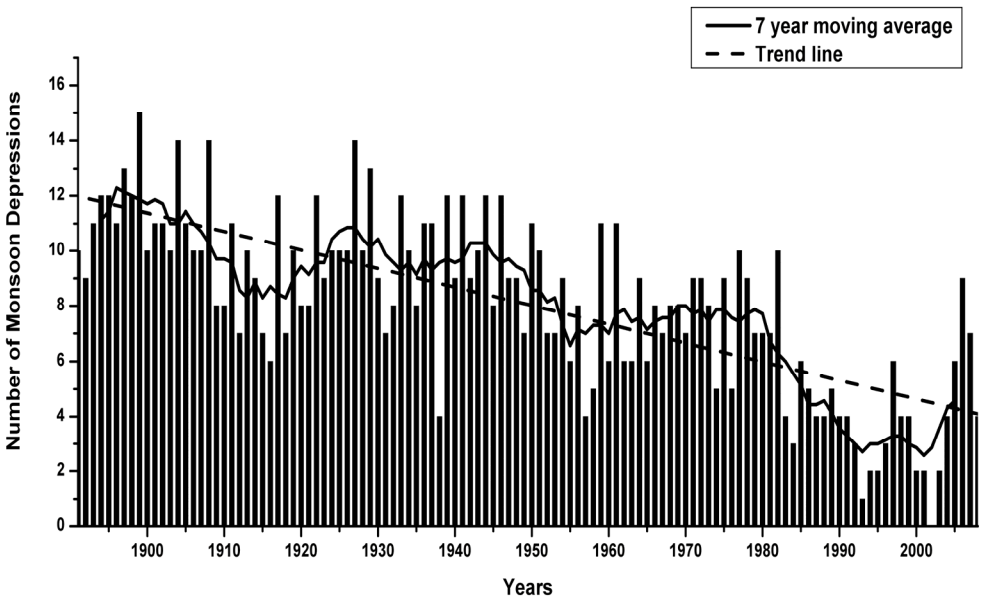

Fig.1.10 : The frequency of Monsoon Depressions in each monsoon season of 1891 to 2007. Seven year moving average and long term linear trend are marked. (Data from IMD)

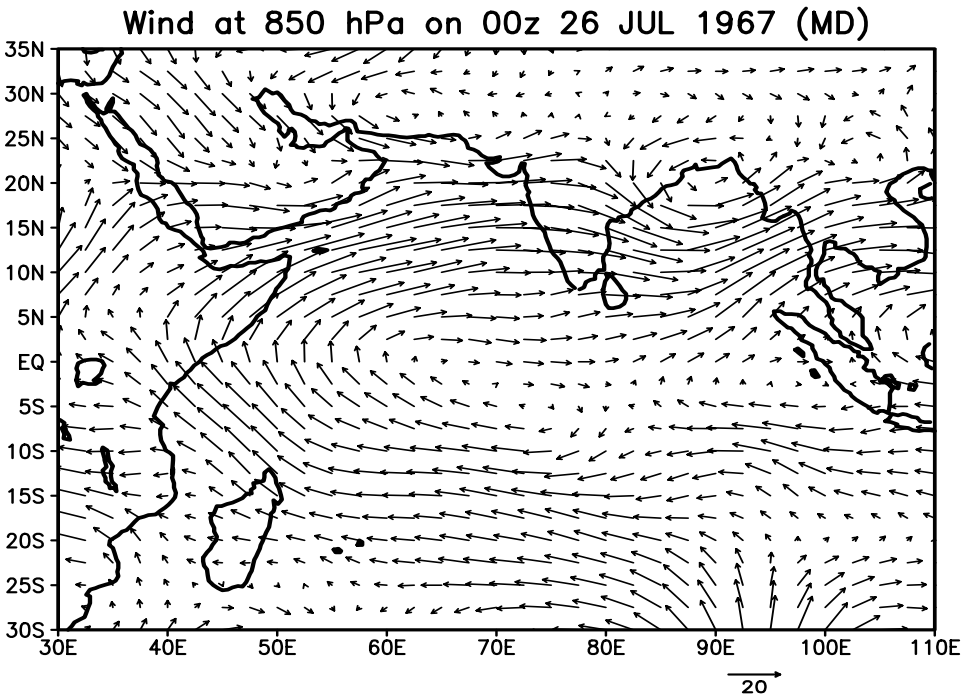

Fig. 1.11a : Monsoon Depression Vortex 26 july 1967

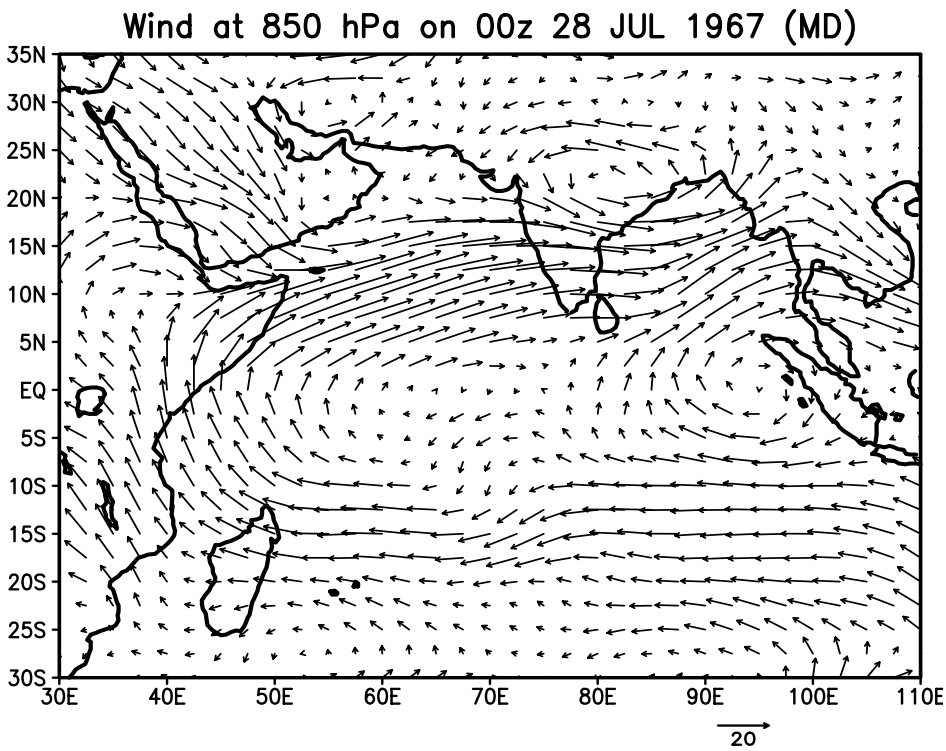

Fig 1.11b : Monsoon Depression Vortex 48 hours later

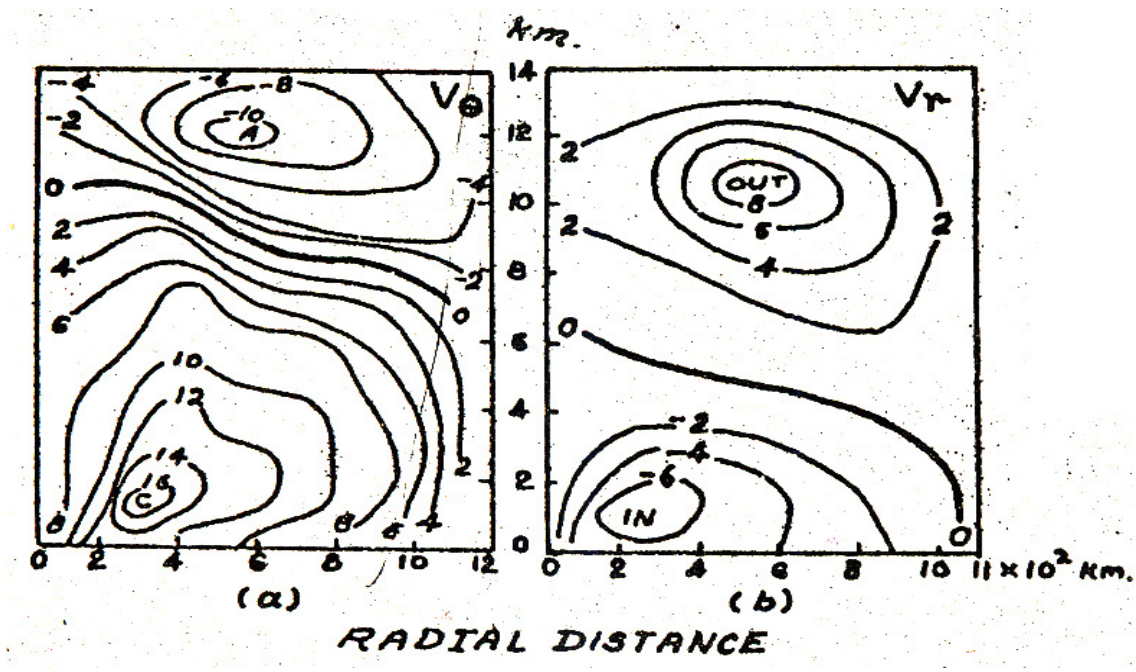

Fig.1.12 : Vertical sections in (a) tangential wind and (b) radial wind in m/s of a composite monsoon depression (from Sikka, 1977)

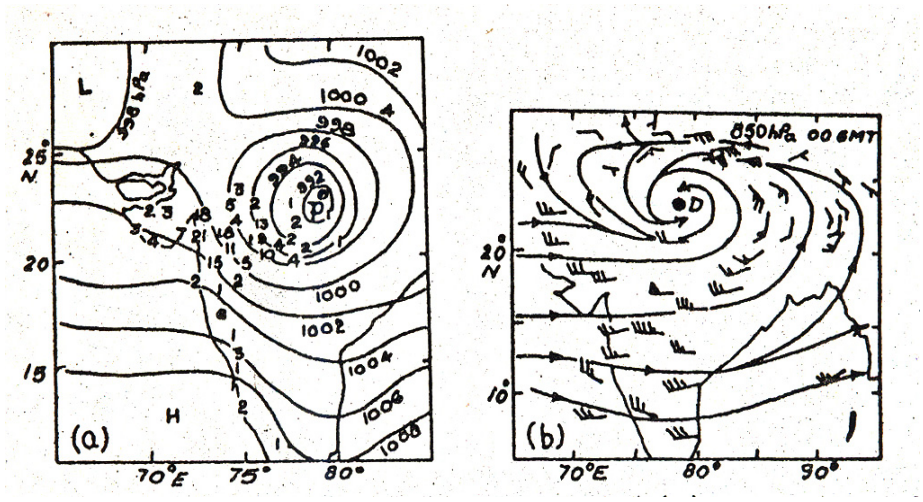

Fig.1.13 : (a) Sea level isobars in hPa and 24 hour rainfall and (b) 850 hPa wind field of a typical monsoon depression

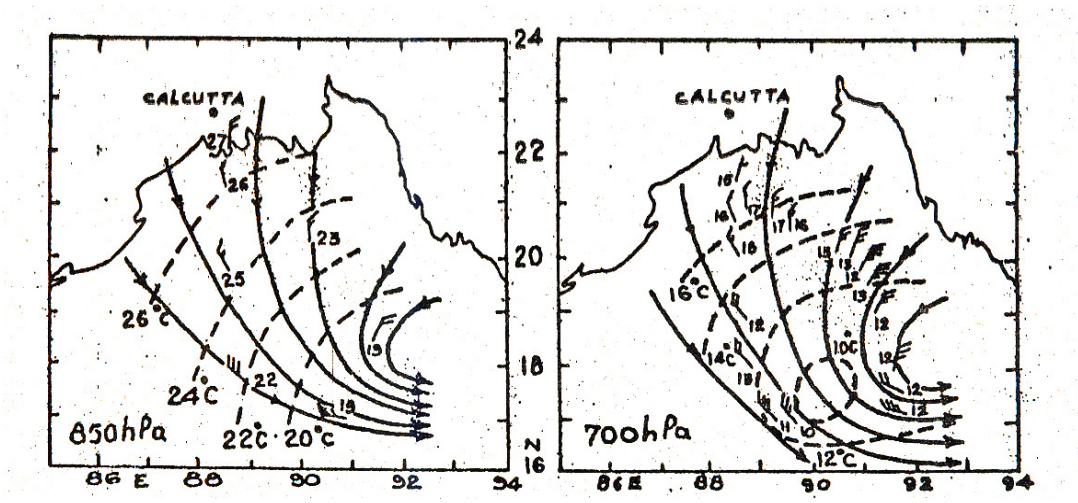

Fig.1.14 : Wind and air temperature at (a) 850 hPa and (b) 700 hPa of a monsoon depression monitored by aircraft in MONEX-1979 – from Joseph and Chakraborty (1980)

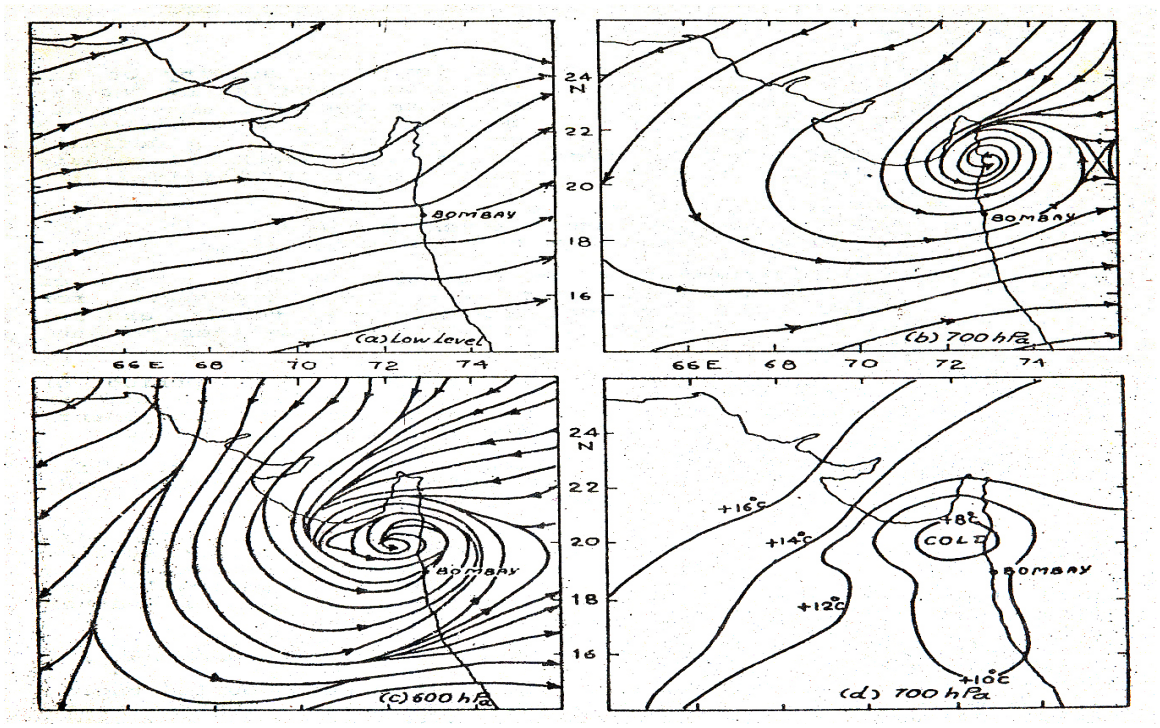

Fig.1.15 : Streamline analysis of a composite MTC at (a) low level, (b) 700 hPa and (c) 600 hPa. Fig (d) gives air temperature at 700 hPa – from Miller and Keshavamurti (1968)

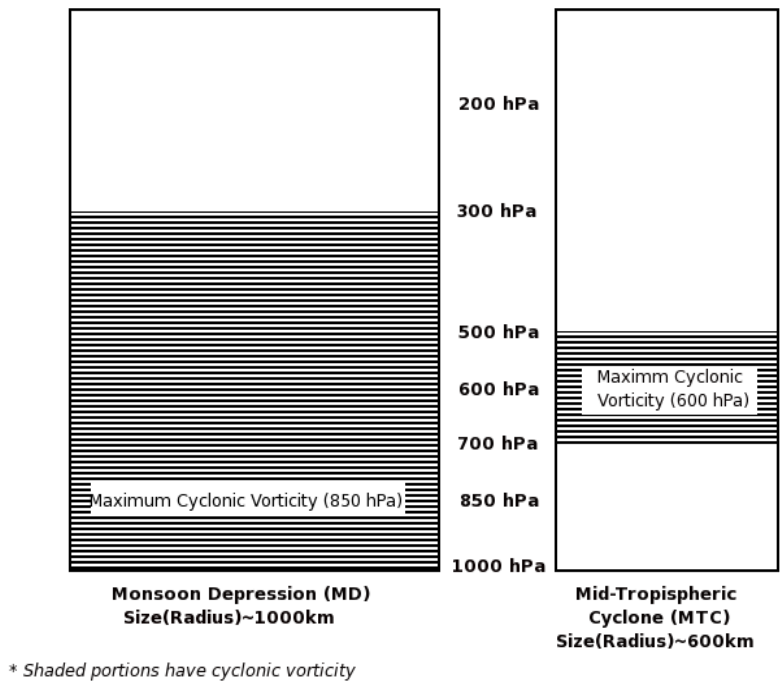

Fig.1.16 : Schematic of some features of MD and MTC that are contrasting

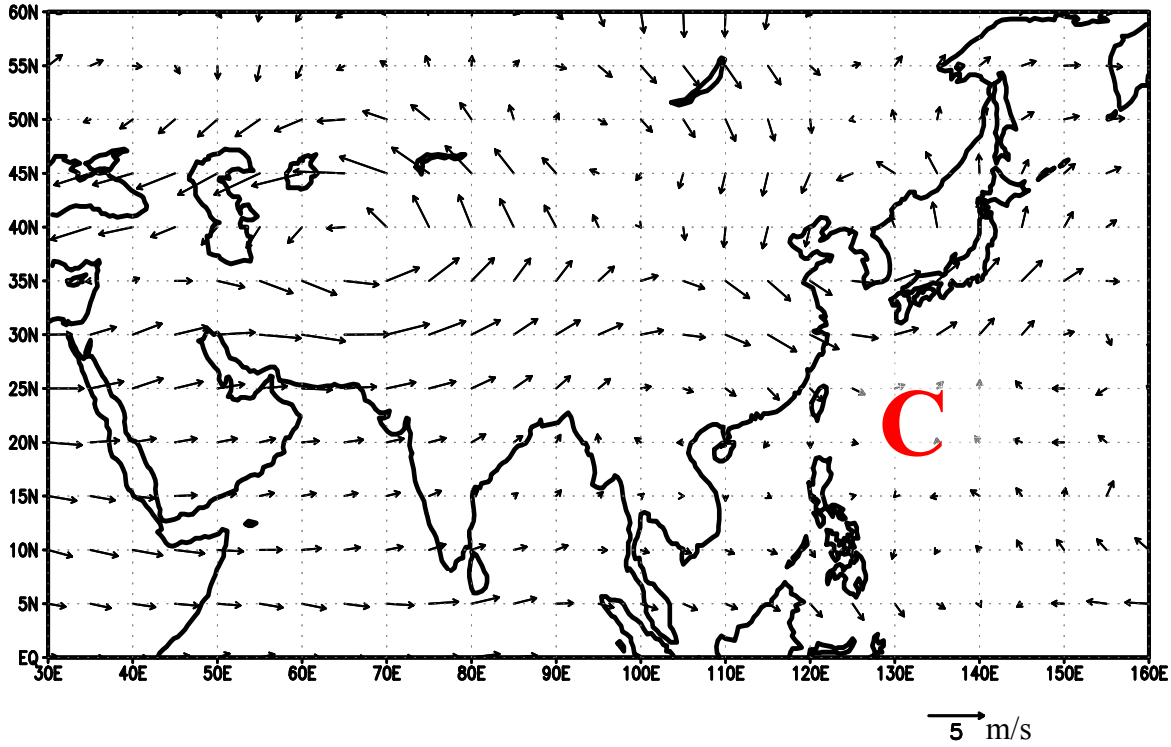

Fig. 1.17a : Composite JJAS 200hPa wind anomaly of 1965, 1972, 1979, 1982 & 1987 (5 DRY monsoons)

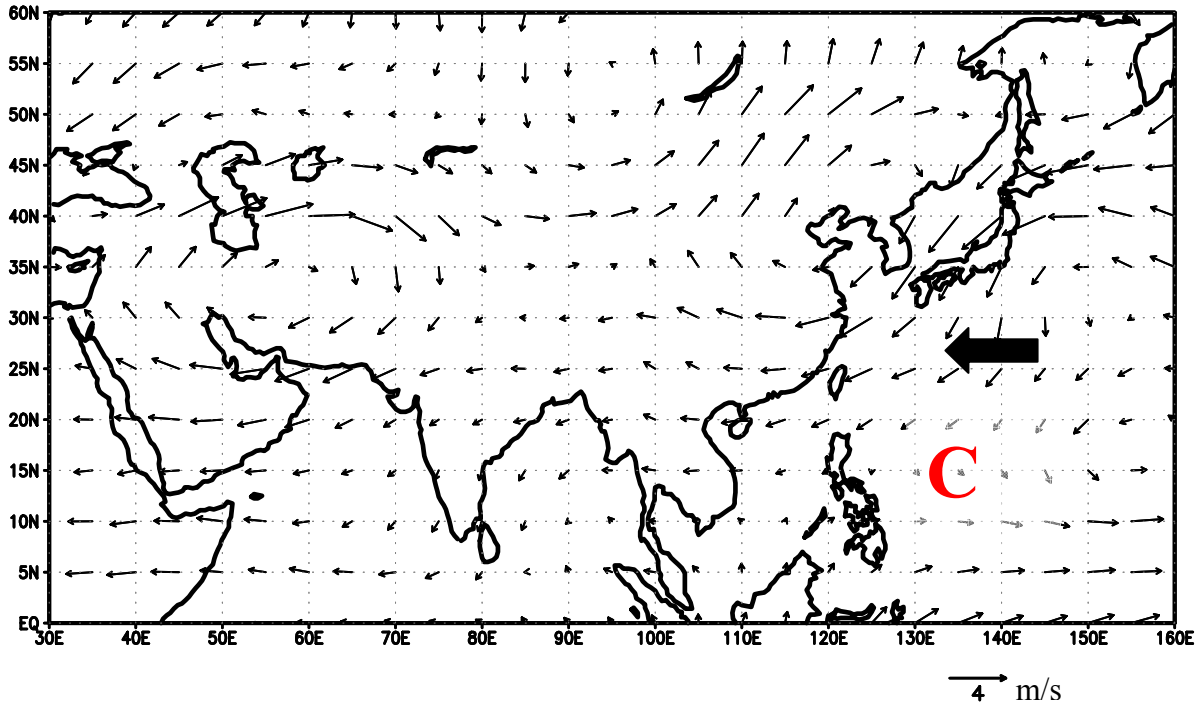

Fig.1.17b : Composite JJAS 200 hPa wind anomaly of 1961, 1970, 1975, 1983 & 1988 (5 WET monsoons)

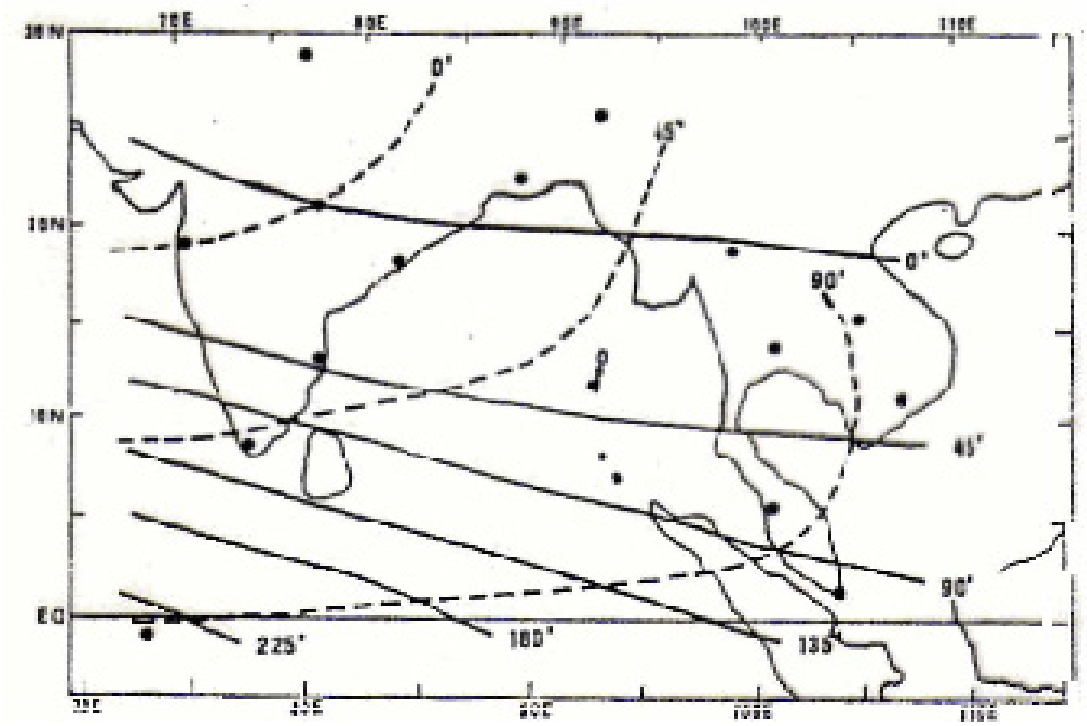

Fig.1.18 : Phase lag relation of filtered 40-day (full lines) and 15-day (broken lines) modes of the geopotential heights of 850 hPa.
The reference point (Phase 0) is at Nagpur - from Yasunari (191)

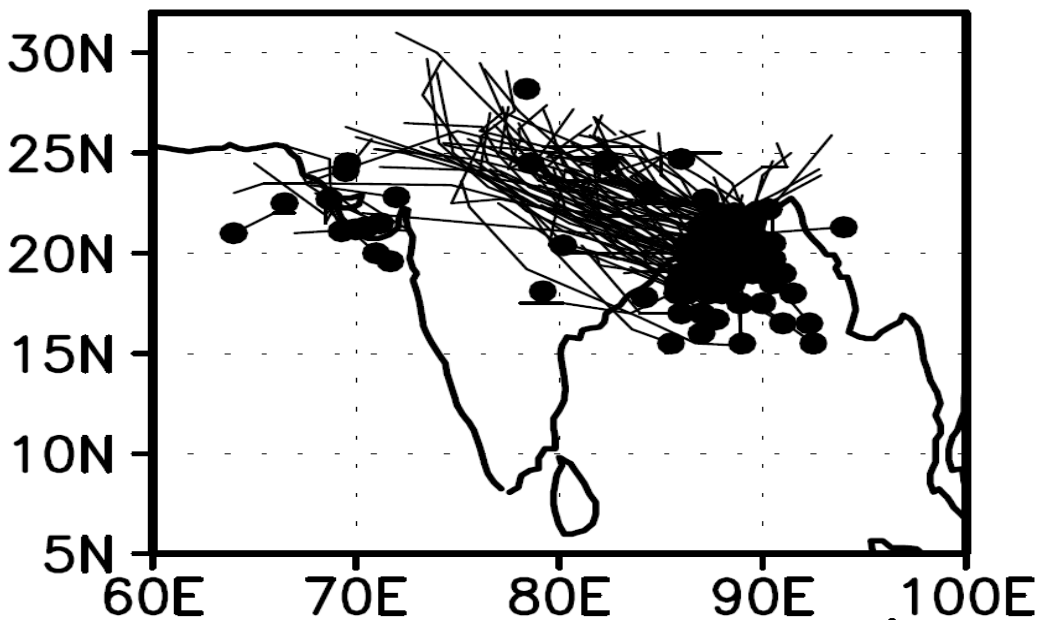

Fig.1.19a : Tracks of monsoon LPS during active phases of monsoon Intra Seasonal Oscillation during 1954-1983. Dots represent genesis point and lines show the tracks of LPS

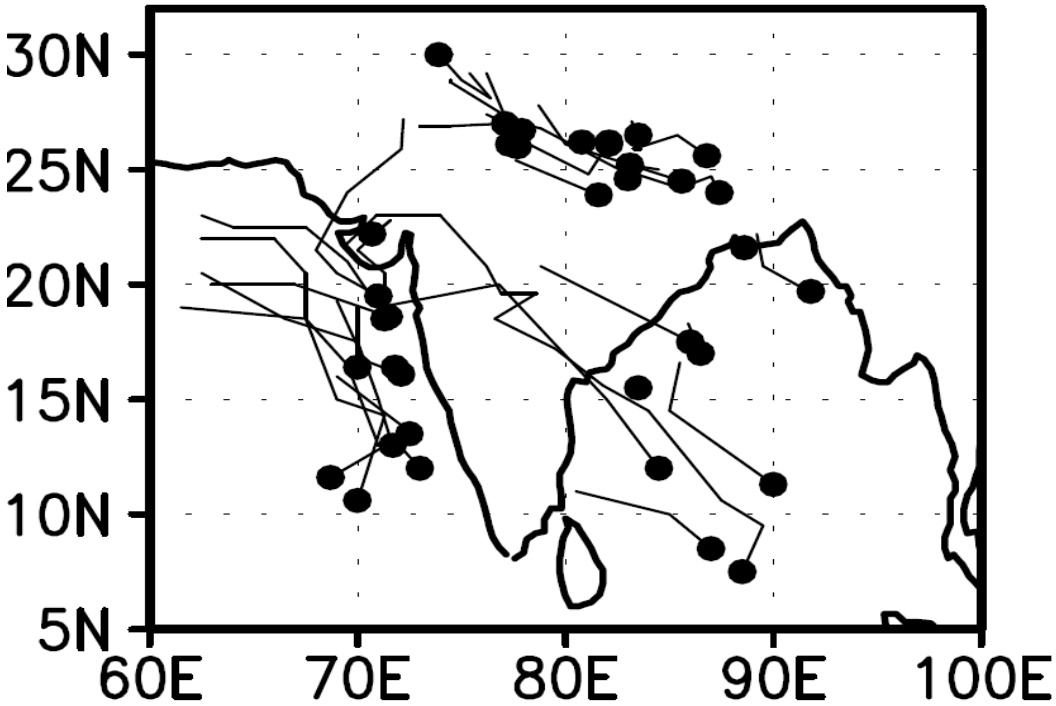

Fig.1.19b: Tracks of monsoon LPS during break phases of monsoon Intra Seasonal Oscillation during 1954-1983. Dots represent genesis point and lines show the tracks of LPS

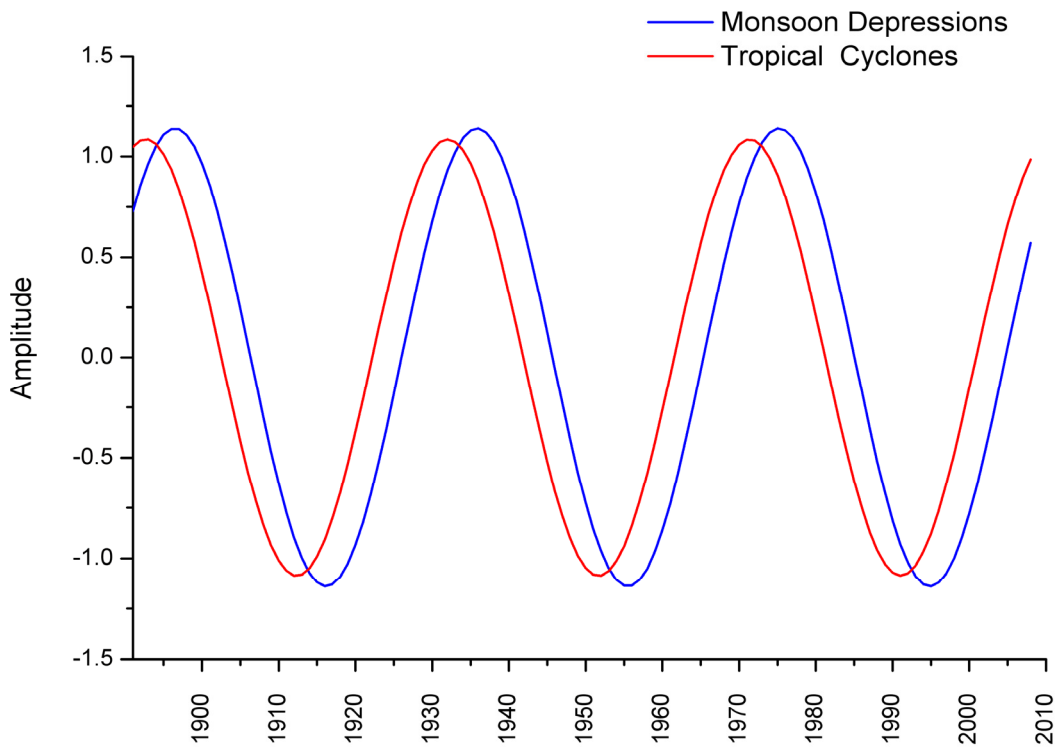

Fig.1.20: Third harmonics (period 39 years) of the time series of number of Monsoon Depressions (blue) and annual number of tropical cyclones (red) of 1891-2007

CHAPTER 2

INDIAN MONSOON VARIABILITY

D. R. Pattanaik

India Meteorological Department, New Delhi

drpattanaik@gmail.com

2.1. Introduction

The word "monsoon" is derived from the Arabic word for season, and the monsoonal regions of the world is delineated by Ramage (1971) on the basis of significant change in the wind direction between winter and summer (with the direction of the prevailing wind within each season being reasonably steady) extends over a large part of the tropics, namely, 25^0S to 35^0N, 30^0W to 170^0E. The Indian sub-continent lies near the centre of this monsoonal region surrounded by ocean on three sides of it, which experiences large seasonal variation in wind direction (Figs. 2.1a,b; based on Rao 1976) between summer and winter. The primary theory behind the cause of monsoon is the differential heating between ocean and land formulated by well known scientist Halley (1686) and subsequently by others (Krishnamurti 1979; Webster 1987). The air-sea interactions play an important role in the monsoon process. As pointed by Pisharoty (1965) the evaporative process over the Arabian Sea plays an important role in contributing to the moisture flux across the West Coast of India and hence in the monsoon circulation. Later, Ghosh et al. (1978) also demonstrated that a large amount of moisture is picked up from the Arabian Sea by evaporation during active monsoon. Like the air-sea fluxes over the Arabian Sea, the sensible heating over the elevated Tibetan Plateau plays a dominant role in the atmospheric diabatic heating of the whole troposphere particularly during the time of onset of monsoon. Diabatic heating over the Tibetan Plateau in the pre-monsoon phase causes horizontal temperature (pressure)

gradients in the upper (lower) troposphere between the surrounding Indian Ocean and the Asian landmass, which facilitates strengthening of southwest monsoon circulation (Ueda and Yasunari 1998).

There is an alternative hypothesis in which the monsoon is considered as a manifestation of the seasonal migration of the intertropical convergence zone (ITCZ; Charney 1969) or the equatorial trough (Riehl 1954, 1979) in response to the seasonal variation of the latitude of maximum insolation. Monsoon circulation is a primary component of the tropical and global climate system and the ability to understand and model its short and long-term variability and evolution is of great interest not only to climate modellers but also to paleo-climatologists.

It is a general perception that life in India revolves around the monsoons. For the millions inhabiting monsoonal regions (particularly the Indian sub-continent), the seasonal variation of the rainfall associated with the monsoon system is of far greater importance than the seasonal variation of wind. Prior to the onset of monsoon, the Indian monsoon zone is characterized by the presence of a heat low centred near the central Pakistan and adjoining northwestern parts of India. Once the monsoon covers the entire country, a tropical convergence zone gets established over the region (Sikka & Gadgil 1980; Krishnamurti and Subramanian 1982; Pattanaik 2003). Over a large part of the Indian region, most of the rainfall (about 80%) occurs in the months of June to September during the summer monsoon. The exception is the east coast of the southern peninsula, where most of the rainfall occurs during October–November during the period of northeast monsoon. The spatial variation of the climatological mean June–September rainfall over the Indian region is shown in Fig. 2.2. Heavy rainfall associated with the monsoon current and synoptic systems are very common during the southwest monsoon over India along the monsoon trough axis. A useful index of the summer monsoon rainfall over the Indian region in any year is the all-India summer monsoon rainfall (AISMR), which is a weighted average of the June–September rainfall obtained from IMD observations. The long period average (LPA) of AISMR based on the period 1941-1990 is found to be 890 mm. During the summer monsoon, high rainfall occurs

along the West Coast of the peninsula (associated with the orography parallel to the coast) and over the northeastern regions as seen from Fig. 2.2. With respect to the monthly rainfall distribution the rainfall during June mainly concentrates over the western coast, northeast states and parts of central India. The peak monsoon months of July and August receive rainfall over most parts of India, whereas, during the withdrawal phase of September the northwestern parts of India receive very little rainfall (Fig. not shown). The space-time variation of rainfall has a large impact on the resources of the region, especially the agriculture sector. Thus, there is a greater need to study the monsoon variability.

2.2. Different temporal scale of monsoon variability

Most of the observational and numerical simulation studies on climate are based on the instrumental records, which are very useful in understanding of the natural variability of climate system and to identify processes and forcings that contribute to this variability. The knowledge of climate variability over the period of instrumental records and beyond on different temporal and spatial scale is important to understand the nature of different climate systems and their impact on the environment and society. Although the Indian monsoon comes with a reassuring regularity, it exhibits a wide range of variability on the spatial, temporal, intra-seasonal, inter-annual, decadal and millennium scale. The large variability in the Asian summer monsoon rainfall on both space and time scales starting from intra-seasonal variation to the Millennium time-scale (Table 2.1) is well known. In addition to these, the monsoon rainfall also exhibits some diurnal characteristics over tropical region. The summer monsoon during June to September is mainly driven by two primary heat sources: sensible heating of the Asian land mass and condensational (latent) heating within the troposphere over the Asian Plateau. Latent heat from moisture collected over the southern subtropical Indian Ocean is transported across the equator and released during precipitation over Asia and Africa. Both sensible and latent heat mechanisms contribute to the land-sea temperature and pressure differences that ultimately drive summer monsoon circulation. Since inter-annual insolation is relatively constant, interannual variability in monsoon strength derives mainly from changes in the latent heat source or other internal feedbacks.

However, over orbital time scales, insolation gradients change is very significant. Hence the monsoon variability at the orbital time scale is thus linked to changes in both the sensible and latent heat sources as well as internal feedback processes, which impact them. The most important scale of the monsoon variability as given in Table 2.1 is the interannual and intraseasonal variability. The coefficient of variability of southwest monsoon rainfall over India during June to September on seasonal scale (AISMR) is shown in Fig. 2.3. Indian summer monsoon exhibits large spatial variability with regions of high rainfall (the West Coast of the peninsula and over the north-eastern regions) are associated with lowest variability and the regions of lowest rainfall (northwestern parts of India) having highest variability as seen from the mean and coefficient of variability maps of AISMR shown in Fig. 2.2 & Fig.2.3 respectively. With respect to the daily variability of AISMR, Fig. 2.4 shows the daily climatological normal rainfall and daily coefficient of variability from 1st June to 30th September. As seen from Fig. 2.4 the daily monsoon rainfall shows highest variability (60% to 70%) during the onset phase of monsoon (during first 15 days of June) followed by about 50% to 60% during the withdrawal phase of September. Fig. 2.4 also shows that the peak monsoon month of July and August shows relatively lower CV (35% to 40%) compared to onset and withdrawal phase of monsoon.

2.3. Interannual variability of seasonal & monthly monsoon rainfall

The interannual variability of monsoon is very crucial as it has a very large impact on agricultural production (Gadgil et al., 1999). It has also been said that the Indian economy is a gamble on the monsoon rains. The interannual variation of AISMR during the last 136 years (1875-2010) is shown in Fig. 2.5. As seen from Fig.2.5 the interannual variation is not very large, with the Standard Deviation (SD) being only about 10% of the mean. The interannual variability of AISMR shows more number of drought years (24 years ≈17.6%) compared to the flood years (19 years ≈ 13.9%) during the period 1875 to 2010. Thus, during the period of 1875-2010, number of deficient years (24) is more than the number of excess years (19). The drought and flood years are identified based on the departure of AISMR beyond ± 1 SD, which is also given in Table 2.2. As seen from Fig. 2.5 among the drought years, 1877 recorded

the lowest rainfall (67% of LPA) during this long history followed by the years 1899 (72% of LPA), 1918 (75.1% of LPA), 1972 (76.1%) and 2009 (78.2%) with negative departures exceeding 2 SD (≈ -20% of LPA) value. Similarly the excess rainfall ever recorded is found to be in 1917 (122.9% of LPA) followed by 1961 (121.8% of LPA) where the positive departures of seasonal rainfall exceeds 2 SD (≈ +20% of LPA) value. As pointed by many earlier studies there is a close correspondence between deficit monsoon rainfall and El Ni˜no (Sikka 1980, Pant & Parthasarathy 1981, Rasmusson & Carpenter 1983). However, Kumar et al. (1999) have suggested that the link with El Ni˜no has weakened in the last decade, and in fact the AISMR anomaly was positive in the recent intense warm event of 1997. Mechanisms leading to the interannual variation of AISMR, including teleconnections with other phenomena (such as the El Ni˜no) are yet to be unravelled. Many other studies have also lined various teleconnection patterns other than ENSO to explain the observed interannual variability of AISMR. Pattanaik et al., (2005) have shown a relationship between AISMR and the evolution of convective activity during winter to pre-monsoon seasons over the Indo-Pacific region and found that the negative OLR (thus, convection) anomalies from January gradually strengthen in a west northwest direction from western Pacific region and get established over the southeast Asian region and adjoining eastern equatorial Indian Ocean by the month of May prior to excess AISMR years indicating a gradual reversal of anomalous rising motion over western Pacific in January to anomalous sinking motion in May over western Pacific region. However, during the deficient AISMR years the negative OLR anomalies established over the western Pacific region in January almost remain active over the same region till the month of May and consequently there is persistent presence of rising motion from northern winter to pre-monsoon seasons over the western Pacific.

Like the interannual variability of AISMR the interannual variability of monthly rainfall during June to September during the period from 1901-2010 for the country as a whole is shown in Fig. 2.6. The contribution of peak monsoon months of July and August to the seasonal total rainfall of 890 mm is found to be about 33% and 29.5% respectively. Whereas, the contribution of June rainfall and September rainfall to the

seasonal total is found to be about 18.5% and 19% respectively. Unlike the Coefficient of Variability (CV) of AISMR, which is close to 10% the CV of monthly rainfall is higher particularly during the withdrawal phase of September (23%) and the onset phase of June (22%), followed by that during August (15%) and July (14%). Thus, the onset and withdrawal phase of monsoon are more variable compared to that of peak monsoon months of July and August. Based on ± 1 SD the excess and deficient monthly rainfall years during the period from 1901 to 2010 are identified and are given in Table 2.1. Being the month of lowest CV, July (Fig. 2.6b) shows most years with normal rainfall, however, there is exceptionally large departure for some years such as (1911, 1918, and 2002 where the negative departures exceed 45%). The active month of August although shows slightly higher CV compared to that of July, the number of excess year is much higher in August compared to that of July as given in Table 2.2 and Fig. 2.6c. Similarly it is also seen from Fig. 2.6a and Fig. 2.6d that the onset and withdrawal phase of monsoon show large variability with many excess and deficient months with rainfall departure exceeding ± 1 SD value.

Although the Figs. 2.5 and Fig. 2.6 indicate large variability of AISMR and monthly rainfall respectively, it does not show any significant linear trend. However, there exists trend in the sub-divisional rainfall (Guhathakurta and Rajeevan 2007). As shown (Fig. 2.7) by Guhathakurta and Rajeevan (2007) during the season as a whole, three subdivisions viz. Jharkhand, Chattisgarh, Kerala show significant decreasing trend and eight subdivisions viz. Gangetic West Bengal, West Uttar Pradesh, Jammu & Kashmir, Konkan & Goa, Madhya Maharashtra, Rayalaseema, Coastal Andhra Pradesh and North Interior Karnataka show significant increasing trends. On monthly scale from June to September, the trend for met subdivision level is shown in Fig. 2.8. June rainfall (Fig. 2.8a) has shown significant increasing trend for the western and south-western parts of the country, whereas significant decreasing trend is observed for the central and eastern parts of the country. July rainfall (Fig. 2.8b) has significantly decreased for most parts of the central and peninsular India but has increased significantly in the Northeastern parts of the country. In July, six subdivisions have shown decreasing trends and eight subdivisions have increasing trends.

In August, four (ten) subdivisions have indicated decreasing (increasing) trends of monthly rainfall. August rainfall has increased significantly for the subdivisions Konkan & Goa, Marathwada, Madhya Maharashtra, Vidarbha, West M.P., Telengana and west U.P and has increased significantly (at 95% significance level) for the subdivisions Konkan & Goa, Marathwada, Madhya Maharashtra, Vidarbha, West M.P., Telangana and west U.P. During the withdrawal phase of September, significant decreasing trend of rainfall is noticed for subdivisions Vidarbha, Marathwada and Telangana and increasing trend (95%) for the subdivision Sub Himalayan Gangetic West Bengal. September rainfall is increasing significantly (at 95% level of significance) in Gangetic West Bengal and decreasing significantly (at 90% level of significance) for the sub-divisions Marathwada, Vidarbha and Telangana.

2.4. Decadal and epochal variability of monsoon rainfall

Although the Indian monsoon rainfall for the country as a whole do not show any trend, however, it is seen that the Indian summer monsoon rainfall displays multi-decadal variations in which there is a clustering of wet or dry anomalies. The decadal mean departure of all India summer monsoon rainfall (AISMR) during last 11 decades from 1901 to 2010 is shown in Fig. 2.9, which indicate the alternating sequence of multi-decadal periods having frequent droughts and flood years. As seen from Fig. 2.9 we can delineate (i) 1901-1930 dry period (ii) 1931-60 wet period (iii) 1961-1990 is also a dry period. Earlier studies by Pant and Kumar (1997) using the data series of Parthasarathy et. al., (1994) also found the similar results of 30 years of alternating sequences of dry and wet period. As also seen from Table 2.2 during the first decade of 1901-1910 there are four deficient years but no excess year. In the decade 1911-1920, there are four deficient and three excess years and during the decade from 1921-1930 there is no deficient year and no excess year. Thus, during the dry period of 1901-1930, we had eight deficient years and three excess years. During the next three decades of wet period (1931-1960), we had two deficient years and five excess years. In the dry period of 1961-1990, there were nine deficient years and five excess years. The recent two decades also witnessed negative composite anomalies with three deficient years

reported in the last decade between 2001 to 2010 and no excess year during this decade.

On monthly scale from June to September the decadal mean percentage departure of monsoon rainfall is shown in Fig. 2.10. As seen from Fig. 2.10a the decadal variability is more in June where alternating sequence of wet and dry periods are seen on almost every decade at least for initial 5 decades till 1950. Subsequently the negative departure persists for two more decades till 1970 followed by positive departure during recent 4 decades. During July (Fig. 2.10b) it is seen that the first two decades show negative composite anomalies and subsequently during the decade from 1921 to 1930 the July rainfall was good with no deficient July as seen from Table 2.2. However, during this decade, in spite of high contribution from July, seasonal rainfall composites became negative (Fig. 2.9) because of high negative contribution of June and August rainfall (Fig. 2.10a & 2.10c). During the subsequent three decades from 1931 to 1960, the mean departure is positive similar to that of seasonal rainfall departure and the subsequent 5 decades from 1961 to 2010 both July rainfall and seasonal rainfall shows negative mean departures for all 5 decades. Thus, except for the decade 1921-1930, behaviour of July rainfall was almost similar to that of monsoon seasonal rainfall shown in Fig. 2.9. In the case of August rainfall (Fig. 2.10c) the six decades from 1931 to 1990 shows good rainfall with positive mean departure and was associated with only five deficient and fourteen excess August rainfall. The recent decade from 2001 to 2010 for August (Fig. 2.10c) witnessed 3 deficient years and associated with mean negative departure of rainfall like that of mean negative seasonal rainfall shown in Fig. 2.9. During September (Fig. 2.10d), the recent 4 decades from 1971 to 2010 experienced mean negative departure of rainfall like that of July rainfall and was associated with 8 deficient month and 5 excess month as shown in Table 2.2.

Thus, it is seen here that the Indian summer monsoon rainfall displays multi-decadal variations in which there is a clustering of wet or dry anomalies. Many other studies (Thapliyal and Kulshrestha 1991; Pant and Kumar, 1997; Hingane, et al., 1985; Rupa Kumar et al., 1992; Rajeevan et al.2006) also indicated a highly variable but trend

less behaviour of the Indian summer monsoon rainfall with a prominent epochal nature of variability. The monsoon rainfall shows the epochal behaviour with altering epochs of above and below normal rainfall. Thapliyal and Kulshrestha (1991) also analysed the climate change and the epochal variations of monsoon rainfall over India and found no systematic climate change or trend over India. Kripalani and Kulkarni (1997) examined the epochal variation of monsoon rainfall and its association with the ENSO-AISMR relationship and showed that the impact of El Nino on the AISMR was more severe during the below normal epochs than during the above normal epochs. To examine the epochs of above and below normal rainfall, 31-year and 21-year running means of AISMR was calculated to isolate low frequency behaviour. These epochs of above and below normal rainfall are shown in Figs. 2.11a,b. The epochal behaviour as shown in Figs. 2.11a,b indicates that as of now the AISMR is in the negative epoch and just entering towards the above normal epoch, although it has not yet entered to above normal epoch. To understand the epochal behaviour of monthly rainfall series for different monsoon months, we have also calculated 31-year running means of each of the monsoon months (Fig. 2.12). It is seen that epochal behaviour of July and September (Fig. 2.12b & 2.12d) rainfall are slightly similar to that of monsoon seasonal rainfall as both are now in negative phase. In August, the above normal or positive phases started from the middle of 1950s and continued till to the end. Both June and August rainfall are in positive phase in the recent period (Fig. 2.12a & 2.12d).

2.5. Inter-annual variability of extreme rainfall

In recent years there have been reports of many exceptionally heavy rainfall events over different stations of India. The recent exceptionally heavy rainfall of 944 mm over Mumbai (Santacruz) on 26-27 July, 2005 was very unprecedented in nature, which led to large scale urban flooding (Bohra 2006, Jenamani et al., 2006; Shyamala and Bhadram 2006; Sahany et al., 2010). Similarly, there are many past instances of Indian stations having recorded as much as half of their annual rainfall, and some times even more than their annual rainfall, in one single day (Dhar and Mandal 1981). The unprecedented rainfall event of 26-27 July 2005 over Santacruz was associated with favourable synoptic conditions such as i) a low pressure area over the northwest Bay of

Bengal and adjoining Orissa-Chattisgarh, ii) intensification of the monsoon trough and development of embedded convective vortices over central India, iii) strengthening of the Arabian Sea current of the monsoon and iv) super-positioning of a meso-scale off-shore vortex over northeast Arabian Sea and its northward movement. After the unusual event of Mumbai rainfall many scientists have performed detailed studies of frequency analysis of heavy rainfall events (Goswami et al., 2006; Rajeevan et al, 2008[a]; Pattanaik and Rajeevan 2010) over the Indian region. The development of a high resolution (1°x1° lat./long.) gridded daily rainfall dataset for the Indian region by National Climate Centre (NCC) at IMD, Pune (Rajeevan et al., 2006) was very helpful in undertaking such studies.

The results presented below are based on the study by Pattanaik and Rajeevan (2010) about the trend and the frequency of heavy rainfall events over the Indian region and its contribution to total rainfall during the southwest monsoon season for a period of 55 years from 1951 to 2005 using the daily gridded (1°x1°) rainfall. Based on the classification by IMD about the rainfall amount in a single day, three categories of rainfall are considered by them to study the variability of frequency of heavy rainfall event such as (i) light to rather heavy rainfall ($0 < R \leq 64.4$ mm), (ii) heavy rainfall ($64.4 < R \leq 124.4$ mm) and (iii) very heavy to exceptionally heavy rainfall ($R > 124.4$ mm) using 55 years of data from 1951 to 2005. In this study the last categories with $R > 124.4$ mm is referred hereafter as extreme rainfall events. In order to see the dominating regions of heavy rainfall events and no rain days the mean frequency in terms of the % days of the whole season of 122 days from 1st June to 30 September for no rain days and three categories of rainy days are shown in Figs. 2.13a-d. The no rain days as shown in Fig. 2.13a gradually increases towards northwest parts of India where the number of rainy days in a season from June to September are less, whereas Fig. 2.13b shows the highest frequency of Category-i rainfall days (more than 70%) over the west coast, eastern and north east regions, gradually decreasing towards the northwest of India. The average frequency of Category-ii and Category-iii rainfall as shown in Fig. 2.13c and Fig. 2.13d respectively is very small compared to the frequency of Category-i rainfall over almost the entire country with the highest frequency over the west coast of

India (more than 10% for Category-ii and more than 3% for Category-iii), northeast parts of India and also some isolated pockets over central parts of India. Thus, it is seen that the highest frequency of extreme rainfall event is mainly observed over the west coast region extending up to the Gujarat coast, northeast parts of the country and some parts of central India. Fig. 2.13d also shows higher frequency of extreme rainfall events over some parts of central India in the belt north of 18°N, which is mainly associated with movement of synoptic scale systems from the Bay of Bengal. It is found that the frequency of extreme rainfall (Rainfall ≥ 124.4 mm) show increasing trend over the Indian monsoon region during the southwest monsoon season from June to September (JJAS) and is significant at 98% level (Figs. 2.14abc). Similarly, on monthly scale the frequency of extreme rainfall events show significant (95% level) increasing trend during June and July, whereas during August and September the increasing trend is not significant statistically (Fig. Not shown). They also found that the increasing trend of contribution from extreme rainfall events during JJAS is (Fig. 2.14c) balanced by a decreasing trend in category-i (rainfall ≤ 64.4 mm/day) rainfall events (Fig. 2.14a). Like the frequency of extreme rainfall event, the contribution of extreme rainfall to the total rainfall in a season is also showing highly significant increasing trend during the monsoon season from June to September and during June and July on monthly scale.

In order to understand the physical reason behind this increase of extreme rainfall event the degree of moist convective instability is calculated over the Indian monsoon region during June to September on each day for the 55 monsoon seasons (June to September) from 1951 to 2005 and the daily mean is calculated over the region by taking the average of 6710 observations (55 years; 55×122 day). Associated with increasing frequency of heavy rainfall event they have also inferred that higher moist convective instability coupled with enough moisture availability during the southwest monsoon season can increase the occurrence of deep convection and hence the frequency of extreme rainfall events. Pattanaik and Rajeevan (2010) also found that the seasonal mean moist convective instability (CI) during JJAS averaged over central India indicates a significant increasing trend (99.9% confidence level) and is basically due to the increasing trend of the number of days with greater degree of moist CI during JJAS,

which may be one possible cause for the increasing trend in the frequency of extreme rainfall events over the region. Thus, the climate change in the form of the increasing trend in the number of above normal unstable days during the monsoon season may be the cause for the increased frequency of extreme rainfall events over the Indian region.

2.6. Intra-seasonal variability of monsoon rainfall

The inter-annual variability of the sub-seasonal fluctuations during the monsoon season is large as seen from the day-to-day coefficient of variability of AISMR in Fig. 2.4. During the summer monsoon season (June to September), a substantial component of the variability of convection and rainfall over the Indian region arises from the fluctuation on the intra-seasonal scale between active spells of rainfall and weak spells or breaks spells of rainfall (Alexander et al 1978, Raghavan 1973, Krishnamurti & Bhalme 1976 etc.). Long breaks in critical growth periods of agricultural crops lead to substantially reduced yield (Gadgil et al 2003). Even in normal monsoon years, an uneven spatial and temporal distribution of rains has an adverse effect on agriculture.

Ramamurthy (1969) defined a break situation as one in which the surface trough (the “monsoon trough’) is located close to the foothills, easterlies disappear from the sea level and 850hpa charts (similar to the situation described by Blanford 1886), provided the condition persisted for at least two days. The breaks in the Indian summer monsoon as a phenomenon was explained initially by Ramaswamy (1962) as of interaction between the easterly and sub-tropical westerly jet stream. The break composite of Ramamurthy (1969) shows large negative rainfall anomalies over a belt around the normal position of the monsoon trough and positive rainfall anomalies near the foothills of the Himalayas and southeastern peninsula. During active monsoon conditions, the monsoon trough is either near the mean position or a little to the south of its normal position and the rainfall anomaly pattern is the opposite of that for breaks. The composite rainfall anomalies during the break monsoon and active monsoon periods as obtained from Rajeevan et al., (2008[b]) using active and break days during the period 1951-2004 is shown in Fig. 2.15 with most of the central India indicating

positive rainfall anomalies during active phase (Fig.2.15b) and just the opposite during the break phase (Fig. 2.15a). Propagation of systems from the Bay of Bengal along the monsoon zone contributes substantially to the rainfall during the summer monsoon. Active spells of the monsoon are characterized by a sequence of time-clustering partly overlapping development of such disturbances (Murakami 1976), whereas no such systems occur over the monsoon zone during breaks as a result large negative rainfall anomalies are reported over central India during break composites and large positive anomalies in case of active composites (Fig. 2.15a, & 2.15b).

The intra-seasonal rainfall distribution over India is influenced by different quasi-periodic oscillations, viz. 3-7 days, 10-20 days and 30-60 days. While 3-7 days periodicity is associated with oscillations of the monsoon trough, the 10-20 days periodicity or quasi-biweekly oscillations are associated with the westward moving waves or synoptic scale convective systems generated over the warm Bay of Bengal and propagating inland towards the main land of India. The 30-60 days oscillations, popularly known as Madden-Julian Oscillations (MJOs, Madden and Julian, 1972) are the dominant component of the intra-seasonal variability (ISV) in the tropical atmosphere. It consists of large-scale coupled patterns in atmospheric circulation and deep convection, propagating eastward slowly (~5 m/s) through the Indian and Pacific oceans where the sea surface is warm. The dominant time-scales of intra-seasonal variation are 10-20 days and 30-60 days with comparable contributions to the total intra-seasonal variability in the Indian region (Goswami 2005 and references therein). While the quasi biweekly (10-20 days) scale is characterized by westward propagations (Krishnamurti and Bhalme 1976, Krishnamurti and Ardanuy 1980, Yasunari 1979, Kulkarni et al., 2006), the 30-50 day scale is associated with northward propagations from the near-equatorial region (Sikka & Gadgil, 1980; Krishnamurti and Subramanian 1982 and Pattanaik, 2003). Subsequent to the classic work of Ramamurthy's (1969), active spells and weak spells/breaks of the Indian summer monsoon have been extensively studied, particularly in the last two decades (e.g. Magana & Webster 1996, Rodwell 1997, Webster et al 1998, Krishnan et al. 2000; Krishnamurthy and Shukla (2000,2007,2008), Lawrence and Webster 2001, Annamalai and Slingo 2001, De and

Mukhopadhyay 2002, Kripalani et al. 2004, Goswami and Ajayamohan 2001, Goswami et al. 2003, Waliser et al 2003, Gadgil and Joseph 2003; Sahai and Chattopadhyay, 2006). Observational studies by Yasunari (1979), Sikka and Gadgil (1980), and Gadgil and Asha (1992) have associated the active and break phases of monsoon with fluctuations in two convergence zones, one over the Indian continent and the other over the Indian Ocean. Although, these studies emphasize the importance of northward propagation, Lawrence and Webster (2001) suggested that the eastward propagation of convection is always related to the northward movement and is fundamental to the variability over both the Indian Ocean and the Indian continent. In addition to the eastward propagation, there also exists some weak westward movement of convection toward the Indian continent (Krishnamurti and Ardanuy 1980, Annamalai and Slingo 2001). Studies by Krishnan et al. 2000, Lawrence and Webster 2002, Annamalai and Slingo 2001, and Annamalai and Sperber 2005 have associated the movements of convection zones over to the Indian continent with the active and break phases of monsoon.

It should be noted that whereas active-weak cycles in the fluctuation of the monsoon rainfall occur every year, breaks do not (Ramamurthy 1969), and long breaks such as the one in 2002 occur only in a few years. Frequent or prolonged breaks during the monsoon season, such as the break in July 2002, can lead to drought conditions. Pattanaik and Rajeevan (2007) found that the long break of July, 2002 (Fig. 2.16c) was accompanied by more typhoon activity in the northwest Pacific and having northerly tracks and associated with above normal convective activity over the northwest Pacific and subsidence over central India. Pisharoty and Desai (1956) found that passage of westerly waves across the Tibetan Plateau and adjoining Himalayas in quick succession leads to 'breaks'. Ramaswamy (1962 & 1965) finds that during 'break' pronounced low index circulation prevails in the middle latitude westerlies north of the Himalayas and large amplitude troughs protrude into Indo–Pakistan area at 500 mb and aloft. Koteswaram (1950) connects 'breaks' in Indian monsoon rainfall with westward moving lows at low latitudes (10^0N in the Bay), prominent at 700 mb and the movement of such lows weakens the north–south pressure gradient over the Peninsula. As

discussed in Rao (1976) and also by many other studies the major difference between the rainfall variation in the good monsoon seasons (1961, 1975, 1988 and 1994) shown in Fig. 2.16 and the poor monsoon seasons (1972, 1987, 2002 and 2009) shown in Fig. 2.17 are the occurrence of a long dry spell or "break" in case of poor monsoon seasons as shown in (Figs. 2.17a-d). As seen from Figs. 16 the major drought years like 1972, 1987, 2002 and 2009 with AISMR departure of about -24%, -19%, -19% and -22% respectively are associated with one or more long break condition where the actual rainfall received is significantly less than that of normal rainfall. However, the day to day variations of rainfall during good monsoon years like 1961, 1975, 1988 and 1994 with AISMR departure of about +22%, +15%, +19% and +12% respectively witnessed most of the days having above normal rainfall (Figs. 2.17).

In spite of the improvement in our understanding there are many unsolved problems exist to understand the fluctuation of monsoon rainfall in the intra-seasonal time scale. The processes that lead to the fluctuation between active and weak spells or breaks, and in particular, factors that trigger the transition between the two, are yet to be adequately understood. Similarly the role of 10-20 (Krishnamurti and Bhalme 1976, Krishnamurti and Ardanuy 1980 and Yasunari 1979) days mode in modulating monsoon, either separate or in conjunction with 30-60 day mode (Sikka & Gadgil, 1980) is still an outstanding problem. There are also large gaps in our knowledge about how these two oscillations interact, how El Nino Southern Oscillation and other low frequency variations can modulate intra-seasonal variations and the extent intra-seasonal oscillations contribute to interannual variability of monsoon. It is difficult to say whether good monsoon force the faster oscillations or whether changes in intra-seasonal variabilities force changes in monsoon strength. More over since these oscillations play significant role in seasonal monsoon strength, if some statistical/ dynamical or combined scheme could foreshadow the behaviour of these oscillations, it will go a long way in serving as a guiding tool for forecasting of monsoon in the intra-seasonal time scale.

2.7. Monsoon Variability on Millennium Time Scale

Modelling of climate variability on inter-decadal to century time scale is a major research area in the field of climatology. The information about climate variability based on instrumental records has both spatial and temporal limitations, as it can provide only a small window to the scope of various climatic processes on a wide spectrum of spatio-temporal scales. Fortunately, nature has plenty of climate-sensitive materials which can be used as "proxy" to get climate information on millennium time scale that contain reliable signatures of past climates. Many long-lived trees grow with annual ring structure and the climatic information recorded by trees growing in stressful forest environments can be extracted from the size, structure and chemical composition of these annual growth rings. In tropical region of south and southwest Asia, number of groups have been working to establish good quality tree-ring data network to understand monsoon variability and related global parameters (e.g. ENSO) in the recent past. Pant et al. (1993) have discussed the long term climate variability and change over monsoon Asia and the mechanisms and importance of extracting climate related information for the last many years using "proxy" sources. Pant et al., (1988) attempted to reconstruct the variability of all India summer monsoon rainfall (AISMR) since last 400 years, using an indirect dendroclimatic approach, based on the fact that the Southern Oscillation (SO) is strongly related to the Indian summer monsoon rainfall. The data of Wright's Index of SO reconstructed back to AD 1602-1960 using tree-ring chronologies from both western-north America and the Southern Hemisphere (Lough & Fritts 1985) have been used to estimate AISMR back to AD 1602. The actual and estimated AISMR series during the calibration period (1870-1960) indicate good agreement with each other. They have also shown that the occurrence of different epochs and major drought events noted from historical and other sources during 19th have also been matching with the reconstructed series during this calibration period.

2.8. Diurnal Variability of Monsoon Rainfall

In addition to the variability of Indian monsoon on different temporal scales mentioned in Table 2.1 and discussed above the diurnal variation is also found to be

prominent over the tropics. Ananthakrishnan (1977) observed the diurnal variation of upper-tropospheric winds over the monsoon domain; however his study was limited because he had access to upper-air data at only selected sites. Later Krishnamurti and Kishtawal (2000) observed the diurnal cycle of monsoon circulation using cloud-tracked winds over 90-min intervals from Meteosat-5. They demonstrated the diurnal amplification and weakening of the Tibetan high circulation and the tropical easterly jet on the southern flank of this anticyclone which, evidently is related to the diurnal response to surface heating, convection, and the buildup and weakening of the thermal winds. Since cumuliform clouds contribute to the major fraction of rain, it is important to study the spatial and diurnal distribution of the probability of occurrence of such clouds (POC). Murakami (1983) used datasets from the Japanese Geostationary Meteorological Satellite to examine the phase and amplitude of the diurnal activity of convection and found that over most of the Asian monsoon landmass of south Asia and Southeast Asia, the diurnal mode of convection is dominated by late afternoon convection and suppressed conditions during the early morning hours.

Some recent studies (Basu 2007; Singh and Nakamura 2010; Takahashi et al., 2010) have also investigated the observational and modelling aspects of diurnal variation of monsoon rainfall. Based on satellite-derived hourly precipitation values over India and neighbouring areas for 2004 monsoon season, Basu (2006) noticed maximum amounts of rainfall recorded over most areas of India during the afternoon hours, coinciding with the maximum in surface temperature, although the pattern is modified in areas where local meso-scale events like katabatic winds or land-sea breezes produce strong convergence. Singh and Nakamura (2010) carried out diurnal variation in summer monsoon precipitation during active and break periods over central India and southern Himalayan foothills using Tropical Rainfall Measuring Mission (TRMM) data for July–August from 1998 to 2007. They found that the precipitation over central India during wet periods is characterized by a large amount of rainfall with a high frequency of rain and a secondary morning peak. The precipitation in dry periods is characterized by a strong diurnal variation with convective rainfall and enhanced electrical activity over central India.

Takahashi et al., (2010) addressed the diurnal cycle of rainfall during the summer monsoon season (May to September) around the Indochina peninsula, with a focus on the diurnal cycle's relationship to terrain by using 10 year (1998–2007) Tropical Rainfall Measuring Mission Precipitation Radar (TRMM-PR) observations. Results revealed that the diurnal variations in rainfall over the Indochina region had three distinct peaks. An early afternoon maximum of rainfall occurred along the mountain ranges and on coastal land. Evening rainfall was observed near the foot of mountain ranges, in a valley, and in a basin-shaped plain; this rainfall weakened before the middle of the night. Heavy rainfall in the early morning was found around the coasts over the eastern Gulf of Thailand and the Bay of Bengal, as well as over the eastern Khorat Plateau. It is seen that nearly half of the total rainfall occurred in the early morning over these regions, which indicated that early morning rainfall significantly contributes to the climatological rainfall pattern. Additional examination of rainfall frequency and rainfall intensity showed that this early morning heavy rainfall was composed of frequent or long-lasting rainfall events with a strong intensity.

References

Alexander, G., Keshavamurty, R. N., De, U. S., Chellappa, R., Das, S. K. and Pillai, P. V., 1978, "Fluctuations of monsoon activity", Indian J. Meteor. Geophys., 29, 76-87.

Ananthakrishnan, R., 1977, "Some aspects of the monsoon circulation and monsoon rainfall", Pure Appl. Geophys., 115, 1209–1249.

Annamalai, H., and Slingo, J. M., 2001, "Active/break cycles: diagnosis of the intraseasonal variability of the Asian Summer Monsoon", Climate Dynamics, 18:85-102.

Annamalai, H., and Sperber, K. R., 2005, "Regional heat sources and the active and break phases of boreal summer intraseasonal (30-50 day) variability", *J. Climate*, 62, 2726–2748.

Basu, B. K., 2007, "Diurnal variation in precipitation over India during the summer monsoon season: Observed and model predicted", Mon. Wea. Rev., 135, 2155-2167.

Blanford, H.F., 1886, "Rainfall of India", Mem. India Meteorol. Dep. 2:217–448.

Bohra A. K., Swati Basu, Rajagopal, E. N., Iyengar, G. R., Das Gupta, M., Ashrit, R. and Athiyaman, B., 2006, "Heavy rainfall episode over Mumbai on 26 July 2005", Assessment of NWP guidance. Current Science, VOL. 90, 1118-1194.

Charney, J.G., 1969, "The intertropical convergence zone and the hadley circulation of the atmosphere", Proc. WMO/IUCG Symp. Numer. Weather Predict., Jpn. Meteorol. Agency III:73–79.

De. U. S. and Mukhopadhyay, R. K., 2002, "Breaks in monsoon and related precursors", Mausam, 53, 309-318.

Dhar, O.N. and Mandal, B.N., 1981, "Greatest observed one-day point and areal rainfall of India", Pure and Applied Geophysics, vol. 119, pp. 922-933.

Gadgil Sulochana and Asha Guruprasad, 1992 "Intraseasonal variation of the Indian summer monsoon 1: observational aspects", J. Metro. Soc. Japan, 517-527.

Gadgil, S, Abrol, Y.P., Rao, P.R.S., 1999, “On growth and fluctuation of Indian foodgrain production”, Curr. Sci. 76(No. 4):548–56.

Gadgil, Sulochana. and Joseph, P.V., 2003, “On breaks of the Indian monsoon”, Proc. Indian Acad.. Sci. – Earth Planet. Sci., 112, 529 – 558.

Ghosh, S. K., Pant, M. C. and Dewan, B. N., 1978, “Influence of the Arabian sea on the Indian summer monsoon”, Tellus 30, 117-124.

Goswami, B.N., 2005, “The Asian monsoon: interdecadal variability”, In the Asian monsoon, Wang B (ed.), Chapter 7. Praxis, Springer: Berlin; 295–327.

Goswami, B.N., and Ajayamohan, R.S., 2001, “Intraseasonal oscillations and interannual variability of the Indian summer monsoon”, J.Climate, 14, 1180-1198.

Goswami, B.N., Ajayamohan, R.S.,.Xavier, P.K. and Sengupta, D.,2003, “Clustering of low pressure systems during the Indian summer monsoon by intra-seasonal oscillations”, Geophys.Res. Letters, 30(8), doi: 10.1029/2002GL016734.

Goswami, B. N., Venugopal, V., Sengupta, D., Madhusoodanan M. S. and Xavier, P. K., 2006, “Increasing trend of extreme rain events over India in a warning environment”, Science, 314, 1442-1445.

Guhathakurta, P.and Rajeevan, M. 2007, “Trends in the rainfall pattern over India”, National Climate Centre Report, India Meteorological Department, Pune, India.

Halley, E. 1686, “An historical account of the trade winds and monsoons observable in the seas between and near the tropics with an attempt to assign a physical cause of the said winds”, Philos. Trans. R. Soc. London, 16:153–68.

Hingane, L.S., Rupa Kumar, K. and Raman Murty, V. 1985, “Longterm trends of surface air temperature in India”, J. Climatology 5, 521-528.

Jenamani, R.K., Bhan, S.C., Kalsi, S.R., 2006, “Observational/forecasting aspects of the meteorological event that caused a record highest rainfall in Mumbai”, Curr. Sci. 90, 1344–1362.

Koteswaram, P., 1950, “Upper level lows in low latitudes in the Indian area during southwest monsoon season and breaks in the monsoon”, Indian J. Met. Geophys. Vol. I, pp. 162–164.

Kripalani, R. H., Kulkarni, A., Sabade, S.S., Revadekar, J. V., Patwardhan, S.K., Kulkarni, J. R., 2004, “Intraseasonal oscillations during monsoon 2002 and 2003”, Current Science, 87, 325–331.

Kripalani, R.H. and Kulkarni, A., 1997, “Climate impact of El Nino/LaNina on the Indian monsoon: A new prespective”, Weather 52: 39–46.

Krishnamurthy, V. and Shukla, J., 2008, “Seasonal persistence and propagation of intraseasonal patterns over the Indian summer monsoon region”, Climate Dynamics, 30, 353-369.

Krishnamurthy, V. and Shukla, J., 2000, “Intraseasonal and interannual variability of rainfall over India”, J. Climate, 13, 4366-4377.

Krishnamurthy, V. and Shukla, J., 2007, “Intraseasonal and seasonally persisting patterns of Indian monsoon rainfall”, J. Climate, 20, 3-20.

Krishnamurti, T.N., Ardanuy, P., 1980, “The 10 to 20 day westward propagating mode and breaks in the monsoon”, Tellus 32:15–26.

Krishnamurti, T.N. and Bhalme, H.N. ,1976, “Oscillations of a monsoon system”, Part 1, Observational aspects, J. Atmos. Sci. 33:1937–54.

Krishnamurti, T. N., (ed.), 1979, “Compendium of Meteorology for Use by Class I and Class II Meteorological Personnel”, vol. 2, pt. 4: Tropical Meteorology.

Krishnamurti, T.N. and Subrahmanyan, D., 1982, “The 30–50 day mode at 850 mb during MONEX”, J. Atmos. Sci. 39:2088–95.

Krishnamurti, T. N., Kishtawal, C. M., 2000, “A Pronounced Continental-Scale Diurnal Mode of the Asian Summer Monsoon”, Mon. Wea. Rev., 128, 462–473.

Krishnan, R., Zhang, C. and Sugi, M. 2000, “Dynamics of breaks in the Indian summer monsoon”, J. Atmos. Sci. 57:1354–72.

Kulkarni, Ashwini, Sabade, S. S. and Kripalani, R. H., 2006, “Intra-seasonal Vagaries of the Indian Summer Monsoon Rainfall”, IITM Research Report No. 114. IITM, Pune, India.

Kumar, K.K., Rajagopalan, B. and Cane, M.A., 1999, “On the weakening relationship between the Indian monsoon and ENSO”, Science. 284, 2156–59.

Lawrence, D.M. and Webster, P.J., 2001, “Interannual variations of the intraseasonal oscillation in the South Asian summer monsoon region.”, J. Clim. 14:2910–2922.

Lough, J. M. and Fritts, H. C.,1985, “The southern oscillation and tree-rings: 1600-1961”, J. Climato. Appl. Met. 24, 952-966.

Madden, R.A. and Julian, P.R., 1972 , “Description of global-scale circulation cells in the tropics with a 40–50 day period”, J. Atmos. Sci. 29:1109–23.

Magana, V. and Webster, P.J.,1996, “Atmospheric circulations during active and break periods of the Asian monsoon”, Preprints Conf. Global Ocean-Atmos.-Land Syst. (GOALS), 8th. Am. Meteorol. Soc., Atlanta, GA.

Murakami, T.. 1976, “Cloudiness fluctuations during the summer monsoon”, J. Meteorol. Soc. Jpn. 54:175–81.

Murakami, M., 1983, “Analysis of the deep convective activity over the western Pacific and Southeast Asia. Part I: Diurnal variation”, J. Meteor. Soc. Japan, 61, 60–77.

Pant, G.B., Parthasarathy, B., 1981, “Some aspects of an association between the southern oscillation and Indian summer monsoon”, Arch. Meteorol. Geophys. Biokl. Ser. B. 29:245–51.

Pant, G. B. and Rupa Kumar, K., 1997, “Climates of South Asia”, John Wiley & Sons, Chichester, 320 pp.

Pant, G.B., Rupa Kumar, K. and Borgaonkar, H.P., 1988, “Statistical models of climate reconstruction using tree ring data”, Proc. Indian Natn.. Sci. Acad., 54, A, No.3, 354-364.

Pant, G.B., Rupa Kumar, K., Sontakke, N.A. and Borgaonkar, H.P., 1993, “Climate Variability over India on century and longer time scales. In: Advances in Tropical Meteorology”, (R.N. Keshavamurty and P.C. Joshi, Eds.). Tata McGraw-Hill Publishing Company Ltd., New Delhi, 149-158.

Parthasarathy, B., Munot, A. and Kothawale, D. R. 1994, “All-India monthly and seasonal rainfall series 1887-1993”, Theoretical and Applied Climatology, 49, 217-224.

Pattanaik, D.R., 2003, “Analysis of moist convective instability over Indian monsoon region and neighbourhood”, Mausam 54, 659-670.

Pattanaik, D. R. and M. Rajeevan, 2007, “North-West Pacific Tropical Cyclone Activity and July Rainfall Over India”, Meteorology & Atmospheric Physics, 95,63-72.

Pattanaik, D. R. and Rajeevan, M., 2010, “Variability of Extreme Rainfall Events over India During Southwest Monsoon Season”, Meteorological Applications, Vol. 17, 88-104. (DOI: 10.1002/met.164).

Pattanaik, D. R., S. R. Kalsi and Hatwar, H. R., 2005, “Evolution of convection anomalies over the Indo-Pacific region in relation to Indian monsoon rainfall”, Mausam, 56, 811-824.

Pisharoty, P. R., 1965, “Evaporation from the Arabian Sea and Indian southwest monsoon”, Proceedings of International Ocean Expedition, 43-54.

Pisharoty, P.R. and Desai, B. N., 1956, “Western disturbances and Indian weather”, Indian J. Met. Geophys, 7, PP. 333–338.

Raghavan, K., 1973, “Break monsoon over India”, Mon. Wea. Rev., 101, 33 – 43.

Rajeevan, M. Bhate, J. Kale, J. D. and Lal, B. 2006. “High resolution daily gridded rainfall data for the Indian region: analysis of break and active monsoon spells”, Current Science, 91, 296–306.

Rajeevan, M., Gadgil, S. and Bhate, Jyoti, 2008[b], “Active and Break spells of the Indian summer monsoon” NCC Research Report No. 7, India Meteorological Department, Pune.

Rajeevan, M., Bhate, J. and Jaswal, A. K., 2008[a], “Analysis of variability and trends of extreme rainfall events over India using 104 years of gridded daily rainfall data”, Geophys. Res. Lett. 35 L18707, doi: 10.1029/2008GL035143.

Ramage, C.S., 1971, “Monsoon Meteorology”, Int. Geophys. Ser., Vol. 15. San Diego, CA: Academic. 296 pp.

Ramaswamy, C., 1962, “Breaks in the Indian summer monsoon as a phenomenon of interaction between the easterly and sub-tropical westerly jet stream”, Tellus, 14, 337-349.

Ramaswamy, C., 1965, “On synoptic methods of forecasting the vagaries of southwest monsoon over India and the neighbouring countries”, Proc. Symp. Met. Results of IIOE, pp. 317–327.

Ramamurthy, K., 1969, “Monsoon of India: some aspects of the ‘break’ in the Indian southwest monsoon during July and August”, Forecasting Mannual 18.3(No. IV):1–57, India Meteorol. Dept., Poona, India.

Rao, Y.P. 1976, “Southwest Monsoon”, Meteorol. Monogr. No.1. India Meteorol. Dept., New Delhi. 366 pp.

Rasmusson, E.M. and Carpenter, T.H., 1983, “The relationship between the eastern Pacific sea surface temperature and rainfall over India and Sri Lanka”, Mon. Weather Rev. 111:354–384.

Riehl, H., 1954, “Tropical Meteorology”, New York: McGraw Hill. p.392..

Riehl, H., 1979, “Climate and Weather in the Tropics”, San Diego/New York: Academic. 611 pp.

Rodwell, M.J., 1997, “Breaks in the Asian monsoon: the influence of Southern Hemisphere weather systems”, J. Atmos. Sci. 54:2597–611.

Rupa Kumar, K., Pant, G. B., Parthasarathy, B. and Sontakke, N. A., 1992, “Spatial and subseasonal patterns of long term trends of the Indian summer monsoon rainfall”, Int. J. Climatol., 12, 257–268.

Sahai, A.K. and Chattopadhyay, R., 2006, “An Objective Study of Indian summer Monsoon Variability Using the Self Organizing Map Algorithms”, IITM Research Report, No-113.

Sahany, Sandeep, Venugopal, V. and Ravi, S. Nanjundiah, 2010, “The 26 July 2005 heavy rainfall event over Mumbai: numerical modeling aspects”, Meteorology & Atmos Phys, 109:115–128.

Shyamala, B. and Bhadram, C.V.V., 2006, “Impact of mesoscale-synoptic scale interactions on the Mumbai historical rain event during 26-27 July 2005”, Current Science, 91, 12, 1649-1654.

Sikka, D.R. and Gadgil, S., 1980, ”On the maximum cloud zone and the ITCZ over India longitude during the Southwest monsoon”, Mon. Weather Rev. 108:1840–53.

Sikka, D.R., 1980, “Some aspects of the large-scale fluctuations of summer monsoon rainfall over India in relation to fluctuations in the planetary and regional scale circulation parameters”, Proc. Indian Acad. Sci. Earth Planet. Sci. 89:179–95.

Singh, P., and K. Nakamura, 2010, “Diurnal variation in summer monsoon precipitation during active and break periods over central India and southern Himalayan foothills”, J. Geophys. Res., 115, D12122, doi:10.1029/2009JD012794.

Takahashi, H. G., Fujinami, H., Yasunari, T. and Matsumoto, J., 2010, “Diurnal rainfall pattern observed by Tropical Rainfall Measuring Mission Precipitation Radar (TRMM-PR) around the Indochina peninsula”, J. Geophys. Res., 115, D07109, doi:10.1029/2009JD012155.

Thapliyal, V. and Kulshreshtha, S. M.,1991, “Climate changes and trends over India”, Mausam 42, 333-338.

Ueda, H. and Yasunari, T., 1998, “Role of Warming over the Tibetan Plateau in Early Onset of the Summer Monsoon over the Bay of Bengal and the South China Sea”, J. Meteor. Soc, Japan, 76, 1-12.

Waliser, D. E., Lau, K.M. and Stern, W., 2003, “Potential predictability of the MJO”, Bull. Am. Meteorol. Soc., DOI:10:1175/BAMS-84-1-33.

Webster, P.J., Magana, V.O., Palmer, T.N., Shukla, J, Tomas, R.A., et al., 1998, “Monsoons: processes, predictability, and the prospects for prediction”, J. Geophys. Res. 103(No. C7):14451– 510.

Webster, P.J., 1987, “The elementary monsoon”, In Monsoons, ed. JS Fein, PL Stephens, pp. 3– 32. New York: Wiley.

Yasunari, T., 1979, “Cloudiness fluctuations associated with the northern hemisphere summer monsoon”, J. Meteor. Soc., Japan, 57, 227-242.

Table 2.1: Temporal scale of monsoon variability along with factors affecting them.

	Intra-seasonal	Inter-annual Variability	Decadal and century	Millennium and Longer
Features	*Active Break cycle of monsoon;*	*Droughts and Floods*	*Changes in the frequency of droughts and floods*	*Changes in the areal extends of monsoon*
Factors	• *Sea surface temperatura /Sea ice* • *Snow cover* • *Soil Moisture* • *Stratospheric Initial conditions* • *The Madden-Julian oscillation*	• *El Nino/Southern Oscillation* • *Local land surface conditions* • *Remote soil moisture/ snow cover* • *Sea ice anomalies* • *Dynamic memory of atmosphere* • *Stratospheric influences*	• *Monsoon circulations variations* • *Deep ocean involvement* • *Human induced changes* • *Green house gases increase* • *Biospheric changes* • *Volcanic eruptions*	• *Global climate excursions* • *Ice ages* • *Warm epochs* • *Extra-terrestrial factor (Sun-earth geometry)*

Table 2.2: Excess and deficient categories of seasonal and monthly rainfall year based on the departure of 1 SD.

AISMR (1875-2010)	Excess	1875, 1878, 1892, 1893, 1894, 1914, 1916, 1917, 1933, 1942, 1955, 1956, 1959, 1961, 1970, 1975, 1983, 1988, 1994 (19 years)
	Deficient	1877, 1899, 1901, 1904, 1905, 1907, 1911, 1913, 1918, 1920, 1941, 1951, 1965, 1966, 1968, 1972, 1974, 1979, 1982, 1986, 1987, 2002, 2004, 2009 (24 Years)
June (1901-2010)	Excess	1909, 1910, 1913, 1916, 1917, 1925, 1936, 1938, 1946, 1956, 1970, 1971, 1978, 1980, 1994, 2001, 2008 (17 years)
	Deficient	1901, 1902, 1903, 1905, 1912, 1923, 1924, 1926, 1931, 1932, 1947, 1958, 1962, 1965, 1969, 1972, 1974,1995, 2009 (19 years)
July (1901-2010)	Excess	1908, 1912, 1914, 1927, 1942, 1944, 1956, 1959, 1961, 1988, 1994, 2005 (12 years)
	Deficient	1901, 1907, 1910, 1909, 1911, 1915, 1918, 1941, 1951, 1955, 1963, 1966, 1970, 1972, 1979, 1982, 1986, 1987, 1992, 2002, 2004, 2008 (22 years).
August (1901-2010)	Excess	1907, 1908, 1910, 1916, 1917, 1919, 1926, 1931, 1933, 1942, 1946, 1953, 1955, 1958, 1961, 1963, 1970, 1973, 1975, 1976, 1983, 1996 (22 years).
	Deficient	1902, 1904, 1905, 1911, 1913, 1920, 1922, 1928, 1930, 1937, 1965, 1966, 1968, 1979, 1993, 1999, 2001, 2005, 2009 (19 years).
September (1901-2010)	Excess	1917, 1924, 1933, 1945, 1947, 1949, 1954, 1955, 1958, 1959, 1961, 1962, 1970, 1975, 1983, 1988, 1993, 1998 (18 years).
	Deficient	1901, 1904, 1907, 1912, 1913, 1918, 1920, 1925, 1928, 1929, 1940, 1951, 1952, 1968, 1972, 1979, 1982, 1986, 1987, 1991, 2001, 2004 (22 years).

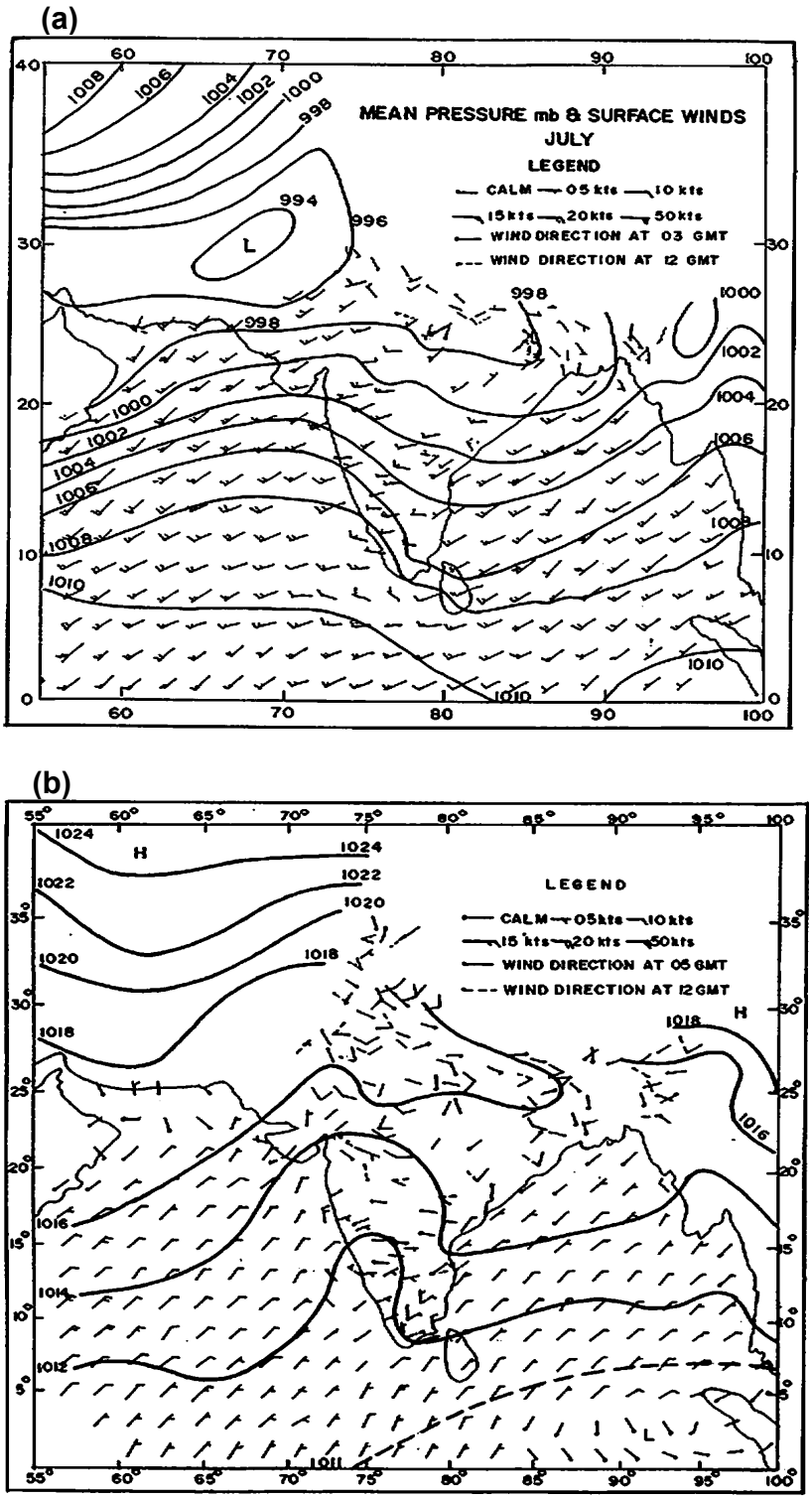

Fig. 2.1 : (a) Mean surface wind and pressure for July; (b) for January (after Rao 1976)

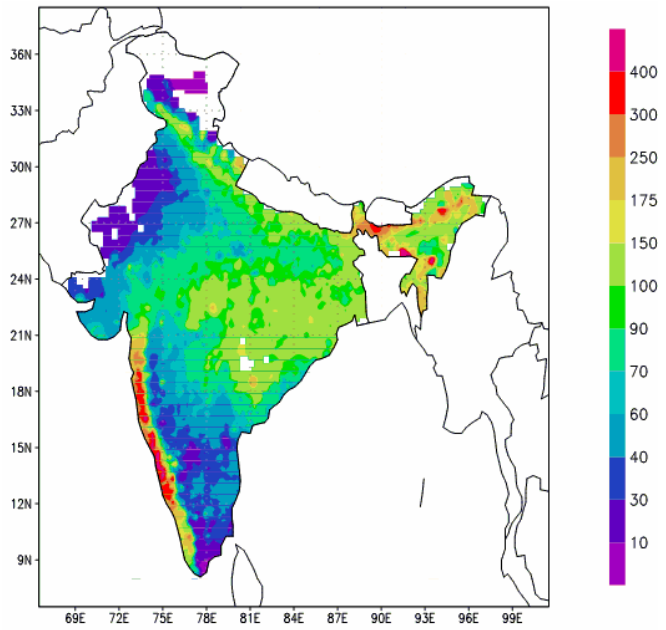

Fig. 2.2 : Mean All India Summer Monsoon Rainfall (AISMR) in cm during 1951-2003.

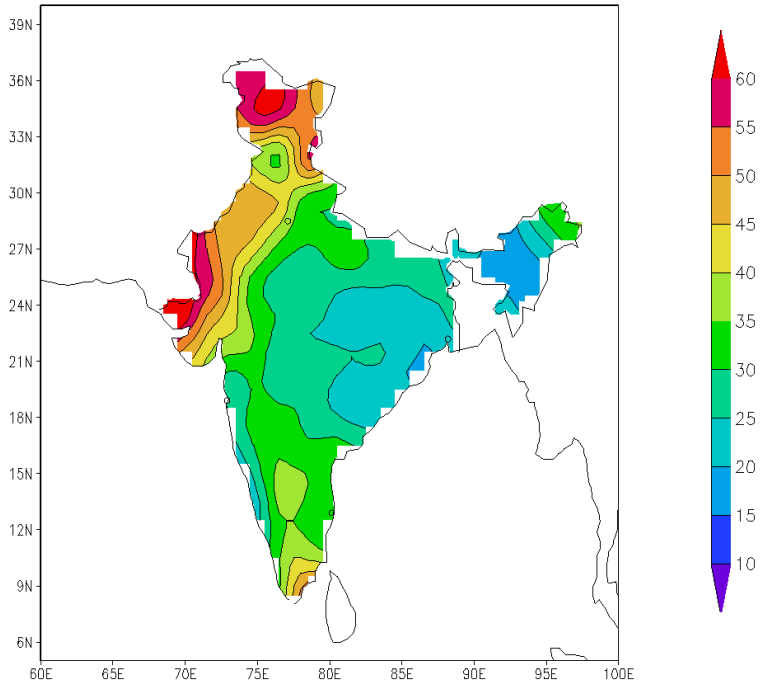

Fig. 2.3 : Mean Coefficient of Variability (%) of All India Summer Monsoon Rainfall (AISMR).

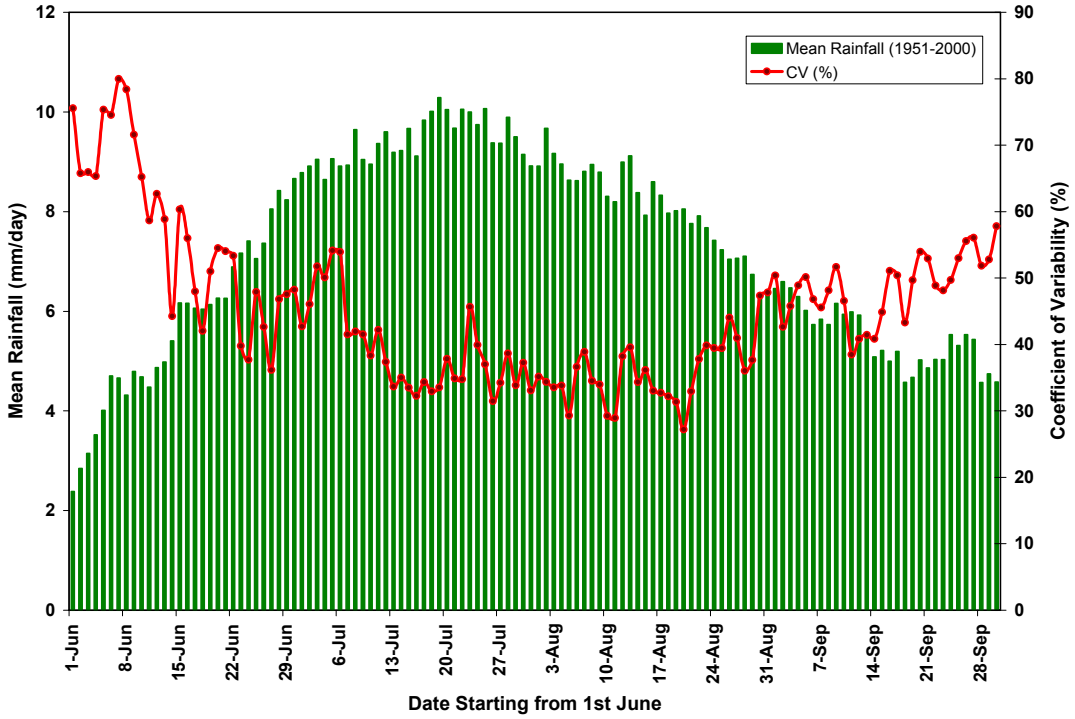

Fig. 2.4 : Daily mean (mm) and daily Coefficient of Variability (%) of all India monsoon rainfall.

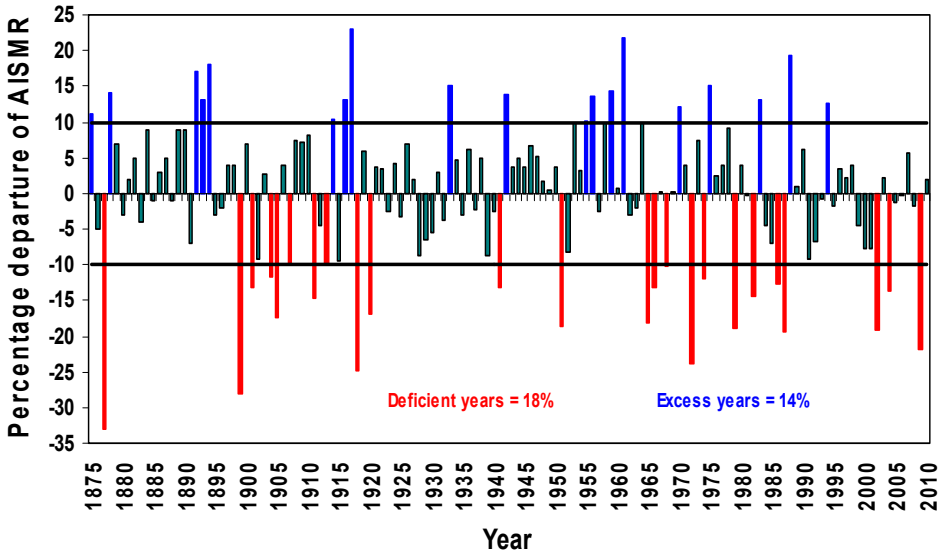

Fig. 2.5 : Interannual variability of AISMR during the period from 1875 to 201

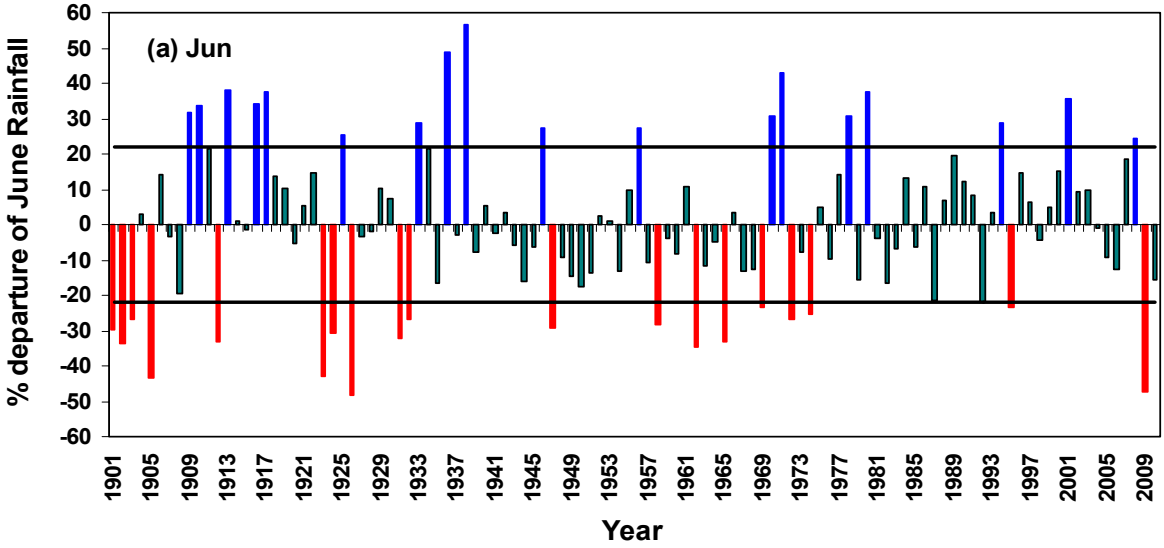
(a) Jun
% departure of June Rainfall
Year

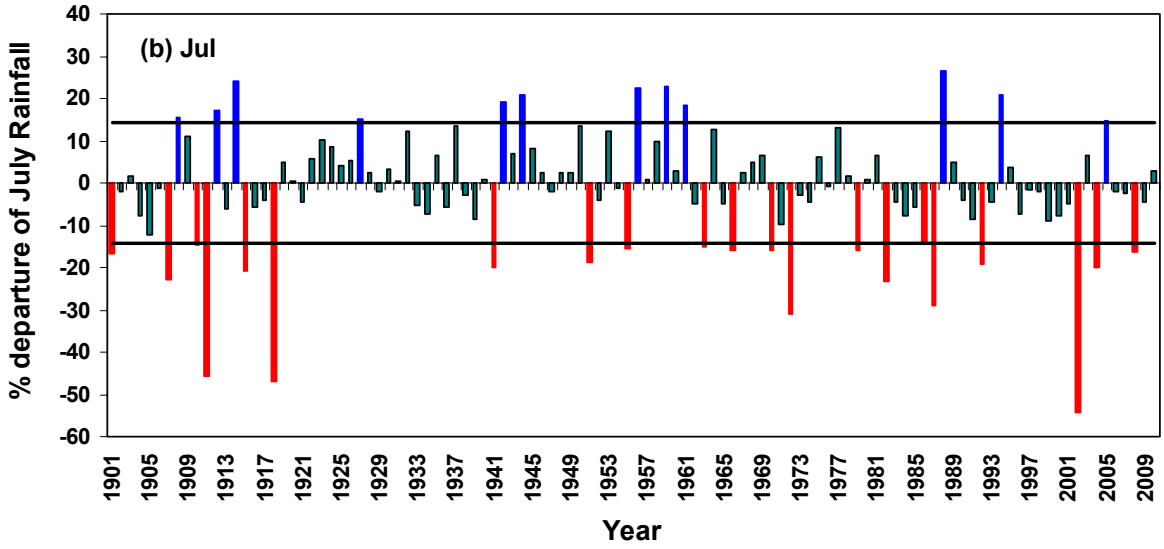
(b) Jul
% departure of July Rainfall
Year

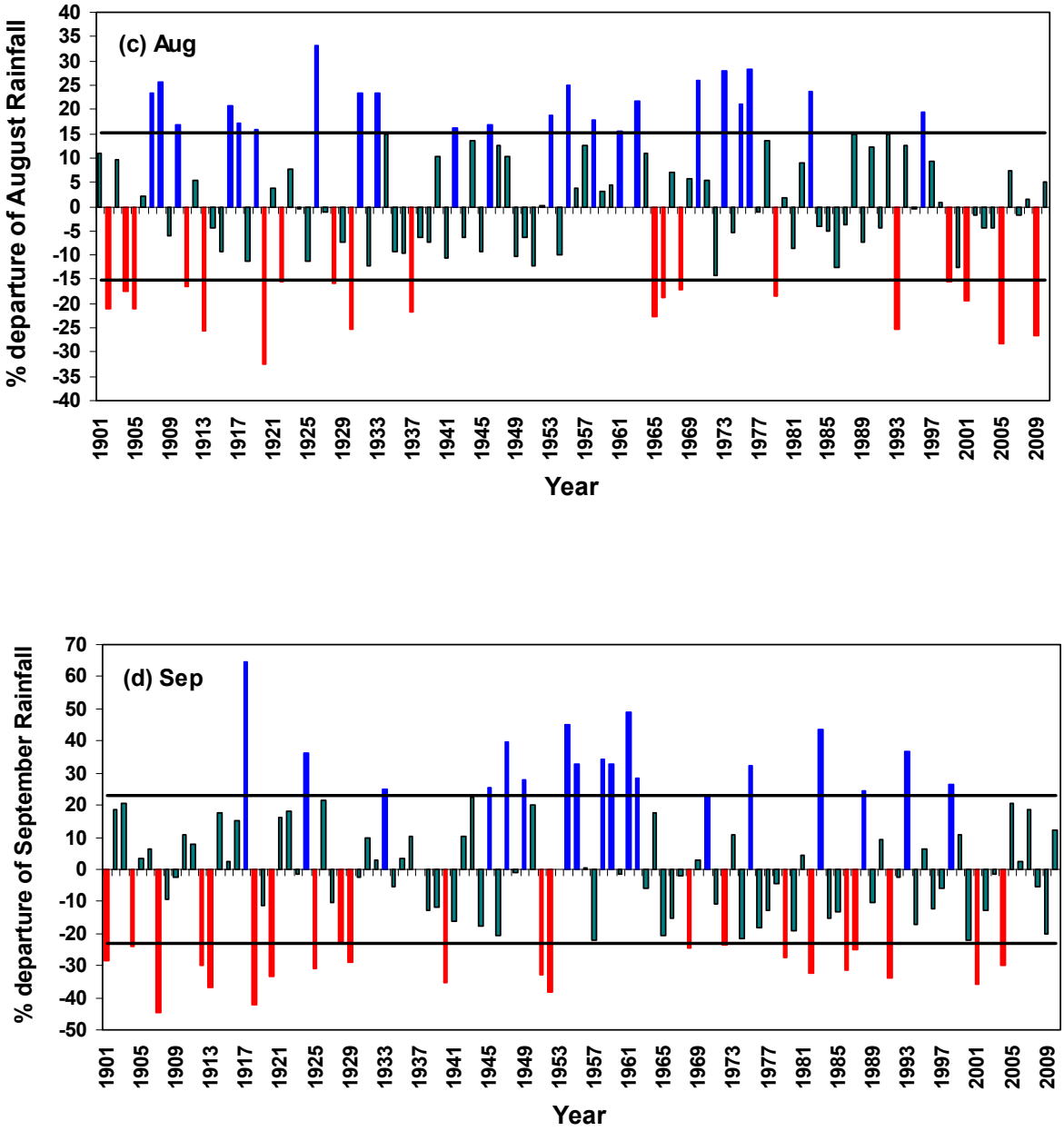

Fig. 2.6 : Interannual variability of all India monthly rainfall during the period 1875-2010 (a) June, (b) July, (c) August and (d) September.

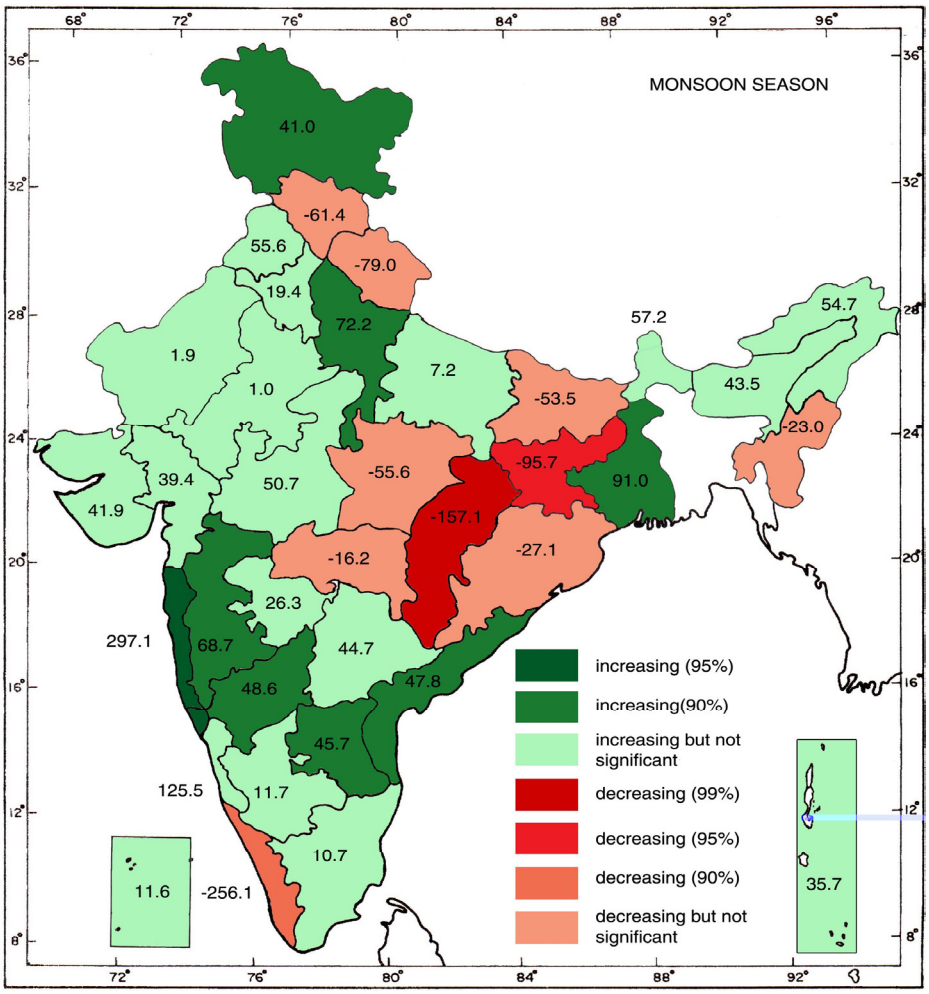

Fig. 2.7 : Increase/Decrease in seasonal rainfall in mm during 100 year for each of 36 meteorological subdivisions for the south-west monsoon season during June to September. Different levels of significance for increasing and decreasing trend are shaded with colours *(Source : Guhathakurta and Rajeevan 2007).*

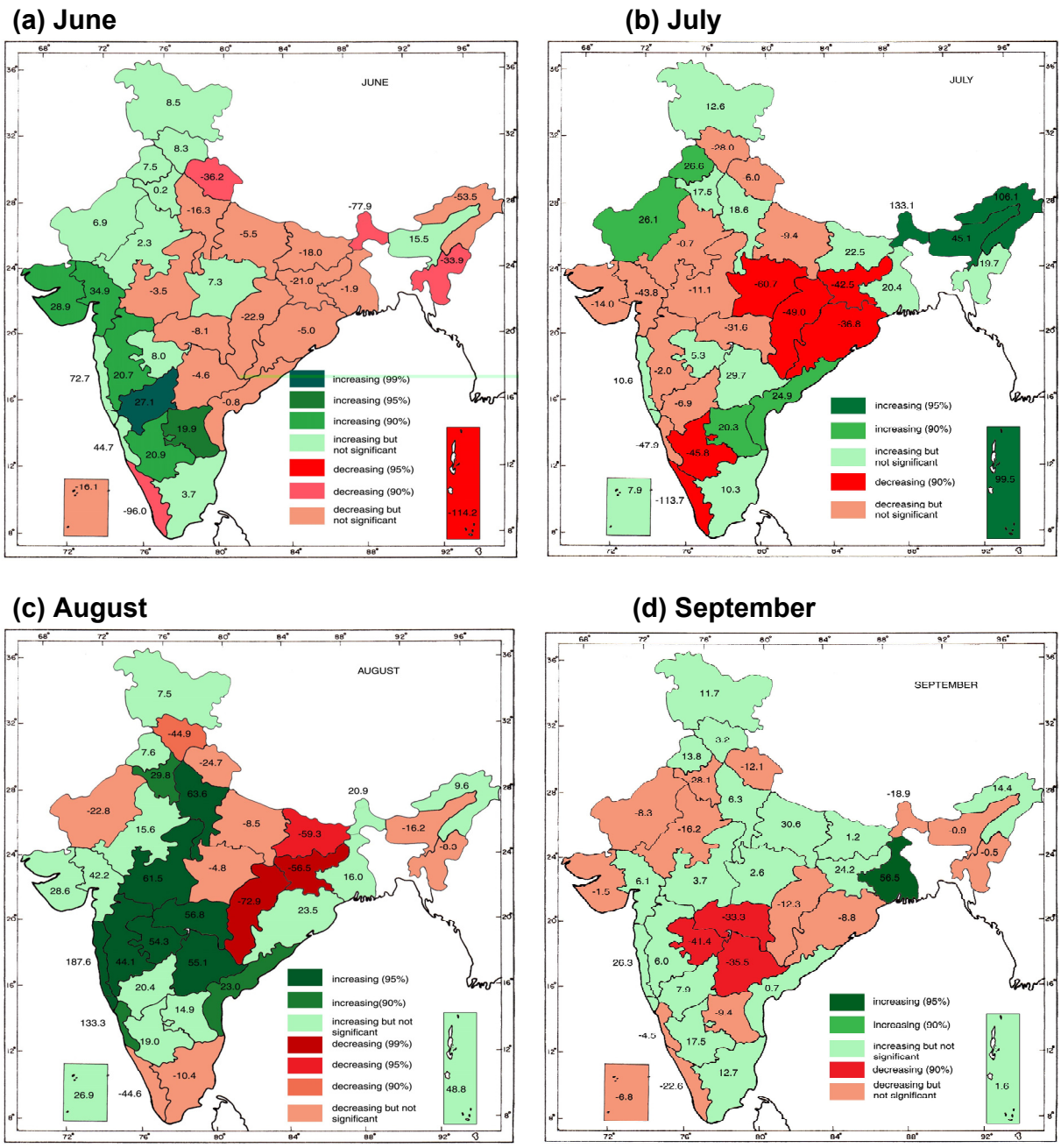

Fig. 2.8 : Increase/Decrease in monthly rainfall in mm during 100 year for each of 36 meteorological subdivisions for the south-west monsoon season (June to September). Different levels of significance for increasing and decreasing trend are shaded with colours *(Source : Guhathakurta and Rajeevan 2007).*

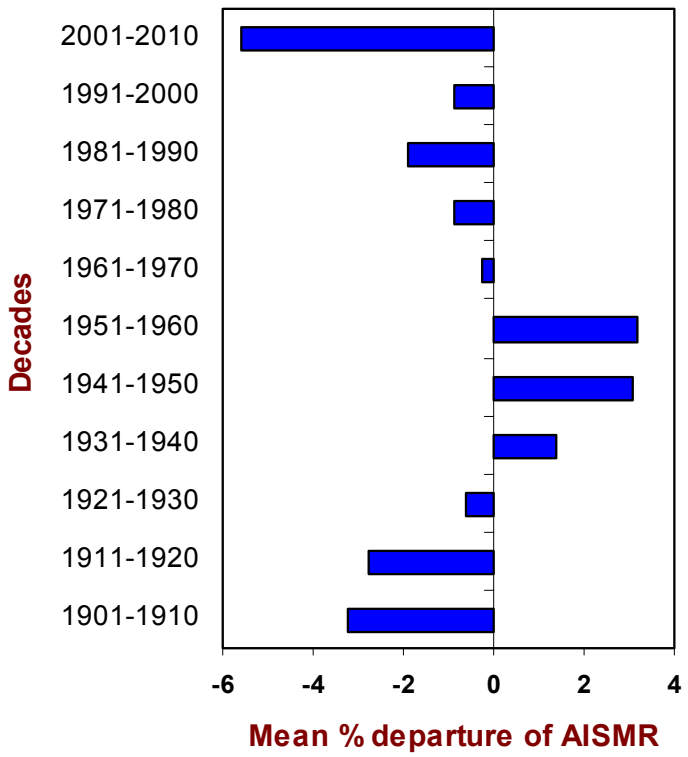

Fig. 2.9 : Decadal composite anomalies of AISMR based on IMD observed rainfall during last 11 decades from 1901-2010.

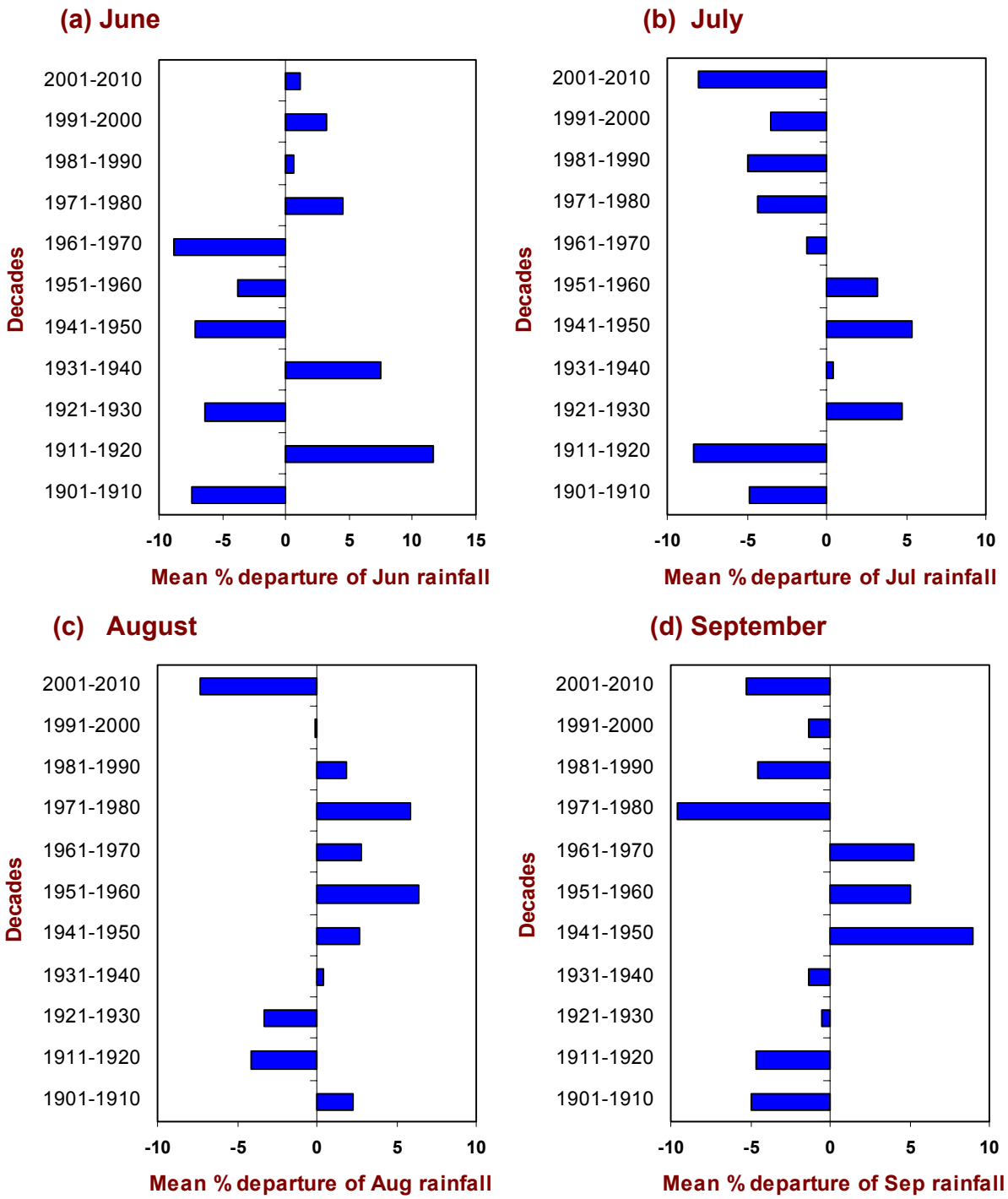

Fig. 2.10 : Decadal composite anomalies of AISMR based on IMD observed rainfall during last 11 decades from 1901-2010.

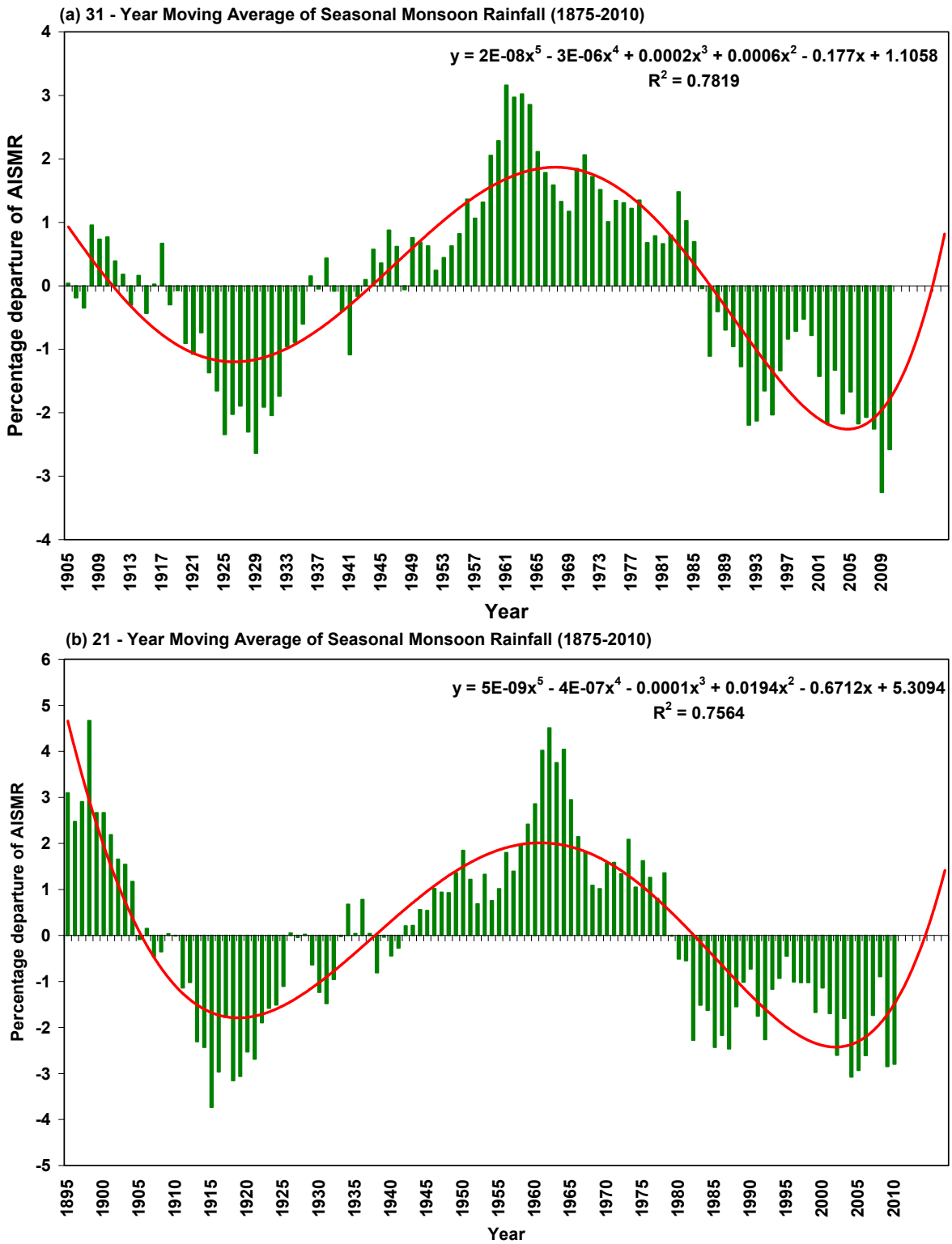

Fig. 2.11 : Epochal variability of AISMR during the period 1875-2010 based on (a) 31-year moving average of AISMR and (b) 21-year moving average of AISMR.

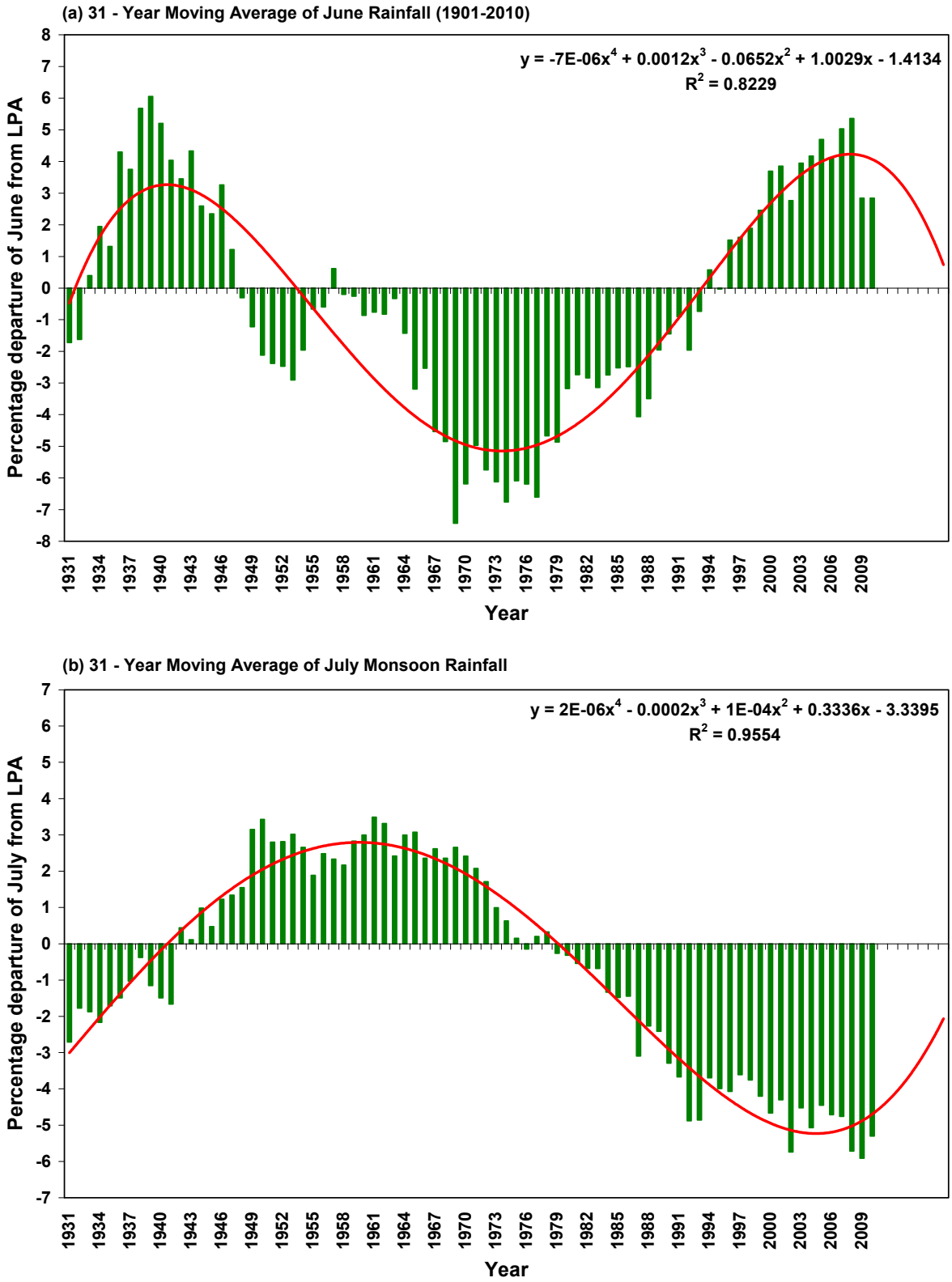

Fig. 2.12 : Epochal variability of monthly rainfall over India during the period 1901-2010 based on 31-year moving average. (a) For monthly June rainfall and (b) for monthly July rainfall.

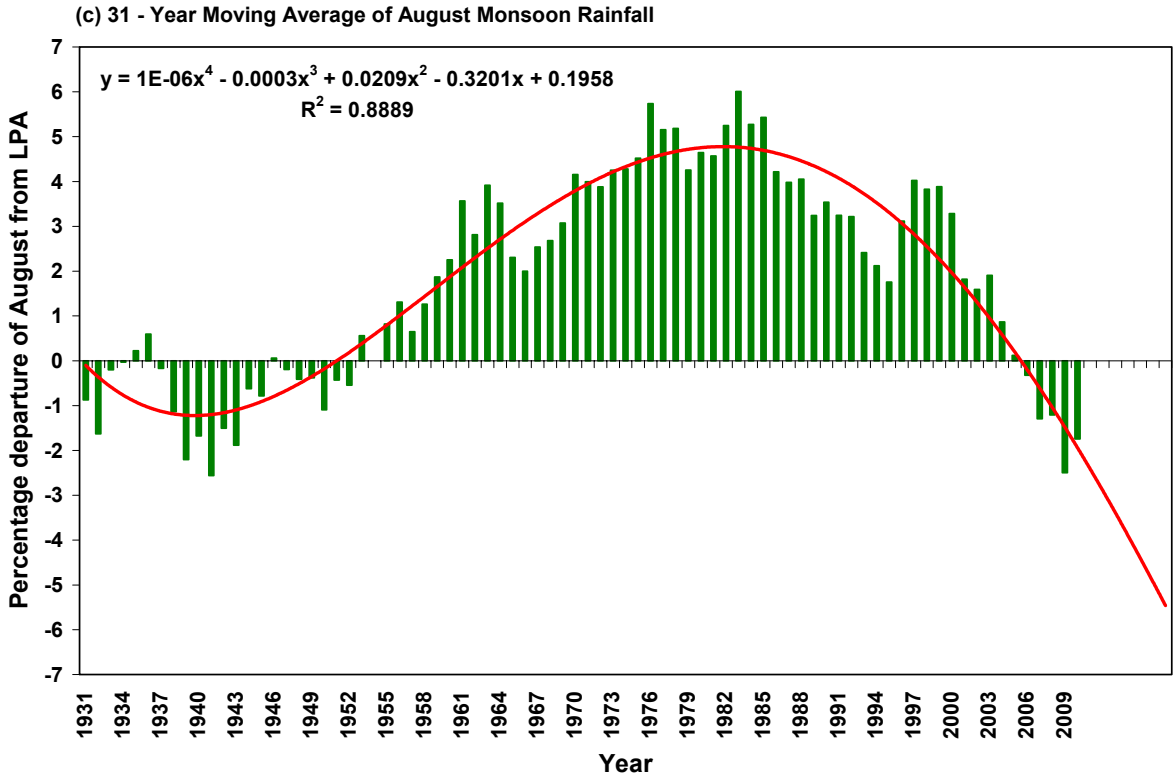

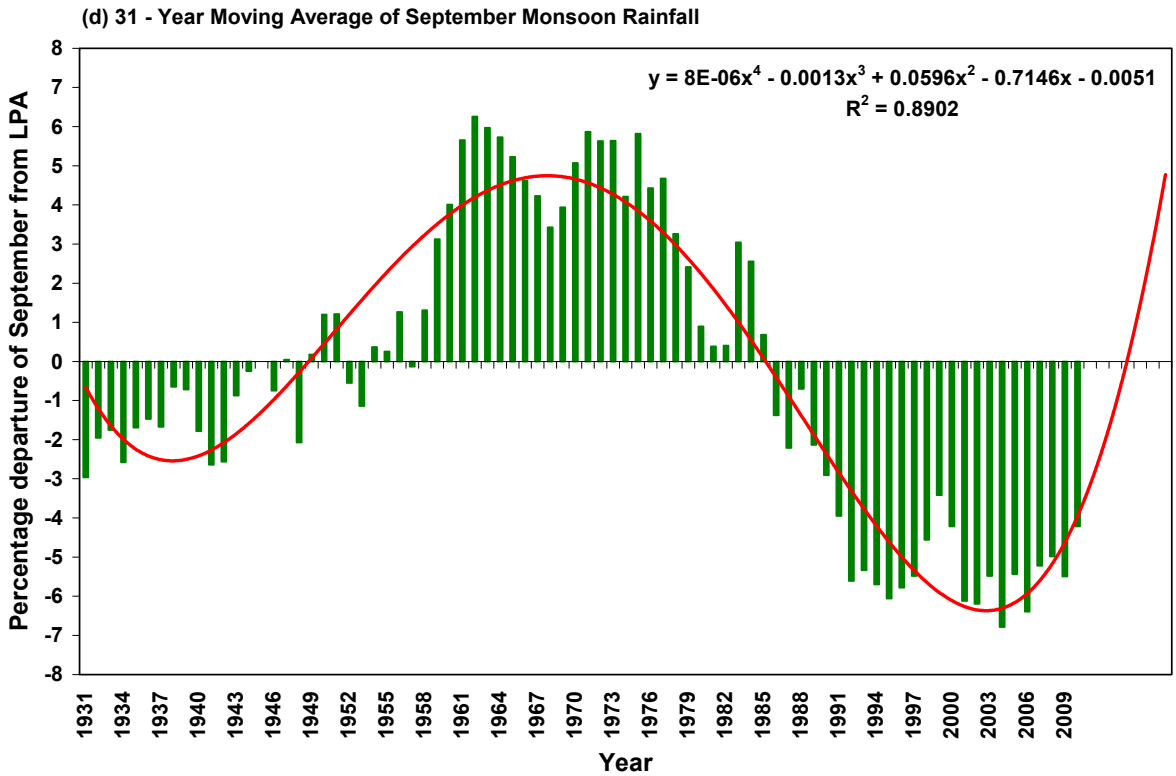

Fig. 2.12 : Epochal variability of monthly rainfall over India during the period 1901-2010 based on 31-year moving average. (c) For monthly August rainfall and (d) for monthly September rainfall.

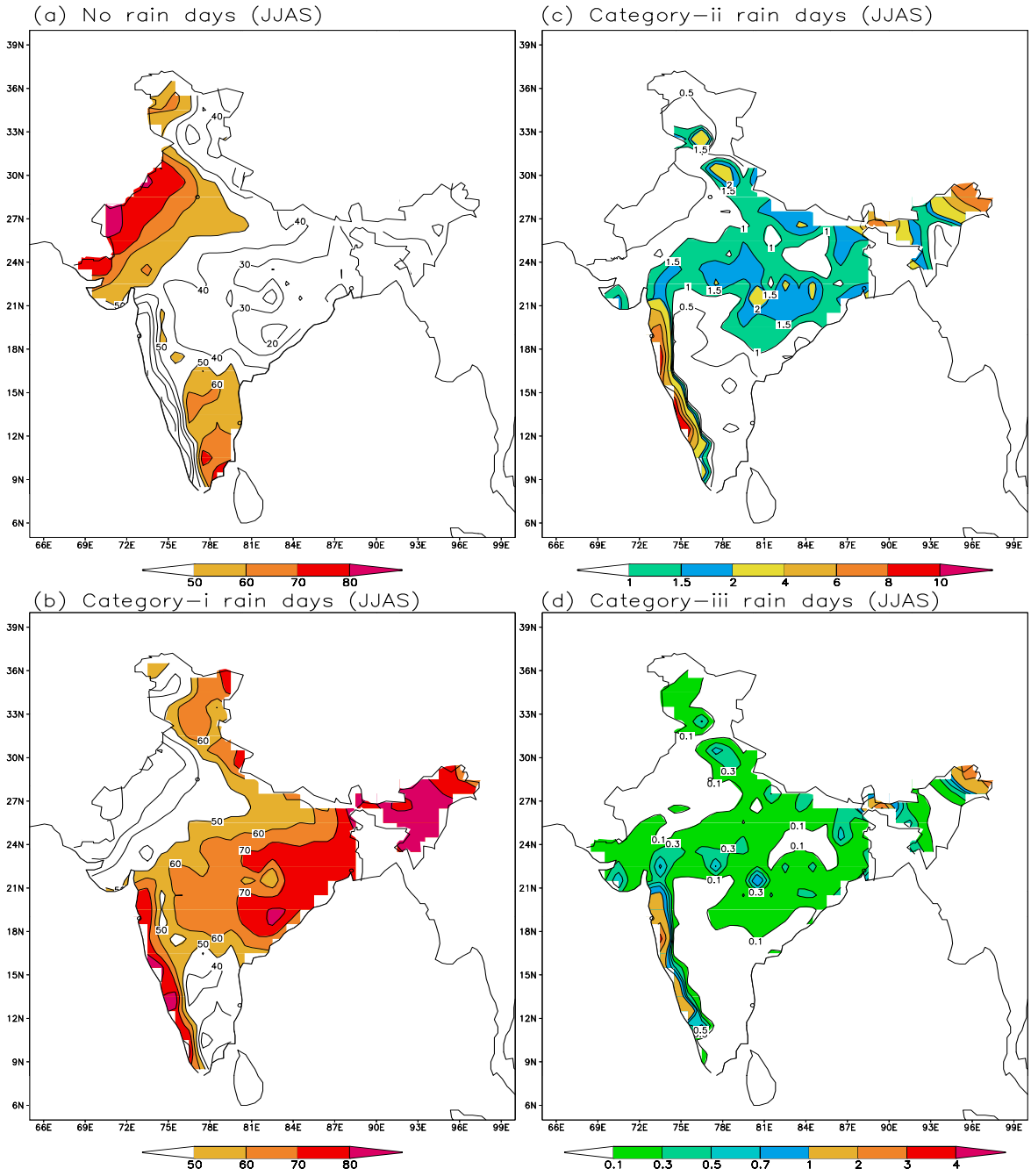

Fig. 2.13 : Average percentage of frequency of no-rain days and different categories of rain days identified in Table I during the monsoon season (June to September) from 1951 to 2005. (a) % of no-rain days, (b) % of Category i rainfall days, (c) % of Category ii rainfall days and (d) % of Category iii rainfall days. Shaded regions are more than 50% in 'a' and 'b', more than 1% in 'c' and more than 0.1% in 'd'. (Source : Pattanaik and Rajeevan 2010)

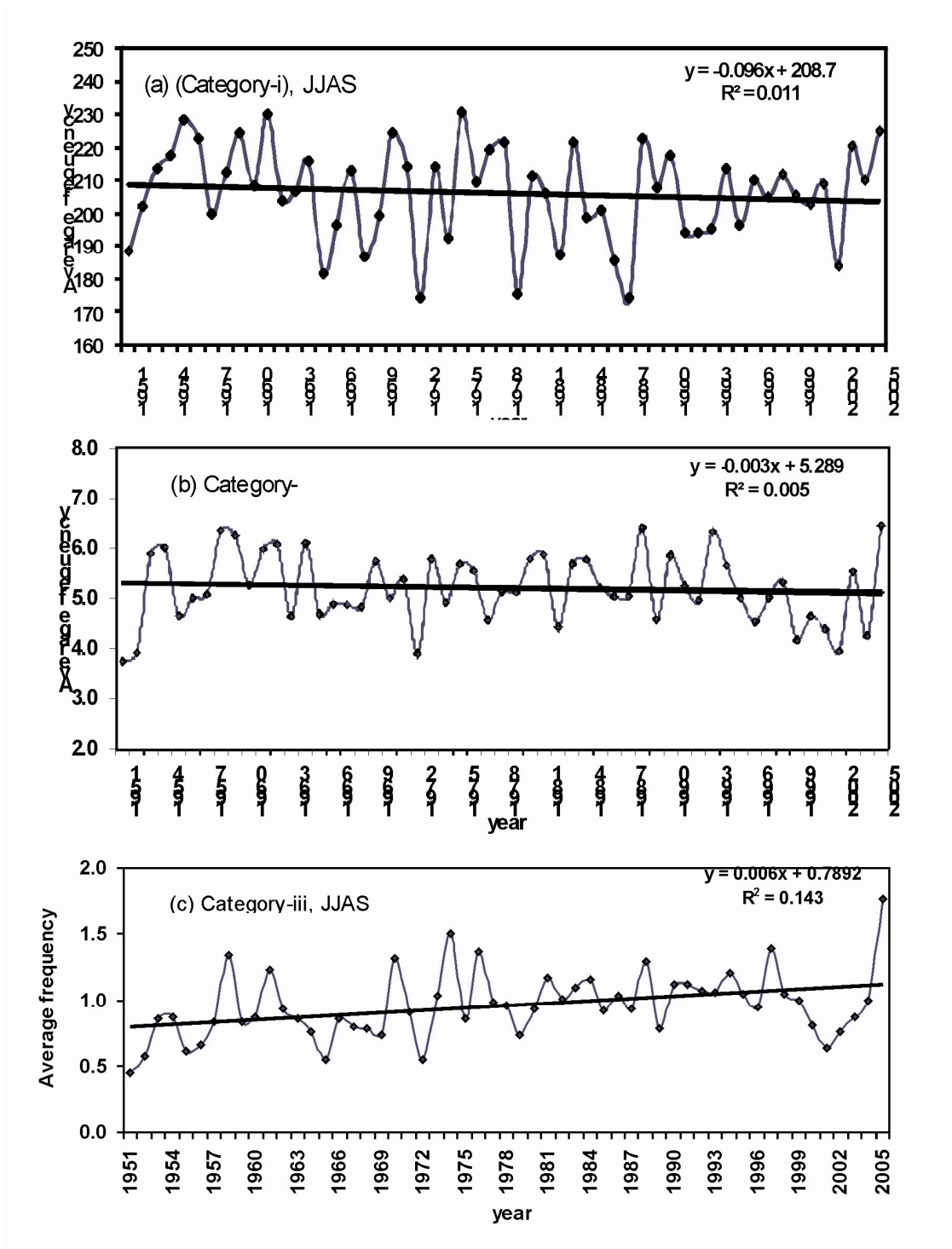

Fig. 2.14 : Average frequency (count per day) of occurrence of different rainfall (R) events during monsoon season (June to September) from 1951 to 2005. (a) Category-i with 'R' ≤ 64.4 mm in a day, (b) Category-ii with 64.4 < 'R' ≤ 124.4 mm in a day & (c) Category-iii with 'R' > 124.4 mm in a day.

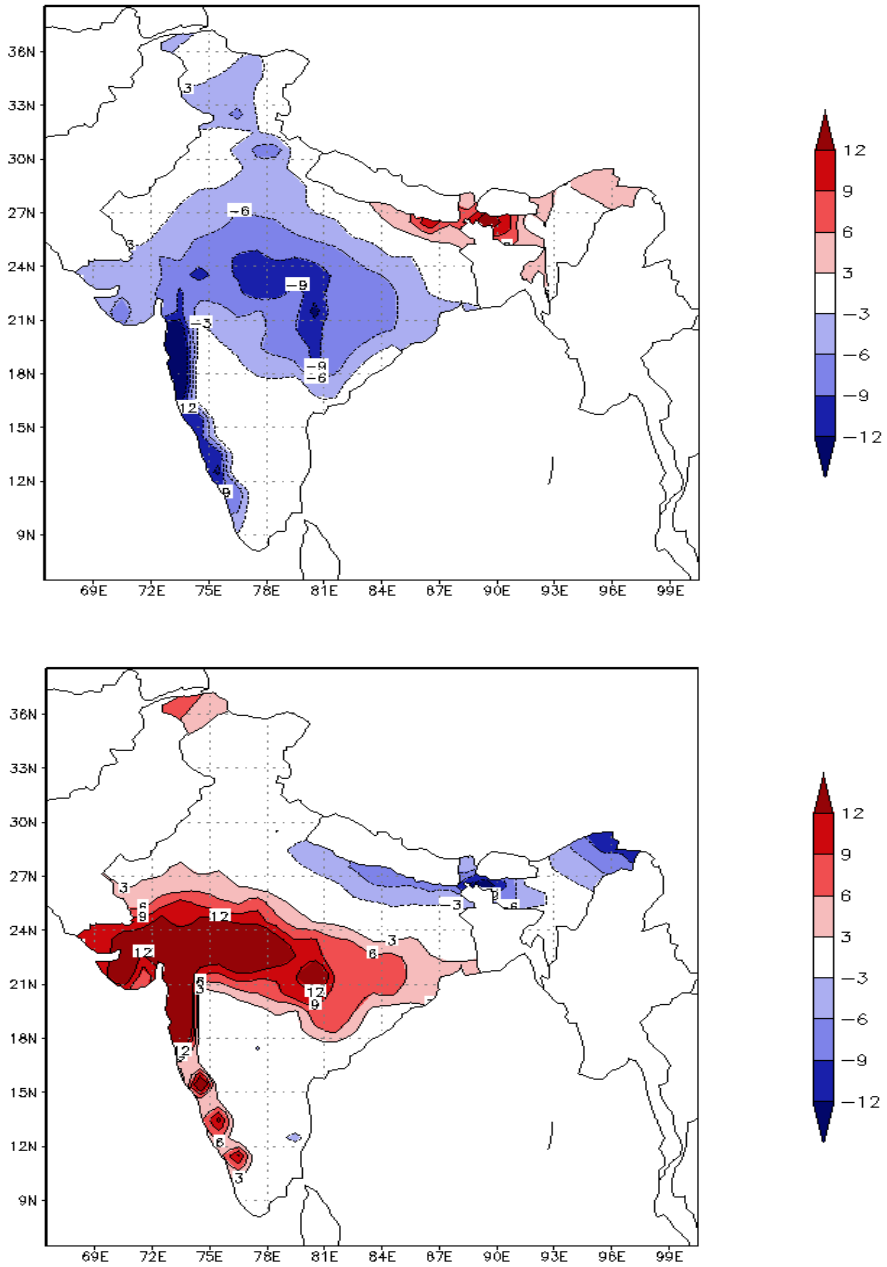

Fig. 2.15 : (a) Composite rainfall anomaly (mm/day) map for the break days (1951-2004) and (b) composite of rainfall anomaly (mm/day) for the active spells (1951-2004).
(Source: Rajeevan et al., 2008)

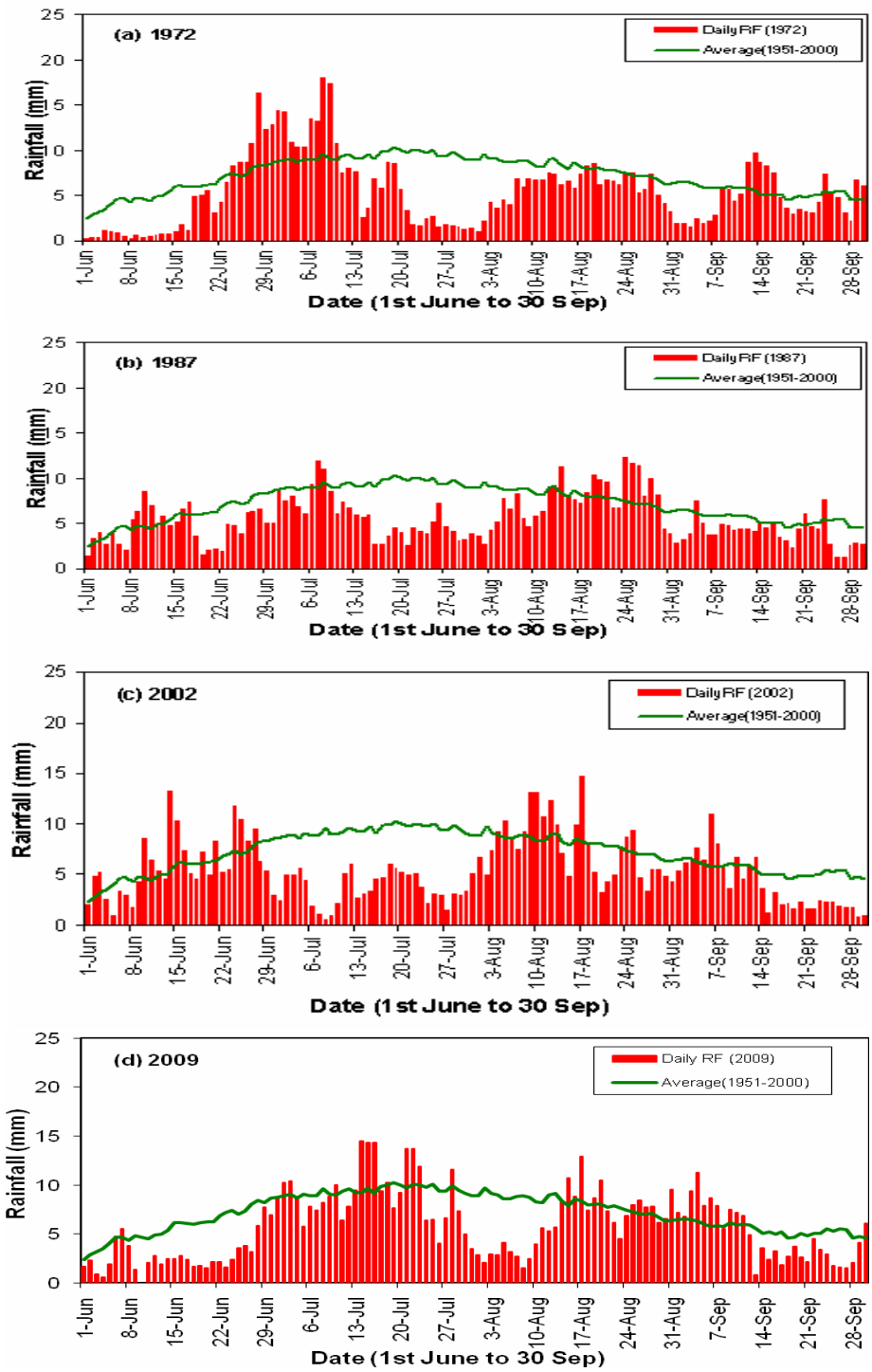

Fig. 2.16 : Daily observed and normal time series of all India monsoon rainfall from June to September during major drought years. (a) 1972, (b) 1987, (c) 2002 and (d) 2009.

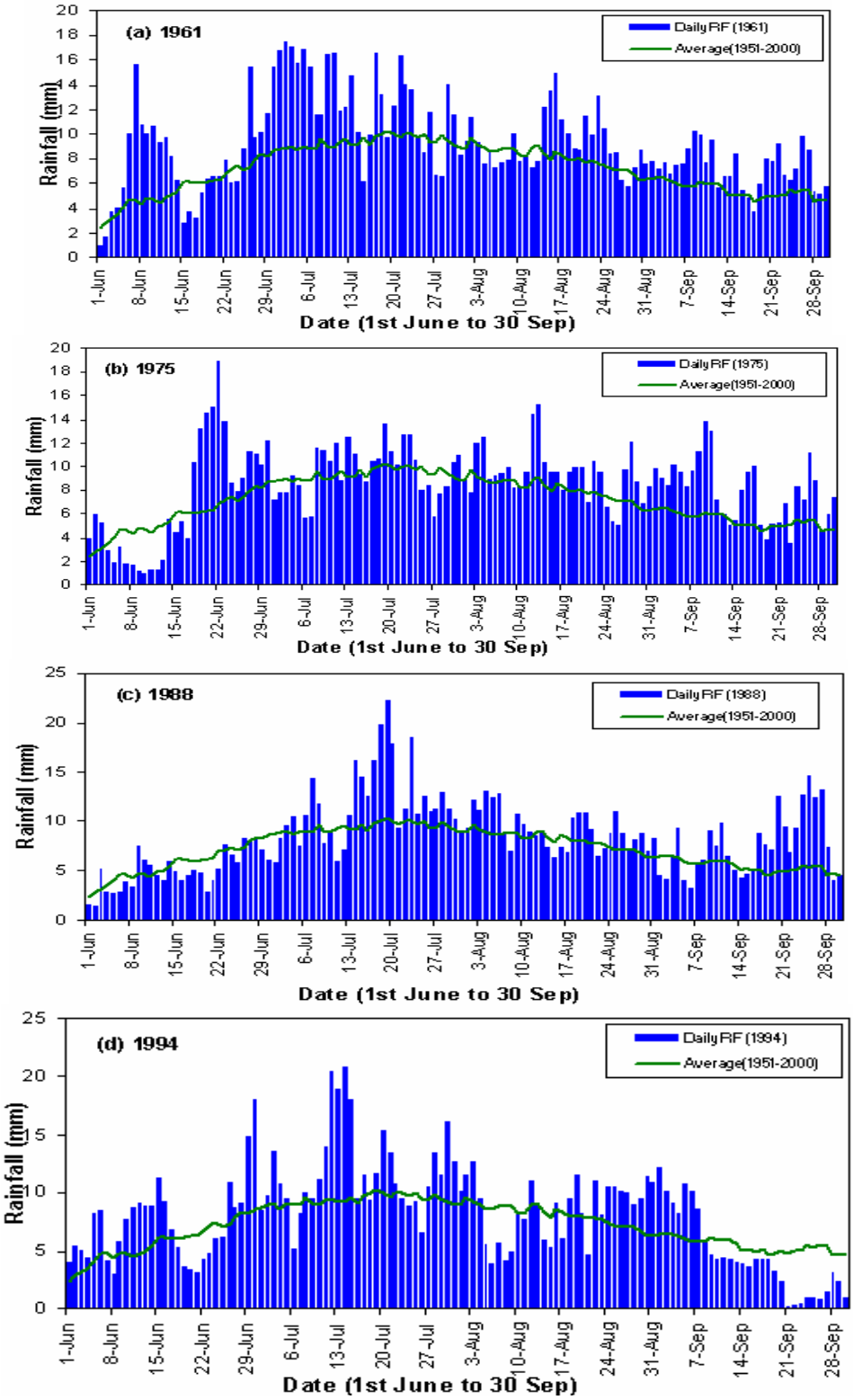

Fig. 2.17 : Daily observed and normal time series of all India monsoon rainfall from June to September during major drought years. (a) 1961 (b) 1975 (c) 1988 and (d) 1994.

CHAPTER 3

GLOBAL TELECONNECTIONS OF INDIAN SUMMER MONSOON RAINFALL VARIABILITY

M. Rajeevan

National Atmospheric Research Laboratory, Tirupati

rajeevan@narl.gov.in

3.1. Introduction

Indian summer monsoon, which is a part of the Asian monsoon, demonstrates perceptible degree of variability on intra-seasonal, inter-annual and multi-decadal scale time scales. Among the wide ranges of timescales, the inter-annual variability of Indian monsoon is the most extensively studied. Inter-annual variation is the yearly deviation of seasonal transition from the mean annual cycle. The pronounced seasonal cycle of Indian monsoon distinguishes it from other monsoon systems in the World that have much weaker annual cycles, for e.g., North American monsoon system (Yang and Lau 2006). Inter-annual variability of Indian summer monsoon rainfall (ISMR) has profound influence on agriculture and national economy. Occurrence of droughts and floods associated with the inter-annual variability of Indian monsoon affects the agriculture, water resources and financial sectors. In spite of an increase in share from the service sector to India's growth, the performance of the agricultural sector is a decisive factor to the growth of GDP of India.

Indian summer monsoon inter-annual variability (IAV) is largely controlled by the internal dynamics of the atmosphere and the slowly varying boundary forcing from the underlying oceans and land surface. Charney and Shukla (1981) hypothesized that the slowly varying boundary conditions at the earth's surface can provide the required memory in the climate system to make it possible to predict the space-time averaged monsoon circulation and rainfall. The lower boundary forcing, which evolves on a slower time scale than that of the weather systems themselves can give rise to significant predictability of atmospheric developments. Among the lower boundary forcings of IAV of the Indian monsoon, sea surface temperature (SST) is perhaps the leading impacting factor.

However, Indian summer monsoon also has vigorous intra-seasonal variability in the form of active and break spells of monsoon rainfall within the summer monsoon season (Ramamurthy 1969, Raghavan 1973, Krishnamurthy and Shukla 2000, Goswami and Ajayamohan 2001, Gadgil and Joseph 2003, Krishnamurthy and Shukla 2007, Rajeevan et al. 2008). A characteristic feature of monsoon season rainfall is the prolonged spells of dry and wet conditions often lasting for 2-3 weeks. These active and break spells are associated with fluctuations of the Tropical Convergence Zone (TCZ) (Yasunari 1979, Sikka and Gadgil 1980). The intraseasonal variation (ISV) of the Indian monsoon has been found to mainly consist of fluctuations on time scales of 10-20 days and 30-60 days. A good review of the ISV of Indian monsoon is given by Goswami (2005) and also in other chapters.

Indian monsoon is related to many large scale anomalies in the general circulation of the atmosphere and oceans, in time and space, which are termed as teleconnections. However, these teleconnections are governed by a variety of complex feedbacks. Indian summer monsoon exhibits several such global teleconnections as revealed by empirical and statistical studies. The origin of the term “Teleconnection” as used in the context of the monsoon is not very certain. Gilbert Walker with those work this term is often associated does not appear to have used it in the several monographs and memoirs that he wrote (Kelkar 2008). The credit for coining this word perhaps goes to Bjerkness (1969). The real monsoon teleconnections refer to those situations or developments in the land-ocean-atmosphere system which occur several months, or may be even years, prior to the onset of the monsoon over India, and are known to exert a strong influence on the monsoon rainfall.

In this review article, important global teleconnections of Indian monsoon identified from empirical and statistical studies are discussed. Relevant model studies related to the observed teleconnections are also discussed. The important teleconnections discussed in this chapter are El Nino/Southern Oscillation (ENSO), Indian Ocean and Atlantic Ocean SSTs, Indian Ocean Oscillation and land surface conditions.

3.2. Inter-annual and decadal variability of ISMR

The inter-annual and decadal variability of ISRM is briefly discussed here. The time series of Indian summer monsoon rainfall (ISMR) (as percentage departure) from 1881 to 2008 is shown in Fig.3.1. The mean ISMR during the period 1941-1990 is 89 cm and the coefficient of variation is about 10%. ISMR does not show any trend and it is mainly random in nature over a long period of time.

The ISMR is said to be normal if the rainfall percentage departure is within ± 10% of long-period mean. Drought is defined if the rainfall departure is less than –10%. Similarly, excess monsoon year is defined if the rainfall departure is more than 10%. During the period, 1875-2008, there were 21 drought years (1877, 1899, 1901, 1904, 1905, 1911, 1918, 1920, 1941, 1951, 1965, 1966, 1968, 1972, 1974, 1979, 1982, 1986, 1987, 2002 and 2004) and 18 excess monsoon years (1875, 1878, 1892, 1893, 1894, 1914, 1916, 1917, 1933, 1942, 1955, 1956, 1959, 1961,1970,1975,1983 and 1988).

From the time series of ISMR (Fig.3.1), significant epochal variations also can be observed. During the epochs of 1901-1930 and 1961-1990, more frequent droughts were observed. During the epoch, 1931-1960, comparatively ISMR performance was above normal with the occurrence of just two drought years. After the drought year of 1987, ISMR was normal or excess, consecutively for 14 years. During the recent years, a severe drought occurred in 2002 and a moderate drought in 2004.

3.3. Relationship with El Nino /Southern Oscillation (ENSO)

The El Nino/Southern Oscillation (ENSO) phenomenon, originating in the tropical Pacific is the strongest natural inter-annual climate signal, which has widespread effects on the global climate system. The Oceanic part of ENSO, El Nino and La Nina are important surface temperature anomalies of the tropical central and eastern Pacific Ocean. The atmospheric part of ENSO, called Southern Oscillation (SO) reflects the fluctuations in the air pressure difference between eastern and western parts of tropical Pacific Ocean. El Nino and La Nina are officially defined as sustained sea surface temperature anomalies of magnitude greater than 0.5^0 C across the central tropical Pacific Oceans. When the condition persists for five months or longer, it is defined as an El Nino or La Nina episode or event. Historically, it has occurred at irregular intervals of 2-7 years and usually lasted 1-2 years.

The relationship between the tropical central and eastern Pacific SSTs and Indian monsoon is the most popular topic studied on monsoon teleconnections. In searching for predictors of the Indian monsoon, Walker (1923, 1924) defined the Southern Oscillation (a sea-saw of sea level pressure between eastern and western equatorial Pacific) which is closely related to the zonal circulation over the equator, called Walker circulation. Later, in a classical paper, Bjerkness (1969) demonstrated that the so-called Walker circulation is strongly coupled with the underlying oceans, especially the SST in the tropical central eastern Pacific. Since 1970s, due to the coordinated observational

(McPhaden et al. 1997) and modeling efforts, we have achieved phenomenal progress in the understanding of the Physics of ENSO, which had led to breakthroughs in seasonal forecasting over the Tropics.

In this section, our present understanding of the teleconnections of Indian monsoon with the ENSO system is discussed in detail. The discussion includes the relationships with SST anomalies over the Pacific, Southern Oscillation, Tropical Pacific upper ocean heat content anomalies, secular variations and predictive relationships.

3.3.1. Relationships with SST anomalies over the central and eastern Pacific

The relationship between El Nino events and Indian monsoon has been studied by many researchers since 1980 (Sikka 1980, Pant and Parthasarathy 1981, Keshavamurty 1982, Rasmusson and Carpenter 1983, Barnett 1983, Mooley and Parthasarathy 1984, Webster et al. 1992, Krishna Kumar et al. 1999, Krishnamurthy and Goswami 2000, Pai 2003, Kane 2005, Krishna Kumar et al. 2006, Rajeevan and Pai 2007). One of the most important results is that there is an inverse relationship between the El Nino events and ISMR. The Indian summer monsoon is weaker than normal during the El Nino years, and that the relationship is opposite for La Nina. On a much broader scale, the monsoon circulation over India is generally weaker (stronger) than normal during El Nino (La Nina) summers. Most of severe droughts over India occurred in association with the El Nino events. However, as discussed below, there is no one-to-one relationship between them.

Fig.3.2 shows the spatial pattern of correlation coefficients (1951-2008) between ISMR and SSTs over the Tropical Pacific during different seasons (MAM, JJA and SON). The patterns show that SSTs over the central and eastern equatorial Pacific during the JJA and SON seasons are negatively correlated with ISMR. Correlations increase in strength from MAM to SON seasons. It may be important to note that during the pre-monsoon season (i.e. in MAM season) correlations are not significant or there is no predictive signal of SSTs over the equatorial Pacific. For monitoring the evolution and progress of El Nino events, four Nino indices are proposed (Trenberth and Stepaniak 2001). They are Nino (1+2) (0-10S, 90-80W), Nino 3 (5N-5S, 150W-90 W), Nino 3.4 (5N-5S, 170W-120W) and Nino 4 (5N-5S, 160E-150W) regions. From Fig 3.2, it can be seen that correlations are the strongest over the Nino 3.4 region.

Monthly variation of correlation (for the period 1951-2008) of ISMR with Nino 3.4 SST from January of the previous year to December of current year is shown in Fig.3.3. Statistically significant inverse relationships between ISMR and ENSO are observed only during and after the monsoon season. During the pre-monsoon period, the correlations between Nino-3.4 and ISMR are weak and cannot be used as a predictor in the long-range forecast models. However, during the El Nino (La Nina) years, there is a gradual shift in the SST anomalies from negative (positive) values to positive (negative) values. This aspect is further shown in Fig.3.4, which shows the evolution of composite SST anomalies during the El Nino and La Nina years during the period 1951-2008. This means, if we take a tendency of SST anomalies of pre-monsoon season (March-April-May) from the winter season (December to February), we will find a positive (negative) value for El Nino (La Nina) years. It is seen that this tendency of SST anomalies from pre-monsoon to winter season has a statistically significant correlation with ISMR. For the period 1951-2008, the correlation of tendency of Nino 3.4 index (from MAM to DJF) with ISMR is 0.45, which is statistically significant.

Table 3.1 shows the relationship between the Warm (El Nino) and Cold events (La Nina) over the equatorial Pacific and ISMR. In this table, a warm event is identified as the event with Nino-3 standardized anomaly more than 1.0 during the June-September period. Similarly, the cold event is identified with Nino-3 less than -1.0 during the same period (Krishna Kumar et al. 2006). The 129 year record (1880-2008) suggests that only less than half of El Nino events are associated with deficient rainfall over India. In other El Nino years, ISMR was normal or excess. This relationship is found to be more or less the same, even if we use the Nino-3.4 index to represent the El Nino event. However, there are exceptions. A typical example is shown in Fig.3.5, in which the June-September SST anomalies are shown for the 1997 and 2002 El Nino years. The El Nino event of 1997 was the most severe El Nino event of the 21st century with the largest Nino-3 standardized anomaly of 3.4^{0}C during the JJAS period. However, ISMR in 1997 was slightly above normal (102% of Long period average, LPA). Comparatively, the 2002 event was a weak El Nino event with modest positive SST anomalies (0.95^{0}C) over the Nino-3 region. However, 2002 was a drought year with seasonal monsoon rainfall deficiency of 19% due to a prolonged break in July, 2002. This important aspect in the El Nino-Indian monsoon will be further discussed in section 3.3.6.

3.3.2. Relationship with Pacific Upper Ocean Heat Content anomalies

Fig.3.3 showed that statistically significant correlations between Nino 3.4 index and ISMR are observed during and after the monsoon season. Therefore, we need to find out any other precursors of the El Nino events, which can indicate a statistically significant correlation with much longer lead time. One such precursor is the upper ocean heat content anomalies over the equatorial Pacific.

Several studies indicated that variability in heat content or its equivalent of volume of warm water (WWV) in the tropical Pacific is important in governing the evolution of the ENSO cycle (Wyrtki 1975; Cane et al, 1986; Jin 1997). Warm water builds up in the equatorial Pacific prior to El Niño and then is transported to higher latitudes during El Niño. It has been suggested that this buildup of the WWV in the equatorial Pacific is a necessary precondition for the development of an El Niño (Wyrtki 1975; Cane et al. 1986). In addition, Meinen and McPhaden (2000) examined the observed changes in surface winds, sea surface temperature (SST) and the WWV in the equatorial Pacific Ocean and found that the magnitude of ENSO SST anomalies is directly related to the magnitude of zonal mean WWV anomalies over the equatorial Pacific. Therefore, zonally averaged WWV changes along the equator are a useful predictor of ENSO time scale SST variations. McPhaden (2003) further demonstrated that, unlike SST, there is no spring persistence barrier when considering upper ocean heat content, which is important for making skillful ENSO forecasts early in the calendar year. Rajeevan and McPhaden (2004) examined the inter-annual variations of WWV in the tropical Pacific and their predictive relationships with ISMR. WWV data are taken from the upper ocean temperature field analysis derived from ship of opportunity XBT measurements and TAO/TRITON moored time series measurements.

Correlation coefficients between monthly WWV anomalies and ISMR using 51 years of data (1950-2000) are shown in Fig.3.6, which indicate a statistically significant (95% level) negative correlation between the ISMR and the WWV anomalies from February to June. The correlations from March to May are significant even at the 99% level. Positive WWV anomalies in the tropical Pacific in boreal winter and spring are associated with below normal ISMR, and vice versa. This is in the same sense as the inverse association between the NINO-3 SST anomalies and ISMR. The correlation between WWV and IMSR weakens during the monsoon season itself, which is consistent with the weak simultaneous correlation between ENSO SST and WWV anomalies in the Pacific at this time of year (McPhaden, 2003).

Further, Rajeevan and McPhaden (2004) observed that the correlations between WWV (FM) and ISMR undergo decadal changes, for the most part hovering at or just below the 95% significance level. However, the IMSR and WWV (FM) 21-year running correlations show a sharp increase beginning in the mid-1980s, opposite to the trend exhibited in the Nino-3 /ISMR correlations (see section 3.3.3). This increase in the correlation between ISMR and WWV (FM) reflects a decadal modulation in the relationship between WWV (FM) and NINO-3 SST for which in certain periods WWV (FM) anomalies are a better predictor of NINO-3 SST (JAS) anomalies than in others. A full understanding of the relationship between these ENSO predictors and ISMR requires improved knowledge of the teleconnections between the Pacific and Indian Ocean regions. However, these results suggest that should the ISMR revert to being more sensitive to ENSO as it was prior to the mid-1970s, WWV may be an even better predictor of ISMR rainfall than it is now. WWV anomalies over the equatorial Pacific Ocean during February and March are being used as one of the predictors in the Long range forecast model for the operational seasonal forecasts (Rajeevan et al. 2006).

3.3.3. Association with the Southern Oscillation Index (SOI)

Plenty of results are available on the space-time variability of the Southern Oscillation (SO). The pioneering work by Bjerkness (1969) and observational analyses by Rasmusson and Carpenter (1982) have shown that the planetary scale tropical sea level pressure anomalies, manifested as a seesaw between the Indian and Pacific Oceans (Southern Oscillation), occur in conjunction with the episodes of large-scale SST anomalies in the tropical Pacific. Walker (1924) was the first one to demonstrate a possible relationship between the Southern Oscillation and ISMR. Several of the predictor parameters used by Walker for long range forecasts of ISMR were some measures of the Southern Oscillation (SO).

In 1980s, more studies were taken up to explore the relationship of ISMR with Southern Oscillation. Pant and Parthasarathy (1981) and Parthasarathy and Pant (1985) studied the association between ISMR and the southern Oscillation index (SOI). The SOI used is the difference of normalized sea level pressure between Tahiti (central Pacific) and Darwin (northern Australia), two stations located in the core regions of the circulation systems associated with the Southern Oscillation. The SOI values of different months and standard seasons show opposite tendencies during the deficient and excess years of ISMR. The correlation coefficient between ISMR and SOI of summer season (JJA),

autumn (SON) and winter (DJF) minus spring (MAM) seasons are significant at the 1 per cent level. The correlation coefficient between the monsoon seasonal rainfall of the subdivisions north of 16^0 N and west of 80^0 E and the SOI series of DJF minus MAM is significant at the 5% level or above. Shukla and Paolino (1983) suggested that correlation between the Southern Oscillation Index (Darwin pressure) during spring and monsoon rainfall over India for an 81-year period is only -0.32, whereas the correlation coefficient between the tendency of the southern Oscillation (MAM-DJF) sea level pressure for Darwin and ISMR for the same 81-year period is -0.46. In 1990s, SOI and Darwin pressure tendency were used as the predictors in long range forecast models (Gowariker et al. 1989, 1991). However, in the forecast models used by IMD in the later years (Rajeevan et al. 2006), this parameter was not used as a predictor due to weakening of its statistical correlation with ISMR.

3.3.4. Secular variation of ENSO- Indian Monsoon relationships

The secular variation of relationships of ISMR with various global predictors has been studied by many researchers (Parthasarathy et al. 1991, Hastenrath and Greischar 1993, Krishna Kumar et al. 1999, Krishnamurthy and Goswami 2000, Rajeevan 2001). They found significant epochal variations in the relationships (measured by correlation coefficient) between many predictors and ISMR. The secular variation of the association between the Southern Oscillation and ISMR was even observed by Walker. The strength of the Southern Oscillation-Indian monsoon rainfall relationship during the late 1800s and early 1900s led Sir Gilbert Walker to discover the southern oscillation (Walker 1924, Walker and Bliss 1932). The next several decades however witnessed a general break down in the SO-Indian rainfall relationship until it was reawakened by the strong Nino of 1957-58 and vigorous El Nino activity in the 1960s. Such epochal variations were noticed with many predictors like 500 hPa ridge position in April, Darwin Pressure Tendency, 10 hPa zonal winds, Bombay mean sea level pressure tendency etc. (Parthasarathy et al. 1991, Hastenrath and Greischar 1993, Rajeevan 2001).

The secular variation of ENSO-Indian monsoon relationship has been studied in detail. Secular variations are generally examined in terms of 21-year moving or sliding correlations. Fig.3.7 shows the spatial pattern of sliding correlations on a 21-year moving window between ISMR and SSTs taken from Yadav (2009) (Fig. 3.3 of the paper). The year indicated in the diagram is the central year of the 21-year period. Areas with correlations significant at 95% (99%) level are shaded light (dark). Negative (positive) correlation is indicated by dotted (continuous) line. SST anomalies showed significant negative correlations over the eastern and central equatorial Pacific and southwest

Arabian sea up to mid 1970s. However, after mid-1970s, correlations over the Pacific have weakened considerably. During the recent years, significant positive correlations are observed only over the north Atlantic. The relationship with north Atlantic SSTs will be discussed later in this chapter. Fig. 3.8 shows the 21-year moving correlations between ISMR and Nino- 3 and Nino 3.4 indices of JJA period using the data of 1901-2008. This diagram clearly shows the multi-decadal variations of the relationships between Indian monsoon and ENSO. During the recent years, the Nino-3 correlations have become statistically insignificant. Even though, the correlation with Nino 3.4 showed significant secular variations, the correlation between Nino 3.4 and ISMR did not become statistically insignificant, as observed for the Nino 3 index. From this diagram, two important inferences may be noted. The weakening of the ENSO-ISMR relationship was observed in the earlier decades, during 1940s and 1950s also. Further, the weakening of the relationship during the recent years is due to just one individual anomalous year of 1997. As we have discussed earlier, 1997 was a severe El Nino event, but ISMR was near normal. To demonstrate this aspect, the moving correlations of Nino 3.4 with ISMR by excluding the year 1997 are shown in green colour in Fig.3.8. This suggests that if we do not consider the anomalous year of 1997, the relationship between the ENSO (Nino 3.4 index) and ISMR is still statistically significant and strong. The analysis of Yadav (2009) revealed the ISMR-ENSO secular variations are observed in the circulation patterns also. For example, during the recent decades, the correlations of ISMR with the cross equatorial flow over the west equatorial Indian Ocean and easterlies over the central Pacific have weakened. Similar secular variations are observed for the winds at 200 hPa level also.

The decadal variation of the ENSO-ISMR relationship was discussed by Pant et al. (1988), Krishnamurthy and Goswami (2000) and Krishna Kumar et al. (1999). Pant et al. (1988) and Krishnamurthy and Gowami (2000) focused on the decadal variability in ISMR and offered explanations in terms of natural modes of low-frequency climate variability. Mehta and Lau (1997) attributed similar variability in ISMR to the influence of solar irradiance. Krishna Kumar et al. (1999) on the other hand claimed that ISMR has been stable through history but has experienced a break down in recent decades due to the effects of global warming. They proposed two mechanisms for this observed secular variation of the relationship. They are a) a southeast-ward shift in the Walker circulation anomalies associated with ENSO events and b) an enhanced land-sea temperature contrast due to the increased winter temperatures over Eurasia. These observations raise the possibility that the Eurasian warming associated with the global warming helps to sustain the monsoon rainfall at a normal level despite strong ENSO events. Kripalani et al. (2001), however, found no evidence of global warming in the weakening of the

relationship. As mentioned earlier, in these papers, the secular variations are examined in terms of 21-year running/sliding correlations. In an interesting paper, Gershunov et al. (2001) discussed the dangers in physical interpretation of low-frequency variability in running correlations, particularly between the indices of inter-annual modes of climate variability. They showed that the decadal modulation of ENSO-ISMR relationship as discussed by Krishna Kumar et al. (1999) simply could be due to stochastic processes. In fact, the specific relationship between ENSO and ISMR is significantly less variable than should be expected from sampling variability alone.

In Fig.3.8, it is observed that the ENSO-ISMR relationship was weaker during 1940s and 1950s also. Therefore, global warming alone cannot explain the observed weakening of the relationship during the recent years. The proposed theory also should explain the weakened relationships observed during 1940s and 1950s. Chang et al. (2001) and Pai (2004) attributed the north Europe circulation patterns for the observed ISMR-ENSO relationship and they could explain the weakening relationship during both the 1940s and the recent decades. Rajeevan et al. (1998) highlighted the significant precursory signals in the surface air temperatures over northwest Europe and Eurasia during winter for the subsequent ISMR. Pai (2004) further observed that the meridional anomaly temperature gradients across Eurasia during January directed towards equator (Pole) is a very good precursor of subsequent excess (deficient) ISMR. This gradient directed towards equator (pole) indicates below (above) normal blocking activity over Eurasia, which leads to less (more) than normal southward penetration of dry and cold mid latitude westerlies over the Indian region, which ultimately strengthens (weakens) the normal monsoon circulation. This temperature gradient is also reflected in the surface pressure anomalies and pressure gradient observed over Europe during the winter season (Rajeevan 2002). Yadav (2008) recently discussed the role of north Atlantic circulation involving Azores high and downstream Rossby wave train over Euarasia in influencing the ISMR variability during the recent years. In section 6, more results will be discussed, highlighting the role of north Atlantic SSTs and circulation in modulating ISMR on inter-annual and multi-decadal time scales.

While the explanation of Pai (2004) was based on surface temperatures, Chang et al. (2001) attributed the weakening of the relationship to the strengthening and poleward shift of the jet stream over the North Atlantic. These changes have led to the recent development of a significant correlation between wintertime western European surface air temperatures and the ensuing monsoon rainfall. This winter signal extended eastward over most of northern Eurasia and remained evident in spring, such that the effect of the resulting meridional temperature contrast was able to disrupt the influence of ENSO on the Indian monsoon.

To conclude, more and more evidences are now showing the secular variations of ISMR-ENSO relationship are due to influence of Indian Ocean (discussed in the next sections) and North Atlantic SST and circulation anomalies. The scientific basis for the hypothesis on the role of global warming is however very weak.

3.3.5. Predictive Relationships of ENSO

As we have seen from Table 3.1, that only 50% of El Ninos are associated with deficient monsoon over India. In remaining El Nino years, Indian monsoon was normal. The best example of the exemption in the relationship was in 1997. In spite of the presence of a major El Nino event, ISMR was slightly above normal. There are many possible theories (Slingo and Annamalai 2000, Srinivasan and Ravi Nanjundiah 2002), explaining how in 1997 ISMR was normal in spite of a severe El Nino event.

Why only some El Nino years cause deficient monsoon over India? Krishna Kumar et al. (2006) addressed this important issue of El Nino-Indian Monsoon relationship using both the observed data and atmospheric model studies. They have shown that the El Nino events with the warmest SST anomalies in the central equatorial Pacific are more effective in focusing drought producing subsidence over India than events with the warmest SST anomalies in the eastern equatorial Pacific. The physical basis for such different impacts is established using atmospheric general circulation model experiments with idealized tropical Pacific warming. The difference in composites of SST anomalies shows that during the El Nino years with droughts, SST anomalies over the central (east) Pacific were larger (smaller) compared to the SST anomalies during the El Nino years with normal monsoon rainfall. The GCM simulations demonstrated the strong influence of the Indian monsoon on the tropical Pacific SST anomaly pattern associated with different El Ninos. The difference in the composites shows a large gradient in the SST anomalies across the equatorial Pacific from central to east Pacific. They suggested that the traditional monsoon forecast methods using predictors that essentially capture the ENSO's strength are likely to be unsuccessful. They further recommended that incorporation of information on the SST configuration in the statistical models should improve the monsoon forecast skill. However, this information is already known in the statistical analysis, which showed that SSTs over the central Pacific Ocean (Nino 3.4 region) have the highest correlation with ISMR, compared to other Nino regions. There were also modeling efforts in this context even in 1980s. For example, Keshavamurty (1982) studied the sensitivity of the SST anomalies over the equatorial Pacific Ocean using the GFDL general circulation model. He concluded that the SST anomalies over the central and west Pacific are more effective in making the influence on the atmospheric circulation.

Rajeevan and Pai (2007) examined the hypothesis made by Krishna Kumar et al. (2006) that incorporation of SST configuration in the statistical models should improve the monsoon forecast skill. The study revealed that composite SST pattern obtained by Krishna Kumar et al. (2006) was not observed in some individual years. A typical example is the case of 1972 and 1997. In both the years, the SST anomaly pattern was the same with the largest SST anomaly over the east Pacific Ocean. In 1997, the SST anomaly over the central Pacific was more than the anomaly in 1972. In spite of the same SST anomaly pattern, 1972 was a severe drought year and 1997 was a normal monsoon year.

Krishna Kumar et al. (2006) suggested that instead of using the strength of SST anomaly alone, the additional information on the SST pattern across the equatorial Pacific may improve the predictive skill. They proposed to make use of the Trans Nino Index (TNI) (Trenberth and Stepaniak 2001) in the prediction models to improve the skill. The TNI is defined as the difference between Nino (1+2) and Nino-4 SST anomalies. Rajeevan and Pai (2007) explored the possibility of including the information on TNI for improving the prediction skill. The analysis showed that there is no statistical relationship between JJAS Nino 3.4 and JJAS TNI and scatter plots do not reveal any clustering of points among the drought years. When Nino 3.4 is more than 1.0, there is a clustering of normal and drought years together, which suggests that additional information of TNI does not help us to separate out the normal El Nino years from the drought years associated with El Nino. This aspect was further examined by calculating a combined index by combining the JJAS Nino-3 and TNI values. The combined index was calculated as a weighted value of Nino-3 and TNI indices. The weights are proportional to the correlation of Nino-3 and TNI with ISMR for the whole period. The weights thus calculated for the period 1880-2004 for Nino-3 and TNI are 0.584 and 0.128 respectively. Fig.3.9 shows the scatter plot between the JJAS combined index and ISMR for the period 1880-2004. This plot does not reveal any significant improvement in the El Nino-ISMR relationship. When the standardized combined index was more than 1.0, there were droughts as well as normal monsoon years. By adding, the TNI, normal monsoon years associated with El Nino could not be separated out as Krishna Kumar et al. (2006) hypothesized. However, the two recent El Nino events of 2002 and 2004 were well discriminated in this analysis. Thus, this study clearly showed that by including additional information on the SST spatial pattern across the equatorial Pacific, the skill of conventional statistical models with precursory signals (like the operational model of IMD) does not improve.

Therefore, there could be some other mechanisms influencing Indian monsoon during the El Nino years, especially in years like 1997. For example, equatorial Indian Ocean can play an important role in modulating ISMR during the El Nino years. The role of Indian Ocean SSTs and equatorial Indian Oscillation on influencing Indian monsoon is discussed in the following sections.

3.3.6. Mechanisms of ENSO influence on Indian monsoon

How El Nino remotely influences Indian monsoon? The physical mechanism through which ENSO is related to the monsoon has been addressed by several studies (for example, Keshavamurty 1982, Shukla and Wallace 1983, Krishnamurthy and Goswami 2000). The sensitivity of equatorial Pacific SST anomalies on the atmospheric circulation was examined by Keshavamurty (1982) using the GFDL atmospheric circulation model. The model response was compared with the variability of the 15-year control run and the statistical significance of the response. He found that the anomalies produce dominant changes in the vertical circulation in the equatorial longitude- height plane. There are global-scale anomalies in the equatorial zonal winds and Walker circulation is significantly altered. He also found that SST anomalies over equatorial central and western Pacific are found to be more efficient in producing atmospheric circulation anomalies compared to equal one over the eastern Pacific. The details of the response are found to be very much longitude dependent. Shukla and Wallace (1983) used the GLAS atmospheric general circulation model to examine the atmospheric response to the SST anomalies over the equatorial Pacific. They found that the eastward shift of the belt of heavy convective precipitation in the western Pacific during the episodes of positive SST anomalies was correctly simulated. The study revealed that associated with positive SST anomalies, the ascending branch of the Walker circulation also shifted eastward and north-south overturning (Hadley circulation) intensified in the central Pacific.

The physical mechanisms of the relationship were examined using the NCEP/NCAR reanalysis data also (Krishnamurthy and Shukla 2000). The inter-annual variation of the Indian monsoon is characterized by fluctuations of a regional Hadley circulation. A strong monsoon is associated with anomalous ascent around 25°N and a weak monsoon is associated with anomalous ascent near the equator. ENSO influences the Indian monsoon not by direct subsidence over the Indian continent region but through an interaction between the equatorial Walker circulation and the regional monsoon Hadley circulation (Krishnamurthy and Shukla, 2000). The decrease in the Indian monsoon rainfall associated with the warm phases of ENSO is due to an anomalous regional Hadley circulation with descending motion over the Indian continent

and ascending motion near the equator sustained by the ascending phase of the anomalous Walker circulation in the equatorial Indian Ocean (Krishnamurthy and Shukla 2000). ENSO can also exert an impact on the Eurasian continent before the monsoon season and the anomalous land surface conditions in turn affect the following monsoon. Experiments with general circulation models can clearly depict this indirect impact of ENSO related SST on the monsoon.

As we have seen, the negative correlation between Indian monsoon and ENSO is the strongest for east Pacific sea surface temperature anomalies (SSTA) that occur during and subsequent months following the monsoon season (June to September). Based on this correlation, one is tempted to speculate that monsoon variability may affect ENSO variability. Since Indian monsoon is correlated more strongly with later months in the year, Normand (1953) suggested that Indian monsoon stands out as an active, not a passive feature in world weather, more efficient as a broadcasting tool than an event to be forecast. Normand (1953) summarized, “Unfortunately for India, the Southern Oscillation in June-August at the height of the monsoon, has many significant correlations with later events and relatively few with earlier events….The Indian monsoon therefore stands out as an active, not a passive, feature in world weather, more efficient as a broadcasting tool than an event to be forecast….”. Based on observations, Webster and Yang (1992) suggested that the monsoon and the Walker circulation appear to be in quadrature and that these two circulations are selectively interactive. During the springtime, the rapidly growing monsoon dominates the near-equatorial Walker circulation. During autumn and winter, the monsoon is weakest with convection fairly close to the equator; the Walker circulation is then strongest and may dominate the winter monsoon.

There are some studies on this interesting aspect of Indian summer monsoon influencing ENSO. Kirtman and Shukla (2000) addressed this issue using 50-year GCM simulations, which suggested that a weak (strong) monsoon results in a weakening (strengthening) of the trade winds over the tropical Pacific. Based on these coupled simulations, they found a variable monsoon enhances the ENSO variability, particularly three to six months after the monsoon ends and can also serve as a trigger mechanism for ENSO. It is found that an ongoing warm (cold) ENSO event is made even warmer (colder) by a weak (Strong) monsoon. Similarly, warm (cold) events are weakened by a strong (weak) monsoon. These results also reproduce the observed lag/lead ENSO-monsoon relation where the maximum negative correlation between the monsoon and the SSTA in the east Pacific occurs 3-6 months after the monsoon season. However, the study by Goswami and Jayavelu (2001) showed that Indian summer monsoon by itself is

unlikely to influence the ENSO significant way. Using the 50-year NCEP/NCAR reanalysis data, they showed that observed surface winds in the central and eastern Pacific associated “purely” with Indian summer monsoon and unrelated to ENSO are very weak. Strong surface winds in the central and eastern Pacific following a “strong” or “weak” Indian summer monsoon noted in some studies are related not to Indian summer monsoon but to the concurrent SST forcing associated with the ENSO.

3.4. Relationship with Indian Ocean SSTs

The role of the sea surface temperature over the Arabian Sea on the southwest monsoon over India has been a subject for a long time (Pisharoty 1965, Saha and Bhavadekar 1973, Shukla and Misra 1977, Weare 1979, Joseph and Pillai 1984). Observational studies on the relationship between the Indian Ocean SST and the Indian monsoon mostly focused on the correlative aspect of the relationships (Saha 1970, Cadet and Diehl 1984, Joseph et al, 1994, Clark et al 2000, Rajeevan et al. 2002). It is important to note that seasonal variations of the SST over this region are very large, but the inter-annual variations are very weak. Rao and Goswami (1988) reexamined the relationship between the Arabian Sea SST and monsoon rainfall by removing the large amplitude high frequency noise and very low-frequency long-term trends. They found there exists a homogenous region in the south-eastern Arabian sea where the March-April (MA) SST anomalies are significantly correlated with the seasonal (June to September) rainfall over India. Verma (1990) addressed the relationship of SSTs over south Indian Ocean with ISMR. Krishnamurti et al. (1989) emphasized the importance of SST anomalies over the equatorial Indian Ocean, which influenced ISMR adversely during the 1987 El-Nino. The study by Shukla and Paolino (1983) suggested that ISMR is correlated more strongly with Pacific SST anomalies than with Indian Ocean SST anomalies.

One of the main objectives of modeling studies in the 1990s was to understand whether the Indian Ocean provides important forcing for the Asian monsoon. Modeling experiments have also focused on the mechanisms for the relationship between the Indian Ocean SST and the monsoon and on the association of this relationship with ENSO. There are some model studies on the relationship between SST anomalies over the Indian Ocean with ISMR (Shukla 1975, Ju and Slingo 1995, Chandrasekhar and Kitoh 1998, Yang and Lau 1998). Meehl (1997) explained the tropospheric biennial component or Tropical Biennial Oscillation (TBO) of the Asian monsoon based on air-sea negative feedback mechanism in which SSTs in the Indian Ocean play an important role.

Rajeevan et al. (2002) analyzed long time series of Indian Ocean SST data to examine the interannual variations of the SST anomalies over the Indian Ocean and the relationship with ISMR using monthly SST data of 49 years (1950-1998). They found a significant positive relationship between ISMR and SST anomalies over the Arabian Sea during November to January and also in May. SST anomalies over the southeast Indian Ocean during February to March are also positively correlated with ISMR (Fig.3.10). The composite analysis revealed that in Non-ENSO drought years, negative SST anomalies are observed over the south Indian Ocean from February which slowly spread towards the equator during the subsequent months. These negative SST anomalies, which persist during the monsoon season, may be playing an important role in modulating ISMR especially in non-ENSO years.

Terray et al. (2003) used the recent historical data sets to assess the relationships between inter-annual variability of the ISMR and SST anomaly patterns over the Indian and Pacific oceans. The focus of this particular study was on the second half (Late) of the Indian monsoon season (LISM). They found that strong (weak) LISMs are preceded by significant positive (negative) SST anomalies in the southeastern subtropical Indian Ocean, off Australia, during boreal winter. These SST anomalies are mainly linked to south Indian Ocean dipole events, studied by Behera and Yamagata (2001) and to ENSO. These SST anomalies are highly persistent and affect the northwestward translation of the Mascarene High from austral to boreal summer. The southeastward (northwestward) shift of this subtropical high associated with cold (warm) SST anomalies off Australia causes a weakening (strengthening) of the whole monsoon circulation through a modulation of the local Hadley cell during the LISM. Furthermore, it is suggested that the Mascarene High interacts with the underlying SST anomalies through a positive dynamical feedback mechanism, maintaining its anomalous position during the LISM. These results also explain why a strong ISM is preceded by a transition in boreal spring from an El Niño to a La Niña state in the Pacific and vice versa. An El Niño event and the associated warm SST anomalies over the southeastern Indian Ocean during boreal winter may play a key role in the development of a strong Indian monsoon by strengthening the local Hadley circulation during the LISM. On the other hand, a developing La Niña event in boreal spring and summer may also enhance the east–west Walker circulation and the monsoon as demonstrated in many previous studies.

Clark et al. (2000) examined the relationships between the variability of IO SSTs and Indian monsoon using the GISST data set of 1945-1994. They found that the boreal fall and winter preceding the Indian summer monsoon, SST throughout the tropical Indian Ocean correlates positively with subsequent monsoon rainfall. Negative

correlation occurs between SST and ISMR in the subsequent autumn in the northern Indian Ocean only. The highest correlation is however found during the post 1977 period. They also examined the inter-decadal variability of the relationships and found that the Indian Ocean has undergone significant secular variations associated with a climate shift in 1976.

Using a long time series of NCEP/NCAR reanalysis data and SST data sets, Li et al. (2001) examined the variability of Indian Ocean SST and found that on the tropical biennial oscillation (TBO, 2-3 years) time scale, the Indian monsoon rainfall has significant positive correlations with the Indian Ocean SST and moisture flux transport in the preceding winter and spring. The effect of this SST influence is different from the remote forcing of the ISMR by the eastern Pacific SST, which is more dominant on the ENSO (3-7 year) time scale. They argued that while the eastern Pacific SST and the Eurasian land temperature both may affect the monsoon on the ENSO time scale, they are not important on the TBO time scale. These results support the tropical and local feedback theories of TBO that this most important component of monsoon variation is largely influenced by the Indian Ocean SST anomalies and interactions within the tropical atmosphere-ocean coupled system.

The recent observational discovery (Saji et al. 1999, Webster et al. 1999) of a remarkable SST dipole (or zonal) mode in the equatorial Indian Ocean (IODM) showed that this zonal SST mode arises from dynamic atmosphere-ocean interactions in the Indian Ocean. IOD has shown large climate impacts (rainfall and temperature) around the globe, especially near the Indian Ocean. Ashok et al. (2001) examined the impact of the Indian Ocean Dipole (IOD) on the relationship between the Indian monsoon rainfall and ENSO using the data of 1958-1997. They found that the IOD and the El Niño/Southern Oscillation (ENSO) have complementarily affected the ISMR during the last four decades. Whenever the ENSO‐ISMR correlation was low (high), the IOD‐ISMR correlation was high (low). The IOD plays an important role as a modulator of the Indian monsoon rainfall, and influences the correlation between the ISMR and ENSO. They discovered that the ENSO‐induced anomalous circulation over the Indian region is either countered or supported by the IOD induced anomalous meridional circulation cell, depending upon the phase and amplitude of the two major tropical phenomena in the Indo‐Pacific sector. In another study, Ashok et al. (2004) further suggested that the anomalous convergence over the western pole of IOD induced by positive dipole events, led to circulation towards India and thus increased precipitation over India. At the same time, the anomalous divergence over the eastern pole induced by positive dipole mode events, decreased the effect of El Nino-induced subsidence over

India. Guan et al. (2003) suggested the increased rainfall in activity over the Indian region during the positive IOD events is through the enhanced cross-equatorial flow to the Bay of Bengal due to strong meridional SST gradient across the east equatorial Indian Ocean.

However, there is a growing evidence indicating that the Asian monsoon is one of the forcing mechanisms for the SST dipole (Li et al. 2003) as this mode grows fast in summer and reaches a maximum amplitude in the autumn. Moreover, the study by Yoo et al. (2006) found that the large-scale maximum variance of Indian Ocean SST does not appear in the regions associated with the Indian Ocean dipole and that the SST variability associated with the dipole does not represent the most dominant mode of the Indian Ocean SST. On the other hand, the Indian monsoon is also strongly linked to the SST of the southern Indian Ocean (Yoo et al. 2006) where large SST variability appears, including the subtropical SST dipole (Behera and Yamagata 2001). At present, there are many questions relevant on the role of Indian Ocean SSTs on Indian monsoon. The results in general indicate a more prominent role of south Indian Ocean SSTs in influencing Indian monsoon.

3.5. Relationships with Indian Ocean Circulation

Using satellite pictures, Saha (1971) demonstrated that the double equatorial cloud band, one to the north of equator and another to the south is a frequent occurrence over the Indian Ocean. The cloud band to the south of equator is referred as Southern Hemisphere Equatorial Trough (SHET) and the other to the north of equator as the Northern Hemispheric equatorial trough (NHET). Using satellite data, Prasad et al. (1988) showed that possible existence of an inverse relationship between the intensity of SHET and southwest monsoon rainfall over India. De et al. (1995) also studied the inverse relationship between SHET and Indian monsoon. Their study also showed that SHET activity is inversely related to the rainfall activity over the Indian sub-continent in general and central Indian in particular. During typical active SHET epochs, the rainfall activity becomes deficient in the central parts of the country. The activity of the SHET is fluctuating in nature. Its duration is prolonged and intensity is increased during the years of major failure. Using 11 years of data, they showed that there is a negative correlation of 0.77 between Indian summer monsoon rainfall and total number of weeks with active SHET during the season.

After the excess monsoon season of 1988, for thirteen consecutive years (1989-2001), monsoon was normal, even during the 1997 El Nino, the strongest El Nino event

of the century. However, a severe drought occurred in 2002 in association with a much weaker El Nino. The intriguing monsoon seasons of 1997 and 2002 triggered studies which suggested a link to events over the equatorial Indian Ocean (Gadgil et al 2003, 2004, Gadgil et al. 2007). If we examine the spatial pattern of Outgoing Longwave Radiation (OLR) anomalies during July of 1997 and 2002, significant differences between 1997 and 2002 can be noticed over the equatorial Indian Ocean (Fig.3.11). In 1997, convection was suppressed over the eastern equatorial Indian Ocean and enhancement over the western equatorial Indian Ocean. On the other hand, in 2002, the pattern is characterized by suppression of convection over the western equatorial Indian Ocean and enhancement over the eastern equatorial Indian Ocean. These observations suggested the important role of the equatorial Indian Ocean. Using the data of 1958-2003, Gadgil et al (2004) showed that in addition to ENSO, the phase of the equatorial Indian Ocean Oscillation makes a significant contribution to the inter-annual variation of ISMR.

The suppression of convection over the eastern (90^0-110^0 E, 0^0 -10^0 S) (EEIO) and enhancement over the western part (50^0 -70^0 E, 10^0 S-10^0 N) (WEIO) are characteristics of the positive phase of the Indian Ocean Dipole /zonal model (IOD/IODZM). Enhanced convection over the western part of the equatorial Indian Ocean and reduced convection over the eastern part are associated with easterly (from the east to the west) anomalies in the equatorial zonal wind, whereas the reverse case i.e., with enhanced (suppressed) convection over the eastern (western) part is associated with westerly anomalies of the zonal wind at the equator. The oscillation between these two states is called the Equatorial Indian Ocean Oscillation (EQUINOO) (Gadgil et al. 2004). Thus, a positive (negative) phase of EQUINOO with enhanced convection over the WEIO is favourable (unfavourable) for the monsoon. A zonal wind index (EQWIN) is defined as a measure of EQUINOO. It is the negative of the anomaly of the zonal component of the surface wind over the central Equatorial Indian Ocean (60^0E-90^0E, 2.5^0S-2.5^0N). Positive values of EQWIN are favourable for the monsoon.

The statistical relationship of ISMR with EQWIN reveals that when EQUINOO is favourable (EQWIN > 0.2), there are no droughts and when it is unfavourable (EQWIN < -0.8) there are no excess monsoon seasons. The ISMR anomaly, the ENSO index and EQWIN for the summer monsoon seasons with the magnitude of the ISMR anomaly larger than one standard deviation (i.e. extremes) during 1958–2004 and the special season of 1997, are shown in Fig. 3.12 in order of increasing ISMR. It is seen that each drought (excess monsoon) is associated with unfavourable (favourable) phases of either ENSO or EQUINOO, or both. In 1997, a normal monsoon year, the two indices were

comparable, but opposite in sign. In 1994, a year with excess rainfall, ENSO was unfavourable, but EQUINOO was favourable. In the monsoon season of 2002, although the El Nino was weaker than that in 1997, EQUINOO was also unfavourable and a severe drought occurred. Thus, with EQUINOO we may explain not only the droughts that occurred in the absence of El Nino or in the presence of a weak El Nino, but also excess rainfall seasons in which ENSO was unfavourable. The worst droughts are associated with unfavourable phases of both the modes.

The oceanic component of the Indian Ocean Dipole Model (IOD) is characterized by anomalies of opposite sign in the SST and sea surface height (SSG) over west equatorial Indian Ocean (WEIO) and east equatorial Indian Ocean (EEIO). This index denoted by DMI is only correlated with September rainfall over India with statistical significance. Ihara et al. (2007) find that in contrast to EQWIN, no skill is added to the specification of ISMR by the DMI when analyzed over the long interval from 1881 to 1998. However, EQUINOO may not be considered as the atmospheric component of IOD (Gadgil et al. 2007).

Fig 3.13 shows the ISMR for the period 1958-2004 in the phase plane of the June to September averages of the ENSO index and EQWIN. The most striking feature of the distribution of extreme years is the clear separation between the years with excess and deficient monsoons. This distribution in the phase plane suggests that an appropriate index would be a composite index, which is a linear combination of the ENSO index and EQWIN. When the value of this index is high (point above the line L) not only is there no chance of droughts but also no chance of moderate deficits. For low values of the index (below the Line L) there is no chance of excess rainfall seasons but a small chance of moderate excess rainfall. However, the strong relationship between extremes of ISMR and this composite index is not predictive but simultaneous.

Ihara et al. (2007) recently analyzed long-term data records to examine the role of Indian Ocean in explaining the ENSO-Indian monsoon relationships. Their results are however consistent with the results of Gadgil et al. (2004). The results of a multiple regression analysis show that the ISMR is better associated with the conditions of the EQWIN and NINO-3 indices than with NINO-3 alone. In particular, there is a negative association between the ISMR and EQWIN during the El Nino years. Negative zonal wind anomalies over the equatorial Indian Ocean are associated with normal or excess summer monsoon rainfall over India despite the presence of El Nino. This association is found to be highly significant during the El Nino events, but the association during neutral and La Nina years is not coherent or significant. They further showed that a significant association between various categories of ISMR and EQWIN during El Nino but not

during La Nina years. On the other hand, the relationship between SST Dipole Mode (IODM), the SST anomaly difference between the western and eastern Indian Ocean and ISMR is weak. However, the hypothesis regarding this 3-way link is only demonstrated with confidence during the El Nino events. It is not clear why the behaviour of EQWIN is not important during the La Nina and neutral years.

As mentioned above, these relationships are concurrent and thus do not have any predictive value. The predictability aspect of the relationship was explored by Gadgil et al. (2007). They explored the possibility of using EQWIN and ENSO indices before the season for prediction about the forthcoming season. However, there appears to be relatively little information about the rainfall for the forthcoming season in the May values of EQWIN and ENSO index. Preliminary results of analysis of rainfall over India, EQWIN and ENSO indices suggest that like in the case of association, the extremes of the mid-season rainfall (July and August) are well separated in the phase plane of the indices for June. So, from the June indices, it is possible to derive useful information about nonoccurrence of extremes (either deficit or excess rainfall) for July and August together. However, more studies are required to assess whether it is possible to predict the EQUINOO for any part of the season and also the impact on the Indian rainfall in that part of the season for a given (predicted) ENSO state.

Similarly, identifying causality in the relationship is an important issue. Negative anomalies of zonal winds over the equatorial Indian Ocean directly may not cause enhanced rainfall over India. Therefore, it is necessary to understand the physical mechanism of the observed relationship through more observational and model studies.

3.6. Relationships with Atlantic Sea Surface Temperatures

Recent studies have shown evidences of the influence of North Atlantic SST anomalies on Indian monsoon, especially on mutli-decadal time scale (Goswami et al. 2006, Li et al. 2008). They showed that the Atlantic Multi-Decadal Oscillation (AMO) produces persistent weakening (strengthening) of the meridional gradient of tropospheric temperature (TT) by setting up negative (positive) TT anomaly over Eurasia. The study by Li et al. (2008) using atmospheric model simulations also showed that warm extratropical North Atlantic SSTs induce an arching extratropical wavetrain response, enhancing Indian monsoon rainfall. Recently, Rajeevan and Latha Sridhar (2008) examined the relationships between ISMR and north Atlantic SST anomalies on the inter-annual time scale.

The spatial pattern of statistical correlations between the SST anomalies and monsoon seasonal rainfall over the coherent monsoon zone (ICMR, consist of central and northwest parts) are shown in Fig.3.14. For examining the changes in the epochal variations, correlation coefficients were calculated for two different periods, 1951-1975 and 1976-2005. The spatial patterns show statistically significant correlations between the SST anomalies over the NW Atlantic Ocean and ICMR during the simultaneous period (JAS). The correlations suggest that the positive SST anomalies over the NW Atlantic region are conducive for above normal monsoon rainfall over the monsoon core region. However, the correlations showed significant epochal variations as shown in Fig. 3.15. The relationships were statistically significant only during the recent period 1976-2005. During the earlier period of 1951-1975, we find that the SST anomalies over the south Atlantic region are well correlated with ICMR (Kucharski et al 2008). However, as shown in Fig. 3.14, those correlations have become weaker during the later epoch, while the SST anomalies over the north Atlantic are better correlated with statistical significance.

To further explore the epochal variations of the relationship and to examine the physical relationship, an index was derived by averaging SST anomalies over the NW Atlantic (30^0-40^0 N, 40^0-65^0W) over the JAS period. The index is termed here as North West Atlantic Index (NWAI). The 21-year running correlations between the NWAI and ICMR are shown in Fig.3.15. For comparison, the correlations between the Nino 3.4 index and ICMR also are shown with the sign of the correlation coefficient reversed. It shows that the correlations between the NWAI and ICMR have strengthened (exceeded 0.50) during the recent years and remained stable, while the correlations between Nino 3.4 and ICMR have weakened during the recent years. It may be noted that the turning points of both 21-year running correlation curves occurred around 1983. The weaker linkage between ENSO and the ISM since 1983 may be due to stronger influence from the North Atlantic to the Indian monsoon in the recent 20 years or so. This aspect was emphasized by Chang et al. (2001) and Pai (2004) suggesting that favourable North Atlantic winter circulation anomalies are responsible for the weakening relationship between ENSO and Indian summer monsoon.

The possible physical relationships between the north Atlantic SST anomalies and Indian monsoon rainfall have been further explored. The analysis showed that the observed SST anomalies are caused by the large scale variations in the Azores High over the North Atlantic. Analysis suggests (not shown here) that the positive SST anomalies over the NW Atlantic are caused by more intense sub tropical Azores High and associated anomalous anticyclonic flow.

Fig. 3.16 a shows the spatial pattern of correlations between the NWAI and vector winds at 200 hPa during the JAS season for the period 1976-2005. Statistically significant (at 95% level) correlation vectors are shown as dark winds. It shows positive NWAI is associated with stronger sub tropical anticyclone including the stronger Tibetan anticyclone. It suggests the shifting of the north Atlantic jet stream to northern latitudes due to stronger Azores high over the north Atlantic. Positive NWAI is associated with a dipole structure of circulation anomalies over Europe; cyclonic circulation over SW Europe and an anticyclonic circulation over North Europe. Near the Caspian sea, cyclonic circulation anomalies are also observed. Fig. 3.16 b shows the spatial pattern of correlations between the NWAI and winds at 850 hPa during the JAS period of 1976-2005. It shows that positive NWAI is associated with stronger cross equatorial flow into Arabian Sea and stronger monsoon westerlies. Positive NWAI is also associated with easterlies over northern plains of India, thus large-scale convergence over the monsoon core zone.

Some previous studies have examined the influence of the mid and high latitude systems on the break/active phase of the Indian summer monsoon on intraseasonal and interannual time scales (Raman and Rao 1981, Kripalani et al. 1997, Rajeevan 2002, Srivastava et al. 2003, Yadav 2008). There are known pathways for the North Atlantic circulation anomalies affecting Indian summer monsoon through the Rossby wave train over Europe emanating from the North Atlantic and propagating along the Asian Jet stream (Branstator 2002, Hoskins and Ambrizzi 1993). The recent study of Ding and Wang (2005) examined the mid-latitude circulation and its influence on Indian summer monsoon. The study reveals a recurrent circumglobal teleconnection (CGT) pattern in the summertime midlatitude circulation of the Northern Hemisphere. The CGT is accompanied by significant rainfall and surface air temperature anomalies over India and has significant correlations with the Indian summer monsoon (ISM). This study also suggested a wave train that is excited in the jet exit region of the North Atlantic may affect the west central Asian High and, thus the intensity of the Indian summer monsoon. Using rainfall data, they have shown that when northwest India and Pakistan experience floods, there is a drought tendency over central-western Europe and a wet tendency in eastern Europe. This feature is clearly observed in Fig. 3.16 a the cyclonic circulation anomaly at 200 hPa over central-western Europe and anticyclonic circulation anomaly over eastern Europe, suggesting deficient (excess) rainfall over central-west (east) Europe. The circumglobal teleconnection pattern discussed in Ding and Wang (2005) is clearly observed in Fig. 3.16 a, showing the correlations of NWAI with wind vectors at 200 hPa.

In the study of Rajeevan and Latha Sridhar (2008), evidence of shifting of the North Atlantic Jet to north Europe during the years with positive NWAI was clearly seen. This is triggered by the upstream disturbances. A Rossby wave train stretching from western Europe to west-central Asia is favoured by the local basic state (Ding and Wang 2005). Accompanying the wave train, strong stationary wave energy is transported from high latitude to west-central Asia, inducing a secondary anomalous high as observed in Fig 3.16 a . Significant anomalous easterlies are also observed over northern parts of India, south of the anomalous sub-tropical high. These easterly anomalies in the upper troposphere reinforce easterly vertical shear over north India. Ding and Wang (2005) discuss the role of enhanced vertical easterly shear on monsoon rainfall. The increased shear may act to confine the Rossby wave response to the lower level and produce a stronger Ekman pumping-induced heating and an enhanced meridional heat flux, both of which would increase the dynamic instability of the atmosphere and thus increase monsoon rainfall over the core region.

NW Atlantic SST and sea level pressure anomalies are used as predictors for the operational seasonal forecasts (Rajeevan et al. 2006).

3.7. Role of Land surface processes including snow anomalies

Indian monsoon is manifested as a land-atmosphere-ocean interaction between continents and oceans in the seasonal cycle. Oceans have large heat content with a longer climate memory for more than a year, while land has smaller heat content and its climate memory is less than a season. Most of the studies on monsoon teleconnection focused on the strong impact of large-scale SST anomalies in the tropical Oceans. Land surface process can affect the Indian monsoon in a very complex way because the interaction between the atmosphere and land surface involves complicated coupling of hydrologic and energy cycles. However, the land-atmosphere interaction cannot be distinguished from ocean-atmosphere interaction because these two processes are strongly coupled to each other (Yasunari 2005).

The physical quantities of the land surface which may posses anomalous atmospheric forcing or climate memory effects can be 1) snow cover and 2) soil moisture and 3) vegetation (Yasunari 2005). Anomalous snow cover can produce anomalous atmospheric conditions through many ways, including the albedo effect and melting process. The melting process has a climate memory even after snowmelt by affecting the soil moisture content near the surface –called the snow-hydrological effect (Yasunari et al. 1991).

Blanford (1884) was the first researcher, who noted the relationship between snow cover and Indian monsoon rainfall. He used the relationship between Himalayan snow cover and ISMR for foreshadowing the ensuing monsoon seasonal rainfall. Walker (1910, 1924) further used this information for preparing long-range forecasts of Indian summer monsoon rainfall. With the availability of satellite based snow cover extent data in 1970s and 1980s, researchers had shown more interest in examining the inter-annual relationships between snow cover and Indian monsoon. Using only 9 years of satellite data, Hahn and Shukla (1976) showed an apparent negative correlation between the satellite-derived winter snow cover extend anomaly over Eurasia and the following ISMR. Since then, several studies (Dey and Bhanu Kumar 1982, Dickson 1984, Bhanu Kumar 1987, Kripalani et al. 1996, Kripalani and Kukarni 1999, Bamzai and Shukla 1999, and Kripalani et al. 2003, Robock et al. 2003) examined these relationships between snow cover/depth and ISMR.

Kripalani (1996) used the SMMR snow depth data and showed that snow depth variations over localized regions of Russia have impact on the subsequent ISMR. Kripalani et al. (1999) studied the long-term data of historical Soviet snow depth data to examine the relationship between snow depth and ISMR. Their results reveal that the wintertime snow depth over western Eurasia surrounding Moscow (eastern Eurasia in central Siberia) shows significant negative (positive) relationship with subsequent ISMR. Following the monsoon, the signs of relationship reverse over both the regions. This correlation structure is indicative of a mid-latitude long-wave pattern with an anomalous ridge (trough) over Asia during the winter prior to a strong (weak) monsoon. As the time progresses, from winter to spring, the coherent areas of significant relationship show southeastward propagation. Empirical Orthogonal Function (EOF) analysis of snow depth reveal that the first mode describes a dipole-type structure with one centre around Moscow and the other over central Siberia, depicting similar pattern as the spatial correlation structure.

Bamzai and Shukla (1999) used satellite derived snow cover data for a longer period of 22 years and snow depth for 9 years over Eurasia to re-examine the possible relationship of snow with ISMR. In contrast to the previous studies that used snow cover averaged over all of Eurasia as a single number, the frequency of occurrence of snow at each grid point over Eurasia is correlated with ISMR. It was found that western Eurasia is the only geographical regions for which a significant inverse correlation exists between winter snow cover and subsequent ISMR. However, composites for high and low snow cover over Eurasia showed spatially homogenous large-scale patterns of snow cover and surface temperature anomalies. Winters of high and low snow cover for Eurasia are

found to be associated with colder and warmer than normal temperatures, respectively for large regions of the Eurasian continent. The inverse snow-monsoon relationship holds especially in those years when snow is anomalously high or low for both the winter as well as the consecutive spring season. Contrary to previous findings, in the analysis of Bamzai and Shukla (1999) no significant relation is found between the Himalayan seasonal snow cover and subsequent monsoon rainfall. On the other hand, the study by Kripalani et al. (2003) revealed an interesting relationship between Himalayan snow cover and Indian monsoon. They studied the relationships of Himalayan snow cover derived from INSAT satellite data with Indian monsoon. The results revealed that the spring snow cover area over western Himalayas has been declining and snow has been melting faster from winter to spring after 1993. Snow cover area during spring is negatively related with ISMR, with May value showing the maximum correlation. However, snow melt during the February-May period is positively correlated with subsequent ISMR, implying that smaller snow cover area during May and faster snow melt from winter to spring is conducive for good monsoon over India. They have found out that the well documented negative relationship between winter snow and ISMR seems to have altered recently and changed to a positive relationship. The changes observed in snow cover extent and snow depth due to global warming may be a possible cause for the weakening of winter snow-ISMR relationship.

Using a long time series of gridded global air temperature data, Rajeevan et al. (1998) examined the relationship between surface air temperature anomalies and ISMR. They found significant precursory signals in the surface air temperatures over northwest Europe and Eurasia for the subsequent ISMR. They observed that during deficient (excess) monsoon years, the meridional gradient in the surface air temperature anomalies over Eurasia during January is directed towards pole (equator). This temperature gradient acts as a precursor for the subsequent mid latitude blocking activity, which ultimately influences the Indian monsoon. The role of blocking highs and large amplitude troughs in westerlies in triggering long duration breaks was highlighted by many researchers (Raman and Rao 1981 and Raman and Maliekal (1985), Rajeevan 1993, Joseph and Srinivasan 2000). A steep pressure gradient indicates strong zonal flow in the circum polar westerlies. On the other hand, when the pressure anomaly gradient reverses, the zonality is disturbed and the circumpolar flow becomes persistently meridional. The observed temperature anomalies over NW Europe may be caused by the different phases of North Atlantic Oscillation (NAO). A positive (negative) phase of NAO is related to positive (negative) temperature anomalies over NW Europe.

Robock et al. (2003) examined the relationship between interannual variations of the strength of the monsoon and land surface conditions. For the periods 1870-1895 and 1950-1995, strong Indian summer monsoon precipitation was preceded by warmer than normal temperatures over Europe and North America in the previous winter and over western Asia in the previous spring, but colder temperatures over Tibet. The European temperature anomalies were related to the positive phase of the North Atlantic Oscillation (NAO). Related negative snow cover anomalies in Europe in winter and central Asia in spring were produced by circulation and temperature anomalies. They argued that the snow-albedo feedback is always operating, but the snow by itself did not physically control the monsoon. Anomalous snow cover impacts on temperature were not prolonged by soil moisture feedbacks because of its short time memory, and there was no obvious relationship between soil moisture and the monsoon. The correlation between ISMR and winter land temperatures and snow cover exists only when interannual variation of the NAO is very strong, and therefore NAO is not robust predictor of the monsoon.

How the climate memory of the snow cover anomaly in winter or spring can influence the monsoon rainfall during June to September? Several groups have investigated the snow-monsoon relationship by means of numerical experiments based on GCMs (Barnett et al. 1989, Yasunari et al. 1991, Zwiers 1993, Vernerkar et al. 1995, and Douville and Royer 1996, Dash et al 2005). Some of these studies concluded that the snow cover-ISMR correlation might result from a common large-scale atmospheric circulation pattern that is responsible both for the snow cover anomaly and the ISMR anomaly. One possible idea is that ENSO-related teleconnection induces anomalous atmospheric circulation over Eurasia, which may fundamentally be responsible for anomalous Indian monsoon activity (Webster et al. 1998). The snow cover anomaly induced by the anomalous circulation may be partly reinforced to produce a weaker monsoon through radiation and energy flux processes.

3.8. Summary

There are known global teleconnection patterns influencing the inter-annual variability of Indian summer monsoon rainfall (ISMR). They are El Nino/Southern Oscillation (ENSO), Indian Ocean sea surface temperatures, Equatorial Indian Ocean Oscillation, North Atlantic SST / circulation anomalies, land surface anomalies including snow cover and snow depth over Eurasia and Himalayas. All these teleconnections are not independent. There are complex interactions and feedbacks among these forcings. For example, ENSO is known to influence Indian Ocean SSTs, which may have direct

influence on Indian monsoon. Similarly, ENSO may cause favourable circulation anomalies over Eurasia causing more snow cover and snow depth, which in turn affect Indian monsoon adversely through land surface processes. The summary of the monsoon teleconnections discussed in this chapter are as following:

1. ENSO is known to be the most important global phenomenon influencing Indian monsoon rainfall. A positive phase of ENSO (positive SST anomalies over the central and east Pacific and negative Southern Oscillation Index) is related to below normal monsoon rainfall and vice versa. However, there is no one to one correspondence between them. Not all the El Ninos cause deficient rainfall over India. Similarly, a drought can occur over India in Non ENSO years also (for example years like 1968, 1974, 1979).
2. Among the different Nino regions, SSTs over the central Pacific (Nino 3.4 region) have the highest correlations with ISMR. However, correlations of these indices during pre-monsoon season with ISMR are statistically not significant and thus no predictability. Statistically significant correlations are observed only during and after the monsoon season.
3. There are secular variations in the relationship between ENSO and Indian monsoon. Statistical analysis shows the relationship weakened during the recent decades, mainly due to the anomalous year of 1997, which was a severe El Nino year. ISMR in 1997 was however near normal. SST and circulation anomalies over the Indian and North Atlantic Oceans may be responsible for the observed weakening of the relationship between ENSO and Indian monsoon. The scientific basis for the hypothesis on the role of global warming on the weakening of the ENSO-ISMR relationship is however weak.
4. There is no convincing answer why only some El Ninos affect ISMR adversely. One of the possible reasons could be the role of SST warming over the central equatorial Pacific. However, inclusion of trans-Pacific SST anomalies (for example Trans Nino Index, TNI) in the forecast models, does not improve the forecast skill as hypothesized by some researchers.
5. On the tropical biennial oscillation (TBO, 2-3 years) time scale, the Indian monsoon rainfall has significant positive correlations with the Indian Ocean SSTs and moisture flux transport in the preceding winter and spring.
6. Some studies suggested that the Indian Ocean Dipole (IOD) and the El Niño/Southern Oscillation (ENSO) have complementarily affected the ISMR during the last four decades. On multi-decadal time scale, it was found that whenever the ENSO‑ISMR correlation was low (high), the IOD‑ISMR correlation was high (low).

7. On the inter-annual time scale, the Indian monsoon is strongly linked to the SST of the southern Indian Ocean where large SST variability appears, including the subtropical SST dipole. On the other hand, the inter-annual relationship between Indian Ocean Dipole Index (the SST anomaly difference between the western and eastern Indian Ocean) and ISMR is rather weak.
8. Recent studies also suggested statistical relationships between Indian monsoon and oscillation in the equatorial zonal winds over the Indian Ocean (EQUINOO). It is seen that each drought (excess monsoon) is associated with unfavourable (favourable) phases of either ENSO or EQUINOO, or both. With EQUINOO we may explain not only the droughts that occurred in the absence of El Nino or in the presence of a weak El Nino, but also excess rainfall seasons in which ENSO was unfavourable. The worst droughts are associated with unfavourable phases of both the modes.
9. Some recent studies highlighted the important role of North Atlantic Ocean as an important source of inter-annual variability of the Indian summer monsoon. There is significant inter-annual simultaneous positive relationship between the SST anomalies over North Atlantic and rainfall over the monsoon core region, but with significant epochal variations. Positive SST anomalies over the North Atlantic Ocean shift the North Atlantic Jet northwards and the associated circulation changes in the upper troposphere influence Indian monsoon through the circumglobal teleconnection across central Asia.
10. There is negative correlation between ISMR and snow cover /depth over NW Europe during winter and spring. However, the correlation between ISMR and winter land temperatures and snow cover exists only when inter-annual variation of the North Atlantic Oscillation (NAO) is very strong.

Unfortunately, the physical mechanisms involved in many teleconnection patterns discussed in this chapter are not understood properly. Unless, we improve the understanding through observations and modeling, we cannot use this information for useful prediction. However, this is going to be a huge task due to the complexity involved in the observed teleconnection patterns. In particular, we need to improve our understanding on the complex interaction of SST anomalies over the central Pacific Ocean and ISMR. Similarly, we need to improve the physical processes involved in the equatorial Indian Ocean zonal wind anomalies and their role on influencing ISMR. This may be achieved through observations and modeling using coupled models. Also, we need better observational system over the tropical Indian Ocean to measure oceanic and atmospheric variables.

References

Ashok, K., Z. Guan, and T. Yamagata, 2001, "Impact of the Indian Ocean dipole on the relationship between the Indian monsoon rainfall and ENSO", Geophys. Res. Lett., 28(23), 4499–4502.

Ashok, K. M., Guan, Z. M., Saji, N. H., Yamagata, T, 2004, "On the individual and combined influences of the ENSO and the Indian Ocean dipole on the Indian summer monsoon", J.Climate, 17, 3141-3154.

Bamzai A. S., and Shukla, J. 1999, "Relationship between Eurasian snow cover, snow depth and the Indian summer monsoon: An observational study", J.Climate, 12, 3117-3132.

Barnett, T. P., Dumenil, L., Schlese, U., Roecker. E. and Latif, M., 1989, "The effect of Eurasian snow cover on regional and global climate variations. J. Atmos. Sci., 46, 661-685.

Barnett, T. P., 1983, "Interaction of the Monsoon and Pacific Trade Wind System at Interannual Time Scales Part I: The Equatorial Zone", Mon.Wea.Rev., 111, 4, 756-773.

Behera, S. K., and Yamagata, T., 2001, "Subtropical SST dipole events in the southern Indian Ocean. Geophys.Res.Lett., 28, 327-330.

Bhanu Kumar, O. S. R. U., 1987, "Seasonal variations of Eurasian snow cover and its impact on the Indian summer monsoon". *IAHS Publ*., 166, 51-60.

Bjerknes, J, 1969, "Atmospheric teleconnections from equatorial Pacific". Monthly Weather Review, 97, 163-172

Blanford, H. F., 1984, "On the connection of Himalayan snowfall with dry winds and seasons of drought in India". *Proc. Roy. Soc*., **37**, 3-22.

Branstator, G., 2002, "Circumglobal teleconnections, the jet stream wave guide and the north Atlantic Oscillation", J.Climate, 15, 1893-1910.

Cadet, D. and Diehl, B., 1984, "Interannual variability of surface fields over the Indian Ocean during recent decades". Monthly Weather Review, 112, 1921-1935.

Cane, M. A., Zebiak, S. E., and Dolan,S. C., "Experimental forecasts of El Nino, 1986, Nature, 321, 827-832.

Chandrasekar, A. and Kitoh, A., 1998, "Impact of localized sea surface temperature anomalies over the equatorial Indian Ocean on the Indian summer monsoon", J.Met.Soc.of Japan, 76, 841-853.

Chang, C.P., Harr, P., and Ju, J., 2001, "Possible roles of Atlantic Circulations on the weakening Indian monsoon rainfall-ENSO relationship", J.Climate, 14, 2376-2380.

Charney, J. G., and Shukla, J., 1981, “Predictability of monsoon, In Monsoon Dynamics”, .Lighthill,J., and Pearce,R. P., Eds, Cambridge University Press, pp.99-108.

Clark, C.O., Cole, J. E and Webster,P. J., 2000, “Indian Ocean SST and Indian summer rainfall: Predictive relationships and their decadal variability”, J. Climate, 13, 2503-2519.

Dash, S. K., Singh, G. P, Shekhar, M. S. and Vernekar, A. D., 2005, “Response of the Indian summer monsoon circulation and rainfall to seasonal snow depth anomaly”, Climate Dynamics, 24, 1-10.

De, U. S., Prasad, O., and Vaidya, D. V., 1995, The influence of southern hemispheric equatorial trough on rainfall during southwest monsoon, Theor.Appl.Climato, 52, 177-181.

Dey, B. and Bhanu Kumar, O. S. R. U., 1982, “An apparent relationship between Eurasian spring snow cover and the advance period of the Indian summer monsoon. J. Appl. Meteorol., 21, 1929-1932.

Dickson, R. R., 1984, “Eurasian snow cover versus Indian monsoon rainfall: An extension of the Hahn-Shukla results.” *J. Climate Appl. Meteorol*., 23, 171-173.

Ding, Q.H. and Wang, B., 2005, “Circumglobal teleconnection in the northern hemisphere summer”, J Climate, 18, 3483-3505.

Douville, H. and Royer, J. F., 1996, “Sensitivity of the Asian summer monsoon to an anomalous Eurasian snow cover within the Meteo-France GCM”. Climate Dynamics, 12, 449-466.

Gadgil, S., Vinayachandran, P. N. and Francis, P. A., 2003, “Droughts of the Indian summer monsoon: Role of clouds over the Indian Ocean.” *Curr. Sci*., 85, 1713-1719.

Gadgil, S., and Joseph, P. V., 2003, “On breaks of the Indian monsoon”, Proc. Indian Acad Science, 112, 529-558.

Gadgil, S., Vinaychandran, P. N., Francis, P. A. and Gadgil, S., 2004, “Extremes of Indian summer monsoon rainfall, ENSO, equatorial Indian Ocean Oscillation” Geophys.Res.Lett., 31, do 10.1029/2004GL019733.

Gadgil, Sulochana, Rajeevan, M, and Francis, P. A., 2007, “Monsoon Variability: Links to major oscillations over the equatorial Pacific and Indian oceans”, Current Science, 93, 182-194.

Gershunov, A., N. Schneider and Barnett, T., (2001) “Low-frequency modulation of the ENSO-Indian monsoon rainfall relationship: Signal or noise?” J. Climate, 14, 2486-2492.

Goswami, B, N., and R. S. Ajayamohan, 2001, “Intraseasonal oscillations and interannual variability of the Indian summer monsoon”, J.Climate, 14, 1180-1198.

Goswami, B. N., and Jayavelu, V., 2001, “On possible impact of the Indian summer monsoon on the ENSO”, Geophys.Res.Letters, 28, 571-574.

Goswami. B. N., 2005, “South Asian Monsoon, Intraseasonal variability in the Atmosphere-Ocean Climate System”, Praxis, Springer Berlin, 19-61.

Goswami, B. N., Madhusoodanan, M. S., Neema, C. P. and Sengupta, D., 2006, “A physical mechanism for North Atlantic SST influence on the Indian Summer Monsoon”, Geophys.Res. Lett., 33, L02706, doi:10.1029/2005GL024803, 2006.

Gowarikar, V., V. Thapliyal, R. P. Sarker, G. S. Mandel and D. R Sikka, 1989, “Parametric and power regression models: New approach to long range forecasting of monsoon rain in India.” *Mausam*, 40, 115-122.

Gowarikar, V., Thapliyal, V., Kulshrestha,S. M., Mandel, G. S. SenRoy, N., and Sikka, D. R., 1991, “A power regression model for long range forecast of southwest monsoon rainfall over India. *Mausam*, 42, 125-130.

Guan, Z, Ashok, K., and Yamagata, T., 2003, “Summer time response of the tropical atmosphere to the Indian Ocean Sea surface temperature anomalies”, J. Met.Soc.Japan, 81, 533-561.

Hahn D. G. and Shukla, J., 1976, “An apparent relationship between Eurasian snow cover and Indian monsoon rainfall”. *J. Atmos. Sci*., 33, 2461-2462.

Hastenrath, S. and Greischar, L., 1993, “The monsoonal heat budget of the hydrosphere-atmosphere system in the Indian Ocean sector”. J. Geophys. Res., 98, 6869-6881.

Hoskins, B. J., and Ambrizzi, T., 1993, “Rossby wave propagation on a realistic longitudinally varying flow”. J. Atmos. Sci., 50, 1661–1671.

Ihara, C., Kushnir, Y., Cane, M. A., La Pena, V. H. De. La, 2007, “Indian summer monsoon rainfall and its link with ENSO and Indian Ocean climate indices”, Int. J.Climatology, 27, 179-187.

Jin, F.-F. 1997, “An equatorial ocean recharge paradigm for ENSO. Part 1: Conceptual model”. J. Atmos. Sci., 54, 811-829.

Joseph, P. V. and Pillai, .P. V., 1984, “Air-sea interaction on a seasonal scale over north Indian Ocean, Part-I: Interannual variations of sea surface temperature and Indian summer monsoon rainfall”, Mausam, 35, 323-330.

Joseph, P. V., Eischeid, J. K., and Pyle, R. J., 1994, “Interannual variability of the onset of the Indian summer monsoon and its association with atmospheric features, El Nino, and sea surface temperature anomalies”. J. Climate, **7**, 81-105.

Joseph, P. V., and Srinivasan, J., 2000, “Rossby waves in May and the Indian summer monsoon rainfall”, Tellus A, 51, 854-864.

Ju, J. and J. M. Slingo, 1995, “The Asian summer monsoon and ENSO”. *Quart. J. Roy. Meteorol. Soc*., 121, 1133-1168.

Kane, R. P., 2005, “Unstable ENSO Relationship with Indian regional rainfall”, Int.J.Climatol, 26,6, 771-783.

Kelkar, R. R., 2008,” Monsoon Prediction”, BS Publications, 234pp.

Keshavamurthy, R. N., 1982, “Response of the Atmosphere to Sea Surface Temperature Anomalies over the Equatorial Pacific and the Teleconnections of the Southern Oscillation”, J.Atmos.Sci., 39, 1241-1259.

Kirtman, B. and Shukla, J., 2000, “Influence of the Indian summer monsoon on ENSO”, Quart. J. Roy Met Soc., 126, 213-239.

Kripalani, R.H., Singh, S. V., Vernekar, A. D. and Thapliyal, V., 1996, “Empirical study on Nimbus-7 snow mass and Indian summer monsoon rainfall”, Int.J.Climatol, 16, 23-34.

Kripalani, R. H. and Kulkarni, A., 1999, “Climatology and variability of historical Soviet snow depth data: some new perspectives in snow-Indian monsoon tele-connections”. Clim. Dyn., 15, 475-489.

Kripalani, R. H., Kulkarni, A., and Singh,S. V., 1997, “Association of the Indian summer monsoon with the Northern Hemisphere mid-latitude circulation”, Int. J.Climatol, 17, 1055-1067.

Kripalani, R. H., Kulkarni, A., and Sabade, S. S., 2001, “ENSO monsoon weakening: Is Global warming really the player?” CLIVAR Exchanges, 6, 11-18.

Kripalani, R.H., Kulkarni,A., Sabade, S. S. and Khandekar, M. L., 2003, “Indian Monsoon Variability in a Global Warming Scenario”, Natural Hazards, 29, 189-206.

Krishna Kumar, K., Rajagopalan, B., and Cane,M. A., 1999, “On the weakening relationship between the Indian Monsoon and ENSO”, Science, 284, 2156-2159.

Krishna Kumar, K., Rajagopalan,B., Hoerling,M., Bates,G., and Cane,M., 2006,. “Unraveling the Mystery of Indian Monsoon Failure during El Nino”, Science doi: 10.1126/science.1131152.

Krishnamurti, T. N., Bedi, H. S., and Subramaniam, M., 1989, “The summer monsoon of 1987”, J.Climate, 2, 321-340.

Krishnamurthy, V. and Goswami,B. N., 2000, “Indian Monsoon–ENSO Relationship on Interdecadal Timescale”, J.Climate, 13,3, 579-595.

Krishnamurthy, V., and Shukla, J., 2000, “Intra-seasonal and Interannual variability of rainfall over India”, J.Climate, 13, 4366-4377.

Krishnamuurthy, V., and Goswami,B. N., 2000, “Indian monsoon-ENSO relationship on Interdecadal time scale”, J.Climate, 13, 579-595.

Krishnamurthy, V. and J Shukla, 2007, “Intraseasonal and seasonally persisting patterns of Indian monsoon rainfall”, J. Climate, 20, 3-20.

Kucharaski, F., Barco, A., Yoo ,J. H., and Molteni, F., 2008, “Atlantic forced component of the Indian monsoon interannual variability”, Geophys Res.Letters, 35, doi 10.1029/2207GL033037.

Li, T., Zhang,Y., Chang, C. P., and Wang, B., 2001, “On the relationship between Indian Ocean SST and Asian summer monsoon”, Geophys. Res. Lett., 28, 2843-2846.

Li, T., Wang, B., Chang, C. P., and Zhang, Y., 2003, “A theory for the Indian Ocean dipole-zonal mode”. *J.Atmos. Sci.*, 60, 2119-2135.

Li, S., Perlwitz, J., Quan.X., and Hoerling,M. P., 2008, “Modeling the influence of North Atlantic multidecadal warmth on the Indian summer rainfall”, Geophys.Res.Letters, 35, doi 10.1029/2007GL032901.

McPhaden, M, J., 2003, “Tropical Pacific Ocean heat content variations and ENSO persistence barriers, Geo. Phys.Res.Letters, 30, No 9, doi: 10.1029/2003GL016872.

McPhaden, M. J., Busalacchi, A. J., Cheney, R., Donguy, J. R., Gage, K. S ., Halpern, D., Ji, M., Julian, P., Meyers, G., Mitchum, G. T., et al., 1998, “The tropical Pacific Ocean-Global Atmosphere observing system: A decade of progress”, J.Geophys.Res., 103, 14169-14240.

Meehl, G. A, 1997, “The South Asian monsoon and the troposphere biennial oscillation”. J. Climate, 10, 1921-1943.

Mehta, V. M. and Lau, K. M., 1997, “Influence of solar irradiance on the Indian monsoon: ENSO relationship at decadal-multidecadal time scales”, Geophys. Res. Lett., 24, 159-162.

Meinen, C. S., and McPhaden, M. J., 2000, “Observations of Warm water volume changes in the equatorial Pacific and their relationship to El Nino and La Niña”, J.Climate, 13, 3551-35559.

Mooley, D. A., and Parthasarathy, B., 1984, “Indian summer monsoon and El Nino”, Pure and Applied Geophys., 121, 339-352.

Normand, C. W. B., 1953, “Monsoon Seasonal forecasting”, Quart.J.Roy.Meteorol. Soc., 79, 463-373.

Pai, D. S., 2003, “Teleconnections of Indian summer monsoon with global surface air temperature anomalies”, Mausam, 54, 407-418.

Pai, D. S., 2004, “A possible mechanism for the weakening of El Nino-monsoon relationship during the recent decade”, Met and Atmos Physics, 86, 143-157.

Pant, G. B. and Parthasarathy ,B., 1981, “Some aspects of an association between the southern oscillation and Indian summer monsoon. Arch. Meteorol. Geophys. Bioklimaatol., 1329, 245-252.

Pant, G. B., Rupa Kumar, K, Parthasarathy, B., and Borgaonkar, H. P., 1988, “Long term variability of the Indian summer monsoon and related parameters”, Adv. Atmos.Sci, 5, 469-481.

Parthasarathy, B. and Pant, G. B., 1985, “Seasonal relationship between Indian summer monsoon rainfall and Southern Oscillation”. J. Climatol., 5, 369-378.

Parthasarathy, B., Rupakumar, K., and Munot, A. A., 1991, “Evidence of secular variations in Indian monsoon rainfall-circulation relationships”, J. Climate, *4*, 927-938.

Pisharoty, P. R., 1965, “Evaporation from the Arabian sea and the Indian southwest monsoon”, Proceedings of International Indian Ocean Expedition (IIOE), P.R.Pisharoty (Eds), 43-54.

Prasad, O., Rama Sastry, A. A., Hansda, A .K., De, U. S., 1988, “Role of southern hemispheric equatorial trough in medium range forecasting”, Mausam, 39, 201-206.

Raghavan, K., 1973, “Break monsoon over India”, Mon Wea Rev, 101, 33-43.

Ramamurthy, K., 1969, “Monsoon of India: some aspects of Break in the Indian southwest monsoon during July and August”, IMD Forecasting Manual, Part IV 18.3, IMD, New Delhi.

Rajeevan, M., Pai, D. S and Thapliyal, V., 1998, “Spatial and temporal relationship between global land surface air temperature anomalies and Indian summer monsoon rainfall”. Meteorol. Atmos. Phys., 66, 157-171.

Rajeevan, M., 1993, “Upper tropospheric circulation and thermal anomalies over central Asia associated with major droughts and floods in India”, Current Science, 64, 244-247.

Rajeevan, M., 2001, “Prediction of Indian summer monsoon: Status, Problems and prospects”, Current Science, 2001, 81,101-107.

Rajeevan, M, Pai, D. S. and Thapliyal, V., 2002, “Predictive Relationships between Indian Ocean Sea surface temperatures and Indian summer monsoon rainfall.” Mausam, 53, 337-348.

Rajeevan, M., 2002, “Winter surface pressure anomalies over Eurasia and Indian summer monsoon”, Geophys. Res. Letters, 29, 10: 1454.

Rajeevan, M., and McPhaden, M., 2004, “Tropical Pacific Upper Ocean Heat content variations and Indian summer monsoon rainfall”, Geophys Res Lett., L18203, doi:10.1029/2004GL020631.

Rajeevan, M., Pai, D. S. and Thapliyal, V., 2002, “Predictive relationships between Indian Ocean sea surface temperatures and Indian summer monsoon rainfall,” Mausam, 53, 337-348.

Rajeevan, M., Pai. D. S., Anil Kumar, R., and Lal. B., 2006, "New Statistical models for long-range forecasting of southwest monsoon rainfall over India", Climate Dynamics, DOI 10.1007/s00382-006-019706.

Rajeevan, M., Bhate, J., J. D. Kale, and Lal, B., 2006, "A high resolution daily gridded rainfall for the Indian region: 297 Analysis of break and active monsoon spells", Curr. Sci., 91(3), 296–306.

Rajeevan, M and Pai, D. S., 2007, "On the El Nino-Indian Monsoon predictive relationships", 2007, Geophys.Res.Letters, Vol.34, doi: 10.1029/2006GL028916.

Rajeevan, M. and Latha Sridhar, 2008, "Inter-annual relationship between Atlantic Sea Surface Temperature anomalies and Indian summer monsoon, 2008", Geophys Res Lett, doi 10.1029/2008GL036025.

Raman, C. R. V., and Rao, Y. P., 1981, "Blocking highs over Asia and monsoon droughts over India". Nature, 289, 271–273.

Raman, C. R. V. and Maliekal, J. A., 1985, "A northern oscillation relating northern hemispheric pressure anomalies and the Indian summer monsoon, Nature, 314, 430-432.

Rao, K. G., and Goswami, B. N., 1988, "Inter-decadal variations of sea surface temperature over the Arabian Sea and the Indian monsoon- a new perspective", Mon.Wea.Rev. 116, 558-568.

Rasmusson, E. and Carpenter, T., 1982, "Variations in tropical sea surface temperature and surface wind fields associated with the Southern Oscillation/El Nino", Mon. Wea. Rev., 110, 354-384.

Rasmusson, E. M. and Carpenter, T. H, 1983, "The relationship between eastern equatorial Pacific sea surface temperatures and rainfall over India and Sri Lanka", Mon. Wea. Rev., 1, 517-528.

Robock, A., M. Mu, K. Vinnikov and D. Robinson, 2003, "Land surface conditions over Eurasia and Indian summer monsoon rainfall". J. Geophys. Res., **108**, 4131-4143.

Saha, K.,1970, "Zonal anomaly of sea surface temperature in equatorial Indian Ocean and its possible effect upon monsoon circulation". Tellus, XXII, 403-409.

Saha, S., and Bavadekar, S. N., 1973, Water vapour budget and precipitation over the Arabian sea during the northern summer, Quart.J.Royal Met. Soc., 99, 273-278.

Saji, N. H., Goswami, B. N., Vinayachandran., P. N., and T. Yamagata, 1999, "A dipole mode in the tropical Indian Ocean". *Nature*, 40**1**, 360-363.

Shukla, J., 1975, "Effect of Arabian sea surface temperature anomaly on Indian summer monsoon: A numerical experiment with the GFDL model". J. Atmos. Sci., **32**, 503-511.

Shukla, J. and B. M. Misra, 1977, “Relationships between sea surface temperature and wind speed over the central Arabian sea and monsoon rainfall over India”. Mon Wea Rev, 105, 998-1002.

Shukla, J. and D. A Paolino, 1983, “The Southern Oscillation and long range forecasting of summer monsoon rainfall over India”. Mon Wea Rev, 111, 1830-1837.

Shukla, J., 1987, “Interannual variability of monsoon”, In *Monsoons,* J.S.Fein and P.L.Stepens, Wiley and Sons, 399-464.

Shukla, J., and Wallace, J. M., 1983, “Numerical simulation response to equatorial Pacific Sea surface temperature anomalies”, J.Atmos.Science, 40, 1613-1630.

Sikka, D.R., 1980, “Some aspects of the large scale fluctuations of summer monsoon rainfall over India in relation to fluctuations in the planetary and regional scale circulation parameters”, Proc. Indian.Acad.Sci(Earth Planet.Sci), 89, 179-195.

Sikka, D. R., and Gadgil, S., 1980, “On the maximum cloud zone and the ITCS over Indian longitude during southwest monsoon”, Mon. Wea Rev, 108, 1840-1853.

Slingo, J. M. and Annamalai, H., 2000, “1997: The El Nino of the century and the response of the Indian summer monsoon”, Mon Wea Rev., 128, 1778-1797.

Srinivasan, J and Ravi Nanjundiah, 2002, “The evolution of Indian sumemr monsoon in 1997 and 1983”, Met and Atmos. Physics, 79, 243-257.

Srivastava, A.K., Rajeevan, M., Kulkarni, R., 2002, “Teleconnection of SST and OLR anomalies over Atlantic Ocean with Indian summer monsoon”, Geophys. Res. Letters., Vol.29, No.8.125-1, 125-4.

Terray, P. Delecluse, P. Labattu, S. and Terray, L., 2003, “Sea surface temperature associations with the late Indian summer monsoon”, Climate Dynamics, doi 10.1007/s00382-003-0354-0.

Trenberth, K. E. and D.P. Stepaniak, D. P. 2001, “Indices of El Nino evolution, J. Climate, 14, 1697-1701.

Verma, R. K., 1990, “Recent monsoon variability in the global climate perspective”, Mausam, 41, 315-320.

Vernerkar, A. D., Zhou, J. and Shukla, J. 1995, “The effect of Eurasian snow cover over on the Indian monsoon”. *J. Climate*, 8, 248-266.

Walker, G. T., 1910, “Correlation in seasonal variations of weather” . *Mem. Indian Meteorol. Dept*, 21, Part 2, 22-45.

Walker, G. T., 1923, “Correlation in seasonal variation of weather”, Memoirs of India Met. Department, 24, 75-131.

Walker, G. T., 1924, “Correlation in seasonal variation of weather, IX: A further study of world weather, Memoirs of India Met. Department, 24, 275-332.

Walker, G. T. and E. W. Bliss, 1932, World weather. *Mem. Roy. Meteorol. Soc.,* 4*, 53-84.*

Weare, B. C., 1979, “A statistical study of the relationship between surface temperature and the Indian monsoon”, J.Atmos.Science, 36, 2279-2291.

Webster, P. J., Moore, A. M., Loschnigg, J. P. and. Leben, R. R., 1999, “Coupled ocean-atmosphere dynamics in the Indian Ocean during 1997-1998”. *Nature*, 401, 356-360.

Webster, P. J. and. Yang, S., 1992, “Monsoon and ENSO: Selectively interactive systems”, Quart.J.Roy.Met.Soc., 118, 877-926.

Webster, P. J., Magana, V. O.,.Palmer, T. N., Shukla,J., Tomas, R. T., Yanai M, and Yasunari, T., 1998, “Monsoons: Processes, predictability and the prospects of prediction”, J.Geophy.Res., 103(C7), 14,451-14,510.

Wyrtki, K., 1975, “El Nino: The dynamic response of the equatorial Pacific Ocean to atmospheric forcing.” *J. Phys. Oceanogr*., **5**, 572-584

Yadav, R. K., 2008, “Role of equatorial central Pacific and northwest of North Atlantic 2-metre surface temperatures in modulating Indian summer monsoon variability”, Climate Dynamics, doi 10.1007/s00382-008-0410-x.

Yadav, R. K., 2009, “Changes in the large scale features associated with the Indian summer monsoon in the recent decades”, Int. J.Climatology, 29, 117-133.

Yang, S. and Lau, K.. M. 1998, “Influences of sea surface temperature and ground wetness on Asian summer monsoon.” *J. Climate*, **11**, 3230-3246.

Yang, S. and Lau., K. M., 2006, “Interannual variability of the Asian monsoon, in The Asian monsoon”, B. Wang (ed), 259-293.

Yasunari, T., 1979, “Cloudiness fluctuation associated with the northern hemisphere summer monsoon”, J. Meteor. Soc. Japan, 57, 227-242.

Yasunari, T., 2006, “Land-Atmosphere interaction, In “The Asian Monsoon” Bin Wang (Ed), Springer, 459-477.

Yasunari, T. A. Kitoch and T. Tokioka, 1991, Local and remote responses to excessive snow mass over Eurasia appearing in the northern spring and summer climate: A study with the MRI GCM. *J. Meteorol. Soc. Japan*, 69, 473-487.

Yoo, S.-H., S. Yang, and C.-H. Ho, 2006, Variability of the Indian Ocean sea surface temperature and its impacts on Asian-Australian monsoon climate, *J. Geophys. Res.*, 111, D03108, doi:10.1029/2005JD006001.

Zwiers, F.W., 1993, Simulation of the Asian monsoon with the CCC GCM-1, J.Climate, 6, 470-486**.**

Table 3.1: EL Nino/La Nina association with All-India summer monsoon rainfall Anomalies during 1880-2008. Based on ERSST data

	Indian Summer Monsoon Rainfall					
	DEFICIENT <-1.0	BELOW NORMAL -1.0 to -0.5	NEAR NORMAL -0.5 to 0.5	ABOVE NORMAL 0.5 to 1.0	EXCESS > 1.0	TOTAL
EL NINO (NINO-3>1.0)	7	5	5	0	1	18
NORMAL	14	13	39	14	6	86
LA NINA (NINO-3<-1.0)	0	0	7	7	10	24
TOTAL	21	18	51	21	17	128

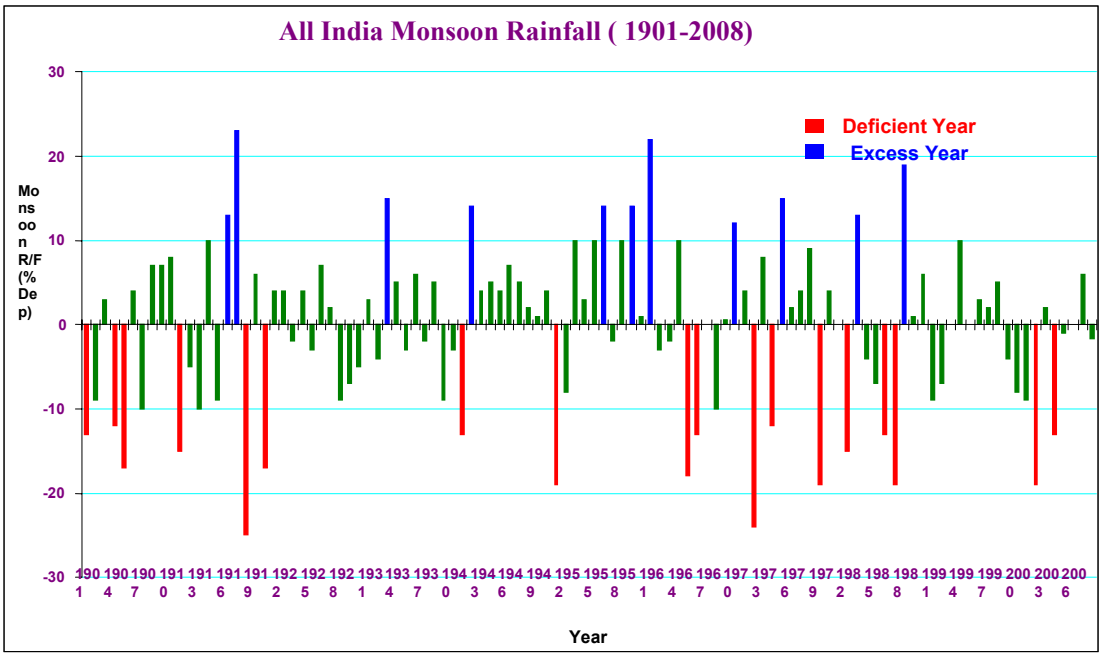

Fig. 3.1 : Time series of all-India Monsoon rainfall as per cent departure for the period 1901-2008.

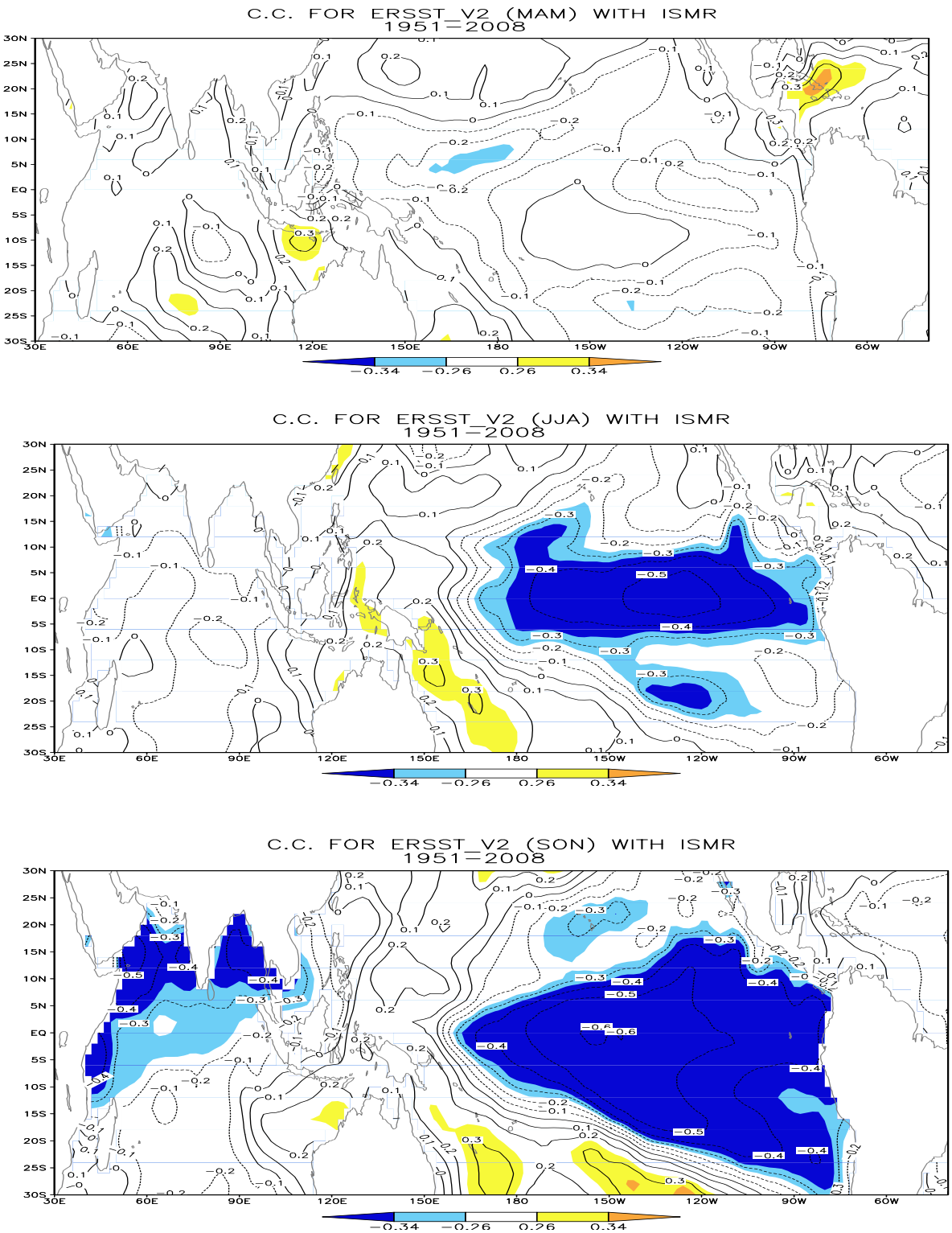

Fig. 3.2 : Spatial correlation of SST anomalies with ISMR during the period 1951-2008 for a) MAM, b) JJA and c) SON seasons. Correlations with statistically significant correlations are shaded.

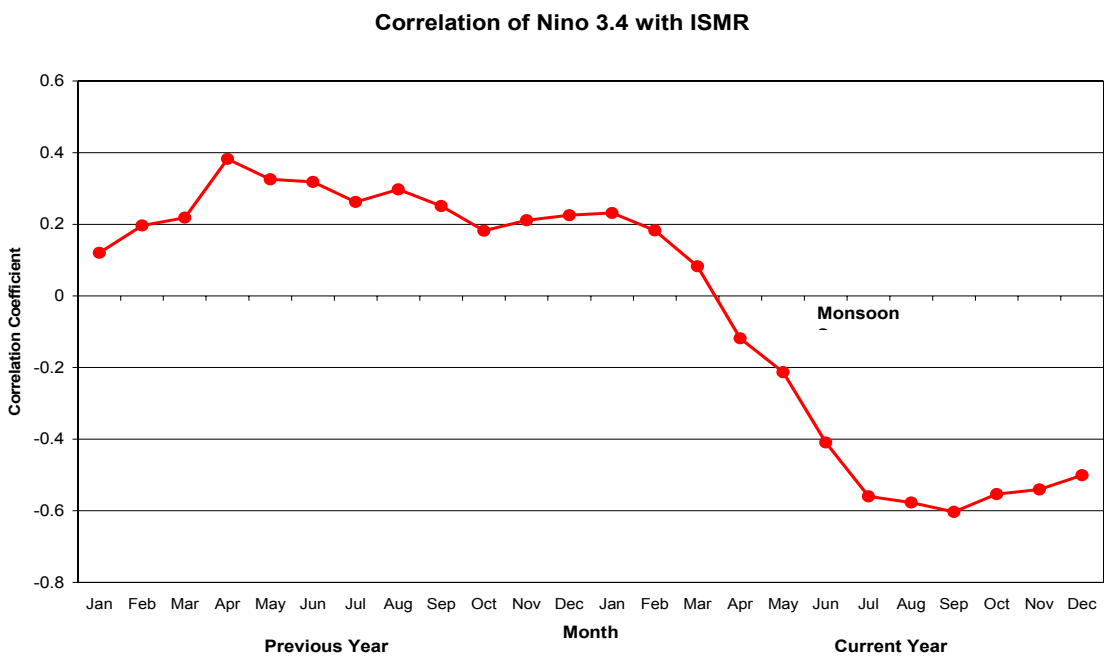

Fig.3.3 : Correlation coefficients between Nino-3.4 SST anomalies and ISMR starting from January of the previous year to December of the monsoon year based on data for the period 1950-2003. The Indian summer monsoon season period is also shown.

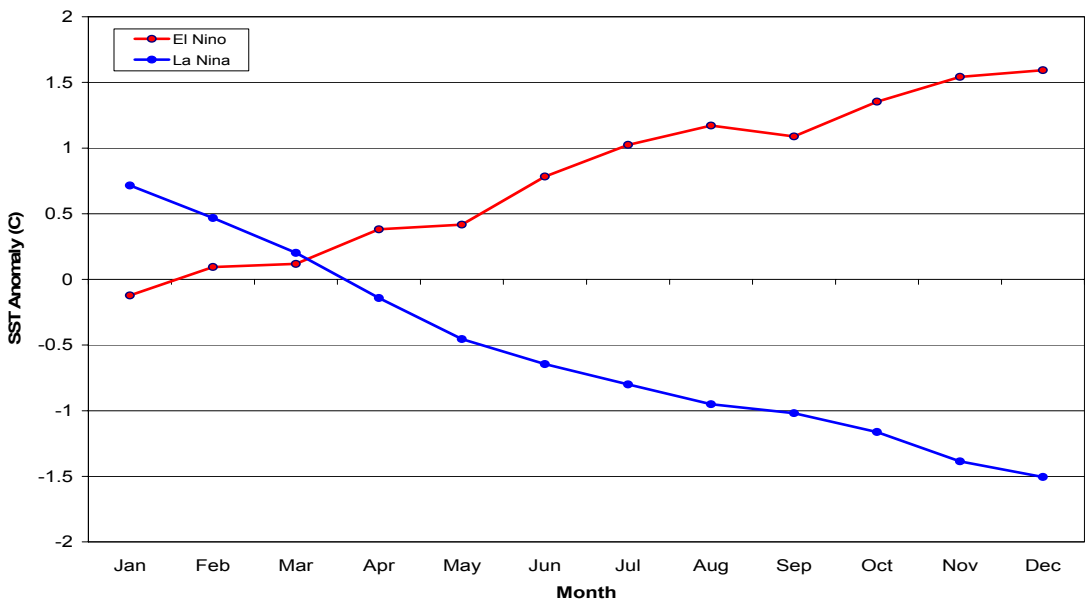

Fig. 3.4 : Time evolutions of composite SST anomalies over the Nino 3.4 region during El Nino (red) and La Nina (Blue) years.

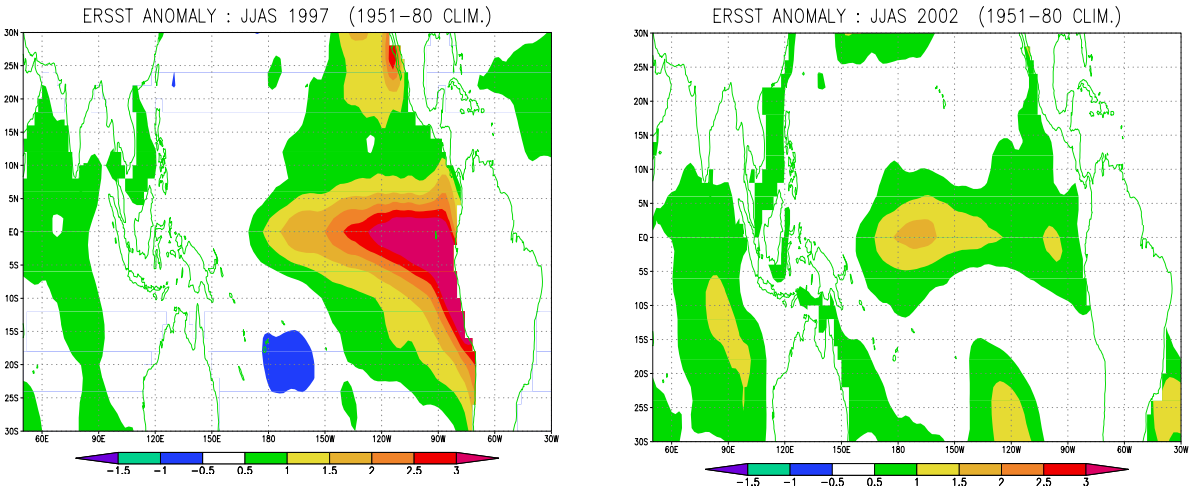

Fig. 3.5 : Spatial Pattern of JJAS SST anomalies during 1997(left) and 2002 (right).

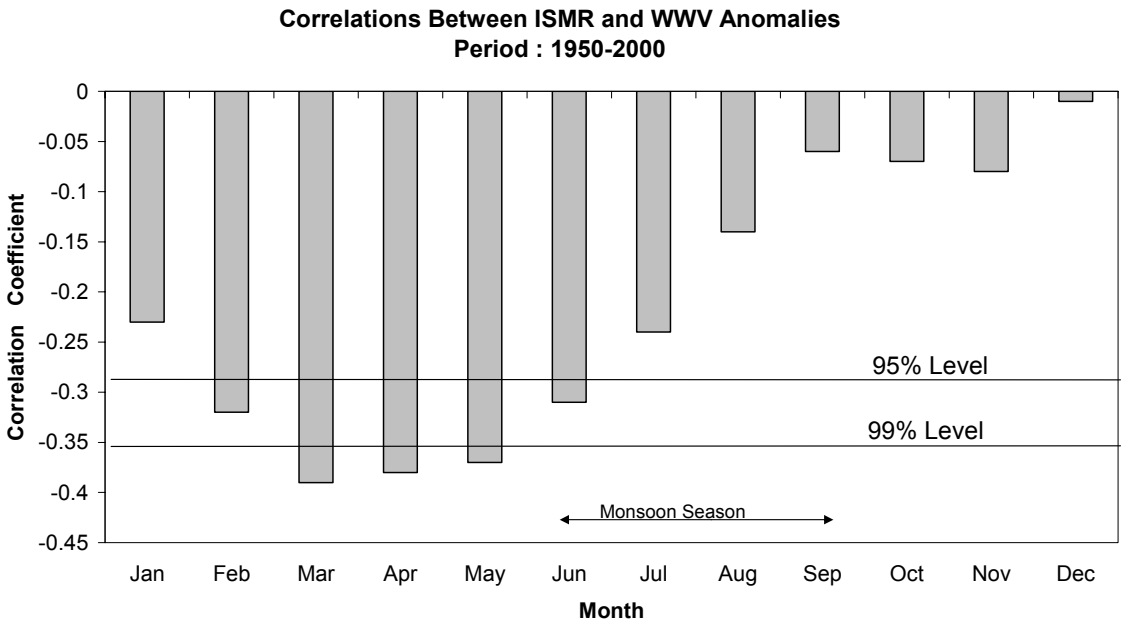

Fig 3.6 : Monthly correlation coefficients between WWV anomaly and ISMR based on data for the period 1950-2000. The 95% and 99% confidence levels are also shown.

Spatial pattern of Sliding correlations on a 21-year moving window between ISMR and SST. The year indicated in these diagrams is the central year of the 21-year period. Areas with correlation significant more than 95% confidence level are colored.

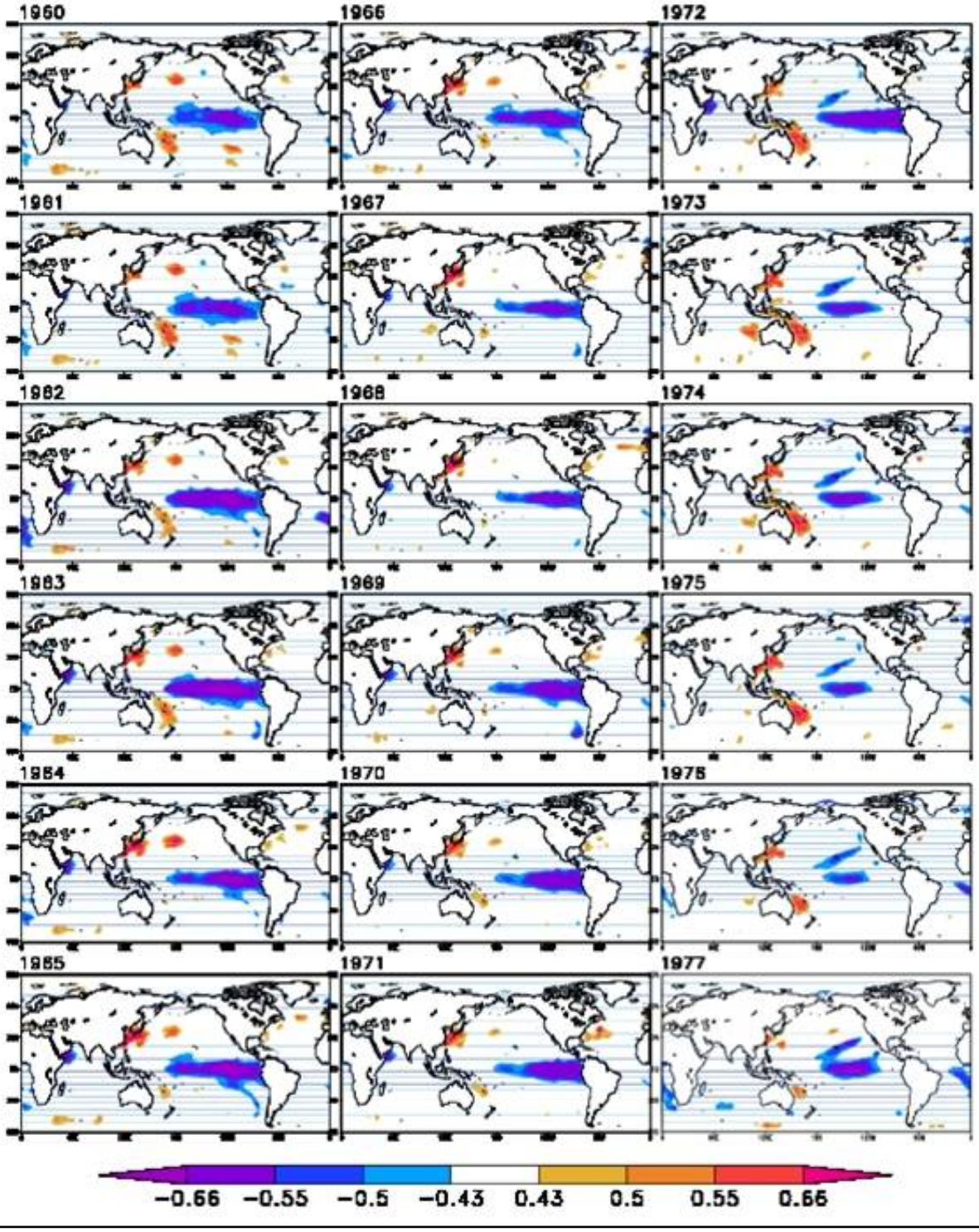

Spatial pattern of Sliding correlations on a 21-year moving window between ISMR and SST. The year indicated in these diagrams is the central year of the 21-year period. Areas with correlation significant more than 95% confidence level are colored.

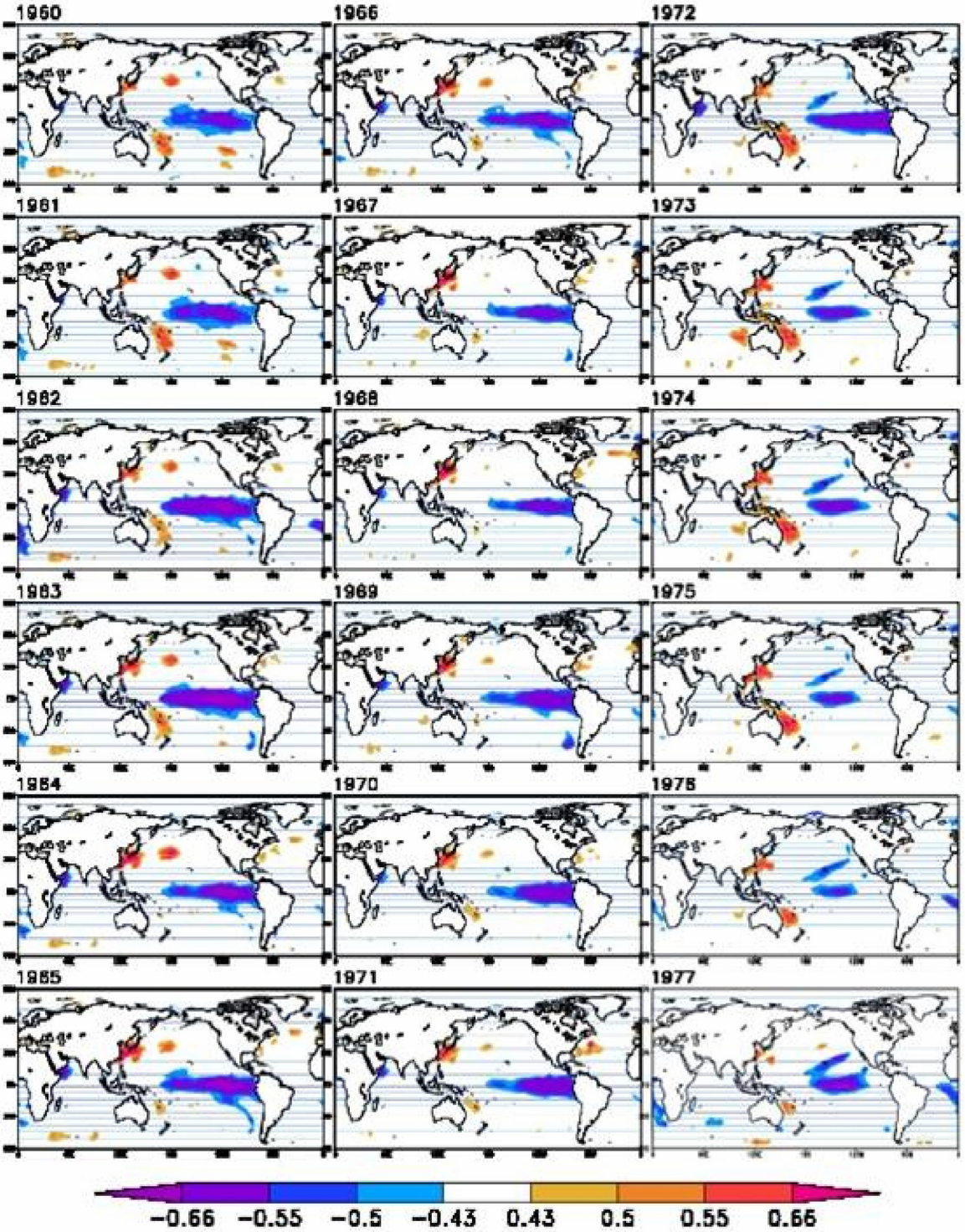

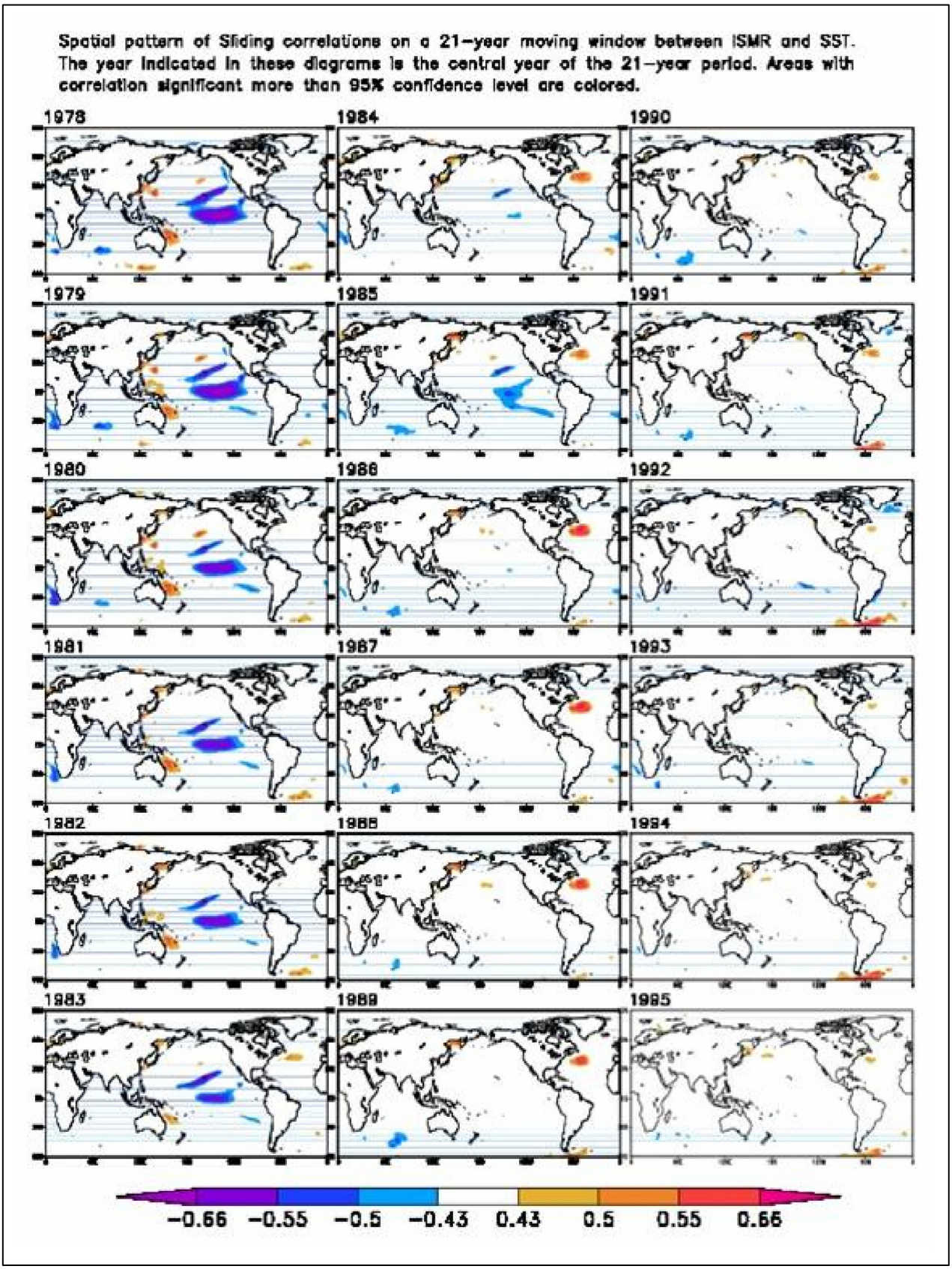

Fig. 3.7 : Spatial pattern of correlations on a 21-year running window between SST and ISMR. The year indicated refers to the central year of the 21-year period. The statistically significant correlations are shaded. (From Yadav 2009)

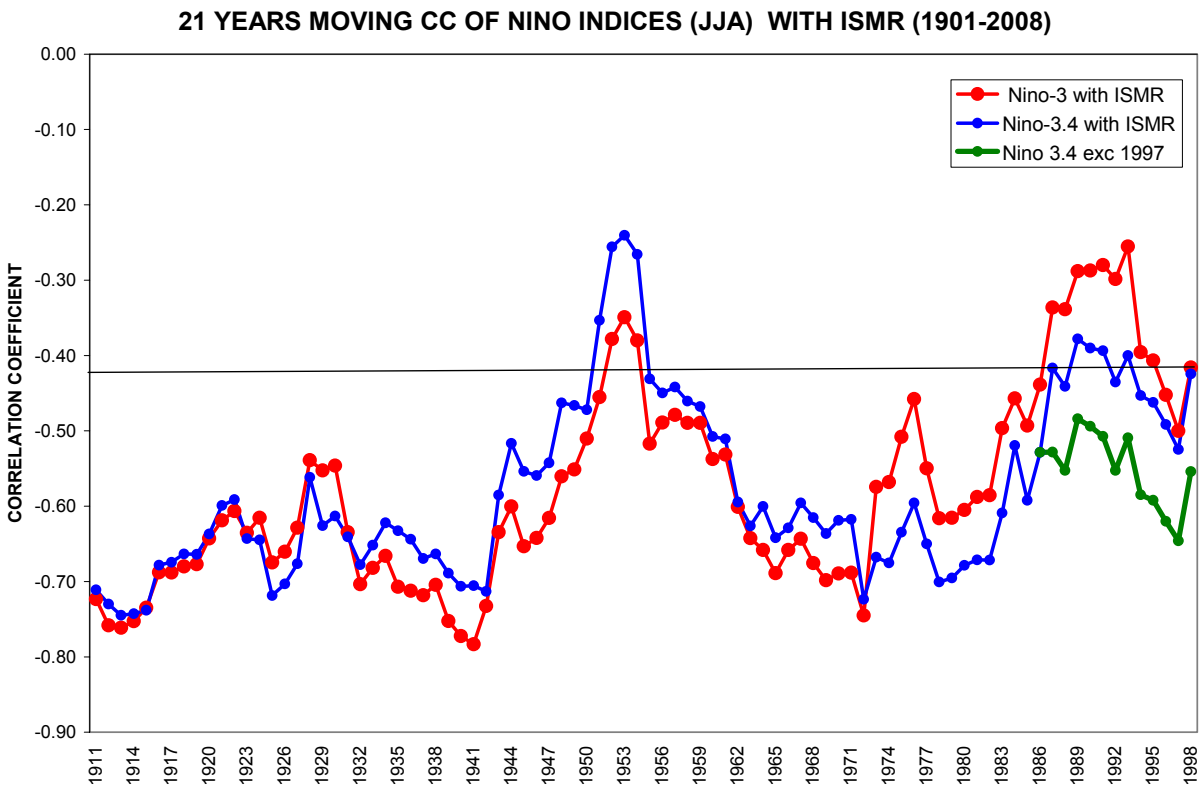

Fig. 3.8 : Secular variations (21 year moving correlations) between ISMR and JJAS Nino 3 (red) and JJAS Nino 3.4 (blue). The CCs with JAJS Nino 3.4 after excluding 1997 are shown as green line. The horizontal line shows the value of significant (95% level) CC for 21-year period.

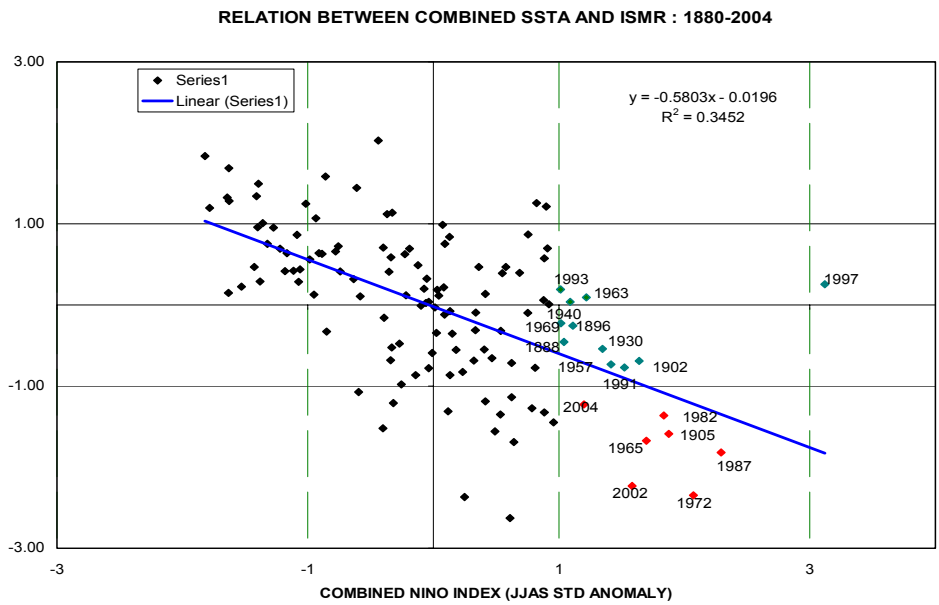

Fig. 3.9 : Scatter plot between JJAS Combined Index and ISMR anomalies (1880-2004)

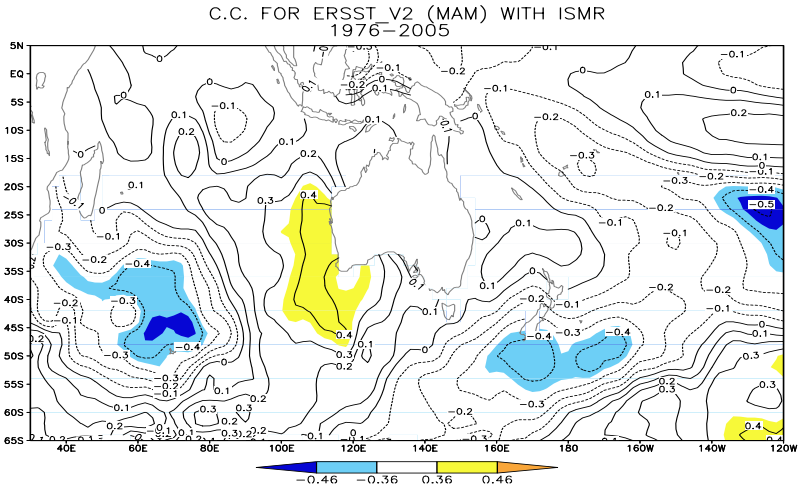

Fig. 3.10 : Spatial patterns of correlations between ISMR and SST anomalies during MAM. Period 1976-2005. Statistically significant correlations are shaded.

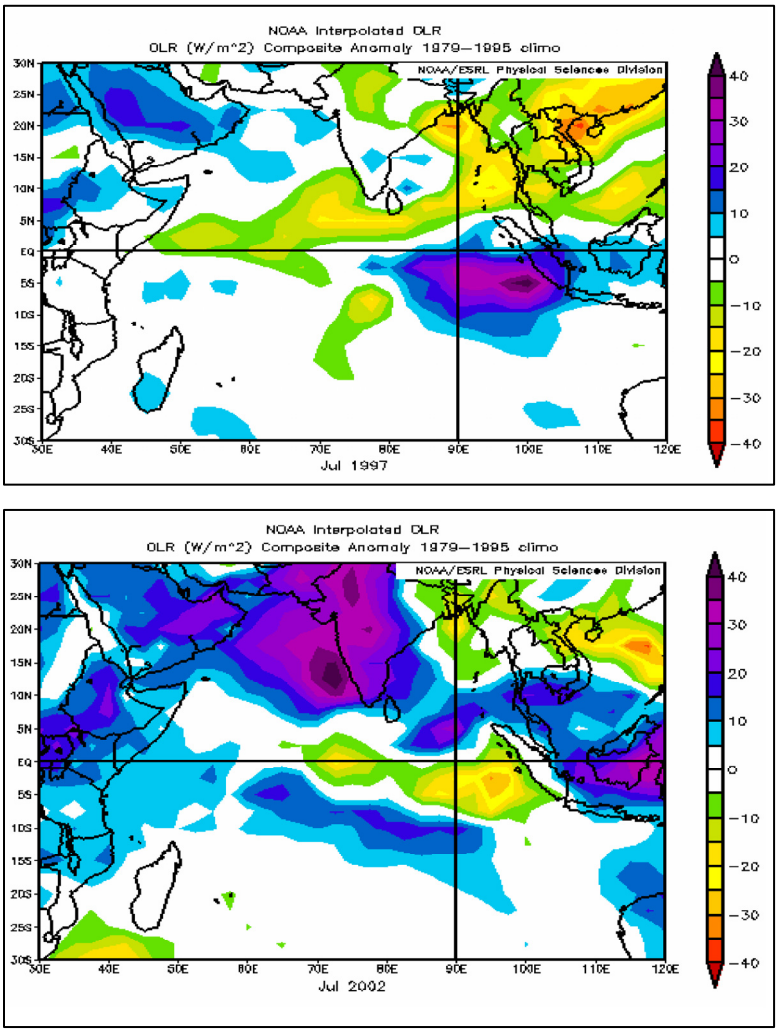

Fig. 3.11 : OLR anomalies (W/m^2) during July 1997 (above) and July 2002 (below).

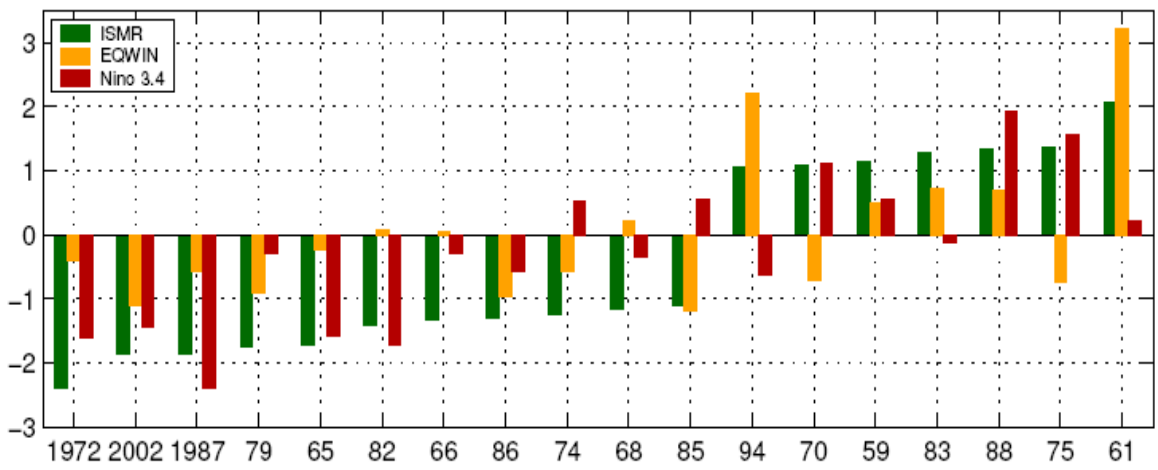

Fig. 3.12 : The ISMR anomaly, EQWIN and ENSO index for all summer monsoon seasons with large deficit or excess during 1958–2004 and 1997. (Gadgil et al. 2004)

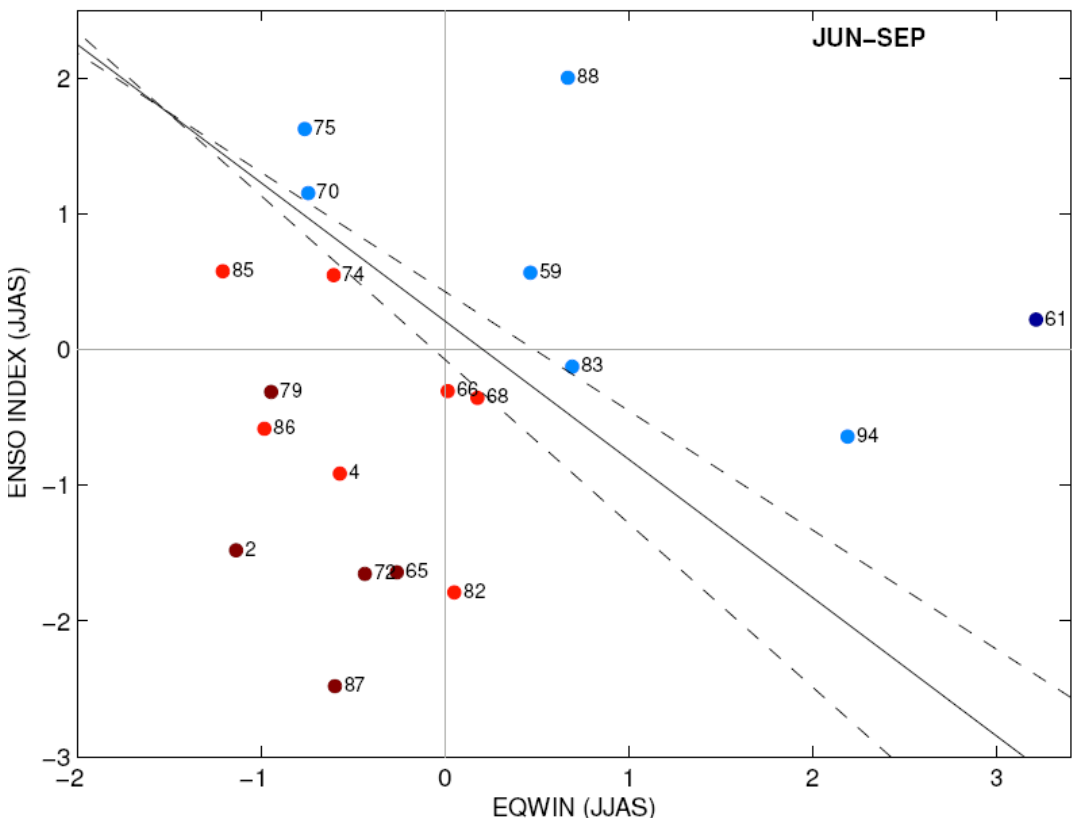

Fig. 3.13 : ISMR in the phase plane of June–September average values of the ENSO index and EQWIN for all the June–September seasons between 1958 and 2004. Red (dark red) represents seasons with ISMR deficit greater than 1 (1.5) standard deviation respectively blue (dark blue) represents seasons with ISMR excess of magnitude greater than 1 (1.5) standard deviation. (Gadgil et al. 2004)

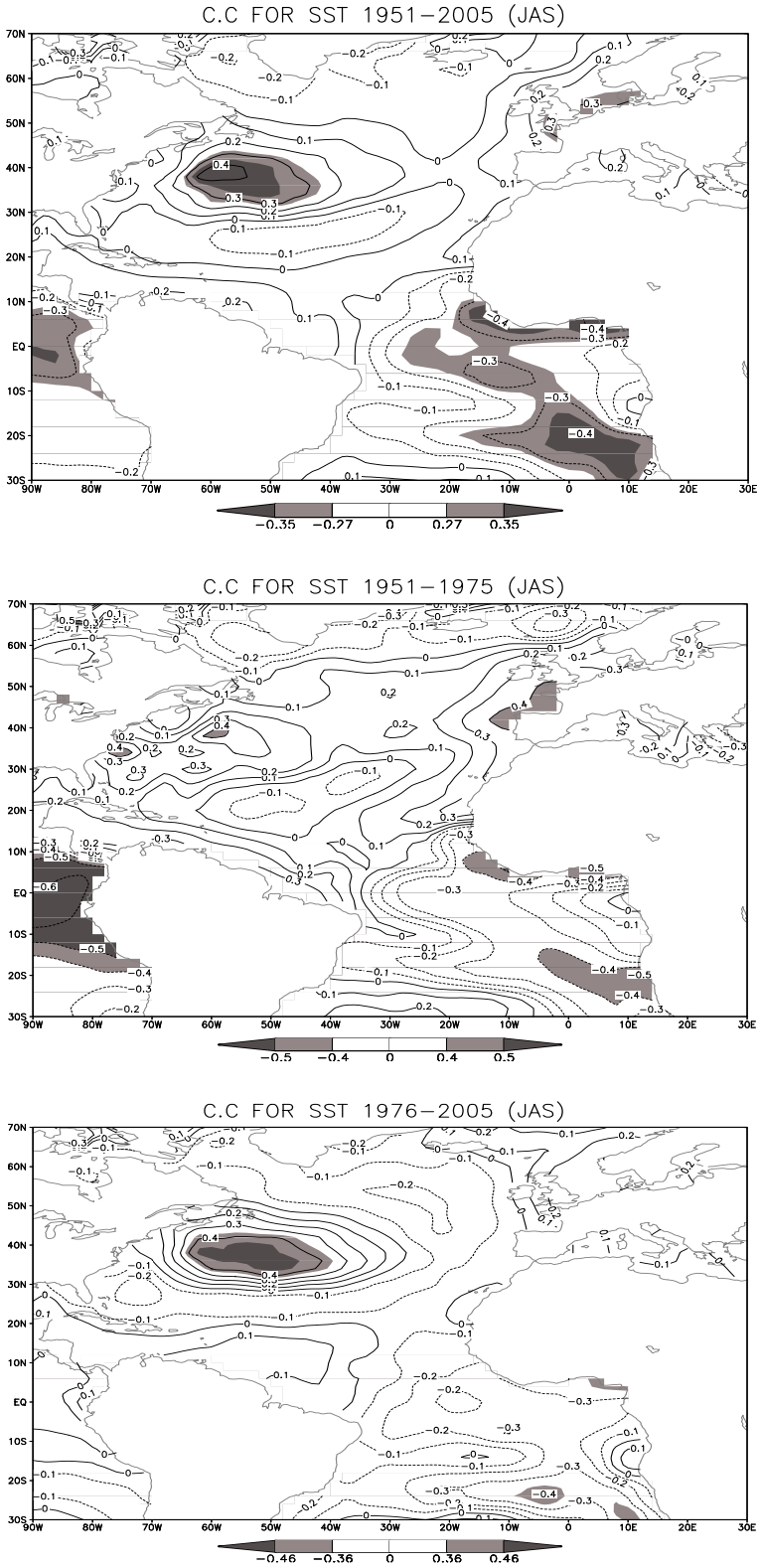

Fig. 3.14: Spatial map of correlation of SST anomalies with ICMR for three different periods, a) 1951-2005 b) 1951-1975 and c) 1976-2005. Correlations significant at 95% (99%) level are shaded light (dark). (Rajeevan and Latha Sridhar 2008).

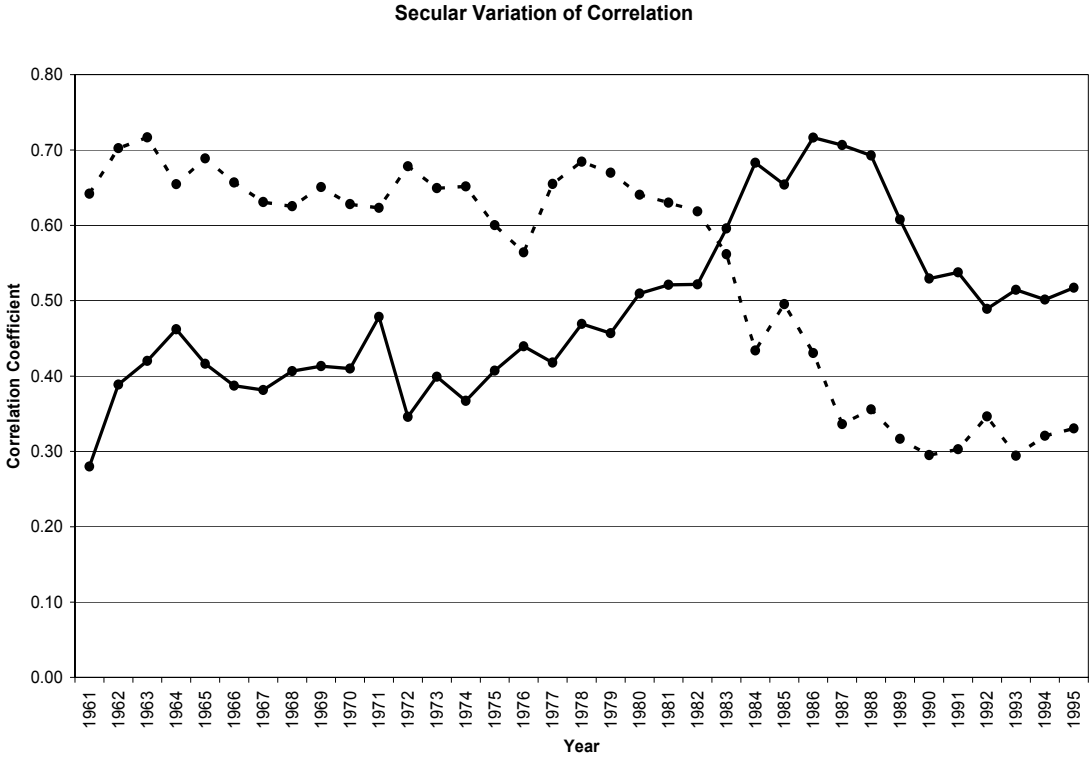

Fig. 3.15 : The 21-year running correlations between the SST index and ICMR (continuous line) and between the Nino-3.4 index and ICMR (dashed line). The sign of the correlation between Nino 3.4 and ICMR has been reversed for comparison. Rajeevan and Latha Sridhar (2008).

(a)

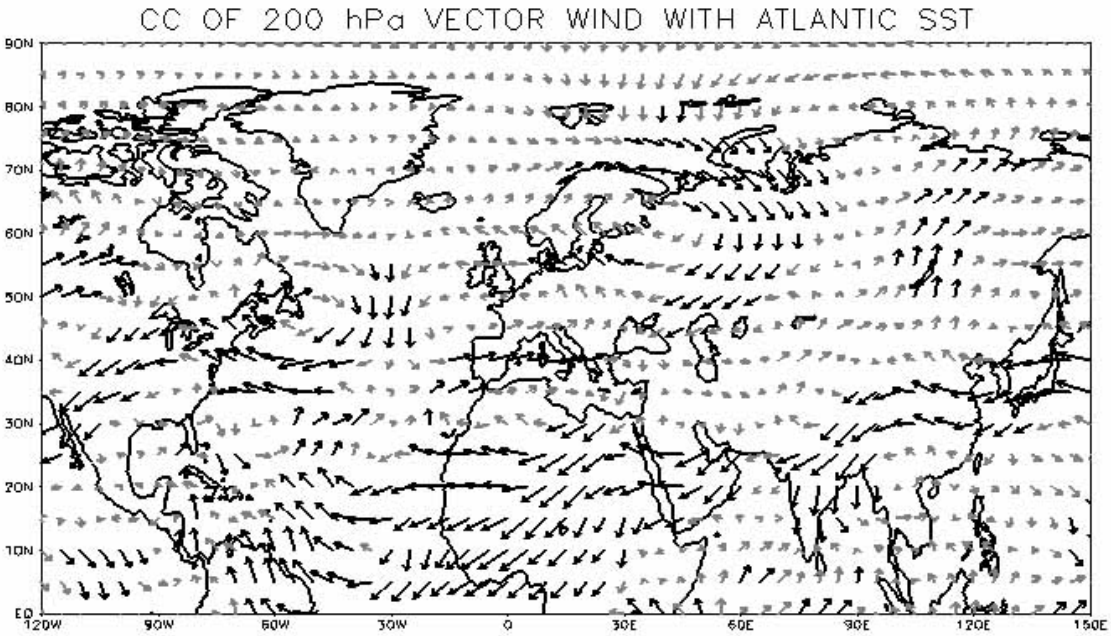

(b)

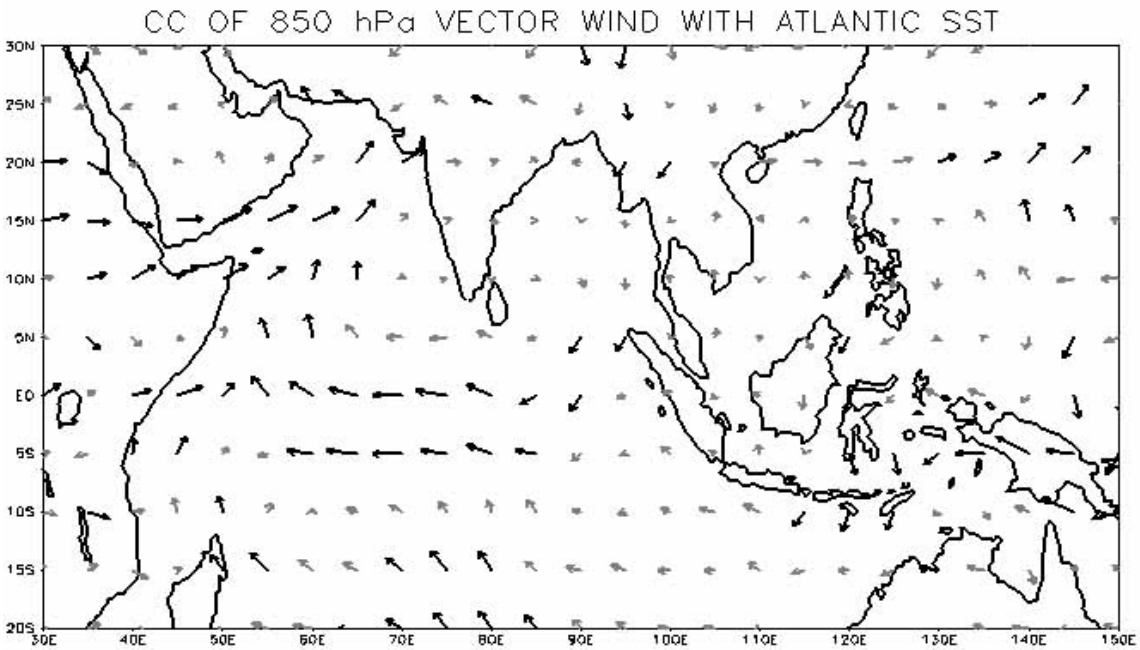

Fig. 3.16: Spatial pattern of correlation between NWAI and vector winds a) at 200 hPa and b) at 850 hPa. Period: 1976-2005. Statistically significant correlations (95% level) are shown in dark. (Rajeevan and Latha 2008)

CHAPTER 4

OCEANS AND THE INDIAN MONSOON

Sulochana Gadgil [1] and P.A. Francis [2]
[1] *Centre for Atmospheric and Oceanic Services, Indian Institute of Science, Bangalore*
[2] *Indian National centre for Ocean Information Services, Hyderabad*

sulugadgil@gmail.com

4.1. Introduction

'I seek the blessings of Lord Indra to bestow on us timely and bountiful monsoons' Pranab Mukherjee, budget speech in the Lok Sabha, February 2011.

This opening remark by the finance minister in his presentation of the budget for 2011-12 in the Lok Sabha, drives home the point that the monsoon continues to have a substantial impact on the Indian agricultural production and the economy, even after six decades of development [Gadgil and Gadgil, 2006]. Thus, understanding and prediction of the variability of the monsoon rainfall over the Indian region is extremely important. In fact, a substantial fraction of the large scale rainfall over the Indian region occurs in association with the propagation of synoptic scale systems from the surrounding seas onto the region. Not surprisingly, the variability of the monsoon is linked to facets of the oceans and events in the atmosphere over the oceans. Hence, even if the focus is the variability of the monsoon rainfall over land, it is essential to consider also the variability of the atmosphere over the oceans as well as variability of the oceans. Here we consider the role of oceans in the nature of the monsoon and its variability on different time scales.

The advent of satellites in the mid-sixties, which made it possible to literally see the evolution of the convective systems over the oceans and their propagations across the oceans onto land, had a major impact on our understanding of the role of the oceans. The first study of the daily satellite imagery over the Indian longitudes

[Sikka and Gadgil, 1980] provided new insights into the links to the oceans of the variability of the monsoon on intraseasonal scale, as well as of the mean monsoon itself. A major advance in our understanding of the interannual variation of the monsoon occurred in the 80's with the discovery (or rediscovery) of a strong link with El Nino and Southern Oscillation, ENSO [Sikka, 1980; Pant and Parthasarathy, 1981; Rasmusson and Carpenter, 1983]. Recent studies [Gadgil et al., 2003, 2004; Ihara et al., 2007] have revealed that one more mode plays an important role in the interannual variation of the monsoon viz. the Equatorial Indian Ocean Oscillation (EQUINOO). The nature of these teleconnections is discussed by Gadgil et al. [2007] and Rajeevan [2011].

In this chapter, we elucidate in brief what we understand about the role of the ocean and the atmosphere over the oceans in the mean monsoon and its intraseasonal and interannual variation, restricting our discussion to the summer monsoon (June-September) in which most of the rainfall is received for the country as a whole. We do not discuss mechanisms proposed for important features of the variability nor the simulation and prediction of the major features with atmospheric and coupled models, because of space restrictions. Information regarding the data used in this study is given in section 4.2. We consider the role of the ocean in the mean monsoon in section 4.3 and in seasonal transitions and intraseasonal variation in section 4.4. The role of ENSO and EQUINOO in interannual variation of the monsoon is discussed in section 4.5. In section 4.6 we discuss the role of the equatorial Indian Ocean in the evolution of EQUINOO. Section 4.7 comprises concluding remarks.

4.2. Data

The following data sets were used in this study (i) monthly all India rainfall from [Parthasarathy et al., 1995] and update from the web site of Indian Institute of Tropical Meteorology (http://www.tropmet.res.in/); the rainfall for 2009 and 2010 from the operational data in Climate Diagnostic Bulletin, India Meteorological Department (ii) NINO 3.4 index i.e., the SST anomaly over the Nino3.4 region (120°W-170°W, 5°S-5°N), obtained from Climate Analysis Section, National Center for Atmospheric Research, USA (http://www.cgd.ucar.edu/) (iii) the outgoing longwave radiation (OLR) data from Climate Diagnostic Center, USA

(http://www.cdc.noaa.gov/) (iv) the surface wind data and vertical velocity data from National Center for Environmental Prediction [Kalnay et al., 1996] (http://www.cdc.noaa.gov/) , (v) weekly mean optimal interpolated SST data from Climate Diagnostic Center, USA [Reynolds et al., 2002, http://www.cdc.noaa.gov/] , (vi) HadISST [Rayner et al., 2003] data from (http://badc.nerc.ac.uk) and (vii) Simple Ocean Data Assimilation [SODA, Carton and Giese, 2008] data archived at http://www.apdrc.soest.hawaii.edu.

4.3. The basic system

Over three hundred years ago, Halley [1686] suggested that the primary cause of the monsoon was the differential heating between ocean and land and the monsoon was considered to be a gigantic land-sea breeze. Differential heating of the land and sea is still considered as the basic mechanism for the monsoon by several scientists [e.g. Webster, 1987]. There is an alternative hypothesis in which the monsoon is considered as a manifestation of the seasonal migration of the intertropical convergence zone [ITCZ, Charney, 1969] or the equatorial trough [Riehl , 1954, 1979], in response to the seasonal variation of the latitude of maximum insolation. It is important to note that whereas the first hypothesis associates the monsoon with a system special to the monsoonal region, in the second, the system responsible is the planetary scale system associated with the major tropical rainbelt (ITCZ/equatorial trough) and the monsoonal regions differ from other tropical regions, only in the amplitude of the seasonal migration of the basic system. The two hypotheses have very different implications for the variability of the monsoon. For example, in the first case we expect the intensity of the monsoon to be directly related to the land-ocean temperature contrast.

Simpson [1951] was perhaps the first to question the importance of the role played by land-ocean temperature contrast. He pointed out *" It is only when one points out that India is much hotter in May before the monsoon sets in than in July when it is at its heights-or draws attention to the fact that the hottest part of India-the northwest gets no rain at all during the monsoon- or shows by statistics that the average temperature is much greater in years of bad rains than in years of good rains, that they begin to doubt whether they know the real cause of the monsoon*."

Subsequent studies have clearly shown that the land surface temperature is higher when there is less rainfall during the summer monsoon and lower when the rainfall is higher [Kothawale and Kumar, 2002]. Thus, rather than the land surface temperature determining the amount of rainfall via the impact on the difference between land and ocean temperature, the land temperature is determined by the rainfall (or lack thereof).

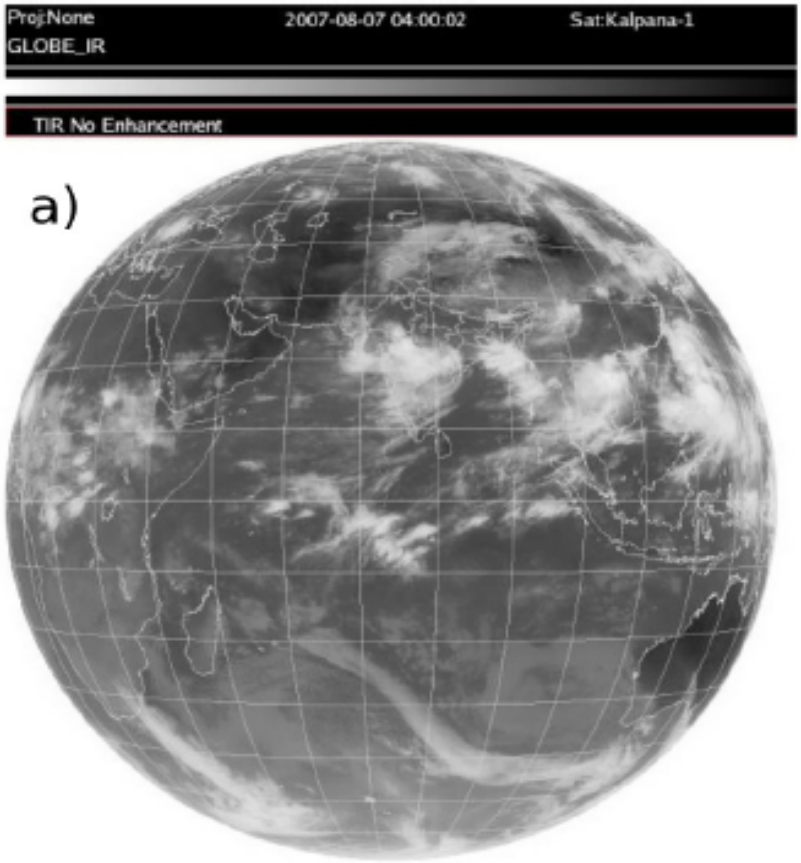

Fig. 4.1a : Infrared imagery of 7 August 2007 from Kalpana.

Sikka and Gadgil's [1980] study of the daily satellite imagery over the Indian longitudes lent support to the second hypothesis in which the monsoon is associated with the ITCZ. They showed that (i) the cloud band over the Indian subcontinent on an active monsoon day is strikingly similar to that characterizing the ITCZ over other parts of the tropics and (ii) dynamically the system has all the important characteristics of the ITCZ [Charney, 1969] including low level convergence, intense cyclonic vorticity above the boundary layer and organized deep convection (e.g. Fig. 4.1.a,b,c for an active monsoon day). The large-scale rainfall over the Indian monsoon zone (Fig. 4.2a) is directly related to the meridional

shear of the zonal wind just above the boundary layer i.e. the intensity of the continental ITCZ [Sikka and Gadgil, 1978]. The all-India summer monsoon rainfall (ISMR) is highly correlated to that of the rainfall in the monsoon zone on the interannual scale (Fig.4. 2b).

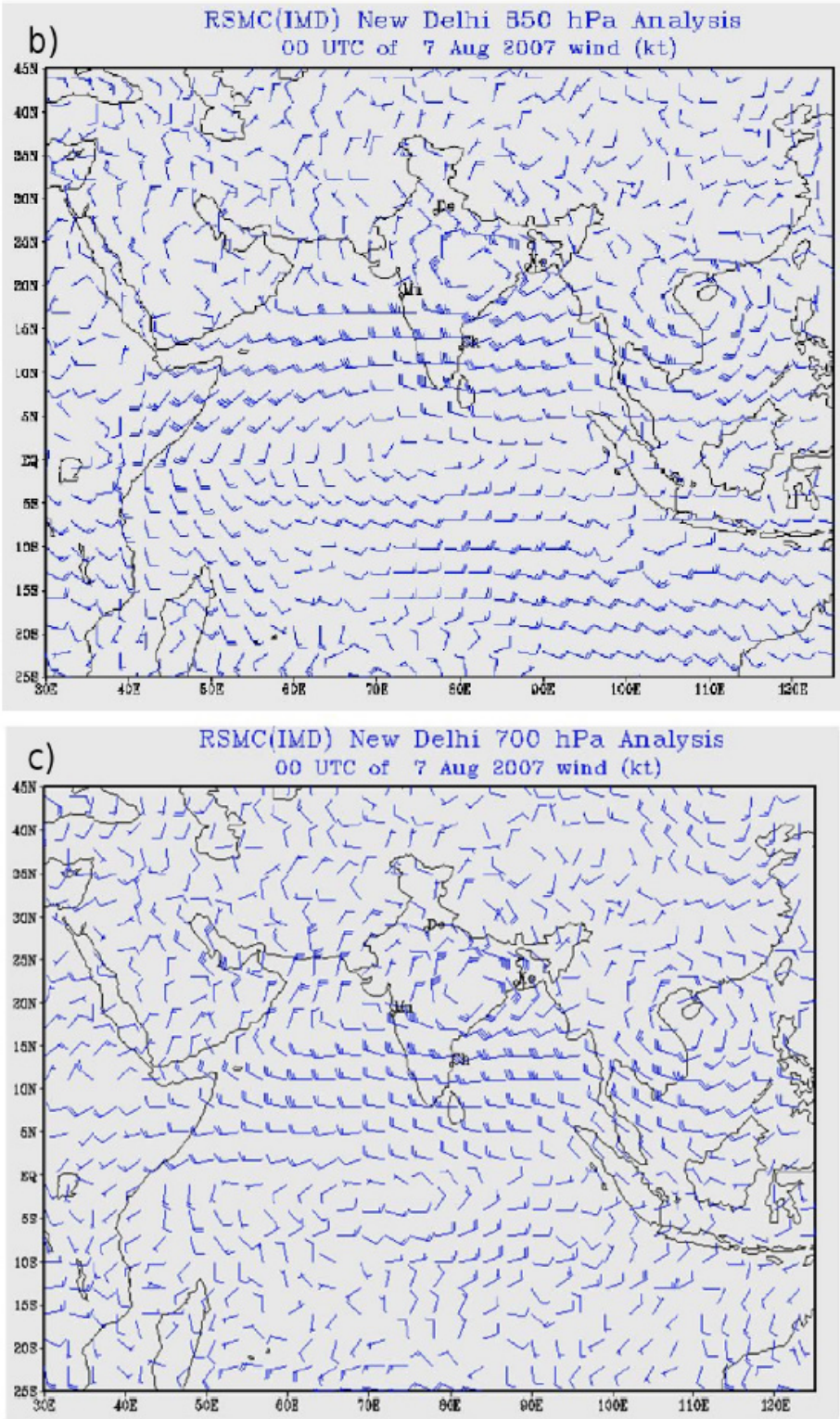

Fig. 4.1 : b) Winds at 850 hPa for 7 August 2007 & c) same as Figure 1b but for 700hPa.

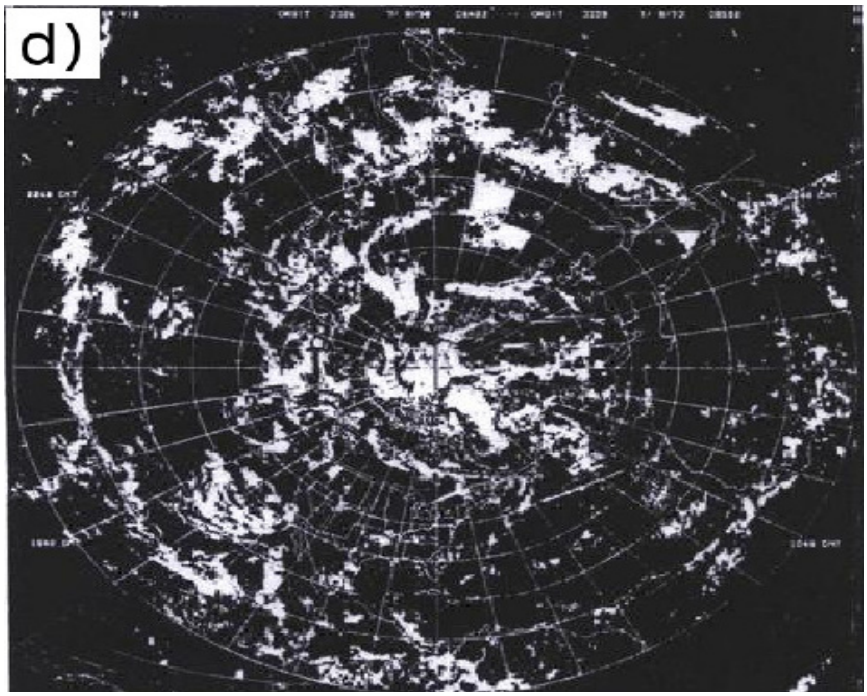

Fig. 4.1d : Visible satellite imagery for the northern hemisphere on 8 July 1973

This continental ITCZ, is called the continental tropical convergence zone (CTCZ) to distinguish it from the more common ITCZ seen over the tropical oceans. It is important to note that the CTCZ is often a part of the planetary scale system stretching across from the Indian region to the tropical Pacific on a daily scale (Fig. 4.1d). The intensity of the CTCZ, i.e. of the associated deep convection and rainfall (which is related to the intensity of the lower tropospheric cyclonic vorticity) is seldom uniform across its large longitudinal extent. Generally synoptic scale disturbances i.e. monsoon lows, depressions, [Joseph, 2011a] are embedded in it (e.g. Fig. 4.1.a, b, c) and the associated rainfall is also organized on the meso-scale. Interactions between the different scales over which convection is organized, play an important role in the variability of the convection on different time-scales.

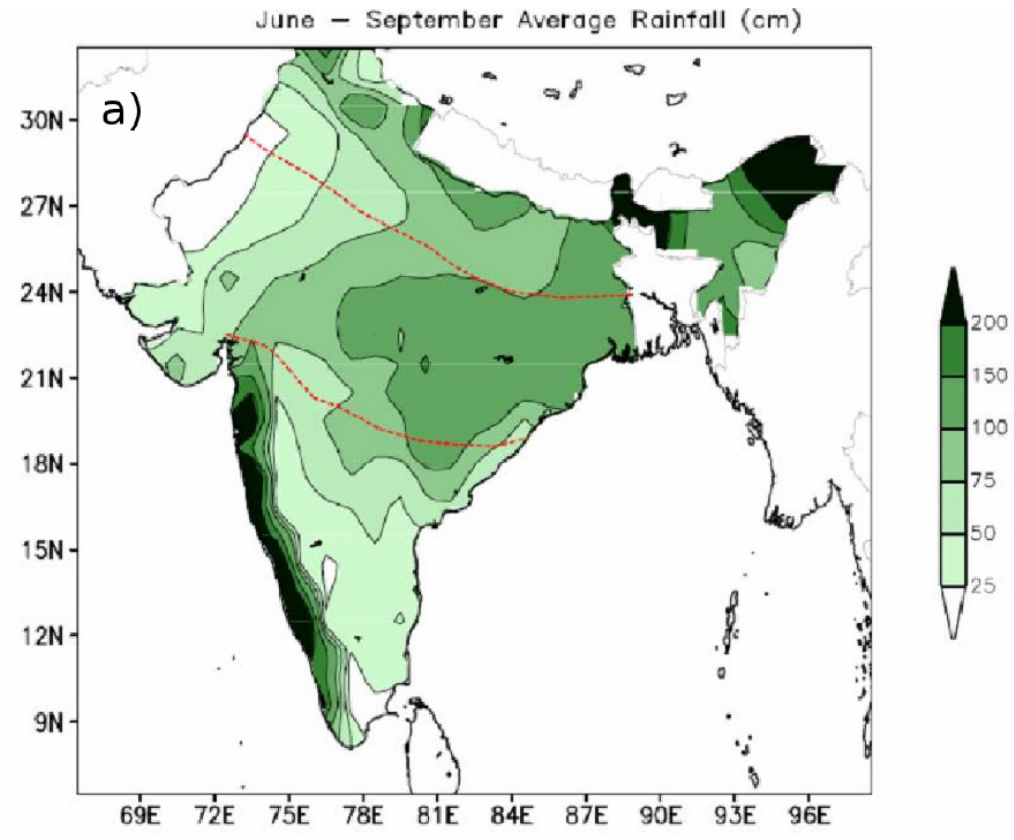

Fig. 4.2a : Mean June-September rainfall over the Indian region (cm); approximate limits of the core monsoon zone indicated by red dashed lines.

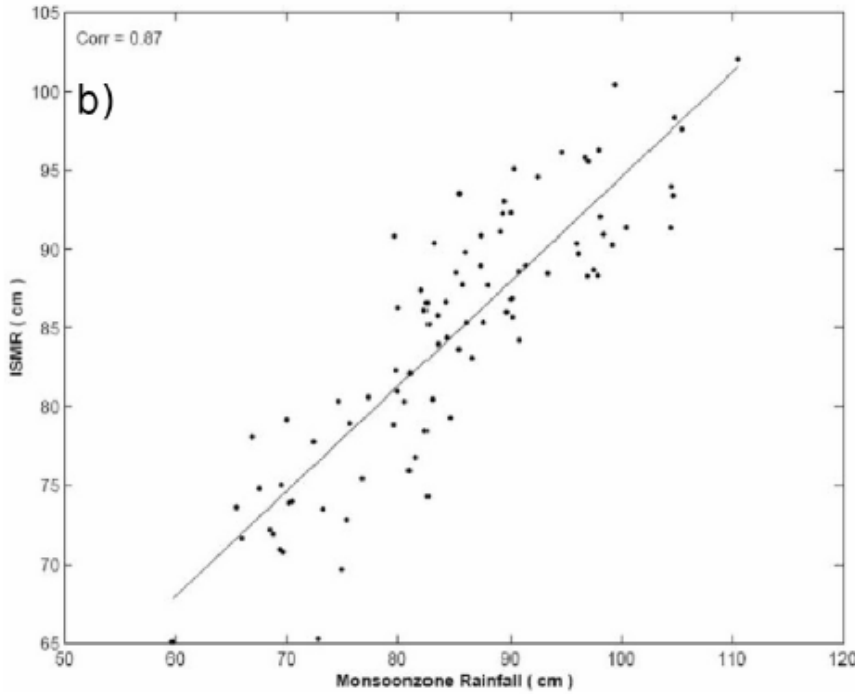

Fig. 4.2 b: ISMR versus the rainfall over the core monsoon zone.

The monsoon is thus a manifestation of the seasonal migration of the ITCZ in response to the seasonal variation in the radiation from the sun and monsoon variability is associated with the space-time variation of the CTCZ. Important feedbacks, such as cloud radiation feedbacks or the feedback between vertical stability of the moist tropical atmosphere and midtropospheric heating by the deep clouds [Krishnamurti and Bhalme, 1976] will operate for the CTCZ as well as the oceanic ITCZ. In addition, processes special to the CTCZ such as land surface processes will play a role in determining the variability.

4.4. Seasonal transitions and intraseasonal variation

The onset of the summer monsoon over Kerala (southern tip of the peninsula) around the beginning of June, marks the commencement of the onset phase of the Indian summer monsoon and the beginning of the rainy season for the country. The northward advance over the subcontinent from its commencement over Kerala to its culmination over the western part of the Indian monsoon zone, takes about 40-45 days [Ding and Sikka, 2006, and references therein]. The CTCZ gets established over the Indian monsoon zone (Fig. 4.2a) in July, at the end of the onset phase of the summer monsoon. Throughout the peak monsoon months of July and August the CTCZ fluctuates primarily over this monsoon zone. The most important feature of intraseasonal (supersynoptic scale) variation is the fluctuation between active and weak spells in July and August [Ramanurthy, 1969; De et al , 1998; Gadgil and Joseph, 2003; Rajeevan et al., 2010, and references therein]. The retreat of the monsoon commences from the western part of the monsoon zone in early September and by mid-October the monsoon retreats from the monsoon zone [Rao, 1976; Joseph, 2011b].

Sikka and Gadgil's [1980] study of the large-scale zonal cloud-bands over the Indian longitudes during the summer, revealed two features which are particularly important in the seasonal transitions as well as intraseasonal variation. Firstly, there are two favourable locations for cloud bands / TCZ, one over the heated subcontinent and another over the warm waters of the equatorial Indian Ocean. Since the convergence in both the zones cannot be intertropical, the term

tropical convergence zone, TCZ (rather than the ITCZ) is used when referring to the Indian longitudes [Gadgil, 1988]. There is a competition between the CTCZ and the oceanic TCZ with active spells of one occurring primarily during weak spells of the other. A major feature of the intraseasonal variation is the series of northward propagations of the cloud bands from the equatorial Indian Ocean onto the Indian monsoon zone at intervals of 2-6 weeks. The prominent cloud band in the satellite imagery (e.g. Fig. 4.1a) can be demarcated as a zone of low OLR from satellite data. The propagations of the cloud band are clearly seen in the variation of such a zone (e.g. Fig. 4.3a). The continental TCZ is maintained partly by these propagations of the oceanic TCZ. Thus the relationship between the TCZs is complex with the oceanic TCZ contributing to the maintenance of the continental TCZ on the one hand and competing with it on the other.

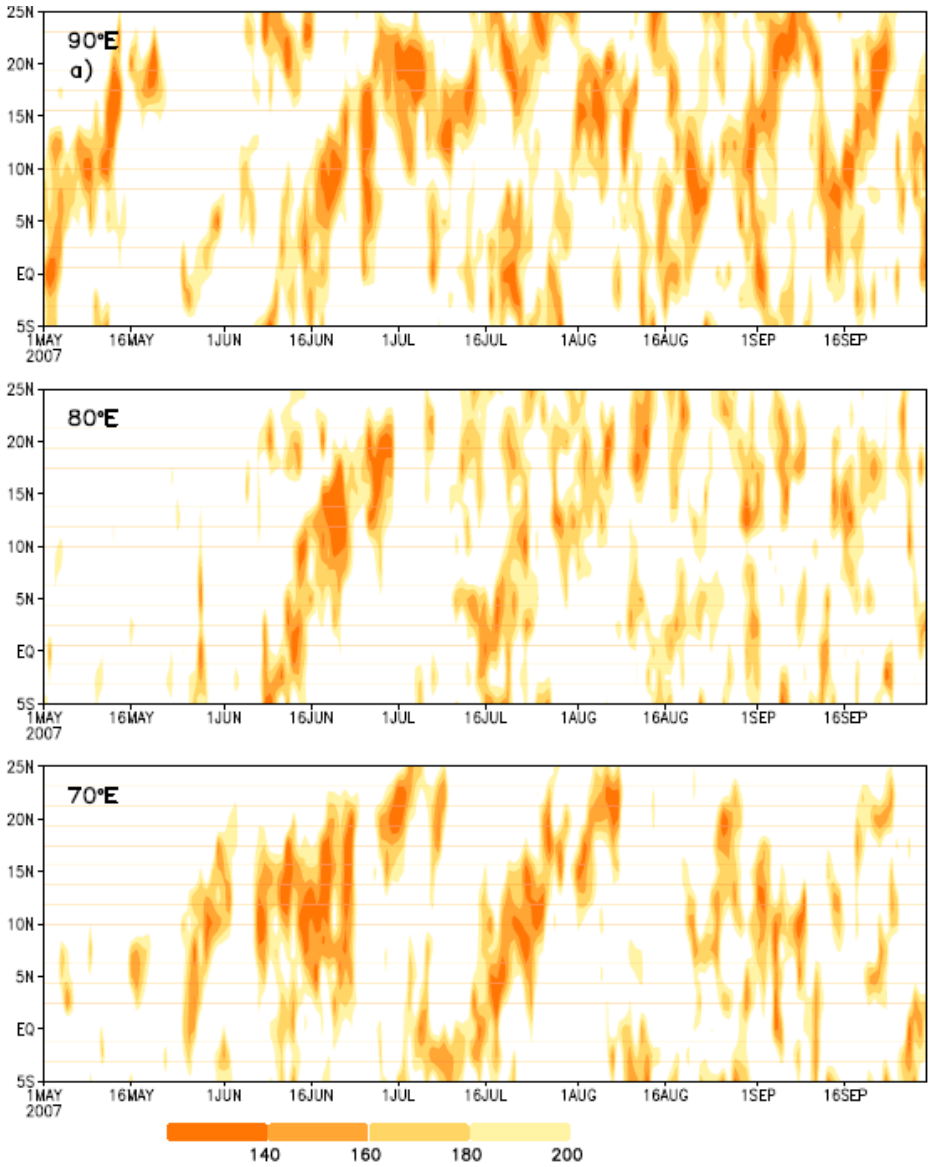

Fig.4.3a : Variation of the low OLR region at 70°, 80°, 90° E during May-September 2007.

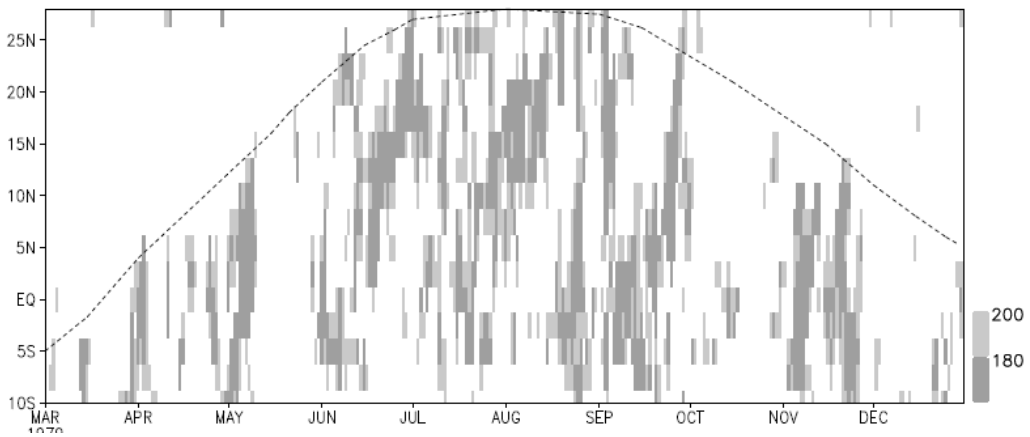

Fig. 4.3b : Variation of the low OLR region at 90E during March-December1979. The seasonal envelope is also indicated. [after Gadgil, 2003].

It is important to note that the seasonal migration of the ITCZ is accomplished by such northward propagations. These propagations culminate farther and farther northward in the onset phase and more and more southward in the retreat phase (Fig. 4.3b). Thus the retreat of the monsoon is not the mirror image of the onset as believed earlier [e.g. Riehl , 1979]. The onset of the monsoon over Kerala is associated with the northward movement of a cloud band generated several days before the onset, over the equatorial region south of the Arabian Sea [Joseph et al., 1994]. The northward advance over the subcontinent generally involves one or more northward propagations, each pushing the limit of the monsoon further northward [Rao, 1976; Sikka and Gadgil, 1980; Webster et al., 1998]. Over the monsoon zone, the onset first occurs over the eastern part. The onset over the western part is often a consequence of westward propagations of synoptic scale systems from the eastern part of the monsoon zone. Thus northward propagations of the cloud systems generated over the equatorial Indian Ocean, Arabian Sea and the Bay of Bengal and westward propagations of systems from the Bay of Bengal (Fig. 4.3c) play a critical role in the seasonal transitions.

There have been a large number of studies of the onset of the monsoon over Kerala [Joseph, 2011b]. The standard deviation of the date of this onset is one week. There is considerable variation from year to year in the advance of the monsoon after the onset. For example in June 2009, the monsoon did not advance north of the peninsula until 24 June. This resulted in a massive deficit in the all-India rainfall of 54% of the long term average for this period. The all-India rainfall for the month of June was rather close to the lowest recorded rainfall (50% in June 1926) since 1871. Francis and Gadgil [2009, 2010] have shown that, in this period, the meridional SST gradient across the eastern equatorial Indian Ocean and the Bay of Bengal was reversed with the Bay being cooler than the equatorial Indian Ocean. They attributed the suppression of convection over the Bay (and hence the large deficit in monsoon rainfall) to the eastern equatorial Indian Ocean being more favourable for convection due to this SST gradient. However, such a reversal of SST gradient is a very rare event. It is important to understand the major factors leading to the observed variability in the advance process for improving predictions of this seasonal transition.

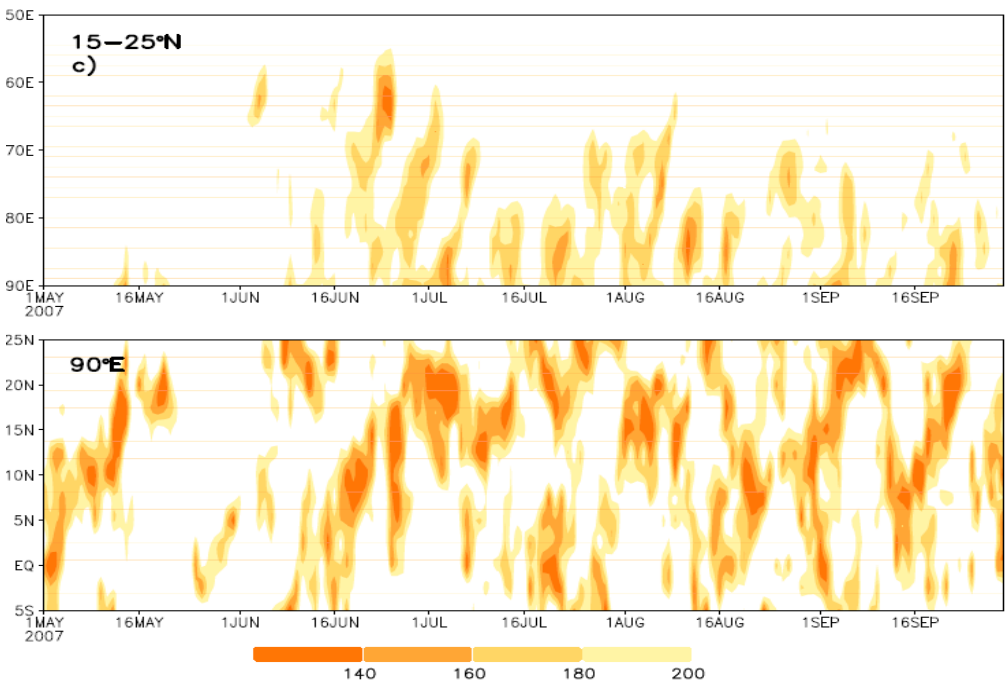

Fig. 4.3c : Variation of the low OLR region for 15o-25oN and 90o E during May-September 2007.

Active spells, weak spells and breaks have been identified by Rajeevan et al. [2010] on the basis of the rainfall over the monsoon zone derived from the high resolution daily gridded rainfall dataset over India [Rajeevan et al., 2006]. The rainfall anomaly composites are shown in Fig. 4.4 and the OLR anomaly composites in Fig. 4.5.

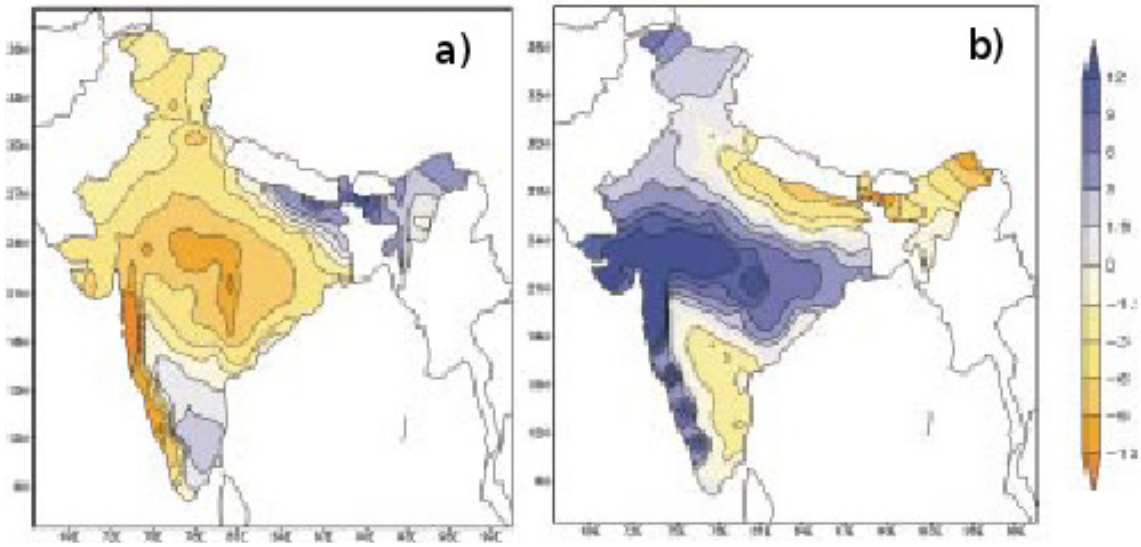

Fig. 4.4 : Rainfall anomaly composites in mm/day for (left) break and (right) active spells (after Rajeevan et. al 2010)

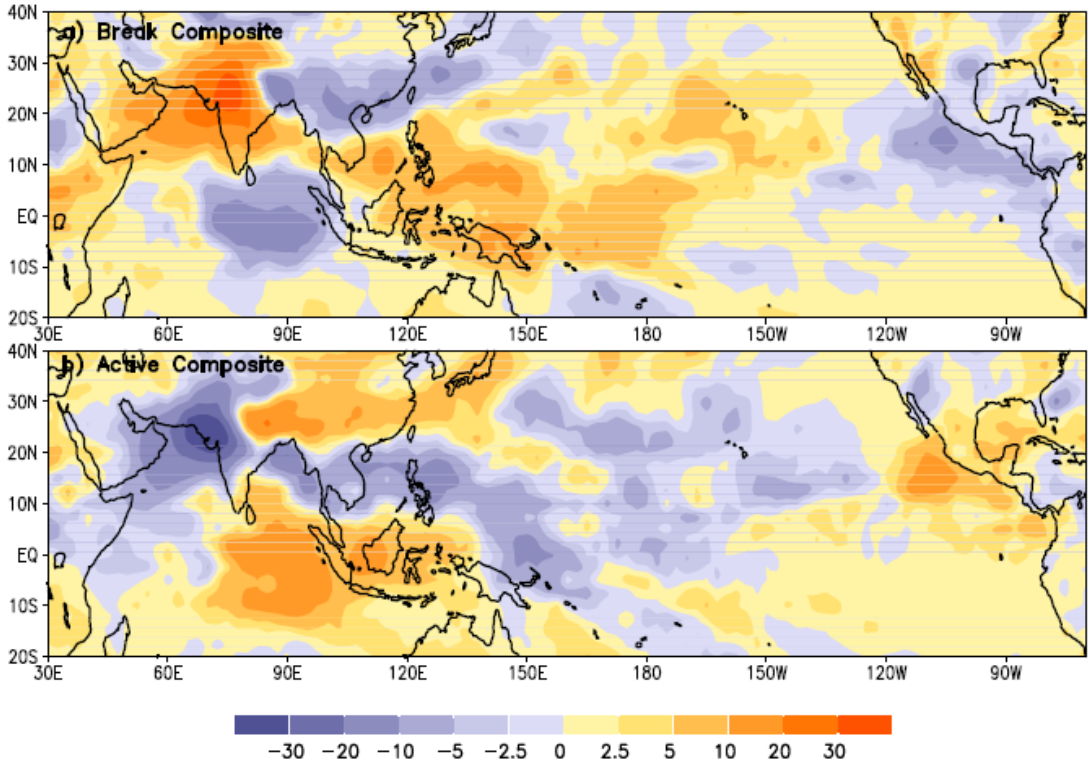

Fig. 4.5 : OLR anomaly composites in Wm□2 for (a) break and (b) active spells [after Rajeevan et al., 2010].

As in the OLR composites of Gadgil and Joseph [2003], the most prominent signal is over the eastern equatorial Indian Ocean, with intensification of convection in breaks and suppression in active spells. It, therefore, appears that the competition of the CTCZ with the oceanic TCZ on the intraseasonal scale is primarily with the TCZ over the eastern equatorial Indian Ocean. The negative OLR anomaly characterizing the active spells is seen to be a coherent band which extends from the Arabian Sea, across the monsoon zone, head of the Bay of Bengal up to the west Pacific. Westward of the dateline also there is large area with enhanced convection over the equatorial Pacific during active spells. Thus, in addition to the links with the Indian Ocean, there appear to be direct links between intraseasonal monsoon variability and the deep convection associated with the ITCZ over the Pacific.

4.5. Interannual variation of the monsoon

A useful index of the summer monsoon rainfall over the Indian region in any year is the Indian summer monsoon rainfall index (ISMR) which is a weighted average of the June-September rainfall at 306 well-distributed rainguage stations across India [Parthasarathy et al., 1992, 1995]. The variation of ISMR anomaly during 1871-2009 is shown in Fig. 4.6. Since the standard deviation is about 10% of the mean, droughts are defined as seasons with deficit in ISMR greater than 10% of the mean [Sikka, 2011] and excess monsoon seasons as those with ISMR anomaly larger than 10% of the mean. Although the interannual variation is not very large, it is important to understand the factors leading to it and thereby improve the redictions, since the impact is large.

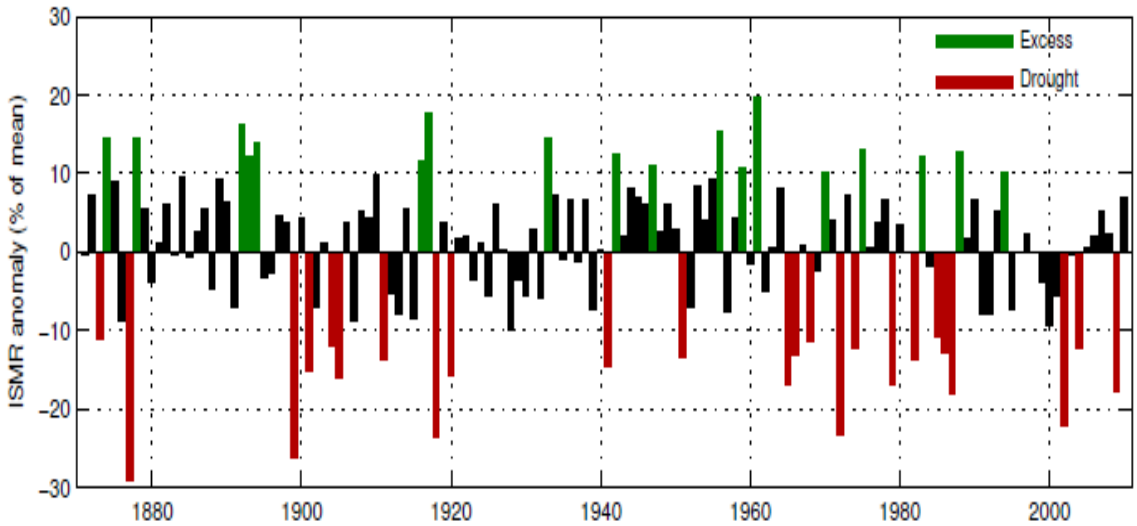

Fig. 4.6 : Variation of Indian summer monsoon rainfall (ISMR) anomaly during 1871-2009; Droughts (red) are defined as seasons with ISMR anomaly< -10% and excess monsoon seasons as those with ISMR anomaly > 10 %.)

Since the theme of this chapter is monsoon and the oceans, we will not attempt a comprehensive review of the interannual variation of the monsoon which is also known to be related to several other factors such as the Himalayan snow cover, Eurasian winter/spring snow-cover, the northern hemispheric temperature in winter and the surface air temperatures over north-west Europe and Eurasia which may be caused by the different phases of the North Atlantic Oscillation [Sikka, 2011, and references therein]. Here we focus on the links of the monsoon variability to the atmospheric events over the oceans. The correlation between ISMR and the OLR

over the Indo-Pacific region for the summer monsoon (June-September) is shown in Fig. 4.7. It is seen that there is a large negative correlation between the ISMR and convection/rainfall over the central Pacific. This is a manifestation of the link between the Indian summer monsoon and El Nino and Southern Oscillation [ENSO, Philander, 1990]. ISMR is also highly correlated with convection/rainfall over the western equatorial Indian Ocean and negatively correlated with the convection/rainfall over the eastern equatorial Indian Ocean (Fig. 4.7). This is a manifestation of the link of ISMR with EQUINOO. In this section we discuss the links interannual variability of the monsoon to the two important modes viz. ENSO (5.1) and EQUINOO (5.2).

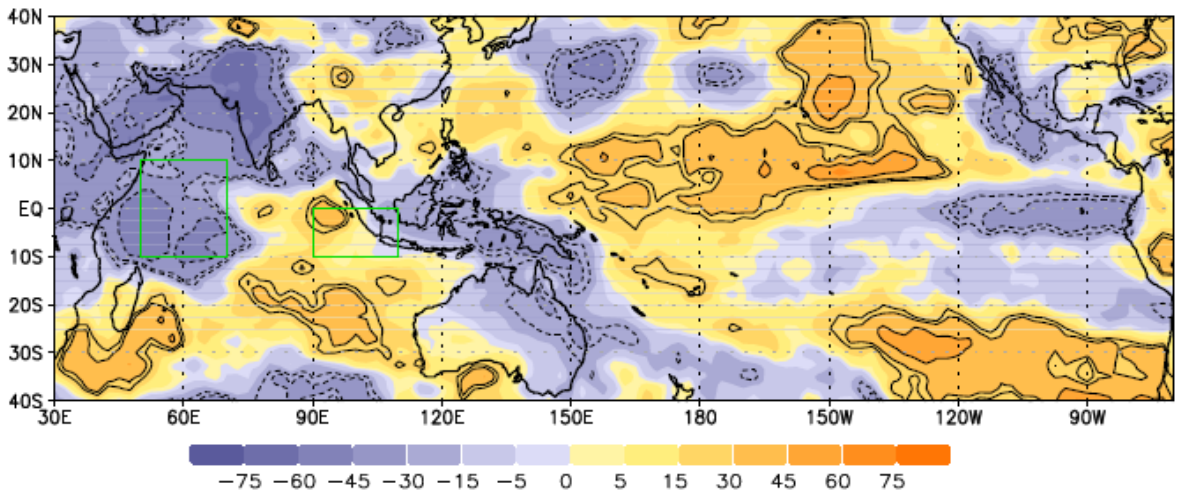

Fig. 4.7 : Correlation (x 100) between OLR (JJAS) and ISMR; the western (WEIO) and eastern (EEIO) equatorial Indian Ocean regions shown as green boxes

4.5.1. Monsoon and ENSO

ENSO involves oscillation between a warm phase, El Nino, characterized by abnormal warming of surface ocean waters of the central and eastern Pacific and enhanced convection in the atmosphere above, and a cold phase, La Nina, characterized by abnormal cooling of these waters and suppressed convection in the atmosphere above. Studies by Sikka [1980]; Pant and Parthasarathy [1981] and Rasmusson and Carpenter [1983] showed that there is an increased propensity of droughts during El Nino and of excess rainfall during La Nina. To depict the relationship of the ISMR with ENSO, we use an ENSO index based on the SST

anomaly of the Nino 3.4 region (120°-170°W, 5°S-5°N), since the magnitude of the correlation coefficient of ISMR with the convection over the central Pacific is higher than that with convection over the east Pacific (Fig. 4.7). The ENSO index is defined as the negative of the Nino 3.4 SST anomaly (normalized by the standard deviation), so that positive values of the ENSO index imply a phase of ENSO favourable for the monsoon. El Nino events are associated with ENSO index less than -1.0 and La Nina with ENSO index greater than 1.0.

The relationship of ISMR with ENSO index is shown in Fig. 4.8 in which the droughts and excess rainfall seasons of ISMR can also be distinguished. It is seen that ISMR is well correlated with the ENSO index with a correlation coefficient of 0.54 which is significant at 99%. For the period 1958-2004, when the ENSO index is favourable (>0.6), there are no droughts and when it is unfavourable (< -0.8) there are no excess monsoon seasons. However, for intermediate values of the ENSO index, there are several droughts and excess rainfall seasons.

Some understanding of the nature of the impact of excess (deficit) convection over the central Pacific characterizing an El Nino (La Nina) on the Indian monsoon can be gained by considering the correlation of the ENSO index with OLR over the Indo-Pacific region (Fig. 4.9). It is seen that enhancement of convection over the central Pacific is associated with suppression of convection over the equatorial Indian Ocean, Bay of Bengal and the Arabian sea. Convection over these oceanic regions is the lifeline of the monsoon with most of the rainfall over the Indian region being associated with cloud systems propagating from these oceanic regions. It is, therefore, not surprising that the convection/rainfall over the Indian region is suppressed as well.

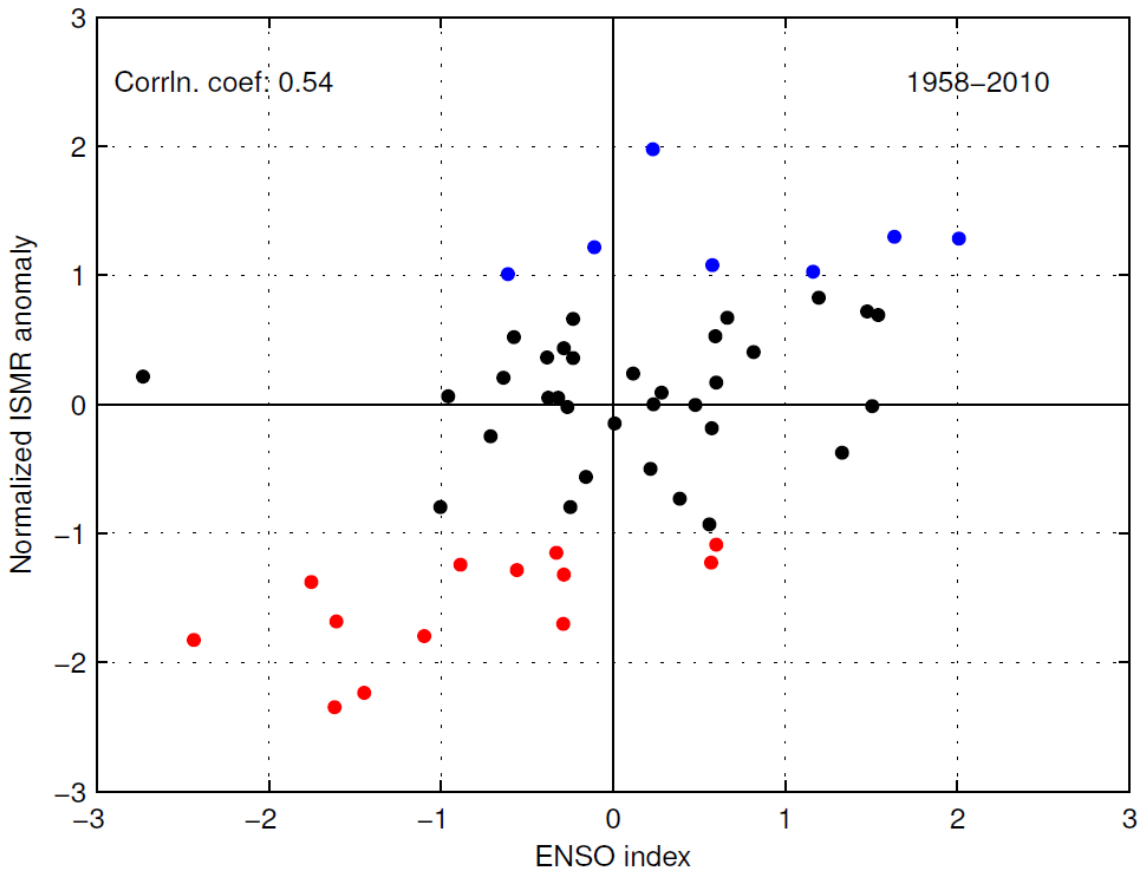

Fig. 4.8 : Normalized ISMR anomaly versus ENSO index defined as the negative of the normalized Nino3.4 SST anomaly for the period 1958-2009.

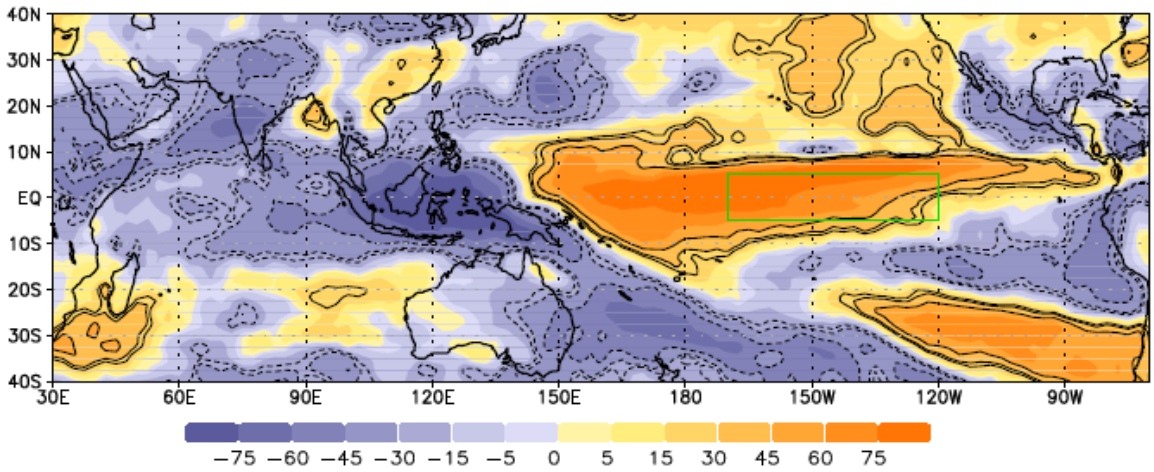

Fig. 4.9 : Correlation (x 100) between OLR (JJAS) and ENSO index for 1979-2009.

Since one of the major achievements of the past two decades is the ability to predict ENSO, it is possible to use this relationship for inputs into the prediction of ISMR. We consider five categories of ISMR viz. large deficit (<75 cm), deficit rainfall (between 75 and 83 cm), normal rainfall (between 83 and 86cm), above normal

rainfall (between 86 and 91cm) and large excess (>91cm) such that all are equally probable (20% chance) for the observed variation during 1958-2009. The chance of occurrence of rainfall in each of these categories when ENSO index is negative or positive is shown in Fig.4.10. It is seen that the probability is substantially different from the climatological one of 20% for the extremes i.e. large deficit and large excess rainfall seasons. Thus, for positive (negative) ENSO index, the probability of a large deficit decreases (increases) to 7% (over 35%), whereas that of large excess increases (decreases) to 30% (4%). However, there is a non-zero probability of large deficits when ENSO index is favourable and for large excess when it is unfavourable. The probability of the intermediate three categories is not substantively different from the climatological probability of 20%.

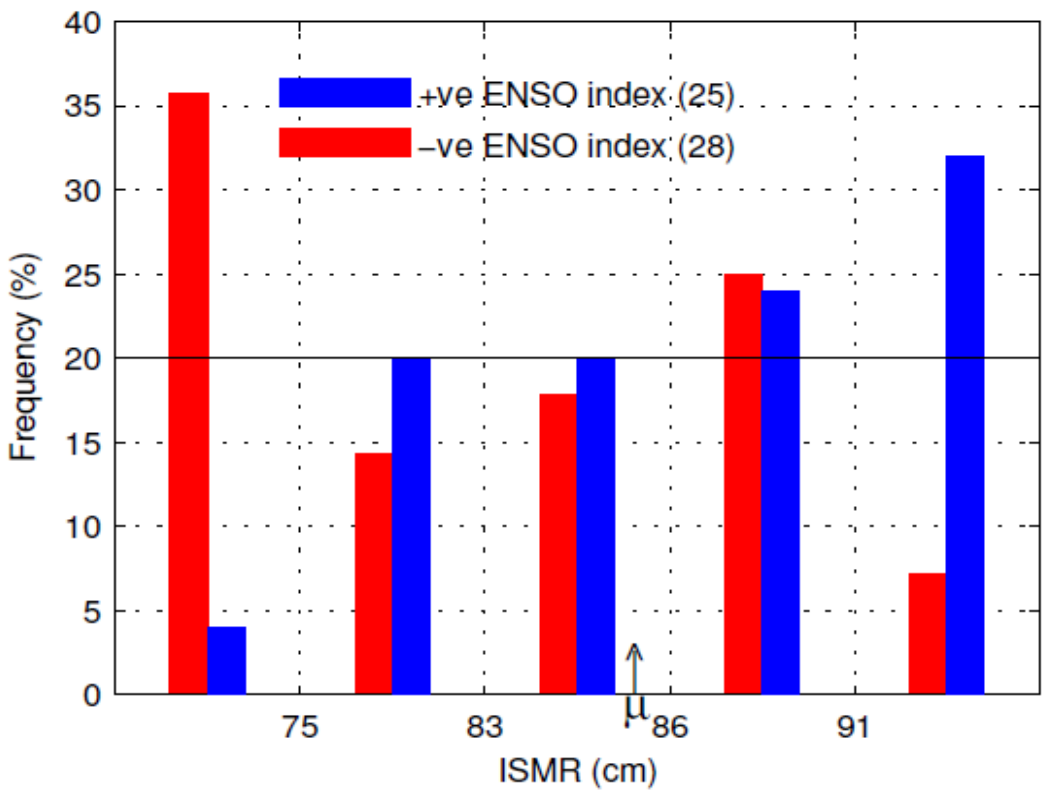

Fig. 4.10 : Frequency of occurrence (as percentage) of different categories of ISMR for negative and positive ENSO index.

So far we have considered only the all-India average summer monsoon rainfall. However, prediction of the spatial pattern is also important. Given a prediction of the phase of ENSO, some clues about the expected spatial patterns of rainfall anomalies can be obtained from Fig. 4.9. It is seen that in association with El

Nino (La Nina), the rainfall is suppressed (enhanced) over most of the Indian region, particularly over the peninsula south of 20°N. However, it is slightly enhanced (suppressed) over the head Bay and adjoining land regions. In fact, anomalies of the summer monsoon rainfall over Bangladesh are of the same sign for the El Nino of 1987 and La Nina of 1988; not surprisingly, its correlation with ENSO was found to be poor [Gadgil et al., 2011]. We find that there is some variation in the nature of the spatial rainfall anomaly patterns associated with ENSO from one month to another (Fig. 4.11). In July and August, the OLR anomaly over the head Bay, is of opposite sign to the OLR anomaly over the Indian region. In September, the entire region has anomalies of the same sign.

Also the largest anomalies are seen over the region south of 20°N in July and August, whereas in June they are larger over the monsoon zone. If we consider the interannual variation of the monsoon and the ENSO index (Fig. 4.12), consistent with the links of the monsoon with ENSO, the El Niño's of 1982 and 1987 were associated with droughts and the La Nina of 1988 with excess rainfall. However, during the strongest El Nino event of the century in 1997, the ISMR was higher than the long term mean and Kumar et al. [1999] suggested that the relationship between the Indian monsoon and ENSO had weakened in the recent decades. Then came the drought of 2002, which occurred in association with a much weaker El Nino than that of 1997. The experience of 1997 and 2002 suggested that the link with ENSO had yet to be properly understood. Such an understanding emerged with elucidation of the role of EQUINOO in the interannual variation of the monsoon [Gadgil et al., 2004, 2007].

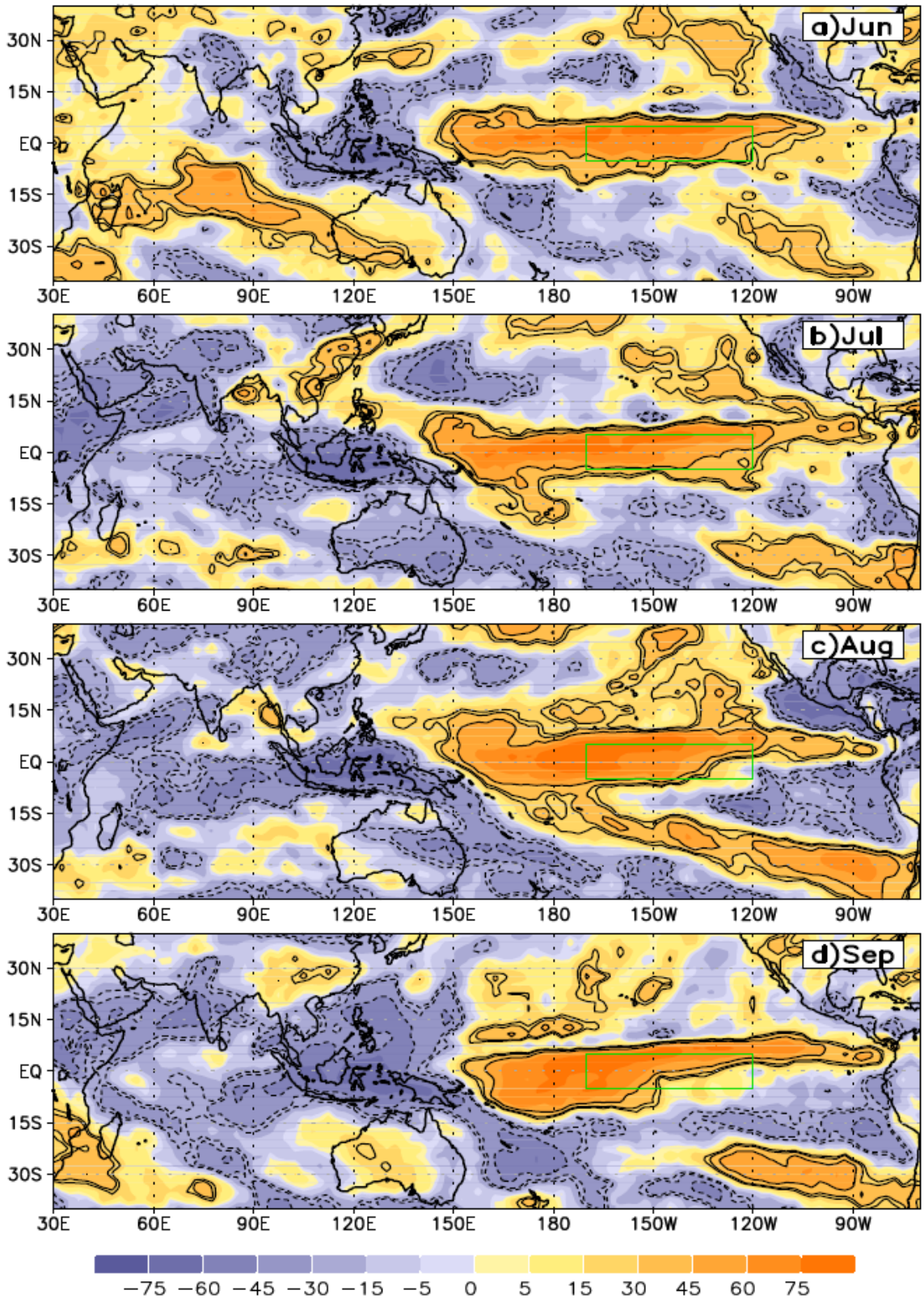

Fig. 4.11 : Correlation (x 100) between OLR (JJAS) and ENSO index for the month of a) June, b) July, c) August, d) September.

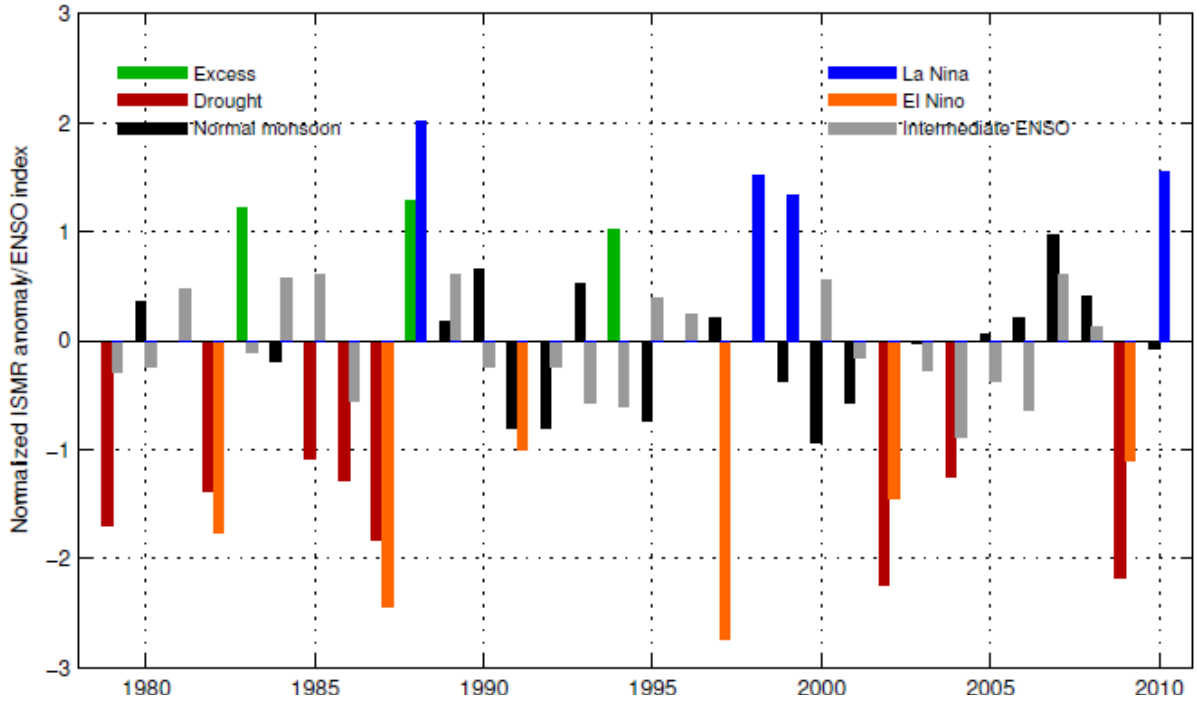

Fig. 4.12 : Variation of ISMR anomaly (normalized by the standard deviation) and the ENSO index during 1979-2010. The first bar indicates the ISMR anomaly, in red for droughts (<-1.0), in green for excess rainfall seasons (>1.0) and in black otherwise. The second bar indicates the ENSO index, in orange for El Nino (<-1.0), in blue for La Nina (>1.0) and grey otherwise.

4.5.2. EQUINOO and the monsoon

The OLR anomaly patterns for July 1997 (for which the all-India rainfall was close to the normal) and 2002 (for which the all-India rainfall was deficit by a massive 49%) are shown along with the mean OLR for July in Fig. 4.13. As expected, in association with El Nino, there is enhancement of convection over the equatorial regions of central and eastern Pacific in 1997 as well as 2002. However, there is a major difference between the OLR anomaly patterns of the two years over the equatorial Indian Ocean. Whereas in July 1997, the convection is enhanced over the western equatorial Indian Ocean and suppressed over the eastern equatorial Indian Ocean, the reverse is the case for July 2002.

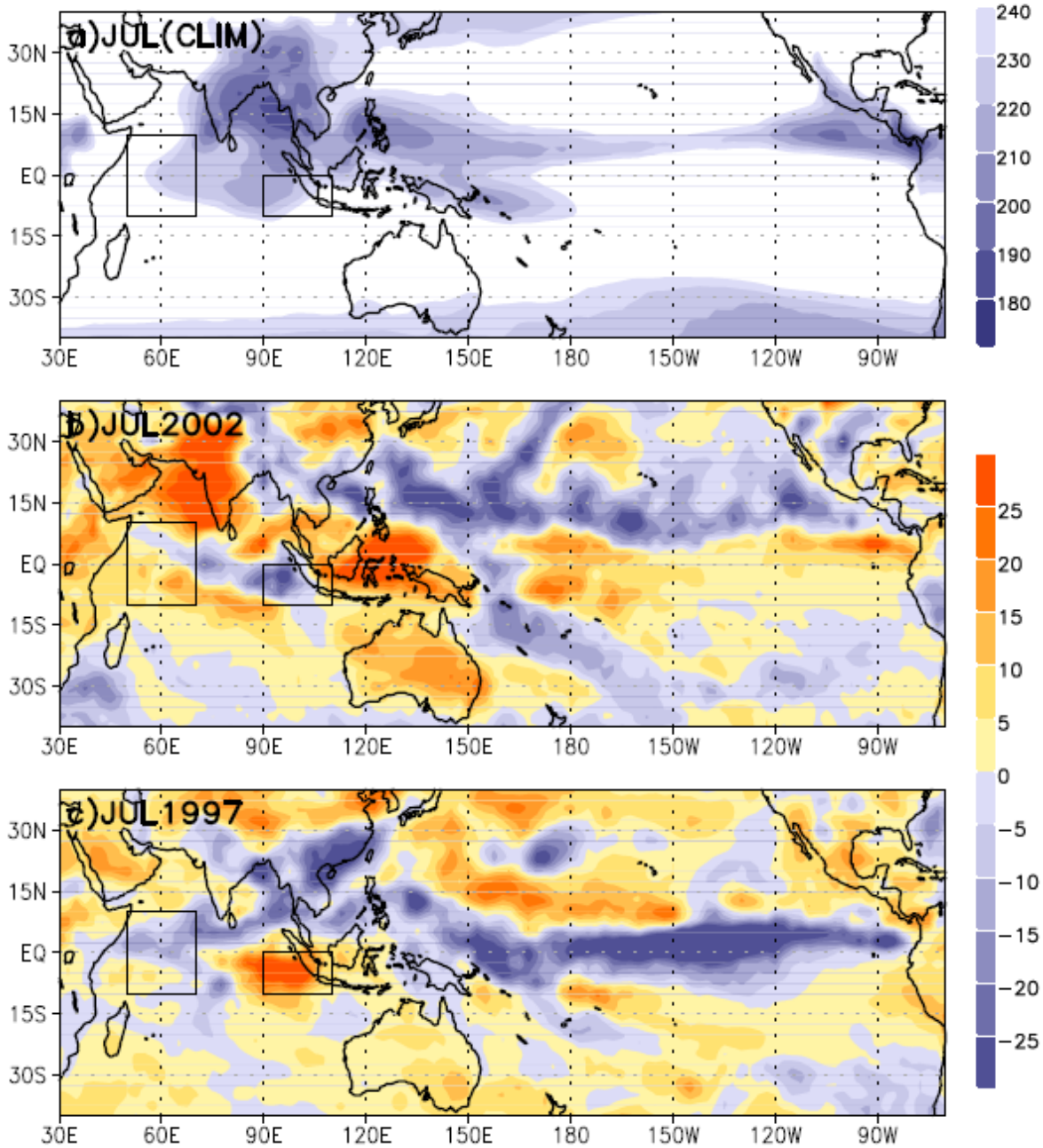

Fig 4.13 : a) Mean OLR (Wm^{-2}) for July. OLR anomaly (Wm^{-2}) for b) July2002 and c) July 1997

Suppression of convection over the eastern equatorial Indian Ocean (90°-110°E, 10°S-EQ, henceforth EEIO) tends to be associated with enhancement over the western equatorial Indian Ocean (50°-70°E,10°S-10°N, henceforth WEIO) and vice versa (Fig. 4.14). EQUINOO is the oscillation of a state with enhanced convection over the WEIO and reduced convection over EEIO (positive phase) and another with anomalies of the opposite signs (negative phase). The positive phase of EQUINOO is associated with easterly (i.e. from the east to the west) anomalies

in the equatorial zonal wind; whereas the negative phase (i.e. with enhanced (suppressed) convection over the EEIO (WEIO)), is associated with westerly anomalies of the zonal wind at the equator. It is seen from Fig. 4.13 that while the phase of ENSO in 1997 is the same as that in 2002, the phase of EQUINOO is positive in 1997 and negative in 2002. Comparison with the mean July pattern shows that while a negative EQUINOO is associated with enhancement of the climatological zonal gradient in convection, a positive phase involves a weakening or reversal of this gradient.

That a positive phase of EQUINOO with enhanced convection over WEIO is favourable for the monsoon is clearly seen from the pattern of the correlation of ISMR with OLR (Fig. 4.7). It should be noted that the magnitude of the correlation of ISMR with the convection over WEIO is comparable to that with the convection over the central Pacific corresponding to the link with ENSO. We use an index of the EQUINOO based on the anomaly of the zonal component of the surface wind over the central equatorial region (CEIO, 60°E-90°E, 2.5^{o}S-2.5^{o}N), which is highly correlated (coefficient 0.79) with the difference between OLR of WEIO and EEIO. The zonal wind index (henceforth EQWIN) is taken as the negative of the anomaly so that positive values of EQWIN are favourable for the monsoon.

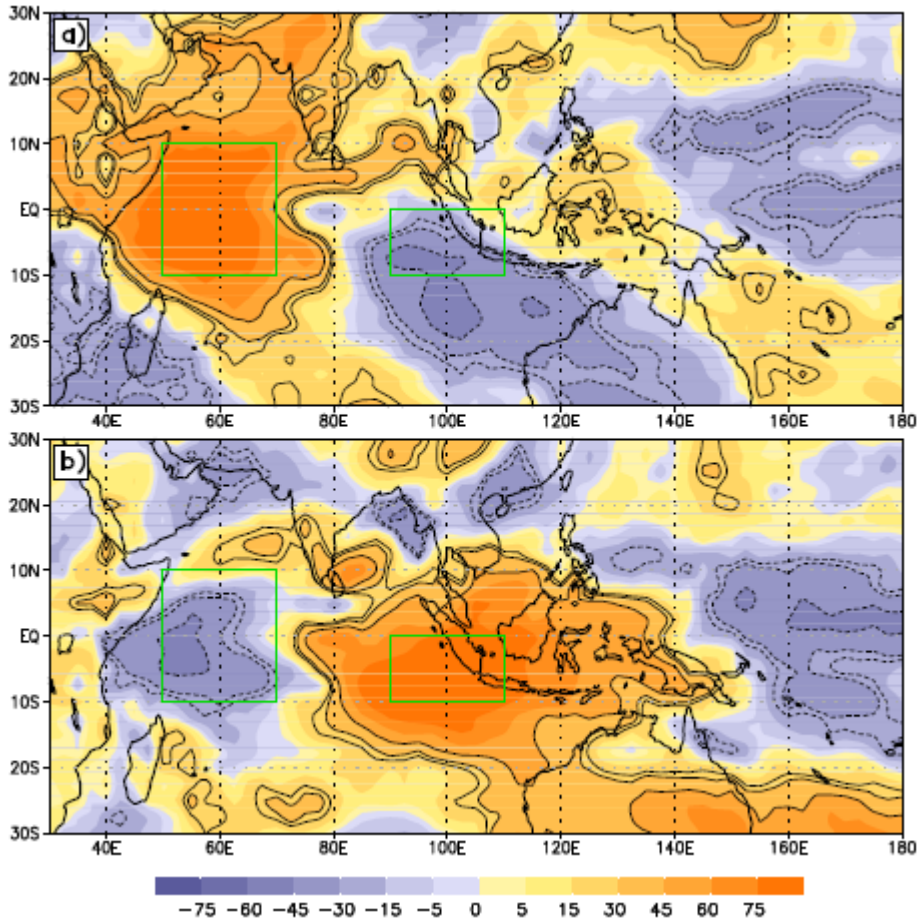

Fig.4.14 : a) Correlation (x100) between average OLR over WEIO and OLR for JJAS, b) Correlation (x100) between average OLR over EEIO and OLR for JJAS.

he spatial pattern of rainfall anomalies over the Indian region associated with strong positive and negative phases of EQUINOO can be deduced from Fig.4. 15a depicting the correlation of EQWIN with OLR over the Indo-Pacific region. It is seen that the largest anomalies occur over the Indian monsoon zone. Note that the anomaly is of the same sign over the head Bay as well, which is different from the pattern associated with ENSO. The relationship of ISMR with EQWIN is shown in Fig. 4.15b. The correlation of ISMR with EQWIN is positive and significant at 99%. The most striking feature of the figure is the asymmetry about zero EQWIN. It is seen that when EQWIN is positive (i.e. favourable) and reasonably strong (EQWIN is >0.2), the ISMR anomaly is either positive or close to zero. There are very few cases in which the ISMR anomaly is large and negative when EQWIN is positive. On the other hand, when EQWIN is negative (i.e. the zonal gradient in convection has the same sign as climatology), there is a large spread in the ISMR values. However, when EQWIN< -0.8, there are no excess monsoon seasons.

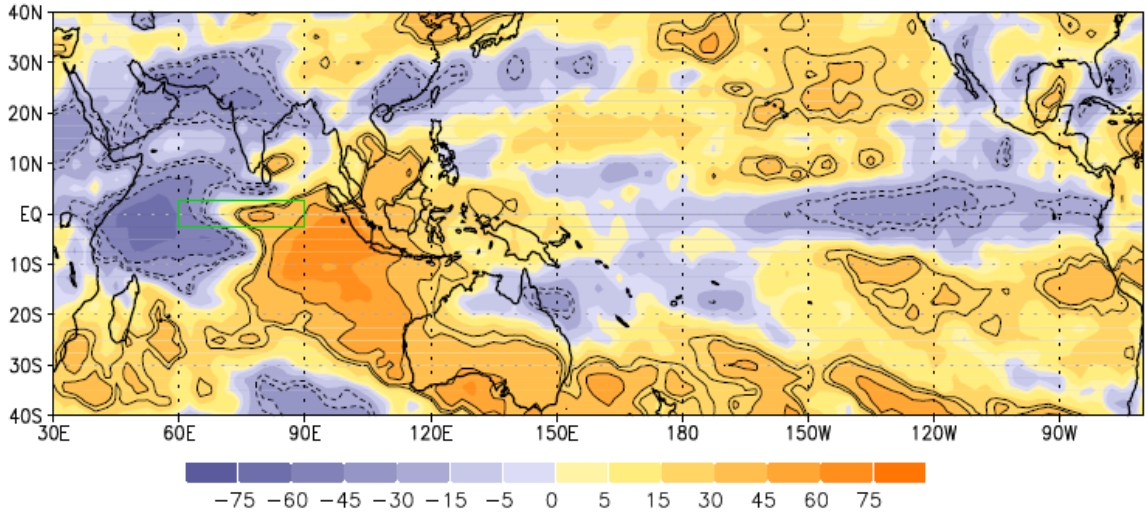

Fig. 4.15a : Correlation (x 100) between EQWIN and OLR (JJAS).

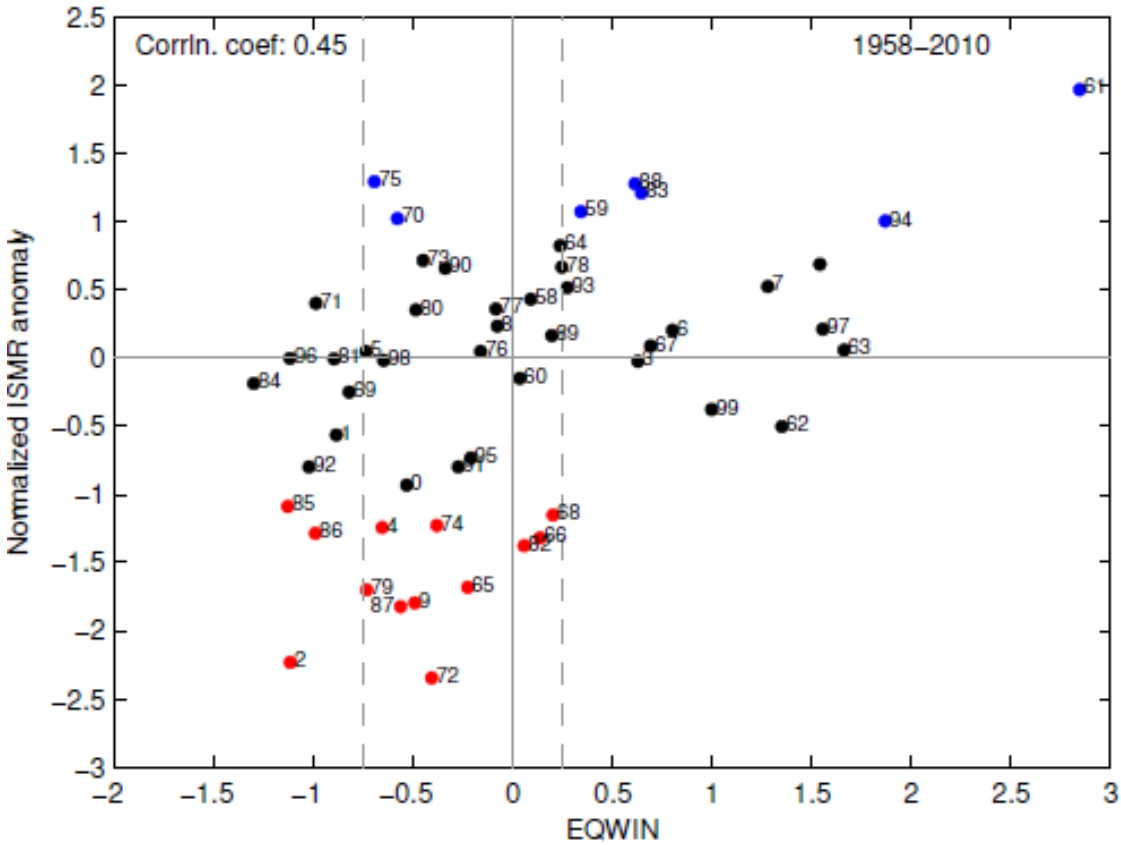

Fig. 4.15b : Normalized ISMR anomaly versus EQWIN for period 1958-2010.

In fact, for June-September the correlation between the ENSO index and EQWIN is not significant (coefficient: 0.052), suggesting that they can be considered as independent modes. The ISMR anomaly, the ENSO index and EQWIN for the summer monsoon seasons with the magnitude of the ISMR anomaly larger than one standard deviation (i.e. extremes) during 1979-2010 and the special season of 1997, are depicted in Fig. 4.16 in order of increasing ISMR. It is seen that each drought (excess rainfall season) is associated with unfavourable (favourable) phases of either ENSO or EQUINOO, or both. In 1997, the two indices are comparable, but opposite in sign and the ISMR anomaly is small. In 1994, ENSO is unfavourable and the excess rainfall can be attributed to the favourable phase of EQUINOO. Clearly, favourable phase of EQUINOO has contributed significantly to ISMR of 1997 as well as 1994. In the monsoon season of 2002, although the El Nino is weaker than in 1997, EQUINOO was also unfavourable and a severe drought occurred.

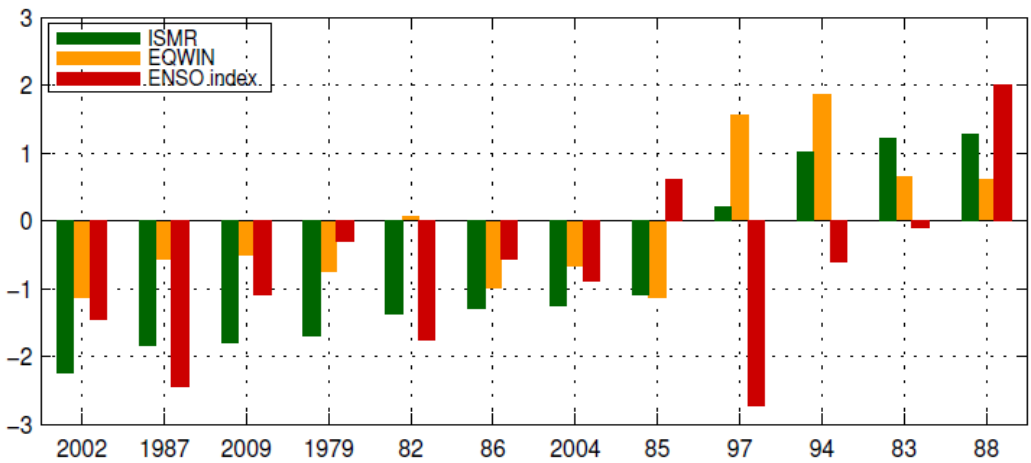

Fig. 4.16 : ISMR anomaly, ENSO index and EQWIN for all the droughts and excess rainfall seasons during 1982-2009 in order of increasing ISMR and also for the special season of 1997.

Thus with EQUINOO we can 'explain' not only the droughts that occurred in the absence of El Nino or in the presence of a weak El Nino, but also excess rainfall seasons in which ENSO was unfavourable. The worst droughts are associated with unfavourable phases of both the modes. In Fig. 4.17a, the ISMR for all the extreme summer monsoon seasons during 1958-2010, is shown in the phase plane of the June to September averages of the ENSO index and EQWIN. The most striking

feature of the distribution of extreme years is the clear separation between the years with excess and deficits with each of the surplus (drought) years located above (below) a certain line in the phase plane (the line 'L' in Fig. 4.17a). Furthermore we find that there are no seasons with even moderate deficits (between half and one standard deviation) above the line and only two seasons with moderate excess below this line [Gadgil et al., 2007]. This distribution in the phase plane suggests that an appropriate index would be a composite index, which is a linear combination of the ENSO index and EQWIN. When the value of this index is high (i.e. point above the line L) there is no chance of droughts. For low values of the index (i.e. below the line L) there is no chance of excess rainfall seasons. It is important to note that the strong relationship between extremes of ISMR and this composite index is not predictive but simultaneous.

We find the extremes of the July-August rainfall are also well separated in the phase plane of the concurrent values of the ENSO index and EQWIN (Fig. 4.17b). Note that the separation for July-August is larger than that for June-September.

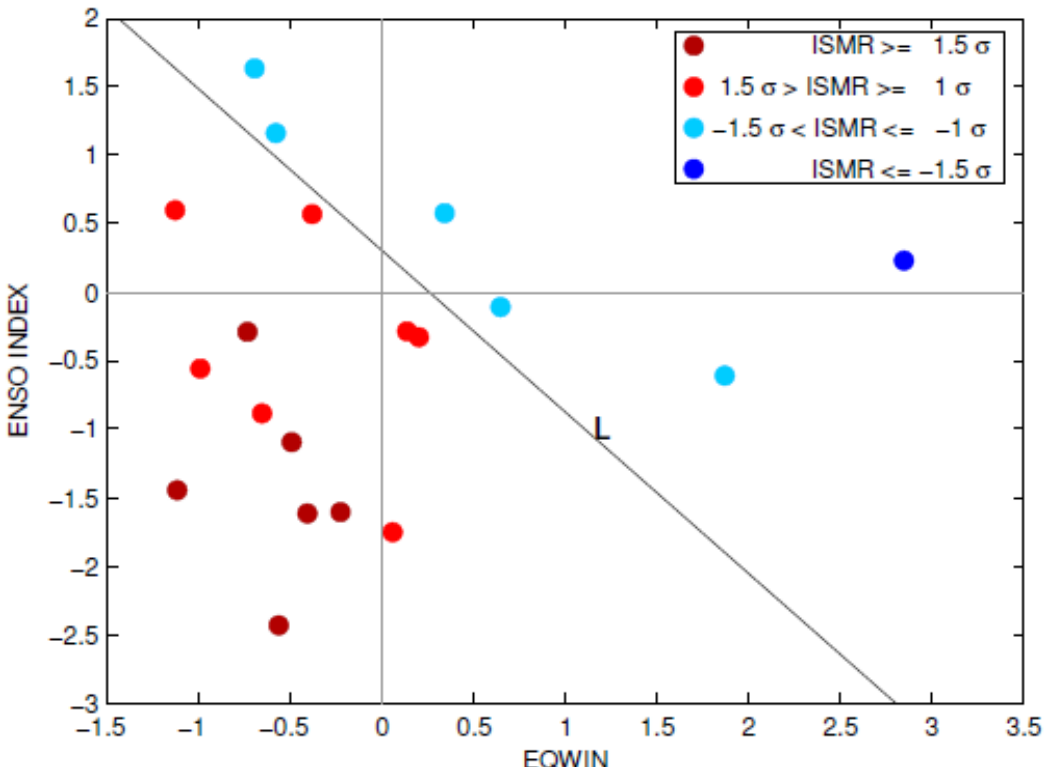

Fig. 4.17a : ISMR is represented in the phase plane of June-September average values of the ENSO index and EQWIN for all the seasons during 1958-2010;

σ represents the standard deviation

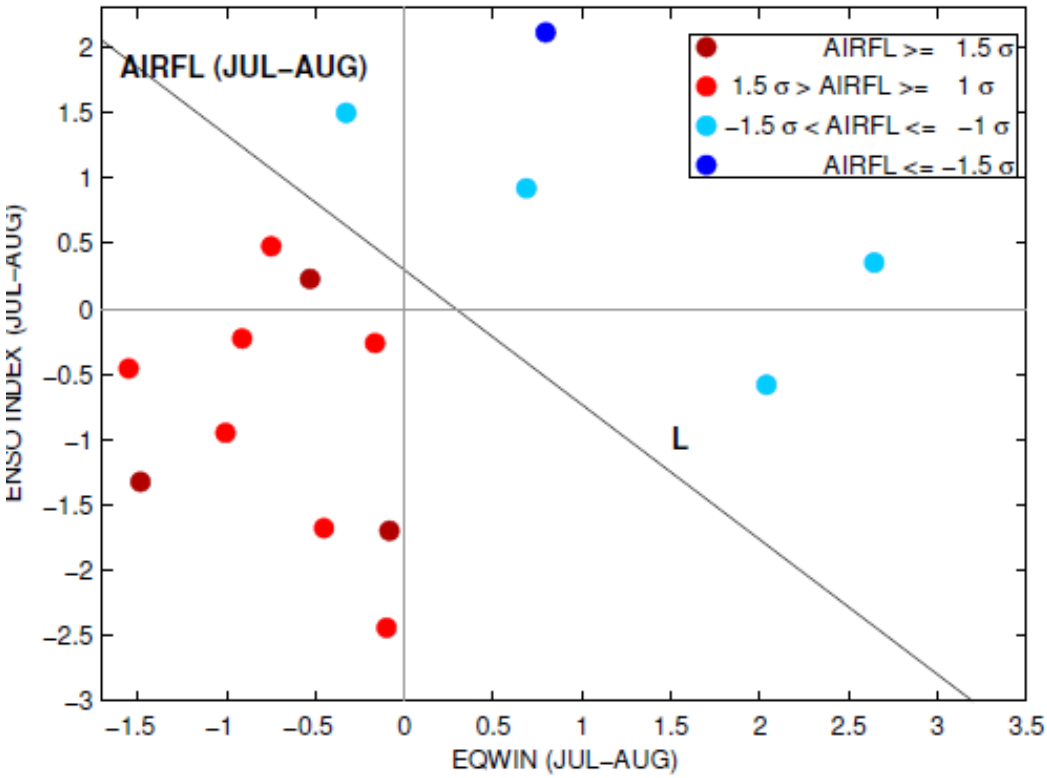

Fig. 4.17b : July-August rainfall is represented in the phase plane of July-August average values of the ENSO index and EQWIN for all the seasons between 1958 and 2010. σ represents the standard deviation of the all India rainfall in July-August.

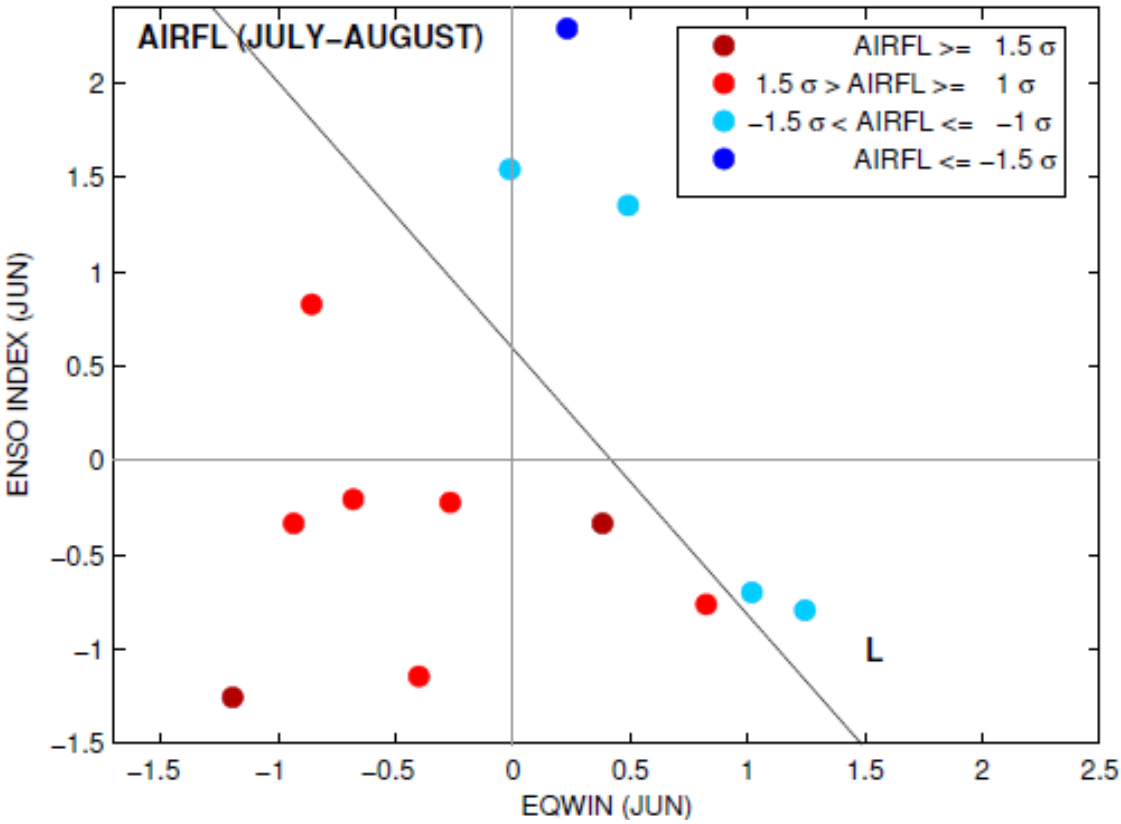

Fig. 4.18 : July-August all India rainfall is represented in the phase plane of the ENSO index and EQWIN for the month of June for all the seasons between 1958 and 2010. σ represents the standard deviation of the all India rainfall in July-August.

In fact, the extremes of July-August rainfall are also separated in the phase plane of the June values of EQWIN and ENSO index (Fig. 4.18). Hence it should be possible to utilize this in prediction of July-August rainfall in June.

If it becomes possible to generate realistic predictions of EQUINOO in the near future, the strong relationship of the ISMR anomalies with ENSO and EQUINOO and hence the composite index, could be used for predicting the likely distribution of ISMR (Fig. 4.19). A reliable prediction of the sign of the composite index would rule out the chance of one of the extremes (i.e. of a large deficit if the sign is positive and large excess if the sign is negative). Furthermore, if the sign is positive the chance of below normal rainfall is also almost halved from the climatological probability.

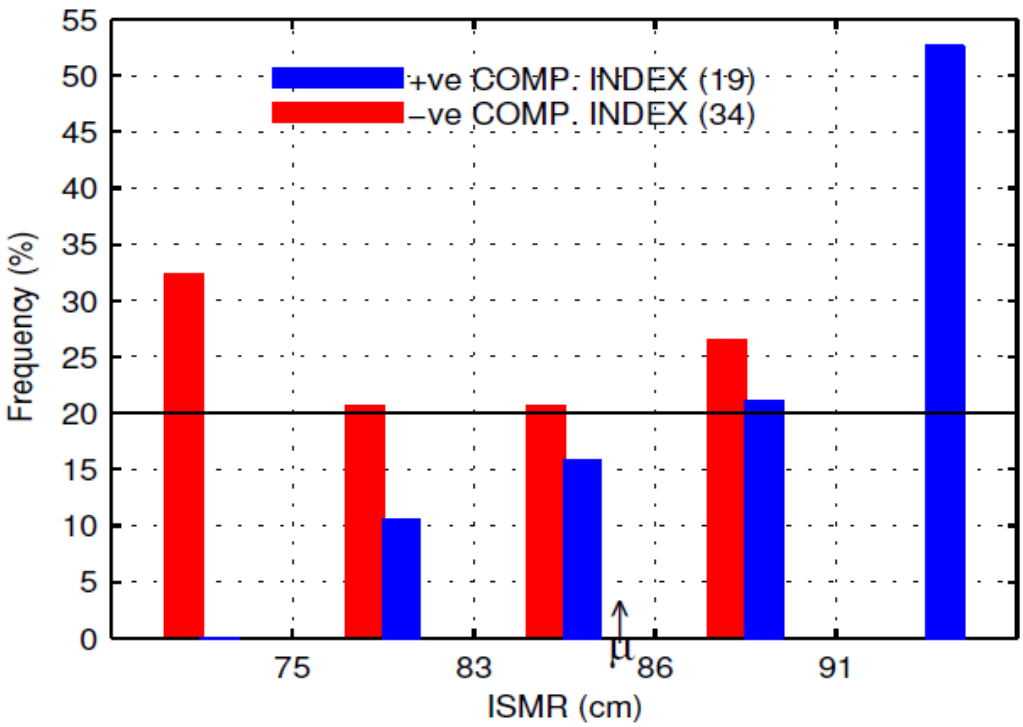

Fig. 4.19 : Frequency of occurrence (as percentage) of different categories of ISMR for positive and negative EQWIN

4.6. EQUINOO and the equatorial Indian Ocean

In this section we elucidate the important features of the evolution of the EQUINOO, since understanding this evolution is a prerequisite for understanding (and hence predicting) the interannual variation of the Indian summer monsoon

rainfall. The seasonal OLR anomaly over EEIO and that over WEIO for each summer monsoon of 1982-2010 is depicted in Fig. 4.20. In this figure, seasons with positive phase of EQUINOO (i.e. negative OLR anomalies over WEIO and positive OLR anomalies over EEIO) appear in the top left quadrant, whereas those with a negative phase in the bottom right quadrant. All the years with positive OLR anomalies over both EEIO and WEIO are El Nino years, with convection suppressed over the entire equatorial Indian Ocean (as well as the Indian region). The La Nina years with enhanced convection over the equatorial region are in the opposite quadrant with negative OLR anomalies over both.

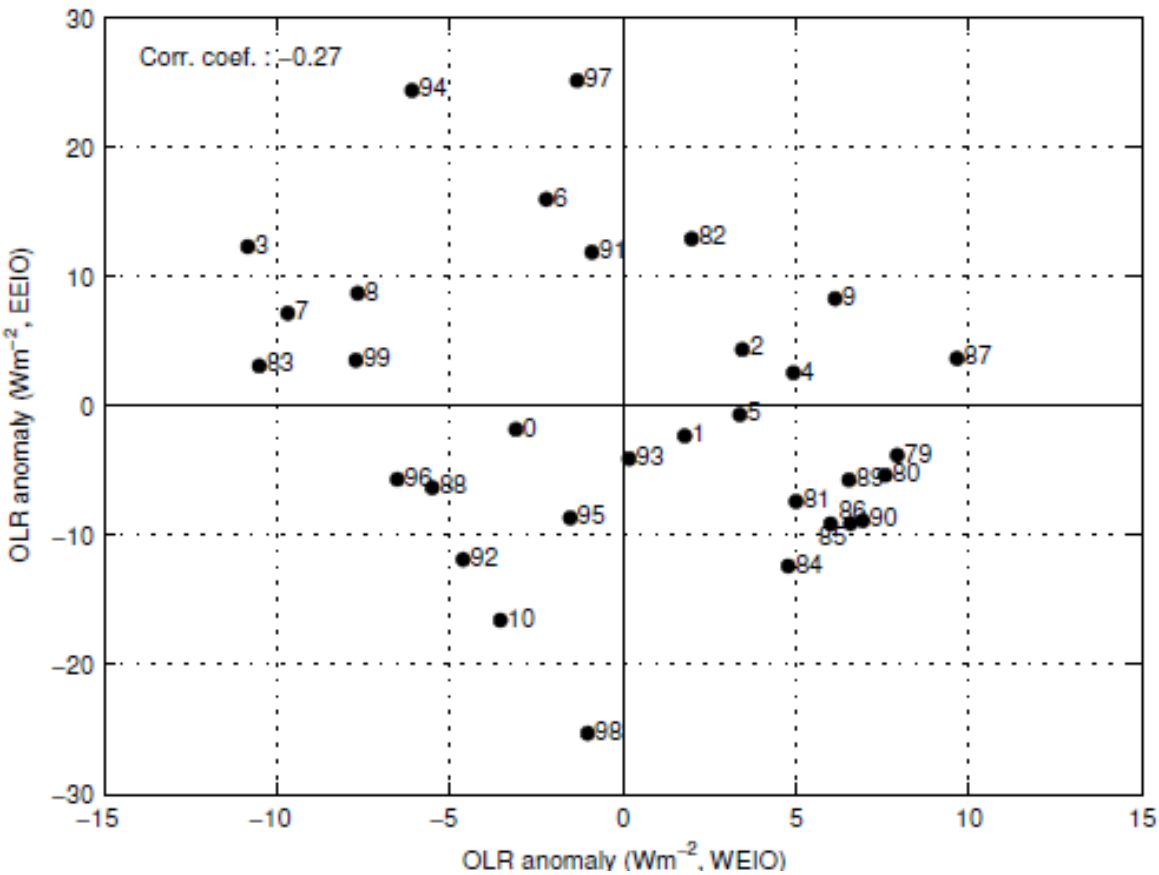

Fig. 4.20 : June-September OLR anomaly over the EEIO and that over the WEIO for all the seasons in the period 1982-2010.

The strong positive phase of EQUINOO with intense suppression of convection over EEIO and some enhancement in convection over WEIO, in the summer monsoon seasons of 1994, and 1997 is associated with the strong positive phase of the coupled Indian Ocean dipole mode [IOD, Saji et al., 1999], which is also known as Indian Ocean zonal mode. Saji et al. [1999] point out that positive

IOD (pIOD) events are characterized by `*a reversal in sign of the SST anomaly across the basin, anomalously low sea surface temperatures off Sumatra and high sea surface temperatures in the western Indian Ocean*' relative to the climatological SST pattern (Fig. 4.21a) with 'accompanying wind and precipitation anomalies' (e.g. for 1994 and 1997 in Fig. 4.21e-h).

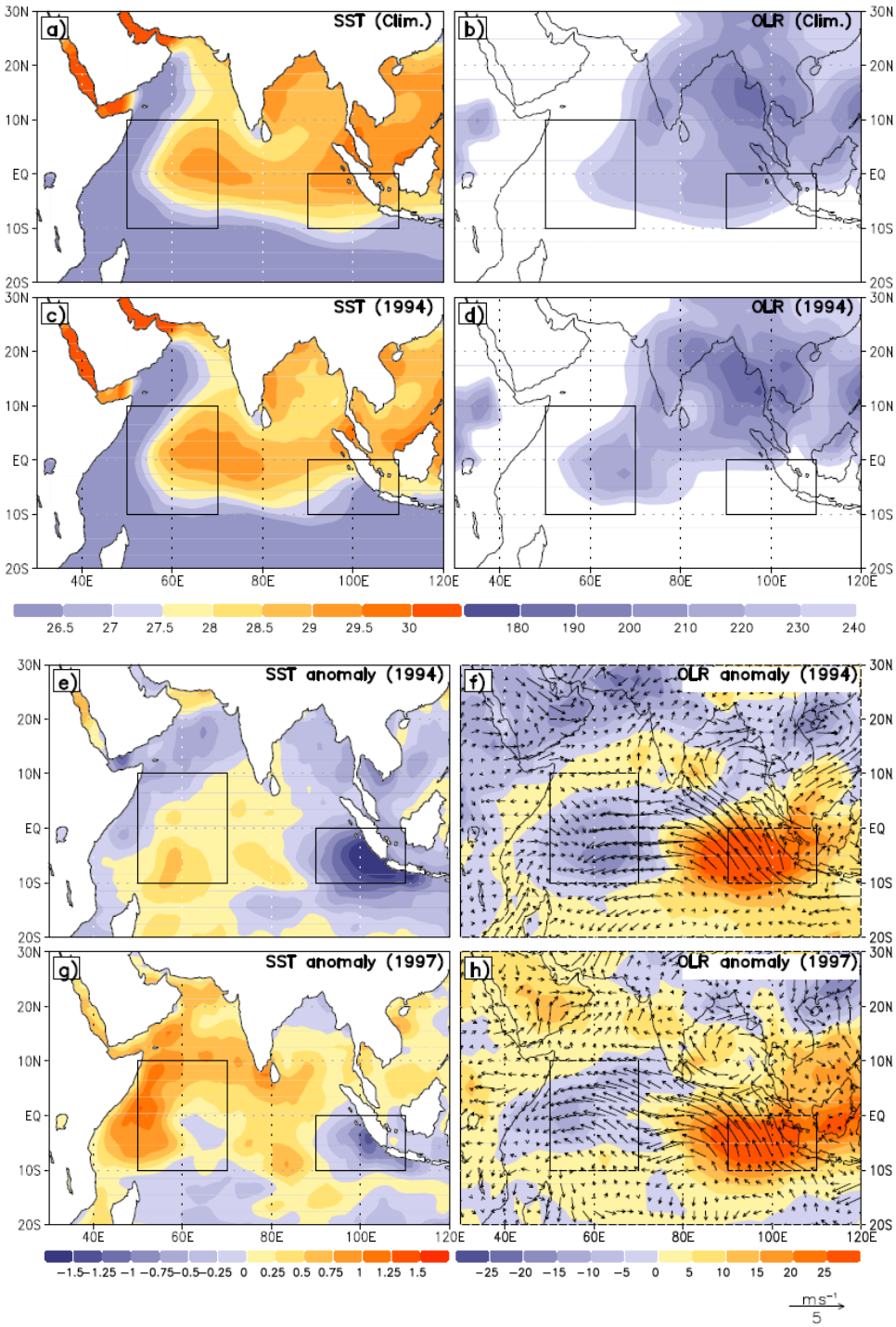

Fig. 4.21 : Climatological pattern of June-September mean a) SST (°C) and b) OLR (Wm^{-2}). June-September mean pattern of c) SST (°C) and d) OLR (Wm^{-2}) for 1994. June-September mean e) SST anomaly (°C) pattern and f) OLR (Wm^{-2}) and surface wind (ms^{-1}) anomalies for 1994; (g,h) same as e) and f) but for 1997.

While pIOD events are associated with a decrease or reversal of the normal zonal gradients of SST, OLR (e.g. Fig. 4.21 c,d for 1994) etc., a negative phase of the IOD involves an intensification of the normal gradients. Hence the major focus has been on understanding the occurrence of pIOD events. We have seen that the strong positive phase of EQUINOO associated with the pIOD events of 1994 and 1997 made a significant contribution to the ISMR. Thus understanding the evolution and occurrence of pIOD events is important for understanding the evolution of EQUINOO.

It should be noted that a positive phase of EQUINOO also occurred in 1983, 2003 and 2007 with larger convection anomalies over WEIO and less suppression of convection over EEIO than for the strong pIOD events of 1994 and 1997. It turns out that on the seasonal scale, there is a strong relationship between the variability of ISMR and the convection over WEIO (Fig. 4.22), with all the droughts being characterized by positive OLR anomaly and all the excess monsoon seasons by a negative OLR anomaly over WEIO. Hence understanding such events with exceptionally high convection over WEIO is also important for prediction of EQUINOO during the summer monsoon.

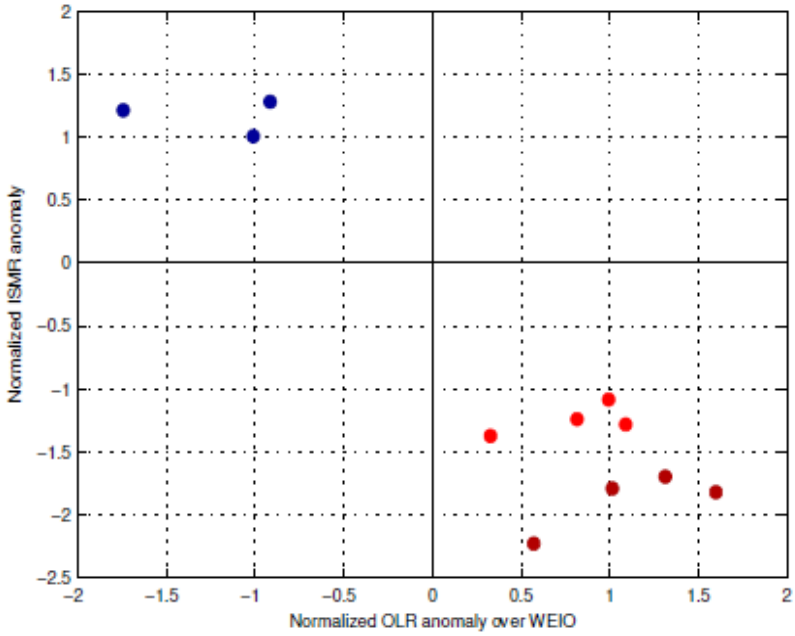

Fig. 4.22: Normalized ISMR anomaly and normalized June- September OLR anomaly over the EIO for of 1982-2010.

5.6.1. The setting: climatology of convection and SST

We discuss in brief the present understanding of the processes involved in the evolution of the mean monthly SST, wind and convection over the EEIO and WEIO (Fig. 4.23). Ocean dynamics plays an important role in the evolution of the SST of EEIO whereas the variation of the SST of WEIO is primarily determined by fluxes at the surface [Murtugudde et al., 2000; Vinayachandran et al., 2002]. The critical role played by the eastern parts of equatorial Indian Ocean in the development of positive IOD events has been pointed out in several studies [Murtugudde et al., 2000; Vinayachandran et al., 2002; Annamalai et al., 2003; Li et al., 2003], so we consider first the evolution of the mean EEIO SST.

From April, the mean wind parallel to the coast of Sumatra is northward, leading to upwelling and hence cooling of the EEIO. The magnitude of this upwelling favourable wind increases rapidly until June and more slowly up to the peak in mid-August (Fig. 4.23a). It starts weakening in mid-September. During spring, WEIO is warmer than EEIO (Fig. 4.23a) and the spring jet in the equatorial Indian Ocean [Wyrtki, 1973] driven by westerlies along the equator (Fig. 4.23a) advects warm water to the eastern Indian Ocean, leading to an increase in the SST of the EEIO and deepening of thermocline [Hastenrath, 2002; Vinayachandran et al., 2002]. Whether the SST of the EEIO increases or decreases, is determined primarily by the balance between the upwelling and advection. Since the mean zonal wind along the equatorial Indian Ocean starts weakening from the beginning of May (Fig. 4.23a), the upwelling due to the wind along the coast of Sumatra dominates and SST of the EEIO starts decreasing (Fig. 45.23a). It reaches a minimum during August-September. By mid-September, the wind parallel to Sumatra starts weakening, the westerly component of the zonal wind over CEIO increasing and the SST of EEIO starts increasing.

Before consideration of the variation of the SST of WEIO, we consider the variation of the mean convection over EEIO and WEIO, since atmospheric fluxes are known to play an important role in determining the SST variation of WEIO. The variation of the mean OLR over EEIO and WEIO during May-November is shown in Fig. 4.23b. We note that the average OLR over WEIO decreases up to the end of

May, oscillates around 240 Wm^{-2} up to the end of August, increases in September and remains high until the end of November. The SST of WEIO decreases rapidly with the increase of convection from May to August and then increases until the end of November. From mid-May until the end of November the mean SST of EEIO is higher than that of WEIO. It is seen that climatologically throughout April-November, the OLR over EEIO is less than that over WEIO, implying that there is more convection over EEIO than over WEIO throughout this period. Consistent with this, the mean sea level pressure over the EEIO is lower than that over WEIO and the mean zonal component of the wind over CEIO is westerly (Fig. 4.23a).

From mid- May-to mid-August, the average OLR and the vertical velocity over WEIO are close to that over EEIO (Fig. 4.23) and the atmospheric conditions appear to be almost equally favourable over the two regions for supporting convection. The strength of the climatological westerly winds over CEIO, which reflects the east-west gradient in the convection, also decreases from mid-May and the magnitude is small (less than 1 ms^{-1}) during June-August (Fig. 4.23a). However, from September onwards, the EEIO is more favourable for convection than WEIO.

The evolution of IOD is strongly locked to the seasonal cycle [Saji et al., 1999; Vinayachandran et al., 2010, and references therein]. Typically, a pIOD event is triggered in April-May, matures during September to November and most of the anomalies disappear by January of the following year [Saji et al., 1999; Annamalai et al., 2003]. Thus the mature phase of a pIOD event, with an intense suppression of convection over EEIO, occurs in the boreal autumn when climatologically, convection over EEIO is favoured.

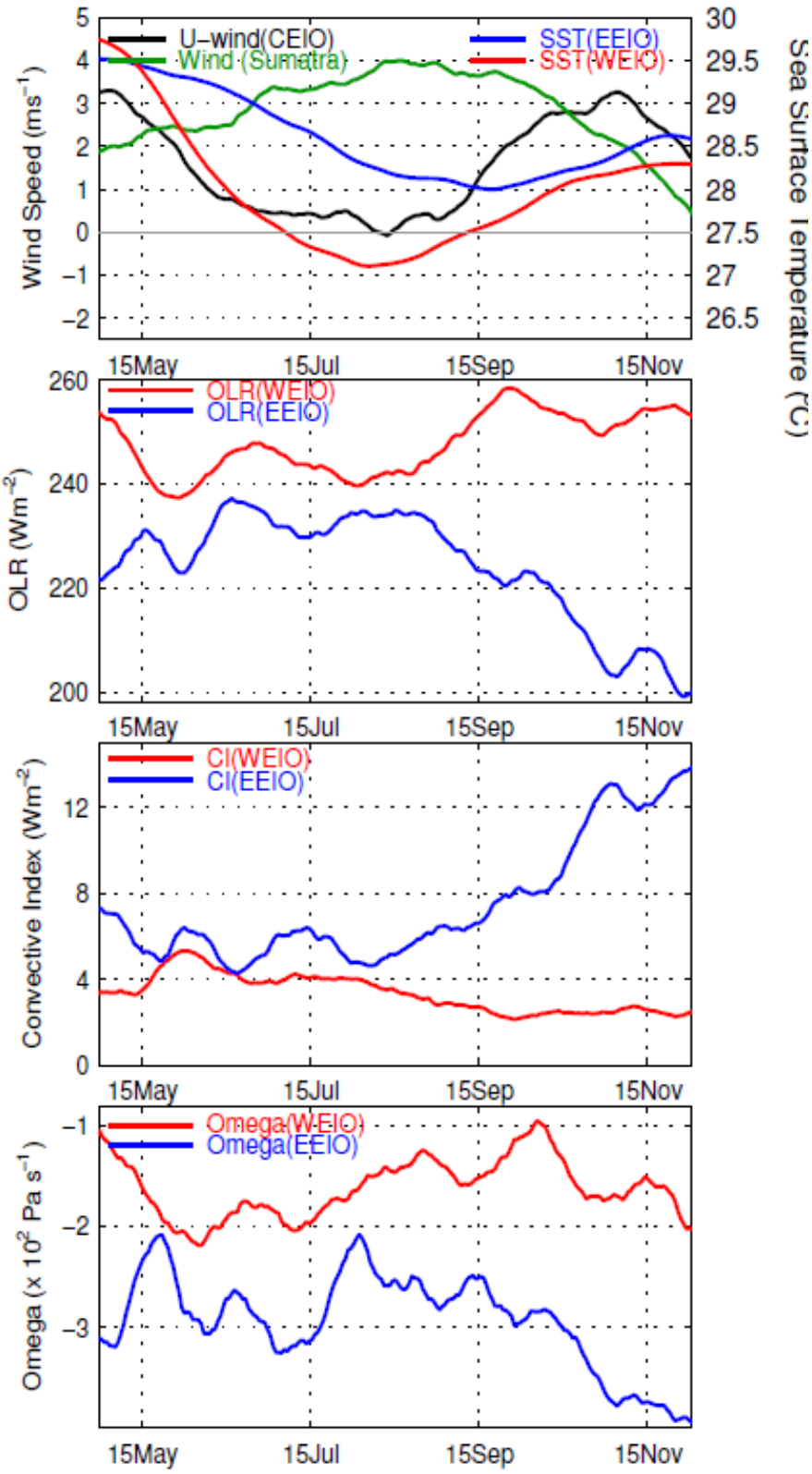

Fig. 4.23 : Variation of the mean of SST [Reynolds et al., 2002], OLR, CI, OMEGA, zonal wind along the CEIO and wind along the Sumatra coast during May-November.

The most commonly used measure of organized deep convection over a region is the OLR, which is what we have considered so far. The regional average OLR is a reasonable measure of convection and its variability, for regions over which the OLR is uniformly low. However, when a substantial part of the region is cloud-free with large values of OLR, the OLR of the cloud-free part also contributes to the regional average. Thus average values of OLR for a region on the daily/weekly and larger scales can be relatively high despite the occurrence of some days/sub-regions of deep convection over some regions. Hence, indices such as the frequency of highly reflective clouds [HRC Garcia, 1985] have been used for assessing variation of deep convection. We use a convective index (CI), which is a measure of the intensity and the horizontal extent of deep convection over a region based on daily 2.5 x 2.5 deg resolution OLR data. We assume that, on any day, deep convection occurs only over the grid points for which OLR is below 200Wm^{-2} and take the difference of the OLR value from 200Wm□2 to represent the intensity of deep convection over the grid point. The CI for a specific region (such as EEIO), for a particular day, is calculated as the sum of the intensity of convection over all grid points with deep convection [i.e. over all the grid points with OLR less than 200 Wm□^{2}, Francis et al., 2007]. The variation of the mean CI over EEIO and WEIO is seen to be consistent with that of OLR (Fig. 4.23b). It is seen that despite the weekly average OLR over WEIO of 240 Wm□^{2} and higher, there is deep convection as indicated by the non-zero mean value of CI from May to November (Fig. 4.23b).

While convection occurs intermittently over WEIO and EEIO in any season, during a season with a strong positive phase of EQUINOO (e.g. 1994, 1997 in Fig. 4.24) the propensity of convection over WEIO is higher than that over EEIO. On the other hand, in the negative phase of EQUINOO (eg. 1985, Fig. 4.24), the propensity of convection is higher over EEIO compared to that over WEIO. We need to understand the factors that lead to the anomalous suppression/enhancement of the convection over EEIO and WEIO in any season. The important factors could be remotely driven descent or ascent over the equatorial Indian Ocean, as in the case of the impact of ENSO. The SST of the equatorial Indian Ocean could also play a role. For example, it is believed that the suppression of convection over EEIO during the positive phase of EQUINOO in 1994, is associated with the cold SST anomaly of EEIO (Fig. 4.20 e,g). In order to assess the impact of SST anomalies on OLR, consider first the relationship of the convection over the tropical oceans with the SST.

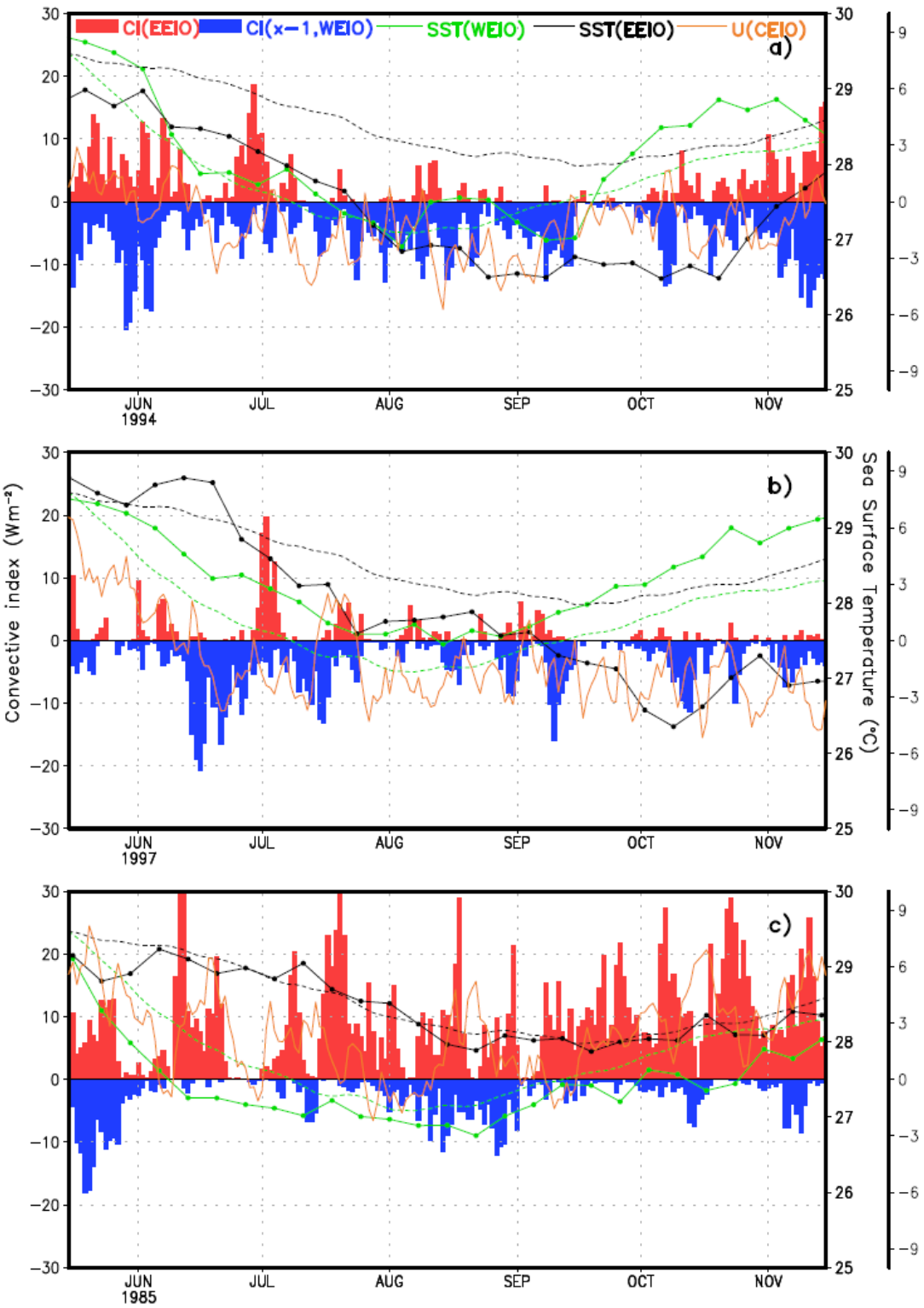

Fig. 4.24 : Variation of the convective index (CI) over EEIO (red) and negative of the CI over WEIO (blue), SST of EEIO (black), mean SST of EEIO(black dashed); SST of WEIO (green), mean SST of WEIO (green dashed);and zonal wind along CEIO (pink)for the years a)1994 b) 1997 c) 1985.

4.6.2. SST-convection relationship

The relationship of convection over the tropical oceans with the SST is known to be highly nonlinear [Bjerknes, 1969; Gadgil et al., 1984; Graham and Barnett, 1987; Waliser and Graham, 1993; Bony et al., 1997; Zhang, 1993; Lau and Sui, 1997]. It has been shown that organized deep convection does not occur over very cold tropical oceans and the propensity for such convection is high over warm oceans with SST above a threshold of about 27.5^{0}C [Gadgil et al., 1984; Graham and Barnett, 1987]. This is clearly seen in the scatter plot of the monthly OLR and SST for each grid point of the Indian Ocean (60°-100°E,15°S-20°N) during June-September 1982-2010 depicted in Fig. 4.25a,b. When SST is below 26.5^{o}C, almost all the grid points are characterized by OLR greater than 240Wm^{-2} (implying absence of deep cloud systems) and the mode is at 255-270Wm^{-2}. The mean OLR decreases rapidly with SST in the critical range 27°C to 28.5^{o}C around the threshold, but hardly changes with SST beyond this range (Fig. 4.25 c,d). The mode shifts across 27.5^{o}C to about 210Wm^{-2} and above this threshold, most of the grid points are characterized by OLR less than 240Wm^{-2}. However, over such warm oceans, there is a large spread in the OLR for a given SST and the relationship between OLR and SST is, at best, weak.

When the SST is above the threshold, whether there is convection or not depends on the dynamics i.e., low-level convergence [Graham and Barnett, 1987]. Hence the local SST plays no role in determining the variability of convection or rainfall when the SST is above the threshold. The mean June-September SST of the Bay of Bengal, eastern Arabian Sea and a large part of the equatorial Indian Ocean is well above the threshold (Fig. 4.21a), and the observed variation is such that it is generally maintained above the threshold year after year [Gadgil, 2003]. Hence the SST is not expected to play a role in the variability of convection over these regions. Thus, although the variability of the monsoon is linked to the convection over the oceans, the correlation between monsoon rainfall over India and SST of the Indian seas on the interannual scale is poor [Shukla and Misra, 1977; Rao and Goswami, 1988]. In fact, the impact of the atmosphere on the ocean comes out as the stronger signal, with SST in the seasons following a good monsoon being lower [Joseph and Pillai, 1986; Shukla, 1987]. However, SST gradients can play a role if they determine where the convergence occurs [Shankar et al., 2007].

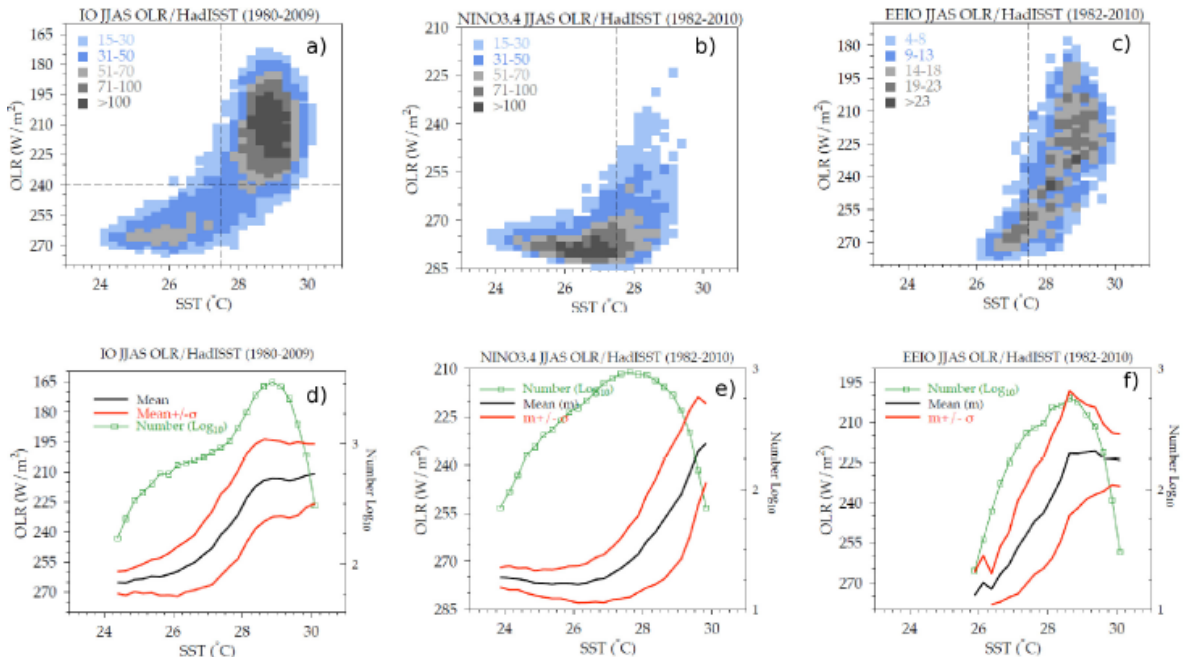

Fig. 4.25 : For June-September of 1982-2009 : number of points in each SST-OLR bin over the a) Indian Ocean b) Nino3.4 region and c) the EEIO. Variation of the mean OLR (black), mean + one standard deviation (red)and mean - one standard deviation (red) of OLR with SST and the variation of the number of grid points (green) with SST for d) the Indian Ocean e)Nino3.4 region and f) EEIO. SST data used here is HadISST.

Variability of the SST of the Nino3.4 region plays a critical role in ENSO. The seasonal mean SST for this region (27°C) is close to the threshold, the observed variation of the SST of this region is generally in the critical range (Fig.4.25 b,e) and the variation of convection over the central Pacific is strongly linked to the variation of the SST. On the other hand, the seasonal mean SST is well above the threshold over almost the entire EEIO region except for a very small part near the southeastern corner (Fig. 4.21a). Hence the mean SST averaged over EEIO at 28.38^{o}C is well above the threshold and the mean OLR is 233 Wm^{-2}. It is seen from Fig. 4.25 c,f that for EEIO, the SST is above the threshold for a majority of the points and there is a large variation in OLR for such warm SST values. For the few points for which it is below the threshold, the OLR is high. However, comparable values of OLR also occur for higher SSTs. Thus, although a cold EEIO (with SST below the threshold) is associated with high OLR i.e. suppressed convection, the general relationship between convection and SST for the EEIO region is not strong.

The variation of the monthly OLR anomaly over EEIO with the SST of EEIO for all the months in the period 1982-2009, is depicted in Fig. 4.25g. It is seen that the relationship between OLR and local SST during June-September for the Indian Ocean region depicted in Fig. 4.25a, is also valid for the average OLR above EEIO and the average SST of EEIO for all months of the year. For SSTs above the threshold, there is a large spread with OLR anomalies ranging from 30 Wm^{-2} to -30 Wm^{-2} suggesting that variation of convection is not linked with the variation of the SST when it is above the threshold. Note that the most intense suppression with OLR anomalies greater than 45 Wm^{-2} occurs when SST is less than the threshold of 27.5°C. However, while all the points with SST is less than 27.5°C, are characterized by OLR anomalies greater than 20Wm^{-2}, comparable OLR anomalies also occur for higher values of SST. When the SST is maintained below the threshold over several weeks, we expect sustained suppression of convection over EEIO (e.g. 1994,1997 in Fig. 4.24). Thus cooling of EEIO to SST below the threshold is an important attribute of strong positive IOD events.

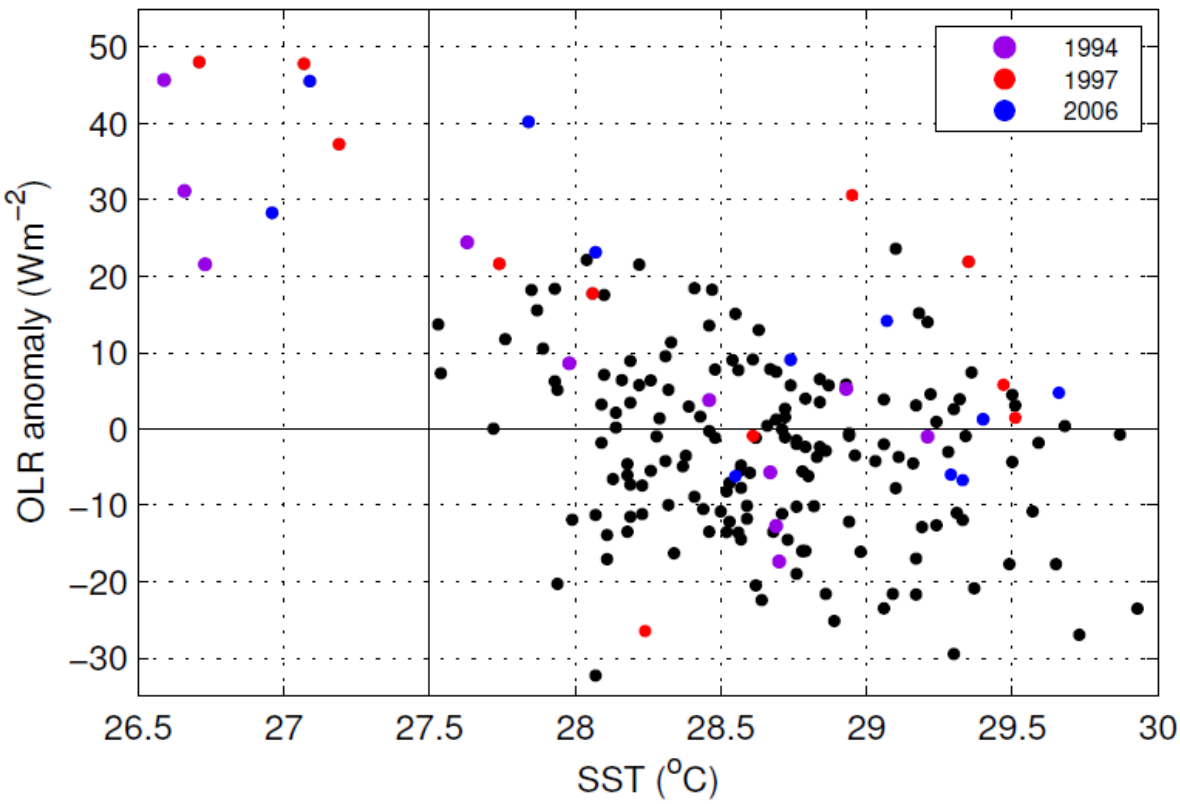

Fig. 4.25g : Monthly mean values OLR anomaly over the EEIO and SST of the EEIO for 1982-2010. Data considered is Reynolds SST and NOAA interpolated OLR.

4.6.3. Coupling of EQUINOO with the ocean component of IOD/Z Mode

Saji et al. [1999] suggested that equatorial zonal wind anomalies co-evolve with the ocean component of the IOD and EQUINOO has been considered to be the atmospheric component of IOD just as the southern oscillation is the atmospheric component of the coupled ENSO mode over the Pacific. We consider the relationship between EQUINOO and the ocean component during the summer monsoon season. The index suggested by Saji et al. [1999] for IOD is the Dipole Mode Index, DMI, which is defined as the difference in the SST anomalies of WEIO and EEIO. DMI is thus the index for the oceanic component of IOD. Note that the difference in the SST anomalies is equal to the anomaly of the difference in the SST of the two regions. Since SST gradients can directly influence the dynamics, anomaly of the gradient may be a better interpretation of DMI. We define DMI as the difference in the SST anomalies normalized by the standard deviation. Positive and negative IOD events are characterized by large positive/negative values of DMI respectively, continuously for several months. In the variation of DMI during 1982-2010 (Fig. 5.26) the events of 1994 and 1997 are seen to be the strongest pIOD events.

It turns out that that the relationship between DMI and EQWIN in the summer monsoon season is not strong (Fig. 4.27). In fact, EQWIN and DMI are of opposite signs in 18 out of 52 years and the correlation coefficient is only 0.5 between the indices suggesting that EQUINOO and the oceanic mode of IOD are not tightly linked. On the other hand, there is a tight linkage between the southern oscillation in the atmosphere and the fluctuations between El Nino and La Nina in the ocean, with the southern oscillation index being highly correlated to the different El Nino indices (correlation coefficient of 0.86 for the Nino3.4 index). The difference between the strength of the coupling between the atmospheric and oceanic components of these two modes is consistent with the difference between the strength of the coupling of the convection over the central Pacific to the SST and that of the convection over EEIO with the SST.

However, strong positive IOD events are associated with a strong phase of EQUINOO. Hence, understanding the evolution of such events is important for understanding and predicting the EQUINOO in the summer monsoon season.

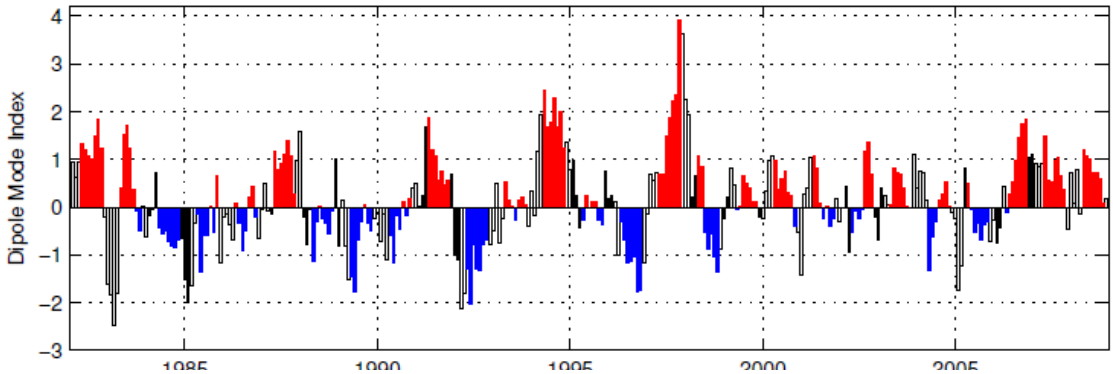

Fig. 4.26 : Variation of the monthly values of DMI for the period 1982-2010. Values between May-November are highlighted by filled bars

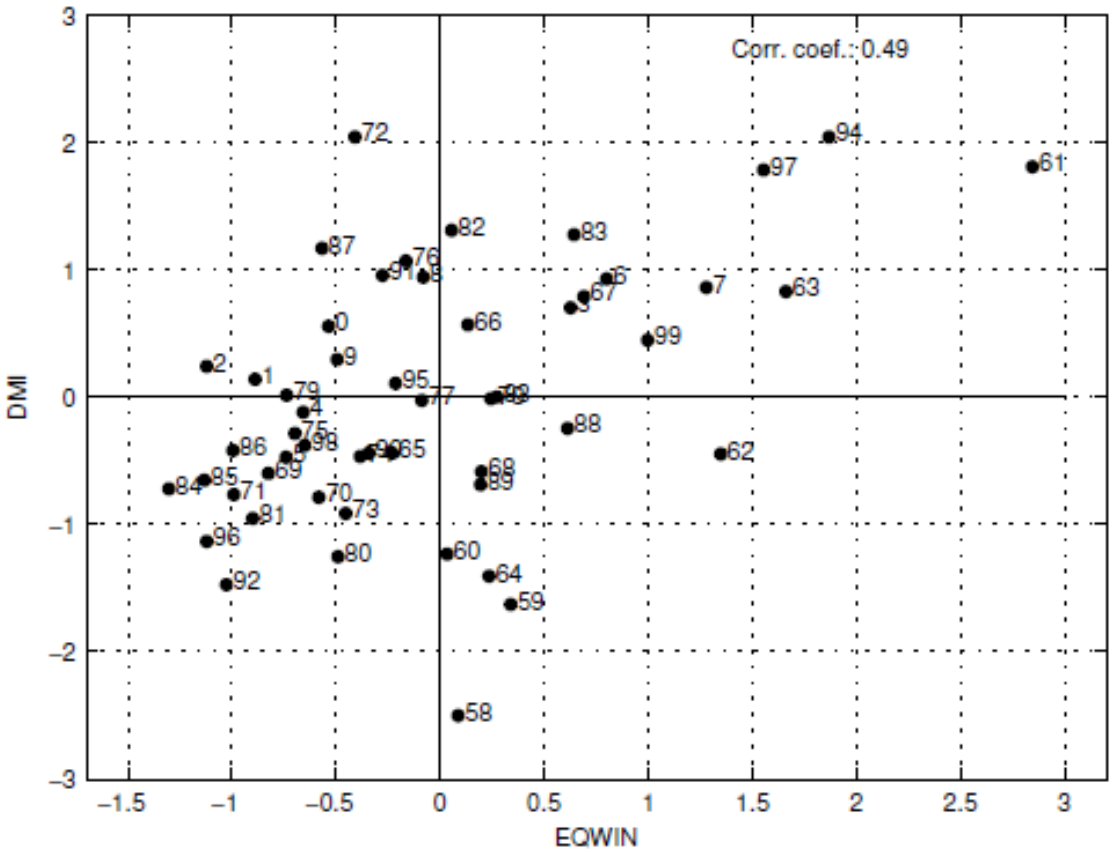

Fig. 4.2 : June-September mean values of DMI is plotted against EQWIN for the period 1958-2009

4.6.4. Evolution of the positive phase of EQUINOO

We consider first the evolution of the positive phase of EQUINOO associated with pIOD events. Here we consider the pIOD events in the satellite era i.e. 1982 onwards (Fig. 4.26). It is seen that in the period up to 1999 DMI is consistently larger than 1.0 during May-November 1982, March to December of 1994 and July-December 1997 and they have been identified as pIOD events [Yamagata et al., 2002; Vinayachandran et al., 2007]. During the strong pIOD events of 1994 and 1997, very large values of DMI occurred for several months. In 2003, a pIOD event was triggered, DMI was positive and large (but smaller than 1.0) from June to August; but midway through the season, the event was terminated [Rao and Yamagata, 2004]. A pIOD event occurred during the latter part of the summer monsoon season and autumn of 2006, with large values of DMI from September onwards [Vinayachandran et al., 2010, and references therein]. Recently, Cai et al. [2009] have suggested that 2007 and 2008 were also pIOD events. In fact, in these years positive phase of the IOD occurred during the summer monsoon season and the autumn. However, DMI exceeded 1.0 only in May and September of 2007 and during May-July of 2008. Hence by our definition, 2007 cannot be considered as a pIOD event, while 2008 could be considered as one with an exceptionally small life span.

An important attribute of the Indian Ocean Dipole is the out of phase relationship between the SST anomalies of EEIO and WEIO. We focus on the summer monsoon season. The June-September SST anomalies of EEIO and WEIO for 1958-2009 are depicted in Fig. 4.28. It is seen that the SST anomalies over the two regions are out of phase in only 17 out of 52 years. In a majority of the years, the anomalies are in phase, as expected from the association with ENSO. Thus the SST anomalies are in phase for the ENSO events of 1987, 1988, 1998 and 2010. While the ENSO mode accounts for about 30% of the variance, the IOD mode accounts for about 12% [Saji et al., 1999]. Of the seasons associated with negative SST anomalies of EEIO and positive anomalies of WEIO, DMI and the SST anomaly of EEIO are large for 1994 and 97. Note that for eight years, despite the SST anomalies being positive for EEIO and WEIO, DMI for June-September is positive and, for four of them (1983, 87, 2003,7), higher than 0.5. Thus if

'anomalously low sea surface temperatures off Sumatra' (i.e. negative SST anomaly of the SST of EEIO) is considered to be a distinguishing attribute of pIOD, DMI being large and positive is not a sufficient condition for the occurrence of a pIOD, although it is a necessary condition.

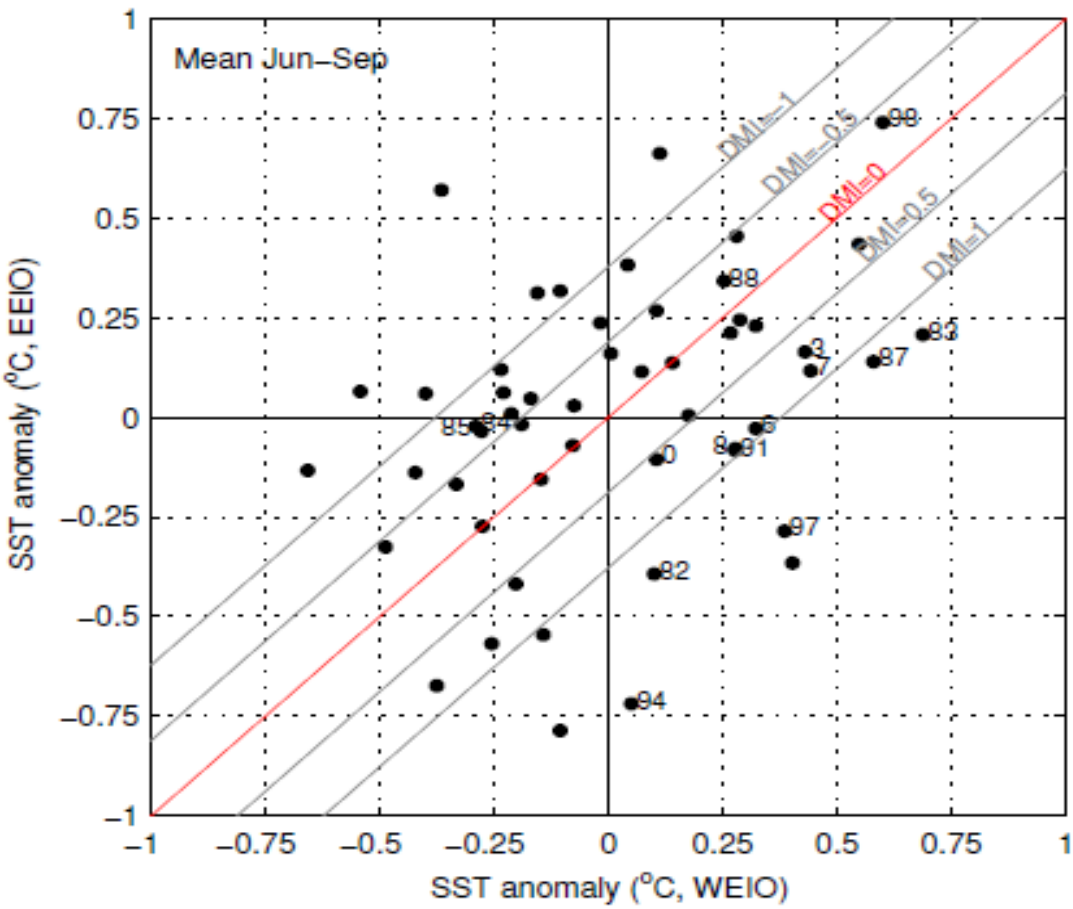

Fig. 4.28 : SST anomaly of the EEIO versus that of the WEIO for all the years in the period 1958-2009. The red line represents DMI=0.

We note that DMI is a measure of the anomaly of the SST gradient between WEIO and EEIO and large positive values are associated with WEIO being anomalously warm relative to EEIO. This can occur with the anomalies being of opposite sign as in the case of IOD events or with positive SST anomalies of both the regions as in the cases mentioned above. In the latter case, DMI is positive because the SST anomaly of the WEIO is larger than that of the EEIO, which could be considered as a positive phase of the zonal mode rather than the dipole mode. We note that of these cases, a strong positive phase of EQUINOO occurred in 2003, 2007 and 1983 (Fig. 4.20). On the other hand, seasons such as 1984, 85 are

characterized by a large negative SST anomaly of WEIO and positive OLR anomaly over WEIO and negative OLR anomaly over EEIO (Fig. 4.23 & 4.26). Thus it appears that the SST of WEIO plays some role in the convection over WEIO during the summer monsoon.

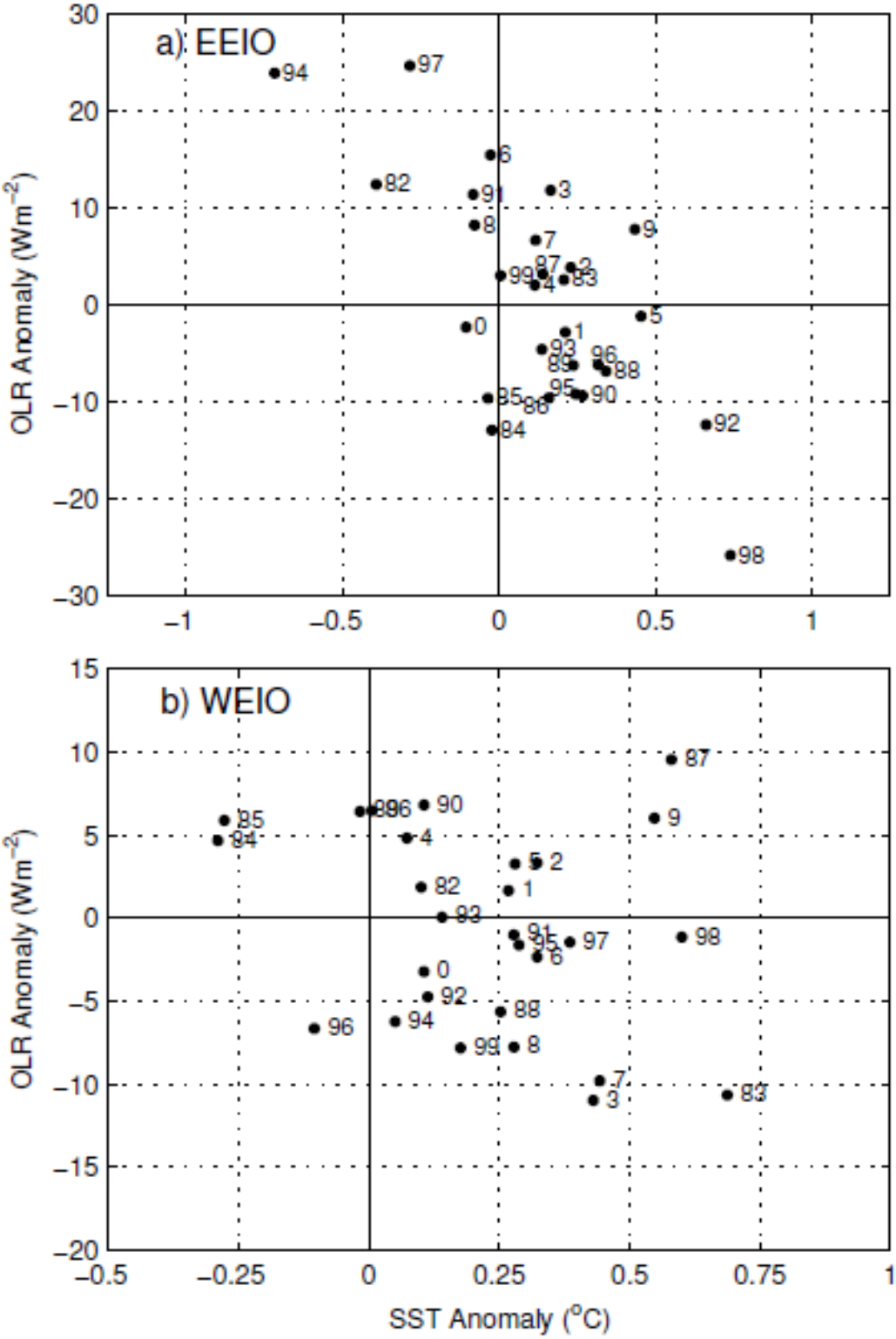

Fig. 4.29 : June to September mean OLR anomaly is plotted against SST anomaly for all the years in the period 1982-2009 for the a) EEIO & b) WEIO

However, it must be noted that the relationship of the OLR over WEIO to the SST of WEIO is much more complex than that for EEIO (Fig. 4.29), because the SST of WEIO is influenced, to a large extent, by atmospheric fluxes. Hence, high (low) SSTs can also result from cloud free (highly convective) conditions over WEIO remotely forced by an El Nino (La Nina) because of the enhanced (decreased) incoming radiation over WEIO. Thus while the seasons with maximum convection over WEIO i.e. 2003, 2007 and 1983 are amongst the warmest seasons for WEIO, the other seasons with very warm WEIO are the El Nino seasons of 1987 and 2009 (Fig. 4.29). These El Nino seasons are characterized by positive OLR anomaly over WEIO which is comparable to or higher than that for the cold SST seasons 1984, 85.

The variation of CI and SST of EEIO and WEIO for 2003, 2007 as well as that for 2008 (for which also EQUINOO was positive (Fig. 5.20) and which has been considered to be a pIOD event with a short life span which ended in August) is depicted in Figure 30. While suppression of convection over EEIO plays a critical role in pIOD events, enhancement of convection over WEIO plays an important role in seasons such as 2003, 2007 and 2008.

Positive IOD events are relatively rare (frequency of occurrence less than 1 in 5 years), and it is believed that they are triggered by some event during April-May [Annamalai et al., 2003; Francis et al., 2007]. The important facets of triggering are (i) suppression of convection over EEIO and (ii) strengthening of the winds parallel to the Sumatra coast. These have been attributed to different factors such as (i) a change in the Pacific Walker circulation [Annamalai et al., 2003] (ii) the intensification of the Hadley cell in the western Pacific between the South China Sea/Philippines Sea (SCS/PS) [Kajikawa et al., 2001] (iii) severe cyclones over the Bay of Bengal during April-May [Francis et al., 2007]. Since in late spring WEIO is also favourable for convection, suppression of convection over EEIO leads to enhancement of convection over WEIO (e.g. 1994 and 1997 in Fig. 4.24). Thus, triggering of a pIOD event by any of the mechanisms suggested, necessarily involves triggering of a positive phase of EQUINOO. *It should be noted that positive phase of EQUINOO is triggered whenever the convection over EEIO is suppressed, irrespective of whether it is accompanied by enhancement upwelling favourable winds i.e. irrespective of whether a pIOD is triggered or not.*

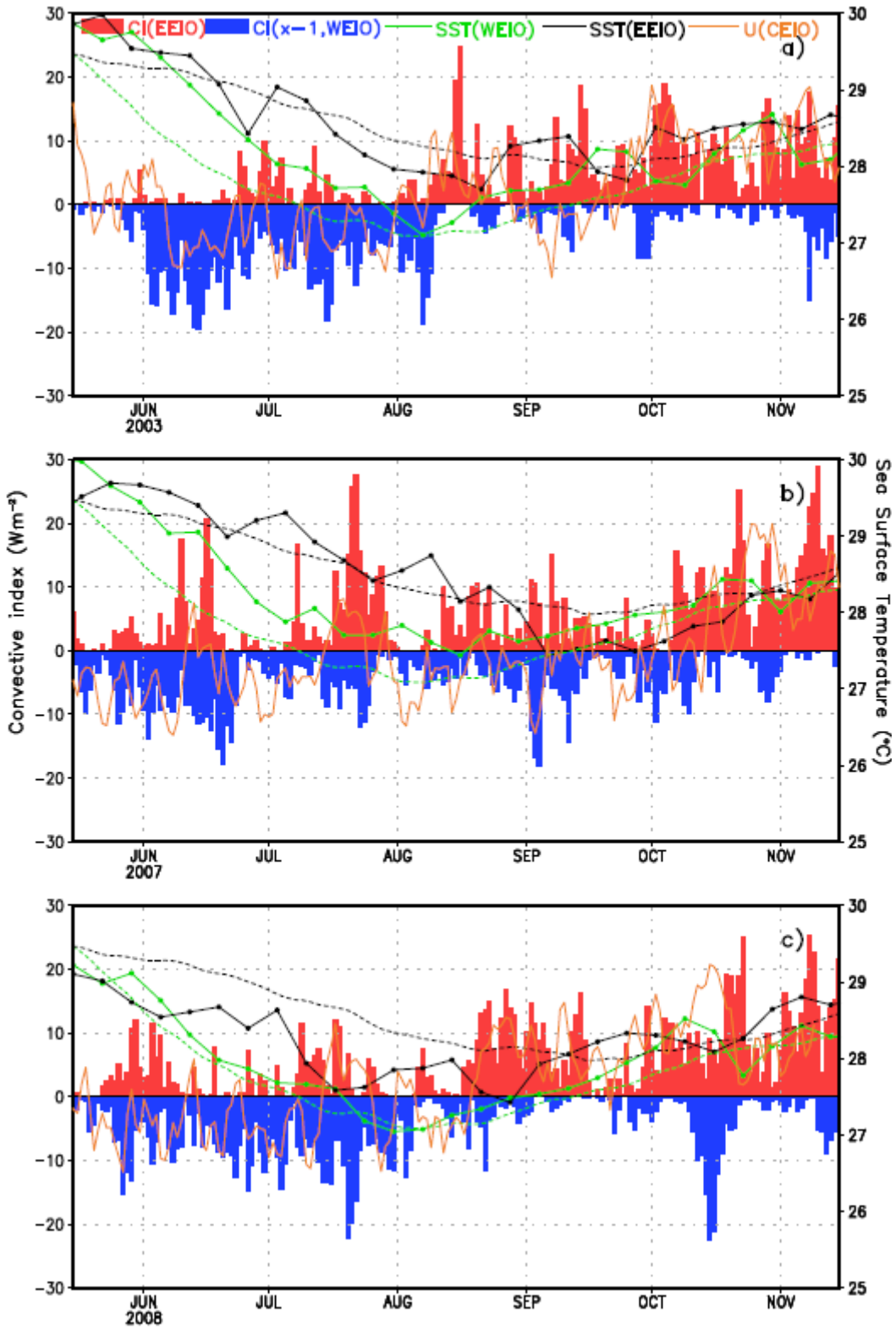

Fig. 4.30 : Variation of the convective index (CI) over EEIO (red) and negative of the CI over WEIO (blue), SST of EEIO (black), mean SST of EEIO(black dashed); SST of WEIO (green), mean SST of WEIO (green dashed);and zonal wind along CEIO(orange) for the years a) 2003, b) 2007 and c)2008.

Once triggered, the evolution of the pIOD involves continued suppression of the convection over EEIO, intensification of the positive phase of EQUINOO and decrease of the SST of EEIO leading to large negative SST anomalies. Weakening of the convection over EEIO and enhancement of convection over the WEIO implies a weakening of surface westerlies over the CEIO and anomalous convergence over the WEIO. This anomalous convergence leads to further enhancement of convection over WEIO, which in turn strengthens the anomalous easterlies over the CEIO further, until the winds become easterly. As the surface easterlies converge over the WEIO, convection is favoured over WEIO relative to EEIO. This east-west gradient in convection maintains the surface easterlies over the CEIO. These surface easterlies trigger upwelling favourable Kelvin Waves in the EEIO and contribute to anomalous cooling of the EEIO. Francis et al. [2007] suggested that this positive feedback between convection and circulation can lead to suppression of convection over EEIO and anomalous cooling of EEIO for periods of several weeks after the event which led to the initial suppression of convection over EEIO. It should be noted that the enhancement of convection over WEIO during this period can occur despite an adverse SST gradient between EEIO and WEIO as in 1997 (Fig. 4.24).

During this positive phase of EQUINOO, the WEIO cools rapidly because of the enhanced convection and the SST of EEIO also decreases rapidly because of the enhanced upwelling/mixing. Depending on the initial SST anomalies and the rates of cooling of the two regions, the SST gradient between them changes during the season. The rates of cooling depend on the forcing (i.e. upwelling favourable winds over EEIO, convection over WEIO) as well as the depth of the thermocline and heat content of the upper layers of these regions. We elucidate the roles of the different factors by an analysis of the different cases.

We can get an insight into the role of the SST gradient as well as the SST of the EEIO by comparing the pIOD event of 1997 with the aborted event of 2003 (Fig. 4.24 & Fig. 4.30). It is seen that in June-July, convection over EEIO was suppressed and convection over WEIO was high. However, convection over WEIO was more intense in 2003, relative to that in 1997, perhaps because of the high SST. In 1997, EEIO was warmer than WEIO in June and most of July; the SST of

the two regions was close in August. In September while the SST of EEIO decreased to values below the threshold, WEIO warmed and the SST gradient was reverse of the climatological gradient. The convection over EEIO continued to be suppressed and the favourable SST gradient contributed to the sustenance of convection over WEIO during August-November in 1997. On the other hand in 2003, WEIO cooled more rapidly than EEIO and EEIO was warmer than WEIO throughout the summer monsoon and beyond. Also the SST of EEIO never decreased to values below the threshold in 2003. When the long spell of intense convection over WEIO ended in August, convection revived over EEIO and was sustained there throughout September. Subsequently, although there was intermittent convection over WEIO, the convection over EEIO was clearly dominant. Thus the evolution of the SST in the EEIO and convection over EEIO in 1997 is markedly different from that in 2003 from September onwards. The major difference in the SST evolution is the faster cooling of EEIO in 1997. The thermocline of EEIO was shallow in 1997 compared to climatology whereas that in 2003 deeper (Fig. 4.31a). Hence, although the upwelling favourable winds were comparable [Francis et al., 2007], the SST of EEIO decreased more rapidly in 1997 than in 2003 and became lower than the threshold from September, thereby stabilizing the positive EQUINOO phase and leading to the maturation into the stage of a strong pIOD event.

In 1994 also, the thermocline of EEIO was shallow. In addition, initial conditions played a role. In the beginning of the season, the SST anomaly of EEIO was negative and WEIO positive with WEIO being warmer than EEIO. With intense convection over WEIO from mid-May, the WEIO cooled very rapidly relative to EEIO and became cooler than EEIO in June. At the end of June, the convection over WEIO decreased, SST of WEIO increased and in July with the SST of WEIO close to that of EEIO, convection over WEIO intensified. By the last week of July, rapid cooling of EEIO led to the SST going well below the threshold and convection over EEIO was totally suppressed from then until November. From August onwards WEIO was warmer than EEIO and convection over WEIO continued to dominate over that over EEIO until November. Thus it appears that as in 1997, EEIO cooling below the threshold played an important role in sustaining the positive phase of EQUINOO throughout the summer monsoon of 1994 and beyond.

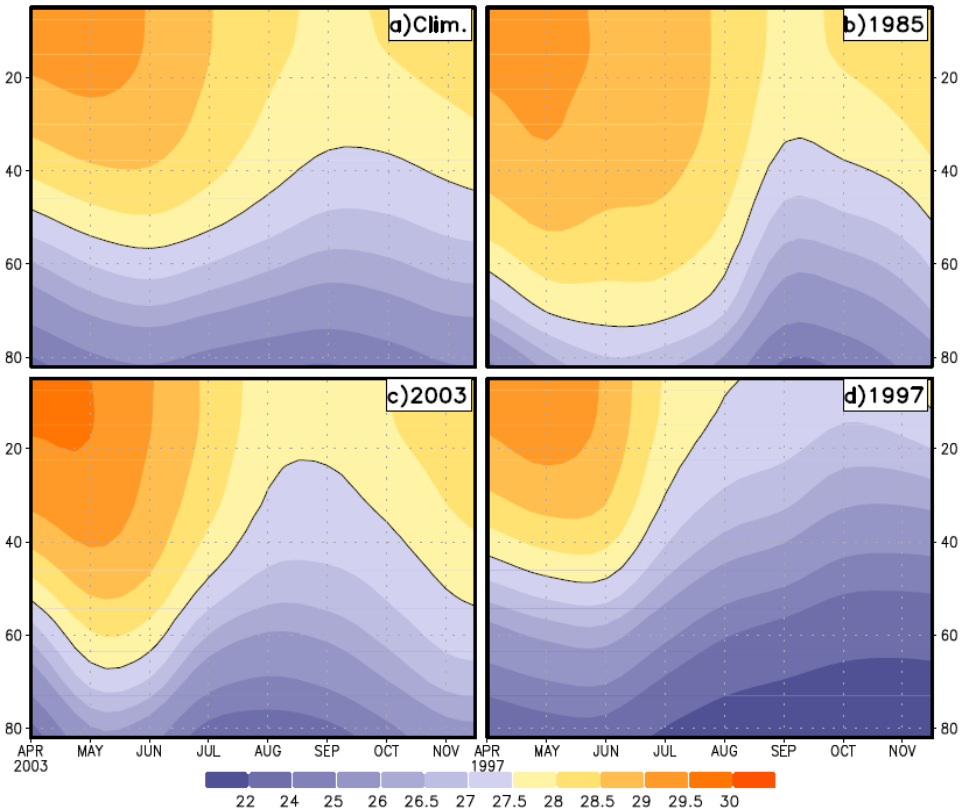

Fig. 4.31a : Time-depth section of temperature (from SODA) in the EEIO for 1985, 2003 and 1997. Climatology is shown in the top left

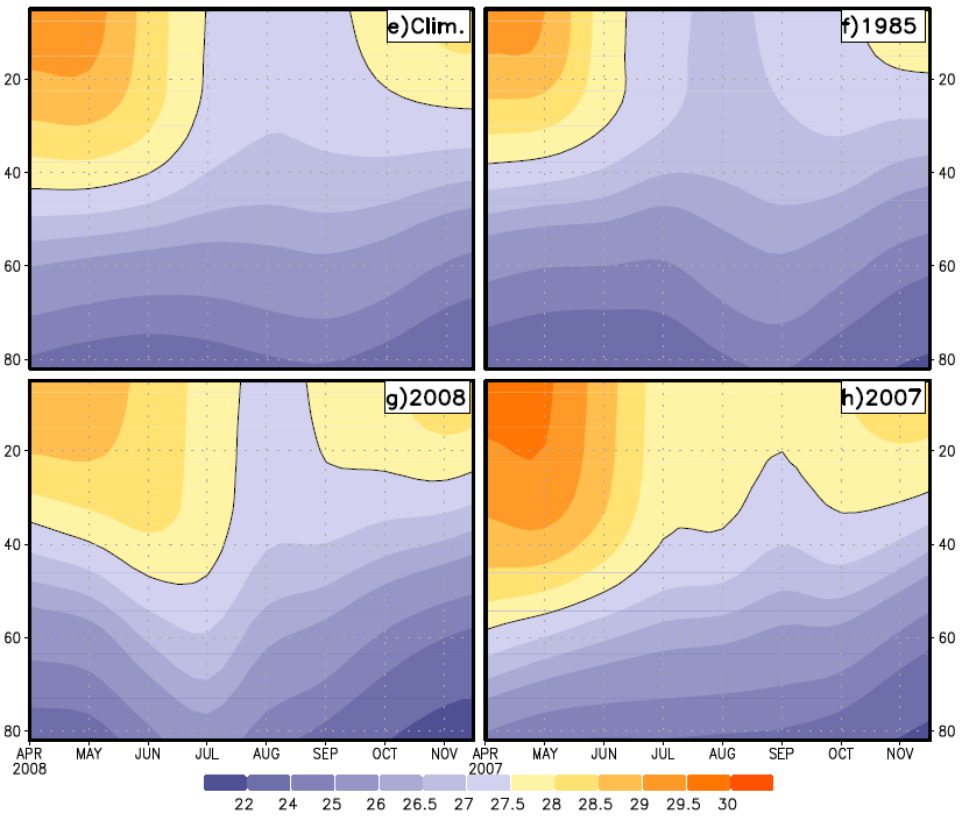

Fig. 4.31b : Time-depth section of temperature (from SODA) in the WEIO for 1985, 2007 and 2008. Climatology is shown in the top left panel.

It is of interest to consider the season of 2007 in which a pIOD event was not triggered but EQUINOO was positive throughout, In 2007, the SST anomaly of WEIO was positive from mid-May to October. The variation of the SST was rather similar to that of the mean SST, with an anomaly around 0.5^0C throughout this period. The EEIO SST was also above normal and higher than SST of WEIO until August. EEIO rapidly cooled in the second half of August and became cooler than WEIO and stayed so until the end of October. Thus in the critical month of September, the SST gradient was favourable for convection over WEIO. There was a high propensity of convection over WEIO throughout the summer monsoon season and the phase of EQUINOO was continuously positive. However, unlike in the cases of strong pIOD (Fig. 4.23), the convection over EEIO was never completely suppressed. Despite the convection over WEIO being maintained above the normal throughout the season, the SST did not decrease rapidly. This is because the thermocline in WEIO was much deeper in 2007 than climatology (Fig. 4.31b).

Thus it appears that once triggered, the convective dynamic feedbacks can sustain the positive phase of EQUINOO despite an unfavourable zonal SST gradient until sometime in August. For sustainenance of the positive phase of EQUINOO after that, the SST gradient has to be favourable (with WEIO warmer than EEIO). If, in addition, the SST of EEIO decreases to values below the threshold (as in 1994 and 1997), the convection over EEIO is totally suppressed and results in a mature pIOD event. However, even when EEIO does not cool to such levels and convection over EEIO is not totally suppressed, the positive phase of EQUNOO can be sustained through September with higher propensity of convection over WEIO than over EEIO as in 2007.

4.6.5. Towards prediction of EQUINOO

It is clear that prediction of the evolution of EQUINOO is a difficult problem. We have seen that some factors can lead to the suppression of convection over EEIO and hence a positive EQUINOO phase towards the beginning of the summer monsoon, which can be sustained for the first half of the season as a result of positive feedbacks between convection and circulation. The SST patterns appear to

play an important role in sustaining the phase in the latter half of the season. Thus, prediction of the SST of WEIO and EEIO for the summer monsoon season is important.

We find that despite the many factors that determine the evolution of the SST of WEIO and EEIO, the SST of these regions in the summer monsoon season is strongly related to that in May (Fig. 4.32). Whether there are other facets of the ocean and atmosphere in the boreal spring that can give a clue about the evolution in the summer monsoon needs to be explored.

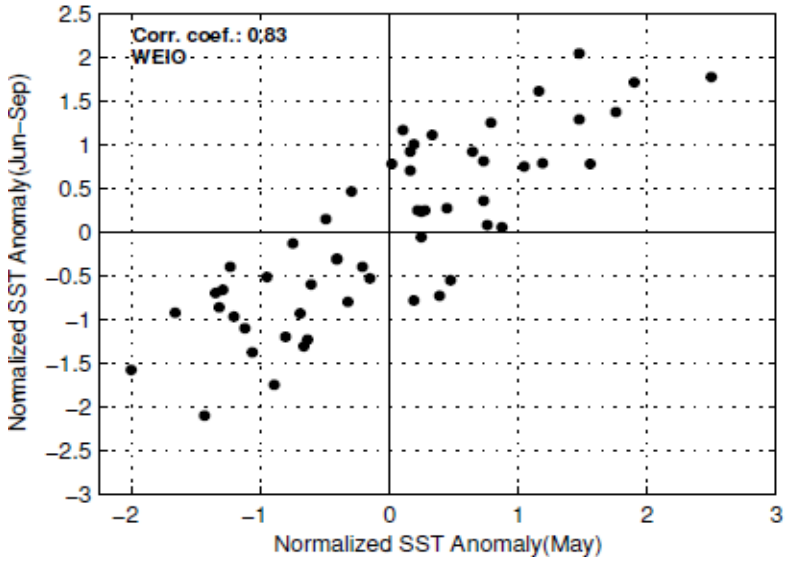

Fig. 4.32a : Normalized June-September SST anomaly of WEIO versus SST anomaly for May of WEIO

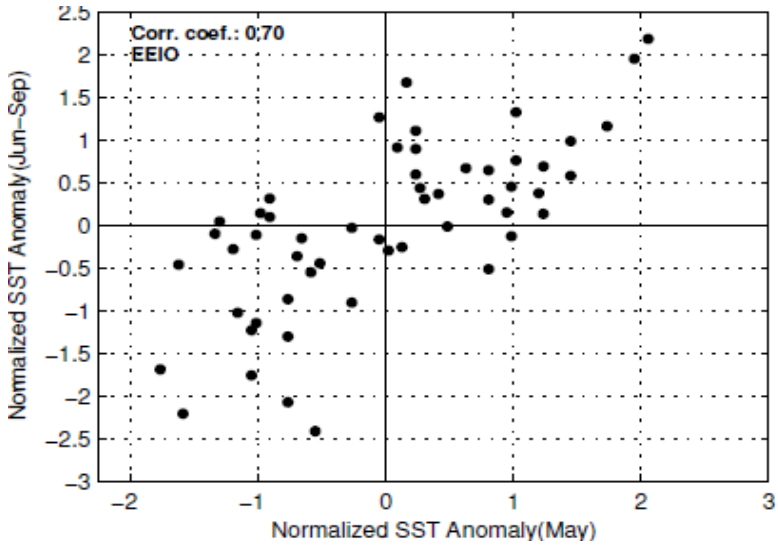

Fig. 4.32b : Normalized June-September SST anomaly of EEIO versus SST anomaly for May of EEIO

4.7. Concluding remarks

We have elucidated the important role of the convection over the equatorial Indian Ocean in the onset phase, in intraseasonal variation between active and weak spells as well as in the interannual variation of the ISMR. The onset phase comprises northward propagation of the TCZ from the equatorial Indian Ocean and westward propagation of synoptic scale systems from the Bay of Bengal. The advance of the monsoon from Kerala can be hampered if the EEIO is warmer than the Bay in May-June as seen in the case of 2009. On the intraseasonal scale, the most dominant signal of the breaks is an enhancement of the convection over EEIO with suppression over WEIO, i.e. negative phase of EQUINOO. On the interannual scale, the worst droughts are associated with an unfavourable phase of ENSO (i.e. El Nino) and negative phase of EQUINOO. On the other hand, enhancement of convection over WEIO is favourable for the monsoon, with no chance of a drought and suppression of convection over WEIO is unfavourable, with no chance of excess rainfall. We believe that the most important impact of the atmosphere over the Indian Ocean (and hence of the Ocean itself) on the monsoon occurs via EQUINOO. Thus monitoring the convection over WEIO and EEIO and, if possible, predicting the evolution of EQUINOO is important for generating predictions of the important phases of the monsoon, on different time-scales.

One of the major achievements of the last two decades has been the unravelling of the critical facets of ENSO made possible by improved observations of the equatorial Pacific and development of models capable of simulating and predicting them. If in addition to a a reliable prediction of ENSO for the forthcoming summer monsoon season, one for the likely phase of EQUINOO can be generated, there will be a marked improvement in the prediction of the Indian summer monsoon rainfall.. The evolution of the convection over the equatorial Indian Ocean depends on convection over regions such as Bay of Bengal and South China Sea/West Pacific (particularly for triggering), as well as more remote factors such as descent over EEIO induced by El Nino. Such factors also have an impact on upwelling favourable winds and hence on the evolution of the SST over EEIO. The SST of WEIO is directly influenced by convection over WEIO. The magnitude of the

response to the atmospheric forcing over WEIO and EEIO depends upon the depth and heat content of the upper layers of the two regions. In addition, the initial SST pattern plays a role in determining the evolution of EQUINOO.

By monitoring the convection over critical regions as well as the detailed profiles of the temperature with depth of EEIO and WEIO, it should be possible to predict the phase of EQUINOO in the forthcoming summer monsoon. This suggests that a buoy network in the equatorial Indian Ocean such as the TOGA-TAO network in the Pacific, could contribute substantially towards making predictions of EQUINOO.

If in the next few years, by improving observations-particularly of the critical oceanic regions, analysis of observations and modelling studies yield deeper insight into the processes that lead to the transition between the phases of the EQUINOO, it may become possible to generate reliable predictions of the evolution of EQUINOO and thereby contribute to generating such predictions of important facets of monsoon variability.

References

Annamalai, H., Murtugudde, R., Potemra J, Xie, S. P., Liu, P. and Wang, B., 2003, "Coupled dynamics over the Indian Ocean: Spring initiation of the zonal mode", Deep. Sea. Res. Part II 50 2305–2330.

Bjerknes J.,1969, "Atmospheric teleconnections from the equatorial Pacific", Mon. Weather Rev. 97, 163–72.

Bony, S., Lau, W.K.M. and Sud, Y. C., 1997, "Sea surface temperature and large-scale circulation influences on tropical greenhouse effect and cloud radiative forcing", J. Climate, **10**, 2055–2077.

Cai W., Pan, A., Roemmich, D., Cowan, T., Guo, X.,2009, "Argo profiles a rare occurrence of three consecutive positive Indian Ocean Dipole events, 2006-2008", Geophys. Res. Lett., 36, 8, L08701,DOI:10.1029/2008GL037038.

Carton, J. and Giese, B. S., 2008, "A Reanalysis of Ocean Climate Using Simple Ocean Data Assimilation", (SODA), Mon. Wea. Rev., 136 (8), 2999-3017.

Charney, J. G., 1969, "The intertropical convergence zone and the Hadley circulation of the atmosphere. Proceedings of WMO/IUGG Symposium on Numerical Weather Prediction", Japan Meteorological Agency, vol. III, pp. 73–79.

De U. S., Lele R. R. and Natu J. C., 1998, "Break in south-west monsoon", India Meteorological Department, Report No. 1998/3.

Ding, Y., and Sikka, D. R., 2005, "Synoptic systems and weather in the Asian monsoon (Ed. B. Wang) Praxis", Ehichester, U.K. 131-202.

Francis, P. A., Gadgil Sulochana and Vinayachandran, P. N., 2007, "Triggering of the positive Indian Ocean dipole events by severe cyclones over the Bay of Bengal", Tellus A59(4) 461–475 doi: 10.1111/j.1600-0870.2007.00254.x..

Francis, P. A. and Sulochana Gadgil, 2010,"Towards understanding the unusual Indian monsoon in 2009", J. Earth Sys. Sci., 119 (4), 397-415.

Francis, P. A. and Gadgil Sulochana, 2009, "The aberrant behaviour of the Indian monsoon in June 2009", Curr. Sci. 97(9) 1291–1295.

Gadgil S., Joseph, P.V., Joshi, N.V., 1984, "Oceanatmosphere coupling over monsoon regions", Nature 312:141–43.

Gadgil, S., 1988, "Recent advances in monsoon research with particular reference to the Indian monsoon", Aust. Meteorol. Mag., 36, 193–204.

Gadgil, S., 2003, “The Indian monsoon and its variability”, Annu. Rev. Earth Planet. Sci., 31, 429–467.

Gadgil, S. and Joseph, P. V., 2003, “On breaks of the Indian monsoon”, Proc. Indian. Acad. Sci. (Earth Planet. Sci.), 112, 529–558.

Gadgil, S, Vinayachandran, P. N. and Francis, P. A., 2003, “Droughts of Indian summer monsoon: Role of clouds over the Indian Ocean”, Curr. Sci. 85 1713–1719.

Gadgil, S., Vinayachandran, P. N., Francis, P. A. and Gadgil Siddhartha, 2004, “Extremes of the Indian summer monsoon rainfall, ENSO and the equatorial Indian Ocean oscillation”, Geophys. Res. Lett. 31 L12213 doi:10.1029/2004GL019733.

Gadgil, S. and Gadgil, Siddhartha, 2006, “The Indian Monsoon, GDP and Agriculture”, Econ. Pol. Wkly., XLI, 4887–4895.

Gadgil, S., M. Rajeevan and Francis, P. A., 2007, “Monsoon variability: Links to major oscillations over the equatorial Pacific and Indian oceans”, current science, 93, 2, 25, 182-194.

Gadgil, S., Rajeevan, M., Zubair, L. and P. Yadav, 2011, “Interannual Variation of the South Asian Monsoon: Links with ENSO and EQUINOO”, The global monsoon system: Research and Forecast, 2nd Edition World Scientific Series on Asia-Pacific Weather and Climate, Vol. 5, 25-42.

Garcia, O., 1985, “Atlas of highly reflective clouds for the global tropics: 1971–1983”, US Dept. Commer. NOAA, Environ. Res. Lab.

Graham, N.E., Barnett, T.P., 1987, “Sea surface temperature, surface wind divergence, and convection over tropical oceans”, Science 238:657–59.

Halley, E., 1686, “An historical account of the trade winds, and monsoons, observable in the seas between the tropics, with an attempt to assign the physical cause of the said winds”, Philos. Trans. R. Soc. London, 16, 153–168.

Hastenrath, S., 2002, “Dipoles, temperature gradients, and tropical climate anomalies”, Bull. Amer. Meteor. Soc. 83 735–740.

Ihara, C, Kushnir, Y., Canea, M. A. and Pena, V. H. D. L., 2007, “Indian summer monsoon rainfall and its link with ENSO and Indian Ocean climate indices”, Int. J. Climatol. 27 179–187.

Joseph, P.V., Pillai, P.V., 1984, “Air-sea interaction on a seasonal scale over north Indian Ocean—Part I. Interannual variation of sea surface temperature and Indian summer monsoon rainfall”, Mausam 35:323–30.

Joseph, P. V., Eischeid, J. K. and Phyle, R. J., 1994, “Inter annual variability of the onset of summer monsoon and its associations with atmospheric features, El Nino and sea surface temperature anomalies”, J. Climate, 7, 81-105.

Joseph P. V., 2011a, “Synoptic Systems during Monsoon season”, Monsoon Monograph, Ed. Asnani et al, India Meteorological Department, N. Delhi, Vol. 1, 554pp.

Joseph P. V., 2011b, “Onset, Advance and Withdrawal of Monsoon”, Monsoon Monograph, Ed. Asnani et al, India Meteorological Department, N. Delhi, Vol. 1, 554pp.

Kalnay, E, Kanamitsu, M., Kistler, R., Collins, W., Deaven, D., Gandin, L., Iredell, M., Saha, S., White, G., Woollen, J., Zhu, Y., Leetmaa, A., Reynolds, R., Chelliah, M., Ebisuzaki, W., Higgins, W., Janowiak, J., Mo, K., Ropelewski, C., Wang, J., Jenne, R. and Joseph, D., 1996, “The NCEP/NCAR 40-Year Reanalysis Project”, Bull. Amer. Meteor. Soc. 77 437–471.

Kajikawa, Y., Yasunari, T. and Kawamura, R., 2001, “The role of local Hadley circulation over the western Pacific on the zonally asymmetric anomalies over the Indian Ocean”, J. Meteorol. Soc. Japan 81, 259–276.

Kothawale, D. R. and Rupa Kumar, K., 2002, “Tropospheric temperature variation over India and links with the Indian summer monsoon: 1971–2000”, Mausam, 53, 289–308.

Krishna Kumar, K., Rajagopalan, B. and Cane, M. A., 1999, “On the weakening relationship between the Indian monsoon and ENSO”, Science, 284, 2156–2159.

Krishnamurti, T. N. and Bhalme, H. N., 1976, “Oscillations of monsoon system. Part I: Observational aspects”, J. Atmos. Sci., 45, 1937–1954.

Lau, W.-K. M., and C.-H. Sui, 1997, “Mechanisms for short-term sea surface temperature regulation: Observations during TOGA COARE”, J. Climate, **10,** 465–472.

Li, T., Wang, B., Chang, C. P. and Zhang, Y., 2003, “A theory for the Indian Ocean dipole-zonal mode”, J. Atmos. Sci. 60 2119–2135.

Pant, G. B. and Parthasarathy, B., 1981, “Some aspects of an association between the southern oscillation and Indian summer monsoon”, Arch. Meteorol. Geophys. Biokl. 29 245–251.

Parthasarathy, B, Munot, A.A. and Kothawale, D,R., 1992, “Indian summer monsoon rainfall indices: 1871–1990”, Meteorol. Mag. 121:174–86

Parthasarathy, B., Munot, A.A., Kothawale, D.R., 1995, “Monthly and seasonal rainfall series for all-India homogeneous regions and meteorological subdivisions: 1871–1994”, IITM Research Report-065, Indian Institute of Tropical Meteorology, Pune, India.

Philander, S. G. H., 1990, “El Nino, La Nina and the Southern Oscillation”, Academic Press, New York, pp. 293.

Murtugudde, R., McCreary, J. P. and Busalacchi, A. J., 2000, “Oceanic processes associated with anomalous events in Indian Ocean with relevance to 1997–98”, J. Geophys. Res. 105 3295–3306.

Rajeevan, M., Bhate, J., Kale, J. D. and Lal, B., 2006, “High resolution daily gridded rainfall data for the Indian region. Analysis of break and active monsoon spells” Curr. Sci., 91, 296 – 306.

Rajeevan M, Gadgil Sulochana, Bhate, J., 2010, “Active and break spells of the Indian summer monsoon”, J Earth Syst. Sci. 119(3):229–247.

Rajeevan, M., 2011, “Global Teleconnections of Indian Summer Monsoon Rainfall Variability”, Monsoon Monograph, Ed. Asnani et al, Indian Meteorological Department, N. Delhi, Vol. 1, 554pp.

Ramamurthy, K., 1969, “Monsoon of India: some aspects of the ‘break’ in the Indian southwest monsoon during July and August”, Forecast. Man. 18.3(No. IV):1–57. India Meteorol. Dept., Poona, India.

Rao, K.G., Goswami, B.N., 1988, “Interannual variations of sea surface temperature over the Arabian Sea and the Indian monsoon: a new perspective”, Mon.Weather Rev. 116(No. 3):558–68.

Rao, S. A. and Yamagata, T., 2004, “Abrupt termination of Indian Ocean dipole events in response to intraseasonal disturbances”, Geophys. Res. Lett. 31 L19306 doi:10.1029/2004GL020842.

Rao, Y.P., 1976, “Southwest Monsoon”, Meteorol. Monogr. No. 1. India Meteorol. Dept., New Delhi. 366 pp.

Rasmusson, E. M. and Carpenter, T. H., 1983, “The relationship between eastern equatorial Pacific sea surface temperatures and rainfall over India and Sri Lanka”, Mon. Weather Rev. 111, 517–528.

Rayner, N. A, Parker, D. E., Horton, E. B., Folland, C. K., Alexander, L. V. and Rowell, D. P., 2003, “Global analyses of sea surface temperature, sea ice, and night marine air temperature since the late nineteenth century”, Journal of Geophysical Research, Vol. 108, No. D14, 4407, doi:10.1029/2002JD002670.

Reynolds, R. W., Rayner, N. A., Smith, T. M., Stokes, D. C. and Wang, W. Q., 2002, “An improved in situ and satellite SST analysis for climate”, J. Climate, 15, 1609–1625.

Riehl, H., 1954, “Tropical Meteorology”, McGraw Hill, New York, p. 392.

Riehl, H., 1979 “Climate and Weather in the Tropics”, Academic Press, New York, p. 611.

Saji, N. H., Goswami, B. N., Vinayachandran. P. N. and Yamagata, T., 1999, “A dipole mode in the tropical Indian Ocean”, Nature, 401, 360–363.

Shankar, D., Shetye, S. R. and Joseph, P. V., 2007, “Link between convection and meridional gradient of sea surface temperature in the Bay of Bengal”, J. Earth System Sci., 116, 385-406.

Shukla, J., Misra, B.M., 1977, “Relationships between sea surface temperature and wind speed over the central Arabian sea and monsoon rainfall over India”, Mon. Weather Rev. 105:998–1002.

Shukla, J., 1987, “Long-range forecasting of monsoons”, In Monsoons, ed. JS Fein, PL Stephens, pp. 523–48. Somerset, NJ: Wiley.

Sikka, D. R and Gadgil, S., 1978, “Large-scale rainfall over India during the summer monsoon and its relation to the lower and upper tropospheric vorticity”, Indian J. Meteorol. Hydrol. Geophys., 29, 219–231.

Sikka, D. R., 1980, “Some aspects of the large-scale fluctuations of summer monsoon rainfall over India in relation to fluctuations in the planetary and regional scale circulation parameters”, Proc. Indian Acad. Sci. (Earth Planet Sci.) 89 179–195.

Sikka, D. R. and Gadgil S., 1980, “On the maximum cloud zone and the ITCZ over Indian longitudes during the southwest monsoon”, Mon. Weather Rev. 108 1122–1135.

Sikka, D.R., 2011, “Scientific Studies on the South West Monsoon – Past, Present and Prospects”, Monsoon Monograph, Ed. Asnani et al, India Meteorological Department, N. Delhi, Vol. 1, 554pp.

Simpson, G., 1921, “The south-west monsoon”, Q. J. R. Meteorol. Soc., 199(17), 150–173.

Vinayachandran, P. N., Iizuka, S. and Yamagata, T.,2002, “Indian Ocean dipole mode events in an ocean general circulation model”, Deep Sea Research Part II, 49, 1573-1596.

Vinayachandran, P. N., Kurian, J. and Neema, C. P., 2007, “Indian Ocean response to anomalous conditions in 2006”, Geophys. Res. Lett., 34, L15,602, doi: 10.1029/2007GL030194.

Vinayachandran, P. N., Francis, P. A.and Rao, S. A., 2009, “Indian ocean dipole: Processes and Impacts, in Current Trends in Science”, Platinum Jubilee Special, Indian Academy of Sciences, p569 589.

Waliser, D. E., and Graham, N. E., 1993, “Convective cloud system and warm pool sea-surface temperature: coupled interaction and self regulation”, J. Geophys. Res., 98,12881-12893.

Webster, P.J., 1987, “The elementary monsoon”, In Monsoons, ed. JS Fein, PL Stephens, pp. 3–32. New York: Wiley.

Webster, P.J., Magana, V.O., Palmer, T.N., Shukla, J.and Tomas, R,A, 1998, “Monsoons: processes, predictability, and the prospects for prediction”, J. Geophys. Res. 103(No. C7):14451–510.

Wyrtki, K., 1973, “An equatorial jet in the Indian Ocean”, Science, 181, 262-264.

Yamagata, T., Behara, S. K., Rao, S. A., Gaun, Z., Ashok, K. and Saji, N. H., 2002, “The Indian Ocean dipole: a physical entity”, CLIVAR Exchanges, 24, 7,2, 15-18.

Zhang, C., 1993, “Large-scale variability of atmospheric deep convection in relation to sea surface temperature in the tropics”, J. Climate, 6, 1898–1912.

CHAPTER 5

MONSOON SIMULATION

R. Krishnan, Ayantika Dey Choudhury,
Rajib Chattopadhyay and M. Mujumdar
Indian Institute of Tropical Meteorological, Pune
krish@tropmet.res.in

5.1. Introduction

The South Asian summer monsoon or the southwest monsoon is one of the most spectacular phenomena of the global climate system characterized by strong seasonal wind reversals and pronounced rainy season. On an average, the mean monsoon precipitation over India during the June to September season accounts for nearly 80% of the country's annual rainfall. Despite the remarkable regularity of the seasonal monsoon circulation, the precipitation distribution undergoes significant inter-annual (year-to-year) variability and exerts profound influence on the agricultural production, economy and human-lives of more than one billion inhabitants in the region. In view of the major socio-economic implications of the monsoon performance during any given year, long range forecasts of the seasonal monsoon rains for the South Asian countries are of paramount importance. While land-sea thermal contrast arising in response to the seasonal variation of the latitude of maximum insolation is necessary for setting up the summer monsoon circulation initially, it is well-recognized that interactions between the monsoonal winds and latent heating from the organized convective systems are crucial for sustaining and driving the seasonal summer monsoon (e.g. Webster et al., 1998, Gadgil, 2003, Goswami, 2005). In other words, the vigor of the monsoon is essentially maintained by the coupling of monsoon circulation and precipitation through convection; and the release of latent heat from organized tropical

convective systems is the major energy source that drives the summer monsoon circulation. From the subsequent discussions, it will be seen that the main challenge in extended prediction of the monsoonal rains mostly arises from the intrinsic complexities of accurately representing the convectively coupled processes of the monsoon system in dynamical forecast models.

5.2. Simulation of mean monsoon

Since the initial development of general circulation models, a large numbers of studies have been carried out to simulate and understand the southwest monsoon system. Manabe et al. (1965) simulated a fairly realistic distribution of tropical precipitation, the Inter Tropical Convergence Zones (ITCZ) and the subtropical dry zones by incorporating the effects of moist convection and hydrological cycle through a 'moist convective adjustment' scheme. The simulation of a realistic ITCZ naturally paved the way to study the simulation of the monsoon climate which also started around the same time. Krishnamurti (1969) tried to predict the scale organization within the ITCZ or low latitudes in general. Washington (1970) experimented with a 5-layer National Centre for Atmospheric Research (NCAR) general circulation model (GCM) which also showed the basic monsoon features like strong cross-equatorial jets near Somalia, formation of Tropical Easterly Jet and appearance of low level westerly over Indian region. Murakami et al., (1970) and Godbole (1973) formulated a simplified model of zonally symmetric motion in two-dimension and conducted several numerical simulations by applying mean conditions at 80°E. Their simulations could capture the principal areas of zonal westerlies and easterlies and their results also brought out the importance of the thermal and dynamical influence of the Himalayas on the development of the summer monsoon circulation. The incorporation of seasonal variation of insolation and sea surface temperature (SST) by Manabe et al. (1974) and convective parameterization further showed some improvements in the seasonal variation of ITCZ, tropical rain-belt and the flow associated with ITCZ. Manabe and Terpestra (1974) and Hahn and Manabe (1975) investigated the

effects of mountain topography on the South Asian monsoon circulation by performing numerical simulations using the Geophysical Fluid Dynamics Laboratory (GFDL) general circulation model (GCM). Their study showed that the Tibetan Plateau acts as an elevated heat-source and maintains the upper-tropospheric anticyclone during the boreal-summer. They pointed out that the inclusion of mountain topography in the GCM resulted in realistic simulations of the South Asian monsoon trough and large-scale stationary flow features around the Tibetan Plateau. Washington and Daggupaty (1975) noted significant improvements in the simulation of monsoon large-scale features using the NCAR 6-layer GCM and a horizontal resolution of 2.5° X 2.5° with detailed physical processes like solar and infrared radiation, cumulus convection, sub-grid scale horizontal and vertical transport of latent heating, sensible heating and momentum. Gilchrist (1977) examined the horizontal distribution of circulation in the lower and upper troposphere, precipitation, sea level pressures using a large number of contemporary models available at that time (GFDL, Rand, NCAR, British Met Office). All the models simulated qualitative aspects of lower and upper tropospheric circulation like the Tropical Easterly Jet, the Somali Jet and the low-level westerly flow in the vicinity of the Indian subcontinent. Due to the coarse model resolution and simplified treatment of physical processes, the simulation of summer monsoon rainfall distribution in the models was rather modest. For example, Gichrist (1977) noted that models particularly underestimated the rainfall around the Western Ghats, Ganges valley and northern India and over estimated the rainfall in the tropical Indian Ocean. This brought out the necessity of improving the monsoon rainfall simulation by enhancing the model resolution and incorporating improved parameterizations of physical processes.

During the 1970s, attempts were made to simulate the evolution of monsoon synoptic disturbances (e.g., lows and depressions) over the Indian region and the associated rainfall distribution using GCMs (e.g. Krishnamurti et al., 1976, 1977). Following the MONEX observational program and the availability of observed global datasets, various studies during the 1980s examined the sensitivity of the

summer monsoon response to cumulus parameterization. These studies clearly hinted the importance of cumulus scale effects on monsoon simulation. Krishnamurti et al (1987) investigated the effects two versions of the Kuo scheme on monsoon onset of 1979. Slingo et al., (1988) using ECMWF operational model showed that monsoon onset as well as the mean July rainfall features clearly depended on the parameterization schemes present in the model. Since latent heat release from cumulus convection is the dominant contributor to diabatic heating, proper representation of cumulus convection in a GCM is a key factor in simulating the observed tropical circulation (Miller et al. 1992). Several simulation studies have documented the importance of cumulus scale effects on the summer monsoon simulation (e.g., Krishnamurti et al. 1987, Slingo 1988, Sud et al. 1992, Zhang 1994, Zachary and Randall 1999, Krishnamurti and Sanjay 2003). Zachary and Randall (1999) showed that the inclusion of stratiform cloudiness parameterization developed by Fowler et al. (1996), led to a reduced precipitation rate and a much more realistic geographical pattern of tropical precipitation.

Over the years, there have been some improvements in simulating the spatial pattern of mean summer monsoon rainfall and associated large-scale circulation features. This is partly due to the improved physical parameterization schemes and partly because of developments in high-resolution modeling using high-speed computers. Fig.5.1a is an example showing the simulation of seasonal mean monsoon rainfall and 850 hPa winds by a high resolution state-of-art atmospheric GCM (Krishnan et al. 2009). The corresponding fields from the observed datasets are shown in Fig.5.1b. It can be noticed that the simulation captures the southwest monsoon low-level cross-equatorial winds over the Indian Ocean; the westerly flow over the subcontinent and the adjoining Arabian Sea and Bay of Bengal. In general, the large-scale semi-permanent features of the monsoon system – viz., Monsoon Trough and associated circulation, Mascarene High, Tibetan Anticyclone, Tropical Easterly Jet, Cross-equatorial flow and low-level jet are well captured in the model simulation (Krishnan et al. 2009). The overall distribution of monsoon rainfall over the Indian region is quite robust in the

simulation. The simulated rainfall clearly shows the precipitation maxima along the west-coast and the head Bay of Bengal; although it may be noted that the model produces excessive precipitation near the Western Ghat Mountains and the Himalayan foothills as compared to observations. Also seen in the simulation is the secondary rainfall maximum between 5°S-10°S over the Indian longitudes which is somewhat underestimated as compared to observations.

Although the state-of-art global high-resolution climate models are able to qualitatively capture the mean summer monsoon rainfall distribution, careful examination reveals that there are deficiencies across models in accurately representing the detailed spatial structure of the mean monsoon rainfall distribution. This is an aspect of major concern for seasonal monsoon prediction using dynamical models. Gadgil and Sajani (1998) examined the simulation of summer monsoon precipitation by 30 different atmospheric GCMs that participated in the Atmospheric model Intercomparison Project (AMIP, Gates, 1992*)*. The AMIP runs were carried out by forcing models with observed monthly SST and sea-ice distribution over a 10-year (1979-1988) period - starting from the atmospheric initial state of 1 January 1979 (Gates 1992). Gadgil and Sajani (1998) noted that the models fell into two distinct classes on the basis of the seasonal variation of the major rain-belt over the Asia West Pacific sector - the first class (class I) comprising models with a realistic simulation of the seasonal migration of the major rain-belt over the continent in the boreal summer; and the second (class II) comprising models with a smaller amplitude of seasonal migration than observed with the rain-belt being almost stationary. Fig. 5.2 shows the July-August rainfall pattern as simulated by the AMIP models as given by Gadgil and Sajani (1998). They noted that models that had a reasonably realistic rainfall pattern over the Indian region could capture the northern propagation of the ITCZ; whereas the rainfall in the remaining models was mostly localized and did not exhibit the northward propagation of ITCZ. Kang et al., (2002) assessed the overall performance of monsoon simulations from 10 different modeling groups that participated in the CLIVAR/Monsoon GCM Inter-comparison Project. They noted

that the overall spatial pattern of summer monsoon rainfall was similar to the observed, although the western Pacific rainfall was relatively weak. All the models reproduced larger amplitudes of the climatological seasonal variation of Indian summer monsoon than the observed, though most models simulated smaller amplitudes in the western Pacific. In noting the above, the main point is that accurate simulation of the mean rainfall distribution over the Indian and East Asian monsoon regions still remains a challenging issue for many state-of-art AGCMs (Gadgil and Sajani, 1998; Kang et al., 2002, Kang and Shukla, 2005). Such biases in accurately simulating the distribution of the climatological mean monsoon rainfall distribution poses a major limitation in seasonal monsoon prediction. This issue will be discussed in the following section.

5.3. Seasonal predictability of monsoon

The possibility of a long range prediction over low latitudes through the time integration of numerical models was envisioned by Charney (1975), Charney et al (1977). The basis for seasonal scale predictability in the tropics arises from the famous hypothesis proposed by Charney and Shukla (1981) based on dynamical and statistical prediction efforts in the 1970s. Numerical prediction experiments with a NASA/GISS atmospheric GCM over the Sahel region was carried out by Charney et al., 1977 to study the sensitivity of rainfall to albedo changes. It was found that after numerical integration of the model for 45 days, the spread of the forecast among the 3 members of the ensemble (measured by inter member variance) was quite small over the Indian monsoon region indicating that the Indian summer monsoon variability in the long range is relatively insensitive to the initial condition as compared to the boundary condition. Around the same time Shukla (1975) examined the sensitivity of the Indian summer monsoon to Arabian SST variations using the GFDL GCM. He found that specification of large positive SST anomalies in the Arabian Sea produced an increased rainfall over India. Empirical studies by Shukla and Misra (1977), Hahn and Shukla (1976) pointed out that large-scale slowly varying boundary condition (e.g. SST, Eurasian snow cover)

could be used as a reliable predictor of the seasonal mean monsoon. The Charney-Shukla hypothesis has been the central paradigm for seasonal monsoon predictability research during the past 3 decades. During the 1980s this hypothesis, backed by empirical seasonal prediction studies which identified robust slowly varying boundary predictors (like SST, snow cover) or atmospheric predictors of Indian monsoon (e.g. Shukla and Paolino, 1983; Gowarikar et al., 1989) created a great enthusiasm in determining the potential predictability and real time prediction skill using dynamical models. During the mid 1980s and the following decades, various coordinated modeling efforts were undertaken (e.g. AMIP, DEMETER, SPIM, etc) to understand the potential of GCMs for seasonal monsoon forecasting. Although the dynamical models have evolved significantly over the years, many models suffer from the inability to reduce large systematic errors caused by deficiencies in treatment of physical processes; and thereby resulting in relatively low seasonal forecast skills over the Indian monsoon region.

The basic premise for seasonal forecasting stems from the memory provided by slowly varying boundary conditions, such as the anomalous SST variations in the tropical Indo-Pacific basin during evolution of ENSO events, which can modulate the large-scale atmospheric circulation and precipitation patterns. Numerous modeling studies using AGCMs have shown that warm SST anomalies in the equatorial central-eastern Pacific can influence the Indian monsoon through anomalous east-west displacement of the ascending and descending branches of the Walker circulation that link the Indo-Pacific climates; and in turn alter the regional monsoon Hadley circulation and rainfall distribution over the subcontinent (e.g., Keshavamurty, 1982; Ju and Slingo, 1995; Soman and Slingo, 1997; Krishnamurti et al., 1989, 1990; Palmer et al., 1992; Chen and Yen, 1994; Nigam, 1994; Sperber and Palmer, 1996; Meehl and Arblaster, 1998; Krishnan et al., 1998; Krishna Kumar et al., 2006). The GCM simulation experiments clearly show that eastward shifts of the rainfall activity to the equatorial central-eastern Pacific during the warm ENSO events force anomalous subsidence and drought conditions over South and South-east Asia. The ENSO-monsoon relationship is better captured in

models that can more realistically simulate the climatological southwest monsoon circulation and rainfall distribution (e.g. Sperber 1999, Kitoh et al., 1999, Lau and Nath, 2000). Modeling studies have also shown that persistent SST anomalies arising from ocean-atmosphere coupled interactions in the tropical Indian Ocean can modulate the regional monsoon circulation and rainfall activity through changes in the monsoon Hadley circulation (e.g., Chandrashekhar and Kitoh, 1999, Krishnan et al., 2003, 2010, Yamagata et al., 2004, Ashok et al., 2004).

In addition to SST, the other boundary forcing that can potentially influence the Indian summer monsoon are the snow-cover and soil moisture. Several studies have investigated the impact of Eurasian snow on the Indian summer monsoon through GCM simulation experiments (e.g., Barnett et al., 1989; Yasunari et al., 1991; Zwiers,1993; Meehl, 1994; Vernekar et al., 1995; Douville and Royer, 1996; Dong and Valdes, 1998; Ferranti and Molteni, 1999; Bamzai and Marx, 2000; Becker et al., 2001; Dash et al., 2005). In general, these studies suggest that excessive snow cover / snow depth over Eurasia in the winter/spring months induces weaker-than-normal summer monsoon circulation through a reduction in the meridional thermal contrast over Asia. Such reductions in the thermal contrast tend to arise either due to (a) Land surface hydrological effects such as snow albedo changes, evaporation of excess water due to snow melt, changes in soil moisture resulting from snow melt etc., or (b) Generation of large-scale mid-latitude circulation anomalies in the middle and upper troposphere which intrude southward and induce anomalous cooling through cold air advection. This leads to suppression of convection over the subcontinent and hence to drought conditions.

Various researches have also suggested significant role of land surface process in shaping the low frequency variability of the Indian monsoon. However, the land surface process affects the Indian monsoon in a very complex way because of the association of the hydrological and global energy cycle. For example, an increase in soil moisture can increase the rate of evaporation and moisten the atmospheric boundary layer thereby assisting the growth of moist

convection and increase of latent heating and rainfall. The source of moisture may be from the natural vegetation (evapo-transpiration), the rivers, lakes and other fresh water source. GCMs employ different parameterization schemes to represent land surface processes in models. Some of the well known schemes are BATS (biosphere-atmosphere transfer scheme) of Dickinson et al., (1986), SiB (simple biosphere) of Sellers et al., (1986) and SSiB (simplified SiB) of Xue et al., (1991), ISBA (Interaction Soil-Biosphere atmosphere, Mahaouf et al., 1995), SECHIBA (Ducoudre et al., 1993) etc. All these schemes calculate the fluxes from the soil and canopy using similar principles with different formulations (varying number of soil and vegetation layers, mosaic approach i.e. fractional coverage of vegetation in a grid box etc). A recent study by Singh et al., (2007) assessed the impact of three different land surface schemes in simulating the monsoon. Based on their analysis they concluded that the features of the Indian summer monsoon, such as strength of the low-level westerly jet, the cross-equatorial flow and the tropical easterly jet, mean rainfall during peak monsoon month (July) were better simulated in one of the land-surface schemes (ie., NoaH) as compared to the two other parameterizations. Alessandri et al., (2007) included a land surface model (LSM) in the Hamburg (ECHAM4) AGCM. Their analysis reveals that the inclusion of LSM schemes has large effects on the simulated boreal summer surface climate of the model especially in the surface energy balance due to changes in the surface latent heat fluxes over tropical and mid-latitude areas covered with vegetation. Rainfall and atmospheric circulation are substantially affected by these changes. They noted that inclusion of LSM schemes helped in enhancing precipitation over the Indian summer monsoon region due to increased evapo-transpiration from the surface.

The other important effect of the land surface comes from the elevated Tibetan plateau situated to the north of Himalayas. The sensible heating from the Tibetan plateau is an important source of diabatic heating over the whole troposphere, particularly during the onset phase of monsoon. GCM simulation suggests that without a Tibetan plateau the rainfall can’t penetrate deep into the

subcontinent. Abe et al., (2003) using an MRI GCM with a varying elevation of the Tibetan plateau concluded that the Indian monsoon became strong gradually with mountain uplift; particularly, in the later stages, the remarkable enhancement was found. With the increase in the height of topography over Tibetan region, an extension of the active convection region was evident and the moist climate in South and East Asian Monsoon region was enhanced along with the increasing strength of circulation such as low-level westerly and upper-level anti-cyclonic circulation. The increase in precipitation, and the enhancement of southwesterly, in the later stages of the mountain uplift, appeared only over India and the south and southeastern slope of the Tibetan Plateau. The analysis shows that the diabatic heating over the Tibetan Plateau also increase the north-south temperature gradient during pre-monsoon and onset phase helping in the development of the seasonal monsoon trough over the Indian region. Further, the strength of monsoon trough is important in determining the seasonal mean monsoon variability over the Indian region.

5.4. Monsoon interannual variability (IAV) in AGCMs and coupled models

In order to get a quick idea about the skill of the current atmospheric models for seasonal monsoon predictions, we shall examine the model simulations conducted under the Seasonal Prediction of Indian Monsoon (SPIM) project. Different modeling groups in India participated in the SPIM project and all AGCMs were run on a single computational platform at CDAC, Bangalore (Gadgil et al, 2009;http://www.clivar.org/organization/aamp/presentations/AAMP9/AAMP9Rajeevan.pdf). The SPIM simulations consist of hindcasts for 20 summer monsoon seasons (1985-2004). For each year, five ensemble member runs were performed starting from the initial conditions of 26-30 April of each year and observed SST were specified as lower boundary condition. Fig. 5.3 shows the time-series of interannual variability of the observed All India Summer Monsoon Rainfall (AISMR) for the period (1985-2004) and the ensemble mean of normalized rainfall anomalies over the Indian region simulated by three different atmospheric models

viz., the Portable Unified Model (PUM), UK Met Office, the Seasonal Forecasting Model (SFM), NCEP and the COLA AGCM. While the monsoon rainfall anomalies were reasonably simulated by the SPIM models during certain years like 1988, the models systematically failed during other years like 1994. In general, it was noted that all the correlation between the observed and simulated rainfall variations was rather modest for all the models.

Some studies suggest that the lack of skill of standalone atmospheric models (AGCMs) to simulate the observed monsoon interannual variability can arise due to the failure of AGCMs to simulate correctly the relationship between the local rainfall and SST variations (e.g., Wang et al., 2005; Kang and Shukla, 2005; Krishna Kumar et al., 2005). AGCM simulations rely on a two-tier approach that presupposes the monsoon variability to be a consequence of solely the atmosphere responding to the specified underlying SST boundary condition. However, such an approach would not be appropriate while dealing with ocean-atmosphere coupled interactions in the monsoon environment; and therefore inclusion of interactive ocean-atmosphere coupling would be essential for improving the skill of monsoon rainfall predictions (Wang et al., 2005, Krishna Kumar et al., 2005). Krishnan et al. (2010) pointed out that standalone AGCMs generally fail to capture anomalous wet Indian monsoons like 1994 which coincided with the evolution of an Indian Ocean Dipole (IOD) event. They suggested that the 2-tier approach adopted in AGCMs does not favour an effective interaction between the large-scale monsoon circulation and the IOD anomalies in the tropical Indian Ocean. Further they pointed out that inclusion of ocean-atmosphere coupling significantly enhances the monsoon large-scale cross-equatorial circulation response; leading to precipitation increase over the subcontinent and rainfall decrease over south-eastern tropical Indian Ocean in a manner broadly consistent with observations.

Coupled models have shown promising skills in predicting IOD events about 2-3 seasons in advance (Luo et al., 2007; 2008); as well as the ability to skillfully predict the evolution of seasonal anomalies over the tropical Indo-Pacific and northwest Pacific with sufficient lead-times (Behera et al., 2006, Chowdary et al., 2009). However, analysis of coupled model forecasts such as the DEMETER multi-model prediction system reveals that the achievable skill of Indian summer monsoon rainfall forecasts using coupled models shows only marginal improvement as compared to standalone AGCMs (e.g., Gadgil et al., 2005,Vinay Kumar, 2008, Joseph et al., 2010). The study by Joseph et al. (2010) attributes the poor performance of the seasonal monsoon forecasts of the DEMETER coupled models to the model's inability to capture the observed relationship between monsoon droughts and very-long breaks; as well the failure of forecasts to realistically represent the air-sea interactions on intra-seasonal time-scales. Pattanaik and Kumar (2010) analyzed the skill of monsoon forecasts generated by the NCEP Coupled Forecast System (CFS) model. They noted that the CFS model forecasts could capture the interannual variability of large-scale monsoon circulation indices fairly well, but the skill of the seasonal monsoon rainfall predictions by the CFS model was not satisfactory. In the next section, we shall discuss about the strong internal dynamics of the monsoon system which is one of the major factors limiting the skill of seasonal forecasts of the monsoon rainfall forecasts over the Indian region.

5.5. Monsoon internal dynamics and sub-seasonal variability

Seasonal rainfall variations over various tropical areas (e.g., Maritime Indonesia, tropical areas in South America and Africa, etc) are significantly modulated by slowly varying boundary conditions and exhibit less dependence on the atmospheric initial-state. However, there is also a growing recognition that the predictability of the seasonal monsoon rains over the Indian region, which is an exception within the tropics, tends to be limited by atmospheric internal-dynamics of the monsoon system (e.g., Palmer and Anderson, 1994, Sperber and Palmer,

1996, Sugi et al., 1997, Goswami, 1998, Kar et al., 2001, Goswami and Xavier, 2005, Krishnan et al., 2009). These studies indicate that the effect of internal-dynamics on the Indian monsoon precipitation variability is non-negligible and compares with the level of externally-forced variability. In other words, the evolution of seasonal monsoon rainfall anomalies over the South Asian region can indeed be quite sensitive to atmospheric initial conditions. Goswami (1998) examined simulations of the GFDL model and estimated that internal-dynamics could contribute to as much as 50% of the total variability of Indian monsoon rainfall. He noted a biennial time-scale oscillation in the model simulations and suggested that such internally-forced variability might arise due to interactions between the sub-seasonal oscillations and the annual cycle. Aspects relating to the monsoon internal dynamics are not yet fully understood. One of the main issues is the long range predictability of sub-seasonal variations of monsoon rainfall associated with the active and break monsoon conditions which can significantly determine the total seasonal monsoon rainfall over India during any particular year (e.g. Goswami and Xavier, 2005).

Observational studies have reported quasi-biweekly monsoonal variations, with time-scale of ~10-20 days, which are characterized by westward propagating circulation and convection anomalies (e.g. Keshavamurty, 1973; Murakami and Frydrych, 1974; Krishnamurti and Bhalme, 1976; Chatterjee and Goswami, 2004 and others). The existence of longer time-scale variability about 30-50 days has been well-documented in observations of winds, cloud-bands and rainfall over the Indian summer monsoon region (e.g., Dakshinamurthy and Keshavamurty, 1976; Yasunari, 1979, 1980; Sikka and Gadgil, 1980; Krishnamurti and Subrahmanyam 1982, Hartmann and Michelsen, 1989 and several others). The convection and circulation features associated with the 30-50 day low-frequency motions show northward propagation from the equatorial region with a typical phase speed of 1° latitude per day. It is known from the above studies that the 10-20 day and 30-50 day monsoon intra-seasonal variations modulate the active and break monsoon cycles over the Indian region.

Northward propagating summer monsoon intra-seasonal oscillations have been noted in zonally symmetric models having varying complexities of interactive feedbacks between convection and large-scale monsoon circulation (e.g., Webster and Chou, 1980, Webster 1983, Goswami and Shukla, 1984, Krishnan et al., 1992, Nanjundiah et al., 1992, Srinivasan et al., 1993, Jiang et al., 2004, Bellon and Sobel, 2008a, 2008b, Chattopadhyay et al., 2008 and others). Webster (1983) simulated a northward propagating biweekly oscillation, using a zonally symmetric model that he attributed to land surface hydrological feedback. The importance of interactive feedbacks between moist convection and large-scale circulation on the low-frequency intra-seasonal variability of the monsoon active / break spells has been discussed by various investigators (e.g. Lau and Chan, 1986; Lau and Peng, 1990; Krishnan and Kasture, 1996; Wang and Xie, 1997; Rodwell, 1997; Krishnan et al., 2000; Kembal-Cook and Wang, 2001; Annamalai and Slingo, 2001; Lawrence and Webster, 2002; Annamalai and Sperber, 2005).

There is a school of thought that emphasizes on the role of atmospheric dynamical processes in driving the summer monsoon low-frequency intra-seasonal variability. For example, Wang and Xie (1997) have highlighted the role of the easterly vertical shear of the zonal wind in the northward propagation of the convection over the Indian region via emanation of Rossby waves. Rodwell (1997) suggested that modifications of the large-scale monsoon flow by remote effects, such as extratropical weather systems in the Southern Hemisphere, can be effective in triggering monsoon breaks over India. Krishnan et al. (2000) showed that forcing by suppressed convection anomalies over the Bay of Bengal leads to development of low-level anticyclonic circulation anomalies as a Rossby wave response, which then propagate northwestward to initiate and force monsoon breaks over India.

The alternative view is that a combination of ocean-atmosphere interactions and convection-circulation feedbacks lead to the northward and northwestward propagation of convection over the Indian and tropical west Pacific sectors during

the boreal summer (Hsu and Weng, 2001, Kembal-Cook and Wang, 2001). Evidence of ocean-atmosphere coupling on intra-seasonal time-scales have been noted both in observational studies (e.g., Krishnamurti et al., 1988, Hendon and Glick, 1997, Sperber et al., 1988, Sengupta et al., 2001, Kemball-Cook and Wang, 2001, Vecchi and Harrison, 2002, Sperber, 2003, Krishnan et al., 2006) and coupled modelling studies (e.g., Waliser et al., 1999, Kemball-Cook et al., 2002, Fu et al., 2003, Fu and Wang, 2004). These studies suggest that positive SST anomalies lead convection by about 10 days and this lead/lag relationship appears to be a factor in the organization and poleward migration over the Indian longitudes.

5.6. Internal feedback mechanisms that can sustain prolonged monsoon breaks

5.6.1. Mid-latitude and monsoon interaction

Several observational and model studies have reported persistent intrusion of mid-latitude and sub-tropical westerly anomalies over West-Central Asia (WCA) and Indo-Pak region during intense monsoon-breaks (e.g. Ramaswamy, 1962, Keshavamurty and Awade, 1974, Ramaswamy and Pareekh, 1978, Kripalani et al., 1997, Raman and Rao, 1981, Krishnan et al., 1998, 2000, 2009, Joseph and Srinivasan, 1999, Krishnan and Sugi, 2001, Ding and Wang, 2007). The large-scale intrusions manifest as anomalous troughs in the westerlies in the middle and upper troposphere over WCA and Indo-Pak, together with a blocking high over East Asia. The advection of cold air in the middle and upper-troposphere from the extra-tropics into northwest and central India produces anomalous tropospheric cooling leading to reduction of the meridional tropospheric temperature gradient (Krishnan et al. 2009). Furthermore, the intrusion of the dry extra-tropical air can suppress the monsoon convection over northern India by weakening the convective instability (Krishnan et al., 2009, Krishnamurti et al., 2010a). Numerical model simulations by Krishnan et al (2009) showed that the suppression of monsoon convection over the Indian region in turn produces an extra-tropical

response over West-Central Asia and allows generation of anomalous circulation patterns thereby facilitating the southward intrusion of cold extra-tropical air. Such an internal feedback between the monsoon and extra-tropical circulation can give rise to long-lasting breaks in the monsoon rainfall (Krishnan et al. 2009). Alternatively, long monsoon-breaks can also be triggered by the eastward propagating Madden Julian Oscillation (MJO) during the northern summer as noted by Joseph et al. (2009). They reported that the passage of suppressed convective phase of the MJO over the eastern equatorial Indian Ocean and west Pacific can trigger westward propagating Rossby waves which then interact with the northward propagating dry-phase over the Indian longitudes thereby giving rise to extended monsoon breaks.

5.6.2. Indian Ocean SST and convection anomalies during prolonged monsoon breaks

Another important issue that needs detailed research is the possible role of Indian Ocean SST and convection anomalies in driving prolonged breaks in the monsoon rainfall over India. Observations indicate that extended monsoon breaks are characterized by a north-south pattern of suppressed monsoon rainfall over the Indian subcontinent and enhanced rainfall over the equatorial eastern Indian Ocean. By conducting GCM simulation experiments, Krishnan et al. (2003) demonstrated that persistent warmer-than-normal SST in the equatorial Indian Ocean can be very effective in prolonging monsoon-breaks. They noted that the near-equatorial warm SST anomalies enhances rainfall over the equatorial oceans and induces anomalous subsidence to the north over the subcontinent, leading to a weakening of the large-scale monsoon reverse Hadley circulation and rainfall reduction over the subcontinent. Krishnan et al. (2006) further examined the mechanisms and physical processes that would result in long lived SST anomaly in the equatorial Indian Ocean during prolonged monsoon breaks. By analysing new data from satellites and direct measurements of oceanic profiles from ARGO floats in the tropical Indian Ocean, they identified an ocean-atmosphere coupling that can

force prolonged SST anomaly over equatorial Indian Ocean. The coupling involves a wind-thermocline feedback on sub-seasonal time-scales and leads to 'long monsoon-breaks' through the regional Hadley circulation which in turn lead to monsoon droughts.

5.6.3. Simulation of monsoon intra-seasonal variability

From the above discussions, it is clear that the summer monsoon intra-seasonal variability (ISV) of active / break monsoon cycles can crucially influence the seasonal monsoon rains over India. Therefore, models must be able to realistically simulate the spatio-temporal characteristics of the summer monsoon ISV with a certain degree of fidelity. Studies have investigated the summer monsoon ISV in different atmospheric models (e.g. Sperber et al., 2001, Kang et al., 2002, Waliser et al., 2003). The results from these studies indicate wide range of variations in the simulated ISV with some models being able to capture the ISV quite reasonably, while others practically fail to simulate it at all. Sperber et al. (2001) observed that even though many models could simulate the dominant mode of subseasonal variability, they did not exhibit the observed spatial rainfall pattern associated with that mode and therefore failed to project the simulated sub-seasonal variability onto the interannual variability. Kang et al. (2002) examined the climatological intra-seasonal oscillations (CISO) in model simulations and noted that models showed robust simulation of CISO over Indian region, but had a much weaker amplitude over the tropical Indian Ocean. Waliser et al. (2003) reported that although some models exhibited northeastward propagation of the summer monsoon ISV, the patterns of ISV were less coherent in terms of the spatial structure (Fig.5.4). It has been reported that improved representation of summer monsoon ISV in model simulations can be achieved through realistic treatment of air-sea interactions in the tropics (Fu et al., 2003, Fu et al., 2007). In a recent study, Joseph et al. (2010) examined the reasons for the poor skill of the DEMETER coupled models in predicting the observed interannual variability of monsoon rainfall over India. They noted that improper representation of air-sea

interaction in most of the DEMETER coupled models resulted in failure to capture the relationship between long monsoon-breaks and droughts over India. Likewise several other studies have shown that the ISV is highly sensitive to tuning of convection parameterization in numerical models (e.g., Slingo et al., 1996, Lee et al., 2001, 2003, Wang, 2004).

5.7. Towards improving the monsoon simulation in numerical models

Accurate simulation of the South Asian monsoon and its variability warrants that the climate models should realistically capture the interactions among different spatio-temporal scales and also the feedback exchanges among the various climate components. The following are some of the key areas where extensive research and development is essential for advancing the current skill of monsoon simulations.

5.7.1. Improving parameterization of cumulus convection and moist processes:

Parameterization of cumulus convection and moist processes over the tropics and monsoon region is perhaps the most fundamental and challenging gap area from the point of monsoon modelling and dynamical prediction. Precipitation processes over the tropics and monsoon region involve interactions among the large-scale, synoptic-scale, meso-scale and cumulus-scale, with feedbacks between dynamics and latent-heating associated with different cloud-types (stratiform, convective); as well as contributions from cloud micro-physical processes. Although different parameterization schemes of tropical convection exist, it is not clear if any single scheme would be adequate to encompass the entire range of scientific problems pertaining to tropical convection. Deficiencies in realistically capturing the monsoon rainfall and its variability arise largely due to improper representation of convective processes in numerical models thereby introducing errors in magnitude and position of the vertical levels of maximum heating which is a major area of concern (Tao et al., 2007).

The launch of Tropical Rainfall Measuring Mission (TRMM) in 1997 has produced a much needed high resolution 4-dimensional observational data of tropical rainfall and latent heating over the entire tropics for more than a decade (http://trmm.gsfc.nasa.gov). This data has helped in understanding various rainfall processes, the partitioning of tropical precipitation into convective and stratiform categories, generation of vertical profiles of hydrometeors. It has also helped the modeling community to validate model results and identify the limitations in simulating the observed tropical heating structure (Shige et al. 2004, 2007, 2008, Krishnamurti et al., 2010). The vertical variation of latent heating significantly influences the structure of the monsoon large-scale response and this sets a strong constraint on the spatio-temporal variability of monsoon. Chattopadhyay et al. (2009) conducted model simulation experiments to examine the sensitivity of the boreal summer monsoon ISV to latent heating from stratiform and convective clouds. They noted that the slow northward propagation monsoon ISV is mainly driven by the stratiform-type latent heating. Choudhury and Krishnan (2011) examined the dynamical response of the South Asian monsoon trough to latent heating from meso-scale convective systems (MCS) by performing GCM simulation experiments. They noted that stratiform-type latent-heating, with a maximum around 400 hPa and a strong vertical heating-gradient, was very effective in promoting mid-level (600-500 hPa) convergence and stretching of cyclonic-vorticity well-above 500 hPa. By varying the population of stratiform and convective rain-types in the simulation, they pointed out that the horizontal-scale of mid-level vorticity response increased significantly as the stratiform population increased. They also observed that the large populations of stratiform-type clouds could extend the mid-level response far to the west over the northern flanks of the African ITCZ.

Krishnamurti et al. (2010b) examined how well some of the current cumulus parameterization schemes (e.g., modified Kuo parameterization, simple Arakawa–Schubert parameterization, and Zhang–McFarlane) perform toward describing the amplitude and the three-dimensional distributions of heating as observed by

TRMM during few days in July 2007. They observed that the Kuo-type scheme which relies on moisture convergence overestimated the rainfall compared to the TRMM estimates. The other schemes used show a slight overestimation of rain rates compared to TRMM. Fig.5.5 shows daily profiles of the vertical distribution of heating Q_1 covering the period 3rd July through 18th July 2007. These are averaged heating rates for the monsoon region between 5°N and 25°N and 70°E and 90°E. It can be seen that there are large errors in the vertical structure of model derived latent heating. For all the days some cumulus parameterization schemes overestimate the amplitude of heating, whereas others carry lower values. The model results also demonstrated large errors in the position of the vertical level of maximum heating.

Strategies to improve cumulus parameterizations in models must be based on rigorous validation of the model simulations against standard bench-marks. For example, modifications in cumulus convection can be targeted towards providing realistic distribution of mean rainfall distribution over west-coast of India, Bay-of-Bengal, Indian landmass, adjoining areas of Mynamar, Indo-China, tropical Indian and Pacific Oceans; as well as realistic pattern correlations of the Indian monsoon rainfall variability with other regions of tropical Indo-Pacific sector. The performance of the cumulus schemes should also be validated for active monsoon phases characterized by synoptic systems (e.g. monsoon lows, depressions, mid-tropospheric cyclones) and large-scale organization of cloud clusters with embedded meso-scale convective systems which produce abundant precipitation over the region. It is also important to partition the rainfall and latent heating into stratiform and convective categories in the model. This can provide valuable insights for improving the representation of cloud structures and their life-cycles through better treatment of cumulus and cloud microphysical processes. Another key element for validating the convection scheme is the northward and westward propagating rainfall bands of the summer monsoon ISV; as well as the super cloud clusters associated with the eastward propagating MJO.

5.7.2. Development of high-resolution global models and regional cloud-resolving models

Observations also show substantial orographic monsoon rainfall concentrated along the narrow mountain ranges of India and Southeast Asia. Very high-resolution global models (at least 25 km mesh), together with regional cloud-resolving models (<3 km grid) will be needed to resolve such fine-scale precipitation features over the monsoon region. Because of the rapid increase in computational power in recent years, there has been considerable interest to employ global cloud resolving models for simulating summer monsoon cloud clusters explicitly. Oouchi et al. (2009) reported simulations for the summer of 2004 by a global cloud-system-resolving model (NICAM) at both 14-km and 7-km horizontal resolution. Results from the NICAM simulation show several features with high precision that resemble the observed northward propagation of the summer monsoon precipitation bands. The 7-km run replicates the summer-mean precipitation maxima in narrow bands along the Western Ghats, and foothills of Himalaya. Also the simulated precipitation exhibits a distinct diurnal cycle and is modulated by synoptic-scale systems and orographic effects. These efforts in ultra high-resolution modeling of the monsoon cloud systems are quite promising and need to be strongly encouraged.

5.7.3. Development of ocean-atmosphere coupled modelling system for monsoon prediction

Another major gap area is the development of a coupled ocean-atmosphere system for seasonal and extended-range monsoon prediction. The importance of ocean-atmosphere coupled interactions in affecting monsoonal variations on intra-seasonal and interannual time-scales has been well-documented. Coupled interactions provide memory to the slow evolution of the atmosphere and ocean anomalies, so that this knowledge could be used to track and predict monsoonal rains. Recognizing the overall lack of observations in the Indian Ocean region, a

new integrated in-situ ocean observing system RAMA (Research Moored Array for African-Asian-Australian Monsoon Analysis and Prediction) has been recently deployed in the Indian Ocean (McPhaden et al. 2009). The RAMA moorings, the network of ARGO floats (http://www.incois.gov.in/incois/argo/argo_dataglobal.jsp), along with the high-quality global coverage of satellite measurements of ocean and atmospheric parameters (e.g., SST, surface winds, sea-level heights, atmospheric temperature, humidity, rainfall, motion-vectors etc) have significantly enhanced the observational coverage in recent years. This has provided a rich source of observations to understand the broad spectrum of phenomena in the monsoon and Indian Ocean region, ranging from diurnal to decadal time-scales that interacts with one another and contributes to the observed variability. These developments in observational monitoring coupled with the rapid strides in data assimilation of the atmosphere (Simmons and Hollingsworth, 2002) and ocean (Derber and Rosati, 1989; Ji et al., 1995) are expected to produce major advances in predicting the coupled ocean-atmosphere multi-scale interactions and monsoon rainfall variability on time-scales of days to weeks during the coming years.

References

Abe, M., Kitoh, A. and Yasunari, T., 2003, "An Evolution of the Asian Summer Monsoon Associated with Mountain Uplift—Simulation with the MRI Atmosphere-Ocean Coupled GCM", *JMSJ*, 81, 909-933.

Alessandri, A., Gualdi, S., Polcher, J. and Navarra, A., 2007, "Effects of Land Surface–Vegetation on the Boreal Summer Surface Climate of a GCM", J. Climate, 20, 255–278.

Annamalai, H., and Sperber, K. R., 2005, "Regional heat sources and the active and break phases of boreal summer intraseasonal (30-50 day) variability", *J. Atmos. Sci.*, 62, 2726–2748.

Annamalai, H., and Slingo, J.M., 2001, "Active/break cycles: Diagnosis of the intraseasonal variability of the Asian summer monsoon", *Climate Dynamics*, 18, 85–102.

Ashok, K., Guan, Z., Saji, N. H. and Yamagata, T., 2004, "Individual and Combined Influences of the ENSO and the Indian Ocean Dipole on the Indian Summer Monsoon", J. Climate, 17 (16), 3141-3155.

Bamzai, A. and Marx, L. 2000, "COLA AGCM simulation of the effect of anomalous spring snow over Eurasia on the Indian summer monsoon", *Quart. J. Roy. Meteor. Soc*., 126, 2575-2584.

Barnett, T., and Preisendorfer, R., 1987, "Origins and Levels of Monthly and Seasonal Forecast Skill for United States Surface Air Temperatures Determined by Canonical Correlation Analysis", Mon. Wea. Rev., 115, 1825–1850.

Barnett, T.P., Dumenil, L., Schlese, U., Roeckner, E. and Latif, M., 1989, "The effect of Eurasian snow cover on regional and global climate variations", *J. Atmos. Sci.*, 46, 661-685.

Becker, B. D., Slingo, J. M., Ferranti, L. and Molteni, F., 2001, "Seasonal predictability of the Indian Summer Monsoon What role do land surface conditions play?", Mausam, 52, 175-190.

Behera, S. K., Luo, J.J., Masson, S., Rao, S. A., Sakuma, H. and Yamagata, T., 2006, “A CGCM study on the interaction between IOD and ENSO”, *J. Climate,* 19, 1608-1705.

Bellon, G. and Sobel, A. H., 2008a, “Poleward-propagating intraseasonal monsoon disturbances in an intermediate-complexity axisymmetric model”, *J. Atmos. Sci.*, **65**: 470–489.

Bellon, G. and Sobel, A. H., 2008b, “Instability of the axisymmetric monsoon flow and intraseasonal oscillation”, *J. Geophys. Res.*, **113**.D07108, doi:10. 1029/2007JD009291.

Chandrasekar A, Kitoh, A. 1998, “Impact of localized sea surface temperature anomalies over the equatorial Indian Ocean on the Indian summer monsoon”, J Meteorol Soc Jpn 76:841–853.

Charney, J. G., and Shukla, J. 1981, “ Predictability of monsoons, in Monsoon Dynamics”, edited by J. Lighthill and R. P. Pearce, pp. 99 – 110, Cambridge Univ. Press, Cambridge, U. K.

Charney J. G., Quirk, W.J., Chow, S. and Kornfield, J.,1977, “ A comparative study of the effects of albedo change on droughts in semi-arid regions”, J Atmos. Sci., 34, 1366-85.

Charney, J.G. 1975, “Dynamics of deserts and drought in the Sahel”,Q J R Meteorol Soc, 101, 193-202.

Chatterjee P. and Goswami, B. N.,2004, “Structure, genesis and scale selection of the tropical quasi-biweekly mode”, *Q. J. R. Meteorol. Soc*. 130, 1171-1194.

Chattopadhyay, R., Sahai, A. K. and Goswami, B. N. (2008), “Objective identification of nonlinear convectively coupled phases of monsoon intraseasonal oscillation, implications for prediction”,J. Atmos. Sci., 65, 1549–1569, doi:10.1175/2007JAS2474.1.

Chattopadhyay, R., Goswami, B. N., Sahai, A. K. and Fraedrich, K. (2009), “Role of stratiform rainfall in modifying the northward propagation of monsoon intraseasonal oscillation”, J. Geophys. Res., 114, D19114, doi: 10.1029/2009JD011869.

Chen T. C. and Yen, M. C., 1994 , " Interannual variation of the Indian monsoon simulated by the NCAR Community Climate Model: Effect of the tropical Pacific SST", J. Climate, 7, 1403-1415.

Choudhury and Krishnan 2011, " Dynamical response of the South Asian monsoon trough to latent heating from stratiform and convective precipitation, (under review, J. Atmos. Sci.)

Chowdary, J. S., Gnanaseelan, C. and. Xie, S.P., 2009, " Westward propagation of barrier layer formation in the 2006-07 Rossby wave event over the tropical Southwest Indian Ocean", *Geophys. Res. Lett.*, **36**, L04607, doi:10.1029/2008GL036642.

Dakshinamurthy, J., and Keshavamurthy, R. N.,1976, " On oscillations of period around one month in the Indian summer monsoon", *Indian J. Meteor. Geophys.,*27**,** 201–203.

Dash S.K., Singh G.P., Shekhar M.S., Vernekar A.D., 2005, "Response of the Indian summer monsoon circulation and rainfall to seasonal snow depth anomaly over Eurasia", *Climate Dynamics* 24,1-10.

Derber, J.C., and Rosati, A.1989, "A global oceanic data assimilation system", J. Phys. Oceanogr., 19, 1333-1347.

Dickinson, R. E., Sellers, A.H., Kennedy P. J. and Wilson, M. F., 1986, "Biosphere-atmosphere Transfer Scheme (BATS) for the NCAR community climate Model", NCAR tech note NCAR/TN-275+STR, 69pp.

Ding, Q. and Wang, B., 2007, " Intraseasonal teleconnection between the Eurasian wave train and the Indian monsoon", J. Climate, 20, 3751–3767.

Ducoudré, N. I., Laval, K. and Perrier, A.1993, "SECHIBA, a New Set of Parameterizations of the Hydrologic Exchanges at the Land-Atmosphere Interface within the LMD Atmospheric General Circulation Model", J. Climate, 6, 248–273.

Douville, H. and Royer, J. F., 1996, "Sensitivity of Asian summer monsoon to an anomalous Eurasian snow cover within the Meteo-France GCM", Clim. Dyn.,12,449-466.

Dong, B.W. and Valdes, P. J., 1998, “Modeling the Asian summer monsoon rainfall and Eurasian winter/spring snow mass”, Quart. J. Roy. Met. Soc., 124, 2567-2569.

Ferranti, L. and Molteni, F., 1999, “Ensemble simulations of Eurasian snow-depth anomalies and their influence on the summer Asian monsoon.*Q.J.R.Meteorol.Soc.*, 125, 2597-2610.

Fowler, L. D., Randall, D. A. and Rutledge, S. A., “Liquid and ice cloud microphysics in the CSU general circulation model, 1, Model description and simulated microphysical processes”, J. Clim., 9, 489- 529, 1996.

Fu, X., Wang, B., Li, T. and McCreary, J. P. 2003, “Coupling between northward-propagating, intraseasonal oscillations and sea surface temperature in the Indian Ocean”, J. Atmos. Sci., 60, 1733 – 1753.

Fu, X., and Wang, B. 2004,“Differences of boreal-summer intraseasonal oscillations simulated in an atmosphere-ocean coupled model and an atmosphere-only model”, J. Clim., 17, 1263– 1271.

Fu, X., Wang, B., Waliser, D. E. and Tao, L.2007, “Impact of atmosphere ocean coupling on the predictability of monsoon intraseasonal oscillations”, J. Atmos. Sci., 64, 157–173.

Gadgil S, Sajani, S. 1998, “Monsoon precipitation in the AMIP runs. Clim Dyn 14, 659-689.

Gadgil S. 2003, “The Indian Monsoon and its Variability. Annual Review Earth Planet. Sci. 31, 429-467.

Gadgil, Sulochana, Rajeevan M. and Ravi S. Nanjundiah, 2005, “Monsoon prediction Why yet another failure?”, *Current Science,* **9**, 88:1389-1400.

Gadgil S, et al, 2009, “Seasonal prediction of the Indian monsoon”, Final project report, Department of Science and Technology, Government of India, pp 1–38.

Gates, W.L., 1992, “AMIP: The Atmospheric Model Intercomparison Project”, Bull. Amer. Meteor. Soc., 73, 1962–1970.

Gilchrist, A., 1977, “The simulation of Asian summer monsoon by General circulation models”, Pure and applied Geophysics, 115-1431-38.

Godbole, 1973, “Numerical simulation of Indian summer monsoon”, Ind. J. Met. Gephys., 24, 1-14.

Goswami, B.N. and Shukla, J., 1984, “ Quasi-periodic oscillations in a symmetric general circulation model”, J. Atmos. Sci., 41, 20-37.

Goswami, B.N., 1998, “Interannual Variations of Indian Summer Monsoon in a GCM: External Conditions versus Internal Feedbacks”, J. Climate, 11, 501–522.

Goswami, B. N., 2005, “South Asian Monsoon”, In: Lau WKM, Waliser DE (eds) Intraseasonal variability in the atmosphere–ocean climate system, Chap. 2, pp 19–61.

Goswami, B. N. and Prince K. Xavier, 2005, “Dynamics of 'Internal' Interannual Variability of Indian Summer Monsoon in a GCM”, *J. Geophys. Res., 110, D24104, doi:10.1029/2005JD006042.*

Gowariker, V., Thapliyal, V., Sarker, R. P., Mandal, G. S. and Sikka, D. R. (1989), “Parametric and power regression models: New approach to long range forecasting of monsoon rainfall in India”, Mausam, 40, 115–122.

Hahn, D.G., and Manabe, S., 1975, “The Role of Mountains in the South Asian Monsoon Circulation”, J. Atmos. Sci., 32, 1515–1541.

Hahn, D.G., and Shukla, J., 1976, “ An Apparent Relationship between Eurasian Snow Cover and Indian Monsoon Rainfall”, J. Atmos. Sci., 33, 2461–2462.

Hartman, D. L., and Michelson, M. L., 1989, “Intraseasonal periodicities in Indian rainfall”, *J. Atmos. Sci.,* **46,** 2838–2862.

Hsu, H.H. and Weng, C.H., 2001, “Northwestward propagation of the intraseasonal oscillation in the western North Pacific during the boreal summer: Structure and mechanism”, *J. Climate*, 14:3834–3850

Hendon, H. and Glick, J., 1997, “ Intraseasonal air–sea interaction in the tropical Indian and Pacific Oceans”, *J. Climate*, **10**:647–661.

Ji, M., Leetmaa, A.and Derber, J., 1995, “An ocean analysis system for seasonal to interannual climate studies”, Mon. Wea. Rev., 123, 460-481.

Jiang, X., Li, T. and Wang, B. 2004, “Structures and mechanisms of the northward propagating boreal summer intraseasonal oscillation”, J. Clim.,17, 1022 – 1039.

Joseph, P. V., and Srinivasan, J. 1999, “Rossby waves in May and the Indian summer monsoon rainfall”, Tellus, 51A, 854–864.

Joseph, S., Sahai, A. K., Goswami, B. N., 2009, “Eastward propagating MJO during boreal summer and Indian monsoon droughts”, Climate Dynamics, 32, June 2009, DOI:10.1007/s00382-008-0412-8, 1139-1153.

Joseph S., Sahai A.K., Goswami B.N., 2010, “Boreal summer intraseasonal oscillations and seasonal Indian monsoon prediction in DEMETER coupled models”, Climate Dynamics, 35, September 2010, DOI 10.1007/s00382-009-0635-3,651-667.

Ju, J. and Slingo, J., 1995, “The Asian summer monsoon and ENSO”, Q.J.R.M.S. Vol. 121, No. 525, pp 1133-1168.

Kang, I, S., et al., 2002, “Intercomparison of the climatological variations of Asian summer monsoon precipitation simulated by 10 GCMs”, Climate Dynamics, 19,383-395.

Kang, I. S., Lee, J.Y. and Park, C.K., 2004, “Potential Predictability of Summer Mean Precipitation in a Dynamical Seasonal Prediction System with Systematic Error Correction. J. Climate, 17, 834–844.

Kang, I. S., and Shukla, J., 2005, “Dynamic seasonal prediction and predictability of the monsoon”, In Asian Monsoon. Bin Wang (eds).585-612 pp.

Kar, S. C., Sugi, M. and Sato, N., 2001, “Interannual variability of the Indian summer monsoon and internal variability in the JMA global model simulations”, J. Meteor. Soc. Japan, 79, 607–623.

Kemball Cook, S. and Wang, B., 2001, “Equatorial waves and air–sea interaction in the boreal summer intraseasonal oscillation”, *J. Climate*, **14**:2923–2942.

Keshavamurty, R.N., 1973, “Power spectra of large-scale disturbances of the Indian southwest monsoon”, Ind. J. Met. Geophy., 24, 117-124.

Keshavamurty, R. N., and Awade, S. T., 1974, “Dynamical abnormalities associated with drought in the Asiatic summer monsoon. Indian J. Meteor. Geophys., 25, 257–266.

Keshavamurty, R.N., 1982, “Response of the atmosphere to sea surface temperature anomalies over the equatorial pacific and the teleconnections of the southern oscillation”, J. Atmos. Sci., 39, 1241-1259.

Kemball Cook, S., Wang, B. and Fu, X. 2002, “Simulation of the intraseasonal oscillation in the ECHAM4 model: The impact of coupling with an ocean mode”, *J. Atmos. Sci.*, **59**:1433–1453.

Kitoh, A., Yukimoto, S., Noda, A., 1999, “ENSO-Monsoon Relationship in the MRI Coupled GCM”, JMSJ, 77,1221-1245.

Kripalani, R. H., Kulkarni, A. and Singh, S. V., 1997, “Association of the Indian summer monsoon with the Northern Hemisphere midlatitude circulation”, Int. J. Climatol., 17, 1055–1067.

Krishna Kumar K., Hoerling M., Rajagopalan B., 2005, “Advancing dynamical prediction of Indian monsoon rainfall”, Geoph. Res. Let., 32, 1-4.

Krishna Kumar, K., Balaji Rajagopalan, Martin Hoerling, Gary Bates and Mark Cane 2006, “ Unraveling the Mystery of Indian Monsoon Failure During El Niño”, Science 314, 115.

Krishnamurti, T. N., 1969, “An experiment in numerical prediction in equatorial latitudes”, QJRMS, 95, 594-620.

Krishnamurti, T. N. and Bhalme, H. N., 1976, “Oscillations of a Monsoon system, Part I Observational aspects”, J. Atmos. Sci., 33, 1937-1954.

Krishnamurti, T. N., Kanamitsu, M., Godbole, R., Chang, C.B., Carr, F. and Chow, J. H. 1976, “Study of a Monsoon Depression (II)”, Dynamical Structure, JMSJ, 54,208-218.

Krishnamurti, T. N., Molinari, J., Pan, H. L., Wong, V., 1977, “Numerical weather prediction relevant to the monsoon problem”, Pure and App. Geophys.115, 1357-1372.

Krishnamurti T. N., Low-Nam, S., Kumar, A., Sheng, J. and Sugi, M. 1987, "Numerical Weather Prediction of Monsoons", Monsoon Meteorology, Oxford University Press.

Krishnamurti, T.N., Dosterhof, D. and Mehta, A.,1988, "Air–sea interaction on the time scale of 30–50 days", *J. Atmos. Sci.*, 45:1304–1322.

Krishnamurti T. N., Oosterhof, D., Dignon, N. 1989, "Hurricane prediction with a high resolution global model", Mon. Weather Rev., 117, 631-669.

Krishnamurti, T.N. 1990, "Monsoon prediction at different resolution with a global spectral model", Mausam, 41, 234-240.

Krishnamurti, T. N. and Sanjay, J., 2003, "A New approach to the Cumulus parameterization issue", *Tellus,* 55A, 275-300.

Krishnamurti, T. N., Thomas, A., Simon, Anu, Vinay Kumar, 2010a, " Desert air incursions, an overlooked aspect for the dry spells of the Indian Summer Monsoon", J. Atmos. Sci., 67, 3423–3441.

Krishnamurti, T. N., Chakraborty, Arindam, Mishra, A. K. 2010b, " Improving Multimodel Forecasts of the Vertical Distribution of Heating Using the TRMM Profiles", *J. Climate*, 23, 1079–1094.

Krishnan, R., Kasture S.V. and Keshavamurty, R.N., 1992, " Northward movement of the 30-50 day mode in an axisymmetric global spectral model", *Current Science*, 62, 732-735.

Krishnan, R., Kasture, S.V., 1996, "Modulation of low frequency intraseasonal oscillations of northern summer monsoon by El Nino and Southern Oscillation (ENSO)", Meteor Atmos. Phys 60(4):237.

Krishnan R., Venkatesan C., Keshavamurty R.N, 1998, " Dynamics of upper tropospheric stationary wave anomalies induced by ENSO during the northern summer, a GCM study, Proceedings of Indian Academy of Sciences (Earth & Planetary Sciences), 107, 1998, 65-90.

Krishnan, R., Zhang, C. and Sugi, M., 2000, "Dynamics of breaks in the Indian summer monsoon", *J. Atmos. Sci.*, **57**:1354–1372.

Krishnan. R., and Sugi, M.,2001, "Baiu rainfall variability and associated monsoon teleconnections", J. Meteor. Soc. Japan, 79, 851–860.

Krishnan, R., Mujumdar, M., Vaidya, V., Ramesh K.V., Satyan, V., 2003, “The abnormal Indian summer monsoon of 2000”, J. Clim. 16:1177–1194.

Krishnan R., Ramesh K.V., Samala B.K., Meyers G., Slingo J.M., Fannessy M.J., 2006, “ Indian Ocean-monsoon coupled interactions and impending monsoon droughts Geophysical Research letters”, 33, L08711 doi:10.1029/2006GL025811.

Krishnan R., Vinay Kumar, M. Sugi and J. Yoshimura, 2009 , “Internal Feedbacks from Monsoon–Midlatitude Interactions during Droughts in the Indian Summer Monsoon”, Journal of Atmospheric Sciences, 66, 553-578.

Krishnan R., Sundaram S., Swapna P., Vinay Kumar, Ayantika D.C., Mujumdar M,. 2010, “Crucial role of ocean-atmosphere coupling on the Indian monsoon anomalous response during dipole events”, Climate Dynamics, 10.1007/s00382-010-0830-2.

Lau N.C., Nath M. J., 2000, “ Impact of ENSO on the variability of the Asian-Australian monsoons as simulated in GCM experiments”, J. Clim 13:4287–4309.

Lau, K.M. and Chan, P.H. 1986, “Aspects of the 40–50 day oscillation during the northern summer as inferred from outgoing longwave radiation”, *Mon. Wea. Rev.*, 114:1354–1367.

Lau, K.M. and Peng, L.1990, “Origin of low frequency (intraseasonal) oscillations in the tropical atmosphere. Part III: Monsoon dynamics”, *J. Atmos. Sci.*, 47:1443–1462.

Lawrence, D. M. and Webster, P. J. 2002, “The boreal summer intraseasonal oscillation: Relationship between northward and eastward movement of convection”, *J. Atmos. Sci.*, 59:1593–1606.

Lee, M. I., Kang, I. S., Kim, J. K. and Mapes, B. E., 2001, “Influence of cloud-radiation interaction on simulating tropical intraseasonal oscillation with an atmospheric general circulation model”, *J. Geophys. Res.,* 106, 14 219–14 233.

Lee, M.I., Kang, I.S., Kim, J.K. and Mapes, B. E., 2003, “Impacts of cumulus convection parameterization on aqua-planet AGCM simulations of tropical intraseasonal variability”, *J. Meteor. Soc. Japan,* 81**,** 963–992.

Luo, J. J., Behera, S., Masumoto, Y., Sakuma, H. and Yamagata, T., 2008, “Successful prediction of the consecutive IOD in 2006 and 2007”, Geophy. Res. Letter, 35, L14S02, doi:10. 1029/2007GL032793.

Luo, J. J., Masson, S., Behera, S.and Yamagata, T.,2007, “Experimental Forecasts of the Indian Ocean Dipole Using a Coupled OAGCM”, *J. Climat*e, 20, 2178–2190.

Mahfouf, J. F., Manzi, A., Noilhan, J., Giordani, H. and De´que´, M., 1995, “The land surface scheme ISBA within the Me´te´o-France climate model ARPEGE. Part I: Implementation and preliminary results”, *J. Climate,* 8, 2039–2057.

Manabe, S., Smagorinsky, J. and Strickler, R.F., 1965, “Simulated Climatology of a General Circulation Model with a Hydrologic Cycle”, Monthly Weather Review, 93(12):769-798.

Manabe, S., Hahn, D.G. and Holloway, J.L., Jr., 1974, “The Seasonal Variation of the Tropical Circulation as Simulated by a Global Model of the Atmosphere”, Journal of the Atmospheric Sciences, 31(1):43-83.

Manabe, S. and Terpstra, T. B., 1974, “ The Effects of Mountains on the General Circulation of the Atmosphere as Identified by Numerical Experiments”, Journal of the Atmospheric Sciences, 31(1):3-42.

McPhaden, M. J., Meyers, G., Ando, K., Masumoto, Y., Murty, V. S. N., Ravichandran, M., Syamsudin, F., Vialard, J., Yu, L. and Yu, W., 2009, “RAMA: The Research Moored Array for African Asian Australian Monsoon Analysis and Prediction”, Bull. Am. Meteorol. Soc., 90, 459- 480.

Miller, M. J., Beljaars, A. C. M. and Palmer, T. N.,1992, “The sensitivity of the ECMWF model to the parametenzation of evaporation from tropical oceans”, J. Clim., 5,418-434.

Meehl, G. A., 1994 , “Coupled land–ocean–atmosphere processes and the South Asian Monsoon Variability”, Science, 266, (5183), 263–7.

Meehl, G. A., and Arblaster, J. M. 1998, “The Asian-Australian monsoon and El Nino- Southern. Oscillation in the NCAR Climate System Model”, J. Clim., 11, 1356-1385.

Murakami T., Godbole, R.V. and Kelkar, R. R.,1970, “Numerical simulation of the monsoon along 80^0E”, Proc. Conf. Summer Monsoon of Southeast Asia, Navy Weather Research Facility, Norfolk, Va., 39-51.

Murakami, T. and Frydrych, M. 1974, “On the preferred period of upper wind fluctuations during the summer monsoon”, *J. Atmos. Sci.* 31, 1549-1555.

Murakami, M., 1977, “Spectrum analysis relevant to Indian monsoon”, PAGEOPH, 115, 1145-1166.

Nanjundiah, R., Srinivasan, J. and Gadgil, S.,1992, “ Intraseasonal variation of the Indian summer monsoon. Part II: Theoretical aspects”, *J. Meteor. Soc. Japan,* **70,** 529–550.

Nigam, S., 1994, “On the dynamical basis for the Asian summer monsoon rainfall–El Niño relationship”, J. Climate, 7, 1750–1771.

Oouchi Kazuyoshi, Akira T. Noda, Masaki Satoh, Bin Wang, Shang-Ping Xie, Hiroshi G. Takahashi, and Tetsuzo Yasunari 2009, “ Asian summer monsoon simulated by a global cloud-system-resolving model: Diurnal to intra-seasonal variability”, Geophy. Res. Lett., 36, L11815, doi:10.1029/2009GL038271.

Palmer T. N., Brankowic, C., Viterbo, P. and Miller, M. J., 1992, “ Modelling interannual variations of summer monsoons”, J Climate, 5, 399-417.

Palmer, T. N., Alessandri, A., Andersen, U., Cantelaube, P., Davey, M., Délécluse, P., Déqué, M., Díez, E., Doblas-Reyes, F. J., Feddersen, H., Graham, R., Gualdi, S., Guérémy, J. F., Hagedorn, R., Hoshen, M., Keenlyside, N., Latif, M., Lazar, A., Maisonnave, E., Marletto, V., Morse, A. P., Orfila, B., Rogel, P., Terres, J.M. and Thomson, M.C., 2004, “Development of a European Multimodel Ensemble System for Seasonal-to-Interannual Prediction (DEMETER)”, Bull. Amer. Meteor. Soc., 85, 853–872.

Palmer, T. N. and Anderson, D. L. T., 1994, “The prospects for seasonal forecasting-A review paper”, *Quart.. J. Roy. Met. Soc. 120,* 755-793.

Pattanaik, D.R. and Arun Kumar, 2010, “Prediction of summer monsoon rainfall over India using the NCEP climate forecast system”, Climate Dynamics Volume 34, Number 4, 557-572, DOI: 10.1007/s00382-009-0648-y.

Raman, C. R. V., and Rao, Y. P., 1981, “ Blocking highs over Asia and monsoon droughts over India”, Nature, 289, 271–273.

Ramaswamy, C., 1962, “Breaks in the Indian summer monsoon as a phenomenon of interaction between the easterly and the subtropical westerly jet streams”, Tellus, 14A, 337–349.

Ramaswamy, C , and Pareek, R. S., 1978, “The south west monsoon over India and its teleconnections with the middle and upper tropospheric flow patterns over the Southern Hemisphere”, Tellus, 30, 126–135.

Robock, A., Mu, M., Vinnikov, K. and Robinson, D., 2003, “Land surface conditions over Eurasia and Indian summer monsoon rainfall”, J. Geophys. Res., 108(D4), 4131, doi: 10. 1029 / 2002JD002286.

Rodwell, M. J., 1997, “Breaks in the Asian monsoon: The influence of the Southern Hemisphere weather systems”, J. Atmos. Sci., 54, 2597–2611.

Sahai, A. K., Chattopadhyay, R. and Goswami, B. N., 2008, “A SST based large multi-model ensemble forecasting system for Indian summer monsoon rainfall”, Geophys. Res. Lett., 35, L19705, doi: 10. 1029 / 2008GL035461.

Sellers, P. J., Mintz, Y., Sud, Y. C. and Dalcher, A.,1986, “ A simple Biosphere Model (SiB) for use within general circulation models”, J. Atmos. Sci., 43, 505-531.

Sengupta, D., Goswami, B. N. and Senan, R., 2001, “Coherent intraseasonal oscillations of the ocean and atmosphere during the Asian summer monsoon”, *Geophys. Res. Lett.*, 28:4127–4130.

Shige, S., Takayabu, Y. N. Tao, W. K. and Johnson, D. E., 2004, “Spectral retrieval of latent heating profiles from TRMM PR data. Part I: Development of a model-based algorithm. *J. Appl. Meteor.*, 43, 1095–1113.

Shige, S., Takayabu, Y. N. and Tao, W. K., 2008, “Spectral retrieval of latent heating profiles from TRMM PR data. Part III: Estimating apparent moisture sink profiles over tropical oceans”, *J. Appl. Meteor. Climatol.*, 47, 620–640.

Shukla, J., 1975, “Effect of Arabian Sea-Surface Temperature Anomaly on Indian Summer Monsoon:A Numerical Experiment with the GFDL Model”, J. Atmos. Sci., 32, 503–511.

Shukla, J., and Misra, B., 1977, “Relationships Between Sea Surface Temperature and Wind Speed Over the Central Arabian Sea, and Monsoon Rainfall Over India”, Mon. Wea. Rev., 105, 998–1002.

Shukla, J., and Paolino, D. A. 1983, “The Southern Oscillation and long-range forecasting of the summer monsoon rainfall over India”, Mon. Weather Rev. 111: 1830–1837.

Sikka, D. R. and Gadgil, S., 1980, “On the maximum cloud zone and the ITCZ over Indian longitudes during the southwest monsoon”, *Mon. Wea. Rev.,* 108, 1840–1853.

Simmons, A. J. and Hollingsworth, A., 2002, “Some aspects of the improvement in skill of numerical weather prediction”, *Q. J. R. Meteorol. Soc.,*128, 647—678.

Singh, A. P., Mohanty, U. C., Sinha, P. and Mandal, M., 2007, “Influence of different land-surface processes on Indian summer monsoon circulation”, 42, *Nat. Hazard*, 423-438.

Slingo J. M., Mohanty U.C., Tiedtke, M., Pearce R.P., 1988, “Prediction of the 1979 summer monsoon onset with modified parameterization schemes”, Monthly Weather Review 116(2): 328-346.

Slingo, J. M., Sperber, K. R. and 22 others, 1996, “Intraseasonal oscillations in 15 atmospheric general circulation models : Results from an AMIP Diagnostic Subproject”, *Climate Dynamics*, 12, 325-357.

Soman, M. K., and Slingo, J. 1997, “Sensitivity of the Asian summer monsoon to aspects of sea surface temperature anomalies in the tropical Pacific Ocean”, Q. J. R. Meteorol Soc. 123: 309-336I.

Sperber, K., and Palmer, T.,1996, “Interannual Tropical Rainfall Variability in General Circulation Model Simulations Associated with the Atmospheric Model Intercomparison Project”, J. Climate, 9, 2727–2750.

Sperber, K. R., 1999, “Are revised models better models: A skill score assessment of regional interannual variability”, Geophys. Res. Lett., 26, 1267–1270.

Sperber, K. R., Brankovic, C., Deque, M., Frederiksen, C.S., Graham, R., Kitoh, A., Kobayashi, C., Palmer, T., Puri, K., Tennant, W., Volodin, E., 2001, "Dynamical seasonal predictability of the Asian summermonsoon", Mon Weather Rev, 129: 2226–2248.

Sperber, K. R., 2003, "Propagation and the vertical structure of the Madden–Julian oscillation", *Mon. Wea. Rev.*, 131, 3018–3037.

Srinivasan, J., Gadgil, S. and Webster, P. J., 1993, "Meridional propagation of large-scale monsoon convective zones", *Meteor. Atmos. Phys.,* 52**,** 15–35.

Sud, Y. C., Chao, W.C. and Walker, G. K., 1992, "Role of a cumulus parameterization scheme in maintaining atmospheric circulation and rainfall in the nine-layer Goddard Laboratory for Atmospheres General Circulation Model", *Mon. Wea. Rev*., 120, 594-611.

Sugi M., Kawamura, R. and Sato, N., 1997, "A study of SST-forced variability and potential predictability of seasonal mean fields using the JMA global model", J. Meteor. Soc. Japan, 75, 717–736.

Tao, W. K., Houze, R. J. and Smith, E. A. 2007, "The fourth TRMM latent heating workshop", *Bull. Amer. Meteor. Soc.*, 88, 1255–1259.

Vecchi, G. A. and Harrison, D. E., 2002, "Monsoon breaks and subseasonal sea surface temperature variability in the Bay of Bengal", *J. Climate*, 15, 1485–1493.

Vernekar, A., Zhou, J. and Shukla, J., 1995, "The Effect of Eurasian Snow Cover on the Indian Monsoon", J. Climate, 8, 248–266.

Vinay Kumar, 2008, "Model studies of droughts in the tropics and sub-tropics", University of Pune, Ph.D. Thesis.

Waliser, D. E., Lau, K. M. and Kim, J. H., 1999, "The influence of coupled sea surface temperatures on the Madden–Julian oscillation: A model perturbation experiment", *J. Atmos. Sci.*, 56:333–358.

Waliser, D. E., Jin, K., Kang, I. S., Stern, S. D., Schubert S. D., Wu, M. C., Lau, K. M., Lee, M. I., Krishnamurthy, V., Kitoh, A., Meehl, G. A., Galin, V. Y., Satyan, V., Mandke, S. K., Wu, G., Liu, Y., Park, C. K., 2003, "AGCM simulations of intra-seasonal variability associated with the Asian summer monsoon", Clim. Dyn. 21:423–446.

Walker, G. T., and Bliss, E. W., 1932, "World Weather", V. Mem. Roy. Meteor. Soc., 4, 53–84.

Wang, B., Kang, I. S. and Lee, J. Y., 2004, "Ensemble Simulations of Asian–Australian Monsoon Variability by 11 AGCMs", J. Climate, 17, 803–818.

Wang, B. and Xie, X., 1997, "A model for the boreal summer intra-seasonal oscillation", *J. Atmos. Sci.*, 54:72–86.

Wang, B., 2004, "The Asian Monsoon", Ed. Bin Wang, Springer/Praxis Publishing Co., NY, pp787.

Wang, B., Ding, Q., Fu, X., Kang, I. S., Jin, K., Shukla, J. and Doblas-Reyes, F., 2005, "Fundamental challenge in simulation and prediction of summer monsoon rainfall", Geophys. Res. Lett., 32, L15711, doi: 10. 1029 /2005GL022734.

Washington, W. M.,1970, "On the simulation of the Indian monsoon and tropical easterly jet stream with the NCAR general circulation model", Preprint Vol., Symp. Trop. Meteor., 2-11 June 1970, Honolulu, Hawaii, Amer. Meteor. Soc., JVI 1-5.

Washington, W., and Daggupaty, S.,1975, " Numerical Simulation with the NCAR Global Circulation Model of the Mean Conditions during the Asian-African Summer Monsoon", Mon. Wea. Rev., 103, 105–114.

Webster, P. J., 1983, "Mechanisms of monsoon low-frequency variability:Surface hydrological effects", *J. Atmos. Sci.,* 40**,** 2110–2124.

Webster, P. J., Magana, V. O., Palmer, T. N., Shukla, J., Thomas, R. A., Yanai, M. and Yasunari, T., 1998, "The monsoon: Processes, predictability and prediction", J. Geophys. Res. 103, 14, 451–14 510.

Webster, P. J. and Chou, L. C.,1980, "Low-Frequency Transitions of a Simple Monsoon System", J. Atmos. Sci., 37, 368-382.

Xavier, P. K. and Goswami, B.N., 2007, “Analog method for real time forecasting of summer monsoon sub-seasonal variability”, Mon. Weather Review 135, 4149-4160.

Xue, Y., Sellers, P. J., Kinter III, J. L. and Shukla, J., 1991, “A Simplified Biosphere Model for global climate studies”, *J. Climate*, 4, 345–364.

Yamagata, T., Behera, S. K., Luo, J. J., Masson, S., Jury, M. R. and Rao, S. A. 2004, “Coupled Ocean-Atmosphere Variability in the Tropical Indian Ocean”, pp. 189-212. Earth Climate: The Ocean-Atmosphere Interaction " Eds. by Wang, C., S.-P. Xie, and J.A. Carton. Geophysical Monograph 147, American Geophysical Union.

Yasunari, T., 1979, “Cloudiness fluctuations associated with the northern Hemisphere summer monsoon”, J. Meteorol. Soc. Japan, 57, 227-242.

Yasunari, T., 1980, “A quasi-stationary appearance of 30 to 40 day period in cloudiness fluctuations during the summer monsoon over India”, J. Meteorol. Soc. Japan, 58, 225-229.

Yasunari, T., Kitoh, A. and Tokioka, T. 1991, “Local and remote response to excessive snow cover mass over Euresia appearing in the northern spring and summer climate:A study with MRI GCM”, JMSJ, 69, 473-487.

Yun, W.T., Stefanova, L. and Krishnamurti, T. N.,2003, “Improvement of the Multimodel Superensemble Technique for Seasonal Forecasts”, J. Climate, 16, 3834–3840.

Zachary, A., Randall, D.,1999, “Sensitivity of the simulated Asian summer monsoon to parameterized physical processes”, J Geophys Res 104:12,177–12,191.

Zwiers F.W., 1993, “Simulation of the Asian summer monsoon with the CCC GCM-1”, J. Climate, 6, 470-486.

Zhang, G. J., 1994, “Effects of cumulus convection on the simulated monsoon circulation in a general circulation model”, *Mon. Wea. Rev*., 122, 2022-2038.

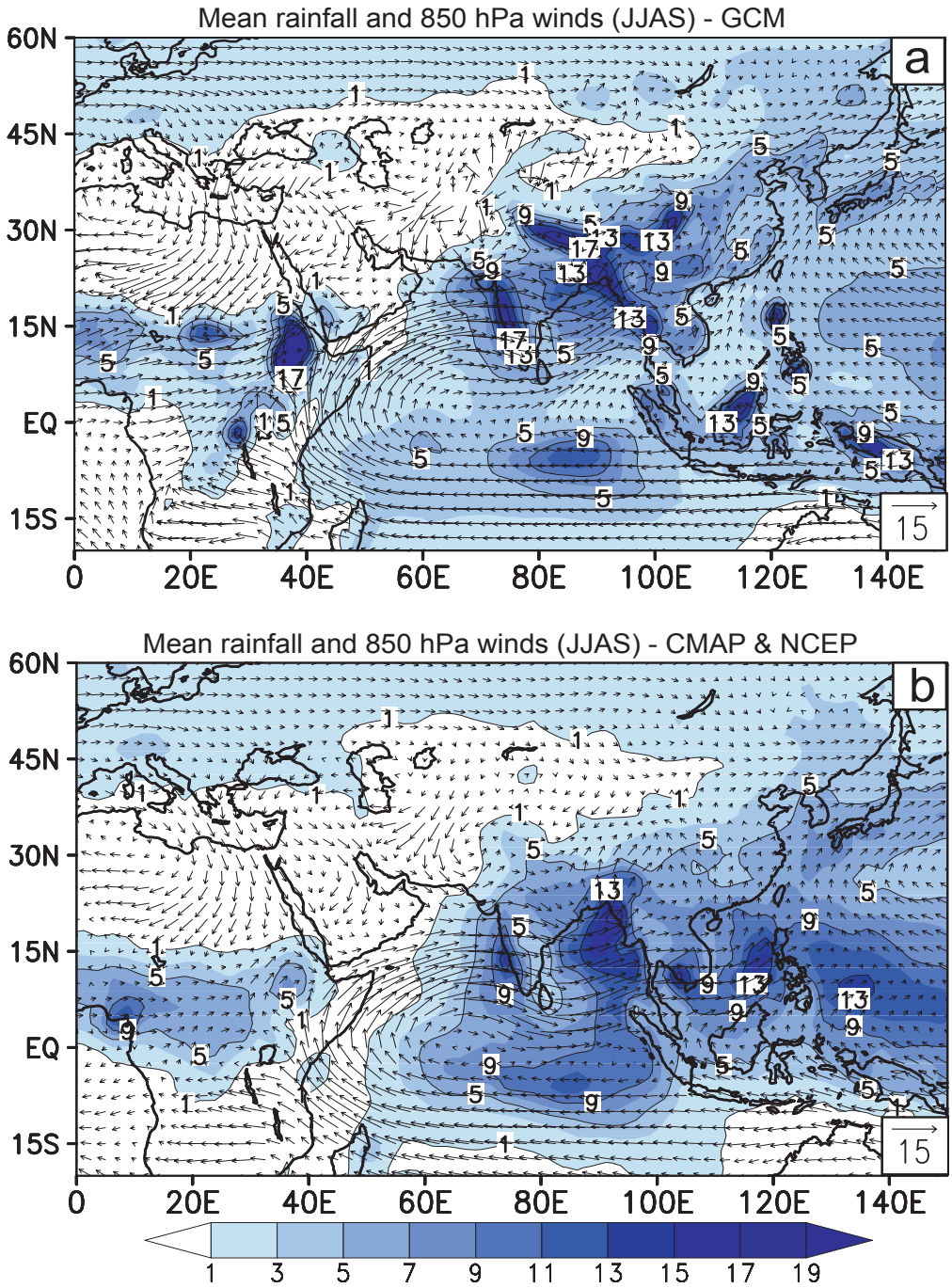

Fig.5.1 : Mean rainfall (mm day^{-1}) and 850 hPa winds (m s^{-1}) for the June-September (JJAS) monsoon season (a) GCM (b) CMAP (rainfall) and NCEP reanalysis winds. The mean fields in the GCM are computed from the 20-year simulation. For the CMAP/NCEP data, the climatology is based on the period (1979-2004).
[Adapted from Krishnan et al. 2009]

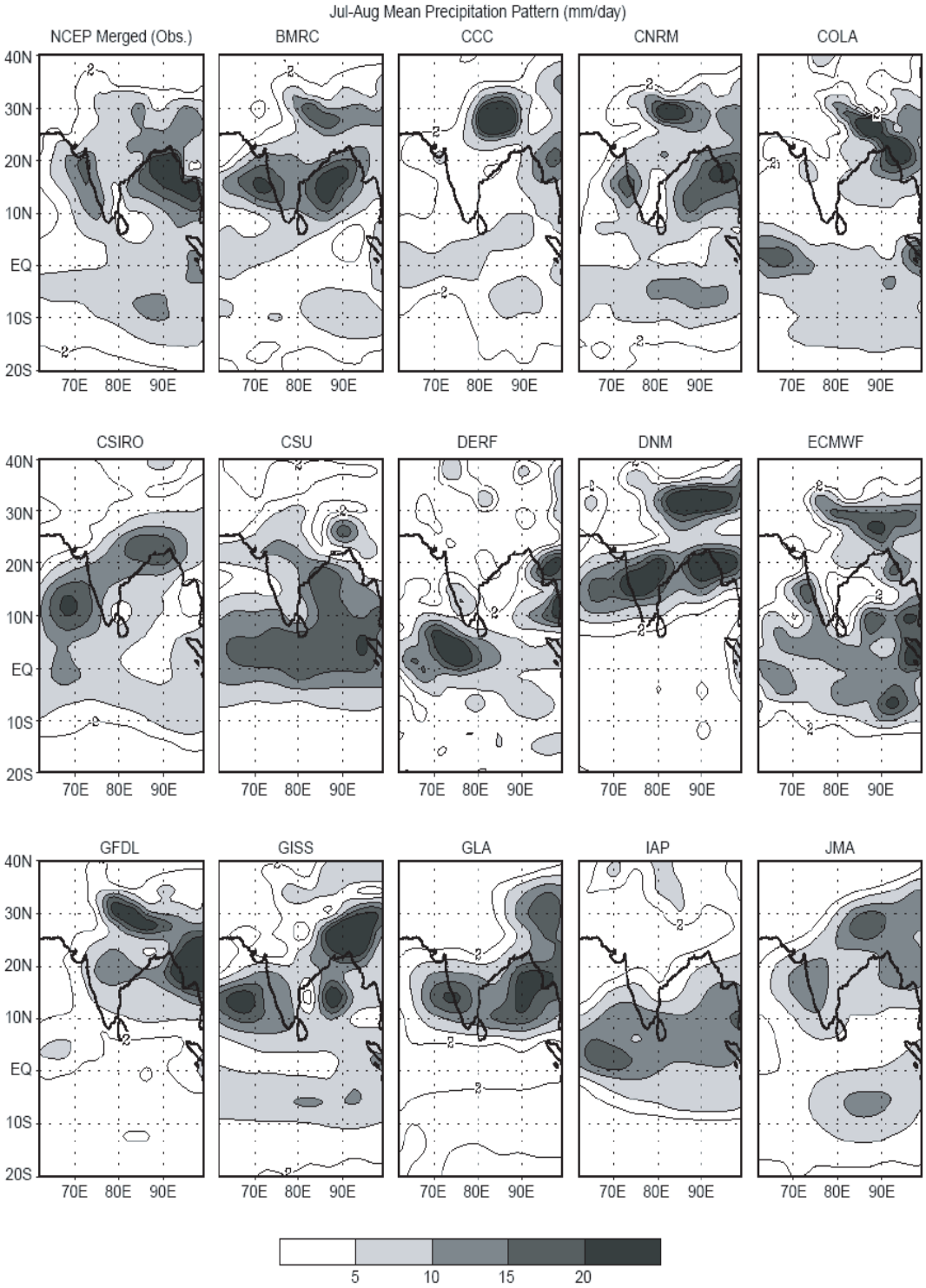

Fig.5.2 : Mean July-August precipitation over the Indian region as simulated by AMIP models. ***[Adapted from Gadgil and Sajani 1998]***

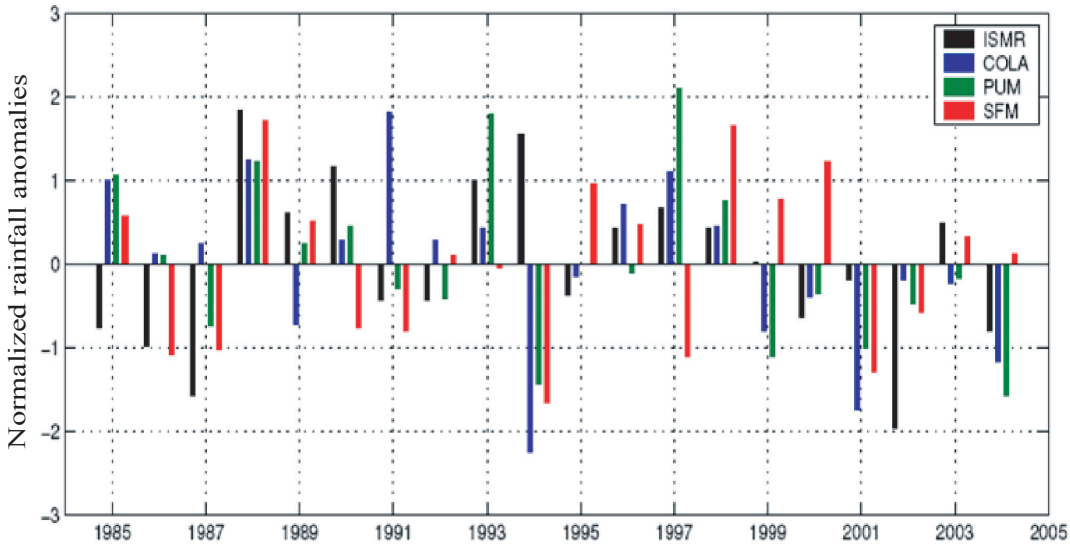

Fig.5.3 : Ensemble mean of simulated rainfall anomalies over Indian region (70°E-90°E; 12°N-32°N) from the Portable Unified Model – PUM, UK Met Office (green bars), Seasonal Forecasting Model - SFM, NCEP (red bars) and COLA AGCM (blue bars). The All India Summer Monsoon Rainfall (AISMR) anomalies are shown in black bars. The rainfall anomalies are normalized by their respective standard deviations.

[Adapted from Gadgil et al. 2009]

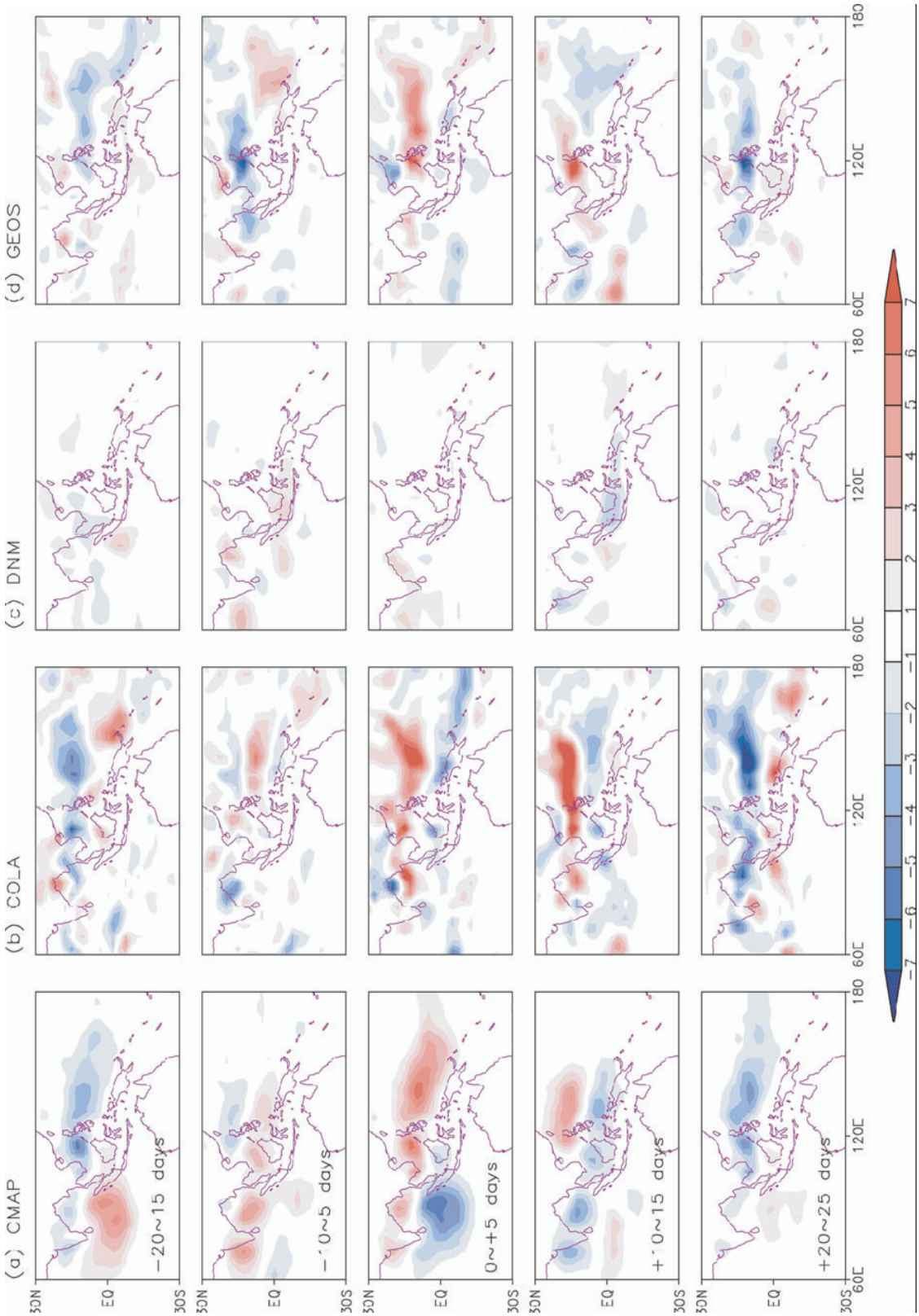
(a) CMAP
(b) COLA
(c) DNM
(d) GEOS
−20~15 days
−10~5 days
0~+5 days
+10~15 days
+20~25 days
30N
EQ
30S
60E
120E
180
−7
−6
−5
−4
−3
−2
−1
1
2
3
4
5
6
7

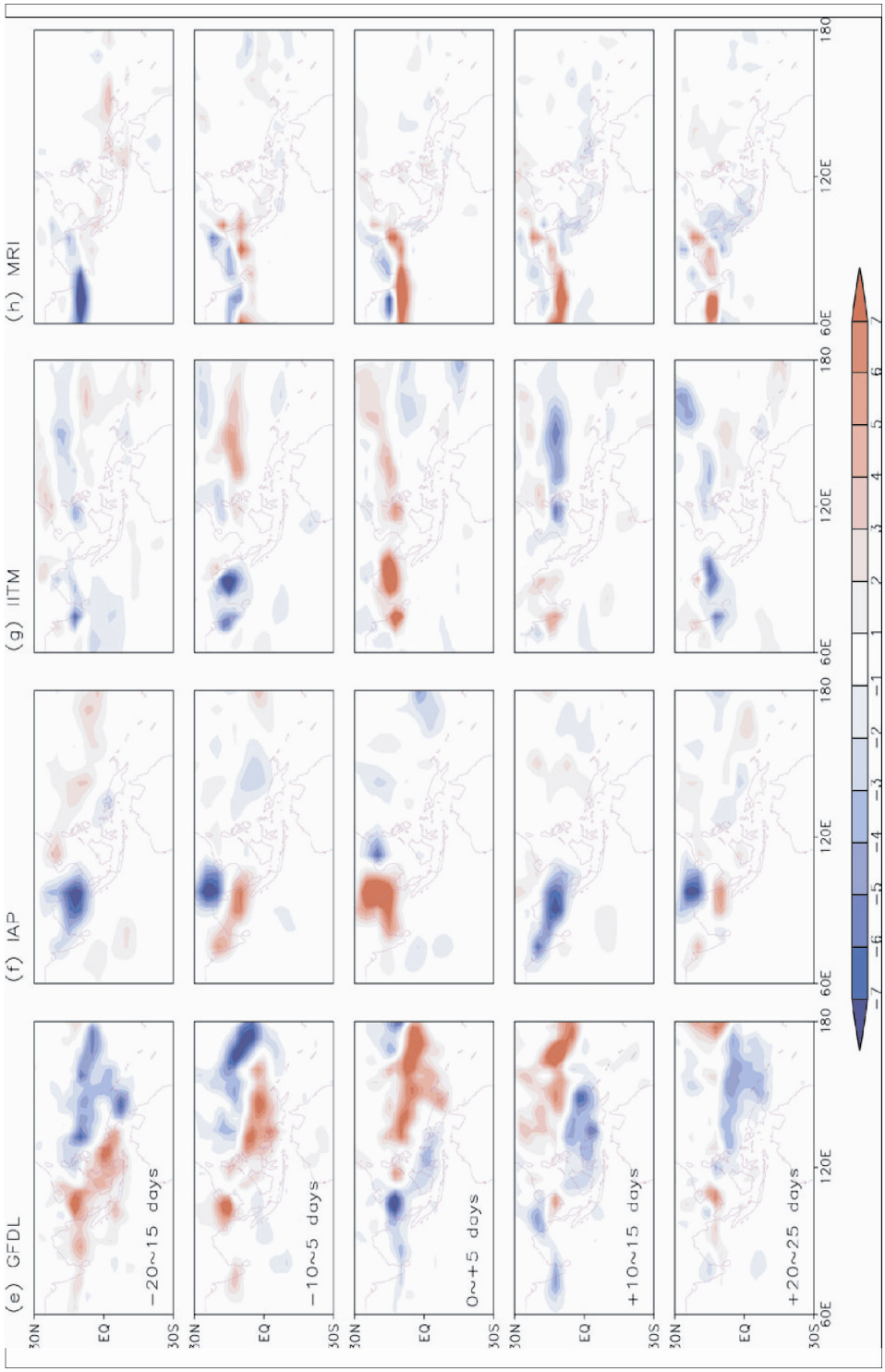

Fig. 5.4 (a-h) : Composite ISO events in terms of rainfall (mm/day) from observations (left) and participating models for the Northern hemisphere summer. Construction is based on identifying event using an extended empirical orthogonal function (EEOF) analysis. The number of events in each composite are given in the parenthesis : CMAP (38), COLA (12), DNM (10), GEOS (11), IAP (18), IITM (16), MRI (18). [Adapted from Waliser et al. 2003]

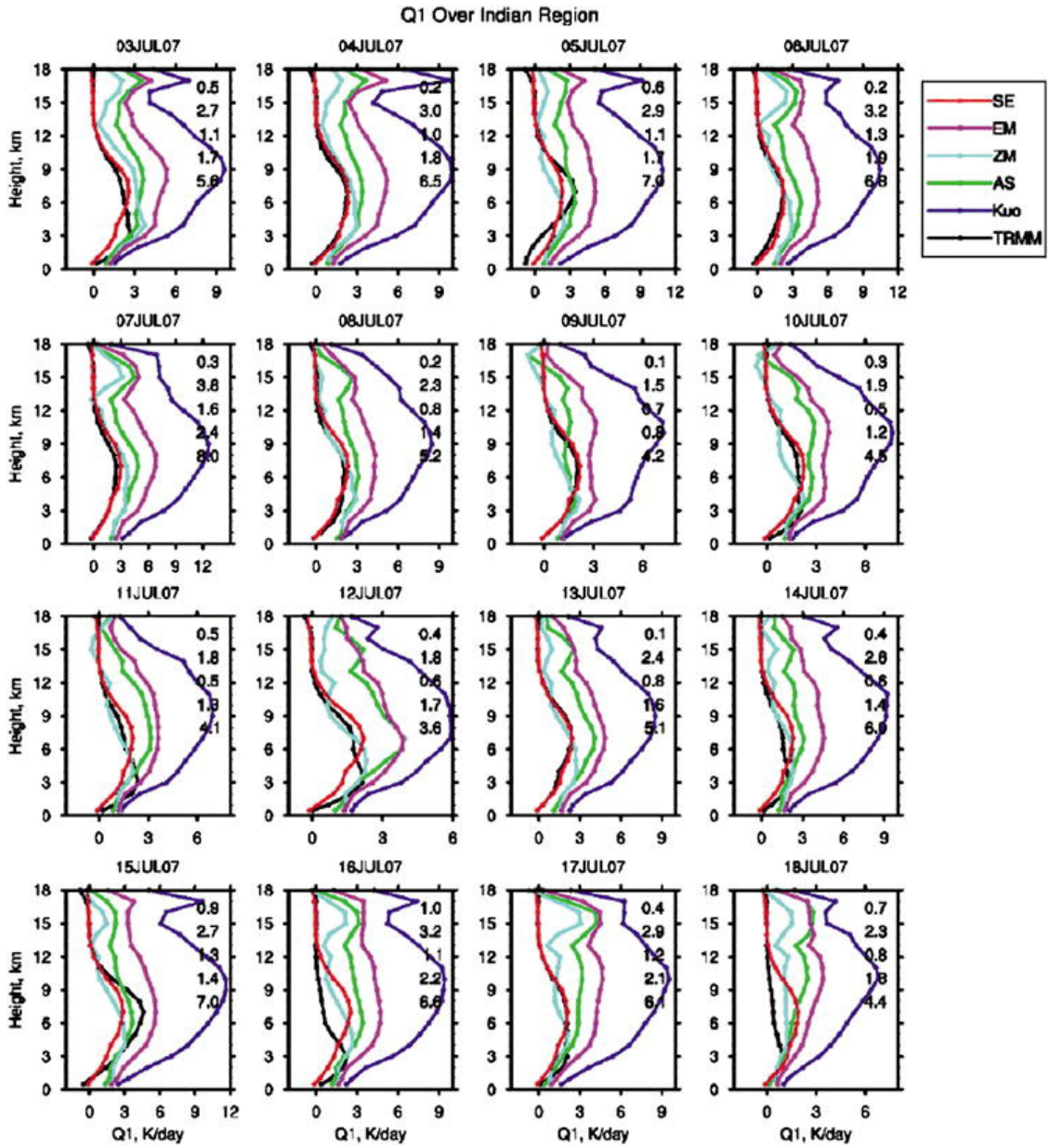

Fig. 5.5 : Vertical profile of Q1 from TRMM PR estimates, and 12–36-h (day 1) forecasts of three member models, their ensemble mean, and the superensemble over the Indian region (5°–25°N, 70°–90°E) during 3–18 Jul 2007. The RMS errors of the forecast fields are indicated as numbers (K day^{-1}) at the top right corner of the panel.
[Adapted from Krishnamurti et al. 2010b]

CHAPTER 6

MODELING OF FORECAST SENSITIVITY ON THE MARCH OF MONSOON ISOCHRONES FROM KERALA TO NEW DELHI, THE FIRST 25 DAYS

T.N. Krishnamurti[1], Anu Simon[1], Aype Thomas[1] , Akhilesh Mishra[1], Dev Sikka[2], Dev Niyogi[3], Arindam Chakraborty[4] and Li Li[5]

[1]Dept. of Earth, Ocean & Atmospheric Sciences,
Florida State University, Tallahassee, FL
[2]Meteorologist, New Delhi
[3]Department of Earth and Atmospheric Sciences,
Purdue University, West Lafayette, IN
[4]Caos, iisc, Bangalore
[5] NRL, Washington

tkrishnamurti@fsu.edu

6.1. Introduction

The annual cycle of the Asian summer monsoon carries the passage of onset isochrones of precipitation. This is a major feature of the monsoon life cycle. Chang (2003) illustrated the march of the principal monsoonal heat source from Indonesia to the eastern foothills of the Himalayas between January and July and a reverse trek during the remaining months of the year. This is the belt of the heaviest monsoon rains that exhibit an annual seesaw in its traverse pattern. This axis should be labeled as a principle axis of the monsoon. A feature that follows this rain belt is the upper tropospheric outflows, that can be seen as a distinct upper anticyclone such as the Tibetan high. During these months the flows exhibit a response to the heating, following the symmetric and antisymmetric heating/circulation scenario of Gill (1980). A clock wise large scale gyre over the southern hemisphere Indian Ocean makes its way well into the northern hemisphere by July, (Fig.6.1). This gyre of clockwise circulation meets the south west coast of India, the Kerala State, during early June normally. Thus the progress of the broadscale differential heating also dictates the onset of the monsoon rains over Kerala, the subsequent progress of the onset isochrones is sensitive to the overall structure of heat sources and sinks. The response of the northward progress of the monsoon to the heating along this principal axis of the monsoon was addressed by Krishnamurti and Ramanathan (1982). They noted that flow features such as those during the onset and active monsoon spells were sensitive

to the location of the heat source of the monsoon. In that sense the heating along the principal axis is also important for the isochrone positions. During the months between May and July these isochrones, plotted at five day intervals (Rao, 1976), show a passage from the Indian Ocean south of India to the foothills of the Himalayas. The standard deviations of the dates of onset over different parts of India have been summarized by Rao (1976). These isochrones are elongated from the south-west to north-east and the onset rains shows a meridional and eventual westward motion. Chang (2005) presented a climatology of the onset isochrones, for the entire Asian monsoon that looks at the east Asian monsoon and the Indian Monsoon in a collective manner, (Fig. 6.2). The Myanmar monsoon onset precedes the Indian monsoon onset by about a month. Lwin (2002) noted that the onset of the Myanmar and the Indian monsoon onset are related to the passages of two successive waves of the ISO (Intraseasonal Oscillation), those strengthen the Myanmar monsoon westerlies during early parts of the month of May and the Kerala onset in India happens during early June from the passage of a second wave of the ISO. Prediction of the passage of the onset isochrones is the same as the prediction of the first rains of the monsoon after a dry season. This does not necessarily convey anything specific about the total rainfall for a season over all of India. From an examination of model outputs and surface and space based observations we noted a scenario that seems to provide an explanation for the meridional motion of the onset isochrones. A typical isochrones during the early parts of the month of June is shown in Fig. 6.3. This illustration is based on the climatological positions of the onset isochrone as defined by the India Meteorological Department. This line is typically found over the southwest coast of India, over the Kerala State, and it extends northwestwards over the Bay of Bengal coast and passes through the central Bay of Bengal and northwards over Bangladesh and northeast Indian states.The India Meteorological Department is routinely providing annual summaries of the onset of the summer monsoon, (Srivastava and Yadav, 2009; Khole et al., 2010, 2011). These carry valuable information. IMD has adopted the following new objective criteria for declaring monsoon onset over Kerala based on rainfall, wind field and OLR data. The criteria are as follows:-

Onset over Kerala is declared on the second day if after 10th May, 60% of the available 14 stations report rainfall of 2.5 mm or more for two consecutive days. The depth of westerlies should also be maintained up to 600 hPa, in the box equator to Lat 10^0N and Long 55^0E to 80^0E. The zonal wind speed at 925 hPa over the area bounded

by 5^0N -10^0N, 70^0E to 80^0E should be at least of the order of 15-20 knots. Another important criteria is that INSAT derived OLR value should be below 200 Wm^{-2} in the box confined by Lat. 5-10^0N and Long 7^0-75^0E. After the onset of Kerala the onset isochrones for the later dates are drawn connecting the places which report rainfall of 2.5 mm or more for two consecutive days. The land mass to the north and west of this line, not having experienced much rain in the spring season, is close to semi arid. The soil moisture over those regions of land are very low with typical values of around 0.15 fraction. A couple of days after the passage of the onset isochrone those values jump up to 0.35 fraction. The soil moisture increase generally starts to occur a day or two before the arrival of the onset isochrone. That has to do with a cloud asymmetry across the isochrone. While the clouds over and behind the isochrone carry a larger proportion of deep convective clouds as compared to startiform clouds the cloud anvils ahead of the isochrone carry a larger proportion of stratiform rain. The anvils are advected in front of the isochrone by the prevailing divergent circulations. The fresh lighter rains from the anvils enhances the soil moisture ahead of the isochrones and the warm day time temperatures facilitate a rapid increase of buoyancy in this region. The enhanced buoyancy results in the growth of newer convective elements ahead of the isochrone. These elements are advected, northwards and or north westwards, by the prevailing divergent circulation that was produced by the heavy rains of the parent isochrone. As the older clouds undergo their life cycle and die, the newer elements grow, the new isochrone and the entire system shows the familiar isochrone motion from south to north and from east to west in northern latitudes. On certain years one notes a stagnation of the onset isochrones that could be related to unusual behavior of the large scale, as reflected by the rotational winds. Those winds around the Tibetan high can at times have a stronger northerly component which can contribute to stationarity of the isochrone. This entire scenario is schematically illustrated in Fig. 6.4. In this chapter, we shall address observational aspects using conventional data sets and vertical cross sections from CLOUDSAT, sensitivity using a mesoscale high resolution WRF model, and a validation of this scenario. The chapter illustrates the major role of soil moisture, stratiform cloud and divergent circulations for the motion of the onset isochrones from Kerala, 10^0N to New Delhi near 25^0 N.

6.2. CLOUDSAT imagery across the onset isochrones

The CLOUDSAT is a NASA satellite that was launched in 2006. The main instrument is millimeter wavelength radar. Ground based radars generally carry a wavelength of centimeter. The mm wavelength radar of CLOUDSAT enables it to detect much smaller particles of liquid water and ice that defines clouds. This cloud radar provides vertical plan views of hydrometeors, (the cloud profiling radar). Two other satellites Aqua (provides water vapor profiling) and CALIPSO (Cloud Infrared Pathfinder Radar Observations) are important for joint studies with CLOUDSAT. Colocated data sets from CLOUDSAT, AQUA and CALIPSO has enabled NASA to develop algorithms to defines the cloud structures and cloud types. These data sets are routinely provided by NASA from their web site. Here we shall illustrate Fig. 6.5 (a-c) typical vertical cross sections from CLOUDSAT that show cloud asymmetry across onset isochrones. In these illustrations, to the right, we show a map of India, with infrared cloud imagery, and the traverse of the satellite. The satellite traverse includes both ascending and descending nodes. To the left are shown the vertical plan view of clouds. A vertical green dotted line provides the location of the onset isochrone (as defined by IMD) for three sample dates. In these cross sections we clearly see a plethora of deep convective elements behind the onset isochrone. The picture ahead of the isochrone generally shows high cloud anvils, cirrus, few towering cumulus and a few cumulonimbus clouds. The NASA classification of cloud types is shown just below each vertical cross section. This region is moistened by the anvil rains, (non convective rains) and the warm surface temperature ahead of the isochrone and the evaporating rain carries large buoyancy. New cloud elements form and grow in this region ahead of the isochrone. We have examined the asymmetry of clouds across the isochrone for different periods of the monsoon, during the last three years and noted very similar structures. This asymmetry is an important characteristic of the newly forming clouds that grow and define a new parent isochrone. The motion of the isochrone seems to be dictated by the divergent circulation that is described in section 6.7.

6.3. Model experiments

6.3.1. The WRF/ARW model

The WRF-ARW model is a collaborative effort among the NCAR Mesoscale and Microscale Meteorology Division (MMM), and NCEP's Environmental Modeling Center (EMC). The WRF model is a fully compressible and nonhydrostatic model (with a runtime hydrostatic option). Its vertical coordinate is a terrain-following hydrostatic pressure coordinate. The grid staggering is the Arakawa C-grid. The model uses the Runge-Kutta 2nd and 3rd order time integration schemes, and 2nd to 6th order advection schemes in both horizontal and vertical. It uses a time-split small step for acoustic and gravity-wave modes. The dynamics conserves scalar variables. We have used the following physics options for this model: Radiation schemes Longwave: rapid radiative transfer model (rrtm) (Mlawer et al., 1997) Shortwave: Dudhia scheme (Dudhia 1989; Grell, 1993), Surface physics: Monin-Obukhov (Janjic) scheme (Monin and Obukhov, 1954), Land surface model: 5 layer thermal diffusion (Skamarock et al., 2005) Planetary boundary layer scheme: Mellor-Yamada-Janjic (MYJ) TKE PBL (Janjic, 1994) Convection scheme: Kain-Fritsch (new Eta) scheme (Kain and Fritsch, 1993), Explicit moisture scheme: WRF Six -class graupel scheme (WSM6) (Hong et al., 2004; Hong and Lim, 2006). The model is run with a single domain at 25km horizontal resolution and 27 vertical levels.

NCEP's GDAS carries a 6 hourly gridded data archive. The GDAS is derived from the NCEP's operational model runs; it is called the final analysis FNL. This includes late conventional and satellite data sets (Petersen and Stackpole, 1989). This assimilation is run 4 times a day, i.e, at 00, 06, 12, and 18 UTC. Model output is for the analysis time and a 6-hour forecast. Precipitation and surface fluxes are only available at the forecast hours. Details of the GDAS are described by Kanamitsu (1989), Derber et al. (1991), and Parrish and Derber (1992). NCEP post-processing of GDAS converts the data from spectral coefficient form to 1 degree latitude-longitude (360 by 181) grids and from sigma levels to mandatory pressure levels. The data are written to the NIC (NOAA Information Center) FTP server (nic.fb4.noaa.gov) in GRIB (GRIdded Binary) format.These data set are used in our study.

6.3.2. The soil moisture parameterization in the WRF/ARW model

In most numerical models the soil moisture algorithm interfaces with the moisture equation of the constant flux layer, thus exchanging precipitation and evaporation relevant to the ground and the atmosphere. The soil moisture algorithm is in fact a time dependent equation for the forecast of soil moisture over four soil layers that carry thicknesses of 10, 30, 60 and 100 cms. The soil model predicts surface skin temperature, total soil moisture, liquid soil moisture in each layer, soil temperature for each layer, the canopy water content (this can be dew or frost intercepted precipitation). These require initial states that are provided by the WPS of the ARW/WRF based on past experimentation. The soil moisture equation is of the form,

$$\frac{\partial s}{\partial t} = \frac{\partial}{\partial z}\left(D\frac{\partial s}{\partial z}\right) + \frac{\partial K}{\partial z} + F_s \qquad (1)$$

where D, K functions for soil texture and soil moisture and Fs represents sources (rainfall) and sinks (evaporation).

The soil temperature prediction equation takes a form

$$C(\theta)\frac{\partial T}{\partial t} = \frac{\partial}{\partial z}\left(K_t(\theta)\frac{\partial T}{\partial z}\right) \qquad (2)$$

where C, Kt are functions for soil texture and soil moisture. Soil temperature information is used to compute ground heat flux.

The surface water budget is estimated from the relation:

dS = P – R - E

where,

dS = change in soil moisture content;

P = precipitation

R = runoff

E = evaporation

Further, the evaporation is a function of soil moisture and vegetation type, rooting depth and the green vegetation cover. This formulation utilizes Noah algorithms of NCAR models, those also include the parameterizations for surface evaporation,

vegetation transpiration and canopy resistance. These details can be found in Chen et al., (1996, 2001).

In our work, we started with experiments that started with this default model from WRF/ARW. For the sensitivity studies on soil moisture, we altered the soil moisture in various experiments, those are described below.

6.3.3. Non-convective rain in weather and climate

The definitions of non convective rain used by radar meteorologists and by numerical modelers appear to be somehwhat distant from each other. Most numerical modelers invoke non convective rain if the location in question carries a dynamic ascent of absolutely stable and near saturated air. Disposition of supersaturation provides a measure of non convective precipitation at that location. Krishnamurti et. al (2006) describe two other, more rigorous, methods for the estimation of non convective precipitation that are variants of this same principle, i.e. the disposition of supersaturation.

The language of the radar meteorologist invokes features such as those shown in Table 7.1 Stano et al. (2002).

Table 6.1: Criteria for determining convective and stratiform rain as seen by TRMM radar

Condition	Convective rain	Stratiform rain
Presence of light bands	×	✓
Absence of bright bands	✓	×
Reflection 20–40 dbz	✓	✓
Reflection >40 dbz	✓	×
Presence of strong gradients of radar reflectivity	✓	×
Absence of reflectivity gradients and reflection>20dbz	×	✓

To expect even after averaging at meso or larger scale grid sizes, for these two methods to match closely would be difficult to achieve. In most of these radar based estimates of convective and non convective rains, parts of the deep convective systems carry anvils and provide stable non convective rains. These are systems where the two coexist in proximity. In large scale models, mostly in the context of large sheets of stratus and altostratus, that span for thousands of miles, in extratropical weather systems, the modeling definition works reasonably well for estimates of non convective rain. However, in the monsoon isochrone context we are dealing with a plethora of deep convection behind, and stratiform anvils ahead of the isochrones. If such coexisting, convective/startiform cloud systems are important for the motion of the isochrones, then a better definition of the stratiform rain may be needed for future modeling. Those can be brought about in cloud resolving, very high resolution models, where the microphysical processes are explicitly tagged. In the current WRF/ARW model that is being presented here, the non convective rain at 25 km resolution comes from the disposition of supersaturartion. Those results are presented in section 6.5.3. In order to see further details on the asymmetry of cloud types across the isochrone, a few experiments were also carried out at a 3 km resolution where explicit clouds, instead of parameterized clouds, were used. Those structures are described in section 6.6.

6.4. A control experiment during a near normal rainfall year

We selected the monsoon season of the year 2000 for the control experiment since the model-based rainfall totals for the first 25 days, all India averaged, were close to the observed totals for the same period. In Fig.6.6 we show, by a dark line, the observed march of the isochrones for the summer monsoon season of the year 2000. This is based on IMD product. The predicted field of the onset isochrones from the mesoscale WRF/ARW model is shown as a red line in Fig 6.6. Here the accumulated precipitation are also shown in each panel, where the panels cover the dates June 1 through 25 at intervals of roughly 5 days. The forecast has many deficiencies; the initial position of the isochrone, observed versus modeled, shows almost a three degree latitude displacement over the Bay of Bengal. Forecasts generally improved during the first 5 days, day 5 forecast showed the least errors and thereafter the model isopleth motion was consistently slower compared to the observed positions. Such errors have

to be expected because the current predictability for tropical rainfall prediction is only of the order of a few days. Through sensitivity studies, shown in the next section, the goal is to find out factors that can either slow down or speed up the motion of the isochrones. This, and two other examples presented below are shown to illustrate the nature of the current prediction using a WRF/ARW model that utilized some default values for various parameters. Overall this is not a very poor forecast for day 25, considering that a northwestward march of the isochrone is implied by this forecast with overall errors that are less than 4 degree latitude.

6.4.1 Modeling isochrone motion during a dry monsoon year:

The observed isochrones for the 2002 season, based on the IMD data sets, are shown in Fig. 6.7 by a dark line. This was a below normal monsoon rainfall year. The march of the isochrones during the first 25 days reflected a slower than normal meridional motion. The accumulated predicted rains preceding the forecast day, in colour shading, are shown at intervals of 5 days, and the predicted isochrones are shown by a red line, in Fig 6.7. The model, in general ,carries a somewhat slower northward and eventual northwestward motion for the isochrone, as a result the control run of the model predicted a somewhat drier monsoon compared to the dry season of 2002. Overall, again this was a very reasonable forecast for the positioning of the isochrone through day 25 of forecast, since the position error were less than 5 degrees in latitude.

6.4.2 Modeling isochrone motion during a wet monsoon year.

This was the 2003 summer monsoon season, the seasonal totals of rains over all India were above normal, but the onset of monsoon over Kerala, the south west coast of India, was delayed by a week. The observed and the predicted isochrones for this experiment are shown in Fig 6.8 . Also shown are accumulated rainfall totals preceding the day for which the forecast is labeled. This was, again a fairly reasonable forecast for the march of the isochrone during the first 25 days of forecast. As in all previous experiments the motion of the predicted isochrone was roughly 3 to 4 degrees latitude slower than the observed positions. Clearly model improvement is called for to speed up the motion of the isochrone somewhat. That is addressed in the next section.

6.5. Sensitivity studies

Observations and modeling suggested that two parameters, the parameterizations of non- convective rain and the representation of soil moisture that carry a strong impact on the meridional motion of the monsoon onset isochrones. These are illustrated in this section.

6.5.1 Variations of soil moisture and precipitation across the isochrones

Fig. 6.9 shows the time variations of the predicted soil moisture (shown along ordinate ,labeled at right) and of the predicted precipitation (shown along ordinate, labeled along left) at two single grid points during the passage of the isochrone. The abscissa shows the latitude normal to the isochrone with respect to a specific location of passage of the isochrone. The data set are simply obtained from model outputs during a forecast for June 2000 onset. The location of the isochrone is marked by an arrow. Both the precipitation and the soil moisture show a drop in values north of the isochrone. This region to the north of the isochrone does not have a very sharp drop of precipitation because of the presence of newly growing cloud elements and the anvil rain. That is also reflected in the slower drop of values of the soil moisture as one proceeds north of the isochrones. Precipitation and soil moisture ahead of the isochrone contributes to an increased buoyancy over theregion immediately ahead of the isochrone where newer clouds can grow. We shall illustrate the typical distribution of buoyancy in the section 6.6.

6.5.2 Enhancing soil moisture by 15 percent over the entire land area of the domain

In section 6.3.1 the current soil moisture scheme is described. That was always used as a default scheme. The results from that scheme were presented in Fig 6.8. After some trial and error it was noted that a uniform 15 percent increase in the soil moisture everywhere compared to what the WRF/ARF provides would reduce the error in the rate of meridional propagation of the isochrones. At each time step after the rainfall (from the model) is computed, the grid-soil moisture was modified by 15%, depending on whether a particular grid point has rainfall. In experiment 1, the soil moisture is increased uniformly 15% at all grid points, and in experiment 2 the soil

moisture is increased by 15% at 5 grid locations north of the raining grid. The soil moisture at the top layer is only modified. As always ocean points carry a tag of 0.9 and above and those were left alone. Those results for the 2003 season are presented in Fig 6.10. The errors in the positioning of the isochrone for most panels are of the order of 2 degrees latitude. This is very promising result. Such an overall enhancement of soil moisture is, however, not necessary, since the motion of the isochrone is most likely affected by what goes on in its immediate vicinity. Our contention, based on observations, was that the region to the immediate north of the isochrone were most important in this regard. Here the enhanced soil moisture contributes to enhanced evaporation over a previously very dry and hot region. That evaporation contributes to formation of new clouds and an enhanced buoyancy over this region to the north of the isochrone, thus permitting further growth and a slow formation of a new position for the isochrone. The isochrone itself moves north and eventually northwestwards because of the orientation of the divergent wind that steers these newly forming elements. The next experiment shows results from an enhancement of soil moisture to the immediate north of the isochrone.

6.5.3. Enhancing soil moisture to the immediate north of the isochrone:

Since what must influence the northward motion of the isochrone is the soil moisture to the immediate north of the isochrone, a simple experiment was designed. Here we increased the soil moisture perpendicular to the leading edge of the isochrone over 5 successive grid points by 15 percent compared to the default values of WRF/ARW discussed in section 6.4. That number 15 percent came from some experimentation, basically that yielded almost the same results as were shown in the previous section where the soil moisture was enhanced by 15 percent over the entire land area of the computational domain. These new results are presented in Fig 6.11. This confirms the notion that the isochrone motion is largely sensitive to the soil moisture to the immediate forward side of the isochrone. This is the region where anvil and newly forming towering cumuli carry some rain and contribute to an enhancement of the soil moisture.

6.5.4. Sensitivity experiment for the enhancement of non-convective rain

Through experimentation, a large sensitivity was noted for the speed of motion of the isochrones of monsoon onset to the parameterization of non-convective rain discussed in section 6.3.2. The disposition of supersaturation asks for a model relative humidity of 100 percent. That being a stringent requirement, since there may be some subgrid scale regions of subsaturation, that threshold value has been reduced in most operational modeling. After some experimentation it was noted that a value of around 85 percent was better suited for anvil rains. The anvil rains occur from pressure levels below 400hPa. Here the criteria for the ascent of absolutely stable and saturated air are met for invoking non-convective rain. It was further noted that even that threshold did not adequately cover the needed enhancement of soil moisture. This leads to an experimentation where the non-convective rain ahead of the leading edge of the isochrone was enhanced by successively by 10, 15 and 35 percent. This enhancement was necessary to account for subgrid scale regions of possible saturation. The best results, Fig 6.11b, came from an enhancement of subgrid scale rains by 15 percent where the observed and the predicted isochrones carried an error in positioning by 2 degrees latitude or less during the 25 day forecast.

6.6. The Buoyancy field ahead of the leading edge of the isohrone

The Buoyancy is defined as follows:

$$B = g\left(\frac{T_v'}{\overline{T_v}} - r_l\right) \qquad (3)$$

where r_l is the liquid water mixing ratio, and T_v' and $\overline{Tv}$ respectively denote virtual temperature values inside a cloud (where r_l > 0.1 g/kg) and outside a cloud (where r_l < 0.1 g/kg). The virtual temperature T_v is defined as

$T_v^* = 1+(r_v/\varepsilon)/(1+r_v)T$, where T denotes air temperature, r_v is the mixing ratio of water vapour and ε is the ratio of molecular weights of water vapour and dry air (ε=0.622).

To illustrate the details of the isochrones evolution we have repeated several of the experiments, presented here, at a 3km resolution. That is particularly useful for seeing the region ahead of the leading edge of the isochrone. Fig. 6.12 illustrates a

typical field of the buoyancy from the model output field. This makes use of the predicted liquid water mixing ratio. This shows several interesting features. It shows a spread of buoyancy ahead of the leading edge of the isochrones. This is the region where the buoyancy helps the growth of a new line of clouds thus establishing a new isochrones in place of the older isochrones. We also see a distribution of positive buoyancy behind the isochrones where the monsoon is active after the onset. Also seen in the illustration were some pre-monsoon onset thunderstorm regions that showed a line of positive buoyancy.

6.6.1. Radar reflectivity cross section across the predicted isochrones

Figure 6.13 shows a vertical cross section, computed inversely, from the model predicted hydrometeors. This is a standard output product that is included for all high resolution forecasts of the WRF/ARW. This model forecast was made at a horizontal resolution of 3km. In this figure the ordinate is a height coordinate and the abscissa denotes longitudes across the isochrone for June 15, 2003. Here we are portraying an isochrones that was located over north eastern India and the forward side of the isochrones is to its west. This was the forecast for day 14, the left half of the diagram denotes the forward side of the isochrone and the right side carries the back side of the isochrone. Of interest here are the radar reflectivities to the forward side that carry some upper clouds and weaker deep convective elements. Those are important features,that were noted in the CLOUDSAT imagery of the radar reflectivity.

6.6.2. Local divergent circulations and the onset isochrones passage

Given the mesoscale model forecasts on the passage of onset isochrones, the post processing of local divergent circulations gives an important perspective for the passage of these isochrones. The divergent circulations roughly emanate from regions of the largest vertical upward motions and heavy rains. This divergent circulation steers the newly forming precipitating elements, that lie ahead of the isochrones in a direction which is roughly perpendicular to the line of heavy rains. The mapping of those features from the model output is illustrated in this section. The divergent circulations are computed from the following equations:

$$\nabla^2\chi = -\left(\frac{du}{dx} + \frac{dv}{dy}\right) \quad (4)$$

Given the horizontal velocity components u and v one can compute the velocity potential χ by soving the above Poisson equation, Krishnamurti and Bounoua (1996). The divergent wind is given by the relation:

$$U_\chi = -\frac{\partial\chi}{\partial x} \quad (5)$$

$$V_\chi = -\frac{\partial\chi}{\partial y} \quad (6)$$

Those divergent wind components were computed, at the 200hPa level, to show the steering for the newly formed precipitating cloud elements ahead of the parent clouds of the isochrone. In Fig 7.14a the divergent winds from the FNL analysis are illustrated on top of the velocity potential χ of the 200hPa surface. These results pertain to June 15, 2003. The weak rains ahead of the isochrone lie in a region that carries strong divergent wind steering directed away from the isochrone. The isochrone is strongly dictated by the steering of newly growing deep convection ahead of the parent isochrone. The rotational part of the wind , not shown here, is nearly always parallel to the isochrone and that stronger wind does not steer the isochrone. The divergent wind is perpendicular to the isochrone , in its vicinity, and is better able to steer the newly growing precipitating cloud elements. As these new elements grow, and the older elements of the isochrone die, a new position of the isochrone is established. Figure 7.14b shows the predicted 200hPa level velocity potential and the divergent wind streamlines. This applies for day 15 of forecast valid on June 15, 2003. These are the results from the mesoscale model forecast from the WRF/ARW. The salient observed features of the divergent wind can be seen here. The model forecast carries a divergent flow that provided the northward steering for the newly forming cloud line that replaces the preceding isochrone.

7. Summary

The chapter addresses the meridional march of the summer monsoon onset isochrones for the first 25 days that covers roughly a passage from Kerala at 7^0N to New Delhi at 27^0 N latitudes. The title of the paper alludes to the first 25 days, that refers to forecast days. The number of days of progress of monsoon from Kerala to New Delhi can vary, on the average it is around 25 days (that is based on the climatological positions of the onset isochrone as shown in fig 7.3. Results show that this speed of northward motion is sensitive to the parameterization of the non-convective rain and to the modeling of the soil moisture. A mesoscale model (WRF / ARW) at a horizontal resolution of 25km and 27 vertical levelsis used that utilizes the initial states and the lateral boundary conditions from the GFS/FNL NOAA model. All experiments cover the period June 1 through June 25 for different years. The model internally carries algorithms for the non-convective rains and the specification of soil moisture. A scenario for the meridional movement of the summer monsoon isochrones over India was developed based on satellite (CLOUDSAT) and reanalysis data sets. That scenario suggested the following ingredients for the motion of the isochrones. There exists an interesting cloud, precipitation and soil moisture asymmetry across the isochrones. The forward side, in the immediate vicinity of the isochrone, experience light rains (partly anvil rains), increase of soil moisture, increase of buoyancy and growth of newly developing clouds. This line of newly forming and growing clouds are steered to the north and eventually to the northwest by a divergent circulation that has its strongest upward motion along the parent isochrone. The rotational part of the wind has less of a role in the steering of the isochrone, since that flow generally appears to be parallel to the isochrone The newly growing clouds slowly replace and become the parent isochrone.And this process repeats itself during the isochrones passage from Kerala to New Delhi. Scientifically this problem is important since the isochrone motions vary from year to year. Further study is warranted on possible strong variations of the rotational wind that can keep an isochrones stationary by having strong rotational winds oppose its meridional motion. The first runs covering the seasons of the years 200, 2002 and 2003 were designated as control experiments since they utilized the default values in the parameterization of the non convective rain and the soil moisture. These experiments clearly showed that forecasts based on the WRF/ARW model carried slower speed for the meridional motion of the isochrones. This was followed up with a

large number of model sensitivity experiments where the intensity of non convective rains and the soil moisture were increased by various percentages compared to the default values of WRF/ARW. Through these sensitivity experiments it was clearly noted that a much improved motion of the model's summer monsoon onset isochrones from Kerala to New Delhi was achievable, compared to the observed estimates of the India Meteorological Department. Thus the results clearly show that the motion of the isochrones from Kerala to New Delhi is very sensitive to the parameterization of soil moisture and the non convective anvil rains to the immediate north of the isochrones. Future modeling will require addressing this problem for operational weather forecasts. The mechanism portrayed here could well apply for the meridional motion of the ISO waves, where the higher frequency motions could be affected by the divergent wind steering and the influences of soil moisture and the stratiform clouds as shown here and the low frequency motions would form the envelope of such events. The mechanism, portrayed here, could also be used for the analysis and interpretations of the dry and wet spells of the monsoon. As a further study it would also be important to examine specific years where unusual stagnation in the progress of monsoon isochrones had been noted. There had been years when the stagnation was noted on more than one occasion in a given year, those are worth examining.

References

Chang, C. P., 2005, "The Maritime Continent monsoon", *The Global Monsoon System: Research and Forecast.* WMO/TD Report 1266, 156-178.

Chen, F., K. Mitchell, J., Schaake, Y. Xue, H. Pan, V. Koren, Y. Duan, M. Ek, and A. Betts, 1996 "Modeling of land-surface evaporation by four schemes and comparison with FIFE observations*", J. Geophys. Res.,* 101, 7251-7268.

Chen, F., R. Pielke, Sr., and K. Mitchell, 2001, "Development and application of land-surface models for mesoscale atmospheric models: Problems and Promises", *Observation and Modeling of the Land Surface Hydrological Processes V. Lakshmi, J. Alberston, and J. Schaake (Editors), American Geophysical Union, 107-135*

Derber, J. C., Parrish, D. F. and Lord, S. J. 1991, "The new global operational analysis system at the National Meteorological Center", *Weather and Forecasting*, 6, 538-547.

Dudhia, J. 1989. "Numerical study of convection observed during the Winter Monsoon Experiment using a mesoscale two-dimensional model", *J. Atmos. Sci.*, 46, 3077–3107.

Gill, A. E., 1980, "Some simple solutions for heat-induced tropical circulation", Quart. J. Roy. Meteor. Soc., 106, 447–462.

Grell, G. A., 1993, "Prognostic evaluation of assumptions used by cumulus parameterizations", *Mon. Wea. Rev.*, 121, 764–787.

Hong, S-. Y., and Lim, J. J-O. 2006, "The WRF single moment 6-Class Microphysics scheme (WSM6)", *J. of Korean Met Soc.* 42, 129-151.

Hong, S-. Y., Dudhia, J. and Chen, S.-H. 2004, "A revised approach to ice microphysical processes for the bulk parameterization of clouds and precipitation", *Mon. Wea. Rev.*, 132, 103–12.

Janjic, Z. I. 1994, "The step-mountain Eta coordinate model: Further developments of the convection, viscous sublayer, and turbulence closure schemes", *Mon. Wea. Rev.,* 122, 927–945.

Janowiak, J. E., and P. Xie, 2003, "A global-scale examination of monsoon-related precipitation", *J. Climate,* 16, 4121–4133.

Kain, J. S. and Fritsch, J. M. 1993, “Convective parameterization for mesoscale models: The Kain–Fritsch scheme. *The Representation of Cumulus Convection in Numerical Models” , Meteor. Monogr*., No. 46, Amer. Meteor. Soc., 165–170.

Kanamitsu, M., 1989, “Description of the NMC Global Data Assimilation and Forecast System”, *Weather and Forecasting*, 4 335- 342.

Krishnamurti, T.N. and R. Ramanathan, 1982, “Sensitivity of monsoon onset to differential heating”, *J. Atmos. Sci.,* 39, 1290–1306.

Krishnamurti, T. N. & Lahouari Bounoua, 1996, “*Model Output Diagnostics : An Introduction to Numerical Weather Prediction Techniques”,* CRC Press, Inc. USA, 259-266.

Lwin T. 2002, “The climate changes over Myanmar during the last decades” *Water Resources Journal* ST/ESCAP/SER.C/212, 212:95–106.

Khole, Medha, Mazumdar A. B. and Sunitha Devi, S., 2010, “Onset, advance and withdrawal of southwest monsoon”, IMD Met. Monogr. Synop. Met. No. 7/2010. Published by India Meteorological Department, pp. 1-13.

Khole, Medha, Mazumdar, A. B., Sunitha Devi, S. and Yadav, B. P., 2011, “Onset, advance and withdrawal of southwest monsoon”, IMD Met. Monogr. Synop. Met. No. 10/2011. Published by India Meteorological Department, pp. 1-20.

Mlawer, E. J., Taubman, S. J., Brown, P. D., Iacono, M. J. and Clough, S. A., 1997, “Radiative transfer for inhomogeneous atmosphere: RRTM, a validated correlated-k model for the longwave”, *J. Geophys. Res.*, 102, 16663–16682, D14.

Monin, A. S. and Obukhov, A. M., 1954, “Basic laws of turbulent mixing in the surface layer of the atmosphere”, (in Russian) *Contrib. Geophys. Inst. Acad. Sci. USSR*, 151, 163–187.

Parrish, D.F. and Derber, J.C. 1992, “The National Meteorological Center's spectral statistical interpolation analysis system”, *Mon. Wea. Rev*. 120, 1747-1766.

Petersen, Ralph A., John, D. Stackpole, 1989, “Overview of the NMC Production Suite”, *Wea. Forecasting*, 4, 313–322.

Rao, Y. P. 1976, “Southwest Monsoon”, *Met. Mon. Synoptic Meteorol.,* India Meteorological Department, 107–185.

Skamarock W. C., Klemp, J. B., Dudhia, J., Gill, D. O., Barker, D. M., Wang, W. and Powers, J. G., 2005, “A description of the advanced research WRF version 2”, NCAR Tech. Note 468+STR, 88 pp.

Srivastava, A. K. and Yadav, B. P., 2009, “Onset, advance and withdrawal of southwest monsoon”, IMD Met. Monogr. Synop. Met. No. 7/2009, Published by India Meteorological Department, pp. 1-7.

Stano, G., Krishnamurti, T. N. Vijaya Kumar, T. S. V and. Chakraborty,. A., 2002, “Hydrometeor structure of a composite Monsoon Depression using the TRMM Radar”, 54(4) 370-381.

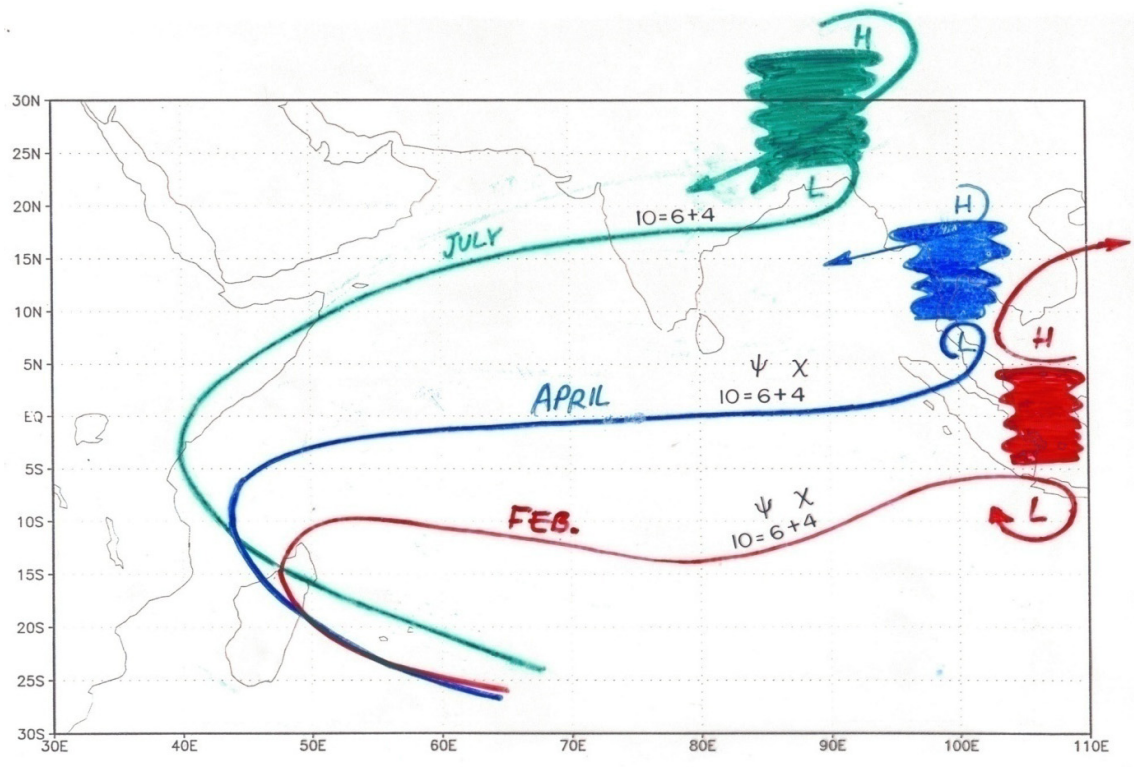

Fig. 6.1 : This shows the northward march of a clockwise flow gyre at 850 hPa level during the months February, April and July. This monsoonal lowlevel flow terminates at the monsoon trough that carries deep convectionand clouds, as shown in the right. Also shown is the upper tropospheric anticyclonic flows.

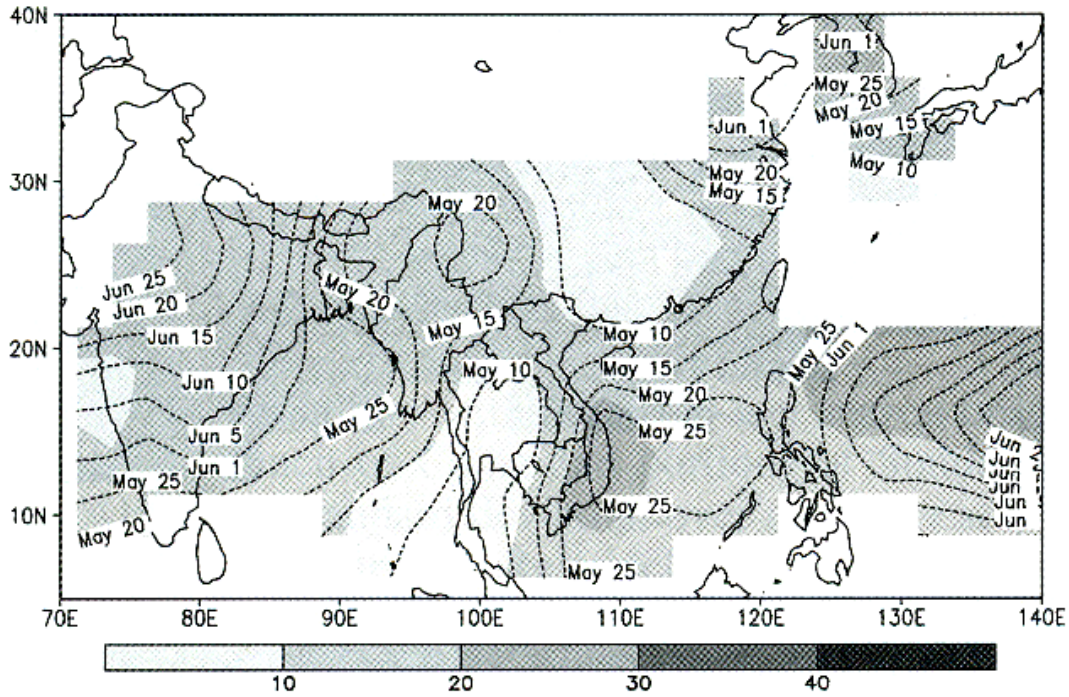

Fig. 6.2 : Climatological isochrones of onset of the Asian Summer Monsoon based on the period (1979-1999). Shading indicates the standard deviation (in days) of the onset date. From Janowiak and Xie (2003).

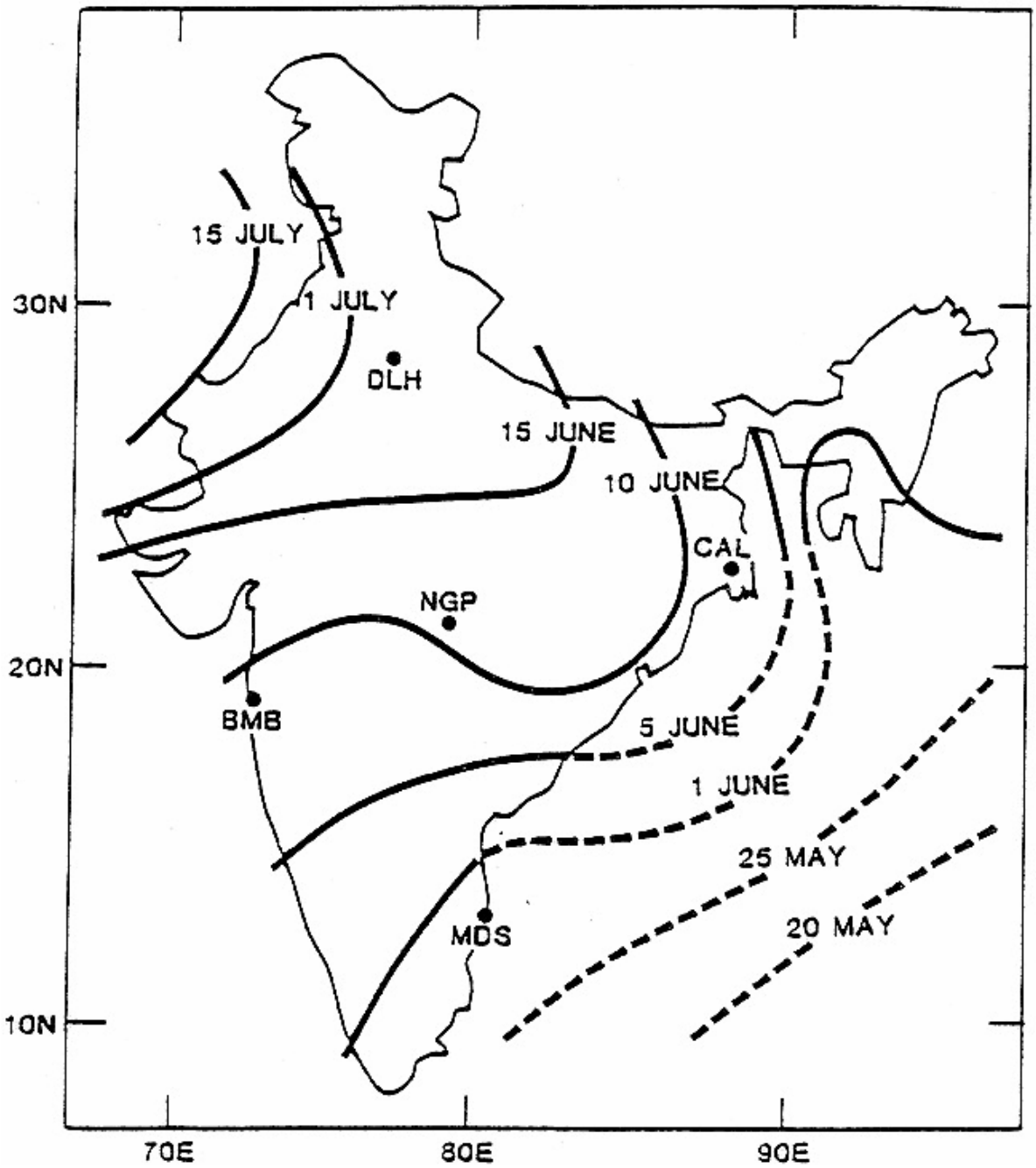

Fig. 6.3 : Climatological positions of the onset isochrones as defined by India Meteorological Department.

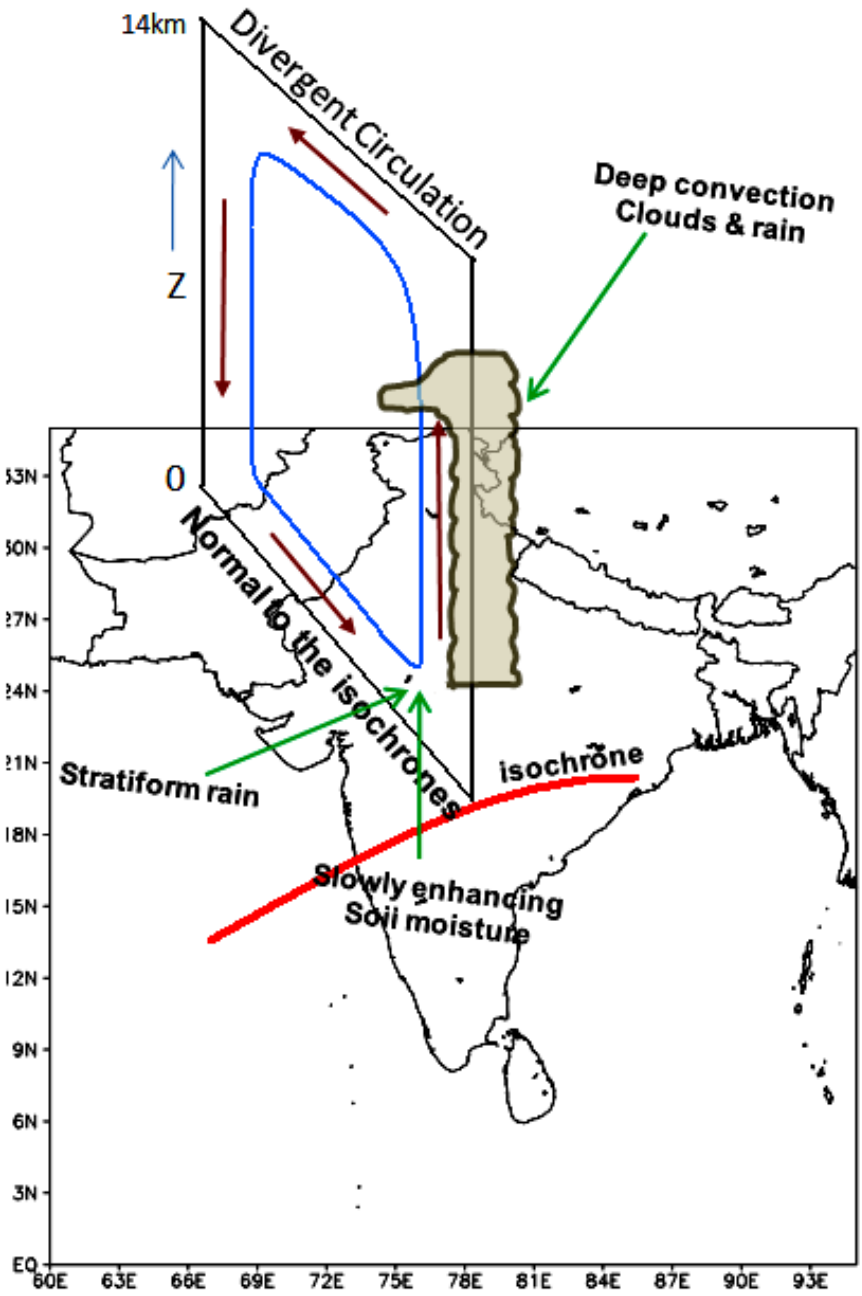

Fig. 6.4 : **This is a schematic of the monsoon onset isochrone, the local divergent circulation, clouds over the parent isochrone, and emphasizing the region immediately forward of the parent isochrone.**

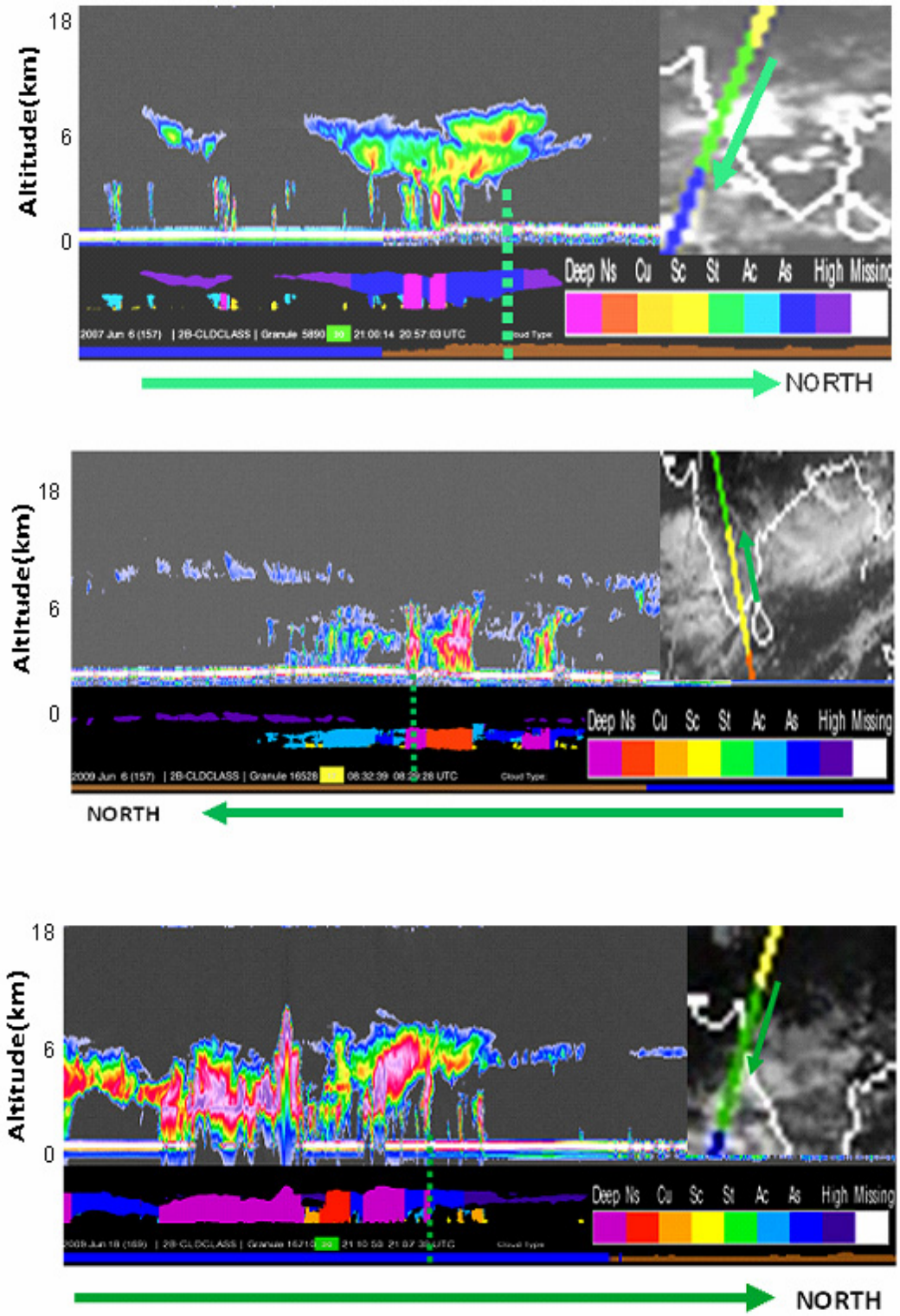

Fig. 6.5(a-c) : The top panel to the right shows the IR imagery from the pole orbiting CLOUDSAT, the radar reflectivity implied from CLOUDSAT and below that are the cloud types as determined by the CLOUDSAT data processing. Three anels show three different examples. The vertical dashed line shows the location of the onset isochrone as determined by IMD. The north is determined by the ascending or the descending node of the satellite motion.

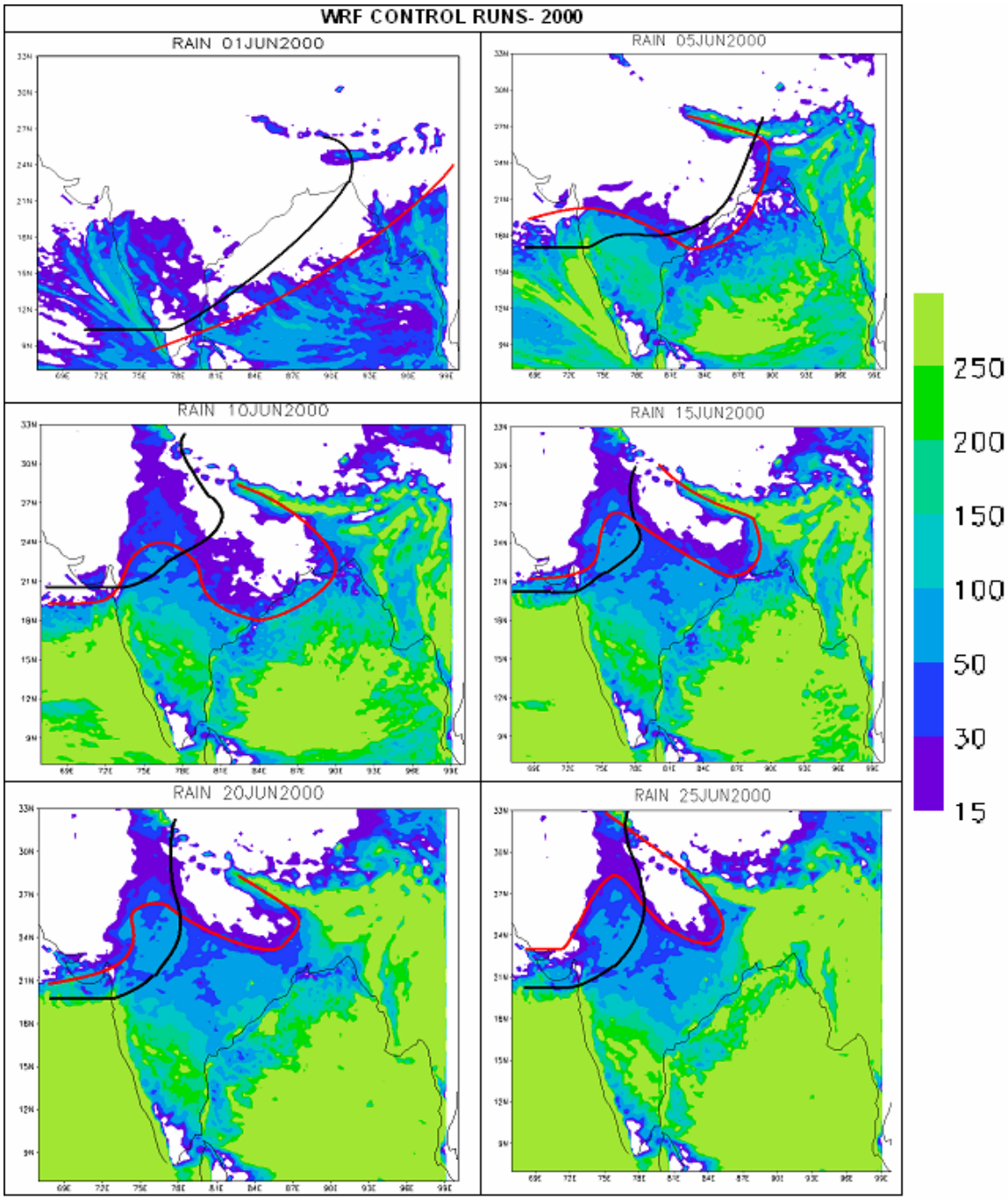

Fig. 6.6 : Accumulated precipitation (mm) for the year 2000.
The IMD onset isochrones is marked as black line and the predicted marked in red.

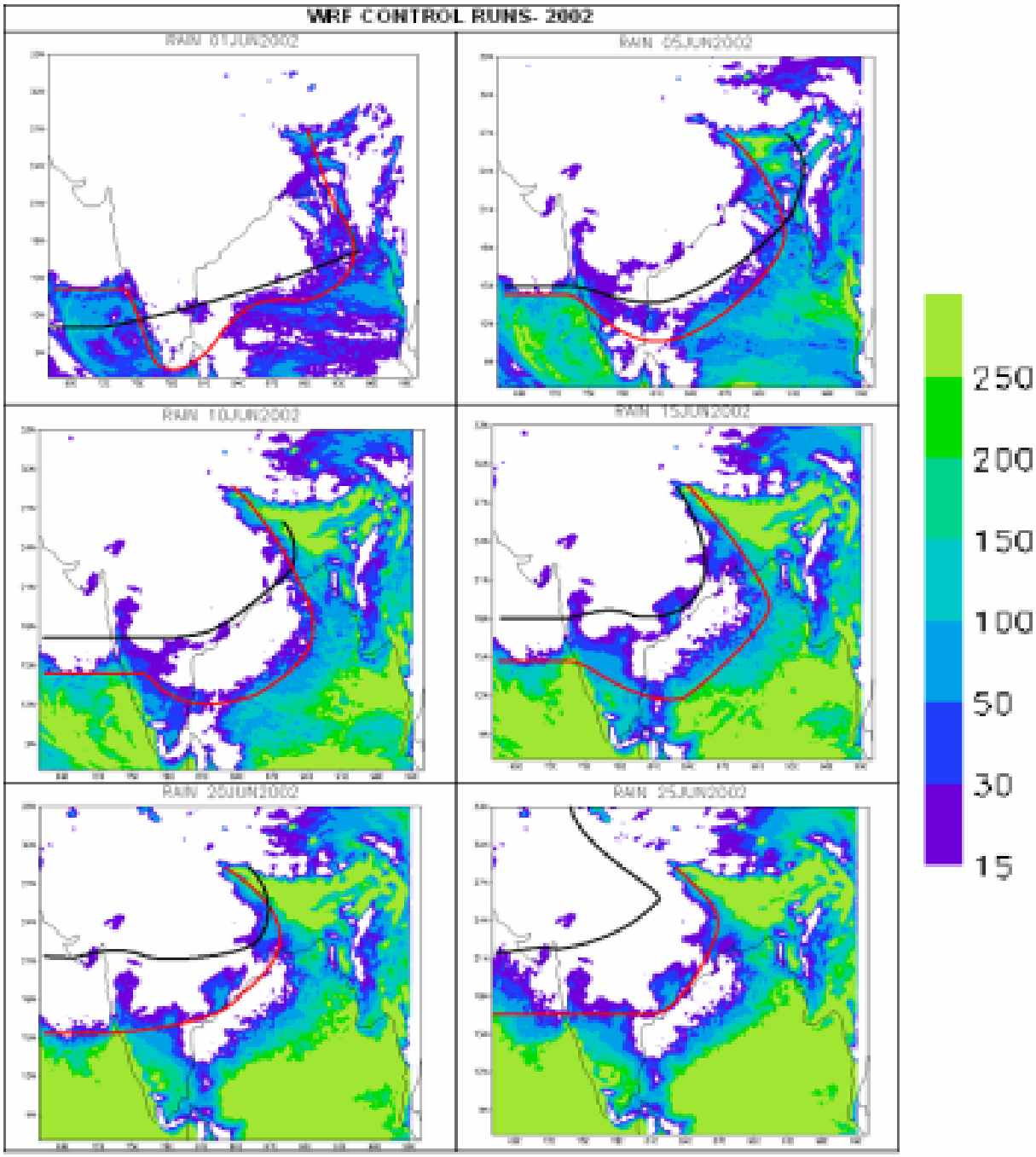

Fig. 6.7: Accumulated precipitation (mm) for the year 2002.
The IMD onset isochrones is marked as black line and the predicted marked in red.

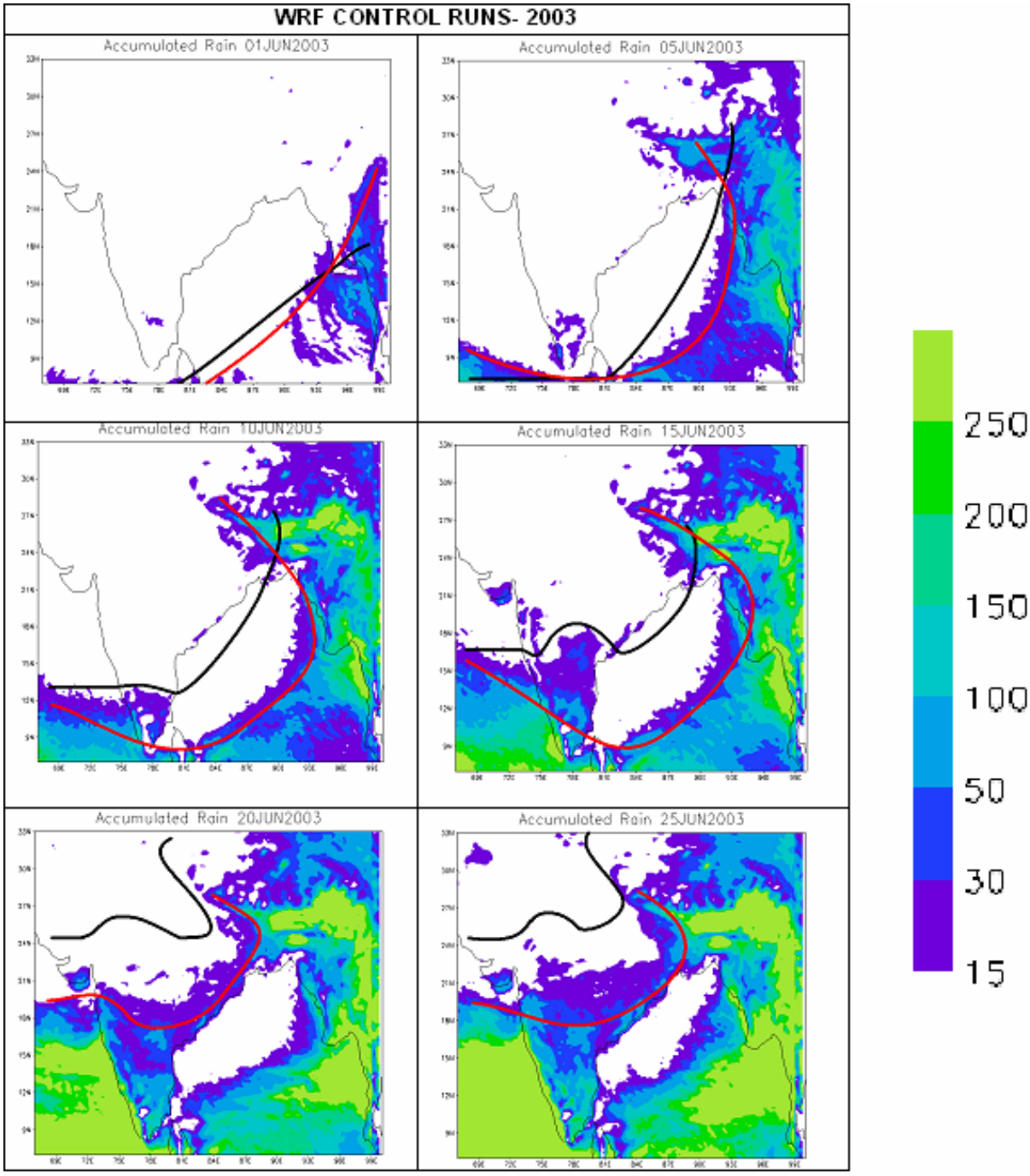

Fig. 6.8 : Accumulated precipitation (mm) for the year 2003.
The IMD onset isochrones is marked as black line and the predicted marked in red.

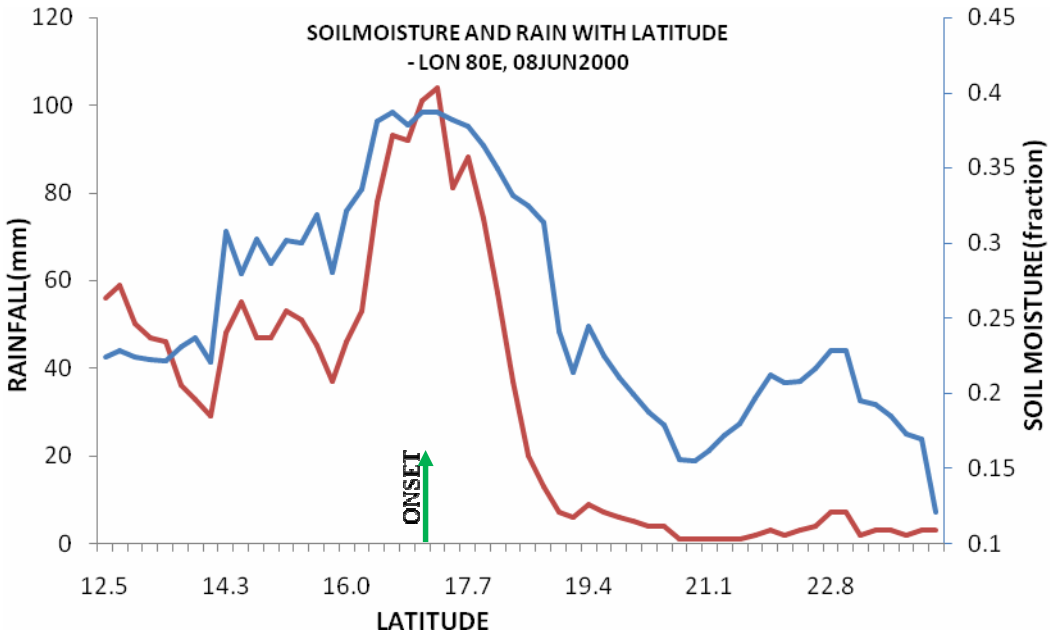

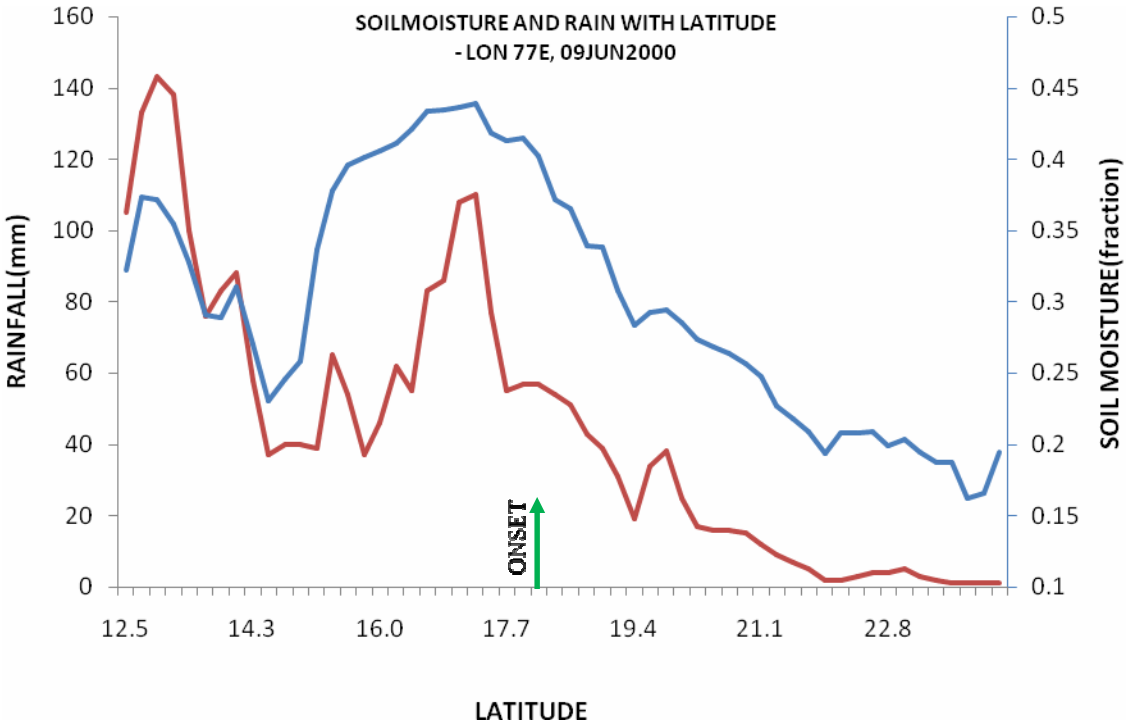

Fig. 6.9 : The variation of soil moisture and rain as a function of latitude. Soil moisture is in raction, and rain in mm/day. These graphs were taken from model output on June 8 2000 at two rid points that experienced a passage of the onset isochrone.
The location of the onset isochrone is marked.

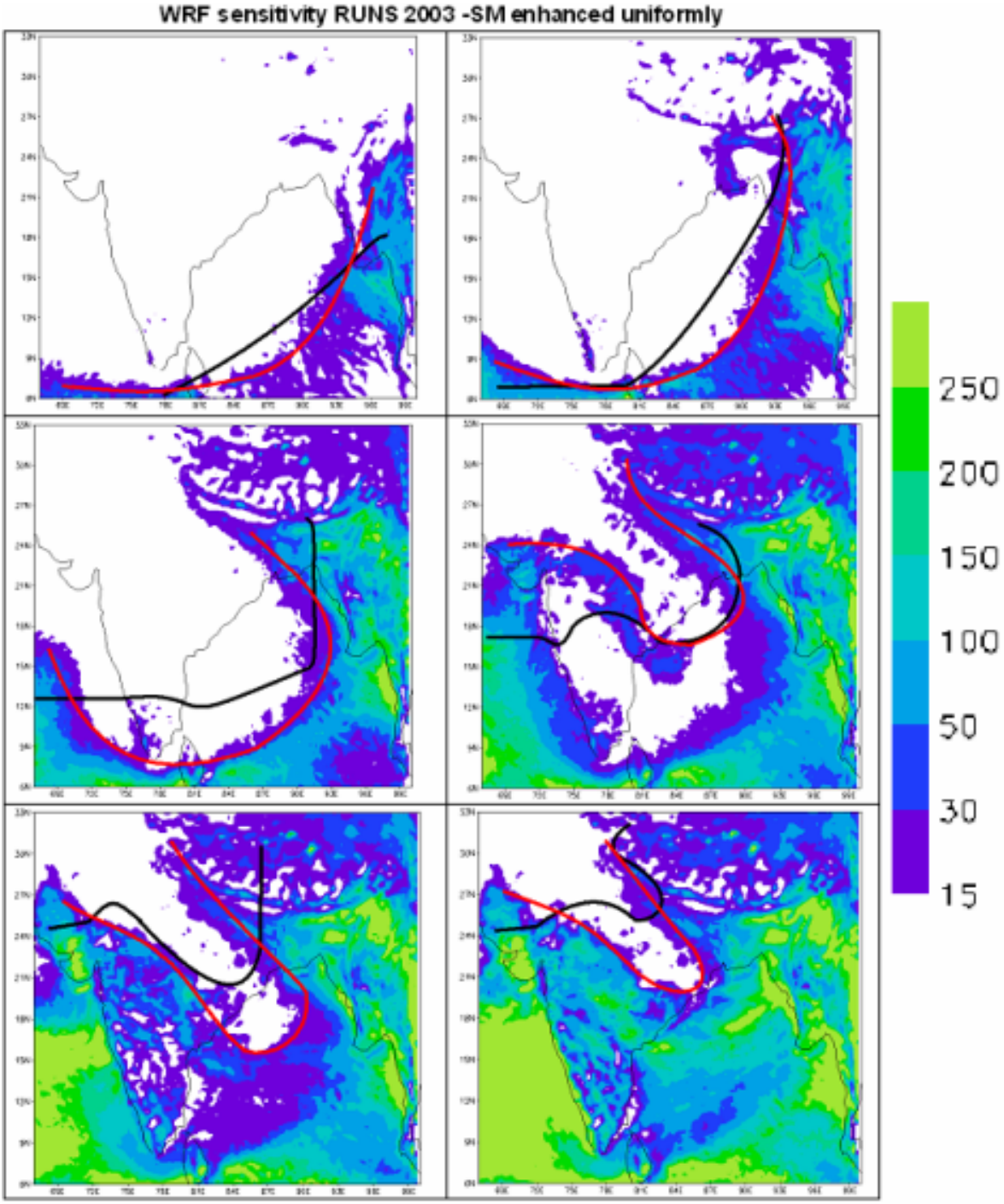

Fig. 6.10 : Accumulated precipitation (mm) for the year 2003 from the WRF/ARW sensitivity experiment of enhancing soil moisture by 15% over the entire land area. The IMD onset isochrone is marked as black line and the predicted marked in red.

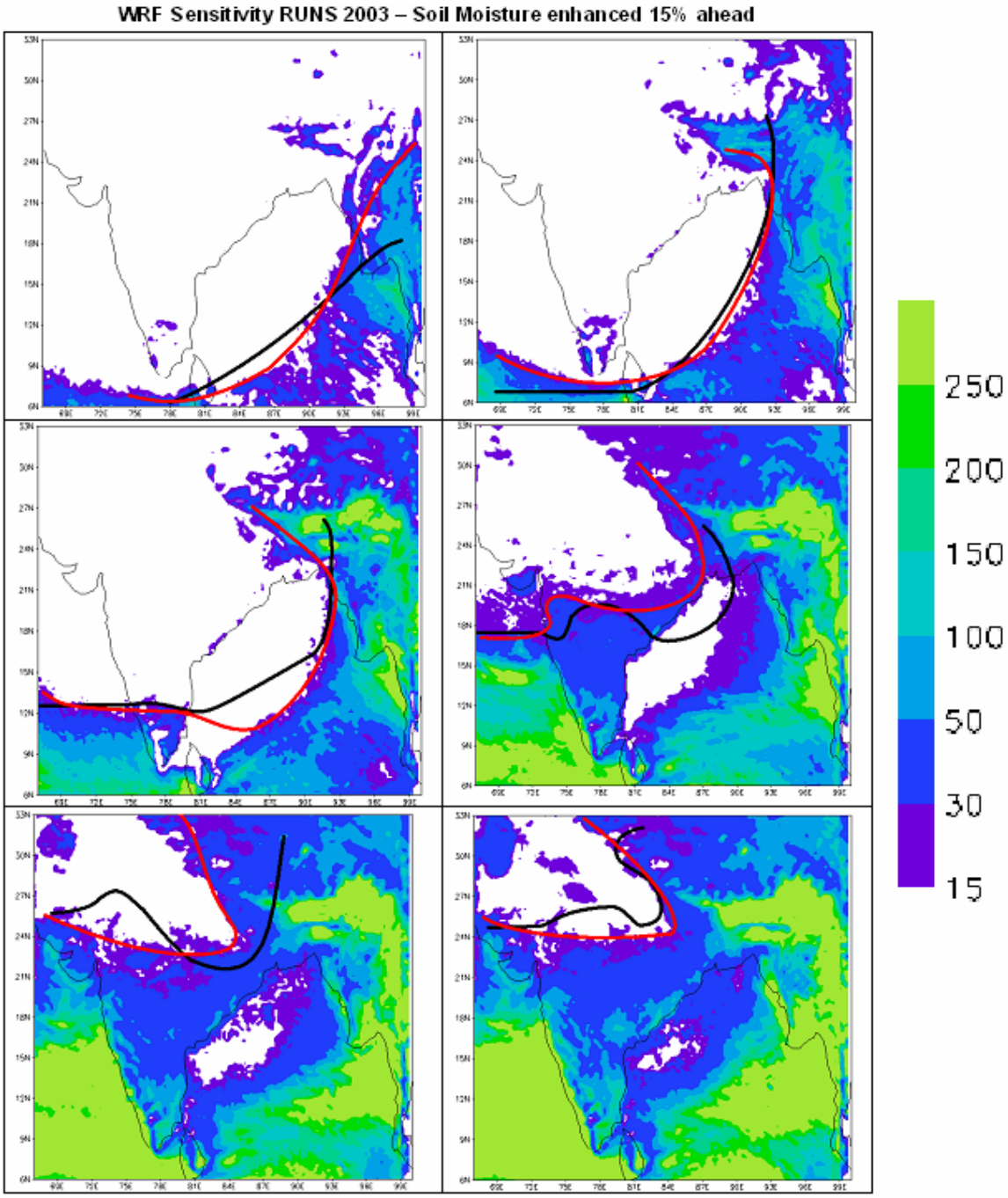

Fig. 6.11a : Accumulated precipitation (mm) for the year 2003 from the WRF/ARW sensitivity experiment of enhancing soil moisture by 15% ahead of the onset isochrone. The IMD onset isochrone is marked as black line and the predicted marked in red.

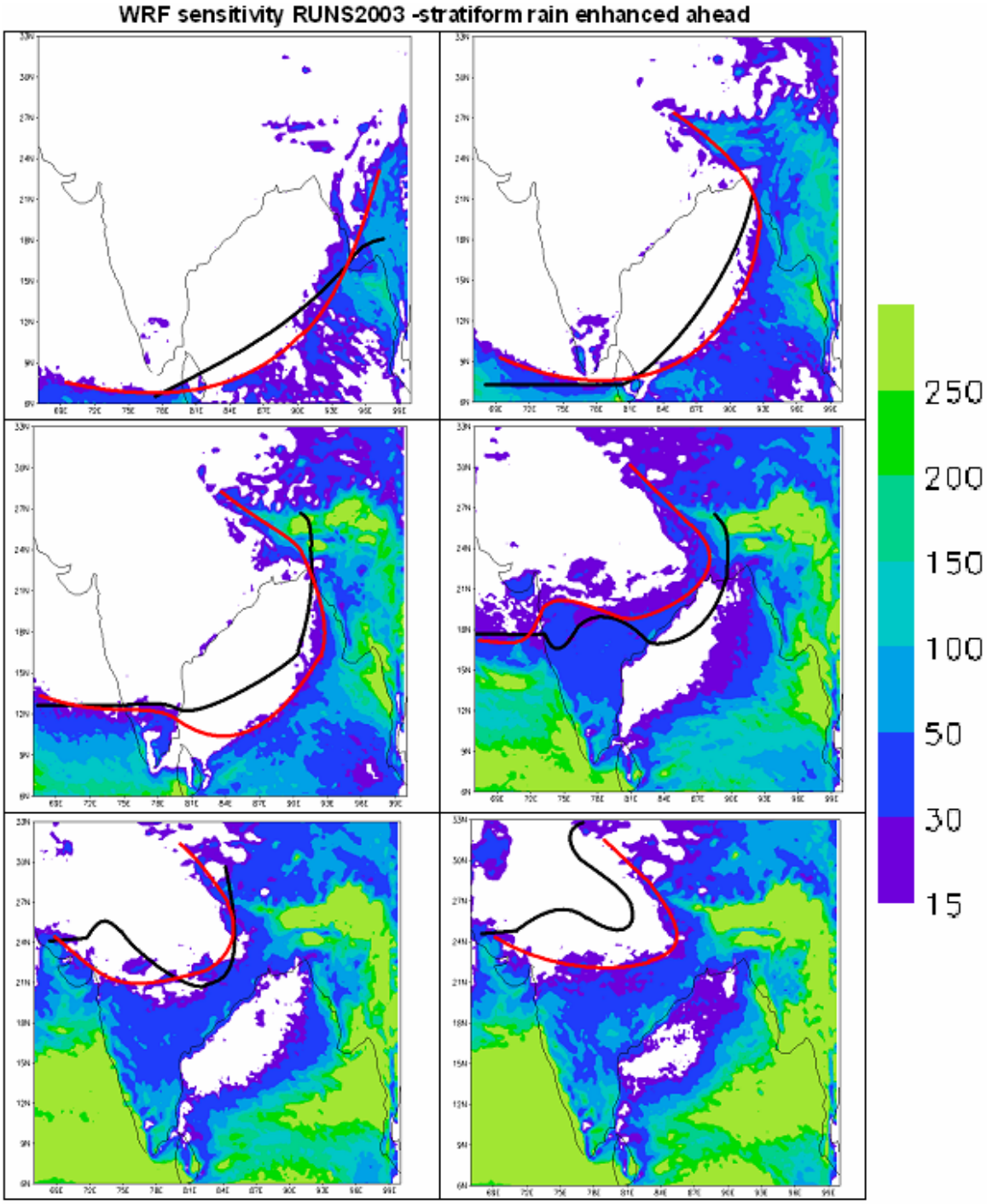

Fig. 6.11b : Accumulated precipitation (mm) for the year 2003 from the WRF/ARW sensitivity experiment of enhancing statiform rain by 15% ahead of the onset isochrone. The IMD onset isochrone is marked as black line and the predicted marked in red.

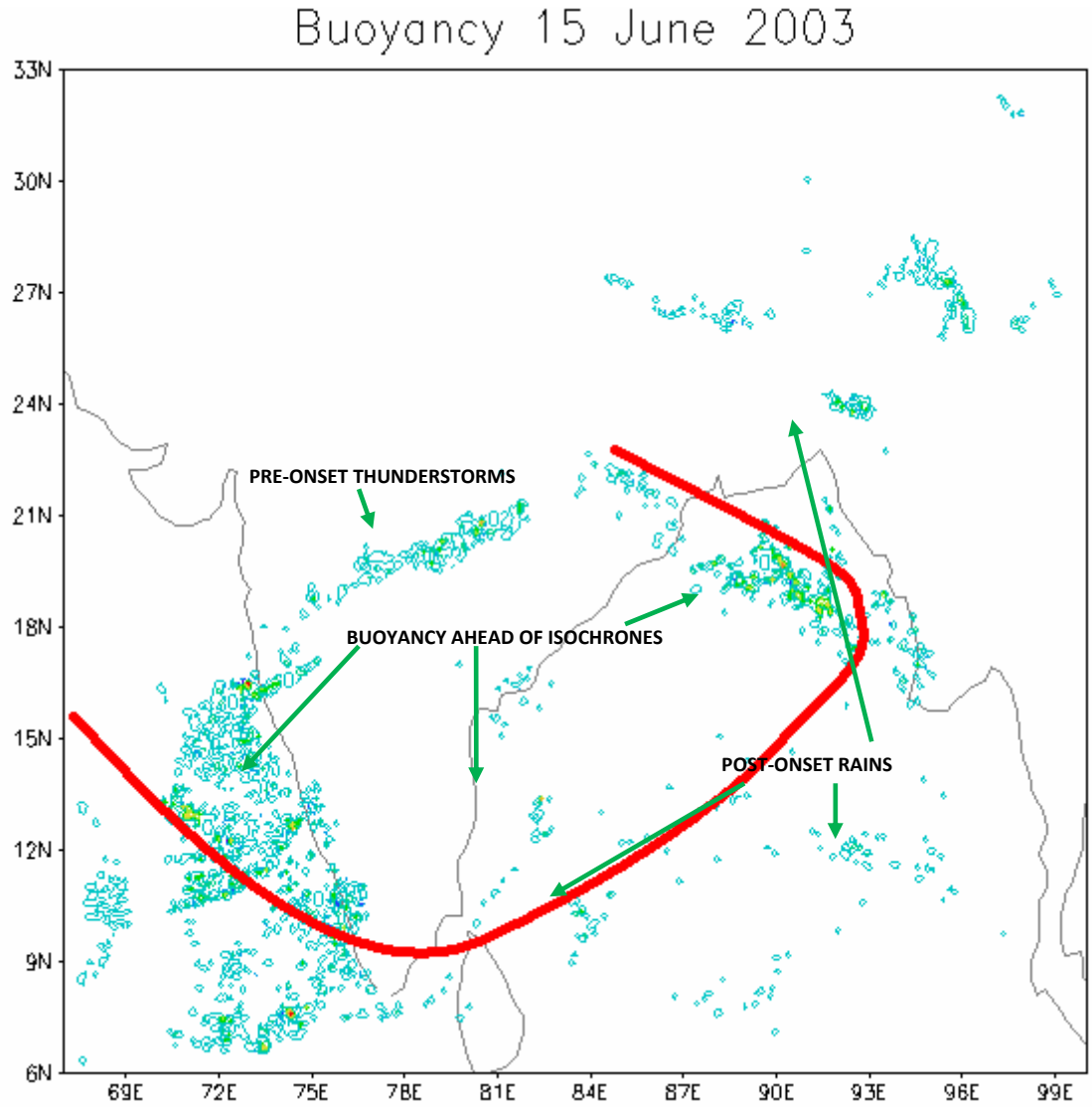

Fig. 6.12 : The buoyancy distribution from the mesoscale forecast for June 15 2003, this is day 14 of the forecast, units of buoyancy are ms^{-2}. The predicted location of the isochrone is shown by red heavy line. Also identified are some features of the buoyancy distribution with respect to the predicted isochrone.

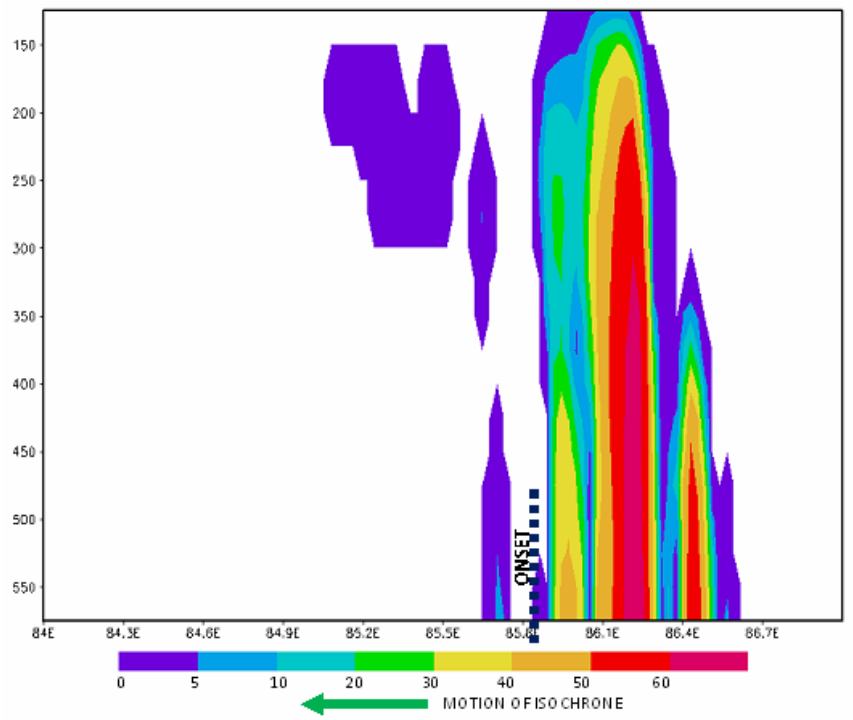

Fig. 6.13 : This illustration shows the model based radar reflectivity cross section across the isochrone, for June 15 2003. The ordinate is height and the abscissa shows longitude normal to the isochrone. Here the left side is the forward side of the isochrone and the right side is to the rear of the isochrone. The lighter cloud reflectivity, ahead of the isochrone, is the important feature here.

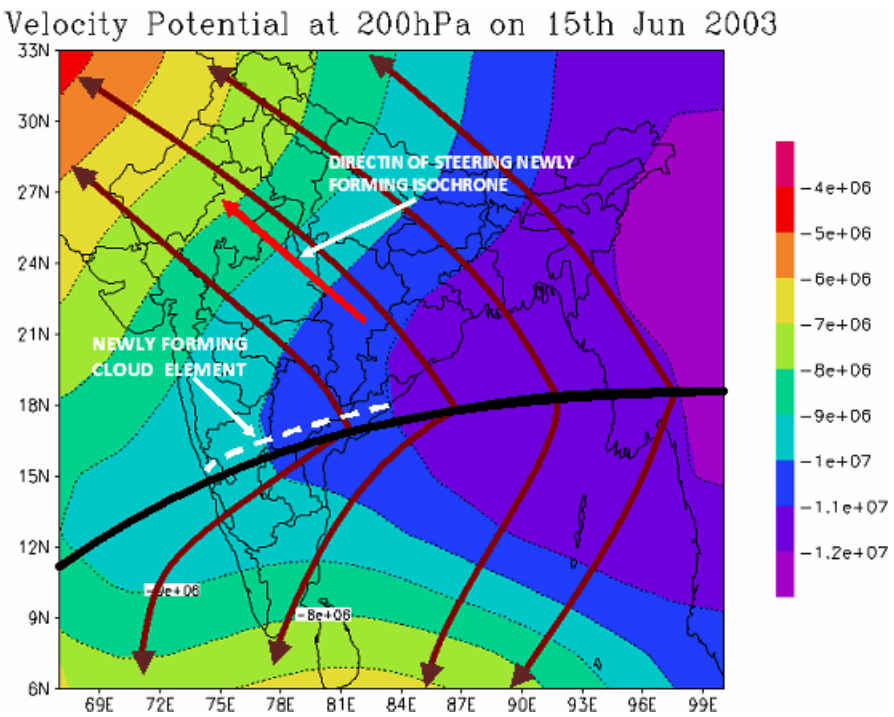

Fig. 6.14a : Velocity potential thin lines with shading. The divergent streamlines are indicated emanating from a line which lies close to the observed isochrone Also marked are some salient features such as the direction of steering of the isochrone by the steering divergent wind. A dashed line shows where newly forming cloud elements , ahead of the isochrone, were noted from the CLOUDSAT.

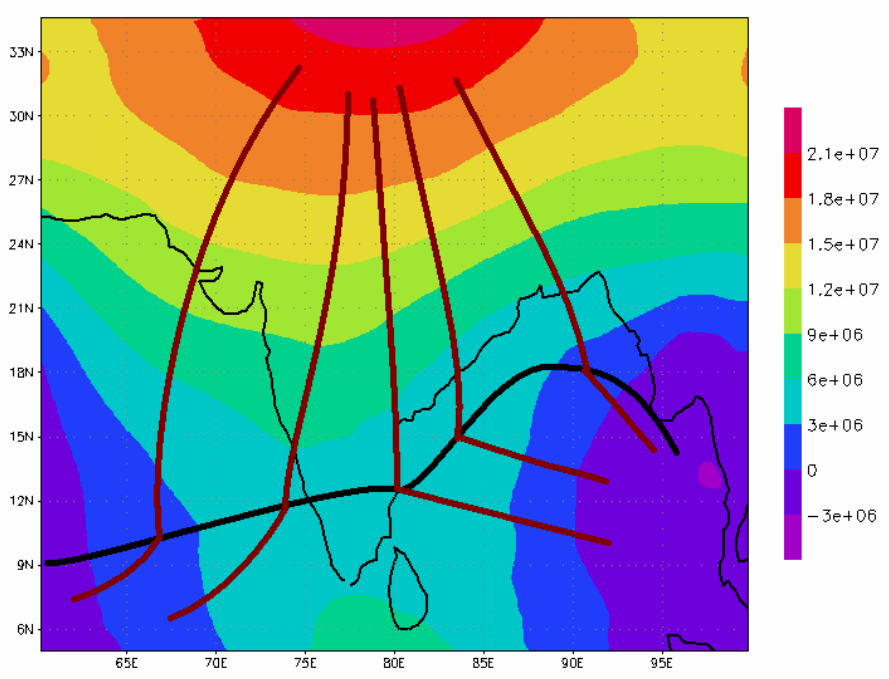

Fig.6.14b : Same as Fig 6.14 a, except this is a forecast product, from the mesoscale model for June 15 2003.

CHAPTER 7

PREDICTABILITY OF THE INDIAN MONSOON IN COUPLED GENERAL CIRCULATION MODELS

V. Krishnamurthy and J. Shukla
Centre for Ocean-Land –Atomshpre Studies Institute of Global Environment and Society, Calverton, Maryland, USA
Department of Atmospheric , Oceanic and Earth Services, George Mason University, Fairfax, Virginia, USA

shukla@cola.iges.org

7.1. Introduction

Because of the tremendous impact of monsoon on various socio-economic aspects of India, the prediction of the monsoon rainfall was recognized to be crucial more than a hundred years ago. The India Meteorological Department (IMD) has long been issuing seasonal forecasts of rainfall using statistical prediction schemes that took firm root with the discovery of significant correlation between the seasonal rainfall and various regional and global climate phenomena by Walker (1923, 1924). Some of these predictors are based on now well-known slowly-varying components of the climate systems such as El Niño-Southern Oscillation (ENSO) (Krishnamurthy and Kinter 2003). Many developing El Niño (La Niña) events have coincided with below-normal (above-normal) seasonal monsoon rainfall (Sikka 1980; Rasmusson and Carpenter 1983). The dynamical basis for long-range prediction of seasonal mean monsoon rainfall was established by general circulation model (GCM) experiments which showed that the tropical atmospheric variability was largely determined by slowly-varying boundary forcings such as sea surface temperature (SST), soil moisture and snow cover (Charney and Shukla 1981).

The Charney-Shukla hypothesis was further supported by observational evidence and was modified by Krishnamurthy and Shukla (2000, 2007, 2008) who suggested that the interannual variability of the seasonal mean monsoon consisted of large-scale seasonally persistent component and a statistical average of intraseasonal variations. They found two nonlinear oscillations, a northeastward propagating mode with an average period of 45 days and a northwestward propagating mode with a period of 30 days, which largely explained the active and break phases of the monsoon. The seasonal mean monsoon, however, was accounted for by two seasonally persisting modes that were shown to be related to ENSO and Indian Ocean Dipole (IOD). The seasonal mean monsoon is determined by the relative strengths of these persistent ENSO and IOD atmospheric modes which can interfere either constructively or destructively. For example, the seasonal rainfall in 1997, the strongest El Niño year on record, was normal because of the counteracting effect of the atmospheric ENSO and IOD modes. The persistent atmospheric modes were shown to have strong lead/lag correlation with the SSTs of the Indian and Pacific oceans (Krishnamurthy and Kirtman 2009), indicating the strong predictive potential of the SST.

The statistical forecasting method employed by the IMD has met with varying degree of success but with no improvement in the forecast skill over a long period (Rajeevan 2001; Gadgil et al. 2005). This method has limitations because it does not provide forecasts with spatial distribution of the rainfall or on sub-seasonal time scales. There are more fundamental problems related to the use of limited amount of data and the choice of the predictors (Lorenz 1962, DelSole and Shukla 2002). On the other hand, the dynamical prediction has evolved over the years to a stage where coupled GCMs are now employed for routine seasonal climate prediction by operational forecasting centers. Earlier studies of dynamical prediction of the Indian monsoon relied on atmospheric GCMs using observed SST as boundary forcing (Palmer et al. 1992; Sperber and Palmer 1996; Krishnamurthy and Shukla 2001; Sperber et al. 2001; Kang et al. 2002). Most of these models simulated the monsoon with deficit rainfall over northern India and excess rainfall over the Arabian Sea and the Bay of Bengal. The interannual variability of the seasonal rainfall in the models showed poor correlation with observations, although SST

seems to have strong influence. Although, this two-tier approach has served useful purpose, Wang et al. (2005) showed that the observed lagged correlation between SST and rainfall was correctly simulated by a coupled GCM but not by an atmospheric GCM forced with observed SST, especially in the subtropical western Pacific where SSTs are primarily forced by the atmosphere. These results emphasize the importance of the coupled ocean-atmosphere interaction in the monsoon region and the need to use coupled GCMs for better prediction. The prediction skill of the monsoon was found to be better with a coupled model compared to that using an atmospheric model (Kumar et al. 2005).

The objective of this review is to discuss the predictability of coupled GCMs in simulating the Indian monsoon. According to Lorenz (1984), the predictability of a system is the degree of accuracy with which it is possible to predict the state of the system in the future. It is worth emphasizing that predictability always refers to the specific model that is used to make the prediction. The relevance of the specific phenomenon, such as monsoon, that is predicted may appear through the time scales and the instabilities involved. The models assessed in this study are advanced coupled GCMs that are used either for operational forecasts of seasonal climate or for developing new approaches to seasonal prediction. The model that is discussed in more detail is the Climate Forecast System (CFS) version 1 of the U.S. National Centers for Environmental Prediction (NCEP). The CFS has been providing operational seasonal predictions since 2004 (Saha et al. 2006). The other models, developed at seven European institutions, come from a project called the Development of a European Multimodel Ensemble System for Seasonal-to-Interannual Prediction (DEMETER) (Palmer et al. 2004). Retrospective forecasts generated by these models have been analyzed to assess their predictability.

The predictability of weather models is usually assessed by analyzing the growth of daily errors and finding the growth rate and doubling time of errors. The daily weather forecasts of the European Centre for Medium Range Forecasts (ECMWF) were examined by Lorenz (1982) who estimated the doubling time of small errors in the midlatitudes to be about 2-2.5 days. Similar estimates were obtained in the subsequent

assessments of the ECMWF weather forecasts (Simmons and Hollingsworth 2002). The Lorenz method was used in recent studies (Rai and Krishnamurthy 2011, Krishnamurthy and Rai 2011) to assess the predictability of the Indian monsoon rainfall and circulation in NCEP CFS. The doubling time of errors was estimated to be about 4-5 days for forecasts initiated during the peak monsoon period. Since these errors saturate in a matter of few days, the analysis of errors in instantaneous states is not suitable for predictability on climate time scales (e.g., seasonal forecasts). For the tropics, Shukla (1998) has shown that the differences between simulations with the same SST forcing are much less than the differences between simulations with different SST forcings, emphasizing the role of slower components in climate predictability. In an analysis of the seasonal forecasts of the monsoon, the CFS was found to predict the ENSO-related features of the monsoon better than the regional features that may not be strongly influenced by SST (Drbohlav and Krishnamurthy 2010).

The predictability of the DEMETER coupled models was compared with the predictability of observed SST forced atmospheric GCMs of the Asia-Pacific Economic Cooperation Climate Network by Kang and Shukla (2006). The atmospheric models produced large systematic errors in the monsoon region, and the predictions showed poor correlation skill. There was no improvement in the correlation skill with the multimodel composite approach. However, the DEMETER coupled models showed better predictability of the seasonal mean rainfall over the monsoon region and western Pacific, indicating the importance of ocean-atmosphere interaction. The multimodel composites of the DEMETER model predictions of the summer season rainfall also had better spatial correlation skill.

In section 7.2, the CFS and the DEMETER models are described along with details of the retrospective forecasts generated by these models. The predictability of the daily rainfall and circulation is discussed in section 7.3. Section 7.4 discusses the seasonal mean monsoon and its predictability. A discussion of the potential for the predictability of monsoon on decadal time scale is provided in section 7.5. A summary is given in section 7.6.

7.2. Models and retrospective forecasts

a. NCEP Climate Forecast System

The NCEP CFS consists of Global Forecast System (GFS) as its atmospheric component (Moorthi et al. 2001) while the Geophysical Fluid Dynamics Laboratory (GFDL) Modular Ocean Model version 3 (MOM3) is its oceanic component (Pacanowski and Griffies 1998). The GFS has T62 horizontal resolution along with 64 sigma vertical layers. The MOM3 has a zonal resolution of 1°, meridional resolutions of 1/3° in the extratropics and 1° in the tropics and 40 layers in the vertical. The atmospheric and oceanic models exchange momentum and heat fluxes once a day with no flux correction. The ocean model is prescribed with observed climatology of the sea ice extent. The initial conditions for the atmospheric model is obtained from the NCEP-Department of Energy Atmospheric Model Intercomparison Project (AMIP II) Reanalysis-2 (R2; Kanamitsu et al. 2002) while the NCEP Global Ocean Data Assimilation System provides the initial conditions for the ocean model. More details of the CFS are given by Saha et al. (2006).

The retrospective forecasts were generated at NCEP by integrating the CFS starting each month for the period 1981-2005. Each ensemble of nine-month long retrospective forecasts consists of 15 members starting from different initial conditions each month. For example, the May forecasts start with the atmospheric initial conditions of 9-13 April, 19-23 April and 29 April-3 May and ocean initial states specified from pentads centered at 11 April, 21 April and 1 May. The forecasts of other months of the year are selected in the same way. For verification of precipitation, the Climate Prediction Center Merged Analysis of Precipitation (CMAP; Xie and Arkin 1996), the R2 precipitation and the gridded daily rainfall data set from the India Meteorological Department (IMD; Rajeevan et al. 2006) are used. The circulation data from R2 reanalysis are used for verifying the horizontal wind fields.

b. DEMETER models

The DEMETER project uses seven coupled ocean-atmosphere models from the following European institutions: (1) European Centre for Research and Advanced Training in Scientific Computation (CERFACS), France, (2) European Centre for Medium-Range Weather Forecasts (ECMWF), (3) Istituto Nazionale de Geofisica e Vulcanologia (INGV), Italy, (4) Laboratorie d'Océanographie Dynamique et de Climatologie (LODYC), France, (5) Max-Planck Institut für Meteorologie (MPI), Germany, (6) Centre National de Recherches Météorologiques (Météo-France), France and (7) Met Office, United Kingdom. Hereafter, these models will be referred to as CERF, ECMW, INGV, LODY, MAXP, METF and UKMO, respectively. The main objective of the DEMETER project was to test the concept of multimodel ensemble prediction. The results of DEMETER have led to routine multi-model ensemble seasonal predictions at the ECMWF. In this study, however, the individual DEMETER models will be compared with each other.

The DEMETER produced 6-month long retrospective forecasts with each model from the initial conditions of 1 February, 1 May, 1 August and 1 November for the period 1980-2001. Each forecast set consists of an ensemble of nine members. Different initial conditions for the nine ensemble members are provided by three different ocean analyses and SST perturbations. The atmospheric initial conditions are taken from the ECMWF 40-year reanalysis (ERA-40). The retrospective forecasts from 1 May initial conditions are used in this study in order to cover the monsoon season. Palmer et al. (2004) have provided the details of the DEMETER models and their retrospective forecasts. For verification purpose in the present study, the precipitation from the IMD data set and R2 reanalysis and SST from the Hadley Centre have been used.

7.3. Daily predictability

The daily mean monsoon rainfall and circulation simulated by the CFS forecasts is discussed in detail by Rai and Krishnamurthy (2011). The daily climatological mean

rainfall and horizontal fields were found to simulate the seasonal cycle of onset, peak and withdrawal of monsoon fairly well. However, the magnitude and the spatial structure of the climatology in the CFS were not found to have good correspondence with the observations. The mean seasonal cycles of the DEMETER model is discussed by Joseph et al. (2010) who show that the multi-model ensemble mean is better compared to the individual models.

In this section, the predictability of the models in forecasting the daily means of rainfall and circulation is discussed in more detail. The predictability of the CFS analyzed by Rai Krishnamurthy (2011) and Krishnamurthy and Rai (2011) is reviewed, and new results on the predictability of the DEMTER models are presented. The errors in forecasts result from the imperfections of the model as well as due to the sensitive dependence on initial conditions in nonlinear systems. Therefore, the predictability of the model can be quantified by the following two measures. One of them is the forecast error defined as the difference between the prediction and observation. The other is the predictability error defined as the difference between two predictions made by the same model. The predictability errors arise solely due to the uncertainties in the initial conditions under the assumption that the model is perfect while the forecast errors are caused by imperfections in both the initial conditions and the model (Lorenz 1982, 1985). The forecast errors and predictability errors give the lower and upper bounds of the predictability of a model, respectively (Lorenz 1982).

For a quantitative analysis of the monsoon predictability, it is useful to work with the following indices of rainfall and circulation over the monsoon region: (1) the Indian monsoon rainfall (IMR) index defined as the rainfall averaged over land points in India, (2) the extended Indian monsoon rainfall (EIMR) index defined as the rainfall averaged over (70°E-110°E, 10°N-30°N) (Goswami et al. 1999), (3) the Asian-Australian monsoon rainfall (AAMR) index defined as the rainfall averaged over (40°E-160°E, 40°S-40°N) (Krishnamurthy and Shukla 2001), (4) the monsoon Hadley (MH) index defined as the meridional wind shear between 850 hPa and 200 hPa averaged over (70°E-110°E, 10°N-30°N) (Goswami et al. 1999), and (5) the Westerly Shear (WS) index defined as the

zonal wind shear between 850 hPa and 200 hPa averaged over (40°E-80°E, 5°N-20°N) (Wang and Fan 1999).

a. Forecast errors

The forecast errors (forecast minus observation) of daily IMR index in individual ensemble members for May and July initial conditions in CFS forecasts are shown as root mean square (RMS) errors in Fig. 7.1 The IMD rainfall data are used as observations. The root mean square (RMS) errors for each ensemble member are computed by averaging the squared forecast errors over the period 1981-2005. The initial size of the errors is in the ranges of 0.6–1.8 mm day^{-1} and 1.8–3.0 mm day^{-1} for the May and July forecasts, respectively. Although the time taken to reach saturation is different for the May and July forecasts, the errors in both cases reach saturation by 1 July. These differences in the error growth are related to the fact that the May and July initial conditions occur during the onset and peak phases of the monsoon. For the EIMR index, which includes part of the oceanic region, Rai and Krishnamurthy (2011) have shown that the errors grow slightly faster for the May forecasts while the errors in the July forecasts are similar compared the error growth of the IMR index. Interestingly, the forecast errors of WS index (zonal circulation index) take about 20-30 days to reach saturation for May forecasts while it seems to take much longer to reach saturation for July forecasts, as shown by Krishnamurthy and Rai (2011).

The overall growth of forecast errors is studied by analyzing the RMS errors obtained by averaging the squared errors over all the ensemble members and over all the years (1981-2005). These RMS errors of the IMR and EIMR indices are shown in Fig. 7.2 for May and July forecasts. The errors in the IMR index shown in Fig.8.2 are with respect to both the IMD observation and R2 analysis whereas the errors in the EIMR index are with respect to R2 analysis only. The initial size of the errors is about 1 and 2 mm day^{-1} for the May and July forecasts, respectively. In the May forecasts, the IMR and EIMR indices take about 60 and 90 days, respectively, to reach saturation, thus indicating different growth rates (Figs. 7.2-a&b). The errors with respect to IMD observations are higher by about 0.5–1.0 mm day^{-1} compared to the errors with respect

to analysis (Fig. 8.2a). In July forecasts, the errors reach saturation in about 30 days for both the IMR and EIMR indices (Figs. 7.2-c&d). The saturation value keeps decreasing steadily toward the end of the monsoon season.

The forecast errors of WS and MH circulation indices were also examined by Krishnamurthy and Rai (2011). Since the magnitudes of the zonal and meridional winds differ widely, the RMS forecast errors of WS and MH indices are shown along with the RMS errors of zonal and meridional winds at 850 hPa and 200 hPa separately in Fig. 8.3 for May and July initial conditions. In May forecasts, the errors in the lower level winds grow at a slower rate and reach saturation in about 40 days (Figs. 7.3-a&b). However, the errors in the upper level winds and the errors in the WS and MH indices grow at a much faster rate at first reaching saturation in about 20 days. Subsequently, the errors decay for a while up to day 130 and then grow again but at a slower rate. The two growing phases happen to occur during the onset and withdrawal phases of the monsoon. The errors in the July forecasts also reveal similar behavior but with some differences (Figs. 7.3-c&d). The WS index, MH index and the horizontal winds at 200 hPa grow at a faster rate and reach saturation in about 20 days. This saturation level lasts for a shorter period of time (compared to May forecasts) and then the errors grow at a slower rate starting from day 60 when the withdrawal phase of the monsoon has started but before the monsoon ends.

The RMS forecast errors of the IMR index in all the DEMETER models are shown in Fig.7.4. The forecast errors are with respect to IMD observed rainfall, and the squared errors are averaged over all nine ensemble members and over the period 1980-2001 to obtain the RMS errors for each model. It should be recalled that all the DEMETER forecasts analyzed here start from 1 May. In general, the error growths in the DEMETER models (Fig. 7.4) are similar to the error growth of the May forecast of the CFS (Fig. 7.1a). While some models (CERF, MAXP, METF and UKMO) reach saturation in about 60 days (by 1 July), other models (ECMW, INGV and LODY) reach saturation by 1 June. MAXP has the lowest saturation value. All models, except UKMO, show an initial slow growth during the monsoon onset period followed by a faster growth rate.

b. Predictability errors

Under the assumption that the model is perfect, the predictability error is the difference between two forecasts of the same model starting with different initial conditions. The predictability errors in the CFS model were analyzed by Rai and Krishnamurthy (2011) following a method used by Lorenz (1982) to determine the predictability of the ECMWF model. The Lorenz method is based on the idea that the one-day forecast of a particular day can be considered to be that day's analysis plus a moderately small error. Thus, the subsequent difference between two forecasts initiated one day apart gives the evolution of a presumably small initial error and will be referred to as 1-day predictability error. Similarly, forecasts starting from initial conditions that are two days apart provide 2-day predictability error, and so on. There are 12 such pairs of forecasts that start one day apart in each month's CFS forecasts. The RMS predictability errors are then computed by averaging the squared errors over all the 12 pairs and over all the years (1981-2005). The RMS 1-day predictability errors of IMR and EIMR indices in the CFS are shown in Fig. 7.5 for May and July forecasts. The general pattern of the growth of predictability errors (Fig. 7.5) is similar to that of the forecast errors (Fig. 7.2). The predictability errors of the EIMR index have a higher saturation value, presumably due to the higher variability of the model forecasts over the Bay of Bengal and the Arabian Sea. The initial size of the predictability errors is large in the July forecasts since they start during the peak of the monsoon season. The growths of 1-day to 4-day predictability errors of IMR, EIMR and AAMR are discussed in more details by Rai and Krishnamurthy (2011).

The predictability errors of the circulation indices in the CFS were also examined by Krishnamurthy and Rai (2011). The evolution of 1-day predictability errors of WS and MH indices are shown in Fig. 7.6 along with those of the zonal and meridional winds at 850 hPa and 200 hPa for May and July CFS forecasts. In this case also, the predictability errors (Fig. 7.6) are similar to the forecast errors (Fig. 7.3). A noticeable difference is in the May forecasts which show less decay after the first saturation (Figs. 7.6-a&b). Also, the slower growths of the upper level zonal wind and the WS index (Fig. 7.6c) start earlier

than in the case of the forecast errors (Fig. 7.3c).

Since all the integrations of the DEMETER models start on the same day (1 May) but with perturbed initial conditions, it is not necessary to follow the Lorenz method to compute the predictability errors in this case. Assuming each ensemble member to be perfect (or assumed to be observation), one at a time, the other members are treated as forecasts. In this way, for each DEMETER model, there are 36 “observation”-forecast pairs for each year. The RMS predictability error of the IMR index is computed from the averages of squared errors over all 36 members and over all the years and is shown for all the DEMETER models in Fig. 7.7. In general, the growth of the predictability errors (Fig. 7.7) is similar to that of the forecast errors (Fig. 7.4). However, the saturation values of the predictability errors are generally smaller than those of the forecast errors. In the case of MAXP, there is no clear error growth which implies that the forecasts of all the ensemble members are close to each other. An examination of the individual forecasts has shown that the daily anomalies of rainfall drift rapidly toward very small values in the IMR and EIMR regions in all the ensemble members. The MAXP model is known to have a large climate drift (Jin et al. 2008). In all the other models, the initial growth of predictability errors is smoother and does not reveal two different growth rates as in the case of forecast errors.

The saturation values reached by the forecast errors and predictability errors depend on the time mean and variance of the observations/analyses and forecasts, respectively. The saturation value of forecast errors (predictability errors) is simply the RMS difference between randomly selected observations (forecasts) and is about $\sqrt{2}$ times the standard deviation of the observations (forecasts). If the observations/analyses and forecasts have same mean and variance, the forecasts errors and predictability errors will reach the same saturation value. In the case of DEMETER models, the saturation values of the forecast errors (Fig. 7.4) are slightly higher than those of the predictability errors (Fig. 7.7). This may imply that the model imperfections have contributed to the increased saturation value in the forecast errors. The seasonal character of the monsoon is reflected in the decreasing saturation level as the monsoon season progresses. In the case of CFS, the forecast errors of the IMR index using the

IMD observation (Figs. 7.2-a&c) seem to saturate at slightly higher values than the corresponding values of the predictability errors (Figs. 7.5-a&c). However, the saturation values of the forecast errors using the analysis (Fig. 7.2) are actually less than those of the predictability errors (Fig. 7.5).The reasons for this behavior may be due to the fact that each ensemble member in the CFS forecasts spans different time periods during the monsoon season and that the analysis may have lower variance.

c. Estimate of error growth rate

In nonlinear dynamical systems, small initial errors first grow exponentially according to linear error dynamics and then slow down during the nonlinear phase of growth before reaching the saturation value (Lorenz 1985; Krishnamurthy 1993). The forecast errors and predictability errors of the models follow the same error growth pattern. To represent this typical error growth in large models, Lorenz (1982) introduced an empirical formula which has been found to be useful in estimating the growth rate of small errors. If the magnitude of the error is E, then the Lorenz error equation is represented by

$$\frac{dE}{dt} = \lambda E - sE^2, \qquad (1)$$

where λ is the growth rate of the error and s satisfies the condition that $E_s = \lambda/s$ is the saturation value of E. λ usually represents the first Lyapunov exponent of the system (Krishnamurthy 1993). If E_0 is the magnitude of the error at an initial time t_0, the solution to Eq. 1 is given by

$$E = \frac{1}{2} E_s \left[1 + \tanh\left[\frac{1}{2} \lambda (t - t_0) - \tanh^{-1}\left(1 - 2\frac{E_0}{E_s} \right) \right] \right]. \qquad (2)$$

The doubling time of small error is given by $t_d = (\ln 2)/\lambda$. The error growth rate can be estimated by fitting the error data to Eq. 2 using a suitable nonlinear least-squares method.

To demonstrate that Lorenz's empirical formula (Eq. 2) is a good approximation, the 1-day predictability error of the EIMR index in CFS May forecasts (from Fig. 7.5b) and its best fit of Eq. 2 are plotted in Fig. 7.8. Using Eq. 2, the nonlinear best fit curve has been extrapolated backward in time so that the initial linear growth is also included and the predictability error has been shifted forward in time in Fig. 7.8. The linear part of Eq. 1 is also plotted in Fig. 7.8 showing the exponential growth. The estimated value of λ is 0.08 which translates to a doubling time of 8.6 days for small errors. Although Eq. 2 is a good approximation, the initial value of the predictability error is found to be large enough to fall in the nonlinear regime of error growth.

All the predictability errors that were discussed earlier were fitted with the Lorenz's empirical formula to estimate the growth rate of small errors. For the predictability errors in the CFS (Fig. 7.5), the doubling times of the IMR and EIMR index are found to be 13.9 and 8.6 days, respectively, for the May forecasts while the corresponding values for the July forecasts are 4.1 and 6.9 days, respectively. These estimates clearly show the difference between the growth of initially small errors during the onset and peak phases of the monsoon. The error growth rates were also estimated for the predictability errors of the IMR index for all the DEMETER models (Fig. 7.7) except MAXP which does not show clear error growth. The doubling time of small errors was found to be 4.6, 3.9, 6.9, 5.0, 4.6 and 4.1 days for CERF, ECMW, INGV, LODY, METF and UKMO, respectively. These values are comparable to the July CFS forecasts. Krishnamurthy and Rai (2011) have shown that two separate empirical formulas with fast and slow growth rates have to be fitted for the predictability errors in the circulation indices of CFS forecasts (Fig. 7.6). For example, the doubling time for fast and slow growth in the 200 hPa WS domain zonal wind of May forecasts (Fig. 7.6a) is found to be 4 and 23 days, respectively.

d. Active and break phases

Some studies (e.g., Waliser et al. 2003, Fu et al. 2007) have reported that the break periods of the monsoon are better predictable than the active periods. Since the CFS forecasts start with initial conditions spread throughout the monsoon season, Rai

and Krishnamurthy (2011) were able to investigate whether predictability depends on the phase of the active/break cycle. Using the IMR index of analysis (R2), the active, break and normal periods are identified by the same criteria used by Krishnamurthy and Shukla (2007) and Rai and Krishnamurthy (2011). The normal periods are further separated by whether the evolution is from normal to active (normal-A) or from normal to break (normal-B). The RMS errors of 1-day predictability errors starting from initial conditions in these four intraseasonal phases are computed separately by using May, June, July and August forecasts.

The RMS predictability errors of IMR and EIMR indices of CFS forecasts initiated during the four phases of the active/break cycle are shown in Fig. 8.9. In the case of the IMR index, the errors starting from active and break phases show similar growth at a faster rate before reaching the saturation level in about 20-30 days (Fig. 7.9a). The doubling time of small errors for these two phases was estimated to be 2.0 days by fitting Lorenz's formula (Eq. 2). The errors starting from both normal-A and normal-B phases grow slowly with an estimated doubling of small errors to be 8.6 days and reach saturation in about 50-60 days (Fig. 7.9a). The predictability errors of the EIMR index starting from all the four phases of the active/break cycle show similar growth behavior. In the case of WS circulation index also, there is no distinction in the error growth patterns from the four phases (Krishnamurthy and Rai 2011). Thus, the CFS does not show any preference in the predictability of either the active phase or the break phase. However, the CFS shows that the forecasts with initial conditions in both the active and break phases have lower predictability than the forecasts initiated during the transition from normal to active and normal to break phases.

7.4. Seasonal predictability

Because of the highly seasonal nature of the monsoon and the dependence of various socio-economic sectors on the entire season's rainfall, prediction of seasonal mean monsoon is very important. In this section, the predictability of the CFS in forecasting the seasonal mean monsoon discussed by Drbohlav and Krishnamurthy

(2010) is reviewed and new results of the seasonal predictability of the DEMETER models are presented. Some aspects of the climatological mean monsoon rainfall and circulation in the CFS forecasts are also described by Drbohlav and Krishnamurthy (2010) and Yang et al. (2008). The June-September (JJAS) climatological means of CFS forecasts show excess rainfall in the Arabian Sea and deficient rainfall in the Bay of Bengal and over India. Although the climatological mean low-level winds are similar to those in the analysis, the forecasts underestimate the magnitude. The analysis of the climatological mean seasonal rainfall in the DEMETER models by Joseph et al. (2010) shows that only INGV and UKMO models realistically capture the spatial pattern over India.

a. Interannual variability

The JJAS seasonal anomalies of rainfall and circulation indices in the CFS forecasts are compared with observations/analysis in Fig. 7.10. The indices of the ensemble means are plotted for forecast leads of one to five months along with observation/analysis (CMAP and R2). The seasonal anomaly of the surface temperature averaged over the Niño-3 region (150°W-90°W, 5°S-5°N) is also shown. The forecasts are less accurate for the indices representing India and its neighborhood (IMR, EIMR and MH; Figs. 7.10-a&c) compared to those representing the Indian and Pacific oceans (AAMR and Niño-3; Figs. 7.10-d&e). These relations are confirmed by the values of the correlation between forecasts and observations (Drbohlav and Krishnamurthy 2010). By examining the composites of strong and weak events based on these various indices, Drbohlav and Krishnamurthy (2010) concluded that the CFS captures more accurately the ENSO-related features of the monsoon than the regionally influenced features of the monsoon.

The DEMETER models also show a similar behavior in the interannual variability of the forecasts. In Fig. 7.11a, the JJAS seasonal anomalies of the EIMR index of ensemble means of the DEMETER models are plotted along with the observed seasonal anomaly (CMAP). Similar time series of the Niño-3 index of the SST is also shown in Fig.

7.11b. While most of the DEMETER models have been able to forecast the interannual variability of the ENSO variability in SST, no model has captured the observed interannual variability of the EIMR index. In fact, the correlations between the model forecasts and the observation for EIMR index are less than 0.35 whereas corresponding correlations for Niño-3 index are in range 0.7−0.8. Another noticeable feature of the Niño-3 index forecasts is that four models (CERF, INGV, LODY and METF) which use the same ocean model (but slightly different versions) are all grouped together (Fig. 7.11b). The relations seen in these predictions indicate that the coupled ocean-atmosphere interactions in the Pacific and Indian Oceans that affect the monsoon need improvement.

b. Forecast errors

The predictability of the coupled models in forecasting the seasonal mean monsoon rainfall is first assessed by examining the forecast errors. The difference in the JJAS seasonal anomaly of rainfall over the monsoon region between CFS forecast and observation (CMAP) is expressed as RMS error by averaging over all ensemble members and over all the years. These RMS forecast errors are plotted in Figs. 7.12-a&c for forecast leads of 1, 3 and 5 months, respectively. In the 1-month lead forecast (Fig. 7.12a), large values (above 3 mm day^{-1}) of the forecast error are in the Bay of Bengal, northeast India, the Arabian Sea along the west coast and the eastern equatorial Indian Ocean. These are the only regions where the magnitude of the error increases (slightly) from 1-month to 5-month lead. In 5-month lead forecast, the errors increase in a small region over the western equatorial Indian Ocean. Over most of the land points in India, the errors are in the range of 0.8–2.4 mm day^{-1} and remain unchanged for all leads. A detailed description of the errors in the forecasts of each month of the monsoon season is provided by Drbohlav and Krishnamurthy (2010).

The RMS forecast errors of JJAS seasonal anomalies of rainfall in DEMETER models are shown in Fig. 7.13. The spatial structure of the errors is generally the same for all the models but the magnitude varies. The common regions of large errors are in northeast India, Bay of Bengal and the equatorial Indian Ocean. Some of these features

are similar to the forecast errors in CFS (Fig.7.12a). The errors are smaller with remarkably similar spatial structure in CERF and METF, perhaps because the two models have the same atmospheric component (ARPEGE) and same oceanic component although with different versions (OPA 8.2/8.0). However, other models (INGV and LODY) that use OPA oceanic component but different atmospheric components do not show the same error structure. It seems that the coupled models with same atmospheric component have similar error structure. Further examples of this behavior is seen in the errors of ECMW and LODY which have IFS as their atmospheric component and in the errors of INGV and MAXP which use ECHAM atmospheric model (different versions). The errors over the land points in India are larger in ECMW, LODY, and UKMO.

c. Predictability errors

The predictability errors of the seasonal mean forecasts under the assumption that the model is perfect are now examined. The predictability errors in the CFS are found by using the method of Lorenz (1982). Two forecasts initiated one month apart are considered and the difference between the JJAS seasonal anomalies of the two forecasts are averaged over all the ensemble members and all the years to obtain the RMS predictability error. The RMS errors, computed as a function of the lead forecast month, are shown in Figs. 7.12-d&f for 1-, 3-, and 5- month lead, respectively. In this case also, large errors (above 3 mm day^{-1}) are in the Bay of Bengal, northeast India, the Arabian Sea along the west coast and the eastern equatorial Indian Ocean. The errors in these regions increase as the forecast lead increases. A detailed description of the predictability errors in the forecasts of each month of the monsoon season is provided by Drbohlav and Krishnamurthy (2010).

For the DEMETER models, the predictability errors are determined by assuming each ensemble member to be perfect, one at a time, while the other members are treated as forecasts. The RMS errors are computed by taking the average over the ensemble pairs and all years. The RMS predictability errors in the DEMETER models are shown in

Fig. 7.14. These predictability errors resemble the forecast errors (Fig. 7.13) in their spatial structure in all the models. In this case also, the models with the same atmospheric component have errors with similar spatial structure and magnitude (CERF and METF; ECMW and LODY). The low values of predictability error over India in MAXP should be treated with caution because the rainfall anomalies of all the ensemble members drift toward small values. Large errors in the equatorial oceanic region are seen in both ECMW and LODY, both of which use the IFS as the atmospheric component. The MAXP model, which has shown quite a different behavior compared to all other models, has been integrated with atmospheric and oceanic initial conditions and perturbation that are different what other models have used.

7.5. Prospects for decadal predictability

Recent years have seen an effort to extend climate prediction from seasonal time scale to decadal and multi decadal time scales. Prediction on decadal time scales is relevant for making long-term decisions to adapt to climate change and natural low-frequency variability of climate. In addition to the external forcing mechanisms, such as the variations in the solar radiation, the interactions within and between climate systems such as the atmosphere and ocean are sources of inter decadal variability. The existence of climate variability on different decadal time scales shown by several ocean-atmosphere coupled models provides hope for predictability at decadal time scale (Latif 1998). There are two different facets of decadal predictability. One is assessing the prediction of the decadal phenomenon itself (e.g., Boer 2000, Troccoli and Palmer 2007) while the other is concerned with the decadal modulation of the seasonal or interannual phenomenon (e.g., Kirtman and Schopf 1998). Although several studies have indicated the possible predictability of phenomena related to Atlantic and Pacific oceans, the decadal prediction is still in infant stages. Because of lack of studies on decadal predictability of the Indian monsoon, a review of the relation of monsoon with known decadal phenomena is presented in this section.

Several studies have provided evidence for decadal variability of the Indian monsoon rainfall and circulation (e.g., Krishnamurthy and Goswami 2000). The IMR index is shown to have a low-frequency variability which alternates between above-normal epochs and below-normal epochs at about three-decade interval. An ENSO-like decadal variability is also known exist in the Pacific Ocean (Zhang et al. 1997). The decadal variations of IMR index and Niño-3 index were shown to vary together most of the time by Krishnamurthy and Goswami (2000). They further suggest that the El Niño (La Niña) may have enhanced relation with droughts (floods) whereas La Niña (El Niño) may not have a significant relation with the monsoon during the warm (cold) phase of the decadal variability. A similar relation was also found by Krishnan and Sugi (2003). In the North Pacific Ocean, the dominant mode of variability is the Pacific Decadal Oscillation (PDO) which varies with a time scale of about 20-30 years. Several studies have established that the North Pacific variability can cause decadal modulation of the variability of the tropical Pacific Ocean or ENSO (e.g., Barnett et al. 1999). This relation implies that the ENSO-monsoon relation can also be modulated by PDO. The influence of PDO on the monsoon variability has not been thoroughly investigated.

Another low-frequency oceanic mode of variability that may influence the monsoon is the Atlantic Multidecadal Oscillation (AMO) which occurs in the North Atlantic with a time scale of about 50-70 years. From model experiments and observations, Zhang and Delworth (2006) have indicated that warm (cold) phase of the AMO enhances (reduces) the Indian monsoon rainfall. They suggest that the warm AMO phase leads to a northward shift in the Intertropical Convergence Zone (ITCZ) which in turn is associated with anomalous southwesterly surface winds. Different mechanisms for the relation between AMO and the monsoon rainfall have been suggested by other studies (e.g., Goswami et al. 2006).

Since the time scales and phases of the AMO, PDO and the ENSO decadal oscillations vary, it is necessary to determine the combined influence of these decadal oscillations on the Indian monsoon. The prospect for decadal prediction of the Indian monsoon depends on the discernable influences of the decadal oscillations of the oceans

and any other slowly varying component of the climate system on the monsoon. So far, not many model experiments have been performed with coupled ocean-atmosphere models to isolate the influences of the decadal variability of the Pacific and Atlantic oceans on monsoon.

7.6. Summary

The predictability of eight coupled ocean-atmosphere models in predicting the Indian monsoon rainfall and circulation has been reviewed. The retrospective forecasts of CFS, the operational coupled model of the NCEP, for the period 1981-2005 were analyzed. The retrospective forecasts of seven coupled models from the DEMETER, a project to test the concept of multi model ensemble prediction, were analyzed for the period 1980-2001. The predictability of these eight models was studied at daily and seasonal time scales. The predictability is expressed in terms of forecast errors which include the imperfections in both the model and initial condition and predictability errors which depend solely on the uncertainties in the initial condition assuming the model to be perfect. The Lorenz method of analysis and the Lorenz empirical formula were used to estimate the error growth rates. The relation between the Indian monsoon and the decadal oscillations of different ocean basins were also discussed.

The forecast errors and predictability errors in the daily forecasts of all the models follow the classic error growth pattern of nonlinear systems. The daily rainfall in the CFS showed differences in the initial size and error growth rate between forecasts with initial conditions in May and July, reflecting the different phases (onset and peak) of the monsoon season. The doubling time of small errors was estimated to be in the rage of 4-14 days for the IMR index and 7-9 days for the EIMR index, depending on the initial month of the forecast. The doubling time of small errors of the IMR index in the DEMETER models, all of which start with 1 May initial conditions, were estimated to be in the range of 4-7 days. The predictability of the horizontal winds in the CFS was found to be somewhat different from that of the rainfall. The error growth in the horizontal winds seems to be governed by two time scales, more pronounced in the upper level than in

the lower level. The analysis of the dependence of predictability on the phase of the active/break cycle did not provide a clear picture. Only in the case of IMR index, there was a difference in the error growth rate between the forecasts initiated in normal phases and those initiated in peak active/break phases.

All the models (CFS and DEMETER) failed to capture the observed interannual variability of the JJAS seasonal anomalies of the rainfall index over the Indian monsoon region, especially during years of developing El Niño and La Niña events. However, all the models were able to predict the seasonal anomalies of the Niño-3 index with very high interannual correlation with observation. These coupled models are successful in simulating the ocean-atmosphere interaction in the Pacific Ocean region but not over the Indian monsoon region. The models still require improvement in capturing the seasonally persistent influences of the slowly varying components of the coupled system according to Charney-Shukla hypothesis. The spatial structures of forecast errors and predictability errors were found to be generally same in all the models. The errors are large in the Bay of Bengal, the Arabian Sea along the west coast of the Indian peninsula and the equatorial Indian Ocean. The analysis of the DEMETER models showed that the models which had the same atmospheric component produced errors with similar structure and magnitude.

The prospect for predicting the Indian monsoon on decadal time scales was addressed by reviewing the known relation between the monsoon and the decadal variability of different oceans. The ENSO-like decadal variability of the tropical Pacific Ocean seems to vary together with the Indian monsoon rainfall and may influence the severity of the droughts and floods. The PDO which influences the ENSO may also affect the variability of the monsoon through ENSO-monsoon relation. The Atlantic Ocean may also affect the monsoon on decadal time scale with the warm (cold) phase of the AMO enhancing (reducing) the Indian monsoon rainfall.

The dynamical seasonal prediction of the Indian monsoon rainfall remains a challenge. Both the AGCMs and the coupled models show large systematic errors in simulating the mean monsoon circulation and rainfall, the statistics of active and break cycles, and the number, intensity and tracks of monsoon lows and depressions. The models are unable to produce realistic simulation of the interannual variability of the monsoon. Even the AGCMs with observed but prescribed SST are unable to simulate the mean monsoon and its interannual variability. This has raised questions about the usefulness of AGCMs with prescribed SST in simulating and predicting the Indian monsoon circulation and rainfall.

Some recent forecast experiments by David Dewitt (personal communication) suggest that the dynamical predictions of seasonal mean monsoon circulation and rainfall from coupled models are indistinguishable from seasonal forecasts if the same SSTs were prescribed (Tier 2). Similar conclusion has been reached by Edwin Schneider (personal communication) in a separate study. These model results, combined with the observational studies of Gadgil et al. (2004) and Krishnamurthy and Kirtman (2009) which showed robust relationships between SST anomalies over the Pacific and Indian oceans and the Indian summer monsoon rainfall, raise the following question which the present study cannot answer: Is the deficiency of AGCMs (with prescribed SST) in predicting the seasonal mean monsoon rainfall primarily due to lack of ocean-atmosphere coupled fluxes or lack of AGCMs ability to simulate the SST-forced response in heating and convergence? Further improvement in observational data network (both atmospheric and oceanic) and advances in numerical modeling technique (including data assimilation) may enhance the accuracy of monsoon simulation as well as our understanding of various physical processes which maintain and control monsoon circulation.

References

Barnett, T. P., Pierce D. W., Latif, M., Dommenget, D. & Saravanan, R., 1999, "Interdecadal interactions between the tropics and midlatitudes in the Pacific basin", *Geophys. Res. Lett*. 26, 615-618.

Boer, G. J., 2000, "A study of atmosphere-ocean predictability on long time scales", *Clim. Dyn*., 16, 469-472.

Charney, J. G., & Shukla, J., 1981, "Predictability of monsoons. *Monsoon Dynamics"*, J. Lighthill and R. P. Pearce, Eds., Cambridge University Press, 99-109.

DelSole, T. and Shukla J., 2002, "Linear prediction of Indian monsoon rainfall", *J. Climate*, 15, 3645-3658.

Drbohlav, H. K. L. & Krishnamurthy, V., 2010, "Spatial structure, forecast errors, and predictability of the South Asian monsoon in CFS monthly retrospective forecasts", *J. Climate*, 23, 4750-4769.

Fu, X., Wang, B., Waliser, D. E., & Tao L., 2007, "Impact of atmosphere-ocean coupling on the predictability of monsoon intraseasonal oscillations", *J. Atmos. Sci.*, 64, 157-174.

Gadgil, S., Rajeevan, M., & Nanjundiah, R., 2005, "Monsoon prediction–Why yet another failure?" *Curr. Sci.*, 88, 1389-1400.

Gadgil, S., Vinayachandran, P. N., Francis, P. A., 2004, "Extremes of the Indian summer monsoon rainfall, ENSO and equatorial Indian Ocean oscillation", *Geophys. Res. Lett.*, 31, doi:10.1029/2004GL019733.

Goswami, B. N., Krishnamurthy, V. and Annamalai, H., 1999, "A broad-scale circulation index for the interannual variability of the Indian summer monsoon", *Quart. J. Roy. Meteor. Soc.*, 125**,** 611–633.

Goswami, B. N., Madhusoodanan, M. S., Neema, C. P., and Sengupta, D., 2006, "A physical mechanism for North Atlantic SST influence on the Indian summer monsoon" *Geophys. Res. Lett.,* 33, L02706, doi:10.1029/2005GL024803.

Jin, E. K. and Co-authors, 2008, "Current status of ENSO prediction skill in coupled ocean-atmosphere models", *Clim. Dyn.*, 31, 647-664.

Joseph, S., Sahai, A. K., & Goswami, B. N., 2010, “Boreal summer intraseasonal oscillations and seasonal Indian monsoon prediction in DEMETER coupled models”, *Clim. Dyn.*, 35, 651-667.

Kanamitsu, M., Ebisuzaki, W., Woollen, J., Yang S.-K., Hnilo, J. J., Fiorino, M., & Potter, G. L., 2002, “NCEP-DOE AMIP-II Reanalysis (R-2)”, *Bull. Amer. Meteor. Soc.*, 83, 1631-1643.

Kang, I. S., & Shukla, J., 2006, “Dynamical seasonal prediction and predictability of the monsoon”, *The Asian monsoon*, B. Wang, Ed., Springer-Praxis, 585-612.

Kang, I.-S., Jin, K., Wang, B.,. Lau, K.-M, Shukla, J., Krishnamurthy, V., Schubert, S. D., Waliser, D. E., Stern, W. F., Kitoh, A., Meehl, G. A., Kanamitsu, M., Galin, V. Y., Satyan, V., Park, C.- K., Liu, Y., 2002, “ Intercomparison of the climatological variations of Asian summer monsoon precipitation simulated by 10 GCMs”, *Climate Dyn.*, 19, 383-395.

Kirtman, B. P., & Schopf, P. S., 1998, “Decadal variability in ENSO predictability and prediction”, *J. Climate*, 11, 2804-2822.

Krishnamurthy, V., 1993, “A predictability study of Lorenz’s 28-variable model as a dynamical system”, *J. Atmos. Sci.*, 50, 2215-2229.

Krishnamurthy, V., & Goswami, B. N., 2000, “Indian monsoon-ENSO relationship on interdecadal timescale”, *J. Climate*, 13**,** 579-595.

Krishnamurthy, V., & Kinter, III J. L., 2003, “The Indian monsoon and its relation to global climate variability”, *Global Climate*, X. Rodó and F. A. Comín, Eds., Springer-Verlag, Berlin, 186–236.

Krishnamurthy, V., & Kirtman, B. P., 2009, “Relation between Indian monsoon variability and SST”, *J. Climate*, 22**,** 4437–4458.

Krishnamurthy, V., & Shukla, J., 2000, “Intraseasonal and interannual variability of rainfall over India”, *J. Climate*, 13**,** 4366-4377.

Krishnamurthy, V., & Shukla, J., 2001, “ Observed and model simulated interannual variability of the Indian monsoon”, *Mausam*, 52, 133-150.

Krishnamurthy, V., & Shukla, J., 2007, “Intraseasonal and seasonally persisting patterns of Indian monsoon rainfall”, *J. Climate*, 20, 3-20.

Krishnamurthy, V., & Shukla, J., 2008, “Seasonal persistence and propagation of intraseasonal patterns over the Indian monsoon region”, *Clim. Dyn.,* 30, 353-369.

Krishnamurthy, V., and Rai, S., 2011, “Predictability of South Asian monsoon circulation in the NCEP Climate Forecast System” , *Adv. Geosci.*, 22, 65-76.

Krishnan, R., & Sugi, M., 2003, “Pacific decadal oscillation and variability of the Indian summer monsoon rainfall” , *Clim. Dyn.*, 21, 233-242.

Kumar, K. K., Hoerling, M., & B. Rajagopalan, 2005, “Advancing dynamical prediction of Indian monsoon rainfall”, *Geophys. Res. Lett.*, 32, L08704, doi:10.1029/2004GL021979.

Latif, M., 1998, “Dynamics of interdecadal variability in coupled ocean-atmosphere models”, *J. Climate*, 11, 602-624.

Lorenz, E. N., 1962, “The statistical prediction of solutions of dynamic equations”, *Proc. Int. Symp. Numerical Weather Prediction*, Tokyo, Japan, 629-635.

Lorenz, E. N., 1982, “Atmospheric predictability experiments with a large numerical model”, *Tellus*, 34, 505-513.

Lorenz, E. N., 1984, “Some aspects of atmospheric predictability, *Problems and prospects in long and medium range weather forecasting”*, D. M. Burridge and E. Kallen, Eds., Springer-Verlag, Berlin, 1-20.

Lorenz, E. N., 1985, “The growth of errors in prediction. *Turbulence and predictability in geophysical fluid dynamics and climate dynamics*, M. Ghil, R. Benzi, and G. Parisi, Eds., North Holland, Amsterdam, 243-265.

Moorthi, S., Pan, H. L. & Caplan, P., 2001, “Changes to the 2001 NCEP operational MRF/AVN global analysis/forecast system”, NWS Tech. Procedures Bulletin 484, 14pp. [Available online at http://www.nws.noaa.gov/om/tpb/484.htm.]

Pacanowski, R. C., & Griffies, S. M., 1998, “MOM 3.0 manual. NOAA/GFDL. [Available online at http://www.gfdl.noaa.gov/~smg/MOM/web/guide_parent/guide_parent.html.]

Palmer, T. N., and coauthors, 2004, “Development of a European multimodel ensemble system for seasonal-to-interannual prediction (DEMETER)”, *Bull. Amer. Meteor. Soc.*, 85, 853-872.

Palmer, T. N., Brankovic, C., Viterbo, P., & Miller, M. J., 1992, "Modeling interannual variations of summer monsoons', *J. Climate*, 5, 399-417.

Rai, S. & Krishnamurthy, V., 2011, "Error growth in Climate Forecast System daily retrospective forecasts in South Asian monsoon", *J. Geophys. Res.*, 116, D03108, doi:10.1029/2010JD014840.

Rajeevan, M., 2001, "Prediction of Indian summer monsoon: Status, problems and prospects", *Curr. Sci.*, 81, 1451-1457.

Rajeevan, M., Bhate, J., Kale, J. D. & Lal, B., 2006, "High resolution daily gridded rainfall data for the Indian region: Analysis of break and active monsoon spells", *Current Science*, 91, 296-306.

Rasmusson, E. M. & Carpenter, T. H., 1983, "The relationship between eastern equatorial Pacific sea surface temperatures and rainfall over India and Sri Lanka", *Mon. Wea. Rev.*, 111, 517-528

Saha, S., Nadiga, S., Thiaw, C., Wang, J., Wang, W., Zhang, Q., Van den Dool, H. M., Pan, H.-L., Moorthi, S.,. Behringer, D, Stokes, D., Pena, M., Lord, S., White, G., Ebisuzaki, W., Peng, P., & Xie, P., 2006, "The NCEP Climate Forecast System", *J. Climate*, 19, 3483-3515.

Shukla, J., 1998, "Predictability in the midst of chaos: A scientific basis for climate forecasting", *Science*, 282, 728-731.

Sikka, D. R., 1980, "Some aspects of the large scale fluctuations of summer monsoon rainfall over India in relation to fluctuations in the planetary and regional scale circulation parameters" , *Proc. Indian Acad. Sci. (Earth & Planet. Sci.)*, 89, 179-195.

Simmons, A. J., & Hollingsworth, A., 2002, "Some aspects of the improvement in skill of numerical weather prediction", *Quart. J. Roy. Meteor. Soc.*, 128, 647-677.

Sperber, K. R., Brankovic, C., Déqué, M., Frederiksen, C. S., Graham, R., Kitoh, A., Kobayashi, C., Palmer, T., Puri, K., Tennant, W., & Volodin, E., 2001, "Dynamical seasonal prediction of the Asian summer monsoon" , *J. Climate*, 129, 2226-2248.

Sperber, K. R., & Palmer, T. N., 1996, "Interannual tropical rainfall variability in general circulation model simulations associated with the Atmospheric Model Intercomparison Project", *J. Climate*, 9, 2727-2750.

Troccoli, A. & Palmer, T. N., 2007, “Ensemble decadal predictions from analysed initial conditions”, *Phil. Trans. Roy. Soc. A,* 365, 2179-2191.

Waliser, D. E., Stern, W., Schubert, S., & Lau, K. M., 2003, “Dynamic predictability of intraseasonal variability associated with the Asian summer monsoon”, *Quart. J. Roy. Meteor. Soc.*, 129, 2897-2925.

Walker, G. T., 1923, “Correlation in seasonal variations of weather. VIII. A preliminary study of world weather” , *Indian Meteor. Memo.*, 24 (Part 4), 75-131. [Also published in *Sir Gilbert T. Walker - Selected Papers*, Indian Meteorological Society, New Delhi, 1986, 120-178.]

Walker, G. T., 1924, “Correlation in seasonal variations of weather. IX. A further study of world weather”, *Indian Meteor. Memo.*, 24 (Part 9), 275-332. [Also published in *Sir Gilbert T. Walker - Selected Papers*, Indian Meteorological Society, New Delhi, 1986, 179-240.]

Wang, B., Ding, Q., Fu, X., Kang, I.-S., Jin, K., Shukla, J., & Doblas-Reyes, F., 2005a, “Fundamental challenge in simulation and prediction of summer monsoon rainfall”, *Geophys. Res. Lett.*, 32, L15711, doi:10.1029/2005GL022734.

Wang, B., and Fan, Z., 1999, “Choice of South Asian summer monsoon indices” , *Bull. Amer. Meteor. Soc.*, 80, 629-638.

Xie, P. and Arkin, P. A., 1996, “Analyses of global monthly precipitation using gauge observations, satellite estimates and numerical model predictions”, *J. Climate*, 9, 840-858.

Yang, S., Zhang, Z., Kousky, V. E., Higgins, R. W., Yoo, S.-H., Liang, J., & Fan, Y., 2008, “Simulations and seasonal prediction of the Asian summer monsoon in the NCEP Climate Forecast System” , *J. Climate*, 21, 3755-3775.

Zhang, R., & Delworth, T. L., 2006, “Impact of Atlantic multidecadal oscillations on India/Sahel rainfall and Atlantic hurricanes”, *Geophys. Res. Lett.*, 33, L17712, doi:10.1029/2006GL026267.

Zhang, Y., Wallace, J. M., & Battisti, D. S., 1997, “ ENSO-like interdecadal variability: 1900–93”, *J. Climate,* 10, 1004–1020.

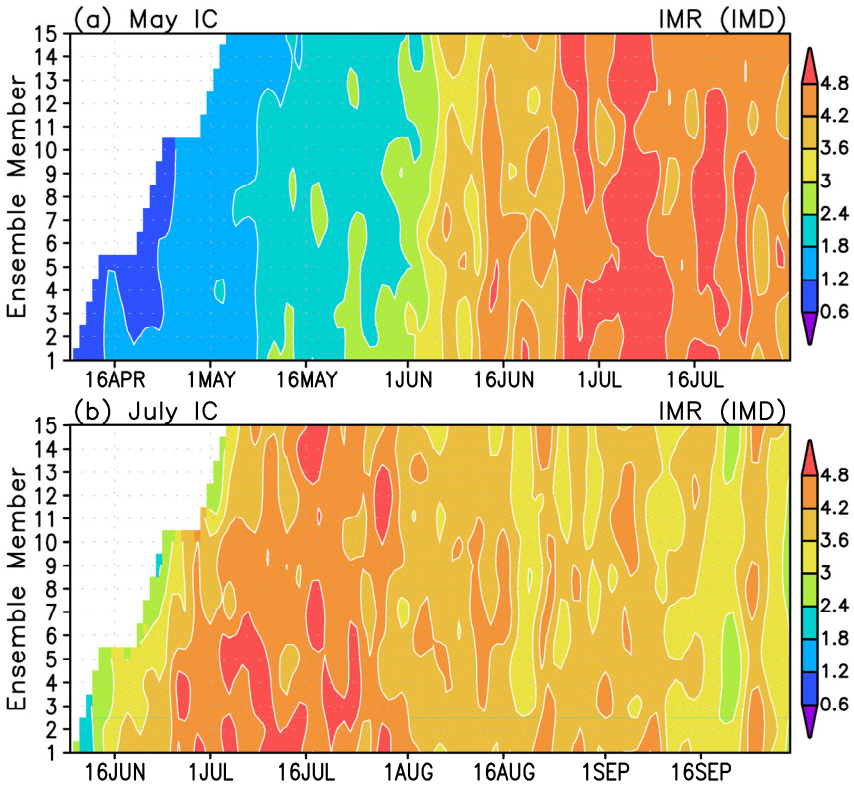

Fig. 7.1 : CFS Forecast errors: RMS errors of IMR index of individual ensemble members starting from (a) May and (b) July initial conditions. The errors are differences between forecasts and IMD observed rainfall. The RMS errors are calculated by averaging the squared errors over the years 1981-2005. Units are in mm day^{-1}.

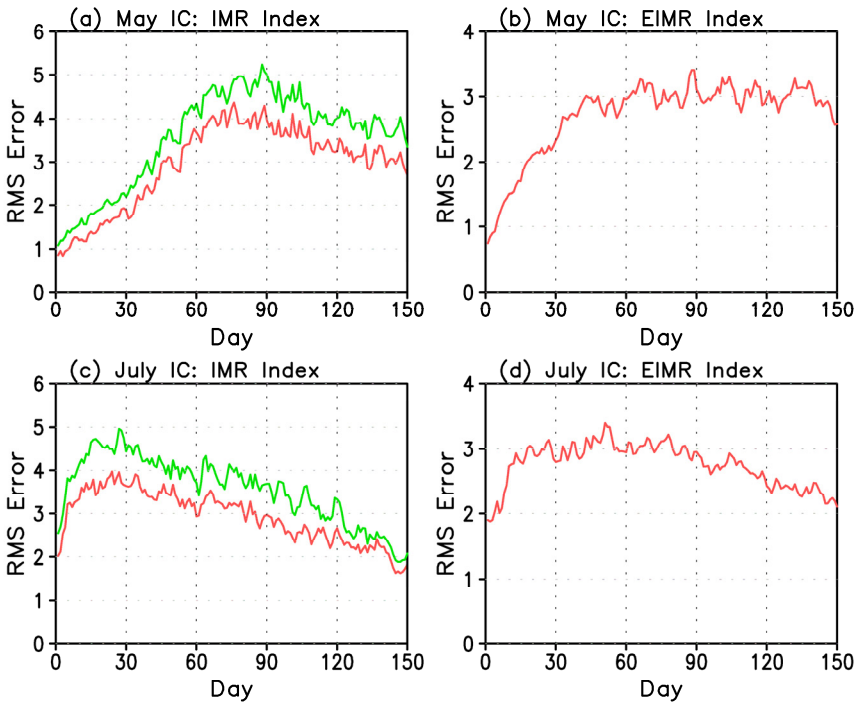

Fig.7.2 : Forecast errors in CFS: RMS errors of IMR index for (a) May and (c) July initial conditions and RMS errors of EIMR index for (b) May and (d) July initial conditions. The RMS errors are computed by averaging the squared errors over all ensemble members and over the years 1981-2005. Day zero refers to the first forecast day of each of the 15 individual ensemble members. Errors with respect to observed IMD rainfall are also shown (green) for comparison with errors with respect to analysis (red). Units are in mm day^{-1}.

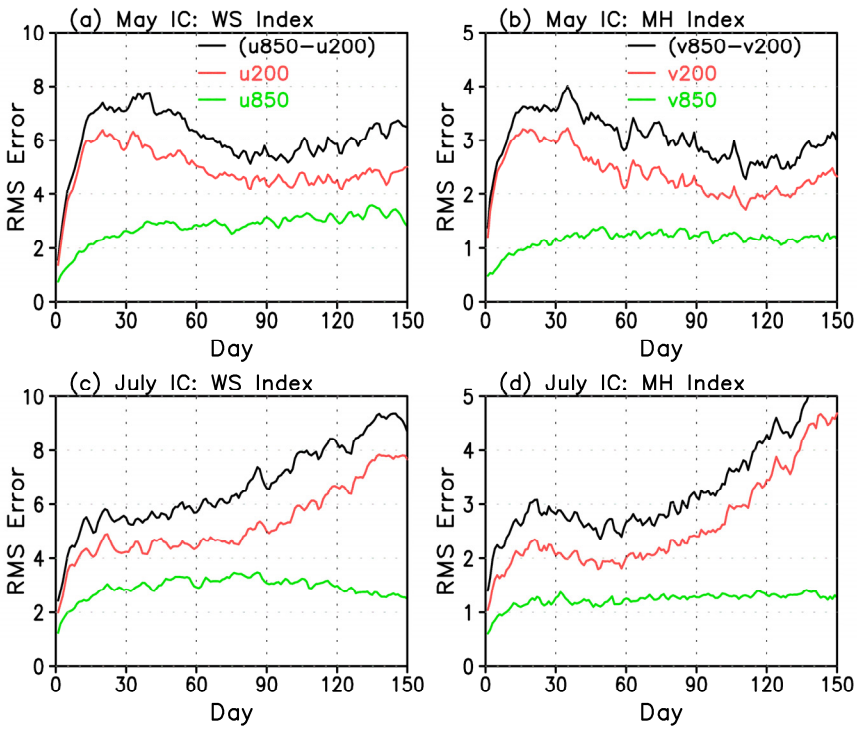

Fig.7.3 : Forecast errors in CFS: RMS errors of WS-domain-averaged *u*850 (green), *u*200 (red) and (*u*850−*u*200) (black) for (a) May and (c) July initial conditions. RMS errors of MH-domain-averaged *v*850 (green), *v*200 (red) and (*v*850−*v*200) (black) for (b) May and (d) July initial conditions. The RMS errors are computed by averaging the squared errors over all ensemble members and over the years 1981-2005. Day zero refers to the first forecast day of each of the 15 individual ensemble members. Units are in m s^{-1}.

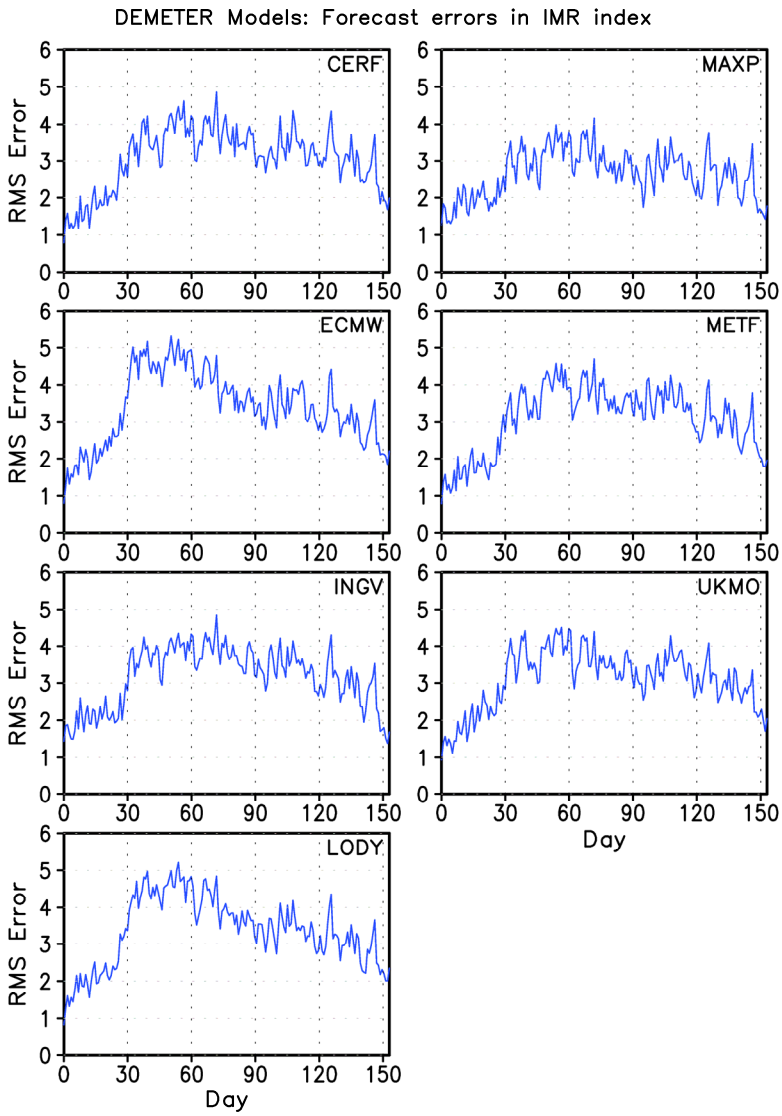

Fig.7.4 : Forecast errors in DEMETER models: RMS errors of IMR index using IMD rainfall data as observation. The RMS errors are computed by averaging the squared errors over all ensemble members and over the years 1980-2001. Day zero refers to the first forecast day of each of the 9 individual ensemble members. The model is identified in the top right corner of each panel. Units are in mm day^{-1}.

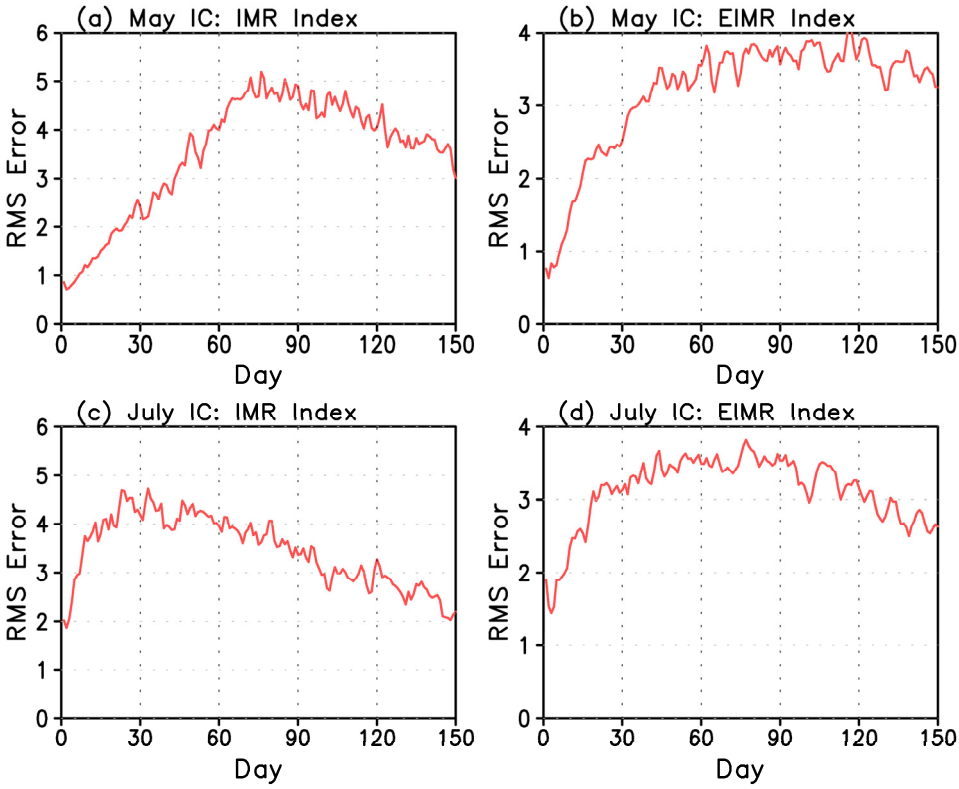

Fig.7.5 : Predictability errors in CFS: RMS 1-day predictability errors of IMR index for (a) May and (c) July initial conditions and forecast errors of EIMR index for (b) May and (d) July initial conditions. The RMS errors are computed by averaging the squared errors over all ensemble member pairs in the 1-day predictability errors and over the years 1981-2005 (see text for details). Units are in mm day^{-1}.

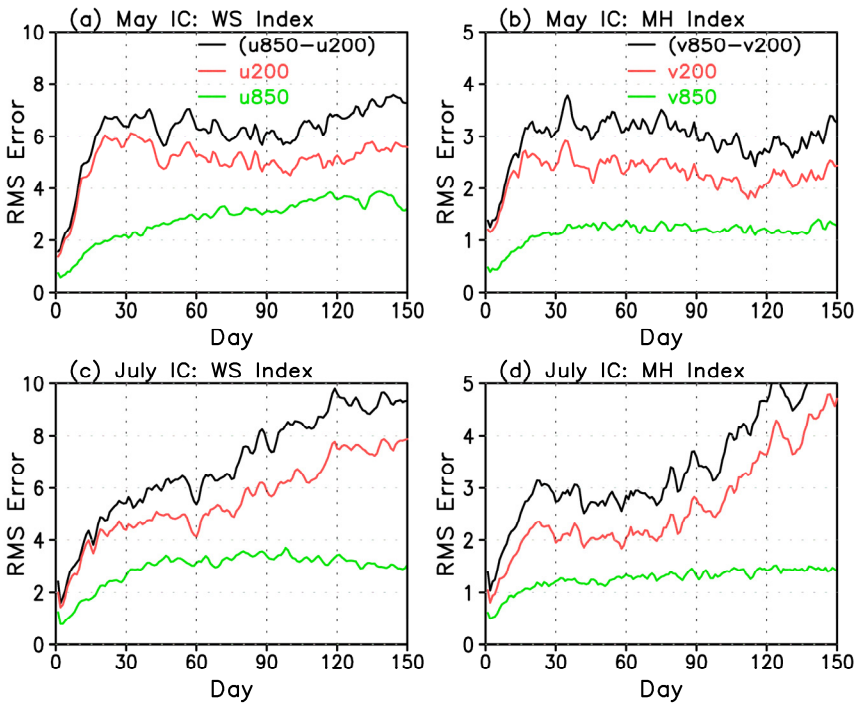

Fig.7.6 : Predictability errors in CFS: RMS 1-day predictability errors of WS-domain-averaged *u*850 (green), *u*200 (red) and (*u*850−*u*200) (black) for (a) May and (c) July initial conditions. RMS errors of MH-domain-averaged *v*850 (green), *v*200 (red) and (*v*850−*v*200) (black) for (b) May and (d) July initial conditions. The RMS errors are computed by averaging the squared errors over all ensemble member pairs in the 1-day predictability errors and over the years 1981-2005 (see text for details). Units are in m s^{-1}.

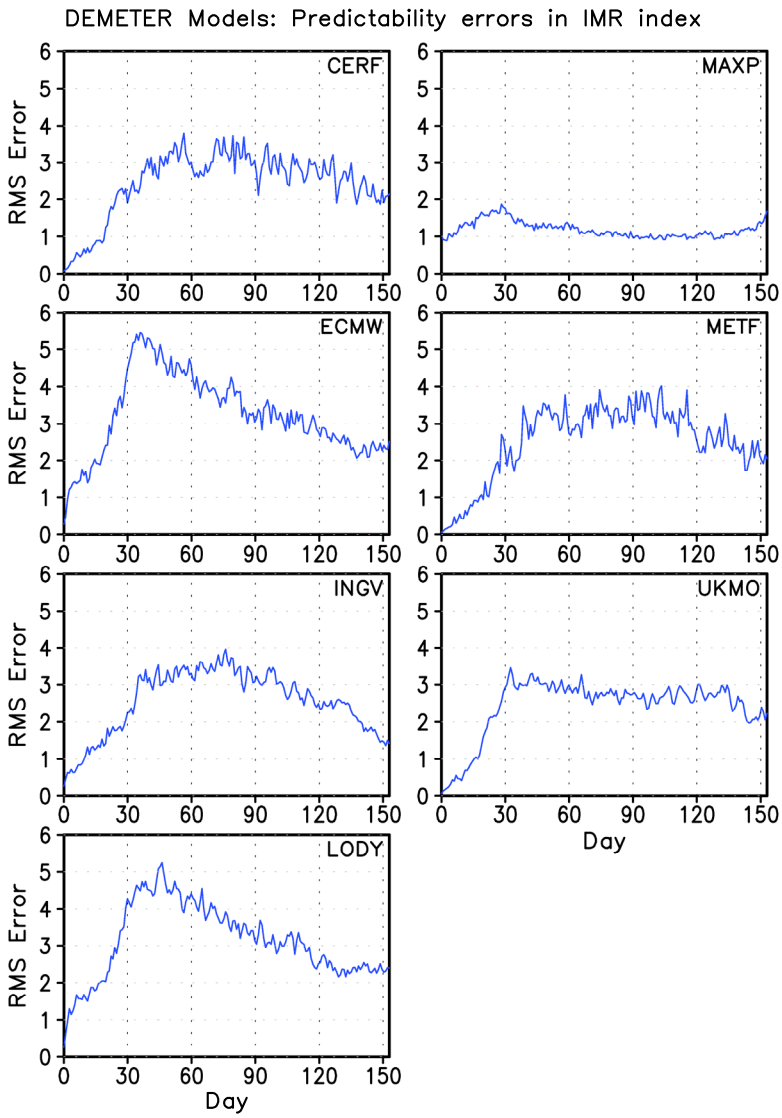

Fig.7.7 : Predictability errors in DEMETER models: RMS predictability errors of IMR index. Units are in mm day^{-1}. The RMS errors are computed by averaging the squared errors over all ensemble member pairs in the predictability errors and over the years 1980-2001 (see text for details). The model is identified in the top right corner of each panel.

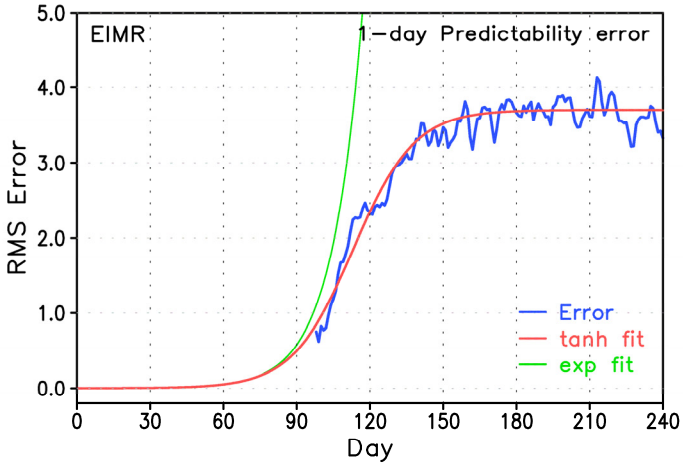

Fig.7.8 : RMS error (blue) of EIMR index, empirical fit (green) according to eq. 2 and empirical fit (red) according to eq. 4. The RMS error is 1-day predictability error in CFS (same as that in Fig. 5b) with May initial condition. The predictability error curve (blue) has been shifted forward in time so that the fitted curves (red and green) are extrapolated back to start with a very small initial error (~10^{-3}) at day zero.

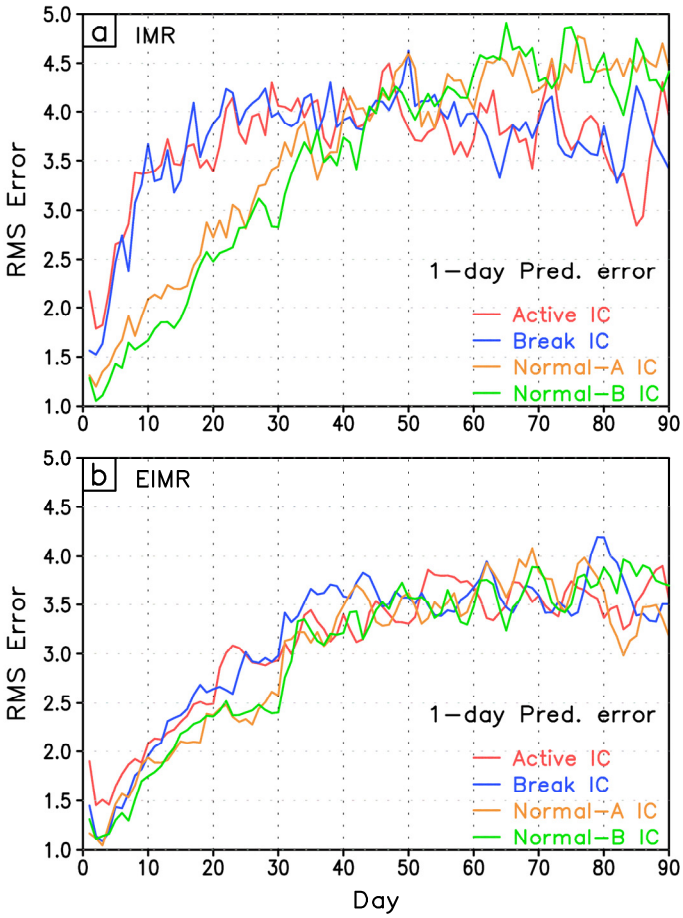

Fig.7.9 : CFS predictability errors: RMS 1-day predictability errors of (a) IMR index and (b) EIMR index shown separately for initial conditions starting from active (red), break (blue), normal-A (orange) and normal-B phases (green). May, June, July and August forecasts are used in computing the RMS errors. The RMS errors are computed by averaging the squared errors over all ensemble member pairs in the 1-day predictability errors and over the years 1981-2005 (see text for details). Units are in mm day^{-1}.

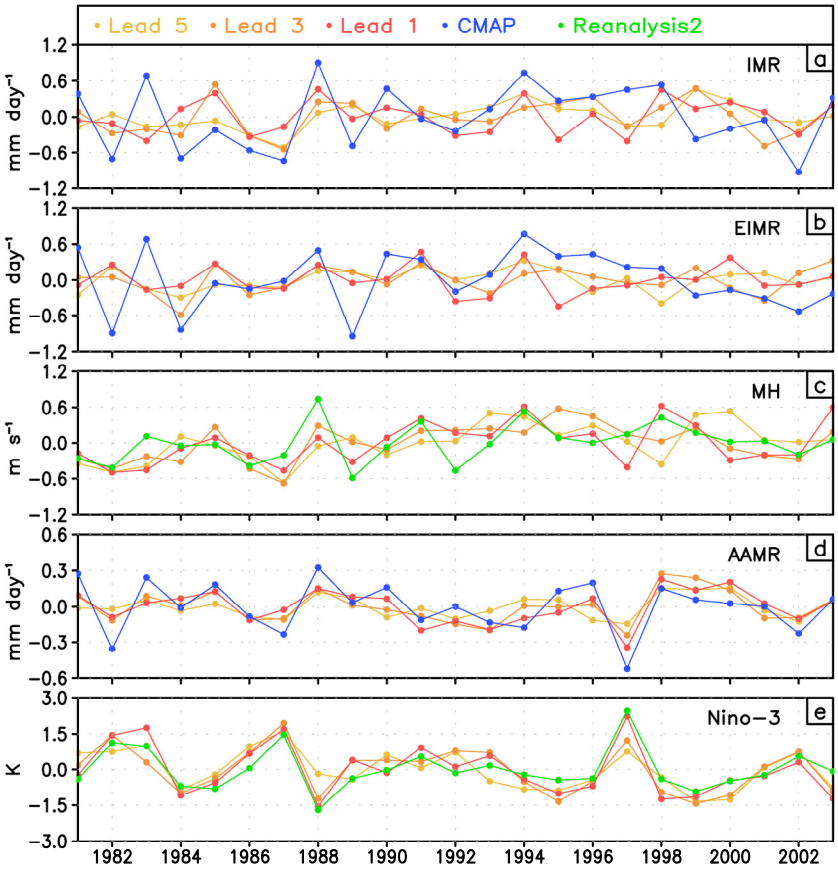

Fig.7.10 : CFS forecasts: JJAS seasonal anomalies of (a) IMR, (b) EIMR, (c) MH, (d) AAMR, (e) WY, and (f) Niño-3 indices in observation (CMAP)/analysis and forecasts for 1-, 3- and 5-month leads.

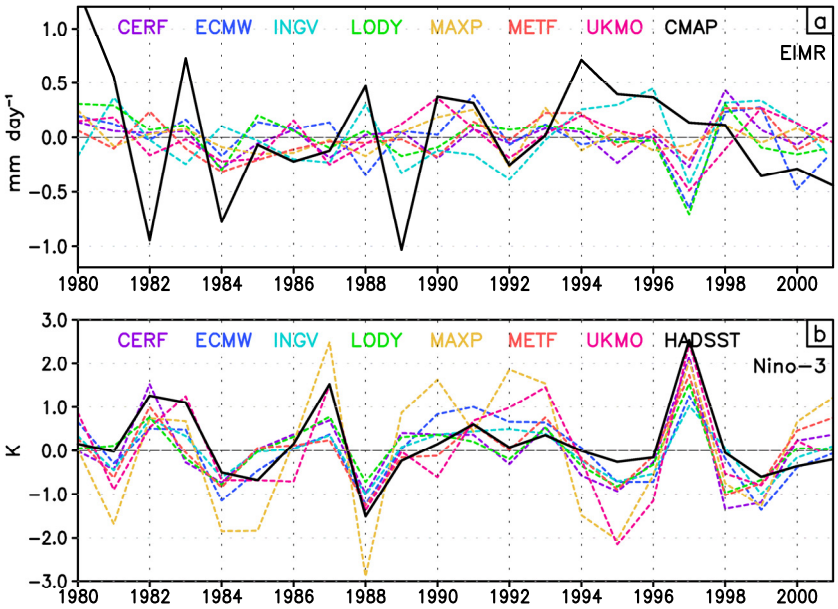

Fig.7.11 : DEMETER model forecasts from 1 May initial conditions: JJAS seasonal anomalies of (a) EIMR and (b) Niño-3 indices in ensemble mean of model forecasts and observations (CMAP for precipitation and HadISST for SST).

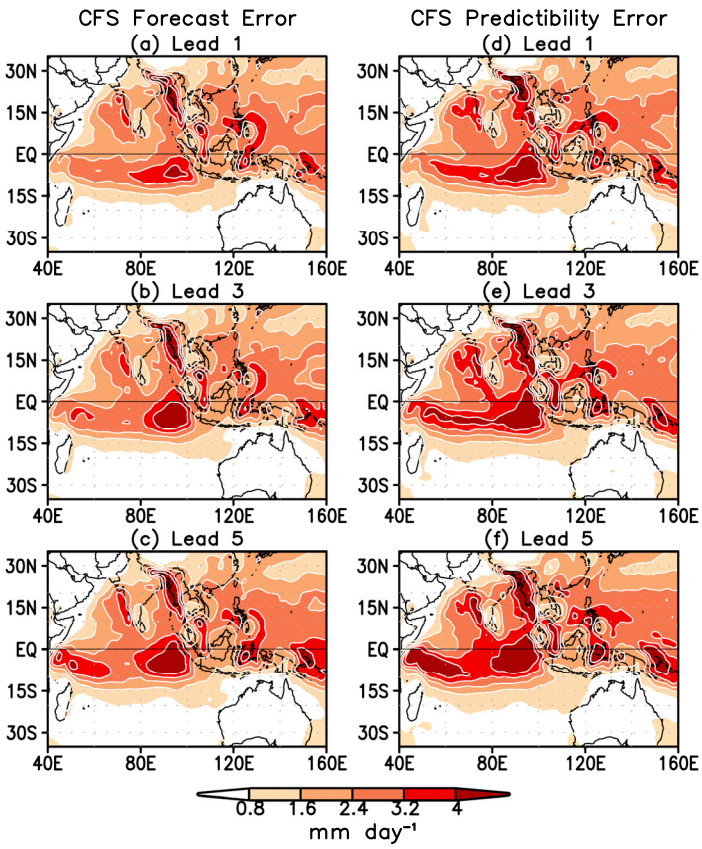

Fig.7.12 : CFS forecasts: Forecast error of seasonal precipitation shown as RMSE of JJAS mean precipitation anomalies between forecast (1-, 3- and 5-month lead) and observation (left panels). Predictability error of the model for *n*-month lead shown as RMSE of JJAS seasonal precipitation anomalies between *n*-month lead forecast and (*n*-1)-month lead forecast (right panels). The RMS errors are calculated by averaging the squared errors over all ensemble members and over the years 1981-2005. Units are in mm day^{-1}.

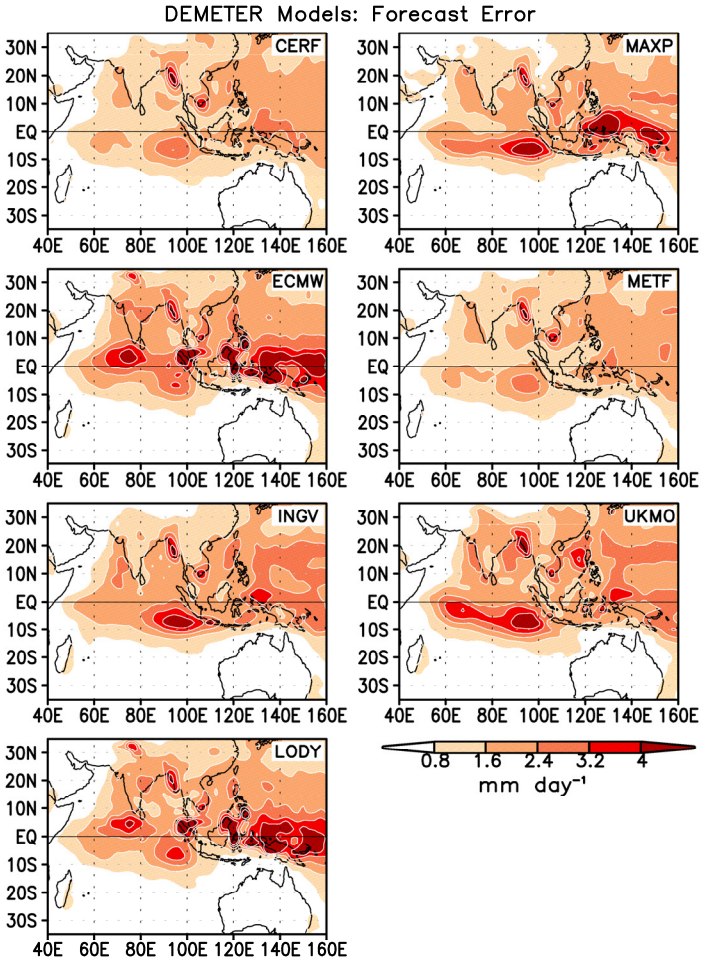

Fig.7.13 : DEMETER model forecasts from 1 May initial conditions: RMS forecast errors of JJAS seasonal precipitation anomalies. Units are in mm day^{-1}. The RMS errors are calculated by averaging the squared errors over all ensemble members and over the years 1980-2001. The model is identified in the top right corner of each panel.

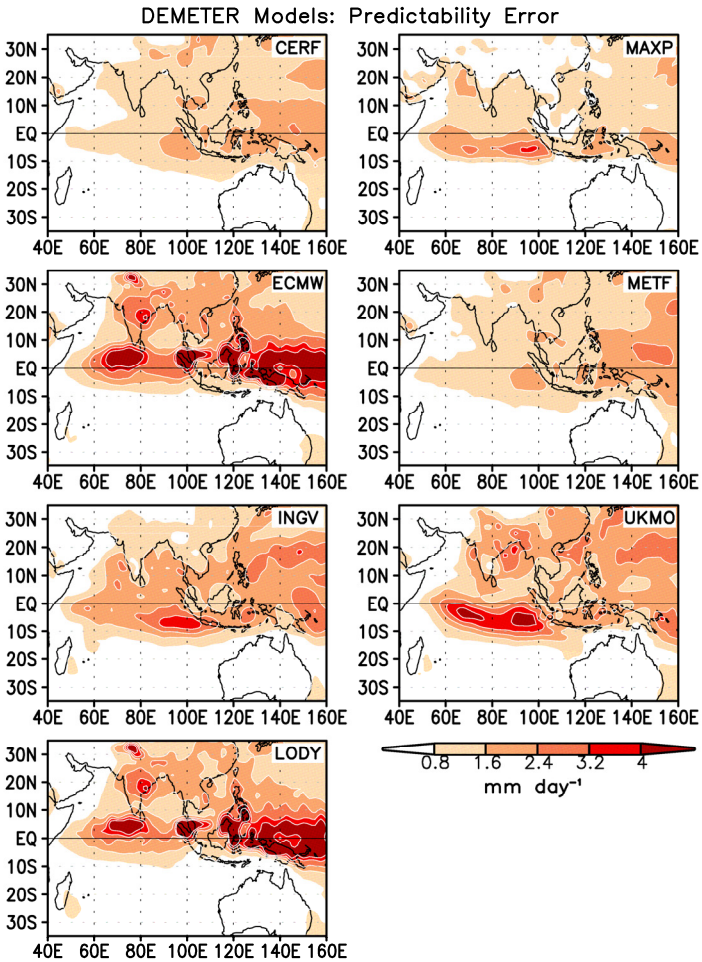

Fig.7.14 : DEMETER model forecasts from 1 May initial conditions: RMS predictability errors of JJAS seasonal precipitation anomalies. Units are in mm day^{-1}. The RMS errors are calculated by averaging the squared errors over all ensemble members and over the years 1980-2001. The model is identified in the top right corner of each panel.

CHAPTER 8

SHORT RANGE FORECASTING OF MONSOON

S.K. Roy Bhowmik
India Meteorological Department, New Delhi

skrb@imdmail.gov.in

8.1. Introduction

Monsoon Forecasting is a challenging problem over the Indian subcontinent where monsoon constitute a major weather system affecting a large population. Short, medium range and seasonal forecasts are essential for various weather sensitive activities such as farming operations, flood forecasting, water resource management, sports, transport etc. Forecasting monsoon weather systems and associated rainfall is one of the difficult areas in Numerical Weather Prediction (NWP) due to complex issues involved. These include impact of topography, treatment of synoptic scale low-pressure systems, mesoscale convective systems and problem of mesoscale good quality observations, particularly over the ocean. In the past, synoptic methods have been the mainstay of tropical weather forecasting (Rao, 1976). Of late, NWP methods have acquired greater skills and are playing increasingly important role in the tropical weather prediction, though the progress of dynamical modelling efforts in the tropics has been rather slow as compared with the extra tropics. This is because of some inherent problems associated with the dynamics of the tropical weather systems. In the extra tropics, the primary energy source for the atmospheric motion is the zonal available potential energy associated with the strong temperature gradients, and there exists a satisfactory dynamical theory of these motions outside the tropics. In the tropics, on the other hand, the storage of available potential energy is very small due to very small temperature gradients. Latent heat release in cumulus convection is the primary energy source. Parameterization of cumulus convection in tropical model is therefore very important, but is a difficult problem. Added to this, there is the problem of large perennial data gaps in the tropical regions, which are largely oceanic. The tropical numerical weather prediction system is required to address these problems adequately. Much progress has been made in recent years in the development of numerical models for low latitudes. The World Weather Watch, now supported by a variety of surface based and space based observing platforms has considerably enhanced the

observational database for numerical weather modelling. The availability of faster computers has enabled large volumes of tests on analysis, initialization, sensitivity to physical parameterization and statistical evaluation of NWP, resulting in an overall improvement in the skill of tropical dynamical models.

Currently, weather forecast services are based on conventional Synoptic Methods supplemented by use of Numerical Weather Prediction products of different centers. In this chapter, use of various NWP products for the short range forecasting of monsoon will be discussed. A brief description of NWP development work in India is given in section 8.2. Section 8.3 describes current operational NWP system and various NWP products used for day-to-day short range (as well as medium range) weather forecasting. The forecast procedure with the use of NWP products is discussed in section 8.4. Current forecast skill and limitations of NWP models are discussed in section 8.5 and the outlook for the future is given in section 8.6.

8.2. NWP Development work in India

The early NWP development works carried out in India was documented by Sarker and Bedi (1987). Very recently, Bohra (2009) made a detailed review of NWP development work of India.

Das and Bose (1958) made the first contribution in India for numerical weather prediction of a monsoon system. Application of computers for numerical weather prediction started in early sixties during the International Indian Ocean Expedition (IIOE) with an IBM 1620 computer. With the availability of IBM 360/44 at the University of Delhi and CDC 3600 computer at Tata Institute of Fundamental Research Bombay, NWP development work in India got initiated. Computer programmes for objective analysis of meteorological data were developed (Datta et al., 1970; Rao et al., 1972; Sinha, 1972; Datta and Singh, 1973). Experiments with Barotropic and Quasi-geostropic models (Shukla, 1972; Datta and Mukherjee, 1972, Mukherjee and Datta, 1973) and diagnostic studies were carried out (Shukla, 1969; Godbole, 1973, Ramanathan and Saha, 1972). With the installation of IBM360/44 at the India Meteorological Department (New Delhi) in July 1973, the work in the NWP field progressed fast (Asnani and Mishra, 1975; Sikka, 1975; Bedi et al., 1976; Bedi,1976;; Ramanathan and Bansal, 1976, Das and Bedi, 1976;1979;1981; Singh et al., 1980; Sinha et al., 1982). Single level preminitive equation spectral model (Bedi 1979) and a three level primitive equation spectral model (Bedi 1985) was attempted. A ten level non-linear balanced model was developed for diagnostic studies in the tropics (Rao et al. 1985). Multilevel models for short range prediction of

flow pattern in the lower troposphere were developed and put in a experimental operational use (Sarker and Bedi, 1987). Krishnamurti (1990) carried out a study on monsoon prediction at different resolution with a global spectral model.

Mountain wave problem addressing properties of mountain waves over Indian region was studied by many authors (like Das, 1964; Sarker, 1965; Sarker et al., 1978; Dutta et al., 2002; Kumar et al., 2006). Das and Bedi (1976) studied the orographic effects by a primitive equation model. Abraham et al. (1996) studied the impact of different types of orography in the simulation of monsoon circulation. Roy Bhowmik (2003) showed that with the enhanced terrain height at the increased horizontal resolution, limited area primitive equation could provide improved heavy rainfall forecast along the Western Ghats of India.

Limited Area Model (LAM) was extensively used in Research and Development mode and for operational forecasting (Singh and Sugi, 1986; Bohra 1991; Prasad et al., 1997; Abraham et al., 1996; Mohanty et al., 1989; 1990). The model is used for general flow pattern, monsoon forecast and tropical cyclone track prediction. In 1988, NCMRWF was established and Global Spectral model T-80 was made operational for the medium range weather forecasting. Florida State University (USA) based LAM was made operational at IMD New Delhi during 1995 (Roy Bhowmik and Prasad, 2001) with initial and boundary conditions from NCMRWF T-80 outputs. Roy Bhowmik and Prasad (2008) attempted to improve LAM analysis and forecast using initial and boundary conditions using operational outputs of Global Forecast System of National Centre for Environmental Prediction, USA (NCEP GFS) instead of NCMRWF T-80 outputs.

A major problem in the use of Numerical Weather Prediction (NWP) model over tropics is the near absence of data over the large oceanic region. In view of the importance of these data in the tropical numerical weather prediction, continuous efforts are being made by NWP community to maximize utilization of various non-conventional data towards improving model initial condition and predictions in global and limited area models (Joshi et al., 1987, Krishnamurti et al., 1995; Bohra et al., 1998; Prasad, 2003; Das Gupta et al., 2003, Kar et al., 2003). Positive impact of these non-conventional observations from Indian satellite was demonstrated in the analysis and forecast of Limited Area Model (Roy Bhowmik et al., 2006; Hatwar et.al. 2005).

Convection plays a dominant role in the tropics, particularly for the development and maintenance of Indian summer monsoon. It affects the tropical circulation through the release of latent heat, vertical transport of heat moisture and momentum and through the interaction of clouds with radiation. Representation of precipitation process in NWP models is known as Cumulus Parameterization (CP). Widely used CP schemes in high-resolution models are: Anthes-Kuo, Arakawa – Schubert, Betts-Miller, Betts-Miller-Janjic (BMJ), Grell scheme (GR) and the Kain-Fritch scheme (KF).

Alapaty et al. (1994) carried out a comparative study on simulation of orographic and monsoon rainfall over Indian region with a limited area model using KF and Kuo schemes. They came to the conclusion that Kuo scheme performs well over the Indian region during monsoon season. Recently, Vaidya (2006) studied the performance of two convective parameterization schemes Kain-Fritsch (KF) and Bette-Miller-Janjic (BMJ) over Indian region using Atmospheric Regional Prediction System (ARPS) model. Rainfall prediction skill is subjectively assessed based on the amount and spatial distribution. They found that out of four cases, in all the cases BMJ scheme produced better results while in one case KF scheme performed better. Ratnam and Cox (2006) tested Grell and Kain-Fritch cumulus schemes using MM5 model for the simulations of the monsoon depression. They found that both the schemes are capable to simulate the large-scale features of monsoon depressions, but failed to capture the correct location of depressions at 24 hours and 48 hours forecast. Results of simulations are very different. Grell scheme tends to overestimate the rainfall. Kain-Fritch scheme could simulate the distribution of rainfall, but location of maximum rainfall was different. These studies conclude that the performance of NWP models depends heavily on initial inputs, model resolution and physics options, especially cumulus parameterizations scheme.

Das et al. (2002) demonstrated impact of various convection schemes in the medium range forecasts of Indian monsoon with NCMRWF T-80 model. Development work on the parameterization of boundary layer physics was carried-out by Basu et al. (1998, 2002). John and Begum (1997) studied impact of different radiation schemes on the simulation of onset of Indian summer monsoon.

The rainfall prediction skill of NWP models is still not adequate to address satisfactorily detailed aspects of Indian summer monsoon. This is because of large spatial and temporal variability of rainfall and some inherent limitations of NWP models. One conventional approach to improve these forecasts is the statistical

techniques such as, Model Output Statistics (MOS). Another potential approach as emerged in recent studies (Krishnamurti et al., 1999) is the Multi-model Ensemble (MME) technique. In the MME approach, forecasts made with different models are combined into a single forecast to partially take into account the uncertainties in the model formulation and initial conditions. This type of ensemble is different from the ensemble forecast of the single model that utilizes a set of different initial conditions where the different initializations constitute the member models (Brooks and Doswell, 1999). Very recently, studies are initiated in India to apply Multi-Model Ensemble (MME) technique (Roy Bhowmik and Durai, 2008; 2010; Roy Bhowmik et al., 2009a) for improving monsoon rainfall forecast in short to medium range time scale.

8.3. NWP Operational System

The NWP operational system is a complete suite of jobs on a high performance computer system. It is centred around the data assimilation scheme and the forecast model itself; other essential components are the database of decoded observations, quality control and pre-processing of observations, data base of post processed products, including graphical and digital outputs, dissemination, verification and archiving. All NWP models in operational use today solve a form of the primitive equations of motion, which being a statement of the basic law of physics, provide a description of atmospheric motion on a very wide range of scales. In addition to the main thermodynamic variables of wind and temperature, the equations also contain humidity as a variable allowing moist diabatic processes to be described. The equations are inherently complex, non-linear and have no analytical solutions, so numerical techniques are used.

Depending on the ranges and regions for which forecast is being made, there are different kinds of models, like a global model for a medium range forecast (4 to 10 days), a regional model (which is also called limited area model) for short range forecast (12 hours to 3 days) and a meso-scale model for a very short range forecast (upto 12 hours). Normally a global model provides boundary conditions for regional model and a regional model provides boundary values for meso-scale model. Again, basically two types of meso-scale prediction models can be identified one, the non-hydrostatic and the other, hydrostatic meso-scale prediction model.

Table 8.1 provides a summary of regional NWP models used in India Meteorological Department. Meteorological Department operationally runs four

regional models, Limited Area Model (LAM) at 75 km horizontal resolution, MM5 model at 45 km resolution, WRF at 27 and 9 km resolutions and Quasi-Lagrangian Model (QLM) for short-range prediction. QLM is used for cyclone track prediction. IMD also runs mesoscale model ARPS in the experimental mode for very short-range prediction.

Table 8.1: Regional models operational at IMD

Grid	LAM	MM5	WRF	ARPS
Horizontal resolution	75 km	45 km	27/9 km	9 km
Vertical Levels	16	23	51	38
Topography	US Navy	USGS	USGS	Terrain data 5 min
Dynamics				
Time integration	Semi-implicit	Semi-implicit	Semi-implicit	Semi implicit
Time Step	600 sec	90 s	90/30 s	30 sec
Vertical Differencing	Centered for all, except humidity which is forward	Arakawa's energy conserving scheme	Arakawa's energy conserving scheme	4 th order
Time Filtering		Rovert's method	Rovert's method	Asselin filter
Horizontal Diffusion	Second order	Second order	Second order over quasi-pressure surface, scale selective	----
Physics				
Convection	Modified Kuo	Grell	Kain Fritsch	Kain Fritsch
PBL	Louis, 1979	MRF (non local closure)	YSU Scheme	1.5 TKE
Cloud microphysics	Based on threshold relative humidity	Simple ice (Dudhia)	WSM 3-Class simple ice	Kain Fritsch warm rain microphysics
Radiation	Long wave (Harshavardan and Corsetti, 1984); short wave (Lacis and Hansen, 1974)	Simple cooling	RRTM (LW), Dudhia (SW)	NASA GSFC (simplified radiation)
Land surface processes	Businger et al. 1971	Five layer soil model	Thermal Diffusion	Noilhn and Planton (1989)

IMD also makes use of NWP products of global models prepared by some other operational NWP Centres like, NCMRWF T-254 model, U.K. (United Kingdom) Met Office, European Centre for Medium Range Weather Forecasting (ECMWF T-799), Japan Meteorological Agency (JMA T-899) and NCEP GFS. IMD receives online the NCMRWF and UKMO model outputs. Under a joint research collaborative project, IMD has been receiving high resolution model outputs (25 km horizontal resolution) of the deterministic model of ECMWF and JMA. NCEP GFS outputs are freely available in the Internet. The outputs of these models are first post- processed using GRIB decoder and then various graphics products are prepared for day to day forecasts.

Considering the need of farming sector, India Meteorological Department (IMD) has upgraded the Agro-Meteorological Advisory Service from agro climate zone to district level. As a major step, IMD started issuing district level weather forecasts from 1 June 2008 for meteorological parameters such as rainfall, maximum and minimum temperature, relative humidity, surface wind and cloud amount up to 5 days in quantitative terms (Roy Bhowmik et al., 2009a). These forecasts are generated through Multi-Model Ensemble (MME) system making use of model outputs of state of the art global models from the leading global NWP centres (NCMRWF, UKMO, ECMWF, JMA and NCEP). The strategy for MME involves two phases. In the first phase, known as training period, utilizes the direct model outputs and the corresponding observed fields to derive the statistics. The weight for each constituent model at each grid point is derived on the basis of correlation coefficients (CC) between the observed values (analysis fields) and forecast values based on the training period datasets. The second phase, called the forecast phase, utilizes the multimodel forecasts and aforementioned weights to obtain the final ensemble forecast (weighted mean).

The member models used in the MME for the district level forecasts during 2008 were: ECMWF, NCEP GFS and JMA. The MME based district level forecast system was further upgraded in 2009 where five models, namely, NCMRWF T-254, ECMWF, JMA, NCEP and UKMO were used as the ensemble member and model weights were recomputed utilizing the data of 2007 and 2008. As the model outputs available are at different resolutions, in the first step, model outputs of the constituent models are interpolated at the uniform grid resolution of 0.25^{o}X0.25^{o} lat/long. for the domain from lat. 0° to 40° N and long. 60° E to 100° E. In the second step, the weight for each model at each grid is determined objectively by computing the correlation co-efficient between the predicted rainfall and observed rainfall. Daily rainfall analysis (Roy Bhowmik and Das, 2007, Rajeevan et al., 2005) at the same resolution

(0.5^ox0.5^o) prepared from the use of rain gauge observations and satellite estimates (INSAT - Kalpana-1) is considered as the observed field. Grid-point weights are computed at the resolution of 0.25^ox0.25^o utilizing dataset of two seasons (1 June to 30 September, 2007 and 2008). The ensemble forecasts (day 1 to day 5 forecasts) are generated at the 0.25^ox0.25^o resolution. The MME forecast fields are then used to generate district level forecasts by taking average value of all grid points falling in a particular district. This resolution is able to cover 585 districts of the country.

8.3.1. Model analysis and forecast fields

A numerical data assimilation scheme provides the initial conditions required to start a numerical forecast, that is, a value for each model variable at the given analysis time at each point of the mode's grid in the horizontal and vertical. Post-processing of model initial fields at the standard pressure level for generation of graphical outputs are called model analysis field at the given observation time.

The operational LAM of IMD consists of real time processing of data received from Global Telecommunication System (GTS) and objective analysis by three dimensional multivariate optimum interpolation schemes. The input data used for the analysis consist of: Surface – SYNOP/SHIP; Upper air – TEMP/PILOT, SATOB; Aircraft reports – AIREP, AMDAR, and CODAR. These are extracted and decoded from the raw GTS data sets. All the data are quality controlled and packed into a special format for objective analysis. The methodology applied for objective analysis scheme is the statistical 3-dimensional multivariate Optimum Interpolation (OI) scheme (Dey and Morone, 1985). The scheme is based on applying correction to a first guess, the corrections being the weighted average of (observation-first guess) residuals at the observation locations. The variables analyzed in this scheme are geopotential (z), u and v components of wind and specific humidity. Temperature (T) field is derived from geopotential field hydrostatistically. Analysis is carried out on 12 sigma (pressure divided by surface pressure) surfaces 1.0, 0.9, 0.8, 0.7, 0.6, 0.5, 0.4, 0.3, 0.2, 0.1, 0.07, 0.05 in the vertical for a regional or limited horizontal domain covering lat. 30 ^{o} S to 60 ^{o} N and long. 0° to 150° E.

Global Data Assimilation System (GDAS) operational at NCMRWF is a six hourly intermittent three dimensional scheme. Main component of GDAS are (i) Data reception and quality control (ii) Data analysis and (iii) the NWP model. Meteorological observations of various observing platform from all over the globe is received at Regional Telecom Hub (RTH), New Delhi through Global Telecommunication System (GTS) and same is made available to NCMRWF. The

data is assimilated four times a day viz, 00, 06, 12, and 18 UTC every day. Data used in the operational assimilation system of NCMRWF are SYNOP/SHIP, BUOY,TEMP, PILOT, AMDAR/AIREP, SATOB from INSAT, METEOSAT at 0° to 60 ^{o} E GMS and GOES. The observations falling within –3 to +3 hours of respective hour of assimilation are being used in the corresponding hour assimilation. A six-hour prediction from the model, with a previous initial condition, valid for the current analysis time is used as the background field or the first guess field for the subsequent analysis. The analysis scheme used is the Spectral Statistical Interpolation (SSI) technique developed at NCEP (Parrish and Derber, 1992). The spectral model at NCMRWF is a T80/L18 spectral global model, the initial version of which is developed at NCEP (Kanamitsu, 1989). The medium range predictions are prepared by integrating the model for 7 days from 00 UTC of each day.

Post-processing of model forecast fields at the standard pressure level for generation of graphical outputs are called model forecast field at the given forecast time.

8.3.2. NWP Products

There are two kinds of NWP products namely; (a) Direct products and (b) Derived Products. NWP products such as wind, temperature, pressure, geopotential height and relative humidity and rainfall, which are directly available as model outputs are called direct products. The outputs such as vorticity, divergence, vertical wind shear, moisture flux, CAPE, CINE etc are called derived products, numerical expression of these derived products are given below:

$$Horizontal \quad - Divergence \quad : \quad \nabla . \mathbf{V} = \frac{\partial u}{\partial x} + \frac{\partial v}{\partial y}$$

$$\mathrm{Re}\, lative - Vorticity \ : \quad \nabla x \mathbf{V} = \frac{\partial v}{\partial x} - \frac{\partial u}{\partial y}$$

Lower tropospheric convergence (negative value of divergence) and vorticity provide information on the intensity of a low pressure system.

$$Vertical\, wind\, shear : \ u500 - u925$$

Precipitable Water Content (PWW in mm):

$$PPW = \frac{1}{g} \int_{1000\,hPa}^{300\,hPa} q\,dp$$

$$Integrated\ horizontal\ moisture\ flux\ divergence:$$

$$Moist\ flux = \frac{1}{g} \int_{\mathbf{1000hPa}}^{\mathbf{300hPa}} \nabla . q\mathbf{V}$$

Precipitable water content and moisture flux convergence (negative value of moisture flux divergence) are useful in quantitative precipitation forecasts. The rate of precipitation is directly related to moisture flux divergence.

$$Convective\ available\ potential\ energy (CAPE):$$

$$CAPE = -\int_{p_f}^{p_n} R_d (T_{vp} - T_{ve}) d \ln p$$

$$Convective\ inhibition\ (CIN):$$

$$CIN = -\int_{p_i}^{p_f} R_d (T_{vp} - T_{ve}) d \ln p$$

Vorticity advection:

$$\frac{\partial (\xi + f)}{\partial t} + \vec{V} \cdot \nabla (\xi + f) = -(\xi + f) \nabla \cdot \vec{V} \quad (Simplified\ vorticity\ equation)$$

positive vorticity advection is related to divergence and negative vorticity advection is related to convergence.

Vertical Motion:

$$where\ the\ vorticity\ advection\ term\ is$$

$$\vec{V} \cdot \nabla(\xi + f) = u \frac{\partial(\xi + f)}{\partial x} + v \frac{\partial(\xi + f)}{\partial y}$$

$$\frac{\partial u}{\partial x} + \frac{\partial v}{\partial y} + \frac{\partial \omega}{\partial p} = 0, \qquad \omega = \frac{dp}{dt}$$

$$\omega(p) = \omega(p_0) + (p_0 - p)\left\langle \frac{\partial u}{\partial x} + \frac{\partial v}{\partial y} \right\rangle$$

Where $\left\langle \frac{\partial u}{\partial x} + \frac{\partial v}{\partial y} \right\rangle$ = mean divergence between levels p_0 *and* p

$$p_0 = 1000\ hPa,\ and\ \omega(p_0)) = 0,\ then$$

$$\omega(p) = (p_0 - p) < \frac{\partial u}{\partial x} + \frac{\partial v}{\partial y} >$$

If div +ve, $\omega(p)$ $ve \Rightarrow$ sinking motion, fair weather

If div -ve, $\omega(p)$ $ve \Rightarrow$ rising motion, weather development

Relative topography (thickness)

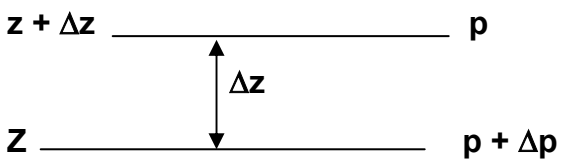

Thickness field between any two isobaric levels can be computed using analysed height fields. It is useful in the study of development processes.

8.4. Monsoon Forecasting – the principal rain producing weather systems

Short-range weather forecasting consists of following steps:

- Identification of weather producing system
- Assessment of intensity, past history and distribution of associated realized rainfall.
- Forecasting movement and intensity of the system
- Forecasting the area and duration of rainfall
- Forecasting intensity of rainfall

Model Analysis fields are used for*:*

- *Identification of weather producing system*
  Mean sea level pressure, lower tropospheric winds, and upper tropospheric winds
- *Assessment of intensity*
  Derived products and associated realized rainfall
- *Deriving past history*
  Time series/ past analysis fields

Model forecast Outputs are used to:

- *Forecast movement, intensity of the system, spatial and temporal characteristics of associated rainfall*

The forecast procedure involves: (i) To make qquantitative assessment of synoptic situations based of direct and derived products of model analysis (such as: 850 hPa wind analysis, vorticity and divergent field, omega field and rainfall analysis), (ii) To make prognostic assessment of prevailing synoptic condition and associated rainfall for forecast up to 3 days, using NWP products of Global/ Regional and mesoscale models, (iii) To use NWP Products of Global models to assess new development and outlook for 3-5 days and (iv) Subjective value addition to numerical guidance based on the forecasters experience and knowledge of the synoptic, topography, climatology and performance statistics of operational NWP models.

Some of the typical case studies of monsoon weather system are presented here.

8.4.1. Monsoon Depression

Monsoon depression is the main rain producing system, which usually forms in the North Bay of Bengal and subsequently moves northwestwards across the country-giving heavy to very heavy rainfall during its passage. West coast of India is another area where heavy rainfall occurs in association with strengthening of low-level westerly winds during the formation of low-pressure system over the Bay of Bengal. The important forecast features of monsoon depression are: genesis, intensification process, track and associated rainfall. Currently most of the operational regional models are capable of predicting initial formation of a low-pressure system as well as the intensification process 3 days in advance, and global models 5 days in advance. But there is a problem in track prediction. Due to mismatch in the track prediction, error continues in the forecast rainfall distribution. Forecaster needs to apply his own experience and wisdom for judicious use of NWP products, particularly for the rainfall forecasts. Moreover, in association with monsoon depression, rainfall of order 40 to 50 cm is a very common weather event. But all NWP models have certain limitations to predict such high amount of rainfall. In this case, knowledge on the model's performance statistics is very essential. Fig.8.1 illustrates distribution of rainfall in the daily rainfall analysis during the passage of a monsoon depression of 14-16 June 2001 (Roy Bhowmik et al, 2005). Gridded rainfall following objective analysis of rainfall observations is called rainfall analysis (Rajeevan et al, 2005; Roy Bhowmik and Das, 2007). Fig.8.2 presents an inter-comparison distribution of rainfall and corresponding precipitable water content (based on model analysis) in association with a monsoon depression of 19 July 2005 (Durai et al., 2007). This information is useful inputs to an operational forecaster.

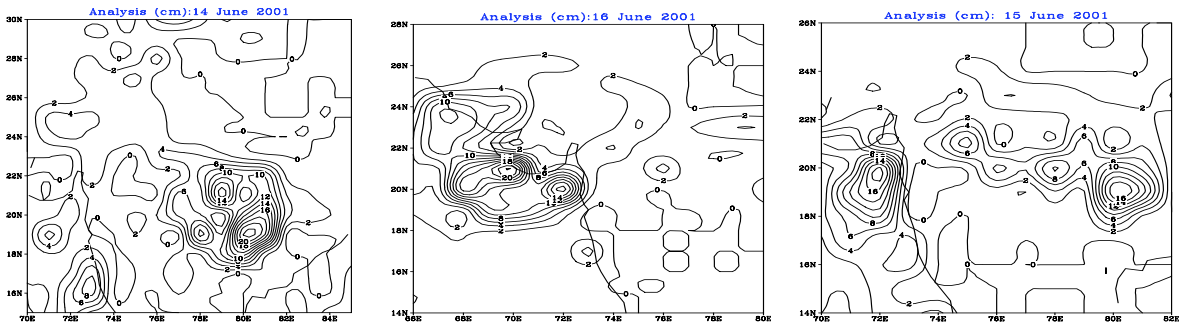

Fig. 8.1 : Rainfall Analysis during the passage of a monsoon depression during 14-16 June 2001

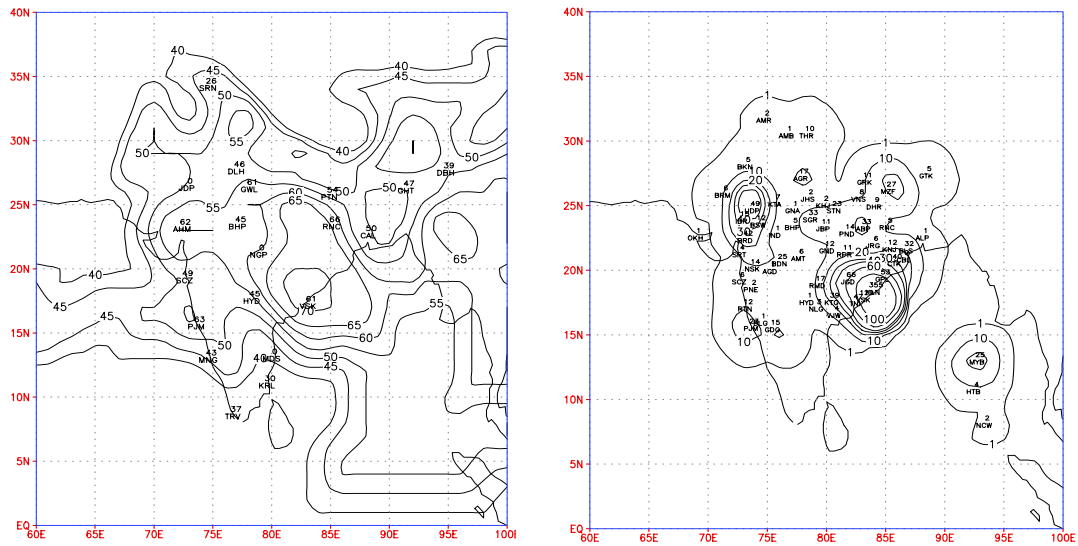

Fig. 8.2 : PWC analysis (mm) with super-imposed computed pwc(mm) from RS observations and corresponding rainfall analysis (mm) with rainfall observations (mm) for 19 July 2005.

Case-1: Deep Depression over Bay of Bengal during 15-17 June 2008.

During 2008, a low pressure area formed over North Bay of Bengal at 03 UTC of 15 June, concentrated into a depression at 03 UTC of 16 June 2008. It continued to move in a northwesterly direction and lay centred at 03 UTC of 17 over Gangetic West Bengal and adjoining Bangladesh. Subsequently, it moved slightly west-northwestwards and lay centred at 03 UTC of 18 over Jharkhand.

Spatial pattern of 850 hPa wind field, 700 hPa relative vorticity, 700 hPa omega field and moisture flux divergence based on LAM analysis of 00 UTC of 15 June 2008, depicting the presence of low pressure area over northwest Bay of Bengal with a trough extending northwest wards are illustrated in Fig. 8.3.

The observed and forecast track by ECMWF, NCMRWF, UKMO and MM5 based on 00 UTC of 16 June along with day-2 forecast of ECMWF, MM5 mean sea level pressure, NCMRWF 850 hPa wind plot valid for 00 UTC of 17 June are given in Fig. 8.4. In this case, all the four models are able to predict the movement of the system northwestwards. However the MM5 initial position was 2-3 degrees south of

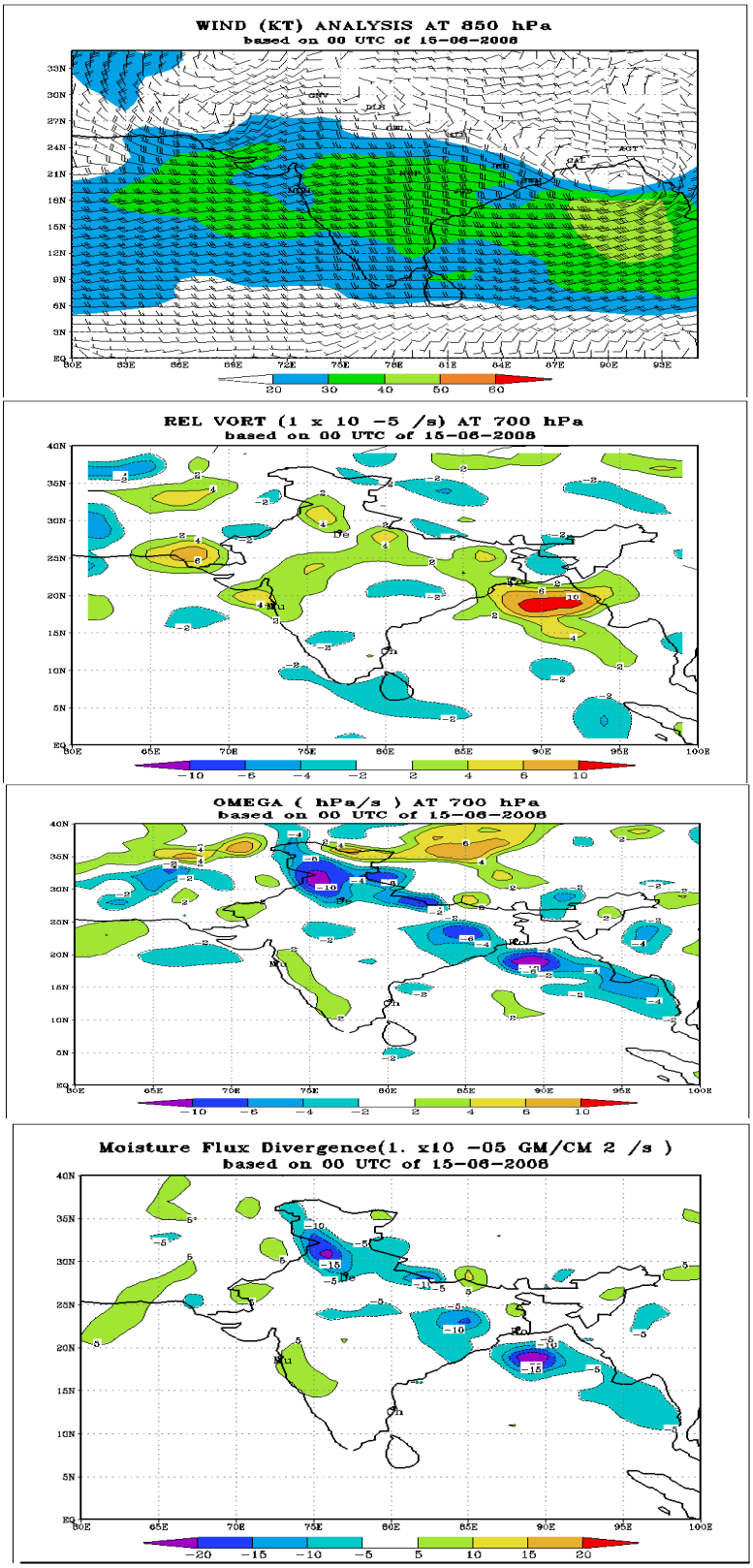

Fig.8.3 : Distribution of 850 hPa wind field, 700 hPa relative vorticity, 700 hPa omega field and moisture flux divergence based on LAM analysis of 00 UTC of 15 June 2008, showing presence of low pressure area over northwest Bay with a trough extending northwest wards.

the observed position and its track forecast was more northerly than the observed northwest track. The MM5 day-2 forecast based on 00 UTC of 15 June valid for 17 June showed the minimum sea level pressure as 994 hPa, where as observed was 990 hPa. The ECMWF was able to predict the track close to the observed with initial error of 50 km southeast of the observed position. The minimum sea level pressure has shown 994 hPa with two closed isobars. The NCMRWF T-254 and UKMO are also predicted the northwest movement of the system. In association of this system, widespread rainfall with scattered heavy to very heavy falls occurred over Gangetic West Bengal, north Orissa and Jharkhand during 16-18 June. The model predicted day-2 rainfall based on 15, 16 June valid for 17, 18 June is given in Fig. 8.5 & 8.6. On both 17 and 18 June, all the models could predict the heavy rainfall over Gangetic west Bengal, north Orissa, Jharkhand and east Utter Pradesh. However MM5 could not predict the heavy rainfall over north Orissa due to the error in the predicted track of the system. Due to this, the heavy rainfall belt also shifted to the wrong place (to the east against the observed location). It is noteworthy that all the models could realistically capture scanty rainfall belt over peninsular India and along west coast.

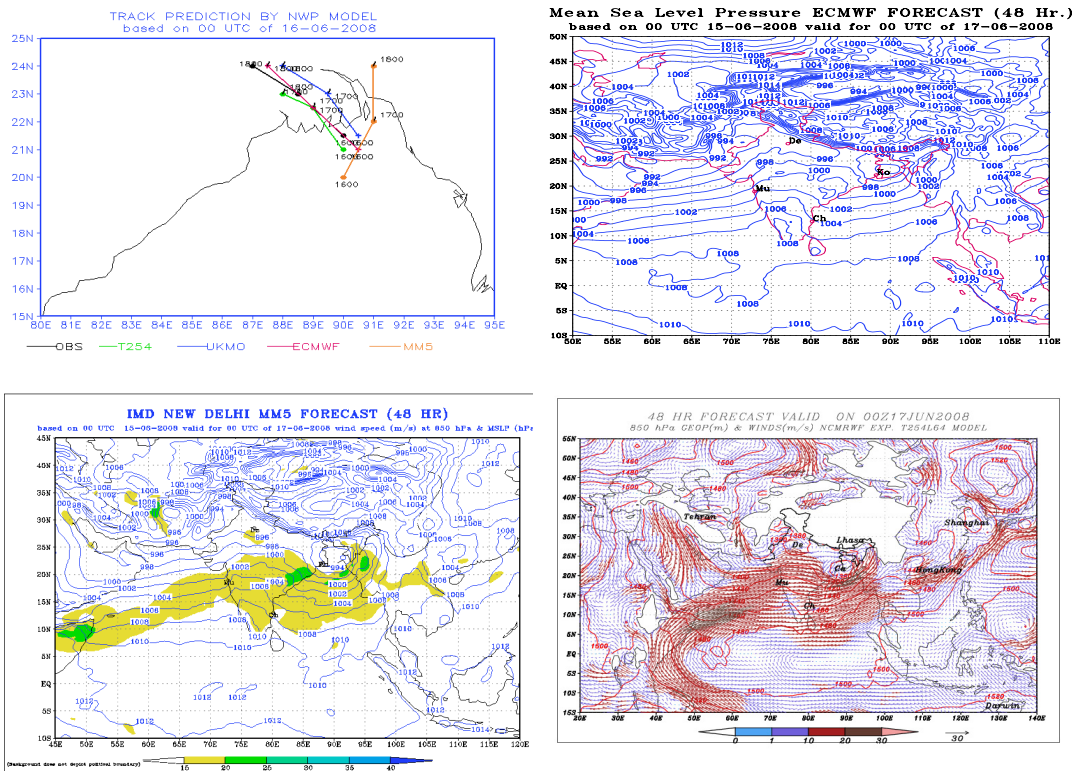

Fig.8.4 : Depression 16-18 June 2008 observed and forecast track by ECMWF, NCMRWF T-254, UKMO and MM5 based on 16 June valid for 18 June and day-2 forecast ECMWF, MM5 mean sea level pressure (hPa), NCMRWF 850 hPa wind plots.

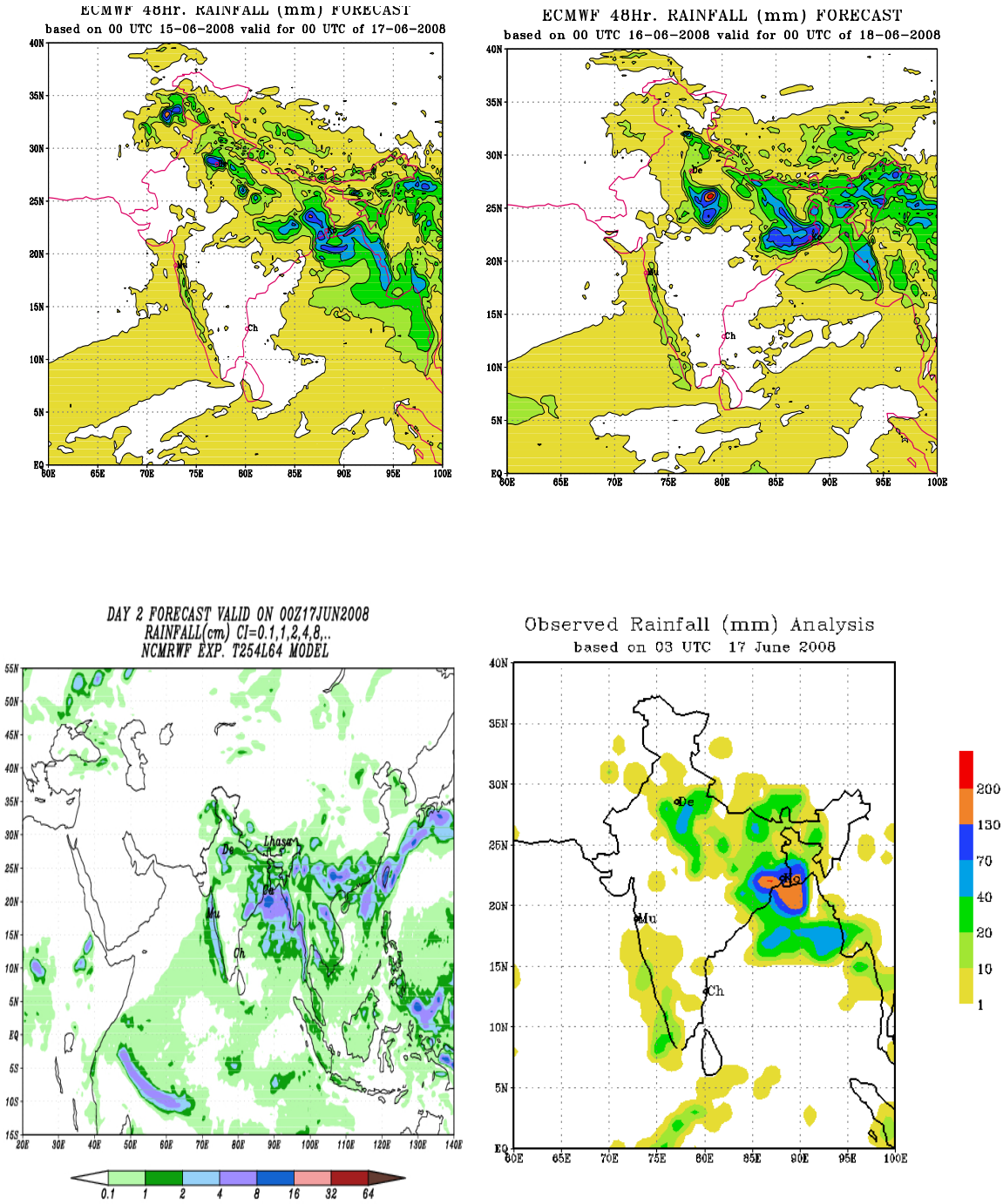

Fig.8.5 : Day-2 rainfall forecast by ECMWF, MM5, NCMRWF and observed grid point rainfall (mm) valid for 17 June 2008.

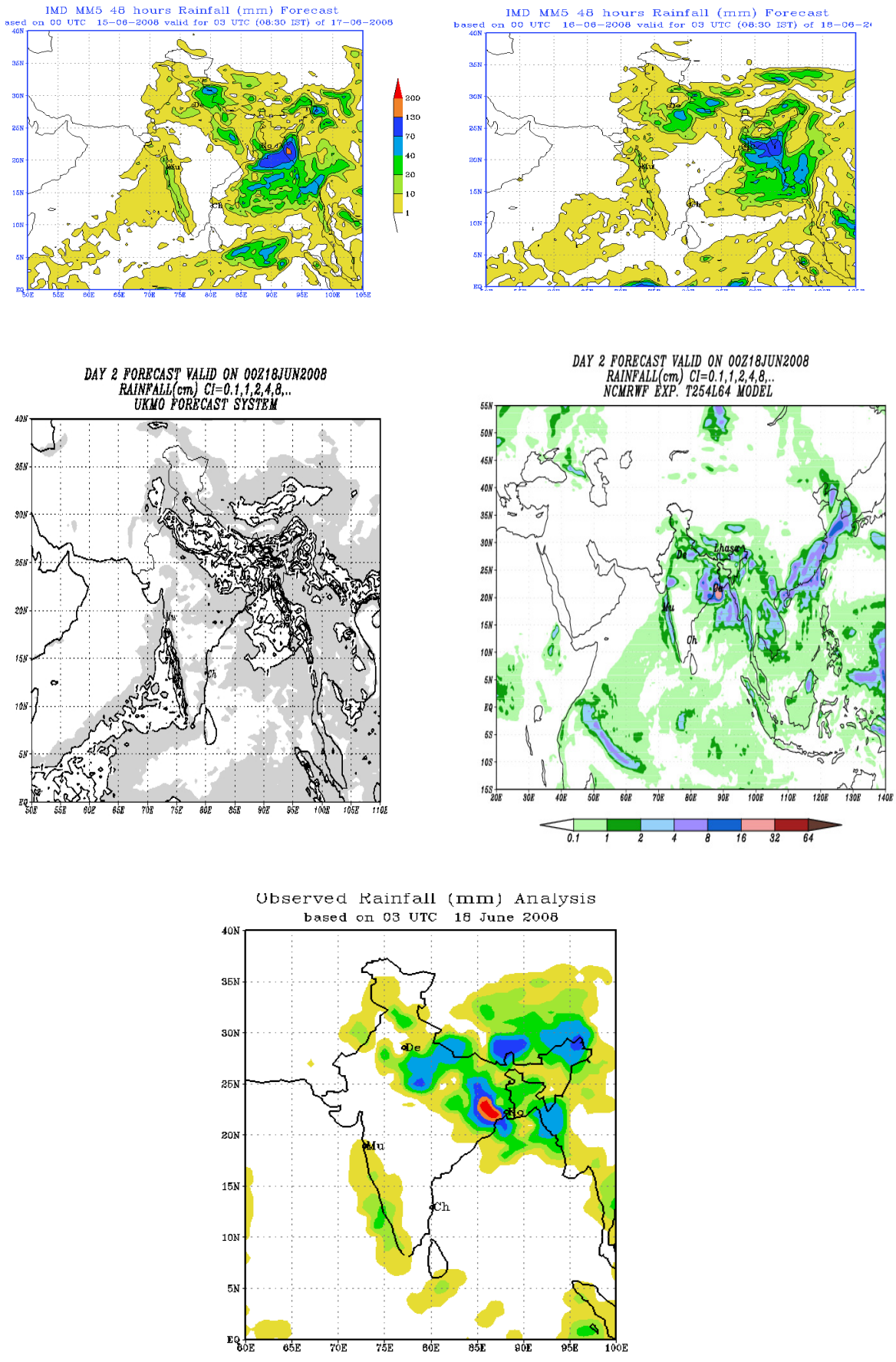

Fig.8.6 : Day-2 rainfall forecast by ECMWF, MM5, UKMO, NCMRWF and observed grid point rainfall (mm) valid for 18 June 2008.

Case-2: Deep Depression over Bay of Bengal 15-19 September 2008

This system formed over the northwest Bay of Bengal, crossed Orissa coast near Chandbali and moved across north Orissa, north Chhattisgarh, northeast Madhya Pradesh and central Uttar Pradesh. Fig. 8.7 presents observed and forecast track by ECMWF, NCMRWF, UKMO and MM5 based on 00 UTC of 15 and

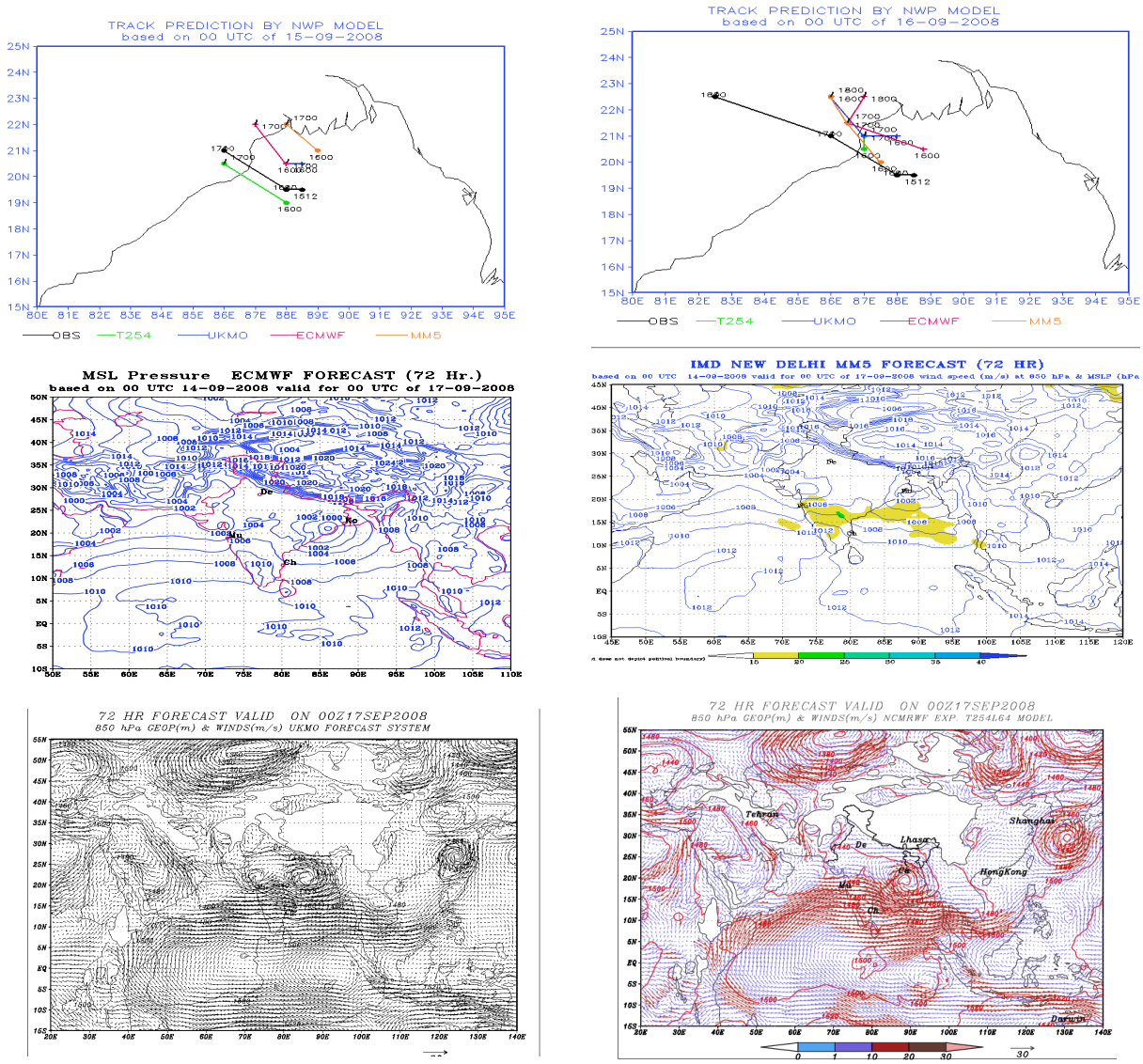

Fig.8.7 : Deep Depression 15-19 September 2008: observed and forecast track by ECMWF, NCMRWF T-254, UKMO and MM5 based on 15, 16 September along with day-3 forecast ECMWF, MM5 mean sea level pressure (hPa), UKMO, NCMRWF T-254 850 hPa wind plots valid for 17 September 2008.

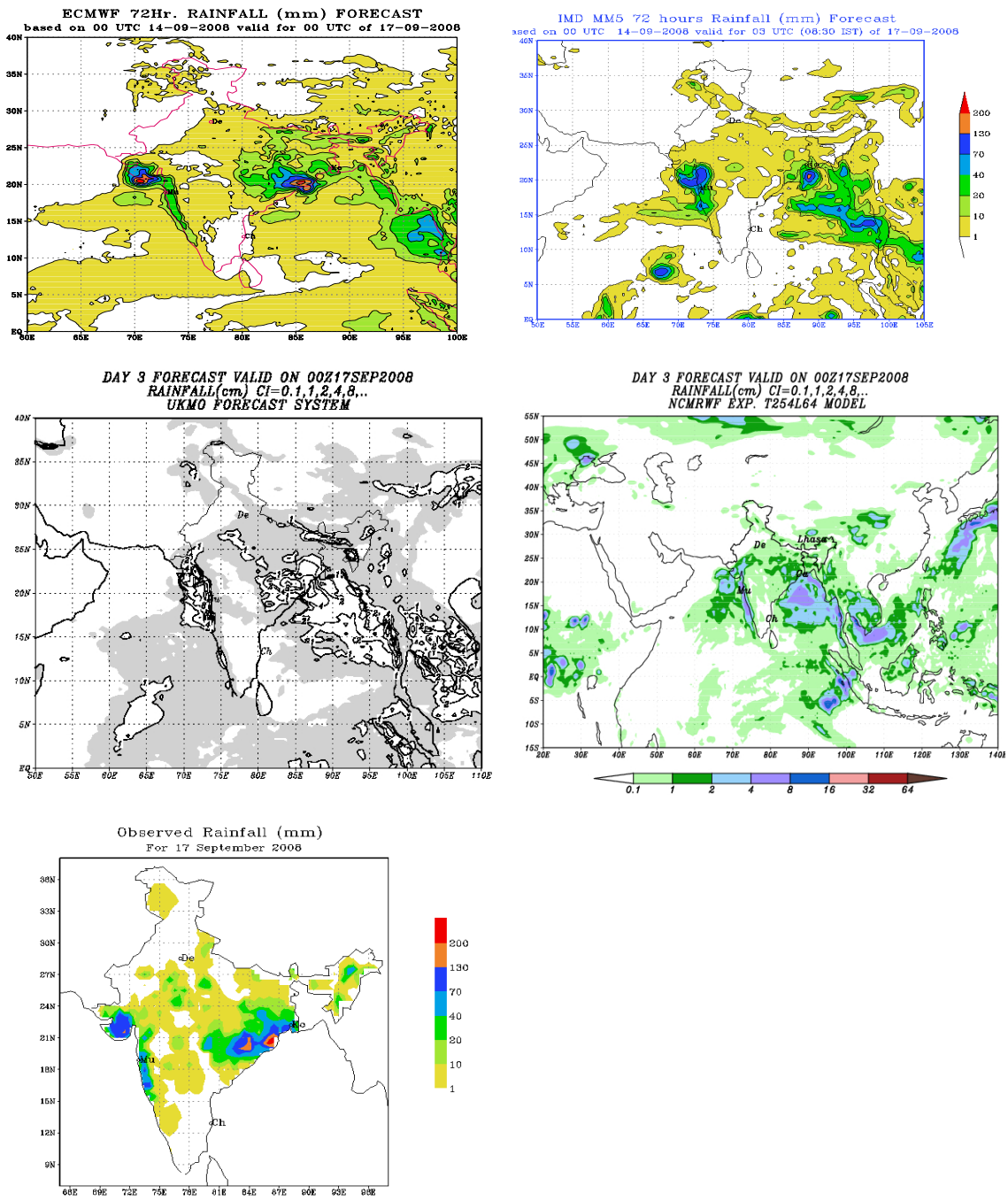

Fig.8.8 : Day-3 rainfall forecast by ECMWF, MM5, NCMRWF and observed grid point rainfall (mm) valid for 17 September 2008.

16 September along with day-3 forecasts of ECMWF and MM5 mean sea level pressure; UKMO and NCMRWF 850 hPa wind plots valid for 00 UTC of 17 September. In this case, all the four models could correctly predict the northwestward movement of the system. However, based on 15 September initial conditions, the forecast showed displacement to the northeast. Based on 16 September the initial position, model predicted day-3 rainfall valid for 17 September

is given in Fig.8.8. In this case, all the models could correctly predict the enhanced rainfall activity over Gujarat, west coast and Orissa. However, MM5 model day-1 forecast could capture heavy rainfall over Orissa and Chhattisgarh (figures not shown), but in day-2 and day- 3 forecasts (figures not shown) the rainfall belt shifted to northeastwards. This is due to the error in the predicted track of the system. Errors are less compared to 15 September, except for ECMWF, which showed northeastward 2-3 degree deviation. The day-3 forecast mslp/wind fields by these models, based on the initial condition of 14 September could predict initial formation of the system. This system caused heavy to extremely heavy rainfall over Orissa and Chhattisgarh leading to severe flood over Orissa. This system subsequently interacted with mid-latitude westerly systems and caused good rainfall over northwest India and led to flood over Haryana and Himachal Pradesh.

Performance of WRF model for this system for 850 hPa wind fields and rainfall fields are illustrated in Fig 8.9-8.14. Inter-comparison of forecasts with the corresponding analysis fields shows that the model could clearly capture the initial formation of the low pressure system over the Bay of Bengal 72 hours in advance. But location of the system was found displaced to the east and the intensity was over estimated. However, 48 hours numerical guidance to predict location of the system and the associated rainfall pattern was very good.

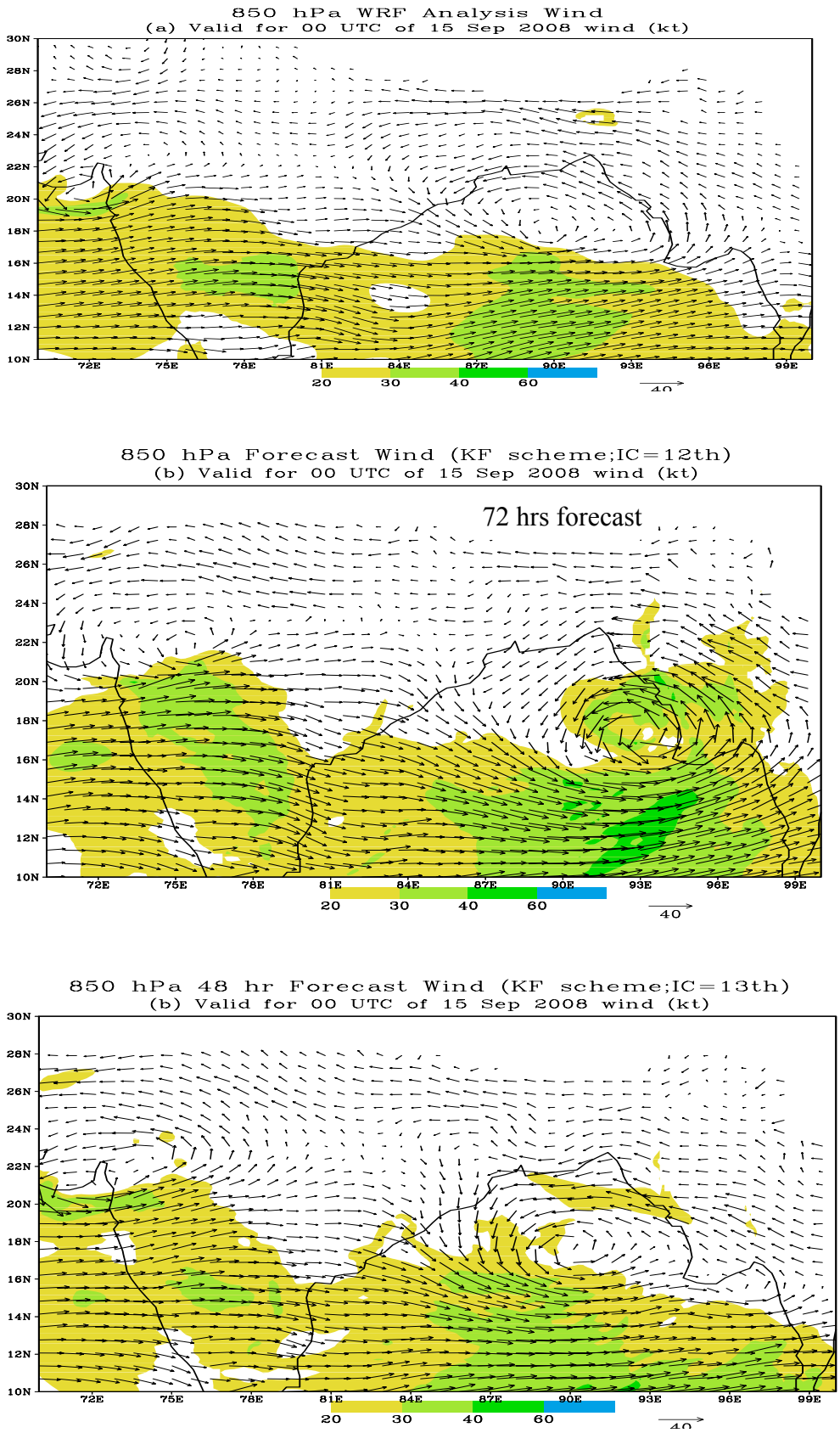

Fig. 8.9 : An inter-comparison of model analysis of 15 September with corresponding 72 hours and 48 hours forecast field of 850 hPa winds

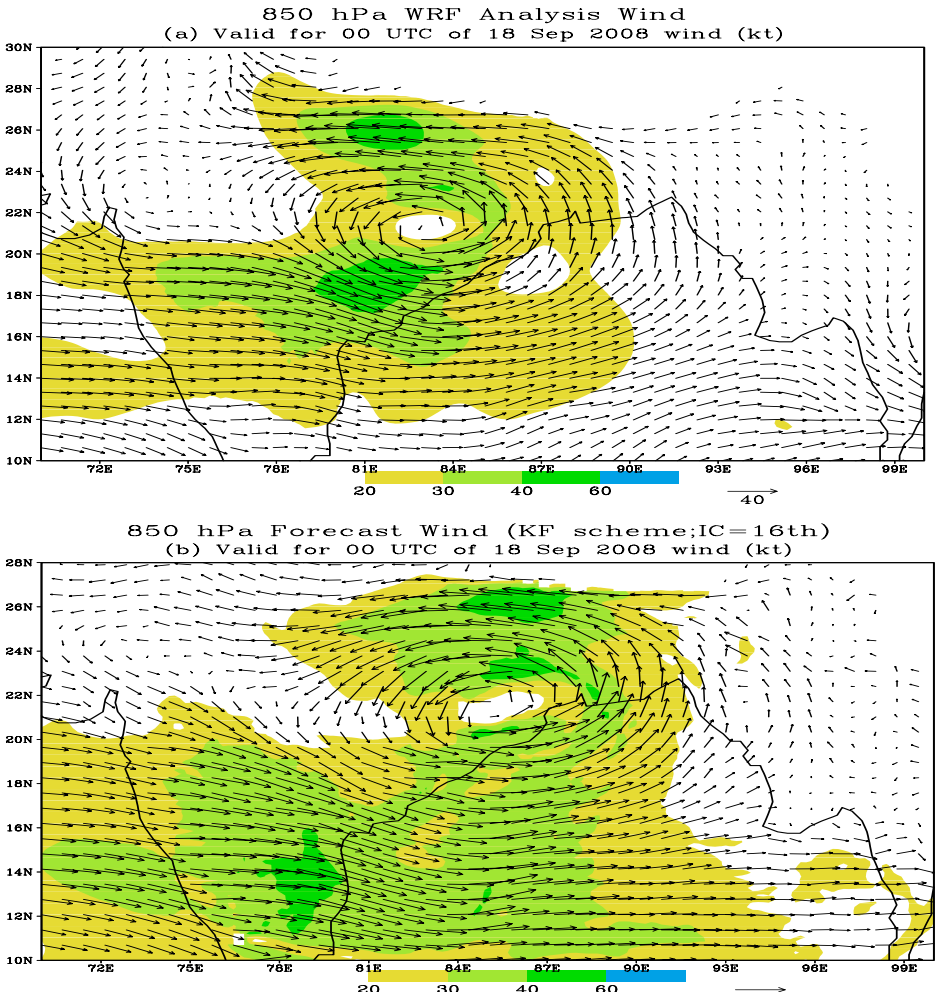

Fig.8.10 : An inter-comparison of model analysis of 18 September with corresponding 48 hours forecast field of 850 hPa winds

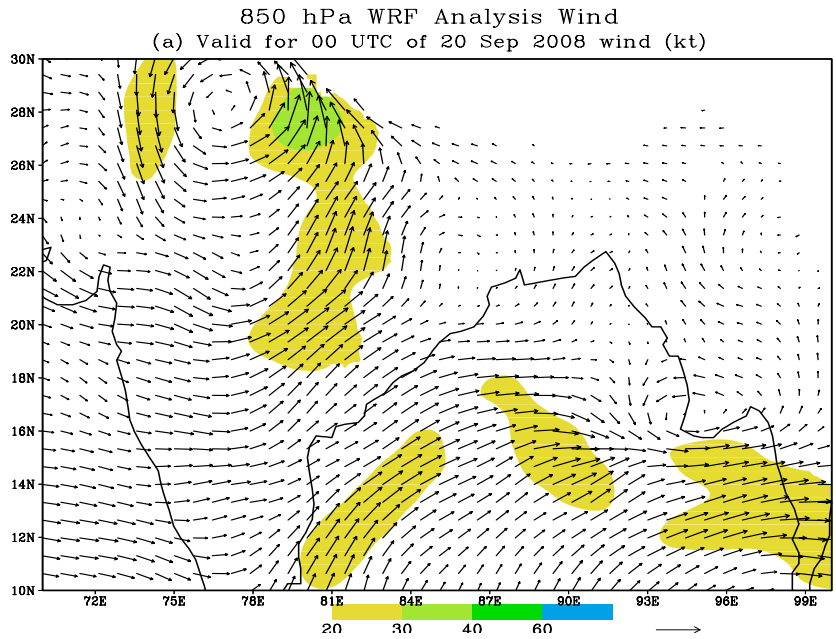

Fig.8.11 : An inter-comparison of model analysis of 20 September with corresponding 48 hours forecast field of 850 hPa winds

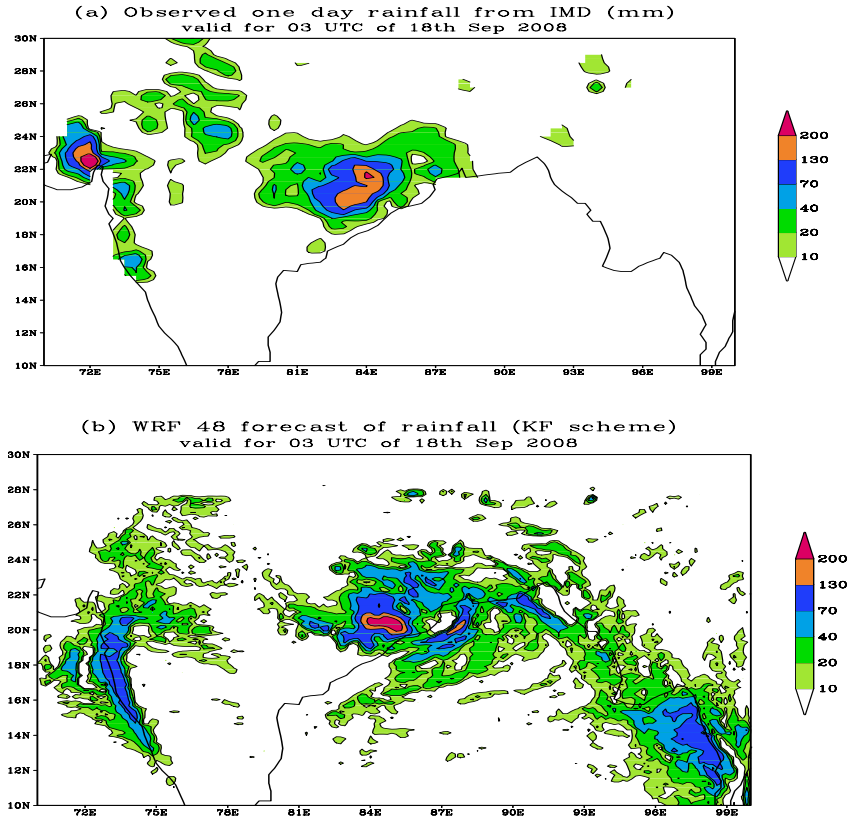

Fig.8.12 : An inter-comparison of rainfall analysis of 18 September with corresponding 48 hours rainfall forecast

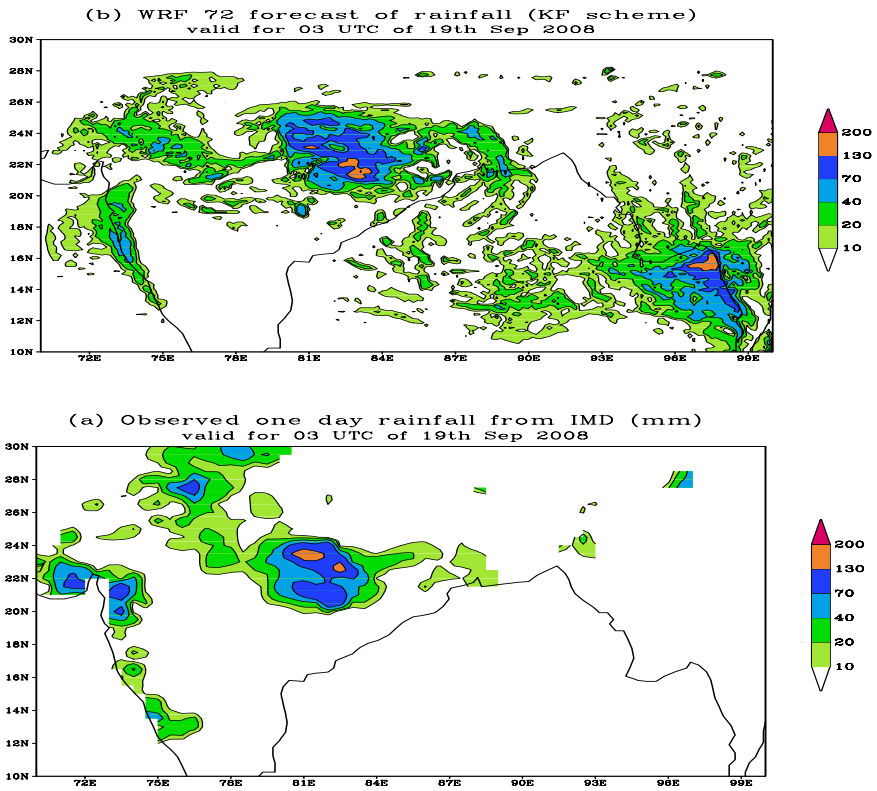

Fig. 8.13 : An inter-comparison of rainfall analysis of 20 September with Corresponding 72 hours rainfall forecast

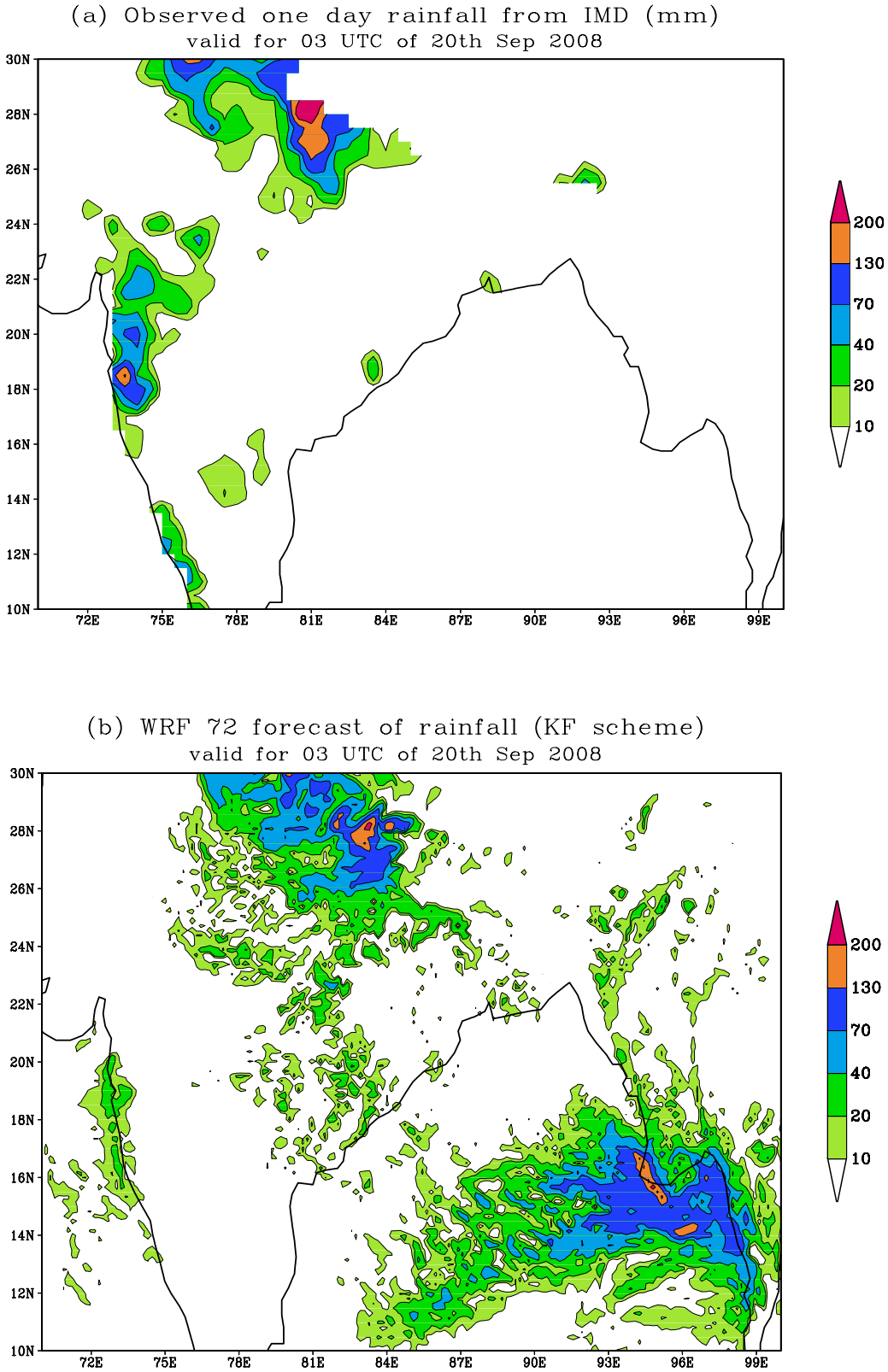

Fig.8.14 : An inter-comparison of rainfall analysis of 20 September with Corresponding 72 hours rainfall forecast

8.4.2. Monsoon Trough

The summer monsoon rainfall in the Indian subcontinent is known to be characterized by active and break/weak spells on a time scale of about two weeks; these active/break spells are the result of fluctuations of the seasonal monsoon trough. Monsoon trough is an extended trough of low pressure, which runs across Gangetic Plains of north India with its western end a chord to the seasonal heat low over northwest India, and Pakistan and eastern end emerges into the head Bay of Bengal. In the mean, the axis of this trough runs from Ganga Nagar in Rajastan to Kolkata via Allahabad. The axis of monsoon trough slopes southward with height and its position at 5 km above mean sea level runs along nearly 20 ^{o}N over the Indian longitudes. The maxima of rainfall lies on the south of its axis.

The monsoon trough is subjected to north and south, meandering and this help in distributing rainfall over the whole Gangetic Plains. These northward and southward movements of monsoon trough axis are generally indicative of the large-scale active and weak monsoon conditions. The position of monsoon trough axis is an important factor in the monsoon activity over the sub continent. When the trough stays in the normal position, this is considered to be an active monsoon situation. The rainfall is well distributed over the northern plains and central parts of the country. When the trough dips into the head Bay, conditions become favourable for the formation of a depression/low in the Bay of Bengal, which eventually moves northwest ward across the main land and produces good rainfall activity. On the other hand, sometimes the axis of monsoon trough shifts northward to the foothills of Himalayas. The northward shift may take place either in its entire stretch from west to east or only in one part. When the trough in its whole stretch shifts northward, the rainfall over the central and northern parts of the country is drastically reduced, but increases along the foot hills of Himalayas. This situation has come to known as a “Break” monsoon condition in Indian Meteorological parlance, so called because of large scale reduction in rainfall over major parts of the country. The break monsoon condition usually lasts for a few days. Prolonged breaks sometimes occur leading to dry condition over the large parts of the country. The monsoon trough often gets completely effaced in the mean sea level and low level wind fields. The trough again shifts to its normal position with the formation of a fresh disturbance in the Bay of Bengal.

During 2008, with the advance of monsoon over the entire country, monsoon trough got established on 10 July. It remained at its near normal position up to 12 July, started shifting northwards from 13 July.

The spatial pattern of mean sea level pressure, 700 hPa wind fields with super imposed relative vorticity, precipitable water content and corresponding rainfall analysis in association with the monsoon trough based on LAM Analysis of 00 UTC 13 July 2008 is illustrated in Fig. 8.15 .

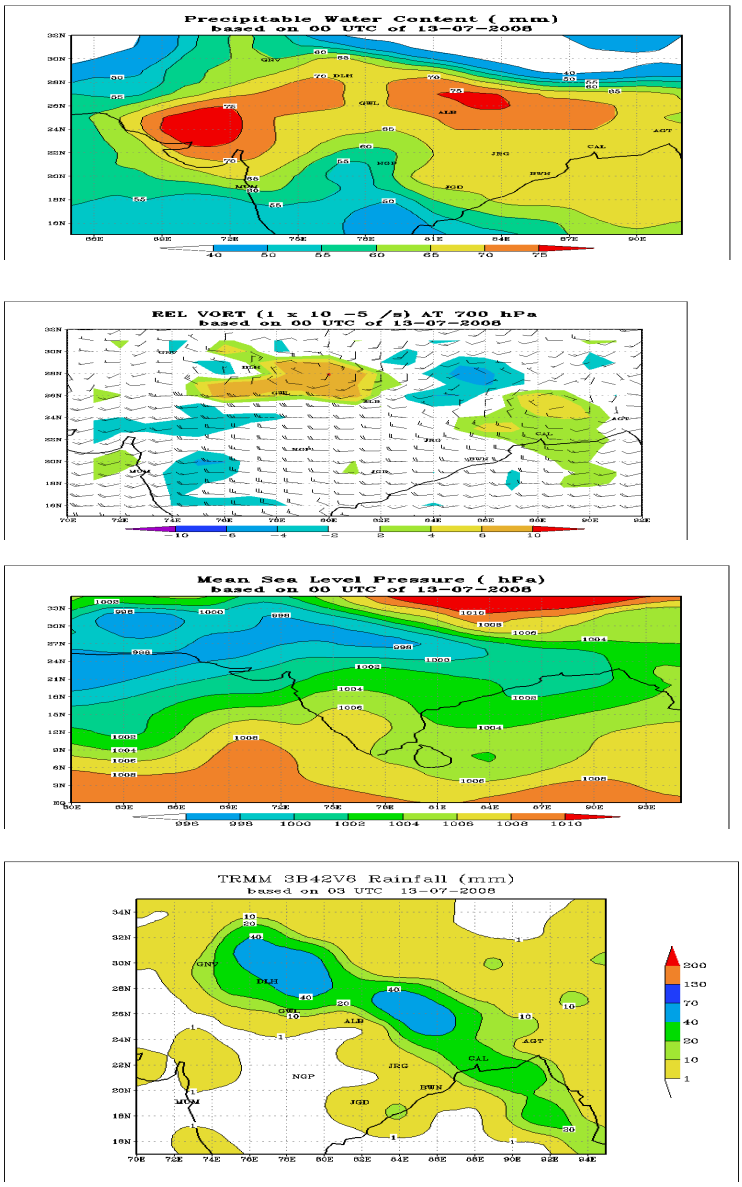

Fig.8.15 : LAM Analysis of 00 UTC 13 July 2008 showing mean sea level pressure, 700 hPa wind super imposed relative vorticity, precipitable water content and corresponding rainfall analysis in association with a monsoon trough

8.4.3. Offshore Trough

Along the west coast of India heavy rainfall often occurs in association with offshore trough. On 8 July 2001, an offshore trough on sea level chart lay off west coast. The corresponding rainfall distribution based on objective analysis of rainfall is presented in Fig. 8.16.

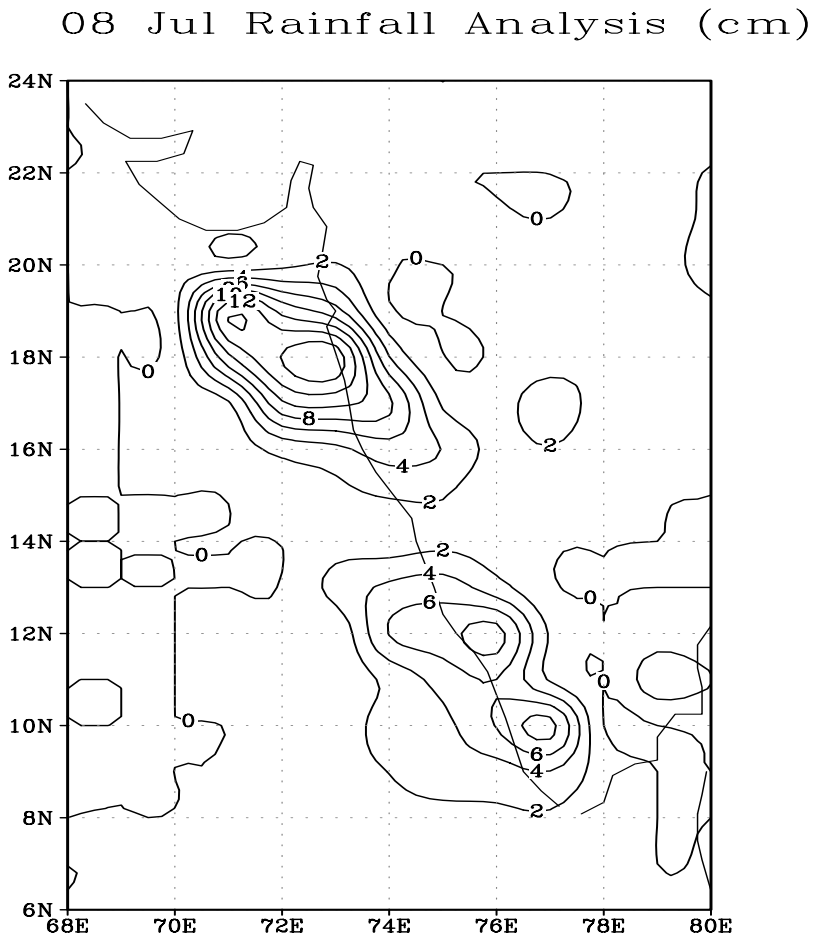

Fig. 8.16 : Distribution of rainfall in association with offshore trough

On 9 June 2008, an offshore trough lay along west coast of India. Fig. 8.17 and 8.18 respectively illustrate corresponding mean sea level pressure field based on ECMWF analysis and ECMWF day-3 rainfall forecast.

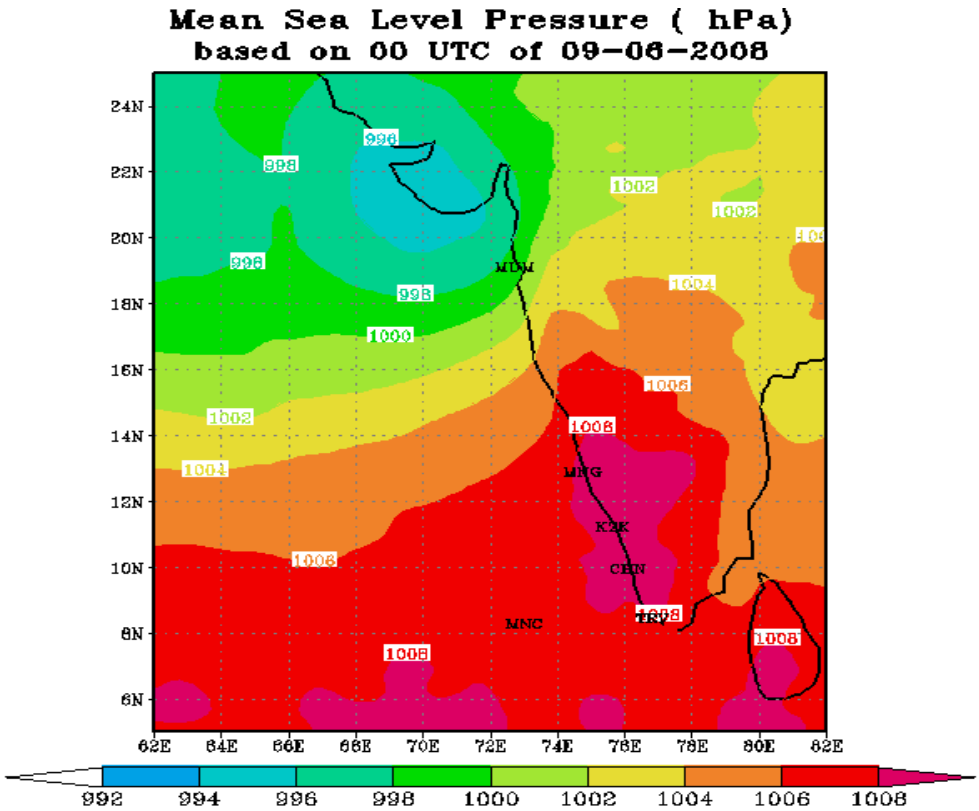

Fig.8.17 : Mean sea level pressure of 9 June based on ECMWF analysis

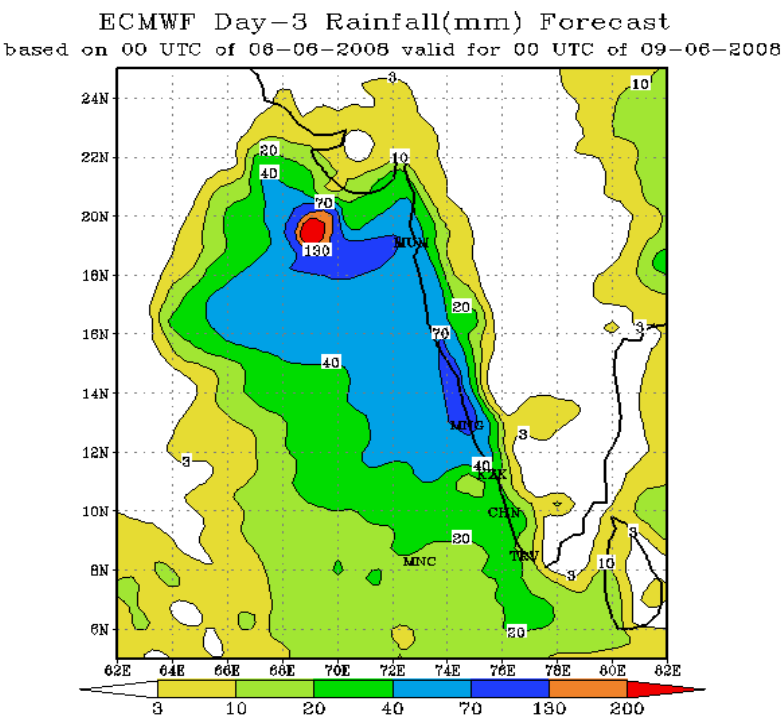

Fig.8.18 : Day-3 rainfall forecast by ECMWF model.

8.5. Forecast skill and limitations of NWP Models

Before one goes for further improvement of a numerical model, an investigation on the performance statistics of the model on temporal and spatial scale is a prerequisite. Several studies (Kanamitsu, 1985; Laurent et al.,1989; Kamga et al.; 2000) revealed that 50 to 80% of the total errors in the ECMWF global model were due the systematic errors of the model. Realizing the importance of performance statistics of operational NWP models, performance statistics of many NWP models have been documented by various authors (Junkar et al., 1989; Mc Bride and Ebert, 2000; Colle et al 2000; Basu, 2003; 2005). Performance statistics of LAM of IMD over Indian region are reported in various studies (Roy Bhowmik and Prasad, 2001; Roy Bhowmik, 2004; Roy Bhowmik et al., 2007). These studies showed that though the model (LAM) is capable to predict important features of south west monsoon such as mean sea level pressure distribution with a heat low over northwest India, monsoon trough separating easterlies to the north and westerlies to the south and its equator ward tilt with height, but rainfall prediction skill continues to suffer. These studies demonstrate that the performance of the model in predicting precipitation varies with month, geographical location and by synoptic system. The model in general is able to reproduce spatial climatlogical pattern of monsoon system but biases of the model fluctuates significantly. In this section performance statistics of various operational NWP models are presented based on forecasts during summer monsoon 2008.

8.5.1. Track forecast errors of monsoon depression

Forecast track verification of monsoon depressions during summer monsoon 2008 has been carried out by computing the direct position error (DPE) – the geographical distance between the predicted location of the system and the verifying position at valid hour. The results are presented in Table 8.2 for the period ranges from initial analysis to 48h for each individual day of all the three cases considered. It is seen that the mean error in the initial analysis is about 110 km, 24 hours forecast is about 165 km, which increases to about 245 km for 48h forecast. The MM5 has shown large errors when the initial state of the system is a weak low pressure and when the system was well defined the track errors reduced considerably. In the case of global models ECMWF, UKMO the initial errors are relatively less. However, the initial errors of 100-150 km are observed even when the system was in a depression stage.

Table 8.2: Direct Position Errors (KM)

Based on 16 June 2008/00 UTC (DPE in kms)

Model	Anal	24hFcst	48hFcst
ECMWF	75	80	65
MM5	166	283	440
UKMO	55	110	120
T254	55	78	157

8 August 2008/00 UTC

ECMWF	---	124	130
MM5	---	283	503
UKMO	---	277	165
T254	---	392	330

09 August 2008/00 UTC

ECMWF	124	175	---
MM5	78	235	---
UKMO	110	60	---
T254	270	290	---

15 September 2008/00 UTC

ECMWF	---	110	157
MM5	---	200	248
UKMO	---	124	230
T254	---	55	75

16 September 2008/00 UTC

ECMWF	110	124	180
MM5	80	90	370
UKMO	166	110	380
T254	55	110	360

8.5.2. Rainfall forecast errors - *Categorical statistics and time series*

ECMWF (T 799) is rated as one of the best models for the forecasts in short and medium range time scales (Roy Bhowmik et al., 2009b). Bias scores of ECMWF rainfall forecast (based on forecasts for the period from 1 June to 30 September 2008) at the rain threshold of 2.5 mm rain, 5 mm rain, 10 mm rain and 15 mm rain for different forecast ranges are shown in Fig. 8.19. The bias score starts from 1.5 and becomes 0.83 at 15 mm rainfall threshold. The bias score becomes perfect (score 1.0) at 10 mm rainfall threshold. For the rain threshold less than 10 mm rainfall, bias score indicates over estimation and for rain threshold more than 10 mm it becomes under-estimation. The results indicate that for the less rainfall amount (less than 1 cm), in general, NWP models over-predict where as for the higher rainfall amount they under estimate. Result of domain (country) mean spatial correlation coefficient (CC) is presented in Fig. 8.20.

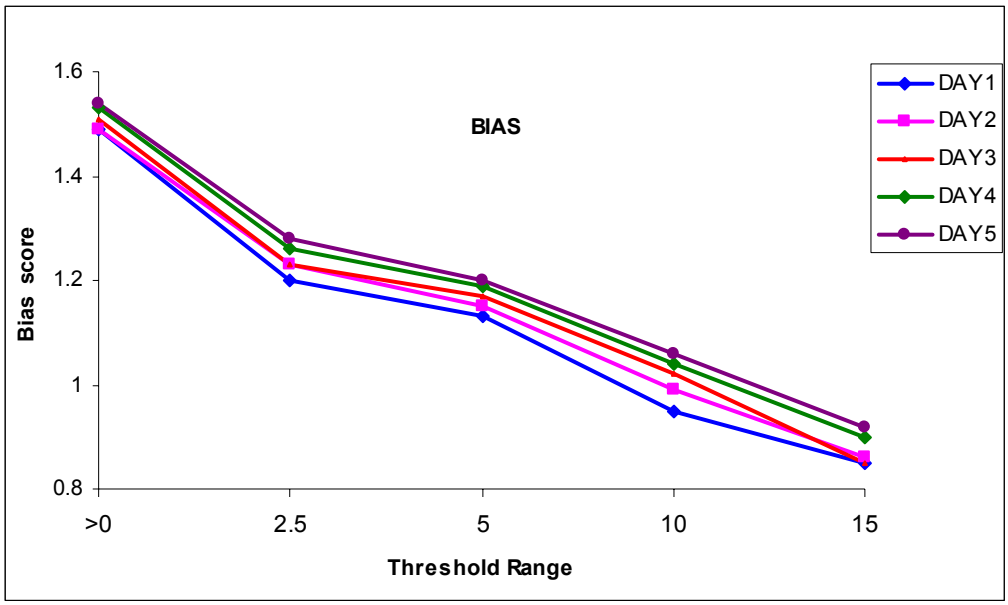

Fig. 8.19 : Inter-comparison of Bias score of day1-day5 rainfall forecasts by ECMWF model at different thresholds for the period from 1 June to 30 September 2008

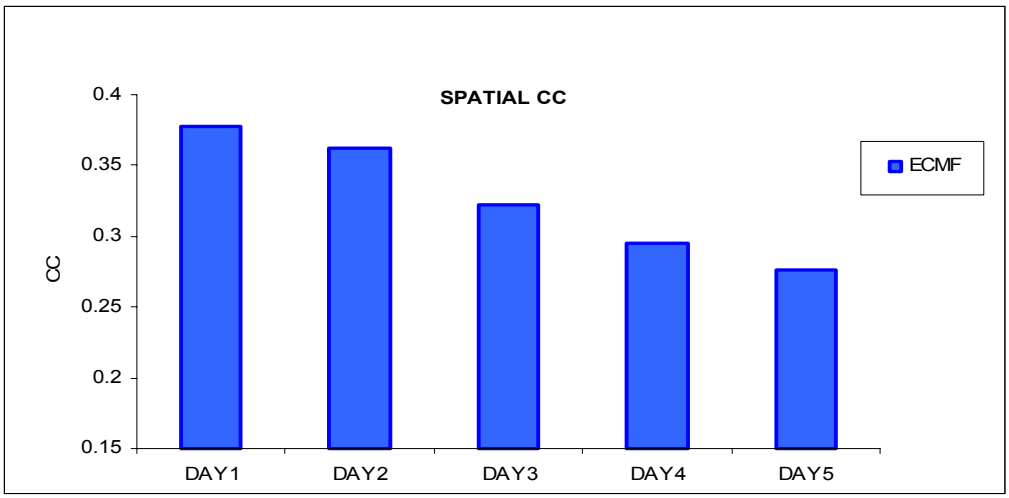

Fig. 8.20 : Inter-comparison of Spatial CC for day1-day5 rainfall forecasts by ECMWF model for the period from 1 June to 30 September 2008. The mean spatial CC shows 0.37 at day 1 forecast, becomes 0.33 at day 3 forecast and 0.28 at day 5 forecast.

Shukla (1987) grouped the entire country into four homogeneous zones based upon common characteristics observed in the inter-annual variability of the monsoon rainfall. Same classification has been used here to examine the performance of the ECMWF model in different homogeneous zone of the country. An inter-comparison of mean spatial CC for the four homogeneous regions of India is presented in Fig. 8.21. The results show that the spatial CC is highest over the south Peninsular India, where spatial CC ranges between 0.47 and 0.45 for day 1 to day 5 forecasts. For the Central India, spatial CC lies between 0.32 and 0.2. For the northwest India the CC ranges between 0.28 and 0.19 and for northeast India the CC is between 0.2 and 0.15.

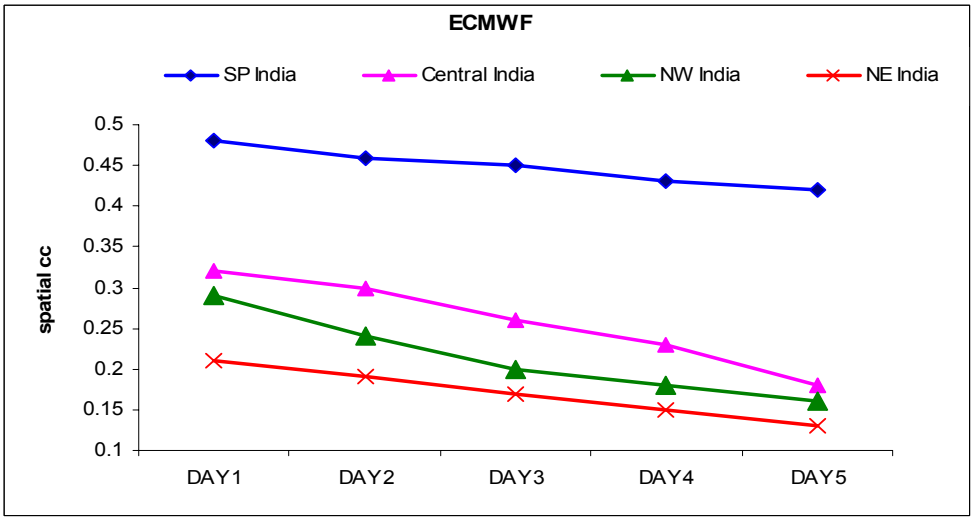

Fig. 8.21 : Inter-comparison of domain mean Spatial CC for day1-day5 rainfall forecasts by ECMWF model for 4 homogeneous regions of India for the period from 1 June to 30 September 2008

As mentioned in section 2, IMD implemented a Multi-model ensemble (MME) forecast from 1 June 2008 based on three member models namely, ECMWF, JMA and NCEP) (Roy Bhowmik et al., 2009b). Fig 8.22 presents an inter-comparison of country mean spatial CC of rainfall forecasts by MME and member models based on the performance during summer monsoon 2008 (1 June to 30 September). The results show that MME is superior to each member model at all the forecasts (day 1 to day 5), followed by JMA, ECMWF and NCEP (GFS). When UKMO and NCMRWF T-254 are included in this comparison (Fig. 8.23), UKMO is found superior to JMA and ECMWF.

Fig. 8.24 and 8.25 illustrate the performance skill of the MME forecasts during 2009 when five ensemble members (NCMRWF, UKMO, ECMWF, JMA and NCEP) were used. Fig. 8.24 presents an inter-comparison of country mean spatial CC of rainfall forecasts by MME, mean ensemble and individual models.

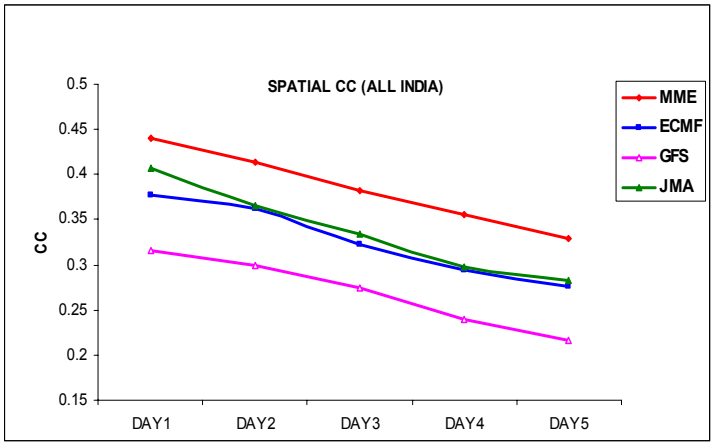

Fig. 8.22 : Inter-comparison of country mean spatial CC of day1-day5 rainfall forecasts by MME and member models for the period from 1 June to 30 September 2008

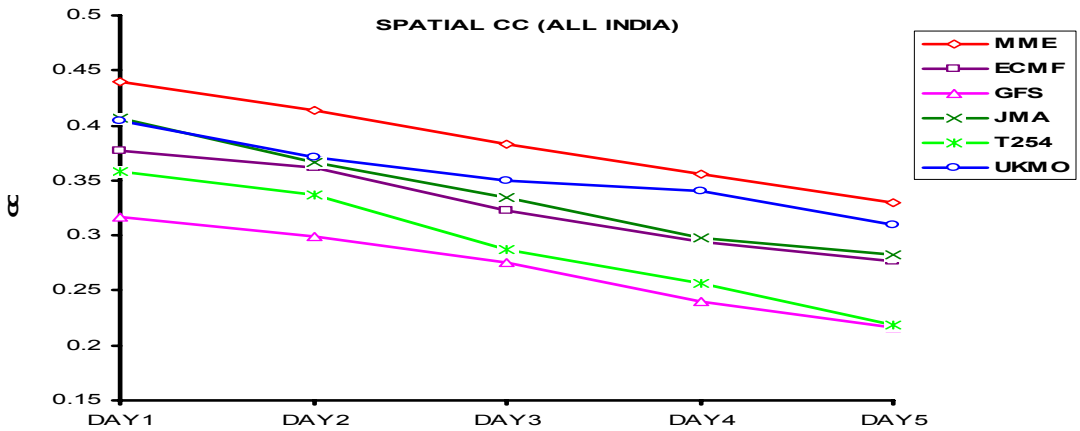

Fig. 8.23 : Inter-comparison of country mean spatial CC of rainfall forecasts by MME, member models and two non member models.

For the NCEP, CC ranges from 0.31 to 0.21 for day 1 to day 5 forecasts, for ECMWF it ranges between 0.35 to 0.27, for JMA between 0.40 to 0.28, for T254 between 0.35 to 0.25 and for UKMO between 0.40 to 0.32. For the MME, CC lies between 0.41 to 0.35 and for the mean ensemble it lies between 0.40 to 0.34. The results show that MME is superior to each member model at all the forecasts (day 1 to day 5). The result of mean ensemble is found to be close to the MME results. Among the individual model, UKMO and JMA are found to be superior, followed by ECMWF, NCMRWF and JMA. Fig 9.25 shows an inter-comparison of country mean root mean square (RMSE) of rainfall forecasts by MME and member models. The RMSE ranges between 15.6 mm to 16.4 mm for NCEP forecasts (day1 to day 5), between 14.4 mm to 15.6 mm for ECMWF forecasts, between 11.6 mm to 12.8 mm for JMA forecasts, between 13.7 mm to 14.6 mm for NCMRWF, between 12.9 mm to 13.6 mm for UKMO forecasts. For the MME, the RMSE lies between 11.6 and 12.2, showing its superiority over the member models. The RMSE for mean ensemble is again close to the RMSE of MME. Among the individual model, JMA and UKMO are found to be the best followed by NCMRWF, ECMWF and NCEP in terms of minimum RMSE.

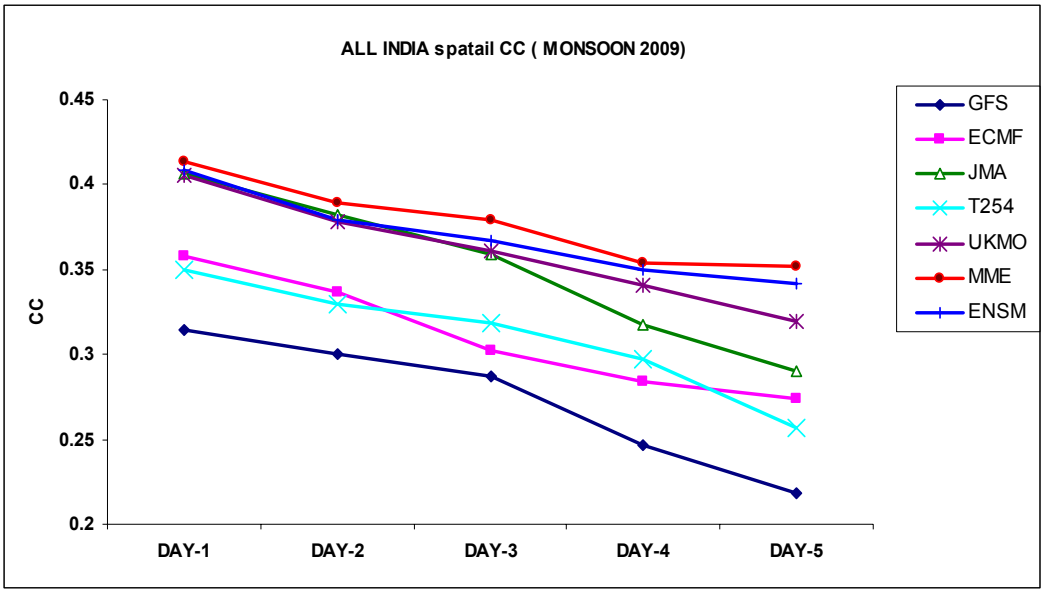

Fig. 8.24 : Inter-comparison of country mean spatial CC of day 1 to day 5 forecasts of rainfall by NCEP, ECMWF, JMA, NCMRWF, UKMO, mean ensemble and MME for summer monsoon 2009

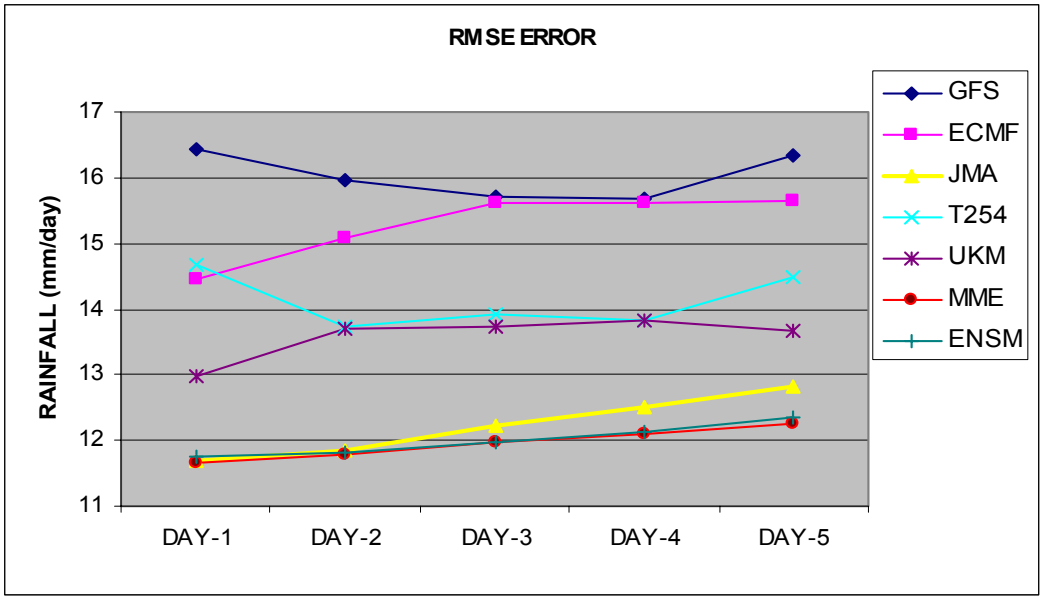

Fig. 8.25 : Inter-comparison of country mean rmse (mm) of day 1 to day 5 forecasts of rainfall by NCEP, ECMWF, JMA, NCMRWF, UKMO, mean ensemble and MME for summer monsoon 2009.

8.5.3. Spatial characteristics of rainfall forecast errors

Fig. 8.26 illustrates the spatial distribution of cumulative rainfall of the season (1 June to 30 September 2008) based on the observations. The observed rainfall distribution shows a north south oriented belt of heavy rainfall along the west coast with a peak of ~ 250 cm. The sharp gradient of rainfall between the west coast heavy rainfall and the rain shadow region to the east, which is normally expected, is noticed in the observed field. Another heavy rainfall belt is observed over the eastern parts of the country with a peak of order 200 – 250 cm to the extreme northeast. The rainfall belt is extended from the North West Bay of Bengal to northwest India along the domain of monsoon trough.

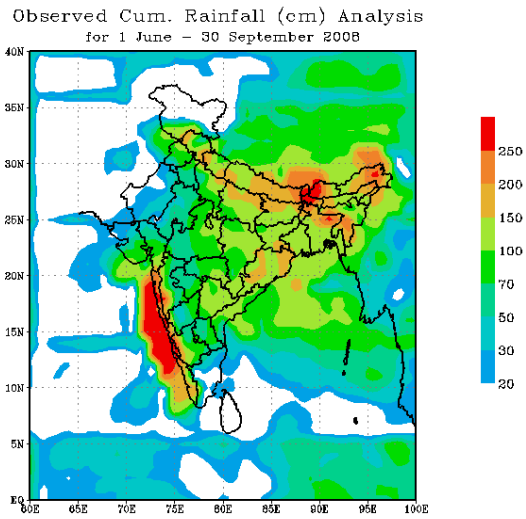

Fig. 8.26 : Mean observed rainfall for the period from 1 June to 30 September 2008

The forecast fields (day 1 to day 3) of cumulative rainfall for the season based on the MME and member models (ECMWF, JMA and NCEP) are shown in Fig. 8.27-8.30. The forecast fields by these models, in general, could reproduce the heavy rainfall belts along the west coast and over the domain of monsoon trough and foot hills of the Himalaya. However, some spatial variations in magnitude are noticed. The inter-comparison reveals that the MME forecasts are closer to the corresponding observed field.

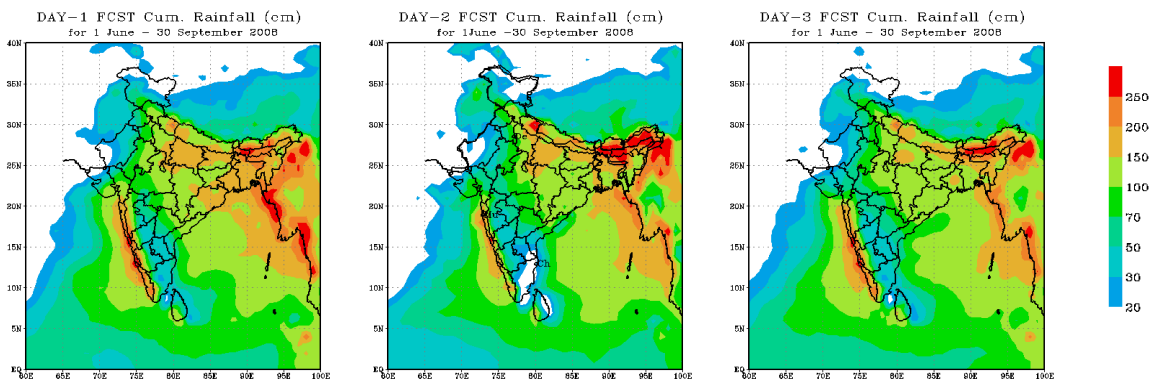

Fig. 8.27: Spatial distribution of cumulative rainfall (cm) based on MME day1-day5 forecasts for the period from 1 June to 30 September 2008

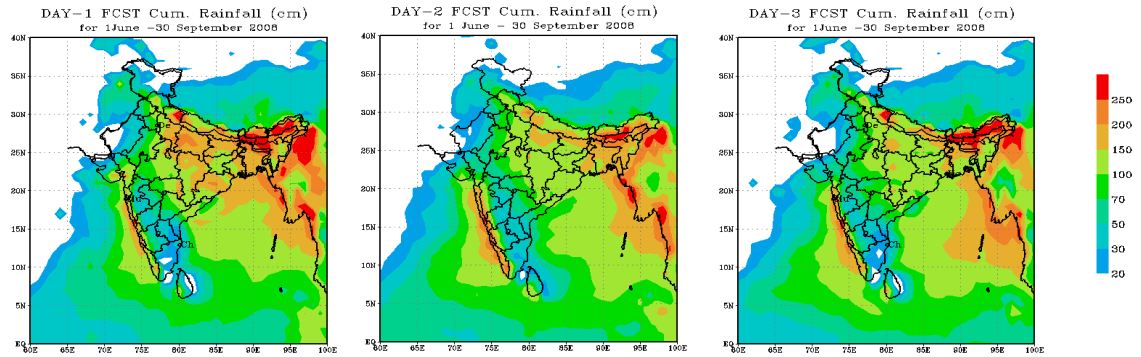

Fig. 8.28 : Spatial distribution of cumulative rainfall (cm) based on ECMWF day1 to day5 forecasts for the period from 1 June to 30 September 2008

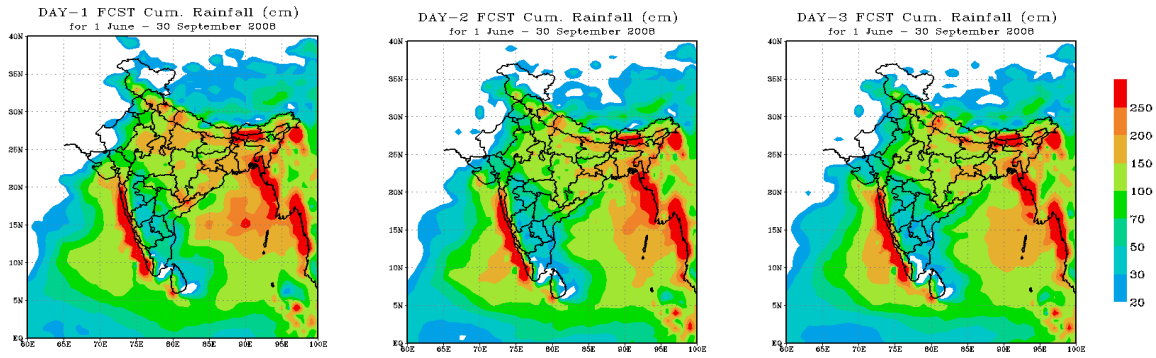

Fig. 8.29 : Spatial distribution of cumulative rainfall (cm) based on NCEP GFS day1 to day5 forecasts for the period from 1 June to 30 September 2008

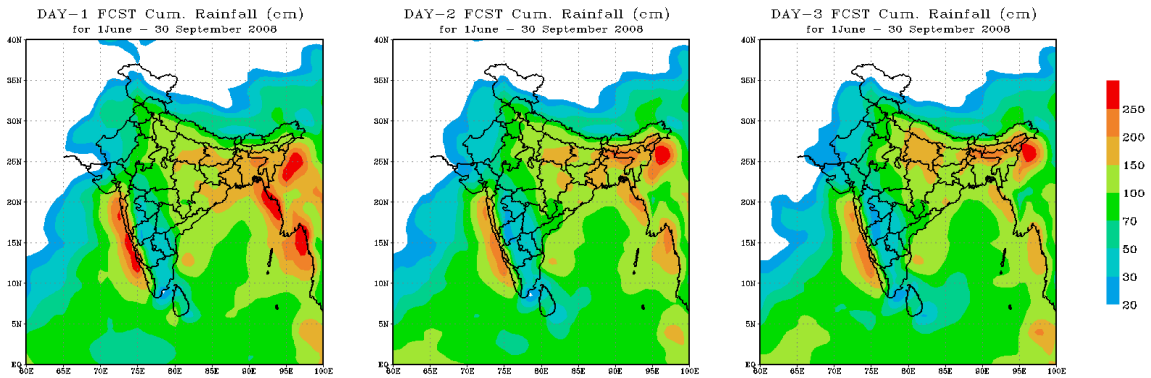

Fig. 8.30 : Spatial distribution of cumulative rainfall (cm) based on JMA day1 to day5 forecasts for the period from 1 June to 30 September 2008

In Fig. 8.31- 8.34, the spatial distribution of mean errors of rainfall for day 1 to day 5 forecasts by these models are demonstrated. Results of MME show mean errors of order -5 mm along the west coast. Otherwise, over most parts of the

country, mean errors are nearly zero mm. For the ECMWF, mean errors of the order of -5 to -10 mm occurred over the west coast of India. GFS shows mean errors of the order of -10 to -15 over the North Bay of Bengal. JMA shows mean errors of magnitude -5 mm along west coast and 5 mm over the North Bay of Bengal. In Fig.8.35 – 8.38**,** the spatial distribution of RMSE of rainfall for day 1 to day 5 forecasts by these models are presented. For the MME, RSME of the order of 20-25 mm prevailed over the domain of monsoon trough, along the foothills of the Himalayas, over the North Bay of Bengal and along the west coast where often-heavy rainfall occurs. Spatial coverage of errors is found to be considerably reduced in the MME forecasts. RMSE generally remained within 10 mm over the rest of the country. For ECMWF and GFS, RMSE has been of the order of 25 – 30 cm over large areas. In Fig.8.39 – 8.42**,** the spatial distribution of anomaly Correlation Coefficients (CC) of these forecasts for day 1 to day 5 by these models are presented. For computation of anomaly CC, observed climatology (on the basis of gridded observed rainfall fields of 15 years) is used. The results show that the anomaly CCs are comparatively higher in the MME forecasts, where anomaly CC of order 0.3 to 0.7 occupy over large areas. Anomaly CC shows sharp decreasing trend from day 4 forecast onwards. Anomaly CC has been very poor by GFS model.

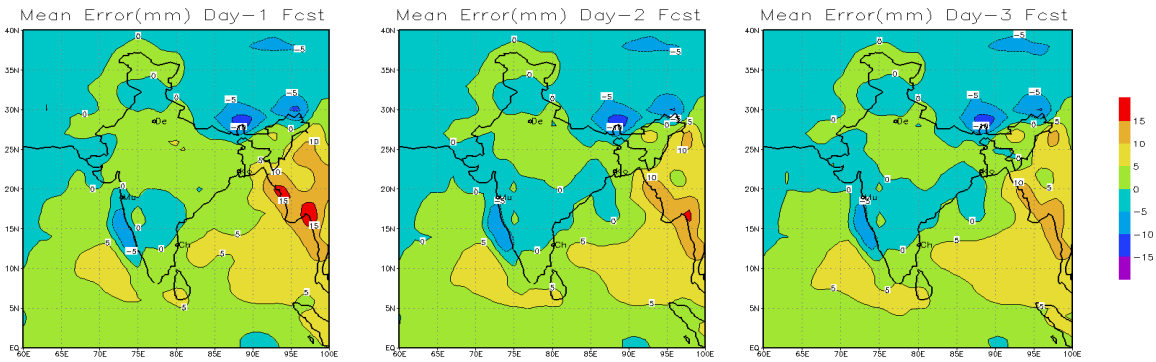

Fig. 8.31 : Spatial distribution of mean errors (forecast-observed) of rainfall (mm) based on MME day1 to day 5 forecasts for the period from 1 June to 30 September 2008

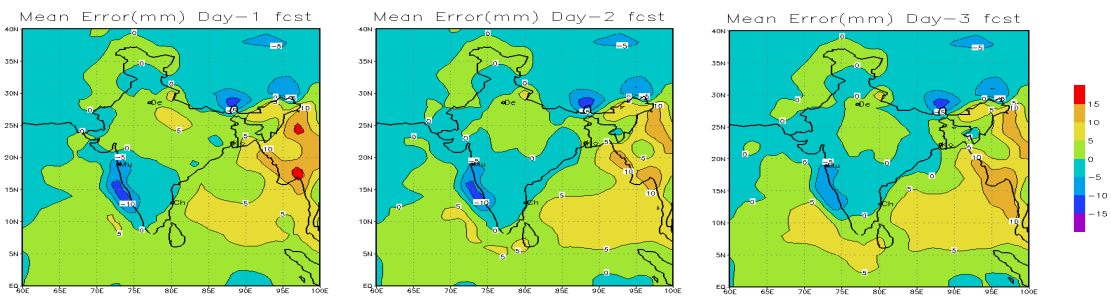

Fig. 8.32: Spatial distribution of mean errors (forecast-observed) of rainfall (mm) based on ECMWF day1 to day5 forecasts for the period from 1 June to 30 September 2008

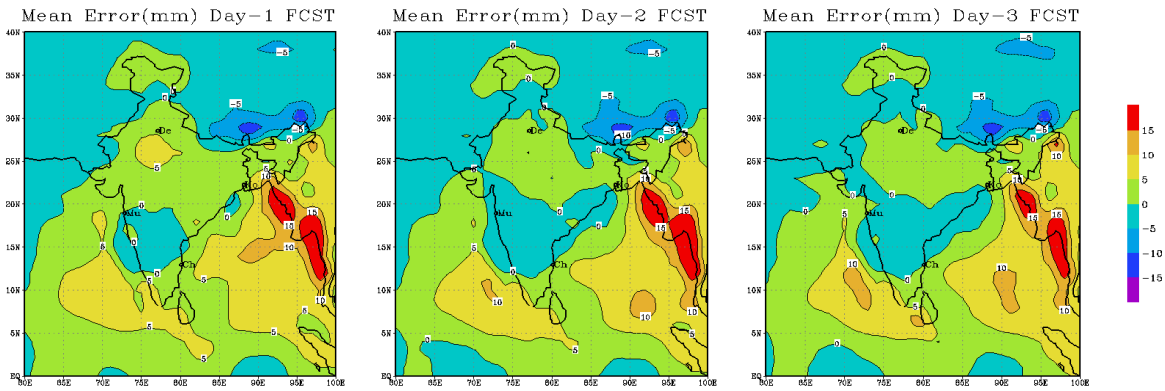

Fig. 8.33: Spatial distribution of mean errors (forecast-observed) of rainfall (mm) based on NCEP GFS day1 to day5 forecasts for the period from 1 June to 30 September 2008

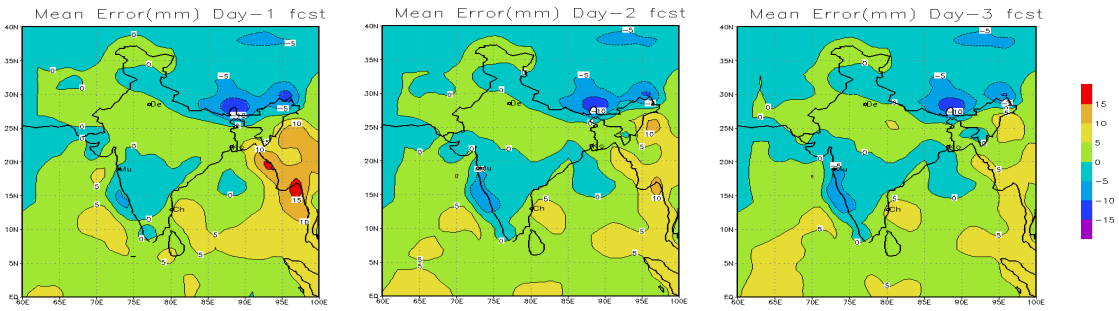

Fig. 8.34: Spatial distribution of mean errors (forecast-observed) of rainfall (mm) based on JMA day1 to day5 forecasts for the period from 1 June to 30 September 2008

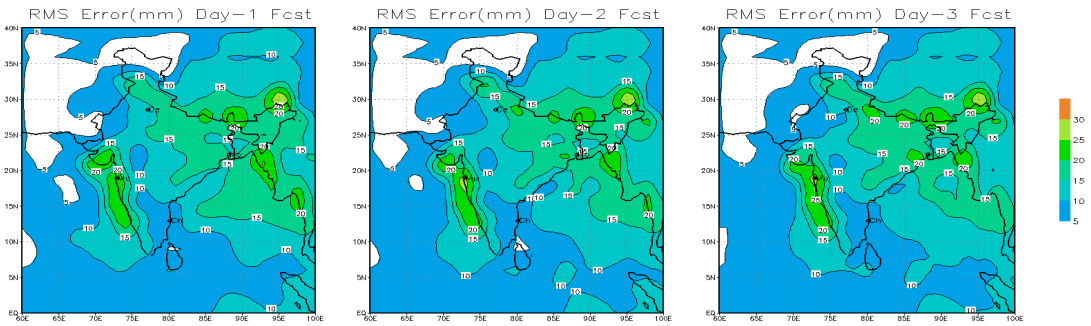

Fig. 8.35: Spatial distributions of root mean square errors of rainfall (mm) based on MME day1 to day5 forecasts for the period from 1 June to 30 September 2008

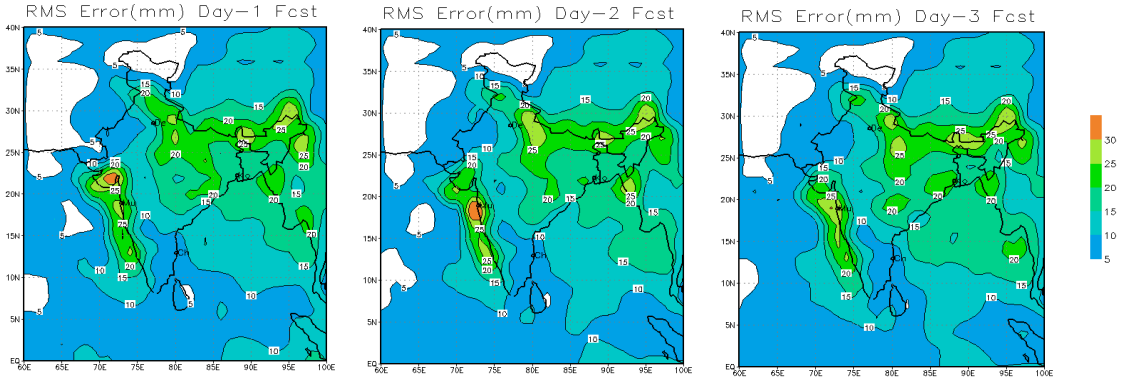

Fig. 8.36: Spatial distributions of root mean square errors of rainfall (mm) based on ECMWF day1 to day5 forecasts for the period from 1 June to 30 September 2008

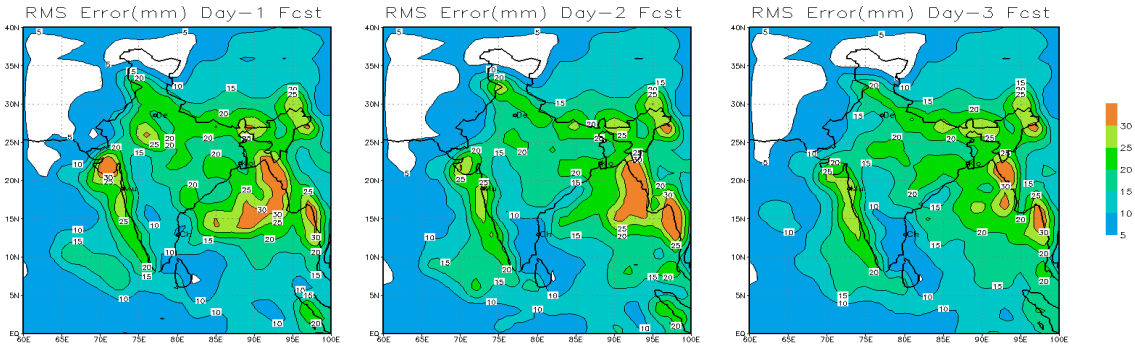

Fig. 8.37: Spatial distribution of root mean square errors of rainfall (mm) based on NCEP GFS day1 to day5 forecasts for the period from 1 June to 30 September 2008

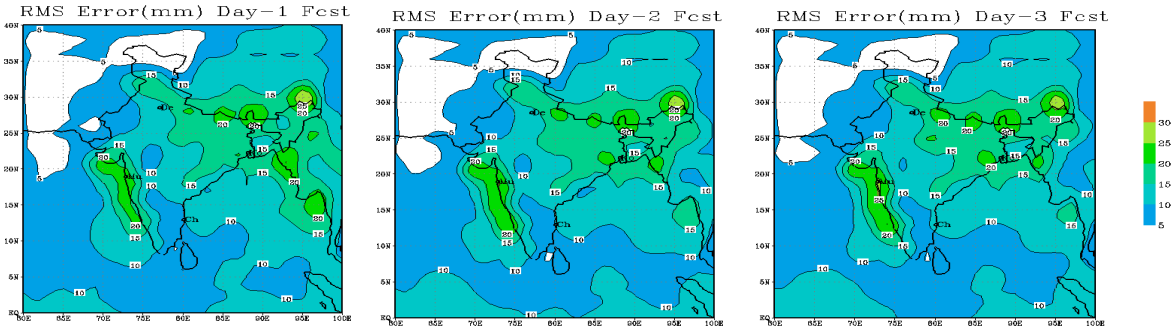

Fig. 8.38: Spatial distributions of root mean square errors of rainfall (mm) based on JMA day 1 to day 5 forecasts for the period from 1 June to 30 September 2008

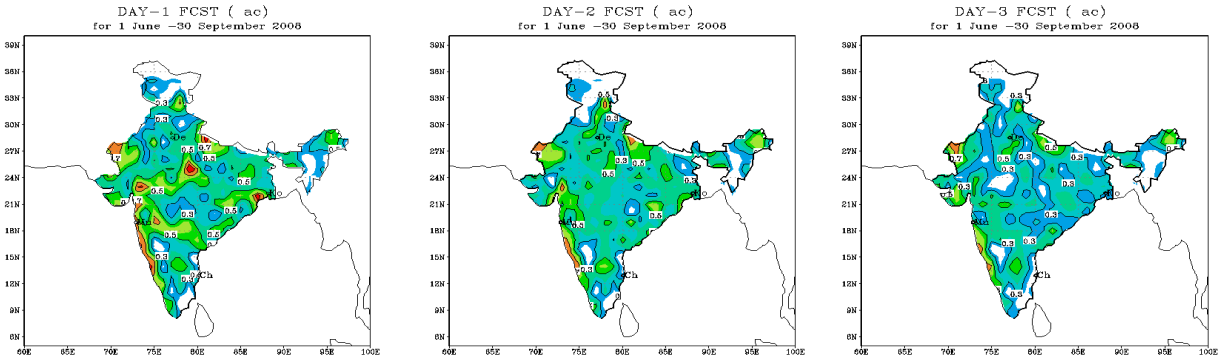

Fig. 8.39 Spatial distribution of anomaly CC of rainfall based on MME day1 to day 5 forecasts for the period from 1 June to 30 September 2008

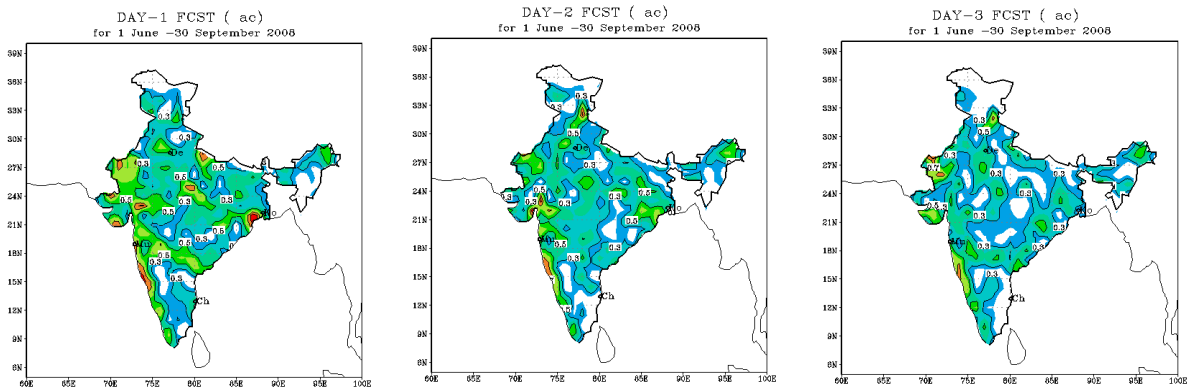

Fig. 8.40: Spatial distribution of anomaly CC of rainfall based on ECMWF day 1 to day 5 forecasts for the period from 1 June to 30 September 2008

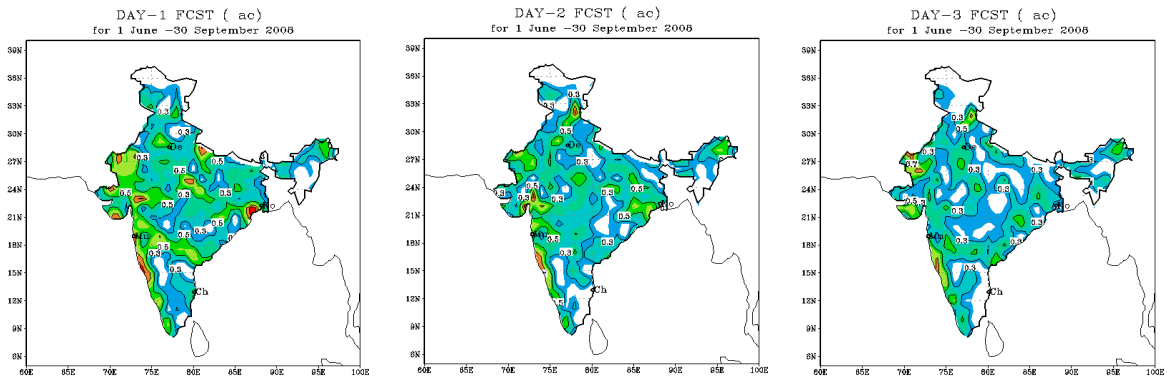

Fig. 8.41: Spatial distribution of anomaly CC of rainfall based on NCEP GFS day1 to day 5 forecasts for the period from 1 June to 30 September 2008

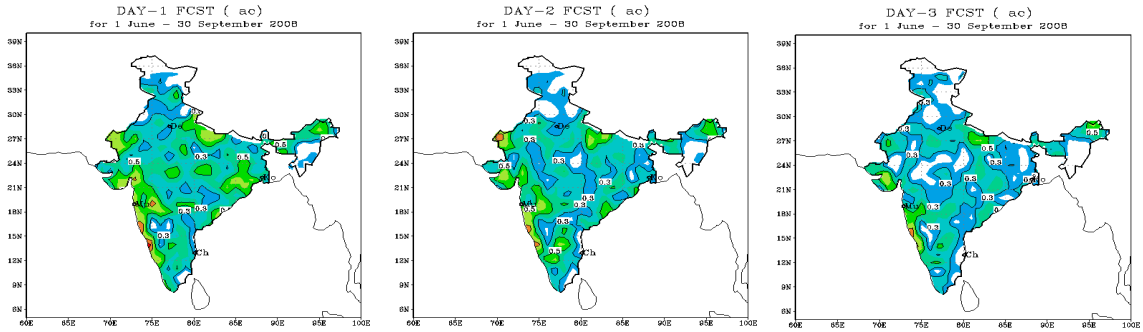

Fig. 8.42: Spatial distribution of anomaly CC of rainfall based on JMA day1 to day 5 forecasts for the period from 1 June to 30 September 2008

8.5. Outlook for the Future

Over the years, NWP models are playing increasingly dominant role in delivering operational real time weather forecasts. Before one uses outputs of a NWP model in the preparation of final forecast, adequate knowledge on the performance skill of the model is a pre-requisite. The results of the case studies and the performance statistics presented in this chapter demonstrate the strength and limitations of operational NWP models in short range time scale. The study will help in updating knowledge of operational forecasters for judicious use of NWP products for delivering improved operational forecast.

There is further scope to improve the forecast skill through the improved mesoscale data assimilation with optimum data ingest from dense conventional and non-conventional data sources. In view of the importance of good quality high-density observations to ingest into assimilation cycle of a high resolution NWP model, IMD has been in the process of implementing a massive modernization programme for upgrading and enhancing its observational system. From this modernization programme good quality observations (both conventional and non conventional) are expected to be available on the mesoscale both in space and time by means of Doppler Weather Radar (DWR), Satellites (INSAT-3D Radiance), wind profilers, meso-network (Automatic Weather Stations), buoys and aircrafts in the real time mode to ingest into the assimilation cycle of global, regional and mesoscale NWP models, with the use of advanced telecommunication system. Three Dimensional Variational Data Assimilation (3 DVAR) (in future 4 DVAR) is a necessary step to obtain improved initial condition.

Currently, under the modernization programme, IMD is equipped with a state of the art High Performance Computing (HPC) system having a peak performance of 14.2 TF at IMD HQ., 1 TF at IMD Pune along with high end servers of 100 GF capacities in major meteorological centers viz. Delhi, Mumbai, Chennai, Nagpur, Kolkata, Guwahati, Ahmedabad, Bangalore, Bhubaneswar, Chandigarh, Hyderabad and Pune for global and regional NWP modeling, particularly for the regional database management, mesoscale data assimilation and high resolution local area model.

With the availability of new observations and infrastructure from the modernization programme of IMD, the near future Weather Forecasting System of IMD would be as briefly given below:

(a) Now-casting and Mesoscale Forecasting System (valid for half hour to 24 hours)

- Processing of Doppler Weather Radar (DWR) observations at a central location (NHAC) to generate 3 D mosaic and other graphics products for nowcasting applications (Sen Roy et al., 2010).
- Enhancing mesoscale forecasting capability of local severe weather by providing 3 hourly area specific rainfall and wind forecasts (up to 24 hours) at the resolution of 3 km from ARPS with the assimilation (hourly intermittent cycle) of DWR, AWS, wind profilers and other conventional and non-conventional observations (Srivastava et al., 2010).

(b) Regional Models for Short Range Forecasting System (valid up to 3 days)

- 72 hours forecasts from WRF model with 3 nested domains (at the resolution of 27 km, 9 km and 3 km). The nested model at the 3 km resolution would be operated at the Regional/State Meteorological Centres at 6 hours interval with 3 DVAR data assimilation.
- 72 hours forecasts from MM5 model with 2 nested domains (at the resolution of 27 km and 9 km) at 12 hours interval with 3 DVAR data assimilation.
- For Cyclone Track Prediction, 72 hours forecasts from Quasi Lagrangian Model (QLM) at 40 km resolution at six hours interval; WRF (NMM) at 27 km resolution with assimilation package of Grid Statistical Interpolation (GSI).
- For Cyclone track and intensity prediction: Multi-model ensemble technique and application of dynamical statistical approach for 72 hours forecasts, forecast would be updated at 12 hours interval (Kotal et al, 2009).

- Development of multimodel ensemble technique for probabilistic forecasts of district level heavy rainfall events.

(c) Global model for Medium range forecasting (valid up to 7 days)

- NCEP Decoding System
- Global Data Assimilation System (GDAS), six hourly cycles with GSI (Grid Statistical Interpolation)
- Global Forecast System (GFS) T-382/L64
- Multimodel Ensemble based district level forecasts.

Fig. 8.43 depicts the short-range forecasting (WRF) strategy at the HQ. Mesoscale data assimilation and generation of high-resolution analysis for RSMC (Regional Specialized Meteorological Centre, Delhi as recognized by WMO) domain at the horizontal grid spacing of 27 km and vertical resolution 51 Eta levels. Time interval would be 6 hourly cycling. Resolution of the forecast fields would be 27 km for RSMC and 9 km for Indian domain. Triple nested (27, 9 and 3 km) model forecast would be made for specific events or expeditions (e.g. Commonwealth Game 2010). Fig.8.44 depicts the short-range forecasting (WRF) strategy at the State Meteorological Centres.

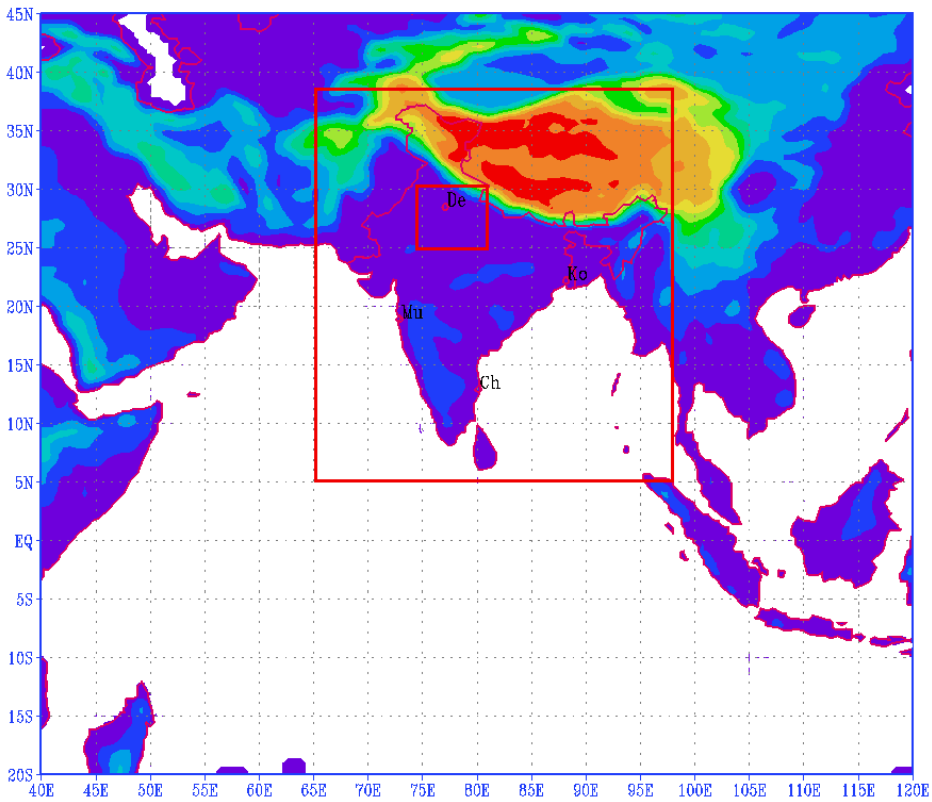

Fig. 8.43: Short-range Forecasting (WRF) Strategy at IMD HQ

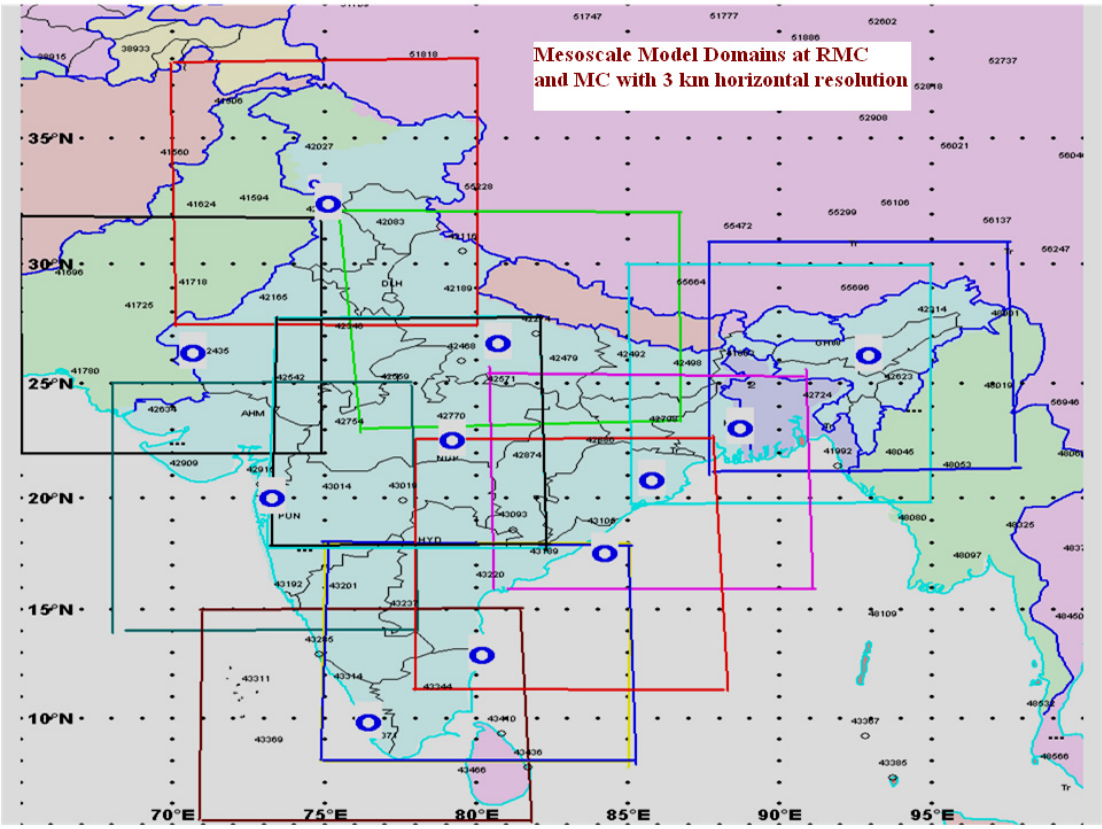

Fig. 8.44: Short-range Forecasting (WRF) Strategy at State Met Centres

IMD is yet to start any Ensemble Prediction System (EPS). The Global EPS have improved during the last a few years, in terms of resolution, ensemble size, length of integration and frequency of forecast cycles. While Singular Vector and Bred Vector methods are still widely used in generating initial perturbations, Ensemble Transform of BV, Ensemble Transform Kalman Filter and Ensemble Data Assimilation are also implemented in various centres. Currently, only ten global centres operate EPS and they exchange EPS outputs (at the native resolution) within themselves. IMD being a RSMC, plans to operate EPS for the forecast up to medium range. In order to get access to EPS outputs of other centre, it is necessary that IMD operates an EPS. IMD has already implement a Global Forecast System (T-382) in experimental model from 15 January 2010, which is expected to be made operational soon. Thereafter, IMD plans towards implementation of an EPS. This would allow IMD to get access to EPS outputs of other Global centres. Current MME System of IMD is based on forecast outputs of five deterministic models. With the availability of EPS outputs from 10 Global centres, IMD may work to develop a MME system based on 10 EPS forecast outputs and there by to develop a Probabilistic Forecast System for better forecasting of monsoon rainfall in short to medium range time scale.

References

Abraham, K. R., Dash, S. K., and Mohanty, U. C., 1996, "Simulation of monsoon circulation and cyclones with different type of orography", Mausam, 47, 235-248

Alapaty, K., Raman Sethu, Madala, R. V., and Mohanty, U. C., 1994, "Monsoon rainfall simulation with the Kuo And Betts-Miller Scheme", Meteor. Atmos. Phys. 53, 33-49.

Asnani, G. C., and Mishra, S. K., 1975, "Diabatic heating model of the Indian monsoon", Mon. Wea. Rev., 103, 115-130

Basu, B. K., 2003, "Verification of model predicted precipitation over India during summer monsoon 1997", Mausam, 54, 359-376

Basu, B. K., 2005. "Some characteristics of model produced precipitation during summer monsoon over India". J. Appl. Met., 44, 324-339

Basu, Swati, Begum, Z. N., and Raja Gopal, E. N., 1998, "Impact of boundary layer Parameterization Schemes on the prediction of the Asian summer monsoon", Boundary layer Meteorology, 86, 469-485

Basu Swati, Iyengar, G. R., and Mitra, A. K., 2002, "Impact of local closure scheme in simulation of monsoon system over India", Mon. Wea Rev, 130, 161-170

Bedi, H. S., Datta, R. K. and Kritchac, S. D., 1976, "Numerical forecast of meteorological elements under the condition of summer monsoon", Meteorologiya i Gilroloyuja, 5, 39-45(In Russian).

Bedi, H. S., 1976, "Spectral representation of hemispheric flow patterns", Indian J.Met. Hydrol. Geophys., 27, 397-405.

Bedi, H. S, 1979, "Spectral integration of hemispheric barotropic model", Indian J.Met. Hydrol. Geophys., 30, 31-38

Bedi, H. S., 1985, "A primitive equation spectral model for study of planetary atmospheric flow", Mausam, 36, 295-300.

Bohra, A. K., 1991, "Forecasting over the monsoon area by a semi implicit semi-Lagrangian regional primitive equation model", Mausam, 41, 223-226

Bohra, A. K., Prasad, V. S., Ramesh, K. J. and Iyenger, G. R., 1998, "Impact of satellite derived temperature profile data in global data assimilation and forecasting system, A case study", The Global Atmospheric and Oceanic System, 5, 345-365.

Bohra, A. K., 2009, "Development of Numerical Weather Prediction in India", Mausam (Diamond Jubilee Volume), 19-32

Brooks, H. E. and Doswell, C. A., 1999, "New technology and numerical weather prediction". Weather, 48, 173-177.

Colle, B. A., Mass, C. F., Westrick, K. J, 2000, "MM5 precipitation verification over the Pacific north-west during 1997-1999 cool seasons", Wea. Forecasting 15, 730-744

Das, P. K. and Bose, B. L., 1958, “Numerical Weather Prediction of movement of Bay Depression”, Indian J.Met. Hydrol. Geophys., 9, 225-252

Das, P. K., 1964, “Lee waves over large circular mountains”, Indian J. Met and Geophys, 15 (4), 547-554

Das, P. K and Bedi, H. S., 1976, “A study of orographic effects by a primitive equation model”. Proceedings of the I.I.T.M. symposium on Tropical Monsoon, Pune, India, 1976.

Das, P. K and Bedi, H. S., 1979, “Numerical simulation of monsoon circulation”, Proc. Indian Acad. Sci., CZ, 17-27

Das, P. K. and Bedi, H. S., 1981, “A numerical model for monsoon trough”, Monsoon Dynamics, Cambridge University Press, 351-364.

Das Gupta, M., Mitra, A. K., Prasad, V. S. and Rajan, D., 2003, “Impact of ATOVS temperature and moisture profile on NCMRWF analysis and prediction”, Mausam,54, 215-224

Das Someswar, Mitra, A. K, Iyangar, G. and Singh, J. V, 2002, “Skill of medium range forecasts over Indian monsoon region using different parameterization of deep convection”, Wea and Forecasting, 17 (6), 1194-1210

Datta, R. K., Chabra, B. M. and Singh, B. V., 1970, “An experiment in objective analysis for 500 hPa”, Indian J.Met. Hydrol. Geophys, 21, 437-442

Datta, R. K. and Mukherjee, T. K, 1972, “Prognosis of 500 mb surface by divergent barotropic model”, Indian J. Met. Geophys., 23, 345-348.

Datta, R. K. and Singh, B. V, 1973, “A scheme for multi-level objective analysis of contour heights”, Indian J.Met. Hydrol. Geophys. 24, 101-108

Dey, C. H. and Morone, L. L., 1985, “Evolution of the National Meteorological Center Global Data Assimilation System”, January 1982- December 1983. Monthly Weather Review 113, 304 -318.

Durai, V. R, Roy, Bhowmik, S. K. and Hatwar, H. R., 2007, “Distribution of precipitable water contents over Indian monsoon region”, Mausam, 58(2), 241-250

Dutta, S. N. Maiti, M. and De, U. S., 2002, “Waves to lee of a mesoscale elliptic orographic barrier”, Meteorl. Atmos. Phys., 81, 219-235

Godbole, R. V., 1973, “Numerical Simulation of Indian Summer Monsoon”, Indian J.Met. Hydrol. Geophys, 24, 1-14

Hatwar, H. R., Rama Rao, Y. V, Roy Bhowmik, S. K., Joardar, D. and Agnihotri, G, 2005, “Impact of ARMEX data in the analysis and forecast of IMD operational NWP model”, Mausam ,56, 131-138

John, P. George. and Begum, Z . N, 1997, “Impact of different radiation schemes in a GCM on the simulation of onset phase of Indian summer monsoon”, Atmosfera, 10, 1-22

Joshi, P. C., Simon, B., Narayanan, M. S, Sharma, O. P and Upadhaya, H. C, 1987, “Assessment of the use of satellite derived winds in monsoon forecasting using a GCM”, Adv. Sys. Res., 7, 353-356

Junker, N. W, Hoke, J. E and Grumm, R.H, 1989, “Performance of NMC's Regional Model”, Wea. Forecasting, 4, 368-390.

Kamga, A. F, Fongang, S. and Viltard, A., 2000, “Systematic errors of the ECMWF operational model over tropical Africa”, Mon. Wea. Rev, 128, 1949-1959

Kanamitsu, M., 1985, “A study of the prediction of the ECMWF operational forecast model in the tropics”, Meteor. Soc. Japan, 63, 779-844

Kanamitsu, M,1989, “Description of the NMC global data assimilation and forecast system”, Wea. Forecasting, 4, 335-342.

Kar, S. C, Patnaik, S., Rupa, .K., Prasad, V. S and Singh S. V,2003, “Impact of surface wind and moisture data from microwave sensors in the analysis and forecast of weather in the Indian Ocean Region”, Mausam, 54, 225-236

Kotal, S. D, Roy Bhowmik, S. K and Mukhopadhaya, B, 2009, “Performance of IMD NWP based objective cyclone forecast system during 2008-09”, IMD Met Monograph, Cyclone Warning No. 4/2009

Krishnamurti, T. N,1990, “Monsoon prediction at different resolution with a global spectral model”, Mausam, 41, 234-244.

Krishnamurti, T. N, Roy Bhowmik, S. K, Ooostered, D., Rohally, R., and Surgi, N., 1995, “Meso-scale signatures within the tropics as generated by Physical initialization”, Mon. Wea. Rev , 123, 2771-2790

Krishnamurti, T. N, Kishtawal, C. M, Larow, T, Bachiochi, D., Zhang, Z, Willford, E. C, Gadgil, S. and Surendran, S, 1999. “Improved weather and seasonal climate forecasts from multimodel super ensemble”. Science 285, 1548-1550.

Kumar Naresh, Ahmed N, Roy Bhowmik, S. K. and Hatwar, H. R., 2006, “Waves drag by two dimensional mountain lee waves”, Mausam, 57, 4 591-596.

Laurent, H. A, Viltard, A and Felice, Z. P, 1989, “Performance evolution and local adaptation of the ECMWF system forecast over north Africa for summer 1985”, Mon. Wea. Rev., 117, 1999-2009.

McBride, J. L and Ebert, E. E, 2000, “Verification of quantitative precipitation forecast of operational NWP model of Australia”, Wea. Forecasting, 15, 103-121

Mohanty, U. C, Paliwal, R. K, Tyagi, A., and John, A., 1989, “Evaluation of a multivariate primitive equation limited area model for short range prediction over Indian region”, Mausam, 40, 34-42.

Mohanty, U. C, Paliwal, R.K, Tyagi, A. and John, A., 1990, “Evaluation of a limited area model for short range prediction of Indian monsoon: sensitivity studies”, Mausam, 41, 251-256

Mukherjee, T. K and Datta, R. K.,1973, “Prognosis of Four-layer quasi-geostrophic model”, Indian J.Met. Hydrol. Geophys., 24, 93-100.

Parrish, D. F and Derber, J. C, 1992, “The National Meteorological Centre’s Spectral Statistical Interpolation analysis system”, Monthly Weather Review, 120, 1747-1763.

Prasad, V. S, 2003, “Impact of high resolution satellite wind vector data on NCMRWF assimilation and forecasting system” , Mausam, 54. 237-246

Prasad, K, Rama Rao, Y. V. and Sen, Sanjib, 1997, “Tropical cyclone track prediction by a high resolution limited area model using synthetic observations”, Mausam, 48, 351-366.

Rajeevan, M, Bhate .J., Kale, J. D and Lal, B, 2005, “Development of high resolution gridded rainfall data for Indian Region”, IMD Met. Monograph No. Climatology 22/2007.

Ramanathan, Y and Saha, K. R, 1972, “Application of primitive equation barotropic model to predict movement of western disturbances”, J. Appl. Meteorl., 11, 268-272

Rao, Y. P, Ramamurti, K. S and Sinha, M. C, 1972, “A scheme of deriving grid point values from observatory reports for numerical weather prediction”, India J.Met. Hydrol. Geophys, 23, 468-478.

Rao, Y. P, 1976, South-west Monsoon, Met Monogram No. 1/1976, India Meteorological Department, New Delhi, 367 pp.

Rao, A.V.R.K, Murty, L. K, Bohra, A. K and Datta, R. K, 1985, “Use of 10 level diagnostic studies of vertical motion in tropic”, Mausam, 36, 135-142.

Ratnam, J. V and Cox, E. A, 2006, “Simulation of monsoon depression using MM5: sensitivity to convective parameterization scheme”, Meteorl. Atmos. Phys., 93(1-2), 53-78.

Roy Bhowmik, S. K and Prasad, K., 2001, “Some characteristics of limited area model precipitation forecast of Indian monsoon and evaluation of associated flow features”, Meteorl. and Atmos. Phys., 76, 223-236.

Roy Bhowmik, S. K, 2003, “Monsoon rainfall prediction with a nested grid meso scale limited area model over Indian Region”, Proc. India Acad. Sc., 112, 499-520

Roy Bhowmik, S. K, 2004, “Systematic errors of IMD’s NWP operational model”, Mausam, 55, 1-14

Roy Bhowmik, S. K., Joardar, D. and Sen Roy Soma, Hatwar, H. R.,.2005, “Meso scale features of monsoon precipitation system as revealed by the objective analysis of rainfall from the use of high dense land rainfall observation” , Mausam, 56, 543-548

Roy Bhowmik, S. K., Joardar, D, Das, Ananda K., Rama Rao Y. V and Hatwar H. R., 2006, “Impact of KALPANA-1 CMV data in the analysis and forecast of IMD operational NWP system”, Mausam, 57, 319-331

Roy Bhowmik, S. K. and Das Ananda K, 2007, “Rainfall Analysis for Indian monsoon region from merged dense raingauge observations and satellite estimates – Evaluation of monsoon rainfall features”, Journal of Earth System Science System, 116(3), 187-198

Roy Bhowmik, S. K, Joardar, D. and Hatwar H. R, 2007, “An evaluation of precipitation prediction skill of IMD operational NWP system”, Meteorl Atmos Phy, 95(3) ,205-221

Roy Bhowmik, S. K and Prasad, .K, 2008, Improving IMD operational limited area model forecasts, Geofizika, 25(2), 87-108

Roy Bhowmik, S. K and Durai, V. R, 2008, “Multi-model Ensemble Forecasting of rainfall over Indian monsoon region”, Atmosfera , 21(3), 225-239

Roy Bhowmik, S. K, Durai, V. R, Das, Ananda K and Mukhopadhaya, .B, 2009a “Performance of IMD Multimodel Ensemble based district level forecast system during summer monsoon 2008”, IMD Met Monograph, Synoptic Meteorology, No. 8/2009

Roy Bhowmik, S. K, Durai, V. R, Das Ananda, K and Mukhopadhaya, B, 2009b “Evaluation of prediction skill of ECMWF forecasts over Indian region in medium range time scale during summer monsoon 2008”, IMD Met Monograph, Synoptic Meteorology, No. 7/2009

Roy Bhowmik, S. K and Durai, V. R, 2010, “Application of multi-model ensemble technique for real-time district level forecasts over Indian region in short range time scale”, Meteorl. Atmos. Phys., 106, 19-35

Sarker, R. P, 1965, “A theoretical study of mountain waves on western ghats”, India J.Met. Hydrol. Geophys,16(4), 563-584

Sarker, R. P, Sinha Roy, K. C and De, U. S, 1978, “Dynamics of orographic rainfall”, India J.Met. Hydrol. Geophys, 29 (1&2), 335-348

Sarker, R. P and Bedi, H. S, 1987, “Operational Numerical Weather Prediction at IMD New Delhi”, Mausam, 38, 275-292

Sen Roy, S, Roy Bhowmik, S. K, Lakshmanan, V, and . Thampi, S. B., 2010, Doppler Radar-based Nowcasting of the Bay of Bengal Cyclone – Ogni of October 2006, J., Earth Sci. Sys (to appear)

Sikka, D. R, 1975, “Forecasting of the movement of tropical cyclone in the Indian Sea by a non divergent barotropic model”, Indian J.Met. Hydrol. Geophys , 26, 323- 325

Sinha, M. C, 1972, “Objective Analysis - a review”, Indian J. Met. Hydrol. Geophys., 23, 241-246

Sinha, M. C., Dayal, V. and Begum, Z. N., 1982, “A package for the objective analysis of isobaric contours”, Mausam, 33 (1),.71-80

Singh, S. S and Sugi, M, 1986, Prediction of monsoon depression with a regional primitive equation model, Mausam, 37, 17-26.

Singh, S. S, Kulkarni, A. A and Sikka, D. R, 1980, “On some aspects of initialization and forecasts in Indian monsoon region”, Mon. Wea Rev., 108, 1315-1325

Shukla, J, 1969, “Numerical experiment on disturbances in the Tropical easterlies”, J. Met. Soc Japan, 48, 405-410

Shukla, J, 1972, “Barotropic model-A review”, Indian J.Met. Hydrol. Geophys., 23, 201-206

Shukla, J, 1987. “Interannual variability of monsoons”. Monsoons, J. S. Fein and P. L. Stephens, Eds., John Wiley and Sons, 399–463.

Srivastava Kuldeep, Roy Bhowmik, S. K, Sen Roy, S, Thampi, S. B and Reddy, Y. K, 2010, “Simulation of high impact convective events over Indian region by ARPS model with assimilation of Doppler Weather Radar radial velocity and reflectivity”, Atmosfera, 23, 53-73

Surgi, N, 1989, “Systematic errors of the FSU global spectral model”, Mon. Wea. Rev, 117, 1751-1766

Vaidya, S. S, 2006,“The performance of two convective parameterization scheme in mesoscale model over Indian region”, Meteorl. Atmos. Phys., 92(3-4), 175-190

CHAPTER 9

MEDIUM RANGE FORECASTING OF SOUTHWEST MONSOON

A.K. Bohra and L. Harenduprakash
Former Head, National Centre for Medium Range Weather Forecasting

akbohra@ncmrwf.gov.in

9.1. Introduction

A Medium Range Weather Forecast (MRF) is defined in the Indian context as a weather forecast with lead-time from 72 hrs to 240 hrs (3 to 10 days). This is the practical definition followed in this discussion. (The ECMWF Charter defines medium range as "the time scale beyond a few days in which the initial conditions are still important"). We consider here only medium range forecast using numerical models that are based on thermo-hydrodynamics of the earth's atmosphere (i.e. using General Circulation Models of the Atmosphere - AGCM). The AGCM is three dimensional in space enclosing the Earth's atmosphere (with a fixed top boundary at around 0.1hPa or less in pressure coordinates). The evolution of the atmosphere is computed forward in time based on the relevant laws of physics and also our scientific understanding of various processes within the atmosphere and its lower and upper boundaries. At the top of the atmosphere the incoming solar radiation (the future values of which are known with sufficient accuracy and is independent of atmospheric processes) is prescribed. This radiation along with the exchanges of momentum, heat and water at its lower boundary are the minimum set of external forcings for the model atmosphere. The details of processes as well as their variety increases with the sophistication of the model. The horizontal and vertical resolutions also increase with the sophistication of the model (the current ECMWF MRF model has an approximate horizontal resolution of 25 km and has 91 levels in the vertical). The present day MRF models are seamless in the sense that the same model, sometimes with minor modifications, is used for short range to climate scale simulations. The current trend in MRF is to evolve towards forecast using Earth System Models, i.e., models that include bio-geochemical processes as well as the ocean with two way interactions.

The present discussion is concerned with medium range weather forecasting during the Southwest Monsoon Season (formally the forecasting of the state of the

atmosphere and hydrometeors during the period 1June to 30 September) as it is currently practiced in India. The discussion focuses primarily on forecasting over the Indian subcontinent but may also cover the larger geographical region bounded by the latitudes 15S and 55N and the longitudes 20E and 140E.

The Southwest Monsoon is a planetary scale phenomenon and an integral and distinct feature of the general circulation of the Earth's atmosphere. Therefore the medium range prediction during the Southwest Monsoon is also carried out using the same analysis-forecast systems as it is done throughout the year - in India as well as elsewhere in the world.

This chapter consists of a brief history of medium range weather forecasting in India, a description of the NCMRWF analysis-forecast systems, the salient features of performance of the forecasts with respect to the Southwest Monsoon and finally the summary and conclusions. Generally we try to present facts and keep the interpretations to a minimum.

In the beginning, studies using monthly, weekly and five days mean and corresponding anomaly charts and statistical analysis of their predictive features were attempted as a tool for medium range forecasting. This met with only limited success (Compendium of Meteorology – 1951, FMU Report on MRF by D. A. Mooley) paving for a more dynamical and physical approach.

9.2. A brief review of the evolution of medium range weather forecasting in India

Medium range weather forecasting in India got a much-needed thrust with the establishment of the National Centre for Medium Range Weather Forecasting (NCMRWF) in 1988. The cardinal purpose of the establishment of NCMRWF was weather forecast support for the Indian agricultural sector. A substantial part of its efforts was in implementing and stabilizing the medium range weather forecast systems, developing operational techniques and procedures for downscaling and customizing the products for use by the farming community and also in establishing a country-wide dissemination system for such products. The latter two functions have since been transferred to IMD in 2008. The stress on agricultural applications has been the defining character of medium range weather forecasting in India to the present and may remain so considering the supreme importance of ensuring food

security of the nation. The research and development efforts carried out at NCMRWF for improving the forecast quality and also the practical value of the forecasts (like downscaling, Statistical Interpretation, Ensemble Forecasting, Multi Model Ensemble, etc) is determined by this guiding principle and is a continuous process. The phenomenological aspects of the Southwest Monsoon are in this context more of utilitarian value - as part of verifying the accuracy of the deterministic forecasts with respect to space and time variability of the Monsoon. The underlying assumption is that an accurate medium range prediction of 10 days will also include all structures and variability of significance - like Monsoon Onset and advancement, genesis, movement and decay of monsoon Lows and Depressions; persistence and cessation of dry spells.

The progress of medium range forecasting of South West Monsoon in the country closely followed the developments at NCMRWF. 1 June 1994 may be considered as the date on which usable real-time medium range forecasts for the monsoon season commenced in India, i.e., when the end-to-end forecast-analysis system based on the T80L18 Global Spectral Model started running in real time and produced medium range global forecasts. Over the years a fully operational location specific forecast system for agriculture was successfully developed on the basis of the T80L18 medium range weather forecasts. This location specific forecasting procedures as well as the Agro Advisory Service Units were transferred to the India Meteorological Department in 2008. Recently, the implementation of the high-resolution, advanced T254L64 forecast-analysis system in 2007 ushered in a significant improvement in the forecast skill compared to the T80L18 forecast system. The current medium range weather forecast system is described below.

9.3. Description of the current NCMRWF Global Data Assimilation - Forecast System

The basic scientific and computational aspects of medium range weather forecasting are now parts of classical meteorology and several specialised books and monographs covering the methods and procedures for medium range numerical weather forecasting are available in print. The present discussion is therefore focused on the specific aspects of the practically realized medium range weather forecasting system in India with particular reference to the Southwest Monsoon season. The forecasts that we discuss here were made in a real world operational regime with a strict data cut off time (that is subject to all types of unaccounted errors in data, fluctuations in data volume and also breaks in the availability of particular

types of data). The particulars provided here may seem inessential but are necessary if one wants to compare the performance of predictions from this system with predictions from other forecast centers and also the improvements in prediction that may take place at NCMRWF in the future.

The operational numerical weather analysis-forecast system of National Center for Environmental Prediction (NCEP), USA - Global Forecast System (GFS) - was acquired by NCMRWF in the year 2007. The GFS was implemented on CRAY-X1E and Param Padma (IBM P5 cluster) computing systems. Observation pre-processing and the post processing of model output are presently executed in Param Padma whereas the analysis system and forecast model at T254L64 resolution are implemented in CRAY-X1E. GFS has the capability to assimilate various conventional as well as satellite observations including radiance observations from different polar orbiting and geostationary satellites.

Data Pre-Processing and Quality Control

The meteorological observations from all over the globe and from various space observation platforms (satellites) are received at the Regional Telecommunication Hub (RTH) IMD, New Delhi through Global Telecommunication System (GTS). These are made available to NCMRWF through a dedicated communication link at half hour interval. Data on a typical Monsoon day is shown in Fig.9.1.

The data decoding part runs 48 times in a day, every half hour, as soon as the GTS data files are received at NCMRWF. The data assimilation steps mainly consist of observation processing, data assimilation and model forecast. In the decoding step, all the GTS bulletins are decoded from their native format and encoded into NCEP BUFR format using the various decoders. Global data assimilation system (GDAS) of T254L64 accesses the observational database at a set time each day (i.e., the data cut-off time, presently set as 6 hour), four times a day and performs a time-windowed (± 3 hours) dump of requested observations. Finally the data pre-processing involves the execution of a series of programs designed to assemble observations dumped from decoder databases, encoding of information about the observational error for each data type as well as the background interpolated to each data location, performing of both rudimentary multi- platform quality control and more complex platform-specific quality control. Quality control of satellite radiance data is done within the global analysis scheme.

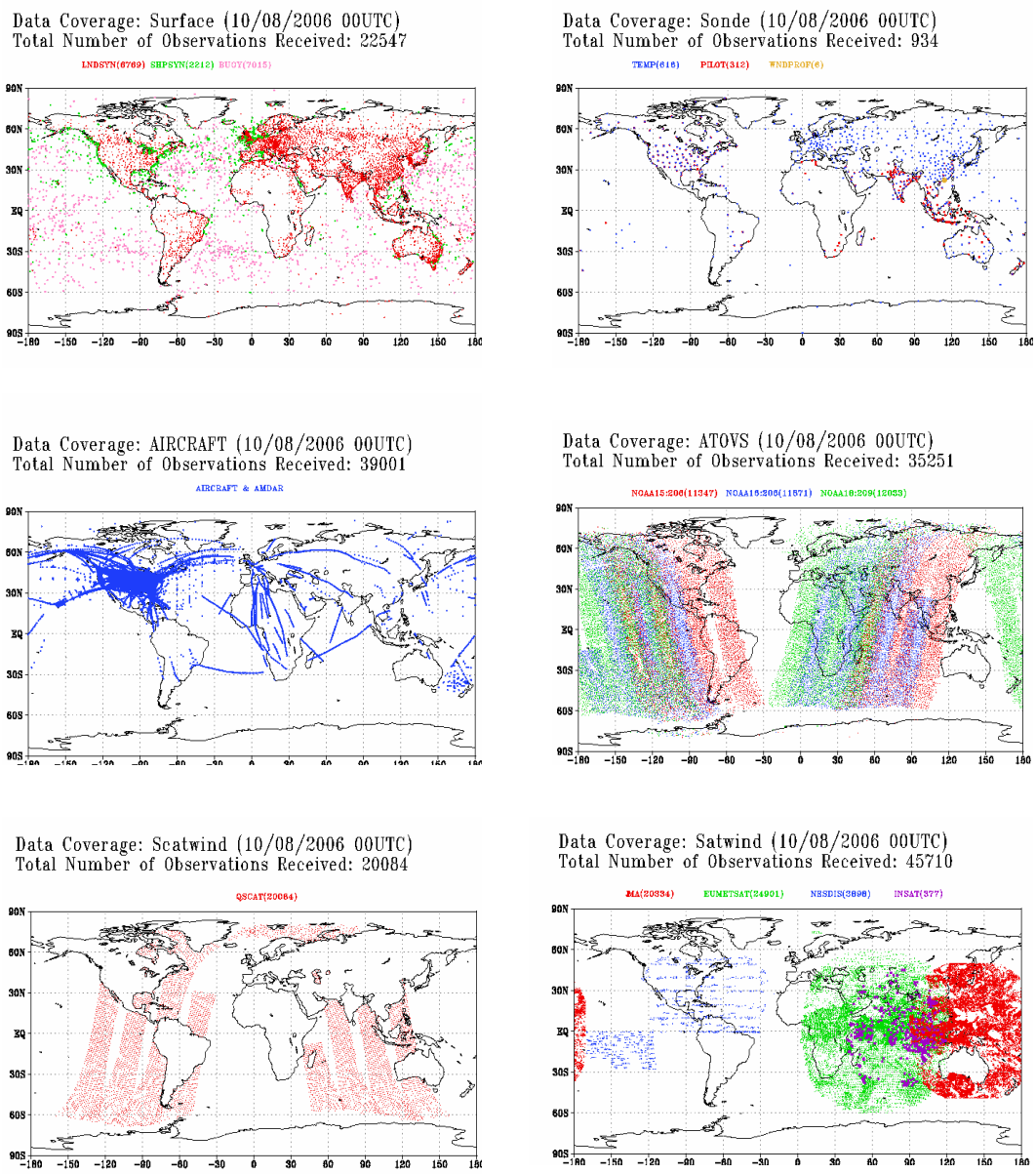

Fig.9.1: Different types of observed data used for 00UTC analysis on a typical monsoon day

9.4. Global Analysis Scheme

The global analysis scheme in the GFS framework is based on a variant of Spectral Statistical Interpolation (called GSI - Grid point Statistical Interpolation) (Parrish and Derber, 1992 and Derber et. al. 1991). The analysis problem is to minimize the equation

$$J = J_b + J_o + J_c \qquad (1)$$

where, J_b is the weighted fit of the analysis to the six hour forecast (background or first guess), J_o is the weighted fit of the analysis to the observations and J_c is the weighted fit of the divergence tendency to the guess divergence tendency. J_c also includes a constraint to limit the number of negative and supersaturated moisture points.

Horizontal resolution of the analysis system is in spectral triangular truncation of 254 (T254). The quadratic T254 Gaussian grid has 768 grid points in the zonal direction and 384 grid points in the meridional direction. The resolution of the quadratic T254 Gaussian grid is approximately 0.5 x 0.5 degree. The analysis is performed directly in the model's vertical coordinate system. This sigma ($\sigma = p/p_s$) coordinate system extends over 64 levels from the surface (~997.3 hPa) to top of the atmosphere at about 0.27hPa. This domain is divided into 64 layers having enhanced resolution near the bottom and the top, with 15 levels below 800 hPa, and 24 levels above 100 hPa.

Meteorological observations from various types of observing platforms, that are assimilated in T254L64 global analysis scheme at NCMRWF are shown Table 10.1. The analysis procedure is performed as a series of iterative problems. There are two main external iterations, which take care of the non-linearity in the objective function J (Eqn. 1). In this external iteration, some parts of the transformation of the analysis variables into the pseudo-observations are linearized around the current solution. In the first external iteration, the current solution is the 6hour forecast (guess). In the later iterations, the current solution is the result from the previous external iteration.

Table 9.1: Observations currently used in T254L64

Observation type	Variables/Sensors
Radiosonde	u, v, T, q, Ps
Pibal winds	u, v
Wind profilers	u, v
Surface land observations	Ps
Surface ship and buoy observations	u, v, T, Ps, q
Conventional aircraft reports (AIREP)	u, v, T
AMDAR aircraft reports	u, v, T
ACARS aircraft reports	u, v, T
GMS, METEOSAT, INSAT,GOES cloud drift IR and visible winds	u, v
NOAA-15,16,18 & Metop-A satellites level 1b radiances	AMSU-A, AMSU-B, & HIRS
NOAA-16 & 17 ozone profiles	SBUV
QSCAT winds	u, v

The use of the level 1b radiance data requires the application of quality control, bias correction, and the appropriate radiative transfer model (Derber & Wu, 1998). The radiative transfer model (CRTM) uses the OPTRAN transmittance model to calculate instrument radiances and brightness temperatures and their Jacobians.

Apart from the increased horizontal (150 km in T80L18 to 50 km in T254L64) and vertical (18 levels in T80L18 to 64 levels in T254L64) resolutions and better quality-control packages for conventional observations in T254L64 GDAS, assimilation of direct radiance is one of the major improvements over the T80L18 data assimilation system.

The Forecast Model

The forecast model is a primitive equation spectral global model with state of the art dynamics and physics (Kanamitsu 1989, Kanamitsu et al. 1991, Kalnay et al. 1990). Model horizontal and vertical resolution as well as their representation is the same as described in the section on analysis scheme. The main time integration is leapfrog for nonlinear advection terms. Semi-implicit method is used for gravity waves and for zonal advection of vorticity and moisture. An Asselin (1972) time filter

is used to reduce computational modes. The model time step for T254 is 7.5 minutes for computation of dynamics and physics. The full calculation of long wave radiation is done once every 3 hours and of shortwave radiation every 1 hour (but with corrections made at every time step for diurnal variations in the shortwave fluxes and in the surface upward long wave flux). Mean orographic heights on the Gaussian grid are used. Negative atmospheric moisture values are not filled for moisture conservation, except for a temporary moisture filling that is applied in the radiation calculation.

Table 9.2: Physical Parameterization schemes in T254L64 & T80 Models

Physics	T254L64	T80L18
Surface Fluxes	Monin-Obukhov similarity	Monin - Obukhov Similarity
Turbulent Diffusion	Non-local Closure scheme (Hong and Pan (1996))	Non-local Closure scheme (Hong and Pan (1996))
SW Radiation	Based on Hou et al. 2002 –invoked hourly	Based on Lacis & Hansen; Harshvardhan et al. (NASA/Goddard) -invoked 12 hrly
LW Radiation	Rapid Radiative Transfer Model (RRTM) (Mlawer et al. 1997). – invoked 3 hourly	Based on Fels & Schwarzkopf – invoked 12 hourly
Deep Convection	SAS convection (Pan and Wu (1994))	Kuo scheme modified
Shallow Convection	Shallow convection Following Tiedtke(1983)	Tiedtke method
Large Scale Condensation	Large Scale Precipitation based on Zhao and Carr (1997)	Manabe-modified Scheme based on saturation
Cloud Generation	Based on Xu and Randall (1996)	Based on Slingo scheme
Rainfall Evaporation	Kessler's scheme	Kessler's scheme
Land Surface Processes	NOAH LSM with 4 soil levels for temperature & moisture Soil moisture values are updated every model time step in response to forecasted land-surface forcing (precipitation, surface solar radiation, and near-surface parameters: temperature, humidity, and wind speed).	Pan Scheme having 1 level of soil moisture & 3-layer soil temperature. Bucket hydrology of Manabe for soil moisture updating

Air-Sea Interaction	Roughness length determined from the surface wind stress (Charnock (1955)) Observed SST, Thermal roughness over the ocean is based on a formulation derived from TOGA COARE (Zeng et al., 1998).	Roughness length determined from the surface wind stress (Charnock (1955)) Observed SST, Bulk formulae for sensible and latent heat fluxes
Gravity Wave Drag	Based on Alpert et al. (1988)	Lindzen and Pierrehumbert Scheme

The physical parameterization schemes used in both the models are summarized in Table 9.2.

The specifications of the surface boundary fields and cloud parameters for T254L64 and T80L18 models are given in Table 9.3.

Table 9.3: Specifications of Initial Surface Boundary fields and Cloud Parameters

Fields	Land		Ocean	
	T254	**T80**	**T254**	**T80**
Surface temperature	Forecast	Forecast	NCEP Analysis	NCEP Analysis
Soil moisture	Forecast	Forecast	NA	NA
Albedo	Climatology (S)	Climatology (S)	Climatology (S)	Climatology (S)
Snow cover	NCEP Analysis	Forecast	NCEP Analysis	Forecast
Roughness Length	Climatology (S)	Climatology (S)	Forecast	Forecast
Plant resistance	Climatology (S)	Climatology (S)	NA	NA
Soil temperature	Forecast	Forecast	NA	NA
Deep soil temperature	Climatology (A)	Climatology (A)	NA	NA
Convective cloud cover	Forecast	Forecast	Forecast	Forecast
Convective cloud bottom	Forecast	Forecast	Forecast	Forecast
Convective cloud top	Forecast	Forecast	Forecast	Forecast
Sea Ice	NA	NA	NESDIS Analysis	NCEP Analysis

(S) --- Seasonal (A) --- Annual

One cycle of analysis (SSI) takes about 70 minutes of computing time in 112 SSPs (Single-Streaming Processor) on Cray X1E compared to 10 minutes for T80L18 SSI on Cray-SV1. The model takes about 100 minutes of computation time in 28 MSPs (Multi-Steaming Processors) of Cray X1E for a 168-hr model forecast

compared to 30 minutes for T80L18 model on Cray-SV1. Due to this large computational time required for T256L64, analysis-forecast system runs 4 times a day for four assimilation cycles (i.e., 0000, 0600,1200,1800 UTC) with a strict data-cut off of 6 hours. In the case of T80L18, though a rapid update cycle with data cut-off of 6-hr runs everyday for 0000UTC cycle, at the end of the day, the entire suit reruns with a large data cut-off (~12 hrs.) and the output from this suit are archived as operational output.

Performance of the Observation Processing and Analysis during Southwest Monsoon

Medium range weather forecast is critically dependent on the observations and the analysis procedure that produce the initial conditions. The whole process - preparation of the initial condition and also the medium range integration of the atmospheric model - can be considered as a single process in which the trajectory of the state of the atmospheric model is corrected using observed data, up to the time of the initial point of the medium range forecast. The medium range forecast is a continuous integration of the model for 168hrs (7 days) forward in time, starting from the initial condition. The forecast also depends on the surface boundary conditions that may have two-way or one-way interaction with the atmosphere. The 'true' state of the atmosphere (or in this case that of the Southwest Monsoon) is what is produced by the analysis procedure. Most of the error calculations of the forecast use the analysis (the term analysis is also used to indicate the state of the atmosphere as produced by the analysis system for a particular time, say 00UTC) as 'truth'. Therefore it is essential to examine the performance of the analysis system before considering the forecasts. This we do using the concrete example of the Southwest monsoon of 2007 when two different analysis-forecast systems were running in parallel. Such a comparison is very instructive in appreciating the dependence of a monsoon analysis on forecast-analysis systems.

Analysis performance

A comparison of Analysis performance between T80L18 and T254L64 global data assimilation systems was carried out by computing root mean square error (RMSE) of both the analyses against the upper air observations (RS/RW and Pilot Balloon) on daily basis for the Southwest Monsoon of 2007. Fig.9.2 shows the RMSE of 00UTC profiles for z, q, u, v, t at different heights. It clearly shows improvement in zonal and meridional components of wind and also the geopotential

height at all levels in the T254L64 system. The same is true for temperature but the improvement is marginal in the middle levels and it is larger in the upper and lower tropospheric levels. In the case of humidity the improvement is confined to 700 – 400 hPa layer only. There is 10 to 30 percent improvement in RMSE of the analysis fields in the case of T254L64 system except for lower level humidity. One may note the fairly large magnitudes of the errors, their variation with altitude and also the difference in errors from one analysis system to another analysis system. It clearly points to the necessity to decrease these errors on a continuous basis by improving the analysis system (by improving the assimilation techniques as well as by increasing the quality, quantity and types of observations).

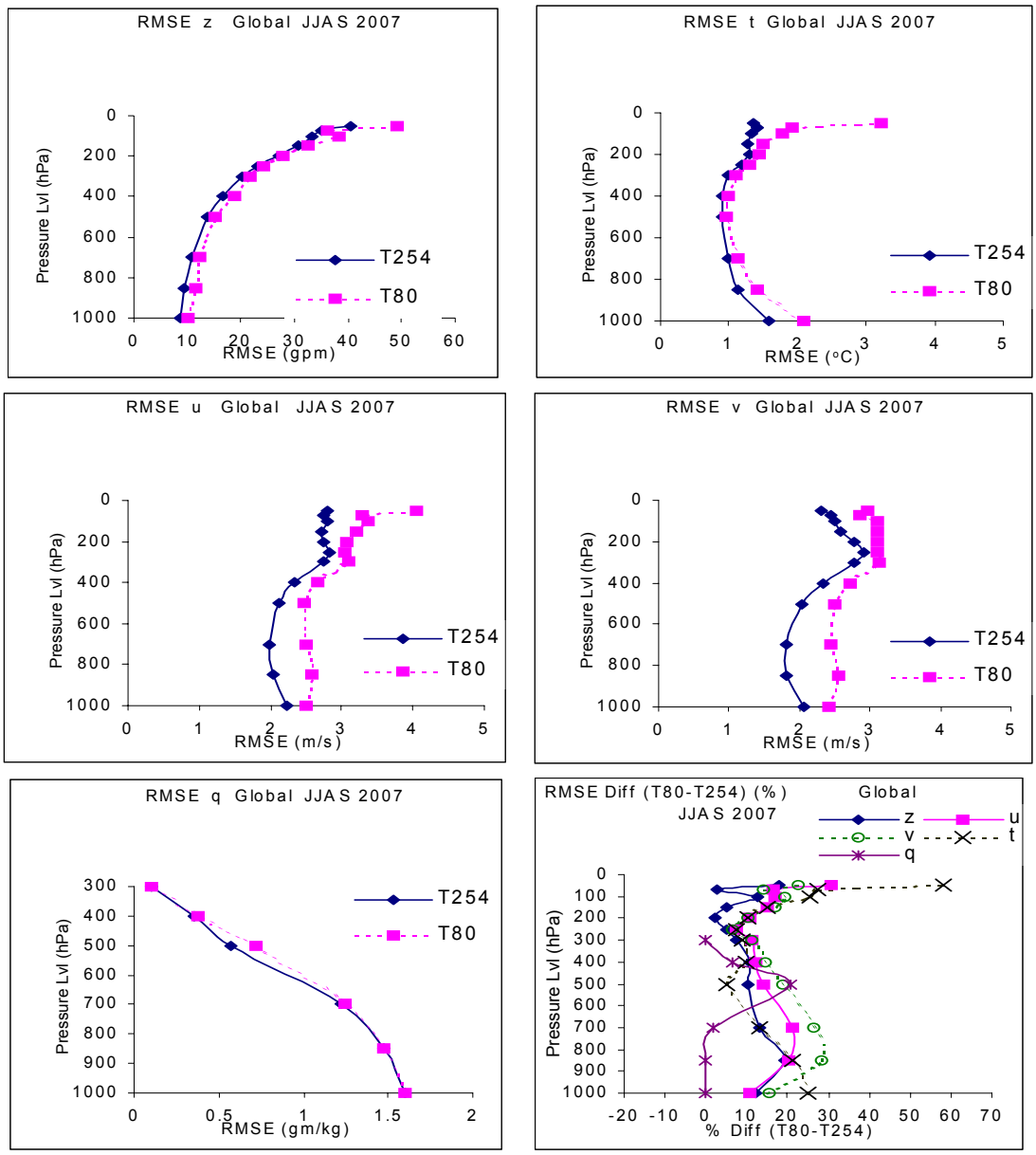

Fig.9.2: RMSE of analysed fields computed against upper-air observations for T254L64 and T80L18 GDAF (averaged for 0000UTC June-September 2007) (a) geo-potential height z, (b) temperature t, (c) zonal wind u, (d) meridional wind v, (e) specific humidity q and (f) change in RMSE (T80-T254)

9.5. Medium Range Forecast of Southwest Monsoon

The numerical forecast gives the values of a large number of variables ranging from the basic ones like temperature, pressure, horizontal wind components and humidity to precipitation, cloud cover, etc. The forecast could further be processed and diagnosed to obtain physically or practically relevant quantitative or qualitative (e.g. the occurrence of fog; maximum and minimum temperature at a location) information. In meteorological practice it is very useful to convert these numerical values into customary forms like weather charts and also describe the state of the atmosphere in terms that are in consonance with commonly used conceptual models. (for example, in terms of 'active' monsoon; intensity of 'heat low', etc.)

Southwest Monsoon is an exceptionally persistent and stable flow structure with clear-cut morphology and it is normally described (very effectively) in terms of a set of so-called semi-permanent and transient features. We follow this tradition in the Indian meteorological practice, while evaluating medium range weather forecasts during the Southwest Monsoon. In some cases the forecasts are considered like values of variables at grid points and in other cases we describe them more in terms of morphologically distinct features that have considerable geographical extent.

Medium range forecast at NCMRWF is carried out for 7 days in to the future. However, the errors beyond 5 days are usually too large and highly variable in the Tropics. The detailed description of errors beyond 5 days has little relevance in the present discussion. We, therefore present error estimates to 5 days (namely, 24hr, 72hr and 120hr forecasts). This is done for the monsoon period of 2008 so as to be representative of the current status of the MRF. There is no single criterion that can satisfactorily measure the error of a forecast. We had used a battery of measures to monitor the errors. However, in this discussion, as a rule, we show the root mean square errors or the changes in mean conditions to keep the size of the discussion within reasonable limits.

9.6. Systematic Errors in the Medium Range Prediction of the Southwest Monsoon

Model forecast errors are usually separated into systematic (time mean) and random errors. The systematic errors are largely owing to the deficiencies in the model formulation. The diagnosis of model systematic errors is essential for

identifying the model deficiencies and improving the skill of model forecasts. The nature and geographical distribution of systematic errors seen in the NCMRWF global T254 model forecasts are discussed below using the seasonal (June-September) means of analyses and medium range (24hr, 72hr and 120hr) forecasts. Before that we consider the mean analysis of wind at 700 hPa isobaric surface and its difference (anomaly) from climatology for July. The anomalies provide an estimate of the magnitude and spatial pattern of the inter-annual variability of the monthly mean conditions as present in the NCMRWF analysis.

Mean Monthly Conditions

The mean monthly conditions during the Southwest Monsoon of 2008 were as given below. Charts are presented for 700 hPa of July only, but the discussion may cover features at other levels and also for other months. The information provided below is relevant while interpreting the information in the subsequent sections.

June: At 850 hPa level, an anomalous cyclonic circulation was seen over the northern Arabian Sea and adjoining parts of Gujarat. This anomalous cyclonic circulation was also observed at 700 hPa level. Anomalous easterlies were observed over the northern plains of India at 850 and 700 hPa levels. At 500 hPa level an anomalous east-west cyclonic circulation is seen over the eastern and central parts of India. These features resulted in a stronger than normal monsoon trough. The central and northern parts of India received more than normal rainfall. At 200 hPa level, the Tibetan anti-cyclone was stronger than normal.

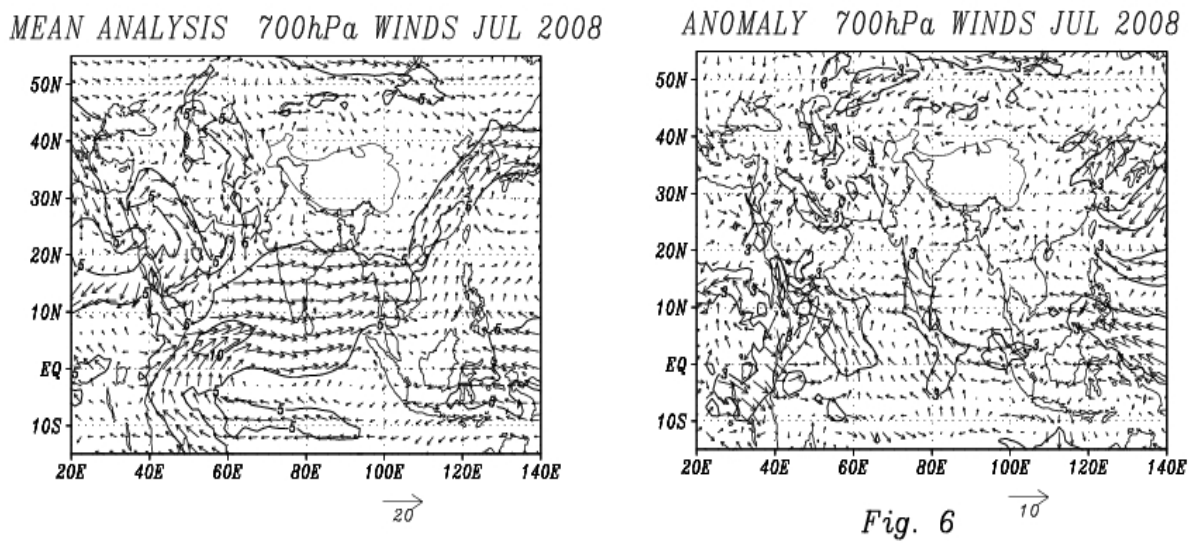

Fig. 9.3: Geographical distribution of mean wind field (a) and anomaly (b) at 700 hPa; for July 2008. Anomalies are departures from the 1994-2003 base period. [Units: m/s, Contour interval: 5m/s for analyses and 3m/s for anomalies]

July: In the lower tropospheric levels (850 and 700 hPa) an anomalous anti-cyclonic circulation was seen over the southern peninsula and adjoining areas (Fig.9.3), resulting in a weakening of the low-level westerly flow. The observed rainfall was deficient over the west coast and central parts of India. Westerly anomalies were seen over the plains of India in the lower tropospheric levels. At 200hPa level the tropical easterly jet was weaker than normal.

August: In the lower tropospheric levels (850 and 700 hPa) anomalous anti-cyclonic circulations were seen over the central Arabian Sea and the central Bay of Bengal. Anomalous easterlies were seen over the northern parts of peninsular India in the lower tropospheric levels. The observed rainfall was in excess over most parts of peninsular India.

September: In the lower tropospheric levels (850 and 700 hPa) anomalous cyclonic circulation was seen over the western parts of India and adjoining areas. An anomalous cyclonic circulation was seen over the eastern parts of India. The observed rainfall was in excess over Gujarat and adjoining areas, the west coast and Orissa. An anomalous anti-cyclonic circulation was seen over the southern Bay of Bengal in the lower tropospheric levels.

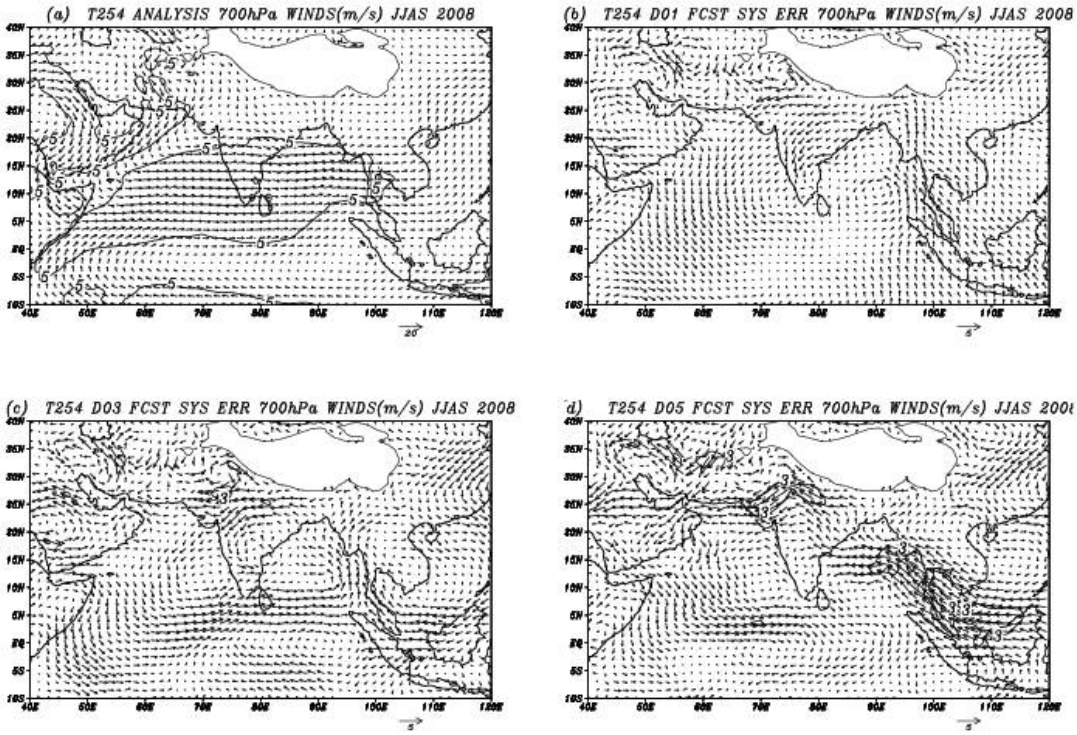

Fig. 9.4: Mean T254 analysed wind field (a) and systematic forecast errors for Day-1 (b), Day-3 (c) and Day-5 (d) at 700 hPa. .
[Units: m/s, Contour interval: 10m/s for analyses and 5m/s for forecast errors]

Systematic Errors

The systematic errors of the 1, 3 and 5 day forecasts are given below. They are shown for the season as a whole for the pressure levels of 850 and 200 hPa. The geographical distribution of the mean analysed wind and the systematic forecast errors for the T254 model at 850 hPa and 200 hPa are shown in Fig.9.4 and Fig.9.5. The notable features seen in the systematic errors of the 850hPa flow pattern are the anomalous easterlies over eastern and central parts of India. This feature is also seen at 700 and 500 hPa levels. An anomalous cyclonic circulation is also seen over the northwest parts of India and adjoining Pakistan at 850 hPa level. The incursion of dry air could be a reason for the scanty rainfall observed in the model forecasts over the northwest parts of India. The low-level jet strength seen in the mean analysis is maintained throughout the forecast period. At 200 hPa, the most significant feature in the systematic errors is the weakening of the Tropical Easterly Jet.

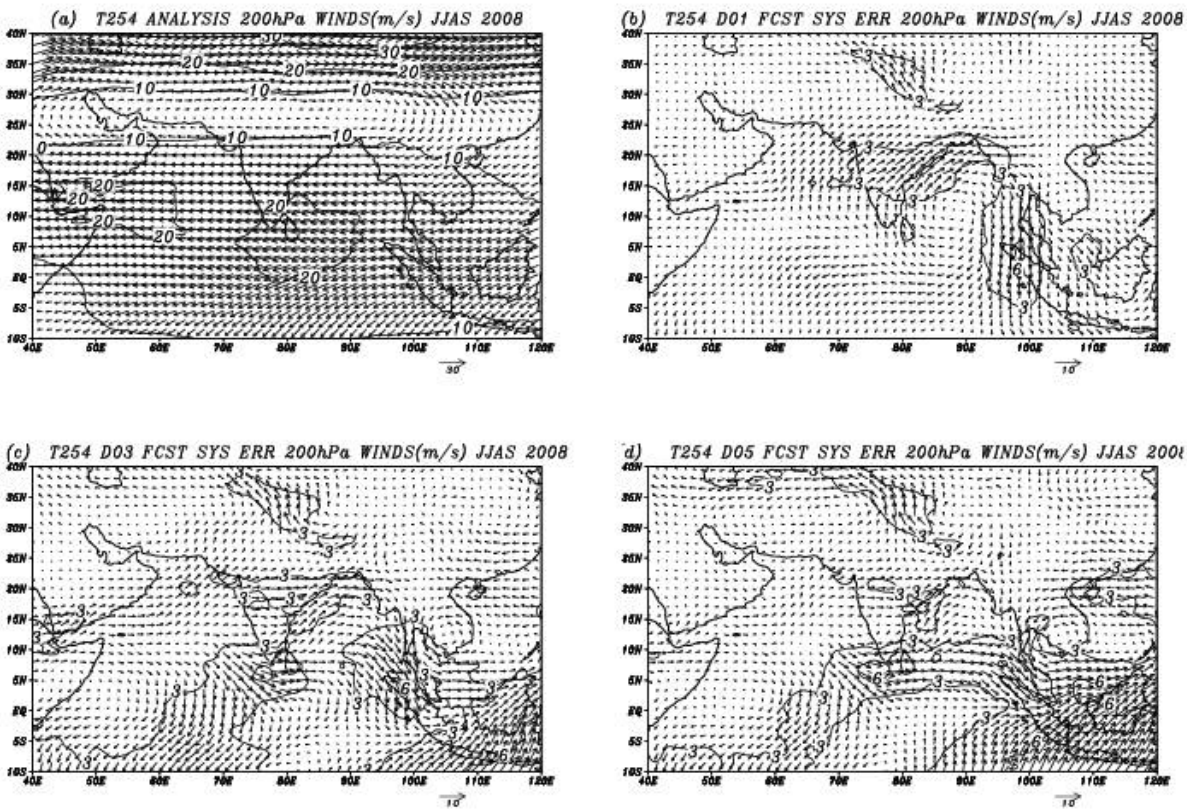

Fig.9.5: Mean T254 analysed wind field (a) and systematic forecast errors for Day-1 (b), Day-3 (c) and Day-5 (d) at 200 hPa. .

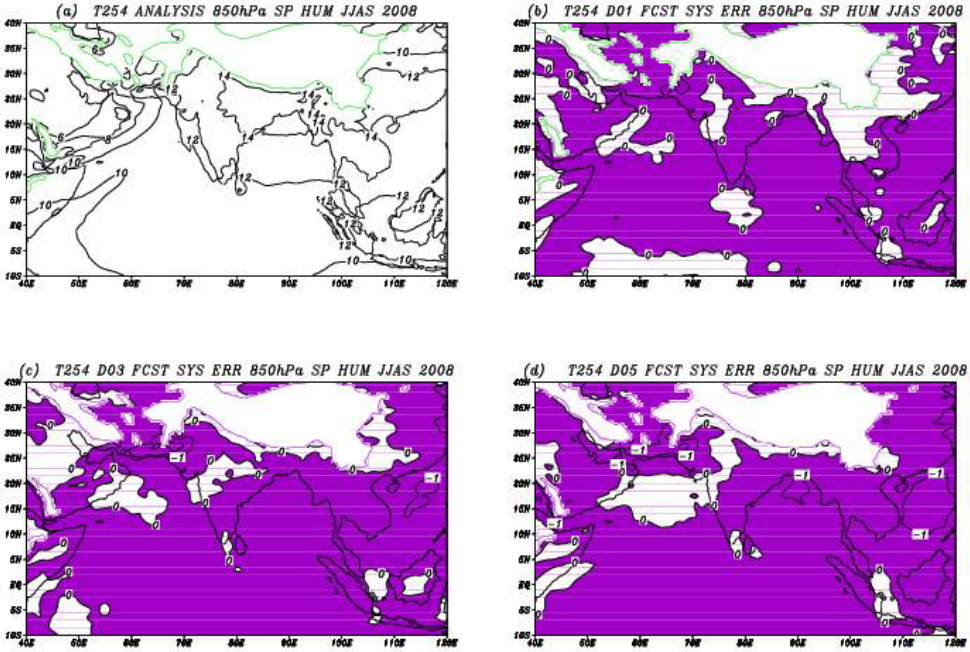

Fig. 9.6: Systematic error of 850 hPa temperature (analysis, 1,3,5 Day forecast)

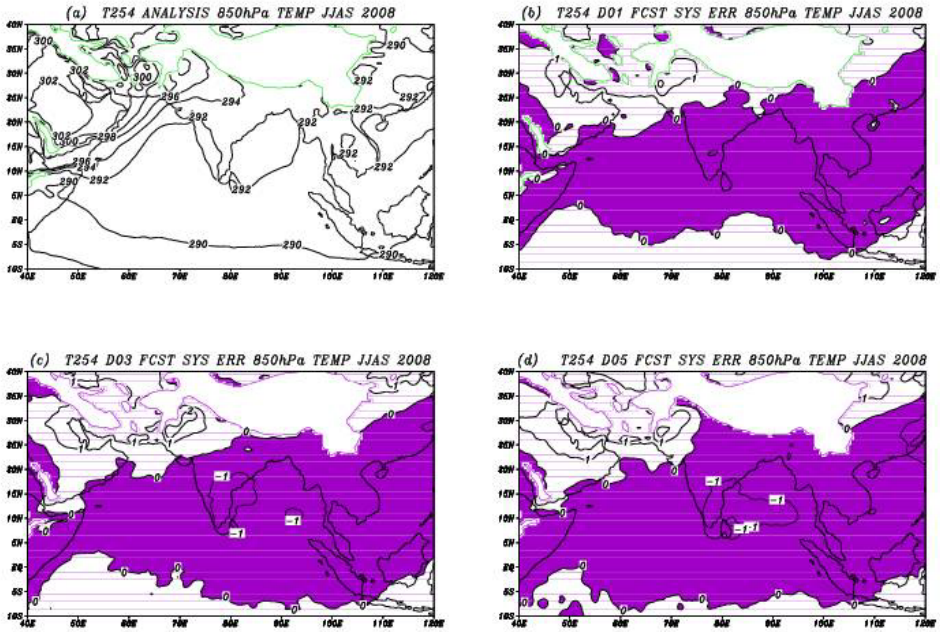

Fig. 9.7: Systematic error of 200 hPa temperature (analysis, 1,3,5 Day forecast)

Geographical distribution of the mean systematic forecast temperature errors for the T254 model at 850 hPa and 200 hPa level are shown in Fig. 9.6(a-d) and 9.7(a-d) respectively. The T254 model forecasts show a warm bias in the lower troposphere over the continents in general, and a cold bias over the oceans. Over the northwestern parts of India, at 850 hPa level a warm bias is seen which is associated with the cyclonic wind errors described in the earlier section. In the upper

troposphere also the T254 model shows a cold bias over the northern parts of India and a warm bias over the central and peninsular India.

9.7. Error Estimates of medium range forecasts

Objective verification scores against the analysis and observations are computed every day valid for 00UTC at standard pressure levels for different areas as recommended by the WMO. Monthly averages are then computed from the daily values of all forecasts verifying within the relevant month.

Fig. 9.8 shows the rmse of the magnitude of the wind vector (RMSEV) for the NCMRWF operational model day 03 forecasts against the radiosonde observations over the Indian Region since January 1999, at 850 hPa level. The most notable feature of the error variation is its seasonal cycle with the winter months having least error and the Southwest Monsoon having the largest error. The increase in errors from winter to summer is 2 m/s, which is about one third of the annual mean error. The winter to summer increase of error is a feature seen in forecasts of other centres as well. However the substantial increase in the errors as well as their magnitudes during Southwest Monsoon demonstrate that it is necessary to greatly improve the accuracy of the forecast-analysis system. It is also seen that there was a continuous increase in error from 2003 to 2006. It is also seen that there is a drop in the error before the beginning of Southwest Monsoon. The reasons for these kinds of changes are not clear. One may also note the significant reduction in the forecast errors accompanying the operationalisation of the T254 forecast-analysis system on 1 June 2007. The errors of the T254 model during monsoon 2008 were less than during monsoon 2007. This reduction in error was brought about mainly because of the improvements in the assimilation system and the use of more data.

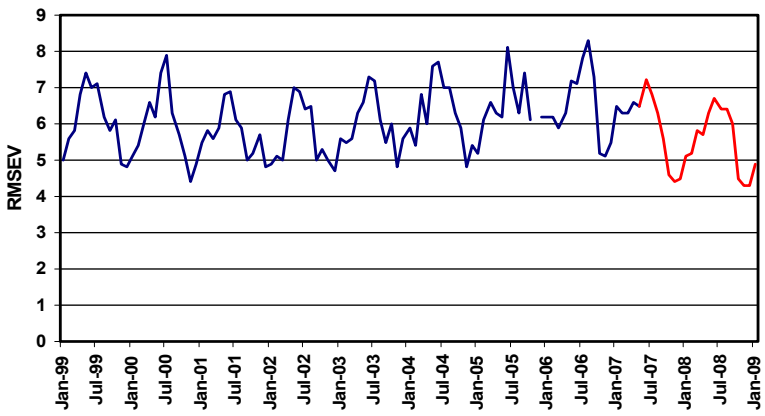

Fig. 9.8: Ten year time series of monthly mean rmse of the vector wind against radiosonde observations in the Indian Region at 850hPa from 1999 (NCMRWF 3day forecast). Blue corresponds to T80 system and red to the T254 system.

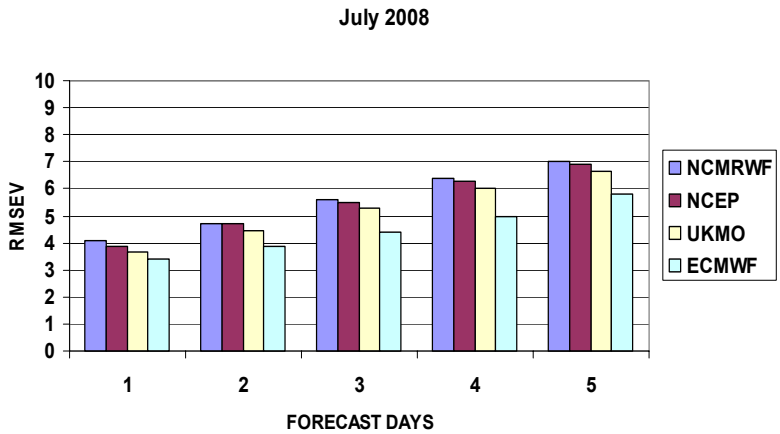

Fig.9.9: RMSEV for 850hPa for the Indian Region July 2008

The status of the errors of the forecasts of NCMRWF during Southwest Monsoon (July 2008) vis-a-vis those of NCEP, UKMO and ECMWF were computed and are shown below. Fig.9.9 shows the RMSEV of winds for the T254, NCEP, UKMO and ECMWF model forecasts against the radiosonde observations over the Asian region (25 - 65 N, 60 -145 E) for the Southwest Monsoon of 2008 at 850 hPa. It is seen that the ECMWF forecasts have the least error among the four models. The NCMRWF forecast errors are comparable to that of NCEP. The differences between the errors of the NCEP,UKMO and NCMRWF are small compared to the magnitude of the errors.

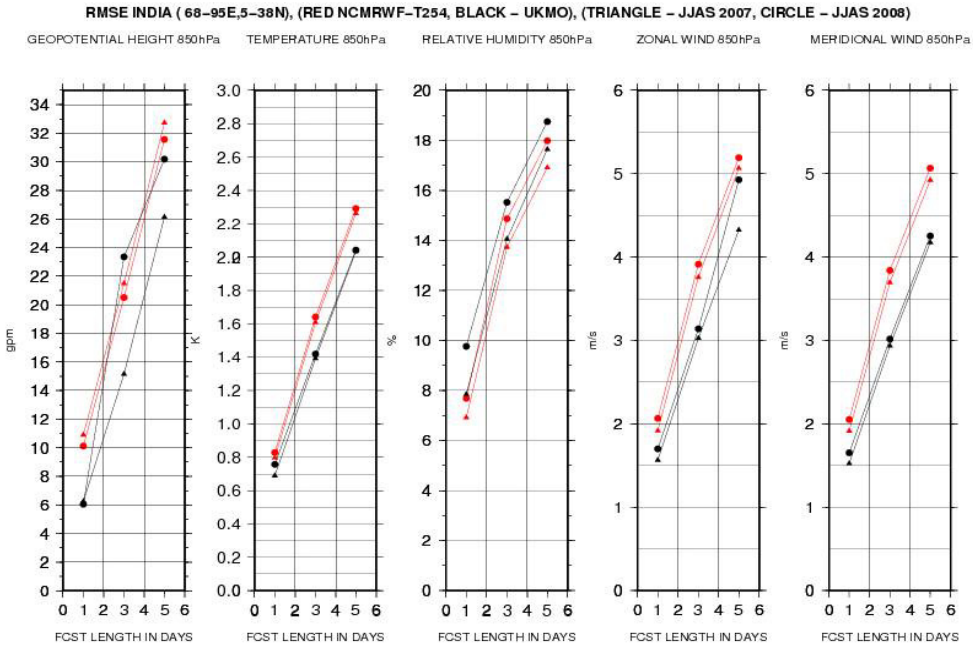

Fig.9.10: RMSE of medium range forecasts over India (see inset map in Fig.9.11). Please see the title of the figure for details. The UKMO forecasts are provided for comparison.

In Fig.9.10 and Fig.9.11 the RMSE of NCMRWF and UKMO forecasts over India (65-95E,5-38N, excluding mountains) for the 2007 and 2008 Southwest Monsoons are given. In these error computations the analysis of the respective systems is take as 'truth'. In Fig.9.10 the RMSE of the forecasts of Geopotential height, temperature, relative humidity and the horizontal components of wind at 850 hPa. The computed errors show that, in general the UKMO forecasts have less error. The sharp increase in error (more than 4 times the error of the 24 hr forecast) by day-5 is seen in all forecasts. We also see year to year changes in errors (for example RMSE of geopotential).

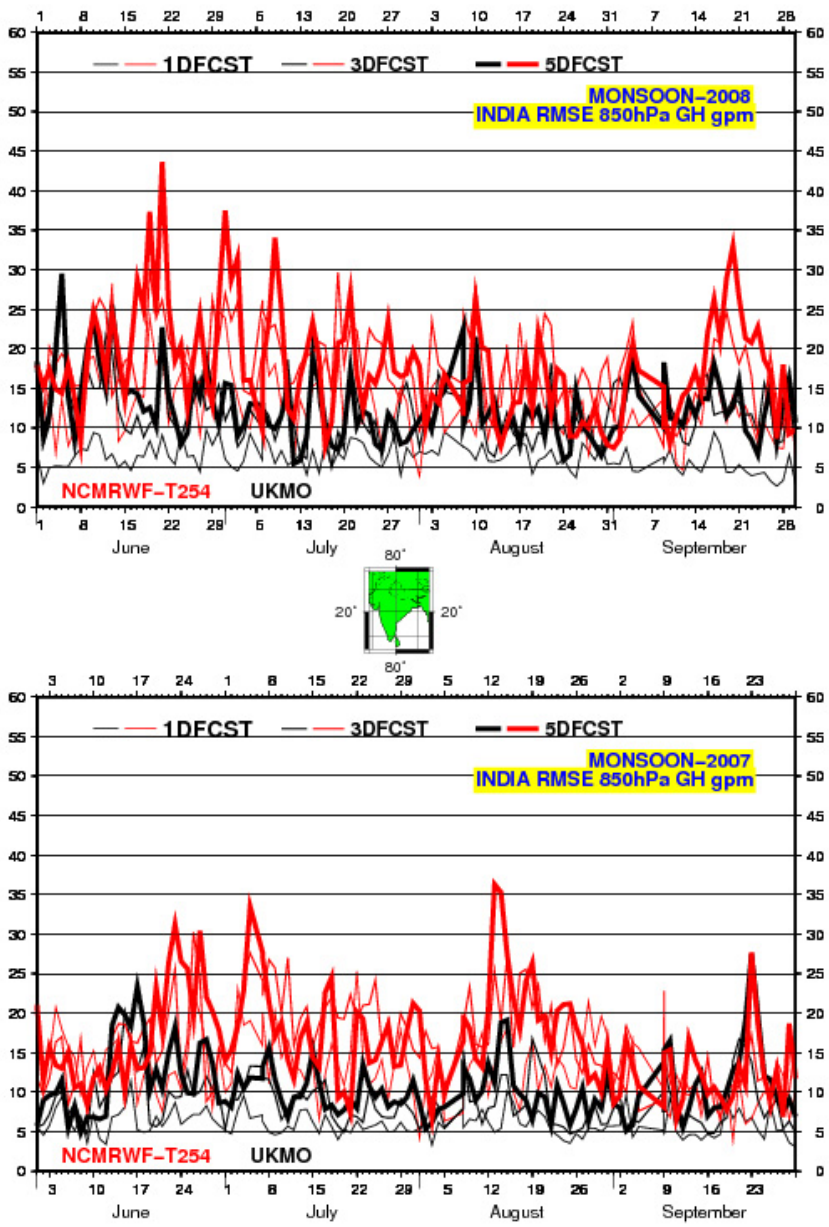

Fig.9.11: Spatial RMSE of 00UTC forecasts. Inset map shows region.

The variation of daily spatial RMSE of 850 hPa geopotential height for India is shown in Fig. 9.11. The most striking feature is the large variation of errors that persist for a period of few to several days. Generally the UKMO forecast errors are less than the errors of NCMRWF forecasts. It is seen that there are occasions when the errors of the 5 day forecasts drops to the error level of 1-day forecasts. This demonstrates that the forecast systems on certain occasions during the monsoon produce fairly accurate deterministic forecasts even with a lead-time of 5 days.

9.8. Monsoon specific forecasts

a. Medium Range forecast of Onset and Advancement of Monsoon

The normal onset date of southwest monsoon over Kerala is 1 June, with a standard deviation of eight days. Monsoon affects not only rainfall but also tropospheric wind, humidity and temperature fields. An objective method for determining monsoon onset, advancement and withdrawal date using dynamic and thermodynamic precursors form NCMRWF T80L18 analysis-forecast system was developed (Ramesh et al. 1996, Swati Basu et al. 1999.) and used since 1995 at NCMRWF. The same has been extended for NCMRWF T254L64 analysis-forecast system 2008.

Rise of kinetic energy (KE) above $60m^2s^{-2}$ at 850 hPa over Bay of Bengal (BOB - as defined in the publications cited above) was noticed first on predictions valid for 12 May and also in the analysis of 12 May. There was a rise in Net Tropospheric Moisture (NTM) above 40 mm on 8 May, followed by a sudden fall at 11-12 May and then further increase thereafter till 10 June. Fall in the mean tropospheric temperature (MTT- as defined in the publications cited above) was also noticed almost around the same time. So, following the objective criteria based on data from NCMRWF T254L64 analysis-forecast system, the date of onset over BOB was determined as 12 May. IMD, based on their criteria, declared the onset over southwest Bay and adjoining parts of Andaman Sea and Bay Islands on 10 May, 2008.

Onset over Kerala (Arabian Sea Branch):

In 2008, according to IMD, monsoon onset over Kerala was on 31 May. The rapid advance of monsoon over Arabian sea (ARB) and adjoining west coast of India

took place mainly due to a depression (5–6 June) over the east central Arabian Sea and a well marked low pressure area (9–11 June) over Saurashtra and Kutch.

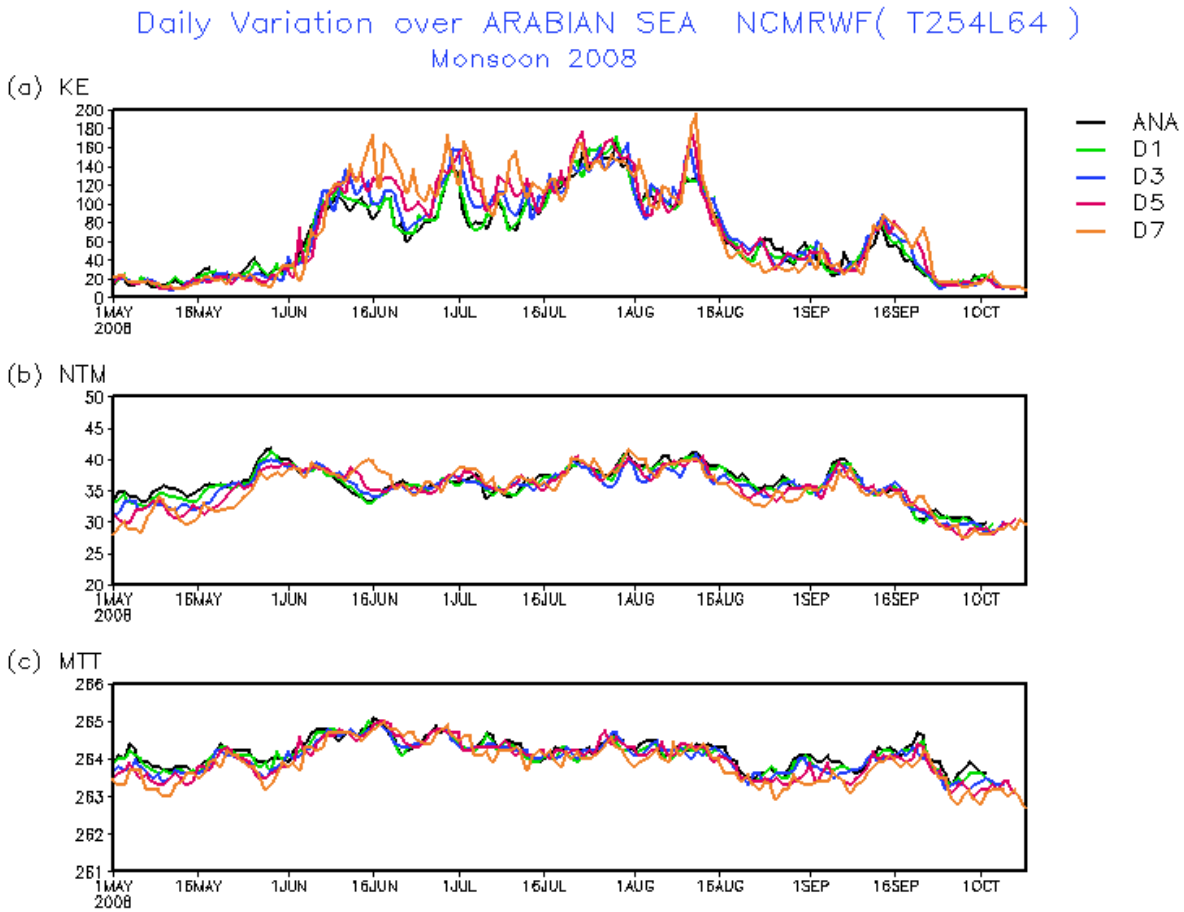

Fig.9.12: Daily variation of (a) Kinetic energy, (b) Net Tropospheric Moisture and (c) Mean Tropospheric Temperature over Arabian Sea

In Fig. 9.12 the daily variations of analysed and predicted KE at 850 hPa, NTM and MTT computed over ARB (0-19.5° N, 55.5°E-75°E) from 1 May onwards are shown. KE at 850 hPa over ARB exceeded the threshold value 60m^{2}s^{-2} on 4 June in the analysis and predictions, and then increased to 120 m^{2}s^{-2} on 6 June. Prior to that, from 28 May onwards, NTM also reached about 40mm and from 4 June onwards the steady decrease in NTM is noticed up to 16 June. This decrease was basically due to occurrence of rainfall associated with monsoon onset over the region. Hence, based on T254L64 analysis-forecast system the onset date of monsoon over Kerala was determined as 4 June.

Advancement of Monsoon

For determining the advancement of monsoon over different locations over Indian mainland, NTM, MTT and wind direction and speed at 850 hPa in analysis and predictions are examined over 43 locations over India. Table 9.4 shows the dates of advancement of monsoon at important locations over India using NCMRWF analysis and forecasts along with the dates according to IMD (as northern limit of monsoon) In 2008, the rapid advancement of monsoon over west coast and monsoon trough region was seen mainly due to formation of two depressions, first over the Arabian Sea during 5th to 6th June and second depression over the Bay of Bengal during 16th to 18th June.

Table 9.4: Date of advancement of monsoon

Locations	Date determined by NCMRWF objective criteria	Date declared by IMD
Cochin	3 June	1 June
Mumbai	5 June	7 June
Gopalpur	8 June	9 June
Kolkata	8 June	9 June
Patna	8 June	10 June
Varanasi	9 June	12 June
Allahabad	9 June	12 June
Agra	12 June	15 June
Delhi	18 June	15 June
Jodhpur	20 June	10 July
Jaisalmer	16 July	10 July

The withdrawal of monsoon was late due to the presence of systems in westerlies over northwest India interacting with the monsoon circulation. IMD declared withdrawal of monsoon from north and northwest India on 29 September. NCMWRF analysis-forecast system suggested the withdrawal of monsoon from north and northwest India on 23 September.

b. Forecast of Monsoon Onset using Monsoon Indices

Forecasts from T254L64 system were used to compute three monsoon indices for monitoring the onset phase of the Southwest Monsoon during 2008. The indices are given in Table 9.5.

Table 9.5: Indices used in the analysis

Name of the Index	Type of Index	Domain of application	Definition in terms of regions	Reference
Wang and Ding	Circulation zonal wind	Tropical South Asia	U850 averaged over (5°N– 15°N, 40°E–80°E)	Wang et al .,2009
Goswami	Meridional wind	South Asia	V850 – V200 over (10°N – 30°N, 70°E – 110°E)	Goswami et al., (1999)
Syroka and Toumi	Circulation zonal wind	Tropical Asia	U850 (5°N – 15°N, 50°E–80°E) – U850 (20°N – 30°N, 60°E –90°E)	Syroka and Toumi (2002)

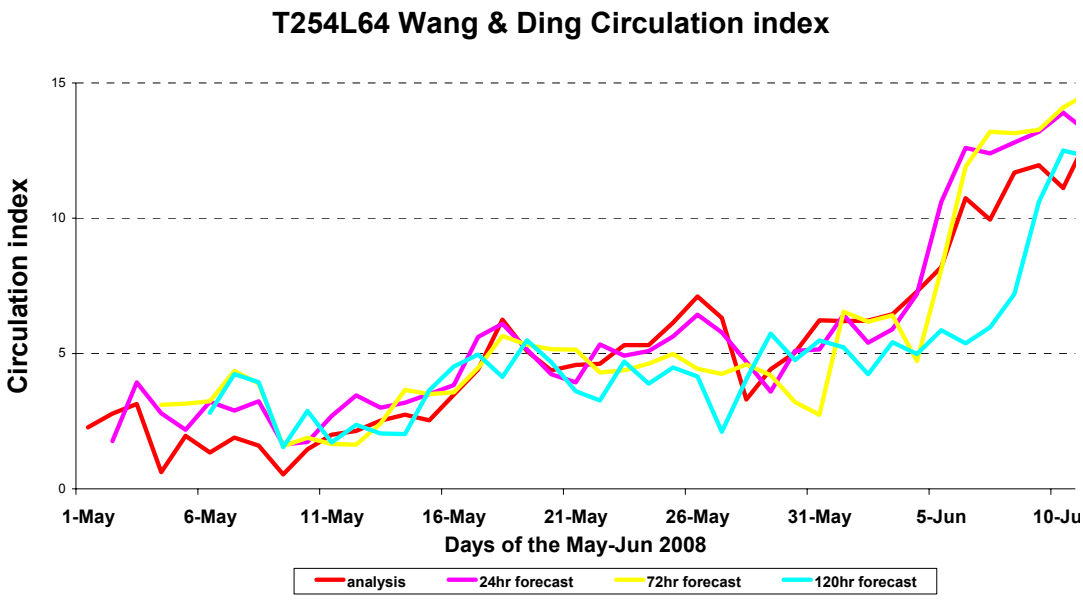

Fig. 9.13

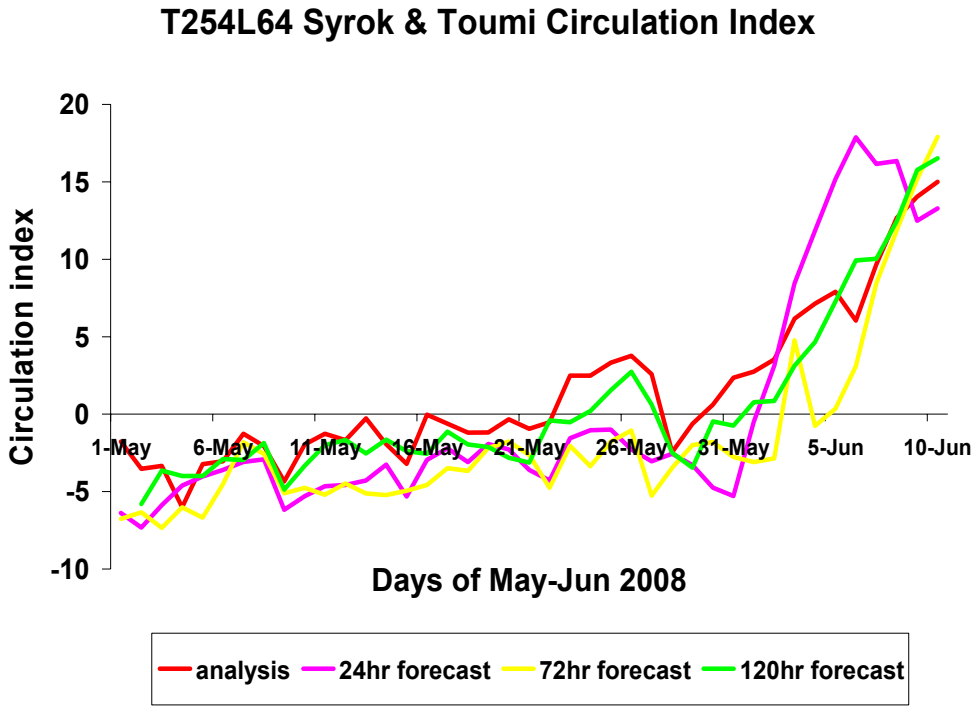

Fig.9.14

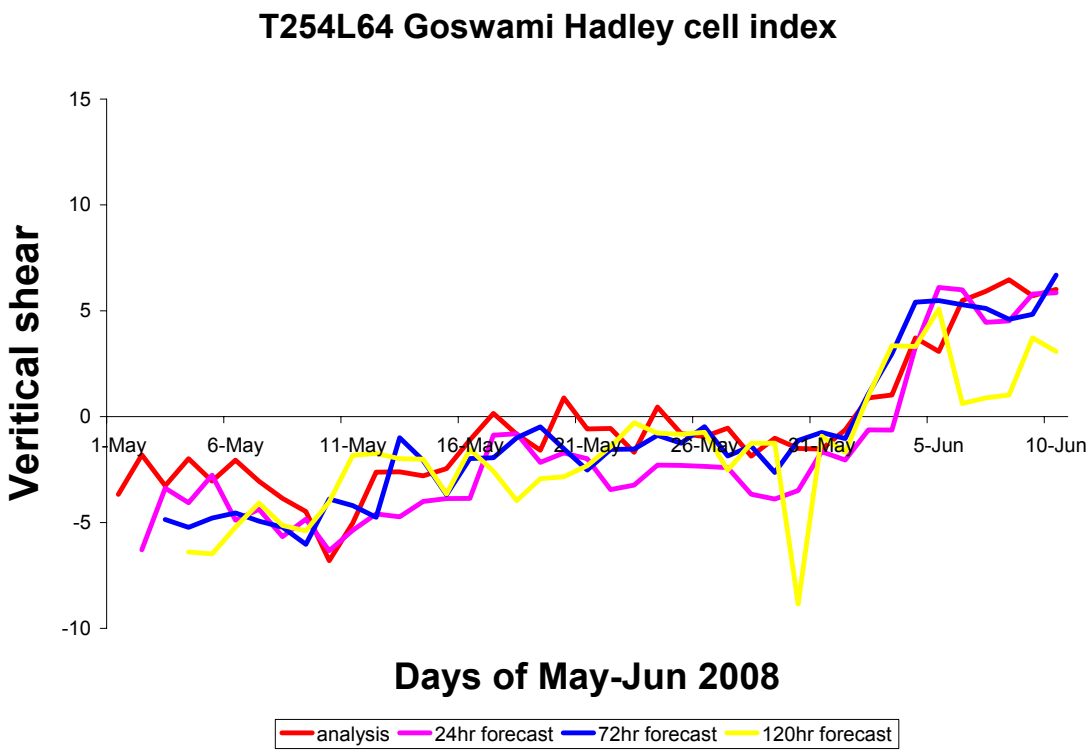

Fig. 9.15

The circulation index according to Wang and Ding (2009) for the analysis, 24hr, 72hr and 120hr are shown in Fig.9.13. The index indicates 31 May as the onset date - by the sustained westerly (U) exceeding 6.2 m/sec and persisting for more than six days i.e. up to 6 June. This high value of U persists beyond 6 June. In the forecasts, broadly, these features are captured well. However 72 hr and 120 hr forecasts have a delay of few days in predicting the onset.

In Fig.9.14 the circulation index of Syroka and Toumi (2002, 2004) for the onset phase is shown. The index based on analysis shows the onset date is around 30 May, because from that day onwards the daily index changes sign from negative to positive. The 24 hr, 72hr and 120hr forecasts also show the change of sign, but with a lag of three days.

The circulation index (vertical shear) based on Goswami et al., (1999) for the onset phase is shown in Fig.9.15. This is known as Hadley cell circulation index. The onset date is later than 31 May and is around 3 June. The index from that day onwards changes sign from negative to positive. The 24hr, 72hr and 120 hr forecasts also have the same trend and change the sign from negative to positive but with a delay of 2-3 days.

In general, the indices are able to distinguish the onset fairly well and are useful for this purpose. However, the MRF generally fails to predict the onset with a lead-time of 3 days.

c. Medium range prediction of Heat Low, Monsoon Trough, Monsoon Lows and Depressions

The deepest low-pressure area over Pakistan and adjoining NW India is known as the Heat Low. The intensity of heat low is a good indicator of the continental heating and land-sea contrast, which drives the monsoon. Deeper (shallower) heat low will usually be associated with stronger (weaker) North-South pressure gradient and enhanced (subdued) monsoon activity.The large-scale monsoon activity is closely associated with the position of the Monsoon Trough. Monitoring and prediction of the position and the intensity of the Monsoon Trough is thus very important for assessment of monsoon activity. The characteristics of these two semi-permanent features, viz. Heat Low and Monsoon Trough in the monthly mean of global model analysis and day-1 forecasts, day-3 forecasts and day-5 forecasts during 2008 are examined here.

d. Heat Low

The intensity of the heat low is represented in this study by the magnitude of the innermost closed isobaric contour on a mean sea level pressure chart. The average heat low centre pressure of NCMRWF T254 model analyses and forecasts for different months during the monsoon season (Fig.9.16) were examined to understand the behavior of the heat low. In all months, the mean heat low position is close to 70ºE, 28ºN in both in the analysis and forecast up to Day-5. In September, the mean MSLP values over this location is well above 1000 hPa. The Day-1, Day-3 and Day-5 forecast position of the heat low for all months, except September, are close to its analysis position.

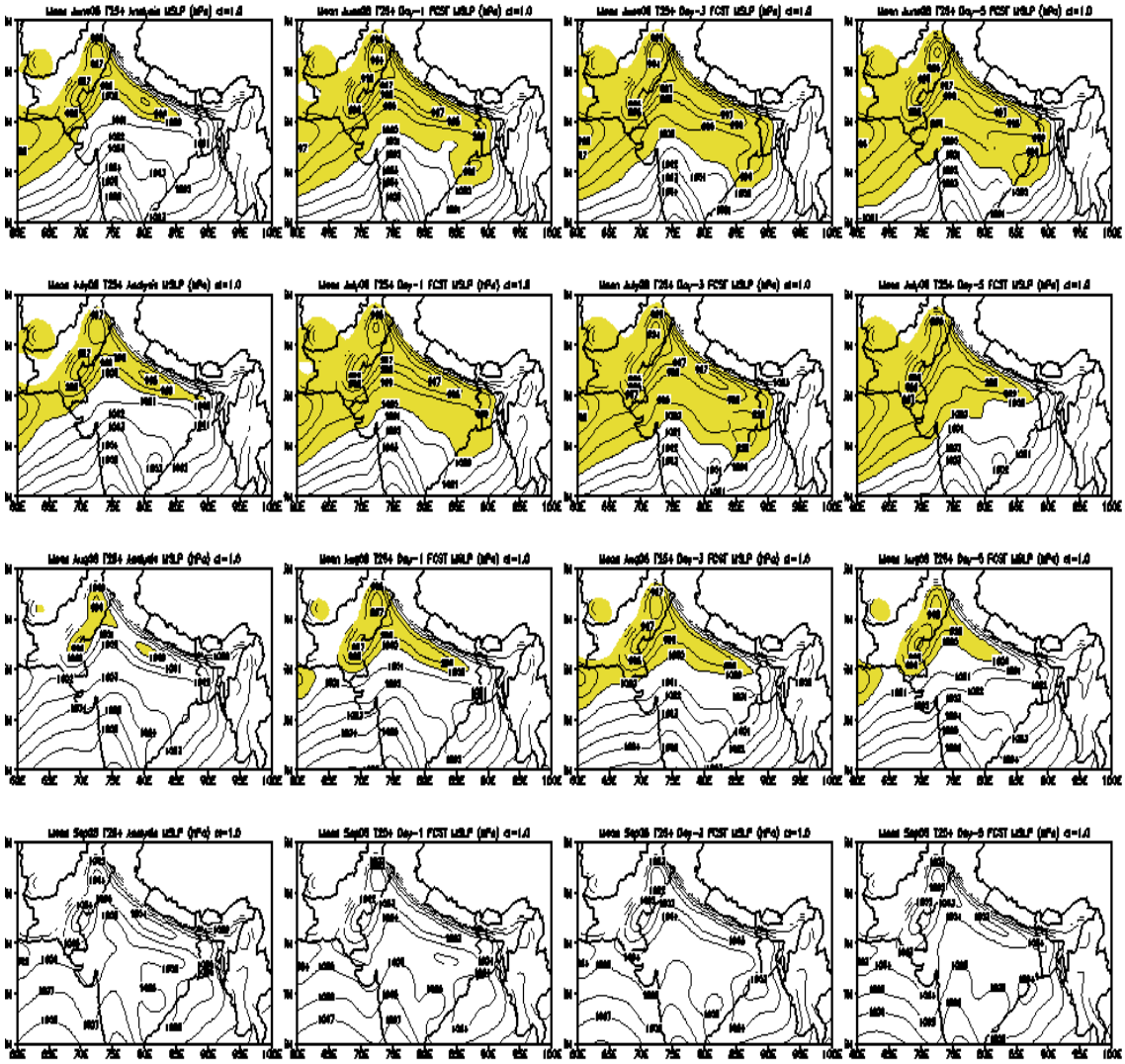

Fig. 9.16: NCMRWF T254 model monthly mean of MSLP analysis and Day-1, 3 and 5 (left to right) forecast over the Indian region for June, July, August and September, 2008 (top to bottom).

In June, the lowest MSLP contour in the analysis is 997 hPa and in the Day-1 forecast it is less (995 hPa). In Day-2 forecast, over the heat low region, MSLP values are around 995 hPa which increases in the Day-5 forecast. In July, MSLP at heat low region is around 997 hPa. As in June, the Day-1 and Day-3 values over heat low region are lower (994 hPa) and higher in Day-5 compared to Day-3 (995 hPa). In August, the heat low becomes weak in both analysis and forecast. The MSLP values in the analysis are around 999 hPa and in the Day-1 and Day-3 forecast the heat low intensified. In the Day-5 forecast, as in the previous months, heat low intensity is reduced (MSLP values are around 998 hPa). In September no heat low is seen in both analysis and forecast. It is seen that the heat low is generally more intense in model forecast as compared to the analysis. Also the Day-1 and Day-3 forecast intensity is greater than that of Day-5 forecast. In general, the model forecast tends to intensify the heat lows, compared to analysis.

e. Monsoon Trough

The strength and position of the monsoon trough at surface level in the T254 analysis and forecast is based on the MSLP charts (Fig. 9.16).

In June, compared to the mean analysis, Day-1, Day-3 and Day-5 forecasts show lower MSLP values over the monsoon trough region. The mean June position of the monsoon trough is the same in both analysis and forecast, up to day-5. During June it is located over the Indo-Gangetic plains close to foothills. In July, in the east the monsoon trough extends up to the head Bay, unlike in June when it extended only up to 86.0^0 E. As in the case of June, the intensity of the monsoon trough is higher in the forecast. The intensity of monsoon trough in Day-1 and Day-3 forecast is higher compared to day-5 forecast. The eastward and southward extension of the trough is also greater up to the Day-3 forecast. In August, the eastward extension of monsoon trough is similar to that of July. However, the MSLP values are much higher over the trough region in August. As in the previous months, in August also the MSLP values over the trough region are lower in the forecast compared to the analysis. In September, the monsoon trough is very weak both in analysis and in the forecasts.

f. Monsoon Depressions

During June-September 2008 four depressions formed. The tracks of all the systems are shown in Fig. 9.17. The analysis and forecasts valid for 00UTC of 18 September are shown in Fig.9.18. It is seen that forecasts reproduce a depression of similar intensity in the analysis and forecasts. The locations also roughly agree. It shows that the medium range forecast system is capable of simulating fairly well a monsoon depression. The prediction of the track of a depression is very useful and required information. In Fig.9.17 the predicted tracks are shown for all the depressions. The tracks predicted using mesoscale models and also the track based on UKMO medium range predictions are shown for comparison.

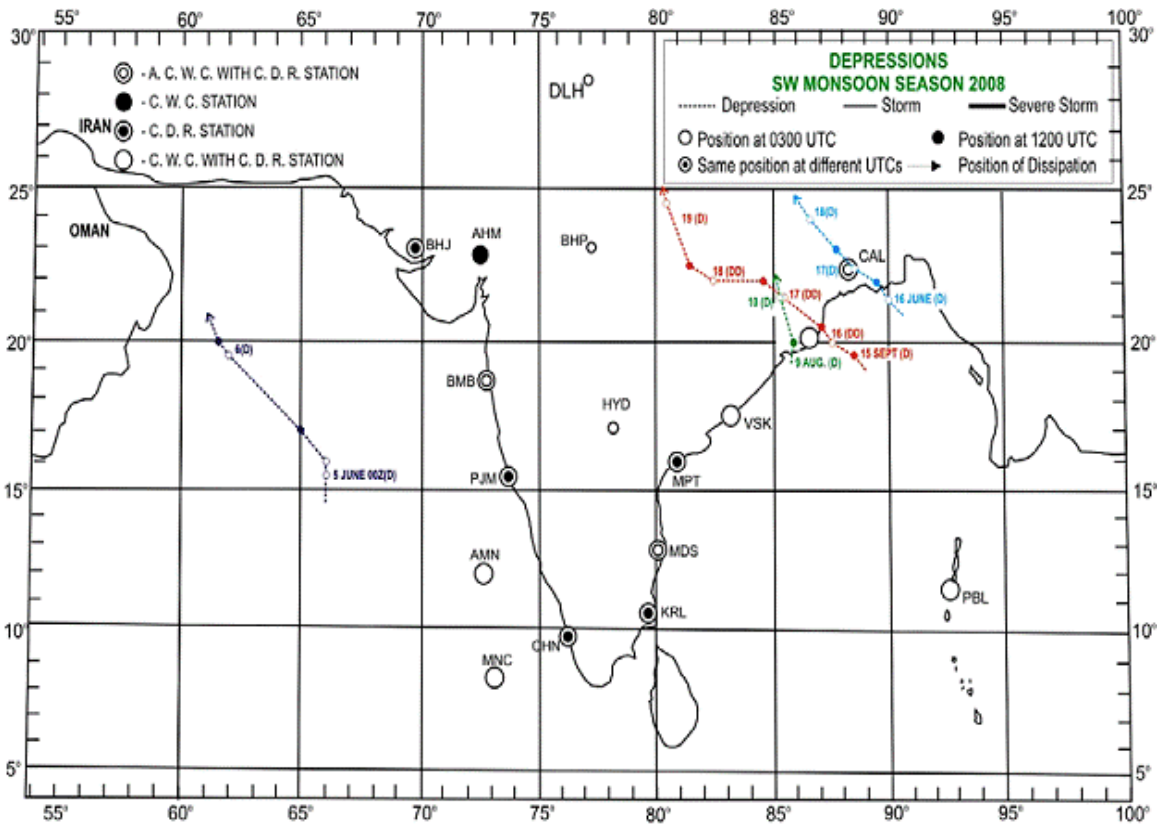

Fig. 9.17: Observed tracks of the Arabian Sea and Bay of Bengal Monsoon depressions during 2008

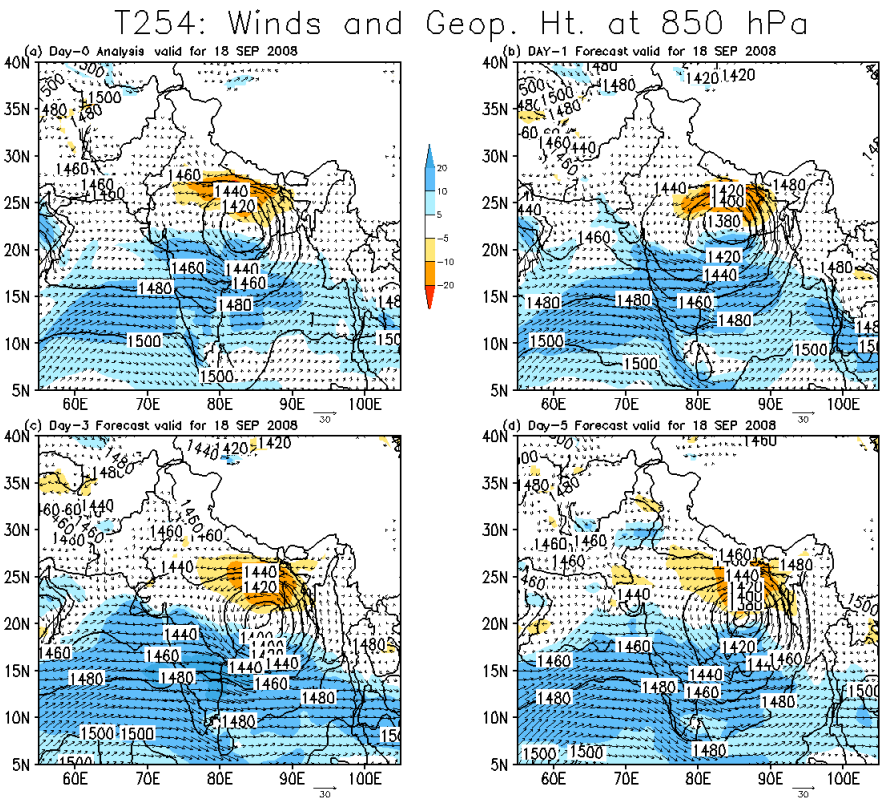

Fig. 9.18: Winds and Geopotential height at 850 hPa in the T254L64 analysis and forecasts valid for 18th Sept 2008.

Tracks of the Arabian sea depression in each of the model forecasts are shown in Fig.9.19. A comparison with Fig. 9.17 clearly shows that none of the models could correctly predict the northwestward trajectory of the system. Eta, T254 and UKMO predicted the movement in the northward direction while WRF and MM5 predicted movement in a wrong direction taking the system closer to the Indian coast. For the Bay of Bengal depression of June 2008, the models indicate a larger spread. The northwestward movement is captured only in the UKMO model. Although T254 also predicted the depression to move northwestward, the track is much to the south of the observed track. The mesoscale models have large errors and they keep the depression towards north. For the August 2008 depression off the Orissa coast, the models show better consensus and the tracks are closely packed. However for the September 2008 depression the models show no consensus. T254 and UKMO show north-west ward movement while the mesoscale models show northward movement.

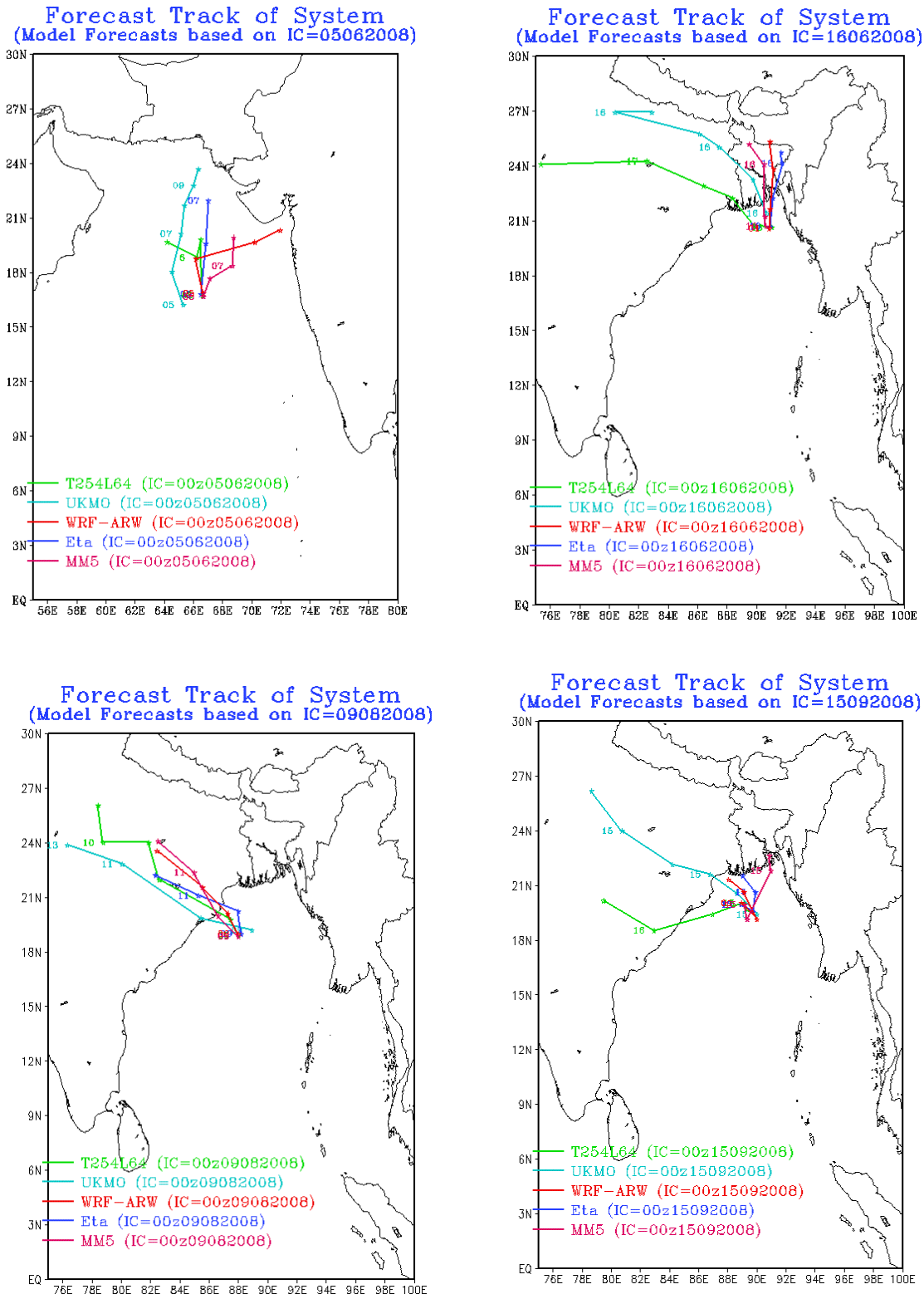

Fig. 9.19: Model predicted tracks of the Monsoon depressions during 2008. The green one is the prediction from the T254L64 system.

g. Mascarene High, Cross-Equatorial Flow, Low-Level Westerly Jet and North-South Pressure Gradient

The performance of the assimilation-forecast system with respect to the Mascarene High (MH), Cross-equatorial flow (CEF), the low level westerly jet (LLWJ) and the north-south pressure gradient along west coast is given below.

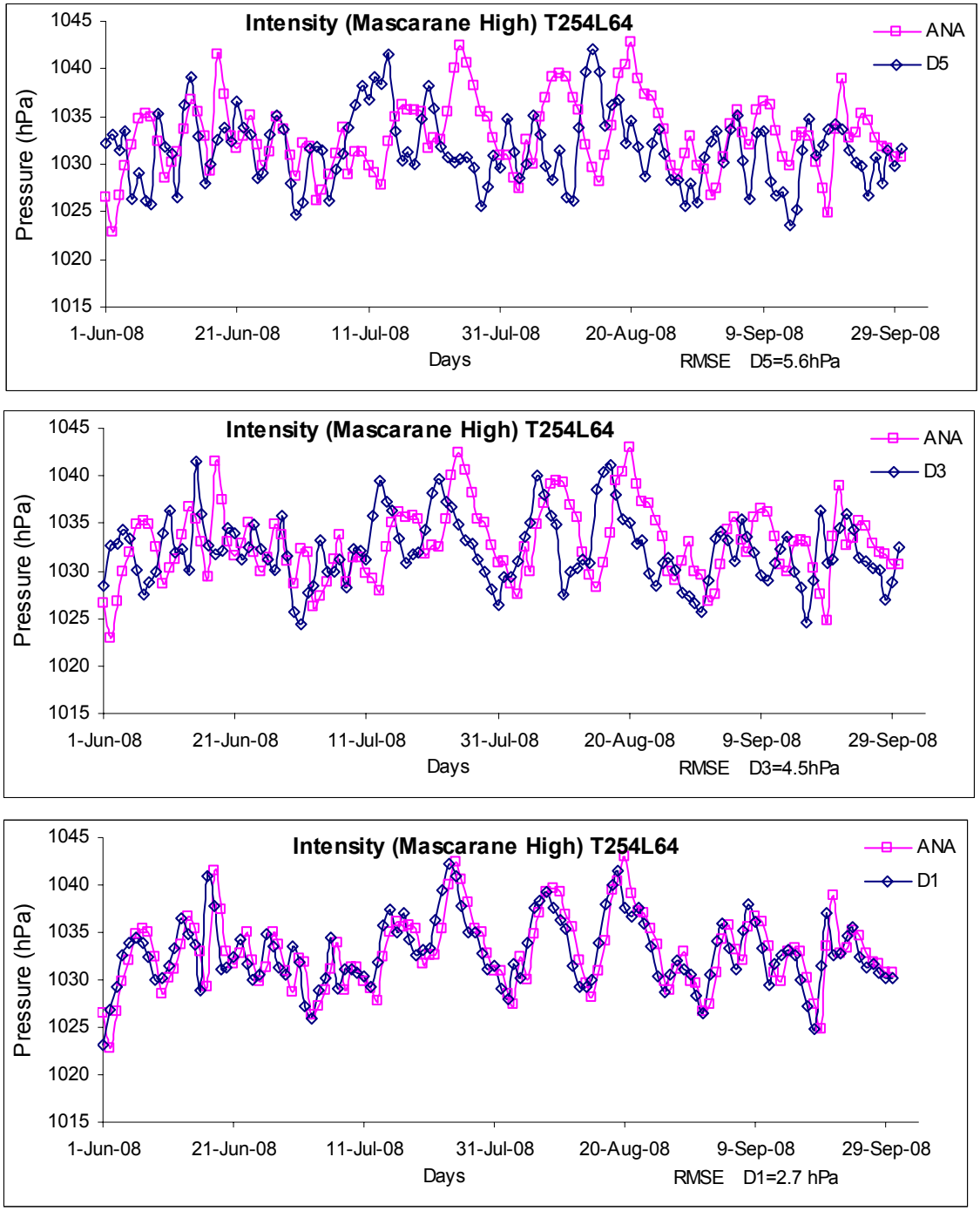

Fig. 9.20: Intensity of the Mascarene high in the analysis against Day-1, Day-3 and Day-5 forecasts during monsoon 2008.

Mascarene High (MH)

During monsoon 2008, the analyzed mean intensity of the Mascarene High was 1032.9 hPa (more intense) and its position was approximately at 70^0 E and 35^0 S. This position is south of the long-term (80 years mean data) observed mean location of 69^0 E, 27^0 S with intensity of 1024 hPa (Gorshkov, 1977). Fig. 9.20 shows the day-to-day variations of the intensity of the Mascarene High. The intensities produced in Day-1 forecasts agree very well with the analysis. For the Day-3 forecasts, good agreement is seen in general, except in the case of a few episodes. In Day-5 forecasts the disagreement is larger compared to Day-1 and Day-3 forecasts. The root mean square errors (RMSE) of the predicted intensity of the Mascarene High for Day-1, Day-3 and Day-5 forecasts are 2.7 hPa, 4.5 hPa and 5.6 hPa respectively.

The longitudinal and latitudinal positions of the Mascarene High (MH) were also analysed (not shown here). The Mascarene High moves west east in association with the passage of westerly waves in the southern hemisphere. The Day-1 forecasts are able to reproduce these variations very well. The agreement between the analysis and the Day-3 forecasts are also generally good, with just few noticeable mismatches. The Day-5 forecasts indicate that the variability in longitudinal positions are captured well, but have more errors compared to the Day-1 and Day-3 forecasts. The RMSE of the predicted longitudinal positions of the Mascarene High for Day-1, Day-3 and Day-5 forecasts are 16.9^0, 24.5^0 and 22.8^0 respectively. The Day-1 and Day-3 forecasts agree well with the analyzed latitudinal positions, except in few cases. In Day-5 forecasts the positional errors are high compared to Day-1 and Day-3 errors. The RMSE of the predicted latitudinal positions of the Mascarene High for Day-1, Day-3 and Day-5 forecasts are 3.6^0, 4.6^0 and 4.5^0 respectively.

Cross-Equatorial Flow (CEF)

The time mean analyzed, Day-1, Day-3 and Day-5 forecasts of the meridional wind at equator over the sector 30^0 E-100^0 E with mean taken over the entire monsoon period (June to September 2008) was computed. In T254L64 model, the analyzed field shows prominent maxima of 14 m/s around 40^0 E at 875 hPa representing the core of the Arabian Sea branch of the cross-equatorial flow and a secondary maxima of 3 m/s between 80^0 E - 90^0 E, representing the Bay of Bengal branch. The dual core of cross-equatorial flow in the Arabian Sea was not seen in this year's analysis, which was observed during monsoon season of 1995 and 1998. This dual core was also absent in recent monsoons of 2005, 2006 and 2007. During monsoon 2008, all the forecasts (day-1 through day-5 predictions) of the cross-equatorial flow (Arabian Sea branch) indicate a slight intensification of the strength of

cross equatorial flow to 15 m/s. The core of the Arabian Sea branch of CEF is well maintained at 15 m/s in a consistent manner. The Bay of Bengal branch of the cross-equatorial flow is also maintained well. Overall T254L64 system well reproduces and maintains the low-level cross equatorial flow both in the Arabian Sea and the Bay of Bengal.

Low-Level Westerly Jet (LLWJ)

The mean analyzed and predicted positions and strength of the low-level westerly jet (LLWJ) in the Arabian Sea at 850 hPa from T254L64 are shown in Fig. 9.21 for the monsoon season as a whole. This diagram brings out clearly the well maintenance of the strength and location of LLWJ in the Arabian Sea throughout the forecast length (day-1 through day-5). The contour of 15 m/s adjacent to Somalia coast in the Arabian Sea is very consistent in analysis and the forecasts. The winds in the Bay of Bengal and peninsular India are also very well maintained

The north-south cross-sections of seasonal mean analyzed and predicted (Day-1, Day-3 and Day-5) zonal component of wind along 54^0 E, a longitude that falls within the climatological location of LLWJ, from T254L64 forecast were examined (not shown here). The observed core of the jet matches with the climatological location. The jet core is observed to be at 16 m/s in T254L64 forecasts. Here the second core (dual core) of 10 mps at around 15^0 N is also seen during 2008 monsoon. The model forecasts (Day –1 through Day –5) agree well with the observed jet strength and position. Even the dual core system is very well maintained in the model. Throughout the forecast length the LLWJ is seen to be very consistent in structure among the forecasts and also with the observed analysis. The strength is seen to slightly intensify from day-1 to day-5 forecasts. In general, the representation and maintenance of LLWJ is good.

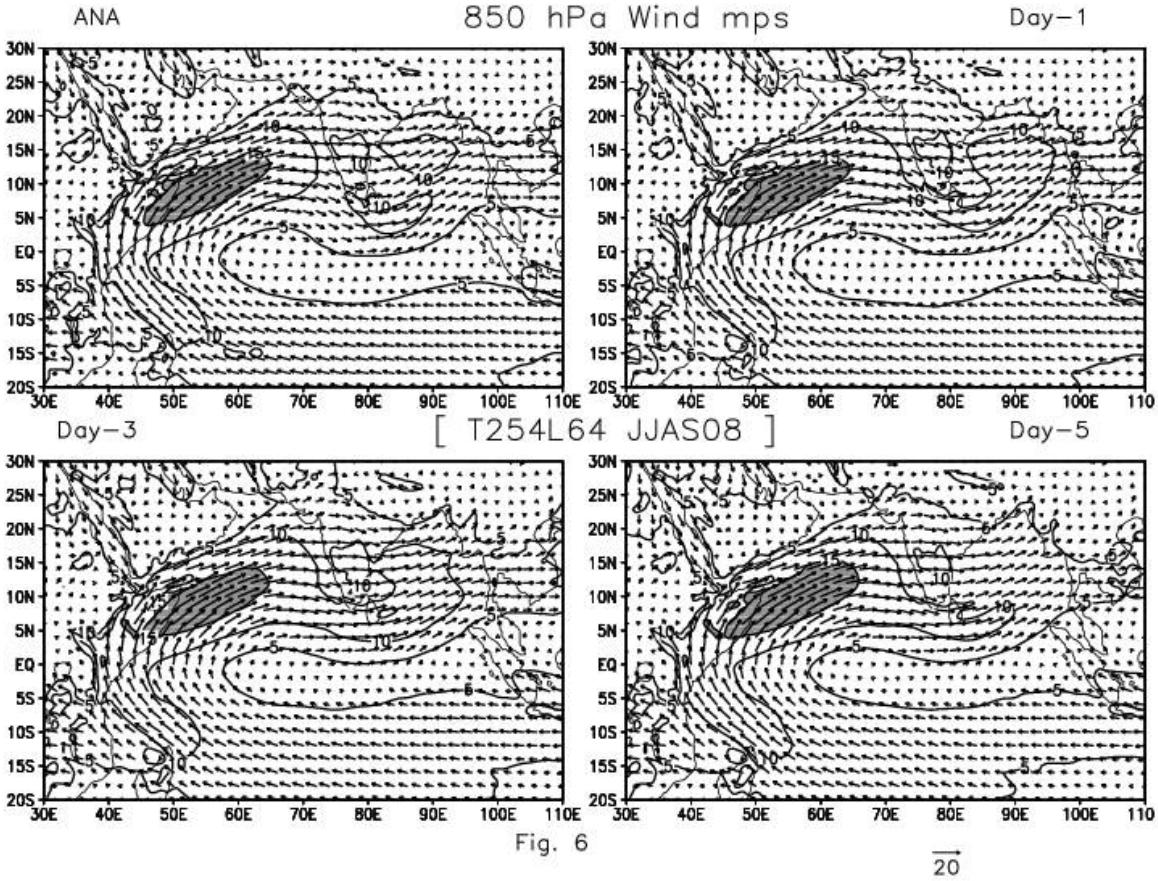

Fig. 9.21: Low Level Westerly Jet during Southwest Monsoon of 2008 in analysis and forecasts (wind speed greater than 15m/s shaded)

The latitude-height cross-sections of seasonal mean analyzed and predicted zonal wind along 75^0 E (a longitude where the low-level westerlies interact with the west coast orography leading to heavy rainfall) from T254L64 system were analysed. The maximum zonal wind in analysis is seen to be between 7 to 8 m/s. The second core at 16^0 N associated with the monsoon trough is seen to be quite strong at 10 m/s. During forecast the strength is well maintained, with slight intensification. The position and intensity of the monsoon trough is also well maintained. The strength of the core at 10^ON is well maintained, but its position is seen to shift southward (from 10^0 N in analysis to 6^0 N in day-5 forecast). This will have impact on the location of the rainfall distribution along the west coast of India in respect to LLWJ.

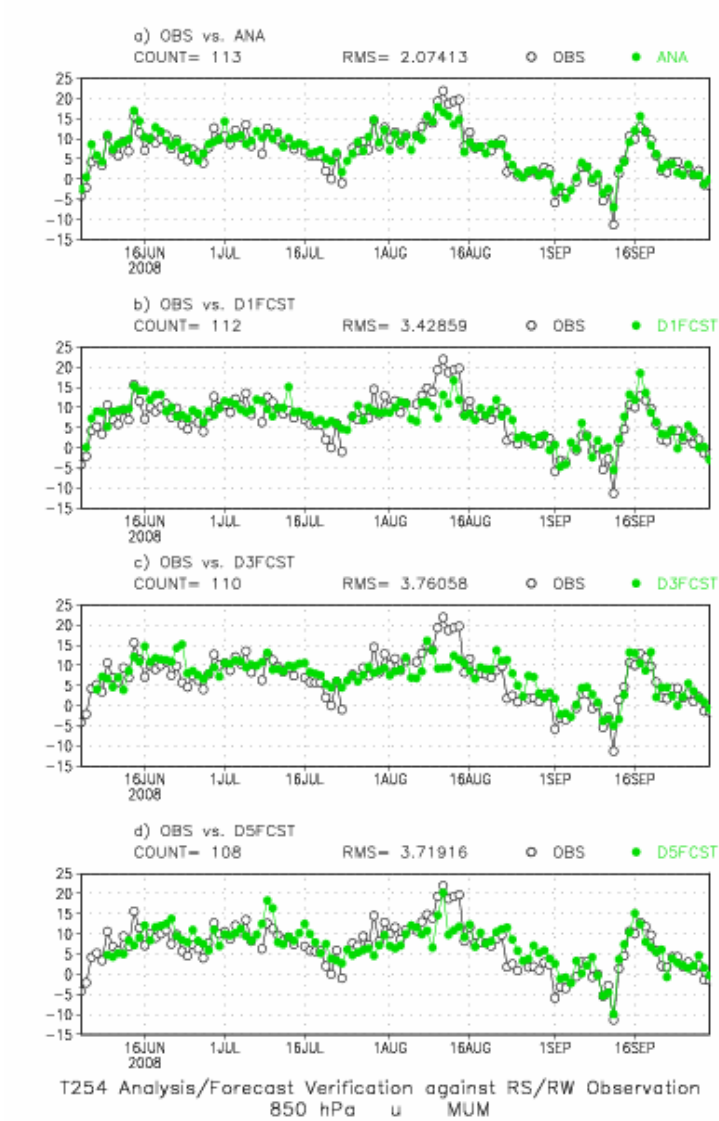

Fig. 9.22: Time series of day-1, day-3 and day-5, forecast zonal winds (u) at a station (Mumbai) against RS/RW observed values during the Southwest Monsoon of 2008, at 850 hPa

In Fig.9.22 is shown the daily verification of day-1, day-3 and day-5 forecasts of the zonal winds (u) at a station (Mumbai) against RS/RW observed values at 850 hPa during monsoon 2008. It is seen that daily variation of wind at a station is captured well in the model forecasts. The RMS errors of the day-1, day-3 and day-5 forecasts are 3.42, 3.76 and 3.71 m/s respectively. The error of the analysis (from the data assimilation system) is 2.0 m/s during the season.

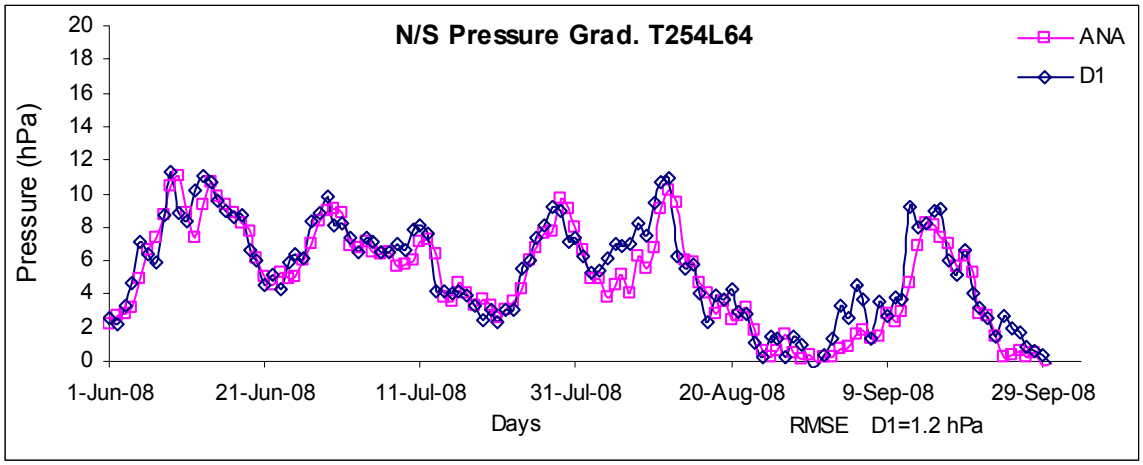

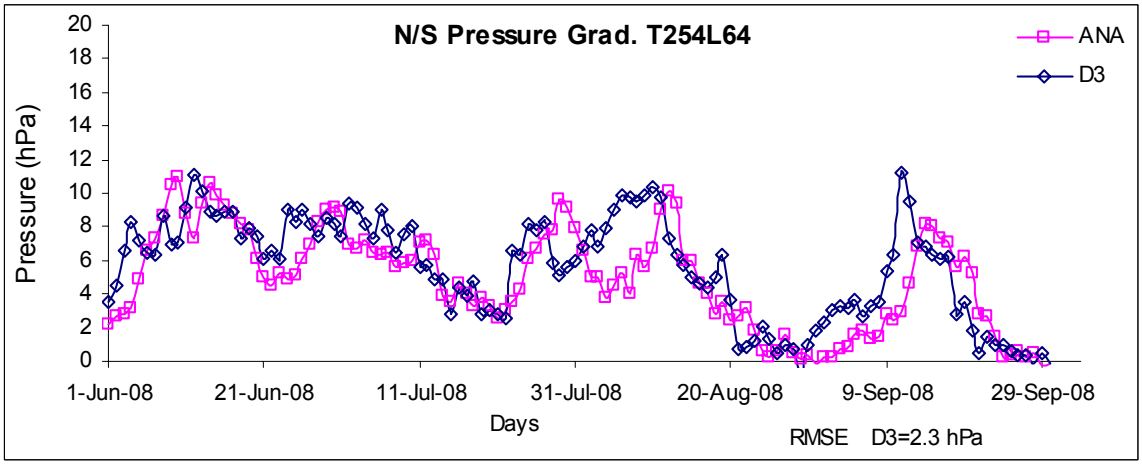

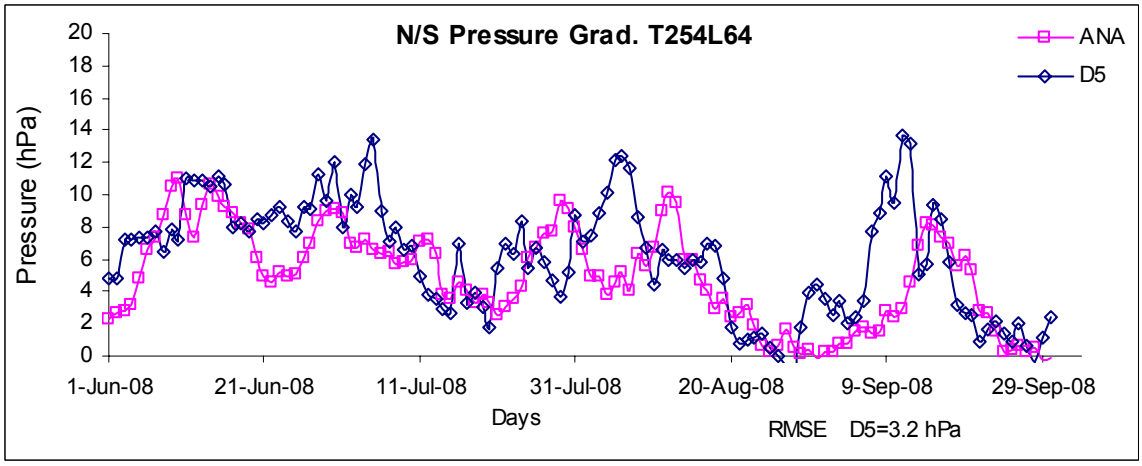

Fig. 9.23: Analyzed, Day-1, Day-3 and Day-5 forecasts of North-South Pressure Gradient along west coast during monsoon 2008

North-South Surface Pressure Gradient over India

The daily variations of analyzed (line with square marks) and predicted (line with diamond marks) values of north-south pressure gradient (Mean Sea Level Pressure difference) along the west coast of India from T254L64 forecast system are shown in Fig. 9.23. The day-1 forecasts match very well with the corresponding analyzed values. In day-3 forecasts the magnitude of north-south pressure gradient along west coast of India is captured reasonably well but the phase is often in error. The day-5 forecasts have large (in amplitude and phases) compared to day-1 and day-3 forecasts. IRMSE of the predicted north-south pressure gradient along the west coast of India for Day-1, Day-3 and Day-5 forecasts are 1.2, 2.3 and 3.2 hPa respectively.

h. Medium range forecast of rainfall

In this section the performance of the global T254L64 medium range rainfall forecasts are discussed. The reference observed rain is the daily gridded merged satellite (Meteosat-7) and gauge data for the Indian region produced by NCMRWF (Mitra et. al. 2003, Basu, B..K. 2007, Mitra et.al. 2009).

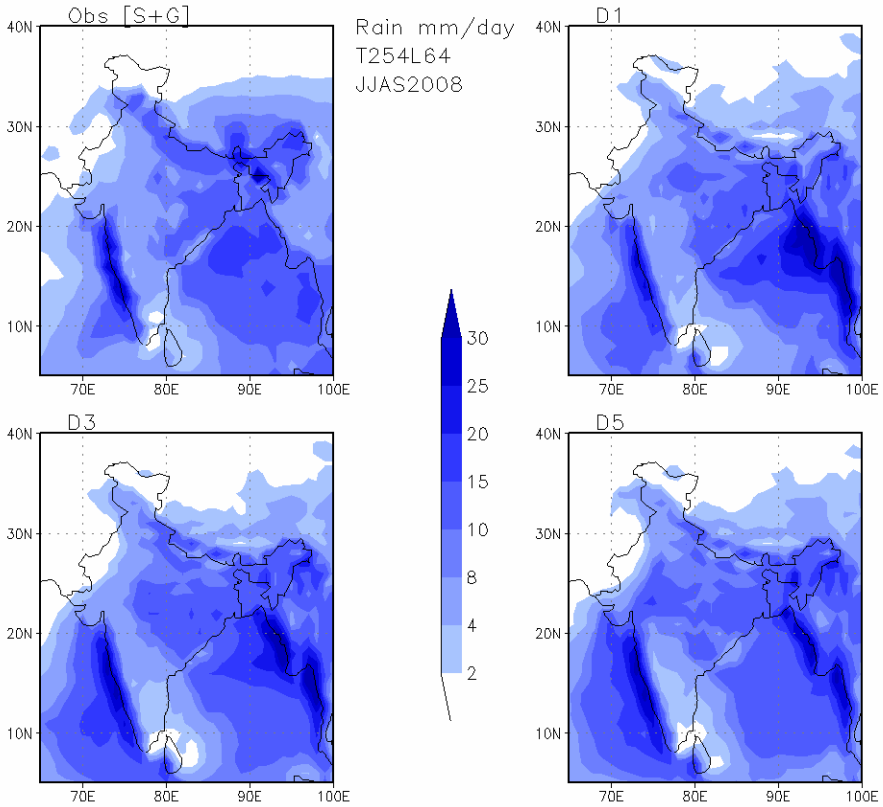

Fig. 9.24: Observed and day-1, day-3 and day-5 rainfall forecasts from the model for the Southwest Monsoon of 2008

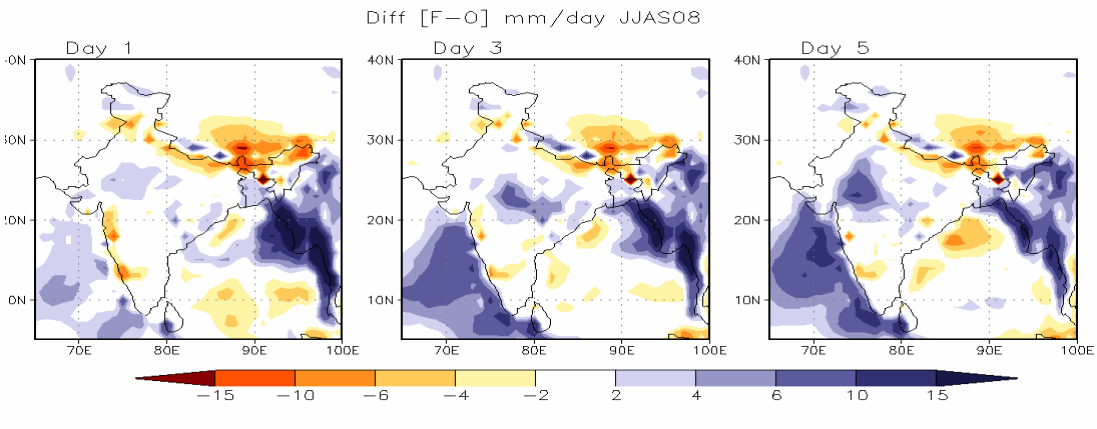

Fig. 9.25: Difference (Forecast - Observation) rainfall for day-1, day-3 and day-5

The Fig.9.24 shows the seasonal total rainfall amounts from observations and model forecasts. Broadly it shows that the model is able to represent the monsoon rain well. In the monsoon trough region, the model forecasts are good only for day-1. In Day-3 and day-5 amounts and locations of maximum rainfall in the monsoon trough zone are different compared to observations. The differences of forecasts (day-1, day-3 and day-5) from the observations are shown in Fig. 9.25, where the differences (errors) are seen clearly. Over central India the error increases with time from day-1 through day-5. The region of the error also moves towards west. Another region with excess rainfall error is the Arakan Coast bordering the northeastern Bay of Bengal.

Different threshold based skill scores for rainfalls for the season are shown in Fig.9.26. These calculations are based on collecting points above a certain intended rainfall threshold amount. We have considered six thresholds of 1 to 6 cm per day.

Equitable threat score, hit rate and bias scores are computed from observed and model rainfall data. Equitable threat score (ETS) is a measure of relative accuracy of the forecasts including chance (expected number of randomly correct forecasts above a threshold) as a parameter. ETS should vary between 0 to 1. Hit rate (HR) also known as success rate is the ratio of number of correctly forecasted points above a threshold to the number of forecasted points above that threshold. HR values are between 0 to 1. Bias score (BS) is the ratio of number of forecasted points above a threshold to the number of observation points above that threshold. If the BS is closer to 1, then it shows that the model rainfall forecast has less bias. Higher values (> 1) means positive (wet) bias, and lower values (< 1) indicated negative (dry) biases.

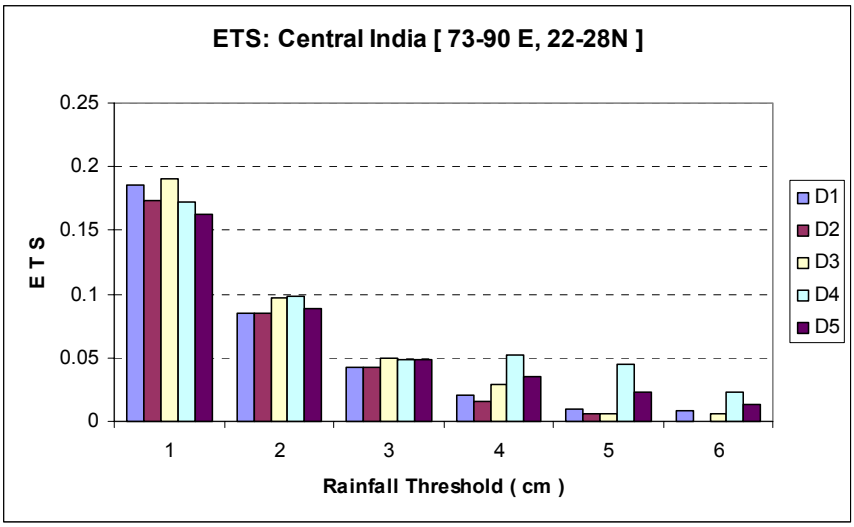

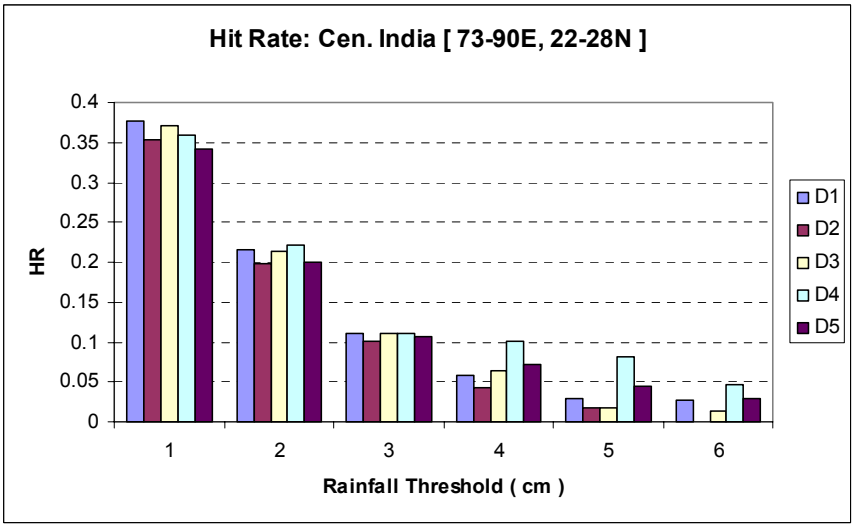

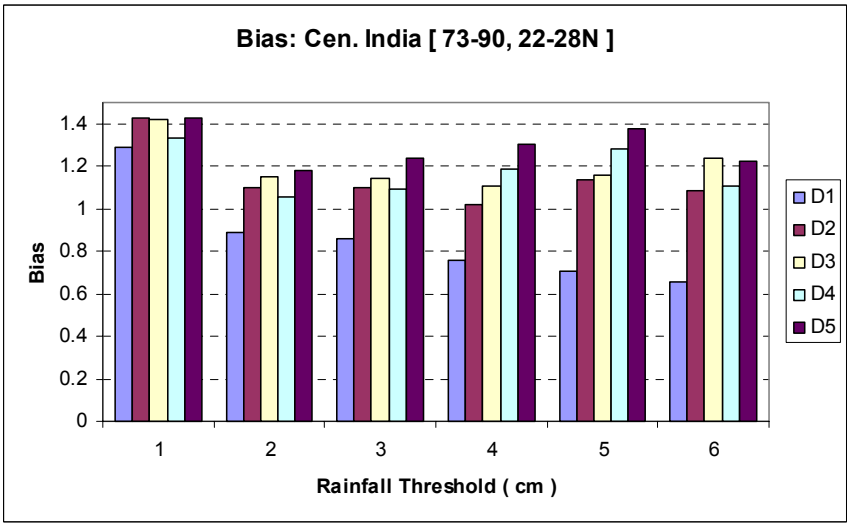

Fig. 9.26: Rainfall threshold based skill scores for Central India (73-90E, 22-28N) for the season (D1 denotes day-1 forecast, etc.)

Fig.9.26 shows the threshold based skill scores for central India region (73-90E, 22-28N). This region is representative of the region where the monsoon trough is generally seen. Most of the models have difficulty in representing this monsoon trough related features realistically. In ETS all scores are below 0.2, and 1 cm threshold shows the highest score. Forecasts for thresholds of 3 cm and above have a poor score of 0.05 or less. The HR for all threshold and all days are below 0.4, showing the below average performance. For threshold of 2 cm and above the scores become 0.2 or lesser. In BS except day-1, for all thresholds and days positive (wet) biases are seen for the central India region.

Estimation of Uncertainty in the Forecast

The atmosphere is a chaotic system, and as a result, small errors in the initial conditions can grow to have a major impact on the subsequent forecasts. The true state of the atmosphere cannot be determined precisely due to observational errors, large data gaps and approximations in the analysis techniques. Therefore, it is essential to provide estimates of the forecast uncertainty while carrying out medium range weather forecasts. This is done using the Ensemble prediction System.

9.9. Ensemble Prediction System at NCMRWF

Ensemble forecasting involves the integration of an NWP model with several perturbed initial conditions. The ensemble of forecasts thus generated, represent the uncertainty in forecast, which may arise due to the errors in the initial conditions, or due to the errors in the model formulation.

There are basically two main techniques for generating the initial perturbations: (i) Breeding technique which identifies the perturbations which grow fastest during the analysis cycle, and (ii) Singular Vectors technique which identifies the perturbation that can grow fastest in the forecasts. The size of the ensembles at various operational centers range from 20 to 50.

At NCMRWF, an eight member Ensemble Prediction System based on the breeding of growing modes (BGM) method has been implemented. The time averaged statistics of the perturbations show that the perturbations represent reasonably well the magnitude and horizontal and vertical distribution of the analysis uncertainty. Experiments with the eight members ensemble have been made for some significant weather systems. This ensemble system is being run on real-time

basis since 2005. Diagnostic studies related to this system have provided a lot of information regarding issues related to monsoon prediction and the systematic errors of the model. It is seen that ensemble prediction also reduces the errors of the forecast in a specified sense.

Fig. 9.27 shows the root mean square error (RMSE) of wind from ensemble mean and Control runs at Day-5 forecasts at 850 hPa. This comparison is made against all radiosonde observations over the Indian region. It is seen that the RMSE is less for the ensemble mean as compared to the Control run. The range of improvement by the EPS is about 1 m/s at 850 hPa.

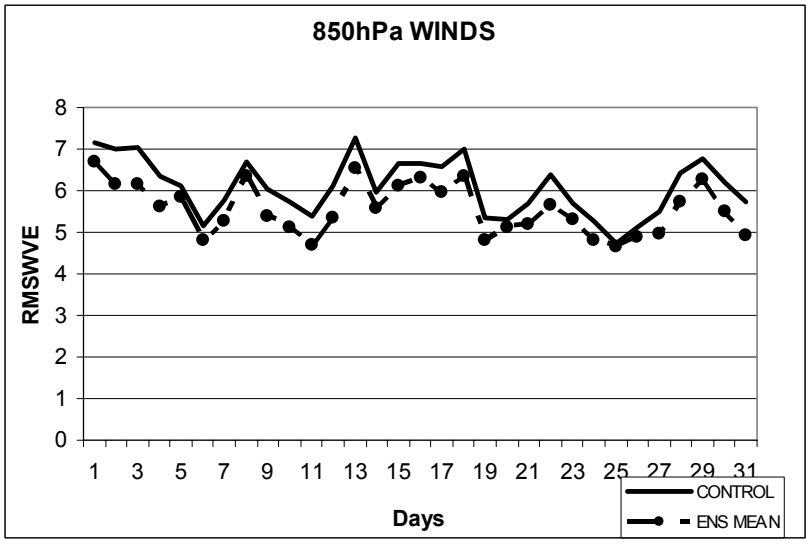

Fig. 9.27: RMSE of wind at 850hPa from ensemble mean and control runs at for July 2006 Day-5 forecasts.

During Southwest Monsoon the uncertainty that results from deficiencies in the model are quite large and also grow at a fast rate. In such conditions the estimation of uncertainties due to the initial conditions may not be of much use. However it is essential that an estimate of the uncertainty is always provided together with the medium range forecast. Its value and requirement will grow with the increase in the accuracy of the deterministic forecasts.

9.10. Improving the Medium Range Weather Forecast products using statistical techniques

a. Multi-Model Ensemble Forecasting

In numerical forecasting there exist uncertainties in the initial conditions, model dynamics and model physics. As a result different models produce forecast values that do not necessarily agree among themselves. In recent years, major operational centers began making their forecast data available for exchange. This has led to the practical realization of the concept of Multi Model Ensemble (MME) forecasting system. In this method observations and forecasts of a variable from different models are used to build statistical relationships between them. Using these relationships and the forecasts from different models the final forecast values are computed. It is found that the method provides forecasts that have less RMSE than forecast from any individual system, in a specified sense. Ministry of Earth Sciences (MoES) initiated a 'multi-model ensemble' (MME) forecasting project at NCMRWF. This MME is a joint activity of NCMRWF, IMD and IITM. Under this project improved forecasts in short and medium range will be made available for operational real time

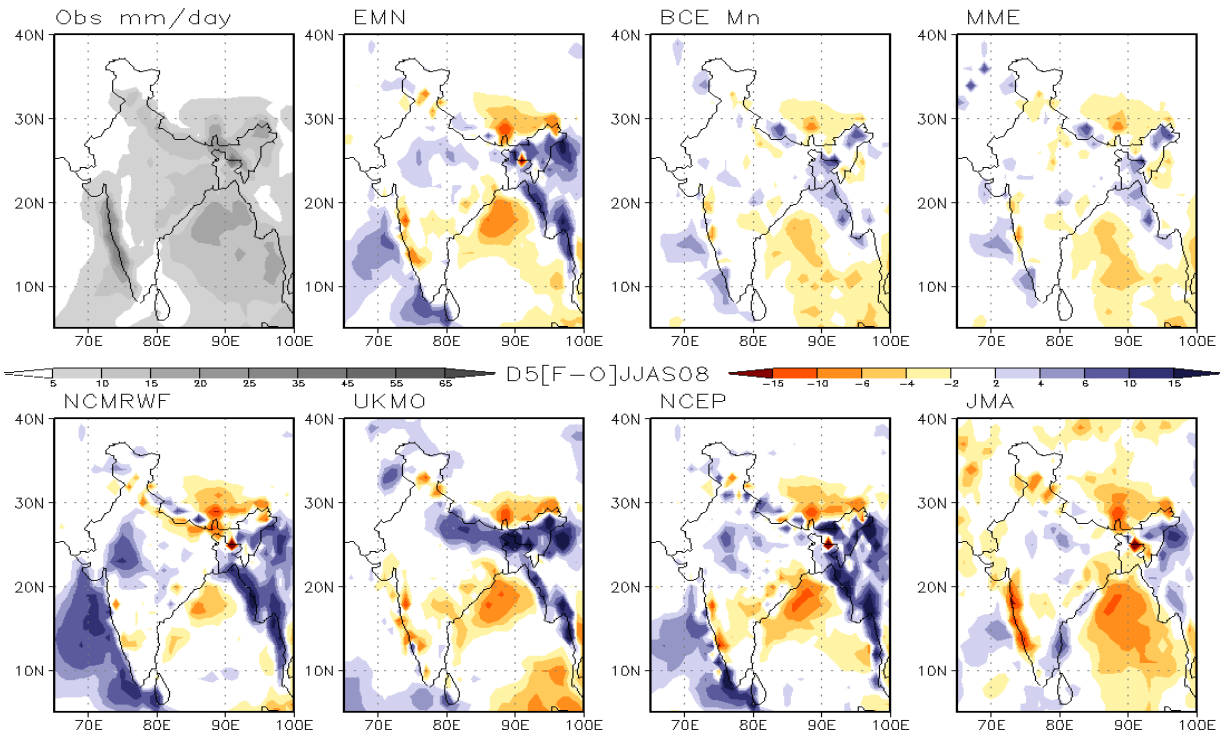

Fig.9.28: Observed Rain (Obs); Error of NCMRWF,UKMO, NCEP and JMA Mean Monsoon Rainfall for 2008 based on 5day forecasts (lower row); Mean of all the forecasts (EMN), Bias Corrected Mean of all the forecasts (BCE Mn) and the Multi Model Ensemble.

use for the Indian region. Initial results are encouraging. Rainfall forecast data from 4 global models (NCMRWF, NCEP, UKMO and JMA) for monsoon 2007 and the observed data were used to develop the MME procedure. Experimental forecasts with MME were conducted during the Southwest Monsoon of 2008 to examine the skills and improvements. In Fig. 9.28 the deviations of day-5 forecast against observed rainfall (analysis) during monsoon 2008 are shown. The multi-model forecasts have less error than the individual model forecasts.

b. Statistical Interpretation Forecast

Basically two methods are used for the statistical interpretation of the deterministic model forecast. One is the Model Output Statistics (MOS), and the other is the Perfect Prog Method(PPM).In MOS equations are developed based on the observed data and the T-80 model forecasts over the last five to six years whereas in PPM equations are developed between the observed and the analysis using past five to six years of data.

At NCMRWF, SI (Statistical Interpretation) forecast model equations are based upon PPM models. The PPM equations are developed for monsoon season using six years(1994-99) of T-80 model analysis(1.5x1.5) data for 30 stations out of these 45 stations (for details of methodology see Rashmi et. al., 2008, Ashok Kumar et. al, 1999,2000). SI forecast for 6 locations in India for the Southwest Monsoon of 2008 is shown in Table 9. 6.

Table 9.6: Skill Scores For Yes/No Day4 Rainfall Forecasts Southwest Monsoon, 2008

STATION	DMO(T-254)		DMO(T-80)		SI (T -80)	
	RATIO	HK	RATIO	HK	RATIO	HK
DELHI	67	0.34	58	0.15	61	0.21
JABALPUR	65	0.28	61	0.21	62	0.24
PUNE	76	0.37	75	0.34	81	0.49
RAIPUR	64	0.23	67	0.24	59	0.21
RANCHI	74	0.19	74	0.13	67	0.30
UDAIPUR	55	0.27	67	0.15	75	0.44

The scores used for verification of rainfall forecast are the ratio score and Hanssen and Kuipers (HK) skill scores. The ratio score (RATI) measures the percentage of correct forecasts out of total forecasts issued. The Hanssen and Kuipers' discriminant (HK) is the ratio of economic saving over climatology. In Table 6 the HK scores and the ratio scores for rain or no-rain forecasts are given. In the case of T254 only the direct model out put (DMO) is considered. It is seen that T254 increased the score of DMO except in the case of Raipur. In three stations (out of six) the T254 DMO forecast skill exceeds the skill of the SI forecast using T80 system clearly demonstrating the improvement in skill associated with the improvement of the deterministic forecast. The utility of the SI for improving upon the deterministic forecast is seen in the improvement of T80 SI forecast with respect to T80 DMO forecast.

9.11. Improving the Medium Range Weather Forecast products using dynamic downscaling

The global model produces forecast that is an average value for the grid with resolution of 50km (100km in the case of the earlier T80L18 system). This resolution cannot account for the differences in atmospheric conditions that will be present in a grid square because of the differing landscapes and orography. There are also weather phenomena (usually extreme weather events like tropical cyclones, squalls, etc) that require inclusion of much more detailed physical processes for their proper simulation than what is present in the global model. Therefore regional (mesoscale) models are used to produce weather forecasts at higher spatial resolution and also with more detailed physical processes than in the global model. Such models are run with initial conditions and boundary conditions taken from the global medium range forecasts. They are especially useful in mountainous territory and also in the case of severe weather. At NCMRWF the MM5 mesoscale model of NCAR and NCEP's Eta model were implemented in 2002 that produce real time forecasts using NCMRWF global model analysis and forecast. Later the WRF model also was implemented. They have been proved useful in the case of mountain weather and also in the case of severe weather. In Fig.10.19 the comparison of these models with respect to the movement of monsoon depressions during 2008 could be seen. Detailed verification and performance analysis is given in Someshwar et. al., 2008.

9.12. Summary and Conclusions

Accuracy of the Medium Range deterministic forecasts during Southwest Monsoon

The current analysis-forecast system at NCMRWF is the T254L64 system. The analysis system is 3D Variational, namely GSI (Grid Point Statistical Interpolation). The forecast model (and also the analysis) has a horizontal resolution of about 50km and it has 64 levels in the vertical. The dynamics and physical processes in the model are state of the art.

The performance of the current analysis system was compared with the earlier T80L18 system. The Global RMSE (with respect to Radiosonde observations) of the analysis during Southwest Monsoon (for Geopotential Height, horizontal Wind Components, Air Temperature and Specific Humidity) shows that there is significant reduction of errors with respect to the T80L18 system. The errors in the analysis, however, are fairly large.

The discussion on medium range forecast of the Southwest Monsoon was done with respect to the year 2008. The monthly mean anomalies (as deviations from the mean conditions based on the previous 10 years) were described before examining aspects of forecast accuracy.

At NCMRWF the medium range forecast is carried out for seven days into the future. The systematic errors for 1,3 and 5day forecasts were examined. Usually the main sources of systematic errors are deficiencies present in the forecast model. It is seen that the errors are spatially coherent over several thousands of kilometers. These error patterns could be visually correlated with the large scale structure of the Southwest Monsoon flow. The temperature and humidity errors also show similar characteristics. The simulation of large-scale flow structure itself is in need of considerable improvement. The magnitude of this type of error becomes quite significant by 72hrs.

The 10year record (1999-2008) of the RMSE (against observations from Indian Radiosonde stations) of the 3day forecasts of the vector winds at 850hPa was prepared to identify the annual and inter-annual variations. These errors include the effects of diverse factors and are strongly dependent on the analysis-forecast system as well as the input data. Therefore the errors do not necessarily reflect the changes

brought about by differences in the atmospheric conditions. However some conjectures on the annual and inter-annual changes in errors could be made from this time series. A striking feature of the time series is that the errors are maximum during the Southwest Monsoon season. It is known that summer errors are the highest in MRF of other centers as well. In the present case the increase of error from winter to Southwest Monsoon is about one third of the annual mean RMSE. The magnitude of the error is large and has an annual cycle. There is significant reduction in error after the introduction of the T254L64 system. These errors are absolute errors and not relative errors. Their actual significance for the predicted weather may be different according to the time of the year.

The RMSE of the vector wind at 850 hPa (against Radiosonde observations in the region 25-65N, 60-145E) for the month of July 2008 was computed for 1 to 5day forecasts of NCMRWF, NCEP, UKMO and ECMWF. It is seen that the NCMRWF forecast is of comparable accuracy as that of NCEP and UKMO. The errors of ECMWF are significantly lower. However the difference in error between the NCMRWF and ECMWF forecasts are about one fifth of the magnitude of the errors. This shows that considerable reduction in errors is still required.

The day-to-day variation of forecast errors (calculated using respective analyses) over India was studied in detail for the Southwest Monsoons of 2007 and 2008. An identical analysis was carried out for the UKMO forecasts. A notable feature is the large variations of errors that persist for a period of a few days to several days. Such variations generally do not have the same pattern in both the systems. Occasionally the errors of the 5day forecasts drop to the error level of 1day forecasts. This demonstrates that the forecast systems under certain conditions during the monsoon produce fairly accurate deterministic forecasts even with a lead-time of 5 days. The seasonal mean of the errors show that the UKMO forecasts have lower errors. However the magnitude of the errors is significant and grows fast from day1 to day5.

In general the error analysis shows that the accuracy of NCMRWF forecasts during the Southwest Monsoon is of the same order as that of forecasts from the leading centres though on the lower side. The errors of the forecasts during Southwest Monsoon are the highest in a year and also are of significantly large magnitudes. This observation applies to forecasts from other centers as well

Accuracy of Prediction of Specific Features of the Southwest Monsoon

The examination of the accuracy of prediction of Southwest Monsoon as a phenomenon is carried out on the basis of some of its characteristics that show variability in the medium range. Longer period variabilities like intra-seasonal oscillations, breaks and active phases of Monsoon rains over India do not fully fall within the medium range. However significant evolutionary phases associated with these variabilities fall within the medium range. It is assumed that, with the improvement of the deterministic global prediction, the evolution of these processes also will be present in the medium range weather forecast. We do not therefore consider those variabilities in our discussion. The features we consider are the onset and advancement; Heat Low, Monsoon Trough, Monsoon Lows and Depressions; Mascarene High, Cross Equatorial Flow, Low level Jet, North-South Pressure Gradient and the rainfall over India.

NCMRWF developed an objective method for determining the onset and advancement of Southwest Monsoon over India based on changes in kinetic energy, tropospheric moisture and temperature. The method identifies with a fair degree of accuracy (as verified against the dates declared by IMD) the date of onset and also the dates of advancement. Forecasts of onset and advancement have the same quality as that of the medium range forecasts. The onset dates are determined with an error range of 2 days. Three other Monsoon indices also show comparable success in identifying the dates of onset over Kerala.

The status and changes of the Heat Low, Monsoon Trough, Monsoon Lows and Depressions are highly useful in describing the monsoon weather conditions and also their evolution. As these features are seen in surface weather charts their practical utility in forecast practice is immense. In the NCMRWF forecasts the Heat Low and Monsoon Trough are simulated well. However with forecast length they become more intense and also the locations show significant shifts. Similarly the Lows and Depressions are simulated well but the forecast of their movement and intensity are not of the desired level of accuracy.

The RMSE of the predicted intensity of the Mascarene High for Day-1, Day-3 and Day-5 forecasts are 2.7 hPa, 4.5 hPa and 5.6 hPa respectively. The RMSE of the predicted longitudinal positions of the Mascarene High for Day-1, Day-3 and Day-5 forecasts are 16.9^0, 24.5^0 and 22.8^0 and the RMSE of the predicted latitudinal positions are 3.6^0, 4.6^0 and 4.5^0 respectively. The phase of the variations have fairly large errors by the third day.

The forecasts (day-1 through day-5 predictions) of the cross-equatorial flow (Arabian Sea branch) indicate slight strengthening of cross equatorial flow to 15 m/s. The core of the Arabian Sea branch of CEF is well maintained at 15 m/s and is consistent among the forecasts. The Bay of Bengal branch of the CEF is also maintained well.

Throughout the forecast length the Low Level Westerly Jet is seen to be very consistent in structure among the forecasts and also with the analysis. It slightly intensifies from day-1 forecast to day-5 forecast. In general, the representation and maintenance of LLWJ is good.

The day-1 forecasts of north-south pressure gradient match very well with the corresponding analyzed values. The phase error is large by the third day and by the fifth day both the amplitude and phase have large errors. RMSE for Day-1, Day-3 and Day-5 forecasts are 1.2, 2.3 and 3.2 hPa respectively.

The most useful parameter in a weather prediction during the Southwest Monsoon is the rainfall. If accurate prediction is given with respect to its magnitude, location and time, in the medium range, it will be of immense value for agriculture and other applications like flood and water management. Though the rainfall simulations look realistic in the gross, the skill of the direct model output is not of the desirable level even for the one-day forecasts (for Central India for the season the highest Equitable Threat Score is less than 0.2 for a rainfall threshold of 1cm; for higher thresholds the score is much smaller). The Hit Rate and Bias Scores also show unsatisfactory levels. In general the rainfall forecast quality is yet to attain the desired levels even for the 24hr forecasts. This highlights the fact that we still have to go a long way before the necessary levels in forecast skill are achieved in the medium range weather forecasting of rain over India during the Southwest Monsoon season. It may be mentioned here that using value addition techniques like Statistical Interpretation of forecast outputs and also Multi Model Ensemble (MME) the skill of the forecast rain is significantly improved. As of now these forecasts are found to be useful when interpreted by an experienced forecaster.

Future Perspectives

A few facts stand out among the foregoing discussion:

a. The present medium range forecasts during Southwest Monsoon in India and also from the other leading centers are of usable quality.
b. There is a large gap between the practical requirements of accuracy and reliability of the forecasts and their current status.
c. It is imperative that substantial progress is made in tackling the central problems of medium range weather forecasts, namely, making the most accurate initial conditions, making correct and accurate deterministic model simulations and estimating uncertainty due to initial conditions and model deficiencies.

The forecasts of the leading centers are better and we know how the errors have been reduced. We also have to follow their path as far as those developments are concerned (4D Variational Data Assimilation, more data (both in quantity and diversity), higher horizontal and vertical resolutions, inclusion of detailed and additional physics). There is also an unknown untapped predictability that may come from ocean-atmosphere coupling. There is, however, no assurance that after all these improvements the accuracy in our region will satisfy our practical requirements. We have to set our goals, therefore, in absolute terms and not in relative terms.

The task of catching up with the progress already made by the leaders in this field is more of a technical problem because we know how those improvements were achieved. But going beyond the present levels of accuracy is a scientific, technical and organizational problem. At NCMRWF some successful and pioneering efforts were made to improve the forecasts. It is seen in Fig.10.8 that the errors during the Monsoons of 2001 and 2002 were the lowest before the introduction of the new T254 system. This reduction was achieved by improvements in the physical processes of the T80 model and also by improving the initial conditions by assimilating new kinds of data, mainly satellite data. The improvements in the model that were carried out were (1) Introduction of a TKE closure scheme for the PBL (2) Changeover to the Harshvardhan parameterization scheme for short wave radiationi (Swati Basu et. al., 2002; Das et. al, 2002; John et. al. 1997). Using the NCEP Daily SST analysis instead of climatological SST modified the ocean boundary condition. The new data that were introduced in the assimilation system (from 2000 Winter) were SSMI Surface Winds and Precipitable Water; Meteosat winds and ATOVS (Bohra et. al.

1988, Prasad et. al.1999). As could be seen from Fig.10.8 these modifications did reduce the errors significantly during the Southwest Monsoon. However, there was a gradual increase in errors from 2003 till the introduction of the new T254 system. This was due to technical problems with the assimilation of the satellite data. After the introduction of the new system in 2007, direct radiance data assimilation was introduced. That resulted in further reduction of the errors seen during the Southwest Monsoon of 2008. Though NCMRWF had developed a T170L28 forecast-assimilation system incorporating the aforesaid improvements in the model, the assimilation system at the higher resolution could not be stabilized. Therefore the full potential of the forecast system was not realized. But this was the first indigenous effort on developing a full forecast-analysis system in India though it gave mixed results.

As far as the scientific aspects are concerned, there are a few perspective areas where the promise of achieving progress is high. They are (not necessarily in order of priority) introduction of 4D Variational Data Assimilation; introduction of cloud resolving models or improvement of parameterisation of convection - including the reproduction of cloud organizations and their interactions Moncrieff (2008), Masato Sugi(2008). It is also necessary that models are evaluated based on the correct reproduction of processes (Catherine Senior et.al (2008), Stuart Bell(2008). In the case of data assimilation, Ensemble Data Assimilation that also takes care of model uncertainties (Palmer, T.N., 2008) has to be developed. Another promising area is that of the introduction of more detailed ocean-atmosphere coupling that is known to be intense during the Southwest Monsoon season.

The efforts for improving medium range weather forecasts have been carried out mainly by international operational / research centers whether in the case of forecast analysis systems or observational systems. The nature of the problem dictates that this situation is going to continue and international cooperation will be a major activity in this field. India, however has a great stake in improving medium range forecasting during the Southwest Monsoon season for obvious reasons. This becomes more significant in the background of possible impacts of a changing climate on weather over our region. The management of unexpected weather patterns may become a real problem in the future. The medium range scale of weather forecast is very crucial in that it provides a reasonable reaction time for taking effective action in many critical situations, if the forecasts are accurate.

It is the foresight of the decision makers of the country that resulted in the establishment of a medium range weather forecast centre in the country about 20 years back. With the enhanced coordination that has been brought to the whole field of earth system sciences with the formation of the Ministry of Earth Sciences along with the significant assets and capabilities in the field of space borne observation systems in India, the chances of meeting the challenges in the field of medium range forecast of the Southwest Monsoon is very bright.

References

Ashok Kumar, Parvinder Maini and Singh, S. V., 1999, "An operational model for forecasting probability of precipitation and YES/NO forecast", *Wea. and Forecasting, 14: 38-48.*

Ashok Kumar, Parvinder Maini, Rathore, L. S. and Singh. S. V., 2000, "An operational medium range local weather forecasting system developed in India", *Int. J. Climatol., 20: 73-87.*

Asselin, R., 1972, "Frequency filter for time integrations", *Mon. Wea. Rev., 100*, 487-490.

Basu, B. K., 2007, "Diurnal Variation in Precipitation over India during the Summer Monsoon Season: Observed and Model", *Monthly Weather Review, 135(6), 2155-2167.*

Catherine Senior, Gill Martin, Alistair Sellar and the HadGEM3, Monsoon Working Group(2008), Model development and evaluation at the Met Office Hadley Centre: Towards Seamless prediction' In Extended Abstracts 'International Conference on Progress in weather and Climate Modelling over Indian Region' held on 9-12 December,2008 at NCMRWF, NOIDA, pp.46-51.

Charnock, H., 1955, "Wind stress on a water surface", *Quart. J. Roy. Meteor. Soc., 81*, 639-640.

Derber, J. C. and Wu, W. S., 1998, "The use of TOVS cloud-cleared radiances in the NCEP SSI analysis system", Mon. Wea. Rev., 126, 2287 – 2299.

Derber, J. C., Parrish, D. F. and Lord, S. J. 1991, "The new global operational analysis system at the National Meteorological Center. *Weather and Forecasting", 6*, 538-547.

Gorshkov, S. G., (Ed.), 1977, "World Ocean Atlas - Atlantic and Indian Oceans, Chief Directorate of Navigation and Oceanography", Former USSR.

Goswami, B. N., Krishnamurthy, V and Annamalai, H 1999, "A broad scale circulation index for interannual variability of the Indian summer monsoon", *Quart. J. Roy. Meteor. Soc.,*125, 611-633.

Hong, S. Y. and Pan, H. L., 1996, "Non-local boundary layer vertical diffusion in a medium-range forecast model", *Mon. Wea. Rev., 124,* 2322-2339.

John, P., George and Begum, Z. N., (1997), "Impact of different radiation transfer parameterization schemes in a GCM on the simulation of the onset phase of Indian summer monsoon", *Atmosfera* , *10,1-22.*

Kalnay, M., Kanamitsu, and Baker, W. E., 1990, "Global numerical weather prediction at the National Meteorological Center", *Bull. Amer. Meteor. Soc., 71*, 1410-1428.

Kanamitsu, M., 1989,"Description of the NMC global data assimilation and forecast system", *Weather and Forecasting, 4*, 335-342.

Kanamitsu, M., Alpert, J. C., Campana, K. A., Caplan, P. M., Deaven, D. G., Iredell, M., Katz, B., Pan, H. L., Sela, J and White, G. H 1991, "Recent changes implemented into the global forecast system at NMC", *Weather and Forecasting, 6*, 425-435.

Mitra, A. K., Dasgupta, M., Singh, S. V. and Krishnamurti, T. N., 2003, "Daily rainfall for Indian monsoon region from merged satellite and raingauge values: large-scale analysis from real-time data", *Journal of Hydrometeorology (AMS), 4(5), 769-781.*

Mitra, A. K., Bohra, A. K., Rajeevan, M. N. and Krishnamurti, T. N., 2009, "Daily Indian precipitation analyses formed from a merged of rain-gauge with TRMM TMPA satellite derived rainfall estimates", J. of Met. Soc. of Japan, 87A, 265-279.

Mlawer, E. J., Taubman, S.J., Brown, P.D., Lacono, M. J. and Clough, S. A., 1997, "Radiative transfer for inhomogeneous atmospheres: RRTM, a validated correlated-k model for the long wave", *J. Geophys. Res., 102*, 16663-16682.

Moncrieff, M. W., (2008) Convective organization and Global Models, Year of Tropical Convection (YOTC) In Extended Abstracts 'International Conference on Progress in weather and Climate Modelling over Indian Region' held on 9-12 December,2008 at NCMRWF, NOIDA, pp.23-28.

Palmer, T. N., (2008) 'Thirty Years of NWP at ECMWF' In Extended Abstracts 'International Conference on Progress in weather and Climate Modelling over Indian Region' held on 9-12 December,2008 at NCMRWF, NOIDA, pp.105-110.

Parrish, D. E. and Derber, J. C.,1992, "The National Meteorological Center's spectral statistical-interpolation analysis system", Mon. Wea. Rev., 120, 1747-1763.

Prasad V. S., Ramesh, K. J., Bohra, A. K. and Bhatia, R. C., 1999: "Assessment of Quality and Impact of Full Resolution TOVS Temperature Profile Data on the Operational Global Data Assimilation-Forecast System of India", *Meteorology and Atmospheric Physics, 68, 197-212*.

Ramesh, K. J., Swati Basu and Begum, Z. N., 1996, "Objective determination of onset, Advancement and Withdrawal of the summer monsoon using large scale forecast fields of a global spectral model over India", Meteor. and atmospheric Physics,61, 137-151.

Rashmi Bhardwaj, Ashok Kumar, Parvinder Maini, 2008, “Statistical interpretation forecast and its skill during monsoon season in India. International Journal of Meteorology”, 34(336),39-47.

Someshwar Das, Ashrit, R., Iyengar, G. R., Saji Mohandas, Das Gupta, M., John, P. George, Rajagopal, E. N. and Surya Kanti Dutta, 2008,”Skills of different mesoscale models over Indian region during monsoon season: Forecast errors”, *J. Earth Syst. Sci.* 117, No. 5, October 2008, pp. 603–620.

Stuart Bell, 2008, “The Met Office NWP System - improving trend and future potential In Extended Abstracts 'International Conference on Progress in weather and Climate Modelling over Indian Region'” held on 9-12 December,2008 at NCMRWF, NOIDA, pp.6-10.

Sugi, Masato, 2008, Climate Change projection with a high resolution AGCM In Extended Abstracts 'International Conference on Progress in weather and Climate Modelling over Indian Region' held on 9-12 December,2008 at NCMRWF, NOIDA, pp.95-100.

Swati Basu, Ramesh, K. J. and Begum, Z. N., 1999, ”Medium Range Prediction of summer monsoon activities over India vis-avis their correspondence with observational features”, Adv. in Atmos. Sci.,16,1,133-146.

Swati Basu, Iyengar, G. R. and Mitra, A. K., 2002, “Impact of non-local closure scheme in simulation of Monsoon system over India”, *Monthly Weather Review, 130 (1), 161-170.*

Syroka, J. and Toumi, R., 2002, “Recent lengthening of the south Asian summer monsoon season”, *Geophy. Res. Lett.,* 29, (DOI: 10.1029/2002/ GL015053).

Tiedtke, M., 1983, ”The sensitivity of the time-mean large-scale flow to cumulus convection in the ECMWF model. *ECMWF Workshop on Convection in Large-Scale Models*”, *28 November - 1 December 1983, Reading, England*, pp. 297-316.

Wang, B., Ding, Q. and Joseph, V., 2009, “Objective definition of the Indian summer monsoon onset using large-scale winds”, *J. Climate* (In Press).

Xu, K. M. and. Randall, D. A., 1996, ”A semi empirical cloudiness parameterization for use in climate models”, *J. Atmos. Sci., 53*, 3084-3102.

Zeng, X., Zhao, M. and Dickinson, R. E 1998, “ Inter-comparison of bulk aerodynamically algorithms for the computation of sea surface fluxes using TOGA COARE and TAO data”, *J. Climate, 11*, 2628-2644.

Zhao, Q. Y. and Carr, F. H., 1997, “A prognostic cloud scheme for operational NWP models”, *Mon. Wea. Rev., 125*, 1931-1953.

CHAPTER 10

EXTENDED RANGE PREDICTION SYSTEM OF INDIAN SUMMER MONSOON

U. C. Mohanty*, P. Sinha, M. A. Kulkarni, N. Acharya, A. Singh, A. Nair and M. M. N. Rao
Centre for Atmospheric Sciences, Indian Institute of Technology Delhi

ucmohanty@gmail.com

10.1. Introduction:

Reliable high resolution weather forecasts are in increasing demand to the governments, industry, traffic, media, farming community and risk management departments of most of the countries worldwide (Majewski, 1997). The Indian Summer Monsoon Rainfall (ISMR) forecast for two weeks to one month in advance is one of the most challenging task to the scientific community due to complex interactions between land-air-sea and also small scale convective activities with large scale flow. The summer monsoon season (June to September) contributes more than 70% of the annual rainfall over India (Parthasarathy et al. 1994). The active equatorial intra-seasonal oscillations (ISO) enhanced the convective activity over the north Indian Ocean and moves northward to the Indian landmass. The onset of Indian Summer Monsoon (ISM) over the southern tip of Indian peninsula marks the beginning of rainfall season and ending of hot summer over the India. Though onset of ISM over Kerala on 1st June is considered the normal date for onset of ISMR according to India Meteorological Department (IMD), it generally occurs during end of May or early June. After the onset of ISM over Kerala, the monsoonal system marches towards the north associated with rainfall. One of the important features of monsoon is the monsoon trough, which, in general passes through the northern part of India such as Punjab, Rajasthan, Uttar Pradesh, Bihar, West Bengal & north of Bay of Bengal. The fluctuation of the ISMR mainly depends on the oscillation of the monsoon trough. In the active

phase of monsoon the trough shifts to south of its mean position causing good amount of rainfall over the country; on the other hand when it shifts to foothills of Himalaya, the rainfall reduces over the central parts of the country and monsoon break occurs. In the second half of September strength of monsoonal westerlies gradually decreases leading to the withdrawal of southwest monsoon.

The Indian summer monsoon plays a crucial role for the agro economic country like India. Major parts of the Indian population (more than 70%) explicitly depend on the agriculture and their economies are highly dependant on the crop productions during the summer monsoon season. Though the monsoonal system is a regular phenomenon, but the Indian summer monsoon has a large abnormality in the global climate systems. This abnormality varies from region to region and time to time. The advance intimation of likely behavior of monthly and seasonal rainfall helps the farmer to avail the opportunities and to make decisions that could enhance the farm productivity and maximize returns or minimize the loss. Among various types of forecasts made for different temporal scales viz. short range, medium range and long or extended range, the extended range forecasts are highly valuable to the farming community, government, industry for long term planning, decision making, management and mitigation. The extended range prediction of monsoon rainfall over smaller regions such as met-subdivision scale (Parthasarathy et al. 1994) is one of the challenging tasks to the scientific communities.

The forecast products from General Circulation Models (GCMs) are being effectively used all over the world for generating seasonal forecasts. The GCMs are the important tools to simulate the atmospheric circulation. Present day, most of the GCMs are coupled with oceanic models to take into account the interactions between the oceans and the atmosphere. Although these numerical tools are required to understand complex interactions between land-ocean-atmosphere systems globally, they are computationally intensive and then, can only produce relatively low spatial resolution simulations which in turn provide data in coarse resolutions on model spatial grid. Therefore, direct application of GCMs output is often inadequate because of their limited

representation of mesoscale atmospheric processes, topography and land sea distribution in GCMs (Cohen 1990; von Storch et al., 1993). Consequently, the performance of these model are poor in capturing small scale physical processes which drive some important local/regional surface variables and their high resolution properties such as precipitation (frequency of occurrence and intensity) and its strong variability (Wood et al, 2004). Also, it is difficult to compare GCMs output to local present observations (Vrac et al., 2007) and even more for extreme climate/weather events (Vrac and Naveau, 2007) due to coarse resolution of GCMs. However, comparison between local observations with the model simulation output is essential to understand physical and dynamical processes of the atmospheric circulation in local scale. In order to overcome these scale issues, it is important to reproduce information from GCMs output in higher resolutions for better understanding the regional/local weather/climatic phenomena though, this reproduced information for specific geographic location may not coincide with the model grid.

A number of methods are used to convert GCMs output to required region. The simplest method is to consider the nearby model grid points as the representative points of the target region. This method often is not able to reproduce realistic features since the representative points are in general, far away from the targeted region and the surface characteristics of the representative points are also different. To improve the nearest point forecast, a number of procedures are present that fall in general calibration and downscaling techniques (Barnston and Smith, 1996; Goddard et al., 2001; Landman and Goddard, 2002; Stephenson et al., 2005). These downscaling techniques work as the bridge between climate forecasts and weather (Wilby and Wigley, 1997; Huth and Kysely, 2000). In other words, downscaling is a technique which links the state of some variables representing large space to the state of some variables representing a much smaller space (Benestad et al., 2008). The field of downscaling is divided into two approaches namely a) “Dynamical downscaling” based on nesting of high-resolution regional climate models (RCMs) to simulate finer scale physical processes consistent with large scale weather evaluation prescribed from a GCM (Giorgi et al., 2001; Mearns et al., 2004; Lim el al., 2007) and b) “Statistical

downscaling" adopts statistical relationships between the regional climate and statistical characteristics of desired fields from the coarse resolution of GCM data (von Storch et al., 1993; Wilby et al., 2004; Goodess et al., 2007). The downscaled high resolution data can be used for forecast and as input into other types of numerical simulation tools such as hydrological, agricultural and ecological models. Therefore, use of proper downscaling techniques is the key issue for extended range prediction systems.

A brief overview has been given in 10.2 on the Extended Range Forecast System (ERFS) and its present status with skill evaluated by various scientists worldwide. Descriptions and methodologies of different downscaling techniques for ERFS have been discussed in 10.3. Preliminary efforts with some experimental results have been given in 10.4. Finally, the conclusions of this study have been presented in 10.5.

10.2. Extended Range Prediction System:

The forecasts are classified in various categories. These categories have mainly defined on the basis of temporal coverage of the forecasts viz. now cast, short range, medium range, extended range, seasonal scale and long range forecasts. The forecasting of the weather for the next six hours is generally referred as now casting. It is easier to forecast in the temporal range of now-casting than the other forecasts because possible occurrence of local weather features such as showers, thunderstorms, snowfall etc. can be predicted upto convincing accuracy by analyzing latest manual observations as well as the latest radar and satellite data sets. The forecasts delivered for a lead time of a day or three are called as short-range forecasts. Medium-range forecasts are made for periods covering 4 to 10 days ahead while the extended range forecasts are made for periods of two weeks to a month. Seasonal forecast refers the prediction of mean weather for seasonal scale. In the long range category, the time scale is more than a year. In short and medium range, local forecasts are most valuable for high impact weather phenomena such as cyclone, thunderstorm, tornado etc which may result in loss of life and property due to wide-spread/heavy rainfall and strong wind.

Present day numerical weather prediction models (NWP) are able to forecast short range atmospheric events with satisfactory accuracy due to improvement of model physics and dynamics and availability of high performance reliable computing systems. Seasonal and extended range forecasts are different from weather forecasts since it involves the prediction of the deviations from the seasonal climate. The skills of different scale of forecasts may be represented in a schematic diagram (based on inputs from various available published work on forecast skill over different temporal scales, researches and forecast application scientists) as Fig. 10.1. It is seen from the Fig.10.1 that though there is a good degree of predictability skill in short-range weather forecast, the skill is waning with time. The seasonal scale forecast which is mainly based on statistical methods has some predictability skills. The extended range prediction is one of the toughest tasks due to inherent complexity of low skill.

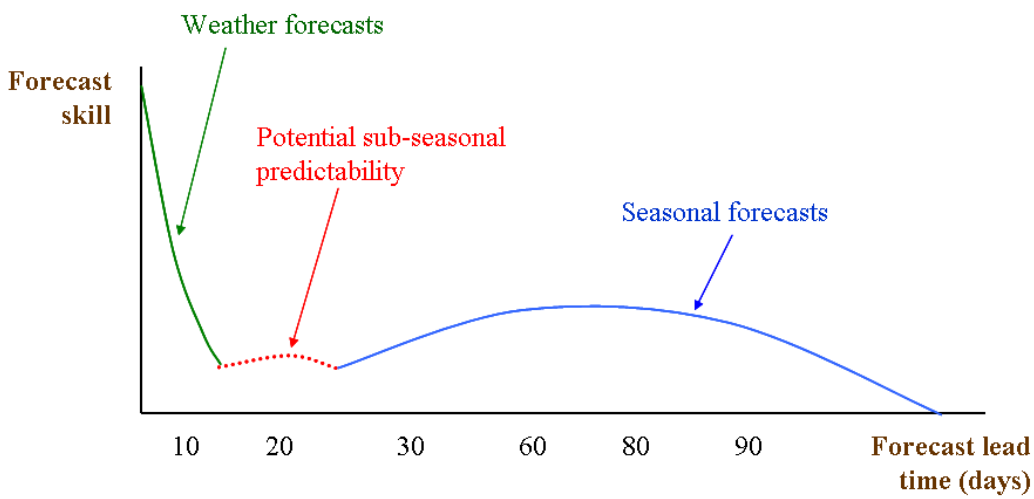

Fig. 10.1: Schematic diagram for skill of different scale forecasts with forecast lead time.

The first long range forecast for ISMR was provided by Blandford in 1886 based on the relationship between Himalayan snow cover and monsoon rainfall (Blandford, 1884). Long range forecasts during initial years were made through subjective and qualitative analysis. Sir Gilbert Walker in 1909 for the first time introduced an objective technique based on correlation and regression analysis (Walker, 1910, 1923, 1924). Walker discovered the link between Indian monsoon with the Southern Oscillation,

which is see-saw of pressure between Darwin and Tahiti in the Pacific Ocean. The first model for long range weather forecast was developed by Walker and it was used for prediction of the Indian summer monsoon rainfall in 1909. He used a linear regression model based on four predictors namely i) Himalayan snow accumulation at the end of May, ii) South American pressure during March–May iii) Mauritius pressure of May and iv) Zanzibar rain in April and May. This was the most important step in the meteorological history for long range weather forecast. In the early and mid of 1930, C-G- Rossby and Jerome Namias had put efforts for long range forecast (Namias, 1955, 1968). Univariate time-series methods and multi-variate statistical and physical methods had been used in different centres for prediction of long range weather in late 60's. In the 70's and 80's research on probabilistic methods continued, and the Monte Carlo Method was developed in the 70's to improve the long range forecast. Till early 1970's, seasonal scale forecast was based mainly on simple regression equations. Along with these statistical techniques, dynamical approaches (using NWP models) were also in use (in R&D mode) for forecasting of weather and climate.

Vilhelm Bjerknes carried out an explicit analysis for weather prediction and divided the rational forecasting system broadly into two sections (Bjerknes, 1904); one is diagnostic section where the initial state of the atmosphere is determined using observations; and next is prognostic in which the state of the atmosphere and its changes can be calculated using the laws of motion. Richardson (Richardson, 1922) had tried to forecast on early 1920's by solving the governing equations numerically, but could not succeeded. In the mid 1930s von Neumann suggested that progress in dynamical forecasting would be greatly accelerated with the availability of faster computing systems that can solve the complex equations numerically. In the mid 1940's, the Institute for Advanced Study in Princeton was the setting for one of the major technological advances in atmospheric science with the advent of numerical prediction on the Eniac, the first high speed computer. The efforts of weather prediction through numerical weather prediction model in the early 1950's had been put forward by Charney and colleagues by solving the complex equations numerically by removing the gravity waves equations using Eniac computing systems. To generate 24 hours forecast

using fastest computing system at that time, it took 24 hours! Moreover, the results were impressive and showed the scope of dynamical methods for numerical weather predictions. With the increase in efficiency of computers and improvements of model physics, the first dynamical seasonal prediction came into picture in the early 1970's using a general circulation model (GCM). Efforts for reliable forecast in extended range weather using dynamical models was taken by European Centre for Medium-Range Weather Forecast (ECMWF) in the mid of 1980's. The improvements of model physics and dynamics, assimilation techniques, more observational data and increase of efficiency of computation systems with time, the skill of seasonal scale predictions have been improved (van den Dool, 1994; Palmer et al 1990) and a number of organizations had started to issue seasonal scale forecast in the late 1990's. In long range forecast, both the statistical techniques and dynamical approaches have similar skills.

In the evolving of seasonal scale prediction which is mainly based on statistical methods, the forecast has some predictability skills over a larger domain. Since the life cycle of a crop is almost completed within a season and evolve through different phases which have two weeks to one month time for each, thus, this seasonal scale prediction of rainfall is not sufficient to the agricultural communities. Therefore, prediction in the scale of two weeks to one month which is known as extended range is highly needed to the farming communities and also for policy planning for agro-economic country India. The short and medium range prediction systems have advanced a great success with the accuracy level nearly 80% for forecast of atmospheric events. This success comes since short and medium range atmospheric events depend largely on its initial values and also with the improvements of observational data sets in higher density. While, the seasonal scale events are mainly governed by seasonal scale features specifically by some large scale features, slowly varying land surface parameters and some semi permanent features, therefore, prediction of seasonal scale events using these features through statistical techniques has some predictability skill. In the context of ERFS programme in India, the predictions of monsoonal rainfall is set for different temporal (two weeks to a month) and spatial (India as a whole, homogeneous and met-subdivision) scales. Earlier studies found that the predictability skill for forecast of

surface air temperature have positive value beyond day 9 (Fig.10.2) and for other weather variables such as total precipitation, surface wind speed etc., the skills are decreasing faster than temperature in the long range forecast. It is also clear from fig.10.1 that extended range prediction has very low skill and that is probably due to characteristics of inherent nature of the prediction systems.

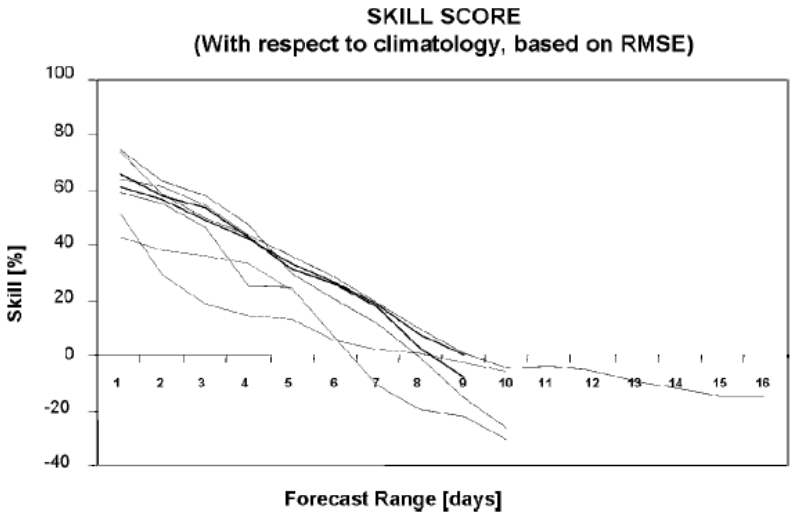

Fig. 10.2 : Skill scores of a set of eight competing forecast of the daily average temperature at London Heathrow. Positive (negative) skill scores indicate that the forecasts are more (less) accurate than long-term climatology. Accuracy was measured by calculating root mean squad errors (RMSE). After Mailer (2010)

10.2.1. Status of Extended Range Forecast:

10.2.1.1. **International**

Present day, a number of organizations/institutes including almost all eminent meteorological organizations such as European Centre for Medium Range Weather Forecast (ECMWF), National Centre for Atmospheric Research (NCAR) (Hack et. al, 1998; Hurrell et. al, 1998 and Kiehl et. al, 1998), UK Met. Office, National Centre for Environment Prediction - Climate Forecast System (NCEP-CFS) (Saha et. al., 2006) , USA, International Research Institute for Climate and Society (IRI) (Li and Goddard, 2005; van den Dool, 1994; Delworth et. al, 2006; Anderson and coauthors, 2005), USA,

Japan Agency for Marine-Earth Science and Technology (JAMSTEC) and APEC Climate Centre (APCC) Korea etc. are issuing a monthly to seasonal scale global forecasts using both dynamical models and statistical techniques. These centres are running coupled (semi or fully) general circulation models and integrations are carried out for several months to generate dynamical output to prepare monthly and seasonal forecasts. The forecasts are mainly generated for precipitation and temperature and issued in each month.

10.2.2.2. National:

As mentioned in earlier section, Blanford (1884), then chief of newly formed India Meteorological Department, was the pioneer in the long range prediction based on inverse relationship between Indian Summer Monsoon Rainfall (ISMR) and preceding winter snow cover over Himalayan region. This relationship was used during the early 1880's for prediction of ISMR in seasonal scale till the discovery of tele-connections with 3 large scale horizontal see-saw oscillations with ISMR by Sir Gilbert Walker (1923, 1924). These pressure oscillations are called the Southern, the North Pacific and the North Atlantic oscillations. Based on this relationship, he made simple regression equation to predict the ISMR in seasonal scale. Further, Sir Gilbert Walker found in-homogeneity in rainfall over India, and divided India as two homogeneous rainfall regions namely North West India and Peninsular India based on the correlation with the predictors and ISMR used for study. This classification on homogeneous region of rainfall was used till 1987 (Gadgil et al, 2005). Till late 1990's, the operational forecasts were generated mainly based on statistical techniques. For this purpose, lot of efforts have been made to find out suitable predictors to improve the seasonal scale forecast (e.g. Walker, 1910, 1923, 1924; Hahn & Shukla, 1976; Banerjee et al., 1978; Shukla and Paolino Jr., 1983; Thapliyal, 1984, 1997; Verma et al., 1985; Bhalme et al., 1987; Hastenrath, 1987; Parthasarathy et al., 1988, 1990). With this, attempt had also been made to develop different forecast techniques (Thapliyal, 1982, 1986; Gowariker et al., 1989). Review on the development of forecasts techniques can be found in some useful literatures (Jagannathan, 1960; Das, 1986; Thapliyal, 1987; Shukla, 1987; Thapliyal &

Kulshrestha, 1992). The developed new models such as Parametric, Power regressions, multiple-regression and Dynamic Stocashtic Transfer etc., have been used since mid 1980's for long range forecasts (LRF). Details of different operational models being used for seasonal forecast of ISMR and methodologies for preparation of forecast over India can be found in Thapliyal (1997). Xavier and Goswami (2007) have developed a OLR based model to predict the monsoon activity (active and dry spells) over India up to 3 weeks. With the development of regional climate models (RCM), an extensive research is going on to downscale coarse resolution coupled general circulation model for forecast in monthly to seasonal scale.

10.3. Methodologies for ERFS

In the last two decades, dynamical numerical models have improved considerably in terms of prediction skill of seasonal scale mean forecast of rainfall over some regions such as over central Pacific; however, not much breakthrough has taken place in improving the prediction skill of Indian summer monsoon rainfall. In recent years, dynamical (with high resolution, improved parameterizations scheme, data assimilation, observed land surface parameters insertion etc.) and statistical (bias corrections, model output statistics, canonical correlation analysis, multi-model ensemble, Bayesian techniques, etc) techniques have shown that the monsoon variability in the tropics can be resolved with reasonable skill in monthly as well as seasonal scale. An extensive research work on dynamical and statistical techniques is required for extended range prediction of rainfall over homogeneous or met-subdivision regions for India.

Present day coupled GCMs produce forecast of atmospheric variables in coarse resolution over grid points, which is insufficient for forecast over smaller regions in extended range prediction. Improvement of forecast in extended range can be made by reproducing global model forecasts in local scale using downscaling techniques. Forecasting of these downscaled variables can be more useful to the application sectors such as agricultural section, hydrology section etc. for planning and

management. There are mainly two kinds of downscaling methods i) Statistical downscaling and ii) Dynamical downscaling which are used to reproduce coupled GCMs data in higher resolutions for extended range prediction.

10.3.1. A review on performances of both techniques over different region worldwide

There are a number of application related criteria that contribute to an appropriate choice of downscaling method in a particular context (Mearns et al., 2004; Wilby et al., 2004). But there are assumptions involved in both techniques (Giorgi et al., 2001) which are difficult to verify a priori and contribute to the uncertainty results. Though statistical downscaling has an advantage over dynamical downscaling for long range forecast, it is not clear which method provides better prediction of localized climate (Benestad et al., 2008). The limitation of statistical methods is that downscaled variables might not guarantee physical consistency between them because it may not be possible fully to include the complex physical processes encompassing nonlinearity in the methods.

Several studies have been carried out to compare dynamical and statistical downscaling methods for various atmospheric phenomena over different regions worldwide. Kidson and Thompson (1998) studied present day climate over stations in New Zealand with the help of a regression-based statistical model and a RCM integration and found that both statistical and dynamical methods gave similar levels of skill in the representation of observed temperature and precipitation anomalies. Similarly, Murphy (1999) found that a regression model for monthly temperature and precipitation anomalies has a comparable performance to a RCM for stations in Europe, but scenarios developed from statistical and dynamical methods differed significantly (Murphy, 2000). Schmidli et al (2007) tested statistical and dynamical methods over European Alps region and stated that none of these methods is superior and performance varies significantly from region to region and season to season. It is also observed from experiments that performance is better for the indices related to the

precipitation occurrence than to the indices related to precipitation intensity. Large differences were also found in precipitation scenarios between a RCM and a multivariate regression model in Scandinavia (Hellström et al., 2001). Charles et al (1999) have studied the stationary of statistical downscaling methods using RCM climate change integration and concluded that a relative humidity predictor is required for the reproduction of RCM simulated changes in precipitation occurrence in global warming scenario. Several inter-comparison studies have adopted dynamical and statistical downscaling for hydrological impact models and significant differences are found between downscaling methods (Hay and Clark, 2003; Wood et al., 2004). Finally, it is accepted that both the statistical and dynamical downscaling methods are capable to capture well the mesoscale atmospheric features that are not captured in GCMs (Schmidli et al., 2007).

10.3.2. Statistical

The basic approach used for application of extended range forecast is tailoring of GCM forecasts in time and space, this approach is often referred as downscaling. These downscaling techniques work as the bridge between Climate forecasts and weather (Wilby and Wigley, 1997; Huth and Kysely, 2000). One of the important techniques for downscaling is statistical downscaling that includes a large number of methods, ranging from simple interpolations to eigen techniques, regression methods (such as Multiple Linear Regression, Principal Component Regression, Stepwise regression etc.), stochastic time series models (Markov Models), artificial neural networks, genetic algorithms etc. (Hewitson and Crane, 1996; Ji and Vernekar, 1997; Wilks 1999; Fuentes and Heimann, 2000; Huth and Kysely, 2000; Huth, 2002; Widmann et al., 2003; Rabiner and Juang, 1986; Zucchini and Guttorp, 1991; Robertson et al., 2004; Kioutsioukis et al., 2008; Feddersen and Andersen, 2005; Coulibaly et al., 2005). These methods are based on finding statistical relationships between sets of predictors and predictands. Usually, predictors are selected from the Global Model output while the predictands are the observed variables for the training period.

The success of downscaling techniques depends on the accuracy of Global Circulation Model's fields. Therefore, Model Output Statistics (MOS) techniques (e.g. Bias Correction, Multi Model Ensemble etc.) must be applied on the model products before applying the downscaling methods.

10.3.2.1. Bias Correction Methods

The term Bias is used to explain an inclination towards a particular perspective or result. Any tendency to favour a certain set of values naturally lead to an uneven dispensation of judgment. Regarding model forecast at a particular time the bias is the difference between estimated parameter and the true value of the parameter. All statistical methods are generally developed with the assumption that errors generated are random in nature and the mean is zero (unbiased estimations). But forecast models have systematic errors. These errors can result in biased forecasts. That means if we have number of simultaneous model simulations and observations then it is essential to check whether the model is biased towards particular range of values, i.e. the model may predict low values of the parameter/s better than high values or vice versa. Then it is very important to remove the bias for the improvement in the quality of the forecast. The best way to handle the issue of bias in forecasts is first estimate the bias and then correct it, before using the data for analysis.

In the case of rainfall there are two characteristics, one is duration/frequency and another is its intensity. Model forecast may be biased for both. In such situations the bias can be corrected in two steps (Ines and Hansen, 2005) viz. frequency correction and intensity correction.

There are two different definitions for the model forecast bias.

According to Wilks (1995)-

Bias is the ratio of number of “yes” forecasts to the number of “yes” observations. That is, if number of “yes” forecast is ‘a’, while number of “yes” observations is ‘c’ then the bias B can be given by following ratio.

$$B = \frac{a}{c}$$

It indicates that if B is 1 then the forecast is unbiased. If B>1 then the forecast is over-estimated and if B<1 then the forecast is under-estimated.

According to Dee and Da Silva (1998)-

A forecast is said to be biased if the mean of forecast error is non-zero. It (the mean of forecast error) is the forecast bias (Dee and Da Silva, 1998). So, forecast bias can be estimated by comparing forecasts with Observations, i.e. from observed-minus-forecast residuals. In such situations we have to assume that observation is the true state of atmosphere.

Some methods for bias correction are given below. Generally bias is corrected by transformation of model output into the corrected one. This correction can also be done without use of transformation functions. In the without transformation methods, the bias is estimated and then corrected but while using transformation methods bias is not calculated explicitly.

Method 1 (without transform):

If F_T is model forecast at time T and O_T is observation at the same time then the model error ε_T will be.

$$\varepsilon_T = O_T - F_T$$

Then the Bias B can be defined as follows.

$$B = \langle \varepsilon_T \rangle$$

Thus, using this definition we can find and remove the general model forecast bias.

i.e. corrected Model forecast = $B + F_T$

But what if the model has different biases for different in range of forecast. In such situation we can find the forecast biases for the different categories of forecast. This technique has been illustrated in following steps.

The model output can be divided into various classes, created using quantiles.

For each and every class, model error and bias can be calculated.

Then the biases may be removed from the respective classes of model output.

One can also fit an equation to find out corrected Model forecast C F_T as follows:

$$C\,F_T = a_0 + a_1\,F_T$$

One way of finding values of a_0 and a_1 is given earlier i.e. substitute a_1=1 and a_0 = $\langle \varepsilon_T \rangle$, this method is also referred as bias corrected individual forecast (Kharin and Zwiers, 2002).

In another technique which is called as regression corrected individual forecast, the coefficients are calculated as following ways:

$$a_1 = \mathrm{Cov}(O_T, F_T)/\mathrm{Var}(F_T) \text{ and } a_0 = \langle O_T \rangle - a_1 \langle X_T \rangle$$

According to Kharin and Zwiers (2002) the regression coefficient a_1 rescales the forecast to correct systematic errors in simulating the atmospheric response to the lower boundary conditions and to minimize the effect of climate noise in the model forecast on error variance. The intercept a_0 removes the bias from the rescaled forecast.

Quantile-Quantile (Q-Q) Mapping Method:

In the quantile mapping method empirical probability distributions of observed and forecasted values are used. The transformed/bias corrected output is inverse of cumulative distribution function (CDF) of observed values at probability corresponds to the model output CDF at the particular value. In quantile mapping method the bias is not calculated explicitly. Suppose we have CDFs, F_o for observed data and F_f for model forecast. Then for a model output X the bias corrected value Y will be as follows:

$$Y = F_o^{-1}(F_f(X))$$

Here F^{-1} is an inverse of CDF. Thus, the quantile mapping procedure is transformation between two CDFs. This method is used and well explained by Wood et al. (2002),

Hashino et al. (2006). The steps that can be followed for this purpose are given as follows. Find empirical probability distribution of the observed as well as model output data. This can be done using simply fitting their histogram and then dividing the frequency of each class by the total number of observations. But for this purpose number of classes created should be large or at least sufficient enough.

This will give us set of probabilities falling in each class say P(xi) where the suffix i =1, ….,n, where n is the number of classes. Now the cumulative distribution function (CDF) will be as follows:

Mathematically we have to write the CDF equation as $C(x_i) = \int f(t)dt$ where f(t) is the probability density function. If we replace the integration sign by summation for the discrete data then it is easier to understand and the function looks as follows.

$$C_i = \sum_{j=1}^{i} P(x_i), \quad i = 1,2,3.....n \qquad \text{----------(1)}$$

Its easy to understand that ∑Ci =1. Also Ci will give us the fraction of total number of data points below the given value i.e. the quantile of the particular class. The inverse of CDF will give us the value at a particular probability. The inverse of CDF is also called as quantile function.

Now one can use the equation (1) written above for getting the bias corrected value of model output. The working of the model output quantile function's mapping on the CDF of observed data can be shown by following fig. 10.3.

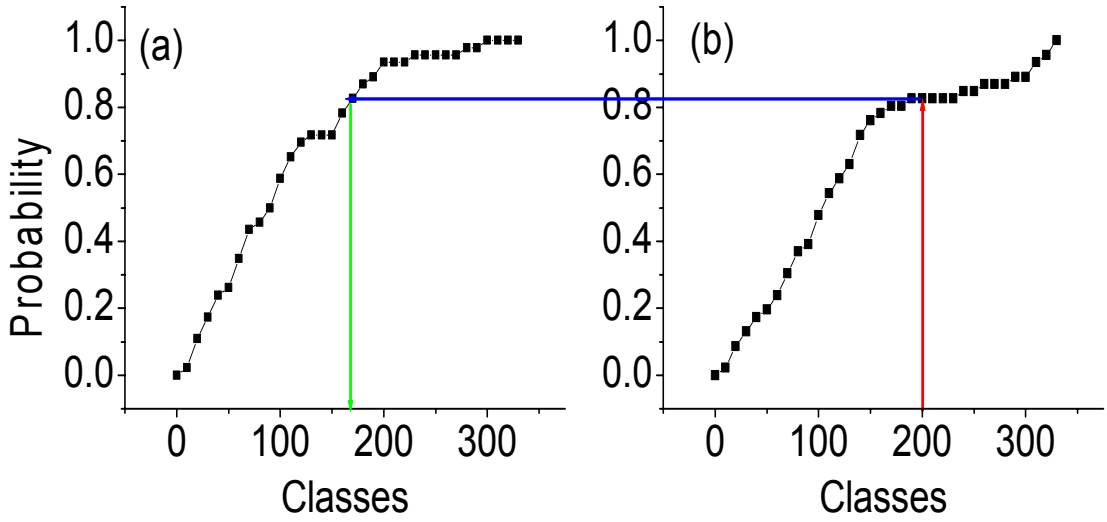

Fig.10.3 : Illustration of quantile mapping for virtual data sets.
The CDF from sub plot (b) is mapped on the CDF of subplot (a)

From the Fig. 10.3 we can easily understand the equation 1 and quantile mapping. In the above Fig.10.3, suppose that Fig. 10.3 (b) is plot of CDF of model output F_f. And Fig. 10.3(a) is the plot of CDF of observed data F_o. Lets consider that the model output is 200 then the from equation 1 F_f (200) ≈ 0.83 (i.e. 0.83 is the probability or 200 is q0.83) and $F_o^{-1}(0.83) \approx 160$. Thus the bias corrected value of model output 200 will be 160.

Regression method:

A regression model is an estimation of expected value. Fitting a regression model is the generally implemented option for the transformation. The regression model is estimated using the observed and simulated datasets from the historical records, i.e. a regression equation is fitted for model output as dependable variable and observed data set as independent variable. In this method the bias is not calculated directly instead, removed indirectly. The regression may be fitted using Locally Weighted Least Square regression approach.

Locally weighted least square method:

If the form of the function f(X,β) is complicated or unknown, then locally weighted least square method can be used. It is also known as LOESS or LOWESS (LOcally WEighted Scatterplot Smoothing). Cleveland (1979) has explained this method in detail. LOESS combines the simplicity of liner least squares and flexibility of nonlinear regression. In this approach, a simple regression equation is fitted to localized subset of the data. First, the data are divided into various subsets and then at each point of the subset, a simple polynomial is fitted using weighted least square technique. Using the response from variables in the neighborhood of the particular point, the weights are calculated i.e. more weightage is given to points near the point and less weightage is given to points which are away. The beauty of this method is user need not specify any particular global function of any form to fit the entire data.
The steps followed in this technique are as follows.

Sub setting the data: it is done by taking the data points close to each other. Actually this can be done by sequential shifting of data points. It means if we have 100 data points, then first we may select 1 to 30 then 2 to 31 till 71 to 100 for fitting the local regression equation.

Then the weightage is given to each point according to the scaled distance.
Weight function (W(x)) as selected. (in general tri-cub). It has following properties

$$W(x) = \begin{cases} (1-|x|^3)^3 & \text{for } |x| < 1 \\ 0 & \text{for } |x| \geq 1 \end{cases}$$

Here, x is the scaled distance.

Then a simple regression equation is fitted using weighted least square method taking W(x) as the weight matrix.

10.3.2.2. Multi Model Ensemble

The skill of climate predictions is limited because of internal atmospheric variability, which is largely unpredictable beyond the deterministic predictability limit of

about two weeks (Kharin and Zwiers, 2002). This variability induces noise in model predictions. Generally model forecasts initiated from different initial conditions as well as different models are averaged using different techniques to reduce this noise in model predictions. This approach is called as ensemble. There are two ways to solve this problem viz. deterministic and probabilistic. The simplest technique is just linearly averaging the model forecasts. Krishnamurti et al., 1999, 2000 have introduced the concept of superensemble approach. This approach has been used by Kar et al. 2010 for precipitation forecast for July month over Indian domain. This approach is briefly discussed below:

Super ensemble:

$$S_t = \overline{O} + \sum_{i=1}^{n} a_i \left(F_{i,t} - \overline{F}_i \right)$$

Where,

St = Super ensemble prediction at time = t.

$\overline{O}$ = Observed monthly mean over the training period.

$\overline{F}_i$ = climatology of the ith model forecast over the training period.

$F_{i,t}$ = ith model forecast for time t.

ai = Regression coefficient (obtained during the training period.)

n = No. of models.

The knack in employing this approach is the estimation of a_i.

The simplest way to do it is ai = 1/n this approach is also known as Simple Composite MME. Another method to calculate ai is singular value decomposition discussed as below.

A covariance matrix is built from the forecast anomalies.

$$C_{i,j} = \sum_{t=0}^{Train} F'_{i,t} \, F'_{j,t}$$

Where,

Train = Training period.

i = ith model forecast.

j = jth model forecast.

F´ = Forecast anomaly

An assumption can be made from the above two equations as O´ = C A. Here A is the column vector containing a_i values.

The matrix C can be written using SVD as C = UWVT. C is a square matrix hence; it is easy to understand that U and V are equal. And a little calculation gives us the vector A.

$$A = V.\left[diag\left(\frac{1}{W}\right)\right].\left(U^T.\tilde{O}\right)$$

Where $\tilde{O} = O' - F'$ while $O' = O - \overline{O}$

Kharin and Zwiers (2002) have applied a slightly different approach called as mutimodel linear regression. These methods can also be used to remove systematic bias from model products. It is given as follows.

$$S_t = a_0 + \sum_{i=1}^{n} a_i \, F_{i,t}$$

In this approach the main trick is to find out the regression coefficients. It can be done by covariance analysis.

Another technique suggested is, synthetic multi model ensemble. In this technique firstly a synthetic dataset is generated using spatial correlation between model forecast and observational data set analysis by principal component analysis and then the MME is performed on the synthetic dataset Yun et al (2005).

10.3.2.2. Probabilistic forecasting

Extended-range prediction is inherently probabilistic. For climate risk management, it is essential that uncertainties in predictions are communicated to user agencies. There are two main approaches for probabilistic forecasting, one is non-

parametric and another is parametric. In non-parametric method, one can just count the number of ensemble members falling in each category and divide them with total number of members to get the probabilities of each category. In parametric method, some distribution is assumed for estimating the probabilities. Here onwards, the discussion is made for the parametric method. In general, the forecast is delivered in three categories (generally terciles) viz. Above Normal, Near Normal and Below Normal. These categories are decided using distribution of observed data in the hind cast period. Afterwards, when the forecast for a particular year will be available, then mean and spread of the forecast distribution is computed using various methods. Once the forecast distribution is known, then chance (probability) of falling the mean of forecast distribution in a particular category is computed. If we have multiple numbers of GCMs then the mean of forecast distribution may be just simple ensemble of all the models while the spread can be computed using the correlation between mean of forecast distribution and observed time series (Tippett et al. 2006).

Downscaling

As mentioned earlier, downscaling is a procedure to find relation between variables at larger spatial and temporal scales to those at smaller scales. The simplest technique is fitting linear regression. In this technique if we choose more than one predictor then it is called as multiple linear regression (MLR). If Y is the predictand and X is set of predictors i.e. model products then

$Y=a_0 + a_1 x + a_2 x + \ldots\ldots\ldots + a_n x$

The coefficients (a_0, a_1,….etc) can be calculated using simplest least square technique. Selection of the best regression equation is the main problem in MLR. Various approaches to select best regression equation can be found in Draper and Smith (1966).

Principal Component Regression (PCR) & Canonical Correlation Analysis CCA:

Principal Component Regression (PCR): If there is very high correlation among the independent variables (predictors) of a regression equation (problem of multicollinearity), then it may lead to unstable regression, in that case, it is essential to remove the correlation among them. This can be done using the Principal Component Analysis (PCA). Some times PCA is also called as Empirical Orthogonal Function (EOF) analysis. Principal components of the independent variables can be used in the regression equation instead of directly using the independent variables. This technique is called as principal component regression. One more advantage of PCR is to reduce the dimension of the independent variables to a large extent which simplify the computation. The steps followed in this procedure are as follows:

Principal component analysis is applied on the set of predictors and the PC's are generated. These PCs are ranked by order of explained variance. This means that the first PCs represent significant variance (which explains the maximum variability among the predictors), and the last unwanted variance or noise. These last PCs are eliminated without losing important information from the data and a new set of independent predictors are generated say 'P'. Afterwards MLR is fitted for 'Y' using 'P' as predictors. Though there doesn't exists any fixed rule to fix the number of PCs to be used, the screen plot of eigen values may be used to identify the number of significant modes.

Canonical Correlation Analysis (CCA): Canonical Correlation Analysis (CCA) is a statistical technique having some similarity with the PCA (Principal Component Analysis). This approach picks out a sequence of pairs of patterns in two multivariate data sets, and constructs sets of transformed variables by projecting the original data onto these patterns. Canonical correlation analysis can also be viewed as an extension of multiple regression (Wilks (1995)) as a multi-component predictors are linearly related to multi-component predictands where, the correlation structure is explained with each successive CCA modes. In CCA, original data sets X (independent) and Y

(dependant) are transformed into new set of variables V_m and W_m respectively, called as canonical variables. These variables are defined as follows

V_m = A X

W_m = BY

Calculation of A and B called as a canonical vector is similar to that of the Principal component analysis.

Then we can write

$W_m = \beta V_m$

It can be easily proved that β = Rc, where Rc is the diagonal matrix of the canonical correlations. Thus Y can be easily found out using the relation Y = $B^{-1} W_m$

Hidden Markov models:

The climate forecasts can also be downscaled to station level using Hidden Markov models. These models have emerged from the Markov processes, in which we assume that the next value in a series is solely depends on its earlier value. But in some cases, the weather patterns that we wish to find out are not completely explained by Markov processes. It means, we don't have all the observations, some of the atmospheric states are hidden (assumed from observations). For example: a person sitting in the house observes that his friend has come to meet him with a wet umbrella, so in this case the hidden state is, it is raining outside. Another example can be given for it as follows: State of a day may be sunny, cloudy or rainy and our observations are dry, slight dry, slight humid, humid. In such cases use of Markov process only based on observations will produce incorrect results. In such situations the observed sequence of states is probabilistically related to the hidden process; and these processes are modeled using a hidden Markov model, in which the underlying hidden Markov process changing over time, and a set of observable states which are related somehow to the hidden states. These Hidden Markov models are further broadly divided into two groups viz. homogenous HMM (referred hereafter as HMM) and Non homogenous HMM

(referred hereafter as NHHM), where HMM is spatial case of NHMM (Hughes and Guttorp 1994).

The development of HMM is explained in detail by Zucchini and Guttorp (1991). In this model the atmospheric states (not observed) are estimated from observations such as rainfall and then these states are verified by plotting some general atmospheric variables. The HMMs are useful for analyzing the multisite sequences of atmospheric variables (generally rainfall). The need of prediction or tailoring of GCM products to station level can be accessed by NHHMs. In NHHM, a relation between atmospheric circulation and a given regional process (GCM product) is worked out to simulate the space-time relation of the regional processes with a particular sequence of atmospheric data. The development of NHMM is explained in detail by Hughes and Guttorp 1994.

Chaos theory (Lorenz model):

A number of attempts have been made for the extended range predictions with the use of the Lorenz model (Lorenz 1963, 1965, 1975) in which the state vector of barotropic model evolves with two characteristic time scales—an oscillation time around the regime centroid, and a residence time within a regime (Palmer 1993). Regime structure in low-order baroclinic models has also been noted (Reinhold and Pierrehumbert 1982, Legras and Ghil, 1985 and Schneider et al., 1991) and it is found that in such models, the faster time scale can be associated with baroclinic instability. Observational studies give some support to this view of the atmosphere. The Lorenz model gave a clear conceptual understanding of results from numerical weather prediction experiments that time averaging alone is of limited value, while ensemble forecasting has greater potential, enabling predictable and unpredictable regime transitions to be recognized a priori. The extended Lorenz model was used to provide a conceptual framework to understand the potentially conflicting GCM results. It is noted that sea surface temperature anomalies can have a statistically significant response in the extended range predictions and the magnitude of low-frequency variability in long integrations

with climatological and interannually varying SST are very similar. Results from the extended range model also indicated that the time-mean response to SST anomalies should have a strong projection onto a preexisting weather regime. The SST anomalies in the extended range model had a strong effect on the probability of residence within these regimes; in practice, estimation of these probabilities can be realized only through ensembles of integrations.

Palmer (1993) has discussed elaborately the physical basis underlying extended-range prediction based primarily on three premises. Firstly, observational (Namias 1955) behavior of synoptic-scale secondly, the definition of deterministic limit finally the slowly varying surface parameters. It is observed that time averages are inherently more predictable than instantaneous fields, that predictability depends very strongly on initial conditions, and that underlying anomalies in the tropical sea surface temperature impart extra predictability to the large-scale extratropical flow. On the one hand, cluster analysis of long hemispheric records of geopotential height indicate the existence of weather regimes (Mo and Ghil 1988; Molteni et al. 1990, 1993; Cheng and Wallace 1993), though they are not as distinct as in the Lorenz model. On the other hand, the nonlinear balance associated with quasi-stationary states in the atmosphere, and the nonlinear interaction between large and synoptic scales, has been very well established from observations (Shutts 1986; White 1990). However, the most important property of the Lorenz model, relevant to the discussion of all three premises for extended-range prediction, is associated with the fact that its local predictability properties vary substantially with position on the attractor; associated with this, phase-space regions where predictability is small are distinct from regions where the flow is quasi-stationary.

10.3.3. Dynamical:

The efforts have been initiated for monthly to seasonal scale prediction more than five decades ago (Namias 1955) and the use of dynamical models for predictions of Asian summer monsoon was initiated around four decades ago (Krishnamurti, 1969). Atmospheric General Circulation Models (AGCM), Global Coupled GCMs (CGCMs) and coupled Atmosphere Ocean GCMs (AOGCMs) are the main tools for dynamical seasonal scale prediction. Numerous groups in USA, Japan, Australia, China and Europe have made major contributions in the area of research and operational practice on Numerical Weather Prediction (NWP). Shukla (1981) has discussed a physical basis for the prediction of monthly means and Miyakoda et al (1983) have represented a skillful dynamical prediction for 30days in early 80's. During last decades, major progresses have been occurred in data quality (those from surface, upper air, automatic weather stations, aircraft and space based) and assimilation techniques which in turn, improved the forecast using NWP models. In recent years, improvement of NWP modeling systems have taken place in terms of resolution, better representation of orography, improvement in physical parameterizations of shallow and deep convection, radiative transfer (treatments of clouds, details of diurnal changes and surface energy balance), surface and planetary boundary layer physics for the fluxes of heat, moisture and momentum, and the inclusion of land surface processes. With the improvements of NWP modeling systems, the forecast skills have also been gradually improving with time. The skill of forecast in case of nowcasting and short range is satisfactory with the use of present day dynamical models and the skill scores has improved by 10 to 30 percent for medium range forecast with the help of multi-model and super ensemble methodology using a number of present day lead models simulations (Krishnamurti et al 1999, 2000a, 2000b, 2001, 2002). Both high-resolution global and very high-resolution regional non-hydrostatic microphysical models have been developed by a number of scientists to address the issues of monsoon life cycle and precipitation which is one challenging concern to the scientific community till date. The scientific basis of dynamical seasonal forecasting is that, in tropics, the lower-boundary forcing (sea surface temperature (SST), sea-ice cover, land-surface temperature and albedo, vegetation cover and type, soil moisture and snow cover etc.),

which evolve on a slower time-scale than that of the weather systems themselves, can give rise to significant predictability of statistical characteristics of large-scale atmospheric events (Charney and Shukla, 1981). Several observational and modelling studies (Charney and Shukla, 1981; Palmer and Anderson, 1994; Shukla et al., 2000b) provide evidence that boundary forcing in the tropics contribute significantly to the internal variability of the tropical and monsoon circulations. A number of experiments have been carried out using a frequency filter (at the initial state to remove all high frequency motions) within a low-resolution global model (Krishnamurti et al., 1982, 1990c, 1992) and simulation results can be used to provide some guidance for the occurrence of the wet and dry spells of the monsoon roughly a month in advance. Impact of resolutions of global models have been studied and improvements have been noticed in the location of monsoon depressions, in the monsoon circulations included distribution of organized convection of mesoscale precipitating rain elements (Krishnamurti, 1990a; Krishnamurti et al., 1998a). It is recognized that the atmosphere is fundamentally chaotic (Houghton 1991) and its evolution is extremely sensitive to initial conditions. By prescribing realistic initial moisture field (from INSAT IR data) over the Bay of Bengal and Arabian Seas, the skill of the precipitation forecast associated with movements of monsoon depression was improved considerably (Rao et al., 2001). Though in dynamical model, significant improvement has been made through the improvement of the model physics and dynamics, but present day AGCM are yet not able to simulate mean and interannual variability of Indian summer monsoon very successfully (Gadgil and Sajani, 1998; Kang et al., 2002). Researches have been carried out using limited area model at low resolution to simulate precipitation during monsoon season over Indian region and results indicate that the orographic rainfall associated with the Western Ghat Mountains is under-predicted, though summer monsoon rainfall in short range is captured well (Roy Bhowmik and Prasad, 2001). With enhanced resolution, the model could capture the heavy rainfall belt along the Western Ghats as well. It is seen that when the orographic rain decreases and the rainfall belt moves to peninsular India, the skill of this model is found to be much higher.

A major emphasis regarding the improvement of extended range predictions is that to identify and finally rectify those aspects of a GCMs climate that deviate significantly from observed climate (i.e. model climate drift). Miyakoda et al (1986) have indicated that most of the error seen in time averaged extended range forecasts is the result of systematic model biases rather than random errors. It is found during mid 80's that significant amount of the systematic errors in GCMs due to probably inaccuracies treatment of convection, cloud -radiation interaction, surface boundary forcing and orography. A lot of efforts have been made to improve atmospheric GCMs through the development and improvement of parameterizations of these physical processes. Forecast skill of the GCMs has improved after inclusion of improved parameterization schemes for orographic gravity waves (Stern and Pierrehumbert, 1988) as well as increase in the model resolutions (Miller and Palmer, 1987).

RCMs are a first approach to develop downscaling methods to generate realistic local time series from large-scale model outputs. For a number of regions of the world, efforts are made to improve regional climate models which can provide monthly to seasonal scale forecasts. Developed nations have put huge resources for real-time regional NWP models for extended range forecast. With availability of enhanced computing and communication resources, efforts on regional numerical prediction for monsoon also have increased in Asia. Basically, regional climate models (RCMs) are limited area models that are driven at their lateral boundaries by reanalysis or GCMs output data (Giorgi 1990). In other way, RCMs can be understood as regional GCMs, i.e., model solving equations of the smaller scale atmosphere dynamics for given regions (Liang et al., 2006). It is accepted that in a RCM model run, the integration time is approximately more than two weeks, so that the sensitivity to initial atmospheric conditions is lost (Jacob and Podzum, 1997). Although, it is found that if the variability of synoptic/large scale features is underestimated or there is a consistent bias in the larger model (i.e. in GCMs), no increased skill would be gained by dynamical downscaling for large scale, but at the same time it is also demonstrated that the RCMs could able to capture better small scale features which have a greater dependence on the surface boundary (Christopher et al., 2005).

A number of RCMs have been developed in different organizations / institutes / centres that can be used as reliable tools for dynamical downscaling (or regionalization) of large-scale climate change signals forced by global climate models (GCMs), to finer, regional scales. For example ARPEGE (Gibelin and Déqué 2003), CHRM (Vidale et al, 2003), CLM (Steppeler et al., 2003), HadRM3H (Buonomo et al., 2006), HIRHAM (Christensen et al., 1996), RACMO (Lenderink et al., 2003), RCAO (Döscher et al., 2002, Jones et al., 2004, Meier et al., 2003), RegCM (Giorgi and Mearns 1999), REMO (Jacob, 2001) and PROMES (Castro et al., 1993) have been used to study the regional scale climate events. Climate version of PSU/NCAR mesoscale model MM5 has been used widely for regional scale simulation (Singh et al 2007). Though Nested Regional Climate Model (NRCM) (Climate version of Weather and Forecast Research model) is under development stage, but NRCM is using by climate scientists for its better performance in finer scale simulation of regional scale events.

The regional climate model Providing Regional Climates for Impacts Studies (PRECIS) is developed by the Hadley Centre of United Kingdom (Simmons and Burridge, 1981; Simon et al., 2004) and has been evaluated its performance through regional scale simulation over various regions such as European region and South Asian region. Regional Spectral Model (RSM) developed at National Centre for Environment Prediction (NCEP) also one important tools for regional scale simulation. Attempts have been made to coupling atmospheric regional climate models with the regional ocean climate models to enhance the performance of the regional climate models (Ratnam et al 2009). Intercomparison of different RCMs (Jacob et al 2007) indicated that most of the models have warm bias in simulation of temperature but precipitation is well simulated in regional scale. Efforts have been made to develop methodologies for the assessment of the quality of a RCM system in the presence of limited predictability (Vidale et al 2003).

Simulation of Indian monsoon carried out by nesting the regional model to the global model indicate that the onset and progress of monsoon and associated rainfall distribution is better in the regional nested model simulation (Kanamitsu and Juang,

1994; Ji and Vernekar, 1997). A number of experiments have also been conducted to simulate monsoon system using non-hydrostatic mesoscale model (Das, 2002) and it is noticed that the skill of the model is increased if surface parameters/characteristics are represented more realistic in the model (Singh et al, 2007). In India, National Centre for Medium Range Weather Forecast (NCMRWF) is using mesoscale Eta model for medium range forecast (Rajagopal and Iyenger, 2002).

Regional climate models (RCMs) are one of the robust tools to downscale coarse resolution GCMs output. The RCM has three basic components: i) Pre-processing of data ii) main code and iii) post processing of model output. In the pre-processing component, a user has to set the domain and resolutions of their interest first. After completing this, interpolation of geophysical data from geological survey, surface data and basic atmospheric fields from GCMs over the each grid point of user's specific domain are carried out. Then vertical interpolation and transformations from pressure co-ordinate to model coordinate (generally sigma or eta coordinate) is performed to prepare the data as input for main model. The main code consists the model dynamics and physics which govern the atmospheric motions and it has a number of different parameterizations schemes such as land surface parameterization schemes, planetary boundary layer schemes, cumulus schemes, radiation schemes, etc. with various options in each schemes. A number of combinations between each scheme have to be tested to tune the model and the results of each combination of the schemes are verified with the observations/verification analysis. Based on the results, the best combination is used to reproduce GCM output to get better simulated results. Optimization of the model can be made through the tuning of scheme so that the efficiency of the model increases. The main code reproduces outputs from the GCMs using the input prepared by Pre-processing component. In the post processing, the output is converted from model coordinates to pressure coordinates for operational applications.

10.3.4. Some empirical methods:

Extensive studies on periodic oscillations between active spells of plentiful rain and break spells of insufficient rain which are one important characteristics during the Indian summer monsoon season have been carried out by many scientists (Rao, 1976; Ramamurthy, 1969; Webster et al., 1998; Goswami and Ajayamohan, 2001; Waliser et al., 2003; Goswami, 2005; Waliser et al., 2009) that can be helpful for the predictions of abundant rain (frequent/prolonged breaks) leading to flood (drought) conditions. Since production of agricultural yields is highly related with the active or break phase of monsoon rainfall, therefore, skillful and timely forecasts of the duration of active/break spells could be of enormous value for agriculture planning, disaster and water resource management. Researches in recent years have exploited the large-scale quasi-periodic character of the monsoon ISOs to develop empirical models for extended range prediction of the Indian summer monsoon ISOs (Goswami and Xavier, 2003; Webster and Hoyos, 2004) and Dwivedi et al (2006) have attempted to develop an empirical technique for extended range prediction of the duration of monsoon breaks from the concept of rules of regime transitions and the duration of regimes in some idealized two-regime dynamical systems such as the Lorenz model (Lorenz, 1963; Evans et al., 2004; Yadav et al., 2005).

A number of methodologies have been developed to predict the 30 to 60 days oscillations of monsoonal Intra-Seasonal Oscillations (ISO) and Madden Julian Oscillations (MJO) (Krishnamurti et al., 1982, 1990c, 1992; Waliser et al 2009, Sperber and Waliser 2008). It is found that ISO has a relation to the dry and wet spells of the monsoon. Therefore, signal of ISO captured by atmospheric models can be useful to predict the dry and wet spells of monsoon. Krishnamurti et al. (1998b) noted a marked predictability for the ISO on a one-month time scale in their integration using atmospheric global model, and concluded that it is possible to address the issues of monsoonal dry and wet spells one month in advance. Goswami and Xavier (2003) noted from an analysis of historical data sets that there is a possible potential predictability exits through almost 20 days in advance for break periods of the monsoon. The potential predictability of active spells is only of the order of 10 days. The former

appears to have large-scale controls (Krishnan and Kasture, 1996), whereas the latter seems to have thermodynamic control as well. Using several different indices of the Indian summer monsoon ISOs, it is noticed that the peak anomaly in an active regime can be used as a predictor for the duration of the following break spell and the stochastically forced Lorenz model may be a useful tool to study some of the salient dynamical properties of the Indian summer monsoon intra seasonal oscillations (Dwivedi et al 2006).

10.4. Preliminary efforts for prediction of Indian summer monsoon:

The Indian summer monsoon is the largest seasonal abnormality of the global climate system. Therefore, the extended range forecast from monthly to seasonal scale in tropics is one of the most challenging tasks in atmospheric sciences. Demand for high-resolution meteorological information is increasing with the increase of economic activity especially in the monsoon region. The climate forecasting of precipitation in monthly to seasonal scale has significant implication in policy planning and national economy for the agro-economic country like India.

India Meteorological Department (IMD) is issuing seasonal scale forecast based on statistical techniques for whole India. Efforts are being made with the use of some statistical methodologies mentioned in previous section to forecast monsoon rainfall in monthly as well as seasonal scale for India and met-subdivisions. Use and development of dynamical methods are in progress.

Development and Application of Extended Range Forecast System for Climate Risk Management in Agriculture (ERFS) – a multi-institutional/organizational project in India has been initiated after the severe drought during 2002 to prevail over the gap between medium range and long range forecast in weather and climate forecast system. In 2002, the deficiency of July was severest for more than a century and had crossed the recorded deficiency occurred during 1877 (-49%). This deficiency had a great impact on the farm productions and need of extended range forecast was realized. A flow chart of the ERFS programme for extended range prediction of monsoon over India

has been shown in fig. 10.4. For this purpose, different Atmospheric GCMs (AGCM) and coupled GCMs (CGCM) outputs from various national and international organizations such as NCMRWF, IRI, ECMWF and NCEP etc. are obtained. Using precipitation and temperature data from IMD surface observational network, model systematic biases are estimated and removed to use as input for statistical and dynamical downscaling. Different methodologies described earlier are being used for predictions of rainfall and temperature in monthly as well as seasonal scale. Final forecast can be generated through probabilistic approaches with the predictions of rainfall/temperature by different statistical and dynamical methodologies.

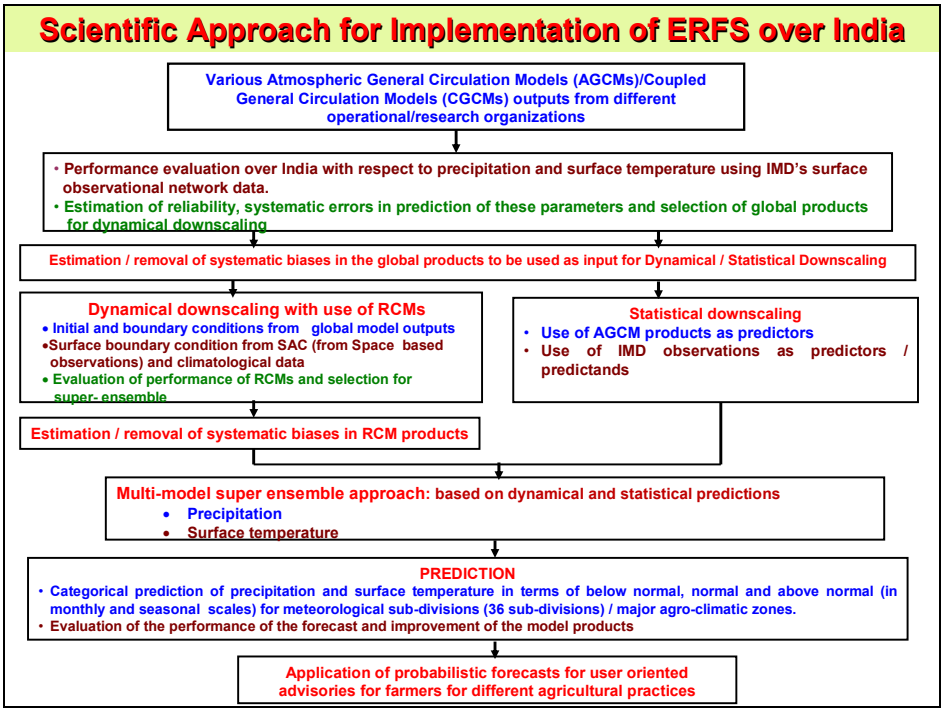

Fig. 10.4: Flow chart of scientific programme for implementation of ERFS project over India.

Experimental test forecast using different techniques for 2010 summer monsoon precipitation and discussions are presented in the next section.

i) Multi Model Ensemble (MME) based model:

An experimental forecast for summer monsoon 2010 (JJAS) is made at each grid point using super ensemble MME approach and given in Fig.10.5. Precipitation forecast from five global models (May start) viz. ECHAM4p5 (2–tier), ECHAM4p5-GML (semi-coupled), ECHAM4p5-MOM3 (1–tier), SINTEXF1 (1–tier) (from Japan Meteorological society) and NCEP-CFS (1–tier) for the period of 1982-2008 are used to generate this forecast. The observed data set used is IMD's 1^0 X 1^0 rainfall. SINTEXF1 is being run at Japan Agency For Marine-Earth Science And Technology (JAMSTEC), Japan and NCEP-CFS model is being run at NCEP, USA while other models run at International Research Institute (IRI) for Climate and Society, USA .

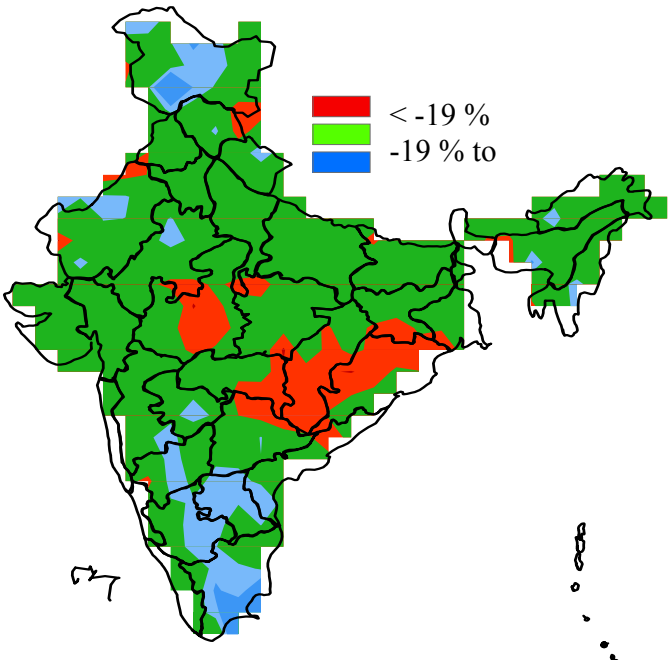

Fig. 10.5: Experimental monsoon rainfall forecast (in % departure) for 2010 using the SVD based multi-model ensemble scheme.

ii) Probablistic Approaches:

Same models (May start) which have been used in the MME scheme also used for probabilistic forecast for summer monsoon (JJAS) 2010 rainfall. The observed data set used is IMD's 1^0 X 1^0 rainfall. The model and observed data sets are normalized to have zero mean and one standard deviation before subjecting to any analysis. As the mean is shifted to zero and standard deviation changed to unity the bounds for the categories become as follows.

Below Normal category: $-\infty$ to -0.43

Near Normal category: -0.43 to 0.43

Above normal category: 0.43 to ∞

The yellow-red colors tell the probabilities of getting below normal rainfall while the shades in gray tells the probabilities for normal rainfall and the shades in blue to pink give the chances of occurring above normal rainfall. It can be observed from the fig. 10.6 that entire Bihar, West Bengal, some part of Uttar Pradesh, Haryana and Uttarakhand may get below normal rainfall, while there are more chances that the southern parts of country will receive above normal rainfall. But over the white region the forecast doesn't have any skill.

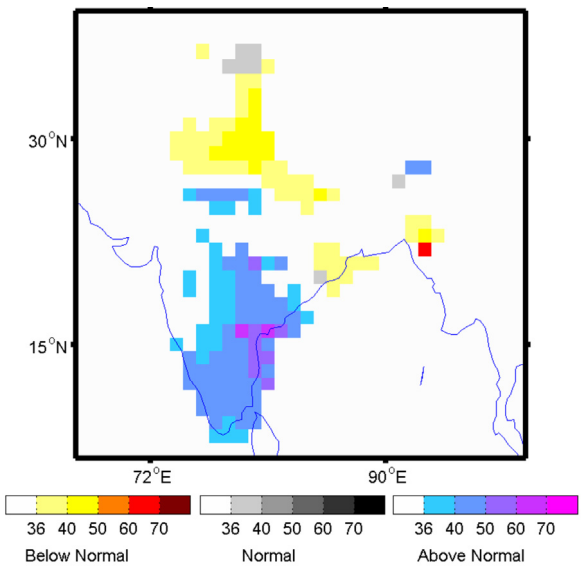

Fig. 10.6 : Experimental Probabilistic forecast for 2010 Monsoon.

iii) Supervised Principal Component Regression (PCR) based model:

In this methodology, the precipitation products from the models used in the earlier method for probabilistic forecasting are considered as predictors (independent variables). These predictors are screened according to their correlation with the observation in hind cast period. After screening, the pool of predictors are gone through the principal component analysis procedure where these variables are made orthogonal to each other. First three principal components are selected on the basis of their correlation with observation. These selected principal components will finally used in the stepwise regression model to generate the forecast. The precipitation forecast generated by this method for 2010 monsoon season is given in fig.10.7. The fig.10.7 indicates that the southern part of country having four subdivisions viz. Tamilnadu, south interior Karnataka, Rayalseema and coastal Andhra Pradesh may get excess rainfall while remaining part of the country may get normal rainfall.

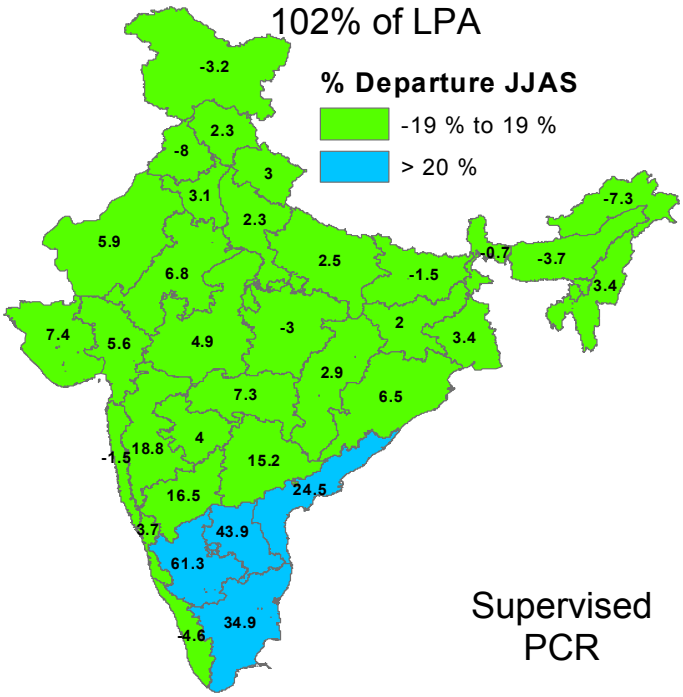

Fig. 10.7: Forecast for 2010 summer monsoon rainfall over different met- subdivisions using supervised PCR

iv) Canonical Correlation Analysis (CCA) based model

JAMSTEC SINTEXF1 model outputs (June start) have been used for experimental forecast of seasonal monsoon rainfall using CCA techniques. Here, model outputs (June start) are considered as predictors to forecast June–September 2010 rainfall over India. Out of all variables of the model output, seven variables (in different regions) are considered as suitable predictors for CCA analysis. These predictors are selected on the basis of the correlation map between predictors and predictand over different domains. The domains and predictors are presented in fig.10.8. It can be noticed from the figure that following seven predictors have been selected. These are:

i) Precipitation (domain1)

ii) Vertically Integrated All Liquid Water Content (domain2)

iii) Specific humidity at 850 hPa (domain2)

iv) Specific humidity at 850 hPa (domain3)

v) Zonal Wind at 850 hPa (domain3)

vi) Meridional Wind at 850 hPa (domain3)

vii) Meridional Wind at 200 hPa (domain2)

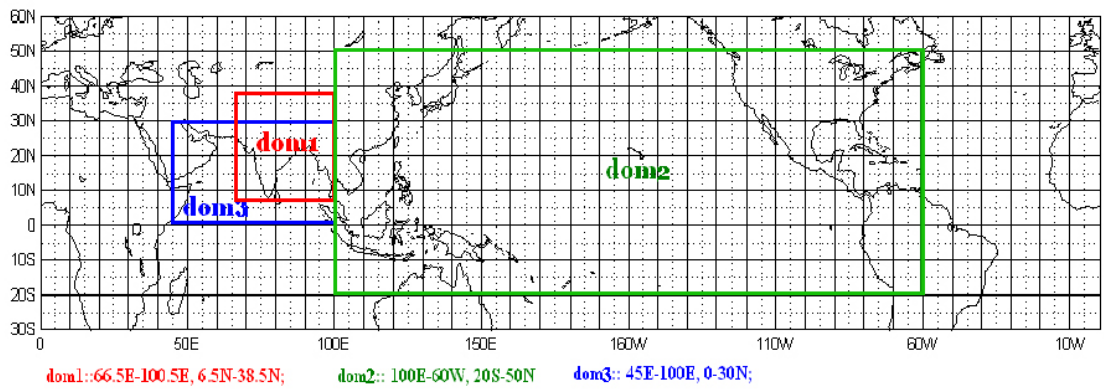

Fig. 10.8: Domains of different predictors for MOS approaches using CCA techniques.

Training period for building up regression equations is considered from 1982-2008 with zero lead (June start time) and IMD rainfall data (1° x 1°) is used as predictand. The data has been normalized before analysis and a composite forecast has been produced using the seven predictors. Experimental test forecast using CCA techniques based on the selected predictors are shown in fig. 10.9. In fig.10.9,

forecasted standardized rainfall anomaly for JJAS 2010 over each grid point has been shown. Results indicate that east part of central India viz. west Bengal, Orissa, Bihar, Uttar Pradesh may get deficient rainfall (seasonal) while North West India (Rajasthan, Gujrat), northern India (Delhi, Himachal Pradesh, some parts of Jammu and Kashmir), north of peninsular India may get excess rainfall.

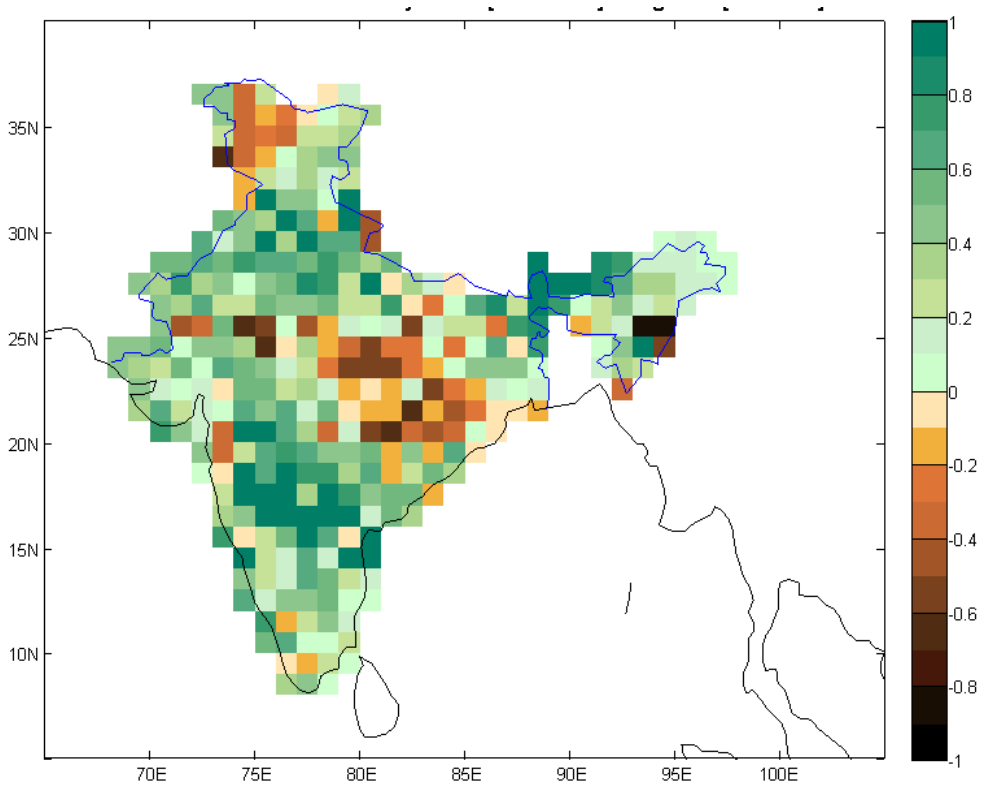

Fig. 10.9 : Forecasted standardized rainfall anomaly for summer monsoon of 2010 using canonical correlation analysis

10.5. Conclusions:

The importance of reliable high resolution forecast and its impact on various sectors of economic activities (especially agriculture) is followed by a broad review of extended range forecast system (not yet comprehensive) and their methodologies are presented. The forecast methodologies are mainly classified into three approaches, statistical, dynamical and dynamical-statistical. Statistical and dynamical downscaling tools on bias corrected GCMs data could able to capture the monthly to seasonal scale

features on regional scale and dynamical-statistical approaches have shown better performance over individual statistical or dynamical methods for prediction of extended range forecast.

The present-day monthly to seasonal prediction has shown some promising features with the advancement of observational network, dynamics and physics of CGCMs/AGCMs, improvement of model initial conditions using data assimilation techniques and availability of high performance computing systems. However, till date, the skill of the Asian summer monsoon rainfall forecast (in particular over Indian sub-continent) sharply decreases after 3-4 days time period. None of the deterministic method could able to improve forecast skill of rainfall remarkably in the medium/extended range time scale over Indian region as compared with the skill of medium/extended range forecast over other regions. Moreover, deterministic forecast is a single value forecast therefore if it fails, it becomes totally wrong. In such circumstances if the accuracy of the forecast is conveyed to user with some confidence then it will be more useful than a single value. This can be achieved using probabilistic forecast. In this study some parametric methods are mentioned, that can be used for probabilistic forecast in tercile categories. This forecast can also be issued in the categories of users' interest. One can use some other parametric as well as non parametric methods for this purpose. In addition to that the Bayesian approach can also be used to generate the probabilistic forecast. In Bayesian approach previous knowledge of the system is used along with some type of linear/non linear models.

Hence, the limitation of the deterministic extended range forecast leads to the greater focus in the development of appropriate probabilistic forecast of different categories of precipitation such as excess, normal, deficient, scanty and so on instead of the location specific and magnitude of rainfall forecast. It is a challenging task and needs concentrated efforts on the improvements of observations as well as the proposed approaches discussed above.

References

Anderson, J. L., and Coauthors, 2005, "The new GFDL global atmosphere and land model AM2-LM2: Evaluation with prescribed SST simulations", J. Climate, 17, 4641-4673.

Banerjee, A.K., Sen, P. N. and Raman, C.R.V., 1978, "On foreshadowing South-west monsoon rainfall over India with mid-tropospheric circulation anomaly of April", Indian Journal of Meteorology, Hydrology and Geophysics, 29**,** 425–431.

Barnston, A. and Smith, T.M., 1996, "Specification and prediction of global surface temperature and precipitation from global SST using CCA", J Clim, 9, 2660-2697.

Benestad, R.E., Hanssen-Bauuer, I.and Chen, D., 2008, "Empirical-Statistical Downscaling", World Scientific Publishing co.. Pte. Ltd.

Bhalme, H.N., Rahalkar, S.S. and Sikdar, A.B., 1987, "Tropical Quasi-Biennial Oscillation of the 10 mb Wind and Indian monsoon rainfall — Implications for forecasting", Journal of Climatology. 7**,** 345–553.

Bjerknes, V., 1904, "Das Problem der Wettervorhersage, betrachtet vom Standpunkte der Mechanik und der Physik, Meteor. Zeit. 21, 1–7; Translation by Y. Mintz: The problem of weather forecasting as a problem in mechanics and physics", Los Angeles, 1954, Reprinted in Shapiro and Grøna˚s (1999), 1–4.

Blanford, H.F., 1884, "On the connection of the Himalayan snowfall with dry winds and seasons of draughts in India", Proc. R. Soc. London, 37, 3-22.

Buonomo E., Jones, R., Huntingford, C. and Hanna ford, J., 2006, "The robustness of high resolution predictions of changes in extreme rainfall for Europe", Quart. J. R. Meteor. Soc., in press.

Castro, M., Fernandez, C. and Gaertner, M. A., 1993, "Description of a meso-scale atmospheric numerical model", In 'Mathematics, Climate and Environment' J.I. Diaz and J.L. Lions (eds.), Masson (ISBN: 2-225-84297-3), 273 pp.

Charles, S.P., Bates, B.C., Whetton, P. H. and Hughes, J. P., 1999, "Validation of downscaling models for changed climate conditions: case study of southwestern Australia", Clim. Res., 12, 1-14.

Charney, J.G. and Shukla, J., 1981, “Predictability of monsoons, in Monsoon Dynamics”, J. Lighthill and R.P. Perce, Ed. (University Press, 1981), pp.99-109.

Cheng, X. and. Wallace, J. M., 1993, “Cluster analysis of the Northern Hemisphere wintertime 500-hPa height field: Spatial patterns”, J. Atmos. Sci., 50**,** 2674–2696.

Christensen, J. H., Christensen, O. B., Lopez, P., Van Meijgaard E. and Botzet, M., 1996, “The HIRHAM4 Regional Atmospheric Climate Model”, Scientific Report, 96-4, 51 pp., DMI, Copenhagen.

Christopher L. Castro, Roger A. Pielke Sr. and Giovanni Leoncini, 2005, “Dynamical downscaling: Assessment of value retained and added using the Regional Atmospheric Modeling System (RAMS)”, J. Geophys. Res., 110, D05108, doi: 10, 1029/2004JD004721

Cleveland, William S., 1979, “Robust Locally Weighted Regression and Smoothing Scatterplots”, J. of the Amer. Statis. Asso. , 74 (368), pp. 829-836

Cohen, S.J., 1990, “was bringing the global warming issue close to home: the challenge of regional impact studies”, Bull. Amer. Meteor. Soc., 71, 520-526.

Coulibaly, P., Dibike, Y. B. and Anctil, F., 2005, “Downscaling precipitation and temperature with temporal neural networks”, J. Hydrometeorol., 6, 483–496.

Das, P.K., 1986, “Long Range Prediction and Predictability”, in ‘Fifth IMO Lecture’, Monsoon, World Meteorological Organisation, No.613, pp.126–136.

Das, S., 2002, “Real time mesoscale weather forecasting over Indian region using MM5 modeling system”, NCMRWF Research Report No. NMRF/RR/3/2002, NCMRWF, New Delhi, India.

Dee, D. P. and Arlindo. M., Da Silva, 1998, “Data assimilation in the presence of forecast bias”, Q. J. R. Meteorol. Soc., 124 (545), 269-295

Delworth, T.L., Broccoli, A. J., Rosati, A., Stouffer, R. J., Balaji, V., Beesley, J. A., Cooke, W. FDixon, ., K.W., Dunne, J., Dunne, K. A. , Durachta, J. W., Findell, K. L., Ginoux, P., Gnanadesikan, A., Gordon, C. T., Griffies, S. M., R. Gudgel, Harrison, M. J., Held, I. M., Hemler, R. S., Horowitz, L. W., Klein, S. A., Knutson, T. R., Kushner, P. J., Langenhorst, A. R., Lee, H. C., Lin, S. J., Lu, J., Malyshev, S. L., Milly, P. C. D., Ramaswamy, V., Russell, J., Schwarzkopf, M. D., Shevliakova, E., Sirutis, J. J., Spelman, M. J., Stern, W. F., . Winton, M.,

Wittenberg, A. T., Wyman, B., Zeng, F. and Zhang, R., 2006: GFDL's CM2 Global Coupled Climate Models. Part I, “Formulation and Simulation Characteristics”, J. Climate, 19, 643-674.

Döscher, R., Willén, U., Jones, C., Rutgersson, A., Meier, H. E. M., Hansson, U. and Graham, L. P., 2002, “The development of the coupled regional ocean-atmosphere model RCAO”, Boreal Env. Res., 7, 183-192.

Draper, Norman R. and Smith Harry 1966, “Applied Regression Analysis”, Wiley publications.

Dwivedi, S., Ashok Kumar Mittal and Goswami, B. N.2006, “An empirical rule for extended range prediction of duration of Indian summer monsoon breaks”, Geophys. Res. Lett., 33, L18801, doi: 10.1029/2006GL027035, 2006.

Evans, E., Bhatti, N., Kinney, J., Pann, L., Pena, M., Yang, S. C., Kalnay, E. and Hansen, J., 2004, “RISE undergraduates find that regime changes in Lorenz’s model are predictable”, Bull. Amer. Meteor. Soc., 85(4), 520 – 524.

Feddersen, H. and Andersen, U., 2005: A method for statistical downscaling of seasonal ensemble predictions, Tellus, Ser. A, 57, 398 – 408.

Fuentes, U. and Heimann, D., 2000, “An improved statistical-dynamical downscaling scheme and its application to the Alpine precipitation climatology”, Theor. Appl. Climatol., 65, 119– 135.

Gadgil, S. and Sajani, S., 1998, “Monsoon precipitation in the AMIP runs”, Climate Dyn., 14, 659–689.

Gadgil, S., Rajeevan, M. and Nanjundiah, R., 2005, “Monsoon prediction – Why yet another failure?” Curr. Sci., 88, 1389-1400.

Gibelin, A.L. and Déqué, M., 2003, “Anthropogenic climate change over the Mediterranean region simulated by a global variable resolution model”, Climate Dynamics, 20, 327-339.

Giorgi, F. and Mearns, L. O., 1999, “Introduction to special section: regional climate modeling revisited”, J. Geophys.Res., 104, 6335- 6352.

Giorgi, F., 1990, “Simulation of regional climate using a limited area model nested in a general circulation model”, J. Climate, 3, 941-963.

Giorgi, F., Hewitson, B., Christensen, J., Fu, C., Jones, R., Hulme, M., Mearns, L., Von Storch, H. and Whetton, P. 2001, "Regional climate information—evaluation and projections, in Climate Change 2001: The scientific basis", p. 944pp, J.T. Houghton et al.

Goddard L., Mason, S.J., Zebiak, S.E., Ropelewski, C.F., Basher, R. and Cane, M. A., 2001,"Current approaches to seasonal-to-interannual climate predictions", Int. J. Climatol, 21, 1111-1152.

Goodess, C.M., Anagnostopoulo, C., Bardossy, A., Frei, C., Harpham, C., Haylock, M.R., Hundecha, Y., Maheras, P., Ribalaygua, J., Schmidli, J., Schmith, T., Tolika, K., Tomozeiu,R. and Wilby, R.L., 2007, "An intercomparison of statistical downscaling methods for Europe and European regions - assessing their performance with respect to extreme temperature and precipitation events", Climatic Change, in press.

Goswami, B.N. and Xavier, P. K., 2003, "Potential predictability and extended range prediction of Indian Summer Monsoon Breaks", Geophys. Res. Lett., 30 (18), 1966.

Goswami, B.N. and Ajayamohan, R. S., 2001,"Intraseasonal oscillations and interannual variability of the Indian summer monsoon", J. Clim., 14, 1180–1198.

Goswami, B.N., 2005, "South Asian Monsoon, in Intraseasonal Variability of the Atmosphere-Ocean Climate System", edited by W. K. M. Lau and D. E. Waliser, pp. 19– 61, Springer, New York.

Gowariker, V., Thapliyal, V., Sarker, R. P., Mandal, G. S. and Sikka, D. R. 1989, "Parametric and power regression models: New approach to long range forecasting of monsoon rainfall in India", Mausam, 40**,** 115–122.

Hack, J. J., Kiehl, J. T. and Hurrell, J. W., 1998, "The hydrologic and thermodynamic characteristics of the NCAR CCM3", J. Climate, 11, 1179–1206.

Hahn, D.G., and Shukla, J., 1976, "An apparent relationship between Eurasian snow cover and Indian monsoon rainfall", Journal of Atmospheric Sciences, 33: 2461–2462.

Hashino, T., Bradley, A. A. and Schwartz, S.S., 2006, "Evaluation of bias-correction methods for ensemble streamflow volume forecasts", Hydrol. Earth Syst. Sci. Discuss., 3, 561–594

Hastenrath, S., 1987, “On the prediction of Indian monsoon rainfall anomalies”, Journal of Climatology and Applied Meteorology, 26, 847–857.

Hay, L. E. and Clark, M.P., 2003, “Use of statistically and dynamically downscaled atmospheric model output for hydrologic simulations in three mountainous basins in the western United Stated”, J. Hydrology, 282, 56-75.

Hellstrom, C., Chen, D., Achberger, C. and Raisanen, J., 2001, “Comparison of climate change scenarios for Sweden based onstatistical and dynamical downscaling of monthly precipitation”, Clim, Res., 19, 45-55.

Hewitson, B.C. and Crane, R.G., 1996, “Climate downscaling: Techniques and application”, Clim. Res., 7, 85– 95.

Houghton, J., 1991: The Bakerian Lecture, 1991, “The predictability of weather and climate”, Phil. Trans. Roy. Soc London A (1991), 337, 521-572.

Hughes, J. P. and Guttorp, P., 1994, “A class of stochastic models for relating synoptic atmospheric patterns to regional hydrologic phenomena”, Water Resour. Res, 30 (5), 1535-1546.

Hurrell, J. W., Hack, J. J., Boville, B. A., Williamson, D. L. and Kiehl, J. T., 1998, “The dynamical simulation of the NCAR Community Climate Model version 3 (CCM3)”, J. Climate, 11, 1207–1236.

Huth, R. and Kysely, J., 2000, “Constructing site-specific climate change scenarios on a monthly scale using statistical downscaling”, Theor. Appl. Climatol., 66, 13–27.

Huth, R., 2002, “Statistical downscaling of daily temperature in central Europe”, J. Clim., 15, 1731–1742.

Ines, Amor V.M. and James W. Hansen, 2006, “Bias correction of daily GCM rainfall for crop simulation studies”, Agricultural and Forest Meteorology, 138, 44–53.

Jacob, D. and Podzun, R.1997, “Sensitivity studies with the regional climate model REMO”, Meteorol. Atmos. Phys., 63, 119-129.

Jacob, D., 2001, “A note on the simulation of the annual and inter-annual variability of the water budget over the Baltic Sea drainige basin”, Met. Atmos. Phys., 77, 61-73.

Jacob, D., Bärring, L., Bøssing Christensen O., Hesselbjerg Christensen, J., de Castro, M., Déqué, M., Giorgi, F., Hagemann, S. Hirschi, M., Jones, R., Kjellström, E., Lenderink, G., Rockel, B., Sánchez, E., Schär, C., Seneviratne, S. I., Somot, S., van Ulden, A. and van den Hurk, B., 2007, "An inter-comparison of regional climate models for Europe: model performance in present-day climate", Climate Change, 81,31–52, DOI 10.1007/s10584-006-9213-4.

Jagannathan, P., 1960, "Seasonal Forecasting in India — A Review", Pune (India): Meteorological Office. 67 pp.

Ji, Y. and Vernekar, A.D., 1997, "Simulations of the Asian summer monsoons of 1987 and 1988 with a regional model nested in a global GCM", J. Climate, 10, 1965-1979.

Jones, C.G., Willén, U., Ullerstig, A. and Hansson, U., 2004, "The Rossby Centre Regional Atmospheric Climate Model Part I: Model Climatology and Performance for the Present Climate over Europe", Ambio, 33:4-5, 199-210.

Kanamitsu, M. and Juang, H. M. H., 1994, "Multi month simulations of Indian Monsoon by the NMC nested regional spectral model", Preprints, 10th conference on NWP, Portland, OR, Amer. Meteor. Soc., 351-352.

Kang, I. S., Jin, K., Wang, B., Lau, K. M., Shukla, J., Krishnamurthy, V., Schubert, S.D., Waliser, D. E., Stern, W. F., Kitoh, A., Meehl, G. A., Kanamitsu, M., Galin, V.Y., Satyan, V., Park, C. K. and Liu., Y., 2002, "Intercomparison of the climatological variations of Asian summer monsoon precipitation simulated by 10 GCMs", Climate Dynamics, 19(5-6), 383-395.

Kar S.C., Acharya. N., Mohanty, U.C. and Kulkarni, M. A. 2010, "Skill of Mean of Distribution of Monthly Rainfall over India during July using Multi-Model Ensemble Schemes", Int. J. Climatol., (Accepted).

Kharin, V. V. and Zwiers, F. W., 2002, "Climate predictions with multimodel ensembles", J. Climate, 15, 793–799.

Kidson, J.W. and Thompson, C.S., 1998, "A comparison of statistical and model-based downscaling techniques for estimating local climate variations", J. Climate, 11, 735-753.

Kiehl, J. T., Hack, J. J., Bonan, G. B., Boville, B. A., Williamson D. L. and Rasch, P. J. 1998, “The National Center for Atmospheric Research Community Climate Model”, J. Climate, 11, 1131–1149.

Kioutsioukis, I., Melasa, D. and Zanis, P., 2008, “Statistical downscaling of daily precipitation over Greece”, Int. J. Climatol., 28 (5), 679-691

Krishnamurti, T. N., Kishtawal, C. M., Zhang, Z., LaRow, T. E., Bachiochi, D. R., Willifor, C. E., Gadgil, S.and Surendran, S., 2000,“Multimodel ensemble forecasts for weather and seasonal climate”, J. Climate, 13**,** 4196–4216.

Krishnamurti, T. N., Kishtawal, C.M., Shin, D.W. and Williford, C. E., 2000b, “Improving Tropical Precipitation Forecasts from a Multianalysis Superensemble” J. Climate, 13, 4217-4227.

Krishnamurti, T. N., Kishtawal, C. M., Zhang, Z., LaRow, T., Bachiochi, D., Williford, C. E., Gadgil, S. and Surendran, S., 2000a, “Multimodel ensemble forecasts for weather and seasonal climate”, J. Climate, 13, 4196- 4216.

Krishnamurti, T. N., Surendran, S., Shin, D. W., Correa-Torres, R. J., Vijaya Kumar, T. S. V., Williford, C. E., Kummerow, C., Adler, R. F., Simpson, J., Kakar, R., Olson,W. S. and Turk, F. J., 2001, “Real-Time Multianalysis-Multimodel Superensemble Forecasts of Precipitation Using TRMM and SSM/I Products”, Mon. Wea. Rev., 129, 2861-2883.

Krishnamurti, T. N., 1969, “An experiment in numerical prediction in equatorial latitudes”, Quart. J. Royal Meteorol. Soc., 95, 594-620.

Krishnamurti, T. N., 1990a, “Monsoon prediction at different resolutions with a global spectral model”, Mausam, 41, 234-240.

Krishnamurti, T. N., and Subrahmanyam, D., 1982, “The 30-50 day mode at 850 mb during MONEX”, J. Atmos.Sci., 39, 2088-2095.

Krishnamurti, T. N., Kishtawal, C.M., LaRow, T. E., Bachiochi, D. R., Zhang, Z., Willifor, C. E., Gadgil, S. and Surendran, S., 1999, “Improved weather and seasonal climate forecasts from multimodel superensemble”, Science, 285, 1548–1550.

Krishnamurti, T. N., Bedi, H. S. and Hardiker, V. M., 1998b, “An introduction to global spectral modeling”, Oxford University Press, 253pp.

Krishnamurti, T.N., Bedi, H.S. and Han, W., 1998a, “Organization of convection and monsoon forecasts”, Meteorol. Atmos. Phys., 67, 117-134.

Krishnamurti, T.N., Lydia Stefanova, Chakraborty, Arun, Vijaya Kumar, T.S.V., David Bachiochi, Steve Cocke, and Brian Mackey, 2002, “Seasonal Forecasts of precipitation anomalies for North American and Asian Monsoons”, J. Met. Soc. Japan, 80, 1415-1426.

Krishnamurti, T. N., Subrahmaniam, M., Oosterhof, D. K. and Daughenbaugh, G., 1990c, “Predictability of low frequency modes”, Meteorol. Atmos. Phys., 44, 63-83.

Krishnamuti, T. N., Sinha, M. C., Krishnamurti, R., Oosterhof, D. and Comeaux, J., 1992, “Angular momentum, length of day and monsoonal low frequency mode”, J. Met. Soc. Japan, 70, 131-166.

Krishnan, R. and Kasture, S. V., 1996, “Modulation of low frequency intraseasonal oscillation of the northern summer monsoon by El Nino and Southern Oscillation (ENSO)”, Meteorol. and Atmos. Phys., 30, 2237-257.

Landman, A., and Goddard, L. 2002, “Statistical recalibration of GCM forecasts over Southern Africa using model output statistics”, J Clim. 15, 2038-2055.

Legras, B. and Ghil, M., 1985, “Persistent anomalies, blocking and variations in atmospheric predictability”, J. Atmos. Sci., 42, 433-471.

Lenderink, G., Hurk, B. van den, Meijgaard, E. van, Ulden A. van and Cujipers, H., 2003, “Simulation of present-day climate in RACMO2: first results and model developments”, KNMI Technical Report, 252, 24pp.

Li, S. and Goddard, L., 2005, “Retrospective Forecasts with the ECHAM4”, 5 AGCM IRI Technical Report 05-02 December 2005.

Liang, X. Z., Pan, J., Zhu, J., Kunkel, K. E., Wang, J. X.L. and Dai, A., 2006, “Regional climate model downscaling of the u.s. summer climate and future change”, J. Geophys. Res., 111, D10108, doi: 101029/2005JD006685, 2006.

Lim, Y. K., Shin, D. W., Cocke, S., LaRow, T. E., Schoof, J. T., O'Brien, J. J. and Chassignet, E. P. 2007, "Dynamically and statistically downscaled seasonal simulations of maximum surface air temperature over the southeastern United States", J. Geophys. Res., 112, D24102, doi: 10, 1029/2007JD008764.

Lorenz, E. N., 1963, "Deterministic non-periodic flow", J. Atmos. Sci., 20, 130– 141.

Lorenz, E. N, 1975, "Climate predictability: The physical basis of climate modeling", WMO, GARP Pub. Sen, 16, 132-136.

Lorenz, E. N., 1965, "A study of the predictability of a 28-variable atmospheric model", Tellus, 17, 321-333.

Mailer, J. P., 2010, "Can we trust Long-range weather forecasts? Management of Weather and Climate Risk in the Energy Industry", NATO Science Series, Springer Academic Publisher (Business Media B.V.).

Majewski, D., 1997, "Operational regional prediction, Meteorology and atmospheric physics 63 (1997) 89-104. Dynamical downscaling: Assessment of value retained and added using the Regional Atmospheric Modelling System (RAMS) Eds.", Cambridge University Press.

Mearns, L.O., Giorgi, F., Whetton, P., Pabon D., Hulme M. and Lal, M., 2004, "Guidelines for use of climate scenarios developed from regional climate model experiments", Tech. rep., Data Distribution Centre of the IPCC.

Meier, H.E.M., Döscher R.and Faxen, T., 2003, "A multiprocessor coupled ice-ocean model for the Baltic Sea. Application to the salt inflow", J. Geophys. Res., 108, C8:3273.

Miller, M. J., and Palmer, T. N., 1986, "Orographic gravity-wave drag: its parameterization and influence in general circulation and numerical weather prediction models. ECMWF Seminar/Workshop 1986 on Observations",Theory and Modeling of Orographic Effects, Reading, Eng., September 15-20, 1986.

Miyakoda, K., Sirutis, J. and Ploshay, J., 1986, "One-month forecast experiments – without anomaly boundary forcings", Mon. Wea. Rev., 114, 2363-2401.

Miyakoda, K., Gordon, T., Caverly, R., Stern W. and Sirutis, J., 1983, "Simulation of blocking event in January 1977", Mon. Wea. Rev., 111, 2363-2401

Mo, K. C. and Ghil, M. 1988, “Cluster analysis of multiple planetary flow regimes”, J. Geophys. Res., 93D, 10 927-10 952.

Molteni, F. and Palmer, T. N., 1993, “Predictability and non-modal finite-time instability of the northern winter circulation”, Quart. J. Roy. Meteor. Soc, 119, 269-298.

Molteni, F., Tibaldi, S. and Palmer, T. N., 1990, “Regimes in the wintertime circulation over northern extratropics. I: Observational evidence”, Quart. J. Roy. Meteor. Soc, 116, 31-67.

Murphy, J., 1999, “An evaluation of statistical and dynamical techniques for downscaling local climate”, J. Clim., 12, 2256-2284.

Murphy, J., 2000, “Predictions of climate change over Europe using statistical and dynamical downscaling techniques”, Int, J. Climatol., 20, 489-501.

Namias, J., 1955, “Long-range weather forecasting”, Sci. Am., 193, 40-44.

Namias, J., 1968, “Long Range Weather Forecasting -History, Current Status, and Outlook”, Bull. Amer.Meteor. Soc., 49, 438-470.

Palmer, T. N., 1993, “Extended-range atmospheric prediction and the Lorenz model”, Bull. Am. Meteorol. Soc., 74, 49– 66.

Palmer, T. N. and Anderson, D. L. T., 1994, “The prospects for seasonal forecasting – A review paper”, Quart. J. Roy. Meteorol. Soc., 120, 755-793.

Palmer, T.N., Brankovic, C., Molteni F. and Tibaldi, S.1990, “Extended-range predictions with ECMWF models: Interannual variability in operational model integrations”, Q. J. R. Meteorol. Soc, 116, 799-834.

Parthasarathy, B., Munot, A. A. and Kothawale, D. R., 1994, “All India monthly and seasonal rainfall series: 1871–1993”, Theor. Appl. Climatol., 49, 217–224.

Parthasarathy, B., Daiz, H. F. and Eischeid, J. K., 1988, “Prediction of all-India Summer Monsoon Rainfall with Regional and Large Scale Parameters”, Journal of Geophysical Research, 93, 5341–5350.

Parthasarathy, B., Rupa Kumar K. and Sontakke, N. A., 1990, “Surface and Upper air temperatures over India in relation to monsoon rainfall” Theoretical & Applied Climatology, 42, 93–110.

Rabiner, L. R. and Juang, B. H., 1986, “An introduction to hidden Markov models”, IEEE Trans. Acoust. Speech Signal Process. 3, 4-16.

Rajagopal, E. N. and Iyengar, G. R., 2002, “Implementation of Mesoscale Eta model at NCMRWF”, NCMRWF Research Report No. NMRF/RR/4/2002, NCMRWF, India, 28p.

Ramamurthy, K., 1969, “Monsoon of India: Some aspects of ‘break’ in the Indian south west monsoon during July and August”, in Forecasting Manual, part IV18.3, India Meteorol. Dept., New Delhi.

Rao, Y.P., 1976, “Southwest Monsoon”, in Meteorological Monograph, Synoptic Meteorol. no. 1/1976, India Meteorol. Dep., New Delhi.

Rao, Y.V.R., Prasad K. and Sant Prasad, 2001, “A case study of the impact of INSAT derived humidity profiles on precipitation forecast by limited area model”, Mausam, 52,647-654.

Ratnam, J. V., Giorgi, F., Kaginalkar, A., Cozzini, S. 2009, “Simulation of the Indian monsoon using the RegCM3 and ROMS regional coupled model”, Climate Dynamics, 33(1): 119.

Reinhold, B. B and Pierrehumbert, R., 1982, “Dynamics of weather regimes: Quasi-stationary waves and blocking”, Mon. Wea. Rev., 110, 1105-1145.

Richardson, L. F., 1922, “Weather Prediction by Numerical Process”, Cambridge University Press, Cambridge, xii+236pp. Reprinted by Dover Publications, New York, 1965, with a new Introduction by Sydney Chapman, xvi+236pp.

Robertson, A. W., Kirshner, S. and Smyth, P., 2004, “Downscaling of daily rainfall occurrence over northeast Brazil using a hidden Markov model”, J. Clim., 17, 4407– 4424.

Roy Bhowmik, S. K. and Prasad K, 2001, “Some characteristics of limited area model precipitation forecast of Indian monsoon and evaluation of associated flow features”, Meteorol. Atmos. Phys., 76, 223-236.

Saha, S., Nadiga, S., Thiaw, C., Wang, J., Wang, W., Zhang, Q., Dool, H. M. van den, Pan, H.L., Moorthi, S., Behringer, D., Stokes, D., Pena, M., Lord, S., White, G., Ebisuzaki, W., Peng, P., Xie, P., 2006, “The NCEP Climate Forecast System” Journal of Climate, 19, 15, 3483-3517.

Schmidli, J., Goodess, C. M., Frei, C., Haylock, M. R., Hundecha, Y., Ribalaygua, J. and Schmith, T.2007, "Statistical and dynamical downscaling of precipitation: An evaluation and comparison of scenarios for the European Alps", J. Geophys. Res., 112, D04105, doi: 10.1029/2005JD007026.

Schneider, E. K., Kinter J. L. and Cehelsky, P., 1991,"Simulation of internal climate variability on long timescales. Proc. Eighth Conf. on Atmospheric and Oceanic Waves and Stability", Denver, CO, Amer. Meteor. Soc, J9-J12.

Shukla, J. and Paolino (Jr), D. A., 1983, "The Southern Oscillation and long range forecasting of summer monsoon rainfall over India", Monthly Weather Review, 111, 1830–1837.

Shukla, J., 1981, "Dynamical predictability of monthly means", J. Atrnos. Sci., 38, 2547-2575.

Shukla, J., 1987, "Inter annual variability of Monsoon; and Long range forecasting of monsoons", In: Fein, J.S. & Stephens, P.L. (Eds), Monsoons, pp. 399–464, 523–547. New York: John Wiley, 632 pp.

Shukla, J., Anderson, J., Baumhefner, D., Brankovic, C., Chang, Y., Kalnay, E., Marx, L., Palmer, T.N., Paolino, D.A., Ploshay, J., Schubert, S., Straus, D.M., Suarez, M. and Tribbia, J., 2000b, " Dynamical Seasonal Prediction", Bull. Amer. Meteor. Soc., 81, 2593-2606.

Shutts, G. J., 1986, "A case study of eddy forcing during an Atlantic blocking episode", Adv. Geophys., 29,135-162.

Simmons, A. J. and Burridge, D. M., 1981, "An energy and angular-momentum conserving finite-difference scheme and hybrid coordinates", Monthly Weather Review, 109, pp. 758–766.

Simon, W., Hassell, D., Hein, D., Jones, R. and Taylor, R., 2004, "Installing and using the Hadley Centre regional climate modelling system", PRECIS, Version 1.1, Met Office Hadley Centre, Exeter, UK.

Singh, A. P., Mohanty, U. C., Sinha, P. and Mandal, M., 2007, "Influence of different land surface processes on Indian summer monsoon circulation", Natural Hazards, 42, 423-438.

Sperber, K. R and Waliser, D. E., 2008, “New approaches to understanding, simulating, and forecasting the Madden-Julian Oscillation”, Bull. Amer. Meteorol. Soc. (submitted)

Stephenson, D. B., Cohelo C.A.S., Dobles-Reyes F.J., and Balmaseda, M., 2005, “Forecast assimilation: a unified framework for the combination of multi-model weather and climate predictions”, Tellus A, 57(3), 253-265

Steppeler, J., Doms, G., Schaettler, U., Bitzer, H.W., Gassmann, A., Damrath U.and Gregoric, G., 2003, “Mesogamma scale forecasts using the nonhydrostatic model LM”, Met. Atmos. Phys., 82, 75-96.

Stern, W. F. and Pierrehumbert, R. T., 1988, “The impact of an orographic gravity wave drag parameterization on extended range predictions with a GCM”, Proceeding of the Eight Conference on Numerical Weather Prediction, Baltimore, Maryland, February 22-26, 1988, 745-750 (WMO technical note, No 20.4).

Thapliyal, V. and Kulshrestha, S. M., 1992, “Recent models for long range forecasting of southwest monsoon rainfall in India”, Mausam, 43**,** 239–248.

Thapliyal, V., 1982, “Stochastic Dynamic Model for long range prediction of monsoon rainfall in peninsular India” Mausam, 33**,** 399–404.

Thapliyal, V., 1984, “Prediction of Indian droughts with lower stratospheric winds”, Mausam, 35**,** 367–374.

Thapliyal, V., 1986, “Long range forecasting of monsoon rainfall in India”, WMO/TD, No 87, pp. 723–732. Geneva: World Meteorological Organization.

Thapliyal, V., 1987, “Prediction of Indian Monsoon Variability: Evolution and prospects including development of new model”, in: Ye, D., Fu, C., Chao, J. & Yoshina, M. (Eds), Climate of China and Global Climate, pp. 397–416. Beijing: China Ocean Press.

Thapliyal, V., 1997, “Preliminary and final long range forecast for seasonal monsoon rainfall over India”, Journal of Arid Environments, 36**,** 385–403

Tippett, M. K., Barnston, A. G. and Robertson, A. W., 2006, “Estimation of seasonal precipitation terciles based categorical probabilities from ensembles”, J. Climate, 20, 2210-2228

Van den Dool, H.M., 1994, “Long-range weather forecasts through numerical and empirical methods”, Dynamics of Atmospheres and Oceans, 20, 247-270

Van den Dool, H.M., 1994, “Searching for analogues, how long must we wait?” Tellus, 46A, 314-324.

Verma, R. K., Subramanian, K. and Dugam, S. S., 1985, “Interannual and long term variability of the summer monsoon and its possible link with northern hemispheric surface temperature”, Proceeding of the Indian Academy of Sciences (Earth & Planetary Science), 94**,** 75–131.

Vidale, P. L., Lüthi, D., Frei, C., Seneviratne S. I. and Schär, C., 2003, “Predictability and uncertainty in a regional climate model’, J. Geophys. Res., 108**,** (D18), 4586, doi:10.1029/2002JD002810.

Von Storch, H., Zorita E. and Cubasch, U., 1993, “Downscaling of global climate change estimates to regional scales: An application to Iberian rainfall in wintertime”, J. Climate, 6, 1161—1171.

Vrac, M. and Naveau, P., 2007, “Stochastic downscaling of precipitation: From dry events to heavy rainfalls”, Water Resour. Res., 43, W07402, doi: 10. 1029/2006WR005308, 2007.

Vrac, M., Stein, M. and Hayhoe, K., 2007, “Statistical downscaling of precipitation through a non-homogeneous stochastic weather typing approach”, Climate Res. in press.

Waliser, D E, Sperber, K.R., Donner, L., Gottschalck, J., Hendon, H., Higgins, W., Kang, I., Kim, D., Legler, D., Maloney, E., Moncrieff, M., Schuber, S., Stern, W., Vitart, F., Wang, B., Wang, W., Weickmann, K., Wheeler, M., Woolnough, S., and Zhang, C., 2009, “MJO Simulation Diagnostics”, J. Climate, 22**,** 3006-3030.

Waliser, D., Lau, K., Stern W. and Jones, C.2003, “Potential predictability of the Madden-Julian oscillation”, Bull. Amer. Meteorol. Soc., 84, 33–50.

Walker, G. T., 1923, “Correlation in seasonal variations of weather. VIII, A preliminary study of world weather”, IMD Mem., 1923, XXIII, Pat IV, pp. 75–131.

Walker, G. T., 1924, “Correlation in seasonal variations of weather IX. A further study of world weather”, IMD Mem., 1924, XXIV, Pat IX, pp. 75–131.

Walker, G. T., 1910, “Correlation in seasonal variation of weather II”, Memoirs of India.

Webster, Magana, Palmer, Shukla, Tomas, Yanai and Yasunari, 1998, “Monsoons: Processes, Predictability, and prospects for prediction”, J.Geophys. Res., 103, 14451-14510.

Webster, P. J., and Hoyos, C., 2004, “Prediction of monsoon rainfall and river discharge on 15– 30 day time scales”, Bull. Amer. Meteorol. Soc., 85, 1745– 1765.

Webster, P. J., Magana, V. O., Palmer, T. N., Shukla, J., Tomas, R. T., Yanai M. and Yasunari, T., 1998, “Monsoons: Processes, predictability and the prospects of prediction”, J. Geophys. Res., 103(C7), 14,451 –14,510.

White, A. A., 1990, “Steady states in a turbulent atmosphere”, Meteor. Mag., 119, 1-9.

Widmann, M., Bretherton C. S. and Salathe, E. P. Jr., 2003, “Statistical precipitation downscaling over the northwestern United States using numerically simulated precipitation as a predictor”, J. Clim., 16, 799– 816.

Wilby, R. L., and Wigley, T. M. L., 1997, “Downscaling general circulation model output: A review of methods and limitations”, Prog. Phys. Geogr., 21, 530–548.

Wilby, R. L., Charles, S. P., Zorita, E., Timbal, B., Whetton, P. and Mearns, L. O. 2004, “Guidelines for use of climate scenarios developed from statistical downscaling methods”, Tech. rep., Data Distribution Centre of the IPCC.

Wilks, D. S., 1995, “Statistical methods in atmospheric sciences (2nd ed.)”, Academic Press. San Diego. US. 467 p. V. 59.

Wilks, D. S., 1999, “Multisite downscaling of daily precipitation with a stochastic weather generator”, Clim. Res., 11, 125– 136.

Wood, A. W., Maurer, E. P., Kumar, A. and Lettenmaier, D. P., 2002, “Long-range experimental hydrologic forecasting for the eastern United States”, J. Geophys. Res.-Atmos., 107, 4429.

Wood, A. W., Leung, L. R., Sridhar, V. and Letternmaier, D. P., 2004, “Hydrologic implications of dynamical and statistical approaches to downscaling climate model outputs”, Clim. Change, 62, 189-216.

Xavier P. K. and Goswami**,** B. N., 2007, “Analog method for realtime forecasting of summer monsoon subseasonal variability”, Mon. Wea. Rev**.,** 135, 4149-4160

Yadav, R. S., Dwivedi, S. and Mittal, A. K., 2005, “Prediction rules for regime changes and length in a new regime for the Lorenz model”, J. Atmos. Sci., 62, 2316– 2321.

Yun, W. T., Stefanova, L., Mitra, A. K., Vijaya Kumar, T. S. V., Dewar, W. and Krishnamurti, T. N., 2005, “A multi-model superensemble algorithm for seasonal climate prediction using DEMETER forecasts”, Tellus, 57A, 280–289.

Zucchini, W. and Guttorp, P., 1991, “A hidden Markov model for space time precipitation”, Water Resour. Res., 27, 1917-1923.

CHAPTER 11

LONG RANGE FORECASTING OF SOUTHWEST MONSOON RAINFALL OVER INDIA

D. S. Pai

India Meteorological Department, Pune

sivapai@hotmail.com

11.1. Introduction

The agricultural practices in India have traditionally been tied strictly to the annual cycle of rainfall. The annual rainfall of the country averages around 1,200 mm. The summer monsoon accounts for almost all the annual rain in 75% of the geographical area and 78% of the gross cropped area. About a third of the cropped area is still rain fed. The most significant feature of the annual cycle of the Indian summer monsoon is its regularity. However, the very regularity of the monsoon makes agriculture susceptible even to the small changes in the annual cycle of the rainfall. Although the Indian summer monsoon rainfall (ISMR) averaged over the whole of India is found to be stable over the past hundred or more years with no noticeable long-term trend, the ISMR has shown considerable interannual variation and major droughts/floods have occurred in some years. Inter-annual variation of ISMR has many social and economic impacts. A year of deficient rainfall can bring great hardship to the large population and cause severe strain on the economy of the country. Therefore, the forecasting of summer monsoon rainfall over Indian has been one of the first targets of endeavors at tropical climate predictions.

As per the World Meteorological Organization (WMO) definition, the forecast from 30 days' up to two year's description of averaged weather parameters is called long range forecast. Although the duration of monsoon over various parts of India varies from about 2 months to 6 months, long range forecasts are generally issued mainly for monthly and seasonal (four months of June to September) scale. Two main approaches were used for the long range forecasting (LRF) of the ISMR. The first approach is based on the empirical statistical method. The statistical approach uses either the historical relationship between the ISMR and predictors derived from

global atmosphere-ocean parameters (Walker 1914 & 1923, Thapliyal 1982, Gowariker et al. 1989 & 1991, Navone and Cecatto 1995, Singh and Pai 1996, Rajeevan et al. 2000, 2004 & 2007, Delsole and Shukla 2002, Sahai et al. 2003, Pai and Rajeevan 2005 etc.) or time series analysis of past rainfall data series (Goswami and Srividya 1996, Iyengar and Raghukanth 2004, and Kishtawal et al. 2003). The statistical method based on the time series analysis use historical rainfall data series only for the prediction of the rainfall in the subsequent years. The second approach towards long range forecasting is based on the dynamical method, which uses General Circulation Models (GCM) of the atmosphere and oceans to simulate the summer monsoon circulation and associated rainfall. In spite of its inherent problems, at present, statistical models perform better than the dynamical models in seasonal forecasts of ISMR. The dynamical models have not shown the required skill to accurately simulate the salient features of the mean monsoon and its interannual variability (Latif et al. 1994, Gadgil and Sajini 1998, Krishnamurti et al. 2000, Kang et al. 2002, Gadgil et al. 2005, Krishna Kumar et al. 2005, Wang et al. 2005).

The India Meteorological Department (IMD) has been issuing operational long range forecasts of the south-west monsoon rainfall since 1886 using statistical methods. The first operational long range forecasting (LRF) of Indian summer monsoon rainfall was issued on June 4th, 1886 using a subjective method. The first objective LRF model based on statistical correlations, however, was resulted from the extensive and pioneering work of Sir Gilbert Walker (Walker 1923 & 1924). Since then, IMD's operational long range forecasting system has undergone many changes in its approach and scope over the years. During 1988-2002, IMD's operational forecasts were based on the 16 parameter power regression and parametric models (Gowariker 1989 & 1991). In 2003, a two- stage LRF strategy was introduced. There are detailed reviews on the long range forecasting of Indian southwest monsoon rainfall can be (Normand 1953, Jagannathan, 1960, Thapliyal and Kulshrestha 1992, Hastenrath 1995, Krishna Kumar et al. 1995, Rajeevan 2001, Gadgil et al. 2005). At present, the forecast for the southwest monsoon season rainfall over the country as a whole is issued using the new statistical forecasting system based on the ensemble method introduced in 2007. Looking into the potential of the dynamical models, IMD also has established an experimental forecasting system based on GCMs.

11.2. Interannual Variability of Indian Summer Monsoon Rainfall

In spite of its regularity, monsoon exhibits large variability in different space and time scales. The space scale varies between as small as a rainfall regime represented by rainfall recorded at a rainguage station to the complete monsoon region. The time-scale varies from daily to interannual to decades, centuries and even millennia.

Fig.11.1a shows the interannual variability of all India area weighted seasonal monsoon rainfall expressed as the percentage departures from long period average (LPA) for the period 1901-2009. The LPA for the period 1941-90 is 890 mm. Fig.11.1b depicts the corresponding monthly rainfall values for the four monsoon months. In Fig.11.1a, the horizontal dashed lines correspond to the ± 10% departure or +/- one standard deviation. The years in which the percentage departures are less than -10% (more than +10%) are called drought (flood) or deficient (excess) monsoon years (Ananthakrishnan & Parthasarathy 1984). Remaining years are called normal monsoon years. It is seen that during the period 1901 -2009, the lowest and second lowest seasonal rainfall have occurred in 1918 (75.1% of the normal) and 1972 (76.4%) respectively and highest and second highest in 1917(122.9%) and 1961(121.8%). There were 13 excess monsoon years and 20 deficient monsoon years in the series. Of the observed 20 deficient years, 6 years (32%) occurred in the first 20 years period (1901-20). During the long intervening period of 1921- 64, there were only two deficient years (1941 and 1951). During the next 23 years period (1965-87), there were 9 deficient years. During the period (1988-2001), there were no deficient rainfall years. During the recent 8 years (2002-2009), there were 3 deficient rainfall years (2002, 2004 & 2009). Two consecutive deficient years, as in 1904-05, 1965-66 and 1986-87 were rare events in the history of ISMR. There were two cases of two consecutive excess years (1916 & 1917, and, 1955 & 1956). The pairs of years 1917-1918, 1941-42,1974-75, 1982-83, and 1987-88 show extreme contrasting events of Indian monsoon rainfall; the interannual difference in the rainfall being highest during 1917-1918 (47.8% of the normal). Also there is no case of the occurrence of three or more consecutive deficient/excess monsoon years. The most noticing point in the rainfall series is that the magnitude of highest negative anomaly is relatively higher than that of the highest positive anomaly. This could be due to the fact that large-scale vertical motion and moisture convergence, which brings rainfall, are suppressed on scale of the country as a whole, under persistent drought conditions. The good rainfall regimes occur on the scale of synoptic scale disturbances, enhancing rainfall over the area of ascent and reducing it over area of descent (Kulshrestha and Sikka, 1989). Table-10.1 shows

the monthly and seasonal rainfall anomalies for excess and deficient rainfall seasons over India for the period 1901-2009. Again it is seen that the deficient years are characterized by persistent negative monthly rainfall anomalies during the entire monsoon season. Excess rainfall years, on the other hand, show greater variability from one to the other monsoon months.

In Fig.11.1a, the red (blue) bars correspond to El Nino (La Nina) years. Out of the 20 drought years during the period of 1901-2009, 13 years (65%) were associated with El Nino events. Similarly out of the 13 excess years, 6 years (46%) were associated with La Nina. This indicates that the association between deficient monsoon rainfall and El Nino is more stronger than that between excess monsoon rainfall and La Nina and that there are forcing other than the SSTs over east Pacific, which can influence the Indian monsoon

11.3. Need and the Basic Premise of LRF

The long-range forecast of ISMR is very crucial as the inter-annual variation of ISMR has many social and economic impacts. Over India, the monsoon rainfall accounts for about 75-80% of the total annual rainfall; in large areas of central and northwest India, the monsoon contribution to the annual rainfall is 90% or more. The total monsoon rainfall during the season has a statistically significant relationship with the crop yield, generation of power, irrigation schedule etc. over the country. In general, a weak monsoon year with significantly low rainfall can cause a low crop yield. On the other hand, a strong monsoon is favorable for abundant crop yield, although sometimes too much rainfall may cause devastating floods. Parthasarathy et al. (1988) and later Gadgil (1996) and Webster et al. (1998) have shown an in phase variation of the rice production in India with the all India summer monsoon rainfall. Fig.11.2 a & b respectively shows the relationship of ISMR with all India major crops production during the concurrent Kharif season and that during the subsequent Rabi season for the period 1966-2008. The crop production time series were first detrended to remove the technology trend from the series and anomalies were computed using normal computed for the base period of 1971-2000. It is seen that there is in phase relationship between the rainfall and the detrended crop production anomalies of the both Kharif and Rabi seasons. This indicates that above normal monsoon rainfall in addition to providing favourable condition for Kharif crops, helps in maintaining improved soil moisture during the subsequent winter season which is vital for the crops during the Rabi season. However, the relationship

between ISMR and Kharif crop production is stronger (C.C. = 0.75) than that between ISMR and Rabi crop production (0.45). The amount of rainfall obtained during the monsoon season is also important for various sectors such as water resources, forestry, hydro-electricity etc. Thus there is a pressing need to understand the Indian monsoon and forecast its interannual variability on long range scale.

The predictability of day-to-day weather patterns in the tropics is restricted to 2-3 days. The seasonal mean monsoon circulation in the tropics, on the other hand, is potentially more predictable. This is because the low frequency component of monsoon variability is primarily forced by slowly varying conditions like sea surface temperature, snow cover, soil moisture etc. Therefore, it is possible to develop models for the long range forecasts of monsoon seasonal rainfall over the country as a whole. However, there is some limit in the seasonal predictability as the mean monsoon circulation is also influenced by the internal dynamics.

11.4. History of LRF in India

In 1877, India experienced a severe famine as a result of highly deficient monsoon rainfall. Subsequent to this, Sir H. F. Blanford, who established India Meteorological Department (IMD) in 1875 and was the first Chief Reporter of IMD, was asked by Government of India to prepare monsoon forecasts. Blanford (1884) used the relationship between winter and spring snow falls over Himalayas and subsequent seasonal ISMR to issue first tentative forecasts from 1882 to 1885. The success of the tentative forecasts encouraged him to issue the first operational forecast for monsoon rainfall of 1886 for the region covering whole India and Burma on 4th June 1886. Since that attempt, the LRF of the monsoon rainfall became one of the important operational duties of IMD. Sir John Eliot who succeeded Blanford as the Head of India Meteorological Department (IMD) in 1895 applied subjective methods such as analogue and curve parallels for the LRF of ISMR. In these methods, he used the weather conditions over whole of India and surrounding regions. From 1895 onwards the monsoon forecasts were based on three parameters, viz. (1) Himalayan snow cover (Oct-May), (2) local peculiarities of pre-monsoon weather in India and (3) local peculiarities over the Indian Ocean and Australia. However, his forecasts of 1899 and 1901 (both drought years) were failures. The efforts for better forecasts continued during the period (1904-1924) of Sir Gilbert T. Walker who took over as the Director General of IMD. Realizing the complexities of the forecasting problem Walker started systematic studies for the development of objective techniques for LRF.

Walker (1910, 1914 & 1923) conducted extensive studies of world wide variations of weather parameters such as rainfall, temperature, pressure etc. He observed that the variations in the monsoon rainfall were connected with widespread and long lasting changes in the pressure distribution over large portions of the global surface. Search for the potential predictors led Walker to identify three large scale seesaw variations in the global pressure patterns. They are North Atlantic Oscillation (NAO), North Pacific Oscillation (NPO) and Southern Oscillation (SO). Walker also introduced the concept of correlation in the field of LRF for the first time to remove the subjectivity in the earlier techniques. He issued the first official forecast in 1909 for the seasonal monsoon rainfall over the whole India based on regression technique. Later, on realizing that the entire country cannot be taken as homogenous rainfall region, Walker (1924) attempted to develop forecasting equations for smaller regions. He divided the country into three homogeneous regions, viz. (1) Peninsula, (2) Northeast India and (3) Northwest India. He developed one regression equation each for the monsoon season (Jun-Sept) for all the three sub-regions and rainfall of the second half of monsoon season (August and September) over Peninsula and Northwest India. These five equations formed basis for the operational LRF in India till 1987. Between 1924 and 1987, operational forecasts were issued for Northwest India and Peninsular India using regression models, which were updated as and when required. Verification of these forecasts (1924-87) revealed that about 63% of these forecasts were correct.

During 1980s attempts were made to overcome the limitations of earlier multiple regression based LRF models by collective use of large number of predictors which are well distributed in time and space and by introducing new techniques. This led to the development of few operational LRF models based on techniques like dynamic stochastic (Thapliyal (1982), power regression and parametric (Gowariker et al. 1989 & 1991). Subsequently, various other models like principal component regression (Singh and Pai 1996, Rajeevan et al. 2000), canonical correlation analysis (Rajeevan et al. 1999; Prasad and Singh 1996), neural network (Navone and Cecatto 1995; Goswami and Srividya 1996; Guhathakurta et al.1999) and power transfer (Thapliyal 2001) were developed.

Between 1988 & 2002, IMD's operational forecasts for the country as whole have been based on the 16-parameter parametric and power regression models. The details of these two operational LRF models used by IMD are discussed in the next section (section 11.5). In view of increasing user demands, from 1999 onwards,

IMD has reintroduced issuing the operational forecasts for three geographical regions of the country, namely, Northwest India, Peninsular India and Northeast India. The areas of these geographical regions were different from that of Walker's geographical regions with the same names.

In 2003, IMD adopted new strategy for issuing LRF for the monsoon rainfall. Accordingly the long range forecasts are issued in two stages (Section 6). The first stage forecast issued in April consisted of forecast for seasonal rainfall over the country as a whole and the second stage forecasts issued in the end of June consisted of update for April forecast along with seasonal rainfall forecast for the geographical sub regions of the country and July rainfall forecast for the country as a whole. During 2003 to 2006, the operational first and update long range forecasts for the seasonal rainfall over the country as a whole was issued using the 8 and 10 parameter models based on power regression and probabilistic discriminant analysis techniques (Rajeevan et al. 2004). In 2004, the country was reclassified into 4 sub geographical regions (Fig.11.3). At present, a new statistical forecasting system based on the ensemble technique introduced in 2007 is used for the seasonal rainfall forecasting over the country as a whole (Rajeevan et al. 2007). In 2009, IMD started to issue forecast for August rainfall over country as a whole along with other second stage forecasts issued in June.

In 2003, IMD implemented an experimental dynamical prediction system based on Atmospheric General Circulation Models (AGCMs). From 2004, forecast for the monsoon season rainfall distribution over India using experimental dynamical prediction system was started.

Though IMD is the only government agency mandated for providing long range forecasts, many institutes in India are involved in the research work related to LRF. Some of these institutes are Indian Institute of Tropical Meteorology (IITM), Pune, Indian Institute of Science (IISc), Bangalore, Space Applications Centre (SAC), Ahmedabad, National Aerospace Laboratories (NAL), Bangalore, Centre for Mathematical Modeling and Computer Simulation (CMMACS), Bangalore, National Centre for Medium Range Weather Forecasting (NCMRWF), Noida and Centre for Development of Advanced Computing, Pune. Many international climate centers are also involved in the research related to seasonal prediction of monsoon rainfall as a part of their efforts to improve global forecasts. IMD makes use of experimental forecasts prepared by these climate research centers both inside and outside India as supportive materials for preparing the operational long range forecasts for India.

11.5. LRF Operational Models for Seasonal Rainfall over the Country as a whole: 1988-2002

11.5.1. Parametric Model

The parametric model was first developed by Gowariker et al. (1989). This model utilized a group of 16 atmosphere-land-ocean parameters and was used by IMD for the operational LRF between 1988 and 1999. In 2000, the model was revised (Thapliyal and Rajeevan, 2002) by replacing its four predictors, namely, April 500 hPa ridge position, 10 hPa zonal wind over Balboa, North India minimum temperature and Darwin spring pressure by four new predictors, namely, Arabian Sea SST, South Indian Ocean SST, Europe Pressure Gradient and Darwin Pressure Tendency. The updated list of 16 predictors is given in Table 11.2. From 2000 to 2002, the forecast was issued based on the revised model.

The parametric model provides categorical forecasts for the summer monsoon rainfall. The model predicts the performance of the monsoon into either of two categories, i.e. wet (normal/excess) or dry (deficient) monsoon. Normal monsoon indicates seasonal rainfall within $\pm$ 10 % of the LPA rainfall for India as a whole. Similarly, the excess and deficient monsoon indicate rainfall > 110 % and < 90 % of the LPA rainfall respectively.

A parameter having positive Correlation Coefficient (C.C.) with the seasonal monsoon rainfall indicates favorable (unfavorable) signal for wet monsoon if its anomaly is positive (negative). Opposite is true for a parameter having negative CC. Using this criterion, the percentage of favorable parameters out of the 16 was determined. The frequency analysis of the signals indicated that whenever more than 70 % of the parameters were favorable, the subsequent monsoon was not only wet on all occasions (100%), but the rainfall was also more than the LPA of the rainfall. On the other hand, when less than 30% of parameters were favorable, there was 83% probability that ensuing monsoon rainfall would be deficient. Thus the confidence on wet monsoon forecast was higher than the deficient monsoon forecast.

11.5.2. Power Regression (PR) Model

Unlike the parametric model in which all the predictors get equal weights, in the PR model, each predictor gets an appropriate weight that depends on the non-linear relationship between the predictors and the ISMR. The general form of the

$$\frac{R + \alpha_o}{\beta_o} = C_o + \sum_{i=1}^{i=16} C_i \left(\frac{X_i + \alpha_i}{\beta_i} \right)^{P_i}$$

Mathematical expression of the PR-model is given below.

Where R is estimated monsoon rainfall over India expressed as the percentage of the LPA of rainfall, X's are the predictors,α's &β's are the scaling parameters and P's & C's are model constants.

11.6. The Two Stage LRF Strategy

Statistical monsoon prediction models are based upon the strong correlations of the monsoon rainfall with certain antecedent atmospheric, oceanic and land parameters. As these correlations can never be 100%, some error is inherent in every statistical model. Another common weakness of all statistical models is that while the correlations are assumed to remain constant in future, they may, and in fact do, change with time and slowly lose their significance. From this angle, in 2003, a critical re-evaluation of the 16-parameter power regression and parametric models was made and it revealed that correlations of 10 parameters had rapidly declined in recent years. Mean while, an extensive search for new parameters which are physically well-related and statistically stable lead to the identification of 4 new predictors of monsoon rainfall. This resulted in building a set of 10 stable parameters (Table 11.3) consisting of 6 out of the earlier 16 parameters and 4 new parameters.

Out of 10 parameters, 8 needed data only up to March and 2 needed data up to June. Using this 10 parameters set, IMD developed two power regression (PR) models, one using 8 parameters needing data up to March and another using the full set of 10 parameters. In addition to these PR models, probabilistic models using the same 8-parameters and 10-parameters respectively were developed to issue qualitative forecast. Based on these models, a two stage forecasting system was

adopted in 2003, for issuing operational forecast for press and public. According to this forecasting system, the first stage LRF for the summer monsoon seasonal rainfall for the country as a whole was issued in the middle of April every year using 8-parameter PR & probabilistic models. In the next stage, LRF update for the first stage forecast was issued in the end of June/beginning of July using the 10-parameter PR & probabilistic models along with monthly forecasts for the country as a whole, and seasonal forecasts for the different broad geographical regions. As of now (2009), the forecasts issued along with update forecast are, forecasts for July and August rainfall for the country as a whole and the season rainfall for the 4 geographical regions(NW India, NE India, Central India and South Peninsula) of the country.

11.6.1. The 8-Parameter and 10-Parameter Power Regression Models for the Seasonal Rainfall for the Country as a Whole

The 8 and 10 parameter PR models were used for issuing quantitative operational forecast of seasonal rainfall over the country as a whole during the period 2003 to 2006. Table 12.3 shows the predictors used for the development of the PR models. The mathematical form of the power regression model is given below.

$$R = C_0 + \sum_{i=1}^{i=n} C_i X_i^{P_i}$$

Where R is the rainfall, X's are standardized predictors, and C's and P's are constants. N is either 8 or 10. The model is non-linear and the power term, P, in the above equation varies between ± 2.

The models were developed using data of 38 years (1958-1995) and independently tested using data of 7 years (1996-2002). The performances of the new 8- and 10-parameter models are given in the Fig.12.4 and Fig.12.5 respectively. Comparison of the model forecasts with IMD's operational forecasts issued using the 16-parameter power regression model during the independent period is given in Table 11.4. It is clear that forecasts from the 8- and 10-parameter models were closer to the actual rainfall than the forecasts from the 16-parameter model. The root mean square error of the operational forecasts by 16-parameter model during the period 1996-2002 was 11% of LPA, while that of the new 8-parameter model and 10-parameter models for the same period was 7% and 6 % of LPA respectively. The model errors of the 8- and 10-parameter models were 5% and 4% of LPA

respectively which are of the same order as the model error of the 16-parameter model at its inception. For more details of these models can be seen in Rajeevan et al. (2004). However, it may be mentioned that though these models showed better performance in general during the drought years in the hindcast mode, they failed to correctly indicate the large rainfall deficiency during 2002 in the hindcast mode and that during 2004 in real time forecast mode.

11.6.2. The 8- Parameter and 10-Parameter Probabilistic Models

The Probabilistic models were based on the statistical linear discriminant analysis (LDA) technique (Wilks 1995, Rajeevan et al. 2000) and used the same sets of 8 and 10 parameters used for the new power regression models. The LDA, first introduced by Sir Ronald Fischer (Fischer 1936), is a useful technique to find out which predictor variables discriminate between two or more naturally occurring (or a priori defined) predictand groups. The LDA also estimate the posterior probabilities for a predictand to fall into each of these groups. The primary assumption for this model is that prior probabilities of all the predictand groups (or quints) are equal. The data for 40 years (1958-1997) were used for the model development and data for 5 years (1998-2002) were used for the model verification. The seasonal rainfall (predictand) was grouped into 5 broad categories of equal probability (20 % each). i.e. each group consisted of 8 years. These categories are deficient (<90% of LPA), below normal (90-97% of LPA), near normal (98-102% of LPA), above normal (103-110% of LPA) and excess (>100% of LPA).

In hindcast mode, the 8- parameter LDA model showed 68% correct classifications, whereas the 10-parameter LDA model showed 78% correct classifications. In hindcast again, both the LDA models correctly gave the highest probability of drought in 8 out of 9 actual drought years except in 2002 (Table -10.5) and no false alarms of drought were generated in any other years.

11.7. The Present Operational Forecasting System

The two stage forecasting system introduced in 2003 (see section 11.6) is still used to issue the operational forecasts for the summer monsoon rainfall. However, from 2007, for preparing the first stage and update forecast for the southwest

monsoon season rainfall over the country as a whole, a new statistical forecasting system based on the ensemble method was used.

11.7.1. New Statistical Ensemble Forecasting System for the Seasonal Rainfall over the Country as a Whole

There were three major changes in the new statistical forecast system used at present (Rajeevan et al. 2007) from that used during 2003 to 2006 which was based on the 8/10 Parameter power regression models. These were: a) use of a new smaller predictor data set b) use of a new non-linear statistical technique along with conventional multiple regression technique c) application of the concept of ensemble averaging. The new ensemble forecasting system introduced in 2007 used a set of 8 predictors (given in the Table 11.6) that having stable and strong physical linkage with the Indian south-west monsoon rainfall. For the April forecast, first 5 predictors listed in the Table-10.6 were used. For the update forecast issued in June, the last 6 predictors were used that include 3 predictors used for April forecast.

In the ensemble forecasting system, the forecast for the seasonal rainfall over the country as a whole was computed as the mean of the two ensemble forecasts prepared from two separate set of models. Multiple linear regression (MR) and projection pursuit regression (PPR) techniques were used to construct two separate sets of models. PPR is a nonlinear regression technique. In each case, models were construed using all possible combination of predictors. Using 'n' predictors, it is possible to create (2^n-1) combination of the predictors and therefore that many number of models. Thus with 5 (6) predictors it is possible to construct 31 (63) models. Using sliding fixed training window (of optimum period of 23 years) period, independent forecasts were prepared by all possible models for the period 1981-2008. For preparing ensemble average, a set of few best models from all possible MR models and another set of few best models from all possible PPR models were selected. The best models were selected in two steps. In the first step, all models (MR and PPR models separately) were ranked based on the objective criteria of likelihood function or generalized cross-validation (GCV) function computed for the period 1981-2007. In the second step, ensemble average of forecasts from the models ranked based on GCV values were computed by using first one model, first 2 models, first 3 models and so on up to all the possible models in the rank list as the ensemble members. The ensemble average for each year of the independent period 1981-2007 was computed as the weighted average of the forecasts from the individual ensemble members. The weights used for this purpose was the C.C

between the actual and model estimated ISMR values during the training period (of 23 years just prior to the year to be forecasted) adjusted for the model size. Mean of the two ensemble average forecasts (one from MR models and another from PPR models) was computed as the final forecast. Performance of the April and June forecast for the independent test period of 1981-2008 computed using the new ensemble method is shown in Fig.11.6 & Fig. 11.7 respectively. The RMSE of the independent April & June forecasts for the period 1981-2008 was 5.9% of LPA and 5.6% of LPA respectively.

11.7.2. Forecasts for the Seasonal Rainfall over the Four Geographical Regions

Since 1999 to 2003, IMD was issuing long range forecasts for seasonal rainfall over the 3 broad geographical regions of India viz., North-west India, North-east India and Peninsula using 3 individual power regression models based on different sets of predictors. In 2004, the country was reclassified into 4 geographical sub regions viz., Northwest India, Central India, Northeast India and South Peninsular India (Fig.11.4). The seasonal forecasts for the 4 geographical regions are issued in June along with the update forecast for the seasonal rainfall over the country as a whole. These forecasts are prepared using separate multiple regression models each based on different set of predictors and with model error of ±8%. The performance of the models for the 4 geographical regions is given in Table 11.7.

11.7.3. Forecast Models for Monthly (July and August) Rainfall over the Country as a Whole

The months of July and August are the rainiest months of the south-west monsoon season. The normal rainfall during July & August months over the country as a whole accounts about 33 % (293 mm) and 29% (263mm) of the monsoon season's total rainfall respectively with a corresponding coefficient of variation of 13% and 14% . The severe drought in 2002 was due to the unprecedented deficient rainfall (46% of LPA) in July 2002, which brought down the country's kharif crop production by 30 million tones below that of the previous year. For the monthly rainfall forecasts over the country as whole, principal component regression (PCR) technique is used. In this method, the principal components of the predictors are used in regression analysis to develop the prediction algorithm. The PCR technique is recommended when there is significant inter-correlation among the independent variables. The PCR model avoids the inter-correlation and helps to reduce the

degrees of freedom by restricting the number of independent variables (Rao 1964). PCR model has been used for the prediction of the seasonal (June-September) ISMR for the country as a whole based on predictors from the Indian Ocean only (Singh and Pai 1996). PCR model has also been used for the prediction of seasonal summer monsoon rainfall over two homogeneous regions of India based on predictors from various observed climatic fields (Rajeevan et al. 2000).

For the forecast of July rainfall over the country as a whole, a set of 5 predictors were used. The model was trained using data for the period 1958-2000 and the model was tested for the period 2001 to 2008. PCA analysis was carried over the predictor set using data for the training period and first three PCs explaining about 89% of the total variability of the predictor data set was retained for multiple regression (MR) analysis. Using the PC loadings of the retained PCs, PC scores were calculated for the independent test period and the same were then used for the prediction of July rainfall for the independent test period. The performance of the PCR model for the July rainfall during the independent test period is shown in Table-10.8. It is seen that, though the model could forecast the sign of the rainfall deficiency during 2002 correctly, it failed to capture the magnitude of deficiency correctly. The RMSE during the training period was 10% of LPA and that during the independent test period was 14.9% of LPA. Relatively large RMSE during the test period was caused by the large forecast error during 2002, when the actual July rainfall was extremely low.

A set of six predictors were used for the forecast of August rainfall over the country as a whole. The model was trained using data for the period 1975-2000 and the model was tested for the period 2001 to 2008. PCA analysis was carried over the predictor set using data for the training period and first three PCs explaining about 75% of the total variability of the predictor data set was retained for multiple regression (MR) analysis. The performance of the PCR model for the August rainfall during the independent test period is shown in Table-10.9. The RMSE during the training and independent test periods was 9.5% of LPA and 10% of LPA respectively.

11.8. Dynamical Prediction

Dynamical models have the capability to generate forecast at smaller spatial scale and to provide forecast at required time interval. There have been several studies that developed and used General Circulation Models (GCMs) for monsoon diagnostic and forecasting studies (Shukla and Fennessy 1994, Ju and Slingo 1995,

Liang et al. 1995, Zhang et al. 1997, Goswami 1998, Webster et al. 1998, Gadgil and Sajani, 1998, Sperber et al. 2000, Ramesh et al., 2000). The studies observed that GCM simulations and forecasts may be sensitive to physical parametrization (Zachary and Randall 1999) and model resolution (Sperber et al. 1994, Lal et al. 1997, Martin 1999). It is essential that Atmospheric General Circulation Models (AGCMs) are able to simulate various features of the summer monsoon such as mean, the intraseasonal variability (ISV) and interannual variability (IAV) with reasonable accuracy for it to be useful for monsoon studies (WCRP, 1992, 1993).

The first systematic efforts to evaluate the performance of the GCMs to simulate the Asian summer monsoon circulation using GCMs were started under the TOGA (Tropical Ocean Global Atmosphere) Monsoon Numerical Experimentation Group (MONEG) program (WCRP, 1992). Under this program, experiments for the monsoon seasons of 1987 & 1988 using the same initial conditions and the same boundary forcing were carried out by several modeling groups worldwide (Palmer et al. 1992, Fennessy and Shukla 1992, Laval et al. 1996, Arpe et al. 1998). Observed SSTs were used as the SST boundary forcing. The results showed that there were significant differences in simulating the mean monsoon by different models. Most models had systematic errors in simulating the regional features of the monsoon. However, a majority of the models could simulate the correct tendency of the inter-annual variability between 1987 & 1988 (Palmer et al. 1992). The results also showed that a large fraction of the simulated Indian monsoon rainfall was forced by the SST variations over the Pacific. It was further observed that over Indian region impact of initial conditions were comparable to the impact of SST anomalies.

The next significant step was the Atmospheric Inter-comparison Project (AMIP), the basic purpose of which was to undertake the systematic intercomparison and validation of the performance of atmospheric GCMs on seasonal and interannual time scales under as realistic conditions as possible, and to support the in-depth diagnosis and interpretation of the model results (Gates 1992, Sperber and Palmer 1996). This attempt provided a unique opportunity to study the potential predictability of interannual fluctuations of the atmosphere based on ensembles of multi-annual integrations. Under AMIP I, the integrations of many of the world's atmospheric general circulation models (AGCM) were carried out over the 3653-day period (1 January 1979 to 31 December 1988, inclusive.) using the observed monthly-averaged distributions of sea-surface temperature and sea ice as boundary conditions. Under AMIP II, the integrations were extended for 7 more years (1989 to 1995). The evaluation of the monsoon precipitation simulated by AGCMs (Sperber

and Palmer, 1996; Zhang et al., 1997; Gadgil and Sajani, 1998) was one of the AMIP diagnostic subprojects that were established to examine model performance in terms of specific process and regional phenomena. Sperber and Palmer (1996) indicated that, for interannual timescales, many AMIP I models simulated the large scale dynamical index and its SST teleconnection pattern realistically, but failed to simulate the mean and Interannual variability of the regional monsoon precipitation with any fidelity. Gadgil and Sajani (1998) analyzed the monthly precipitation simulated by 30 GCMs under AMIP I. They found that while most of the models simulated the seasonal migration of the primary rain belt over the African region and the rainfall patterns associated with the African monsoon in austral and boreal summers, the seasonal variation over the Asia-West Pacific region and the seasonal mean pattern over the Indian monsoon zone were realistically simulated only by some models. The simulation of the inter-annual variability of monsoon rainfall differed widely from one model to another indicating the great sensitivity of this region on resolutions and physical parameterizations of the models.

European Center for Medium Range Weather Forecasting (ECMWF) coordinated a European collaborative Project (Brankovic and Palmer 1997) called PRediction Of climate Variations on Seasonal to inter-annual Time scales (PROVOST). Under this project, a series of ensemble runs using T63L19 ECMWF model were made for each season. For monsoon season, there were nine ensemble members corresponding to 9 different initial conditions starting from 23rd May. The integrations were carried out using the observed SST during the 15-year period of 1979-1993. Fig.12.8. shows the spatial distribution of the ensemble mean model precipitation during the period June-September, averaged over the period 1979-1993 (Rajeevan 2001). The spatial distribution of observed average precipitation (ECMWF reanalysis) for the same period is also shown. It may be seen that the spatial pattern of precipitation over North Bay of Bengal simulated by the model was close to the observed pattern. But model precipitation over Southern Hemisphere (corresponding to the Southern Hemisphere Equatorial Trough) and Northeast India is higher than the observed by 6 mm/day. On the other hand, model could not simulate the precipitation pattern over the West Coast of India as observed. There, the model precipitation was smaller than the observed by 6 mm/day.

The inter-annual variability of Indian summer monsoon rainfall (averaged over land regions between 7.5^{o}N to 30°N, 70°E to 95°E) during the period 1979-1993, for the nine ensemble along with the IMD's observed rainfall anomalies are shown in

Fig.11.9 (Rajeevan 2001). The mean of the ensembles is shown as thick line. The model rainfall anomaly in 1981, 1982, 1985, 1988 and 1992 is very well close to the observed rainfall anomaly. But in some other years (1979, 1980, 1987 and 1990) the model rainfall anomaly is very much different from the observed. For 1979, the model predicated excess rainfall, while the observed rainfall anomaly was deficient.

From Fig.11.9, it can also see that there is a large dispersion among the ensemble members in individual years. This dispersion is quite comparable to the inter-annual fluctuations. Thus, the simulation of the seasonal mean Indian monsoon rainfall is found to be sensitive to small changes in the initial conditions. However, the prediction of the seasonal mean rainfall in other parts of the tropics (Sahel, NE Brazil, equatorial Pacific) does not seem to be sensitive to small changes in the initial conditions (Webster et al. 1998). Due to this dependence on initial conditions, ensemble averages of the predictions based on different initial conditions are more useful for preparing the seasonal prediction of monsoon rainfall. This approach is likely to further refine the model performance.

Recently, the super ensemble method of improving weather and climate forecast using a number of forecasts from a variety of weather and climate models has developed skill. Along with the benchmark observed (analysis) fields, these forecasts are used to derive simple statistics on the past behavior of the models. A super ensemble forecast is prepared by comparing these statistics with model forecasts. Average root mean square error from the multi-model super ensemble predictions was much smaller than the errors from the individual predictions. Further studies are being carried out to bring out the full potential.

11.9. Experimental Dynamical Forecasting System at IMD

Looking at the potential of dynamical models for providing seasonal forecasts for tropical region, IMD in collaboration with Indian Institute of Science (IISc), implemented an experimental dynamical model forecasting system in 2003. The experimental forecasting system established at the National Climate Centre (NCC), Pune is based on the Seasonal Forecast Model (SFM) of the Experimental Climate Prediction Center (ECPC). Preparation of experimental dynamical model forecasts for the monthly and seasonal southwest monsoon rainfall was started in 2005.

The SFM model was originally developed at the National Centers for Environmental Prediction (NCEP) to provide regional details for the Global Spectral Model (GSM). The details of the model are described in Kanamitsu et al. (2002). The model is a non-hydrostatic global spectral model with horizontal resolution T62 and 28 vertical levels. The basic model Physical processes and parameterization schemes were developed from reanalysis-II version of NCEP Medium Range Forecast model. The Model used convective parameterization based on Relaxed Arakawa–Schubert-type (Moorthi and Suarez, 1992), the shortwave Radiation scattering and absorption scheme based on Chou (1992), Long wave radiation flux computation based on Chou and Suarez (1994) and Cloud and large scale precipitation scheme based on Slingo (1987). Land surface scheme of the model is a multilayer soil model with more complex surface layer physics based on Oregon State University (OSU) land surface scheme of Pan and Mahart (1987). The model used refined planetary boundary layer physics of Hong and Pan (1996) and the parameterization of orographic gravity wave drag based on Alpert et al. (1988).

For running the model in the hindcast mode, observed sea surface temperatures (SSTs) were used as the boundary conditions. In the forecast mode, the model used SST boundary conditions created based on persisting SST method. Under hindcast mode, 20 years model climatology (1985-2004) was prepared. The model simulated rainfall climatology is shown in Fig.12.10. The year to year variation of model hindcast rainfall anomaly over India for the period 1985 to 2004 is given in the Fig.11.11. The C.C between the actual and model hindcast rainfall anomalies during the period 1985-2004 is 0.37. It is seen in the Fig.11.11 that the model has useful skill over the Indian region.

In the forecast mode, forecasts for monsoon months (June to September) were prepared twice. To prepare forecast in the month of April, model integration was started from 1st April to 30th September by using SST boundary conditions prepared by persisting March SST anomalies. 10 ensembles were generated using the initial conditions corresponding to 0000Z UTC from 22nd March to 31st March obtained from NCEP reanalysis. Similarly to prepare forecast in June, persistent method based on May SSTs were used and to generate 10 model ensembles initial conditions corresponding to 0000Z UTC from 21st May to 30th May were used. The model forecasts based on persistence method using March and May SSTs for the period 2005 to 2008 is given in the Fig.11.12. Further improvement in the model skill is necessary before the model can be used for operational forecast.

11.10. Operational Forecast Model for the Monsoon Onset over Kerala

Since 2005, IMD has been issuing operational forecast for the onset of monsoon over Kerala using an indigenously developed statistical model (Pai & Rajeevan 2009). The model is based on the principal component regression (PCR) method using 6 predictors. Table-11.10 shows the list of the 6 predictors. Sliding fixed wind period of length 22 years was used for deriving the independent forecasts. According to this method, for the prediction of monsoon onset over Kerala each year, data of 22 years just prior to the reference year was first used for PC analysis of the predictor data series. PC scores were calculated for the reference year using the PC loading matrix and predictor values. Only those PCs that having eigen values more than or equal to 1 were then used as the input to the multiple linear regression equation. For training regression equation also the same 22 years used for PCA analysis was used. In this way, monsoon onset over Kerala was predicted for the period 1997-2008. Before the analysis, the predictors were normalized by 1975-2000 climatology. Fig.11.13 shows the performance of the forecast for the independent test period (1997-2009). The RMSE of the forecast during 1997-2009 is 4 days. With a model error of ± 4days, it can be seen from the Fig.11.13 that, since 2005, all the operational forecasts issued with this model have been accurate.

11.11 Summary and Conclusions

Seasonal forecasting of Indian summer monsoon rainfall (ISMR) over India has been one of the first targets of endeavors at tropical climate predictions. Two main approaches are used for the long range forecasting (LRF) of the ISMR. The statistical approach uses the historical relationship between the ISMR and predictors derived from global atmosphere-ocean parameters (mainly derived from slowly varying boundary forcing). The second approach is based on the dynamical method, which uses General Circulation Models (GCM) of the atmosphere and oceans to simulate the summer monsoon circulation and associated rainfall. The GCM simulation is primarily driven by the sea surface temperature (boundary) conditions provided in the models. In spite of the inherent problems such as epochal variation in the predictand - predictor relationship, intercorrelation between the predicators, changing predictability etc. in the statistical approach, at present, statistical models shows better skill than the dynamical models in long range forecasting of Indian summer monsoon rainfall. The dynamical models have not yet shown the required skill to accurately simulate the salient features of the mean monsoon and its

interannual variability. It has been found that the simulation of the Indian monsoon circulation and rainfall features with coupled ocean-atmosphere models (Latif et al. 1994) is also difficult. Super-ensemble type dynamical model predictions (Krishnamurti et al. 2000) are found to improve the skill in the prediction of monsoon rainfall. Dynamical models are likely to go through several years of development efforts before they can completely replace statistical models. Work on the refinement of statistical models has therefore to continue. Therefore, India Meteorological Department (IMD) has been using statistical methods for issuing operational long range forecast for southwest monsoon rainfall. However, there is necessity of subjecting statistical forecast models for the monsoon to a constant scrutiny. The temporal instability of some predictors does not allow the continued use of such models over a long period of time without change. This throws a challenge to the modeler as good parameters are hard to find. It also creates a dilemma for the operational forecaster who would like to have a time-tested model which he can trust rather than one which is being frequently updated. The periodic revision of models has also to be viewed in the light of the possible impact of global warming and climate change on the inter-annual variability of the Indian summer monsoon rainfall (Krishna Kumar et al. 1999, Kripalani et al. 2003).

At present, IMD issues long range forecasts for southwest monsoon rainfall in two stages according to two stage forecasting strategy implemented in 2003. The first stage forecast issued in mid April consists of quantitative forecast for the seasonal (June-September) rainfall for the country as a whole. The second stage forecast issued in the end of June consists of update for the April forecast, forecast for the monthly (for the rainiest months of July and August) monsoon rainfall for the country as a whole and forecast for the seasonal monsoon rainfall for the four geographical regions (NW India, NE India, Central India and south Peninsula) of the country. At present, the forecast for the southwest monsoon season rainfall over the country as a whole is issued using the new statistical forecasting system based on the ensemble method introduced in 2007.

In addition to the above long range forecasts, IMD also issues operational forecast for the monsoon onset over Kerala in the middle of May. In addition to operational forecasts based on statistical forecasting system, experimental forecasts of monthly and seasonal rainfall over Indian region based on dynamical forecasting system were also prepared. For this purpose seasonal forecast model (SFM) which is an atmospheric GCM originally developed by Experimental Climate Prediction Center (ECPC), USA is used.

Apart from IMD, other research institutions in India and abroad are also involved in long range forecasting research. While preparing, the operational forecasts for southwest monsoon season, IMD also takes into account the forecasts from various other research institutions from India and abroad. IMD makes use of experimental forecasts prepared by these climate research centers both inside and outside India as guidance for preparing the operational long range forecasts for India. It has been found that, there is large divergence in the forecasts provided by dynamical models for the Indian region. Various inter-comparison projects conducted in India and abroad using atmospheric and coupled GCM outputs from various centers, has reported that these models do not have any skill in simulating the climatology as well as the itnerannual variability of monsoon rainfall. There is urgent need for concentrated and continued efforts to develop a dynamical model suitable for long range forecasting of Indian summer monsoon rainfall.

References

Alpert, J. C., Kanamitsu, M.,. Caplan, P. M., Sela, J. G., White, G. H. and Kalnay, E. 1988,"Mountain induced gravity wave drag parameterization in the NMC medium-range model". Preprints, *Eighth Conf. on Numerical Weather Prediction,* Baltimore, MD, Amer. Meteor. Soc., 726–733.

Blanford, H.F., 1884, "On the connection of the Himalayan snow with dry winds and seasons of droughts in India", Proceedings of the Royal Society of London, 37, 3-22.

Brankovic, C. and Palmer, T. N., 1997,"Monthly Wea. Rev.", 125, 859-874.

Chou, M. D., 1992," A solar radiation model for use in climate studies". *J. Atmos. Sci.,* 49, 762–772.

Chou. M, and Suarez,M. J.1994, "An efficient thermal infrared radiation parameterization for use in general circulation models"' NASA Tech. Rep. TM-1994-104606 Series on Global Modeling and Data Assimilation, 85 pp.

Fischer, R. A., 1936, "The use of multiple measurements in taxonomic problems", Ann. Eugenics, 7, 179-188.

Gadgil, S., 1996, "Climate change and agriculture – An Indian perspective, In Climate variability and agriculture", (Eds. Y. R. Abool, S. Gadgil and G. B. Pant), Narosa, New Delhi, India, 1-18.

Gadgil, S., and Sajani, S., 1998, "Monsoon precipitation in the AMIP runs", Climate Dynamics, Clim. Dyn., 14, 659-689.

Goswami, 1998, "Interannual variations of Indian summer monsoon in a GCM: external conditions versus internal feedbacks". J. Clim. 11: 501–522.

Goswami, P., and Srividya, P., 1996, "A Neural Network design for long range prediction of rainfall pattern", Curr. Sci., 70, 447-457.

Gowariker, V., Thapliyal, V., Kulshrestha, S. M., Mandal, G. S., Sen Roy, N., and Sikka, D. R., 1991, "A power regression model for long range forecast of southwest monsoon rainfall over India", Mausam, 42, 125-130.

Gowariker, V., Thapliyal, V., Sarker, R. P., Mandal, G.S., and Sikka, D. R., 1989, "Parametric and power regression models: New approach to long range forecasting of monsoon rainfall in India", Mausam, 40, 115-122.

Guhathakurta, P., Rajeevan, M., and Thapliyal, V., 1999, “Long range forecasting Indian summer monsoon rainfall by a Principal component Neural Network Model”’ Met and Atmos. Phys, 71,255-266.

Hong, S. Y., and Pan, H. L. 1996, ”Non-local boundary layer vertical diffusion in a medium-range forecast model” *Mon. Wea. Rev.,* 124**,** 2322–2339.

Hong, S.-Y., and Pan, H.-L.1996, “Non-local boundary layer vertical diffusion in a medium-range forecast model”. *Mon. Wea. Rev.,* 124, 2322–2339.

Kanamitsu M., Kumar, A., Ming, H., Jung, H.,. Kyung, J., Wang, W.I., Yang, F., Hong, S. Peng, P., Chen, W., Moorthi, S and Ji, M., 2002, “NCEP Dynamical forecast System 2000”, *Bull. Amer. Meteor.Soc.,*83*,* 1019- 1037

Kripalani, R. H., Kulkarni, A., Sabade, S. S., and Khandekar, M.L., 2003, “Indian monsoon variability in a global warming scenario”, Natural Hazards, 29, 189-206.

Krishna Kumar, K., Rajagopalan, B., and Cane, M. A., 1999, “Epochal changes in Indian monsoon ENSO precursors”, Science, 284, 2156-2159.

Krishnamurti, T. N. and co-authors, 2000, “Multimodel ensemble forecasts for weather and seasonal climate”, J. Climate, 13, 4196-4216.

Latif, M., Sterl, A., Assenbaum, M., Junge, M. M., and Maier-Reimer, E., 1994, “Climate variability in a coupled GCM-Part II: The Indian Ocean and monsoon”, J. Climate, 7, 1449-1462.

Moorthi, S., and M. J. Suarez, 1992, “Relaxed Arakawa– Schubert: A parameterization of moist convection for general circulation models”, *Mon. Wea. Rev.,* 120**,** 978–1002.

Navone, H. P. and Ceccato, H. A., 1995, “Predicting Indian monsoon rainfall: A neural network approach”, Climate Dynamics, 10, 305-312.

Pai. D. S. and Rajeevan, M., 2009, ”Prediction of summer monsoon onset over Kerala”, India, J. Earth Syst. Sci. 118, No. 2, pp1–13.

Palmer, T. N., Brankovic, C., Viterbo, P. and Miller, M. J., 1992, “Modeling inter annual variations of summer monsoon”, J. Climate, 1992, 5, 399-417.

Pan, H.-L., and Mahrt, L., 1987, “Interaction between soil hydrology and boundary layer developments”, *Bound.-Layer Meteor.,* 38**,** 185–202.

Parthasarathy, B., Rupakumar, K. and Munot, A. A., 1991, “Evidence of secular variations in Indian summer monsoon rainfall circulation relationships”, J. Climate, 4, 927-938.

Parthasarathy, B., Munot, A. A. and Kothawale, D. R., 1988, “Regression model for estimation of Indian food grain production from Indian summer rainfall”, Agric. For. Meteorol., 42, 167-182.

Prasad, K. D., and Singh, S. V., 1996, “Forecasting the spatial Variability of the Indian monsoon rainfall using Canonical Correlation”, Int. J. Climatol., 16, 1379-1390.

Rajeevan, M, Guhathakurta, P., and Thapliyal, V., 2000, “New models for long range forecasting of monsoon rainfall over northwest and peninsular India”, Met. Atmos. Physics, 73, 211-225.

Rajeevan, M. Thapliyal, V., Patil, S. R., and De, U. S., 1999, “Canonical Correlation Analysis (CCA) models for long-range forecasts of sub-divisional monsoon rainfall over India”, Mausam, 50,145-152.

Rajeevan, M., 2001, “Prediction of Indian summer monsoon: Status, problems and prospects”, Current Science, 11, 1451-1457.

Rajeevan, M, Pai D. S., Dikshit S. K., and Kelkar R. R., 2004, “IMD’s New Operational Models for Long Range Forecast of South-west Monsoon Rainfall over India and their Verification for 2003”, Current Science, V86, pp422-431.

Rajeevan, M, Pai D. S., Anil Kumar R, and Lal B, 2007, “New statistical models for long-range forecasting of southwest monsoon rainfall over India”, Climate Dynamics, V28, pp813-828.

Ramesh, K. J, Rao PLS, Mohanty UC, 2000, “A Study on the performance of the NCMRWF analysis and forecasting system during Asian summer monsoon: thermodynamic aspects”, Clim Dyn 154: 141–162.

Singh, O. P. and Pai, D. S. 1996, “An oceanic model for the prediction of SW monsoon Rainfall Over India, Mausam”, 47, 91-98.

Slingo, J. M., 1987, ”The development and verification of a cloud prediction model for the ECMWF model”. *Quart. J. Roy. Meteor. Soc.,* 113**,** 899–927.

Sperber, K. R and Palmer, T. N., 1996, ”Interannual tropical rainfall variability in General circulation model simulations associated with the Atmospheric model intercomparison project”. J. Climate,

Thapliyal, V. and Kulshreshtha, S., 1992, “Recent models for long-range forecasting of southwest monsoon rainfall over India”, J. Arid. Environ., 43, 239-248.

Thapliyal, V., 1982, “Stochastic Dynamic model for long range forecasting of summer monsoon rainfall in peninsular India”, Mausam, 33, 399-404.

Thapliyal, V., 2001, “Long-range forecast of summer monsoon rainfall over India”, Evolution and development of new power transfer model, Proc.Ind.National.Sci.Acad, 67 A, 343-359.

Walker, G. T., 1910, “Correlation in seasonal variations of weather”, II, Mem. India Meteorol. Dept., 21, 22.

Walker, G. T., 1914, “A further study of relationships with Indian monsoon rainfall”, II, Mem. India Meteorol. Dept., 23, 123-129.

Walker, G. T., 1923, “Correlation in seasonal variations of weather”, VIII, A preliminary study of world weather, Mem. India Meteorol. Dept., 24, 75-131.

Walker, G. T., 1924, “Correlation in seasonal variations of weather”, IV, A further study of world weather, Mem. India Meteorol. Dept., 24, 275-332.

WCRP, 1992, ”Simulation of interannual and intraseasonal monsoon variability” WMO/TD-No. 470, 185pp.

WCRP, 1993, ” Simulation and prediction of monsoons: Recent results”, WMO/TD-No. 546, 73pp.

Webster, P. J., Magana, V. O., Palmer, T. N., Shukla, J., Tomas, R. A., Yanai, M. and Yasunari, T., 1998, Monsoons: Processes, Predictability, and the prospects for prediction, J. Geophys. Res., 103, 14451-14510.

Wilks, D. S., 1995, “Statistical Methods in the Atmospheric Sciences”, Academic Press, 467pp.

Table 11.1: All India monthly and seasonal rainfall anomalies observed during extreme southwest monsoon years for the period 1901-2009.

Excess Monsoon Rainfall Years						Deficient Monsoon Rainfall Years					
Years	Jun	Jul	Aug	Sep	JJAS	Years	Jun	Jul	Aug	Sep	JJAS
1914	1.1	23.9	-4.3	17.6	10.4	1901	-29.9	-16.7	11	-28.4	-13.1
1916	34.3	-5.7	20.6	14.9	13.2	1904	2.8	-7.7	-17.4	-23.8	-11.8
1917	37.8	-4.2	17	64.5	22.9	1905	-43.6	-12.3	-21.2	3.2	-17.4
1933	29	-5.2	23.2	25	15.1	1911	21.7	-45.9	-16.4	7.9	-14.7
1942	3.6	19.2	16.3	10.4	13.8	1918	13.5	-47.1	-11.4	-42.1	-24.9
1955	9.6	-15.4	24.9	32.7	10.1	1920	-5.6	0.6	-32.5	-33.3	-16.8
1956	27.4	22.5	3.7	0.6	13.6	1941	-2.6	-19.8	-10.5	-16.2	-13.3
1959	-3.7	23	3.1	33	14.3	1951	-13.6	-18.9	-12.1	-32.9	-18.7
1961	10.7	18.4	15.6	48.8	21.8	1965	-33.3	-4.8	-22.7	-20.8	-18.2
1970	30.7	-16	26	23.2	12.2	1966	3.6	-15.9	-18.8	-15.4	-13.2
1975	4.9	6	21	32.2	15.2	1968	-12.5	5.1	-17.3	-24.5	-10.3
1983	-6.8	-4.3	23.8	43.5	13	1972	-26.7	-31.2	-14.1	-23.6	-23.9
1988	6.8	26.6	14.9	24.6	19.3	1974	-25.6	-4.4	-5.3	-21.8	-12
1994	29	20.8	12.7	-17.1	10.0	1979	-15.5	-16	-18.5	-27.6	-19
There were 13 Excess monsoon years and 20 deficient monsoon years during the period 1901-2009. A year is said to be excess (deficient) monsoon year when the all India seasonal rainfall departure is more than 10% (less than -10%).						1982	-16.8	-23.1	8.9	-32.2	-14.5
						1986	10.8	-14.2	-12.7	-31.2	-12.7
						1987	-21.6	-28.8	-3.7	-25.1	-19.4
						2002	9.4	-54.2	-1.7	-12.9	-19.2
						2004	-0.8	-19.9	-4.3	-30	-13.8
						2009	-47.2	-4.3	-26.5	-20.2	-21.8

Table 11.2: List of Parameters used in the operational 16 parameter parametric & PR models between 2000 & 2002

Parameter No.	Parameters (Monthly Period)
X_1	50 hPa East-West Ridge (January + February)
X_2	Darwin Pressure Tendency (April-January) (500 hPa Ridge Position (April)*
X_3	South Indian Ocean SST (February +March) (Darwin 09 hrs Pressure (Spring))*
X_4	East Coast Minimum Temperature (March)
X_5	Arabian Sea SST (January + February) (Northern India Minimum Temperature (March))*
X_6	Central India Temperature (May)
X_7	N. H. Temperature (January +February)
X_8	N. H. Pressure (January to April)
X_9	Southern Oscillation Index (SOI) (March to May)
X_{10}	Indian Ocean Equatorial Pressure (January to May)
X_{11}	Himalayan Snow Cover (January to March)
X_{12}	Eurasian Snow Cover (December)
X_{13}	Europe Pressure Gradient (January) (10 hPa Zonal Wind over Balboa (January))*
X_{14}	El Nino (Same Year)
X_{15}	El Nino (Previous Year)
X_{16}	Argentina Spring Pressure

*Parameters which were replaced from the old 16 parameters list

Table 11.3: List of 10 parameters used for developing new LRF models

S.No	Parameter	Period of Data	C.C. with ISMR
1	Arabian Sea Surface Temperature	January+ February	0.55
2	Eurasian Snow Cover	December	-0.46
3	NW Europe Temperature	January	0.45
4	Nino 3 SST Anomaly (Previous Year)	July to Sept	0.42
5	South Indian ocean SST Index	March	0.47
6	East Asian Pressure	February + March	0.61
7	50 hPa Wind Pattern	January +February	-0.50
8	Europe Pressure Gradient	January	0.42
9	South Indian Ocean Zonal wind at 850 hPa	June	-0.45
10	Nino 3.4 SST Tendency	AMJ - JFM	-0.46

Table 11. 4: Comparison of the performance of 16-, 8- and 10-Parameter models (Error = Actual Rainfall – Forecast)

Year	16-Parameter Model	8-Parameter Model	10-Parameter Model
1996	+7	+3	+3
1997	+10	-1	+1
1998	+6	-6	-3
1999	-12	-6	-7
2000	-7	1	0
2001	-7	0	0
2002	-20	-18	-15

Table 11.5: Hindcast probability of drought indicated by the LDA Model

Year	Probability (%)	
	8-Parameter LDA Model	10-Parameter LDA Model
1965	92	96
1966	91	78
1972	89	99
1974	77	66
1979	97	99
1982	79	89
1986	51	55
1987	96	99
2002	20	4

Table 11.6: Details of the 8 predictors used for the new ensemble forecast system

S.No	Predictor	Used for forecasts in	Correlation Coefficient (1971-2000)
1	NW Europe Land Surface Air Temperature (P1)	April	-0.51
2	Equatorial Pacific Warm Water Volume (P2)	April	0.43
3	North Atlantic Sea Surface Temperature (P3)	April and June	0.36
4	Equatorial SE Indian Ocean Sea Surface Temperature (P4)	April and June	0.59
5	East Asia Mean Sea Level Pressure (P5)	April and June	-0.31
6	Central Pacific (Nino 3.4) Sea Surface Temp.Tendency (P6)	June	-0.49
7	North Atlantic Mean Sea Level Pressure (P7)	June	-0.46
8	North Central Pacific wind at 1.5 Km above sea level (P8)	June	-0.44

Table 11.7: A comparison of the performance of forecasts for the seasonal rainfall by MR models for NW India, NE India, Central India and South Peninsula

YEAR	NWI		NEI		CI		SPNI	
	ACTUAL	FORECAST	ACTUAL	FORECAST	ACTUAL	FORECAST	ACTUAL	FORECAST
2001	91.2	90.5	89.3	95.8	95.1	103.8	90.0	98.9
2002	73.9	87.5	93.3	90.6	83.1	98.3	67.5	94.8
2003	107.8	104.9	96.0	100.1	108.3	95.6	88.5	97.7
2004	78.0	80.6	94.0	98.0	89.0	97.1	85.0	93.1
2005	90.0	103.2	80.0	98.9	110.0	99.9	112.0	114.0
2006	94.0	92.3	83.0	97.5	116.0	95.9	95.0	95.7
2007	85.0	93.7	104.0	103.9	108.0	106.8	126.0	109.0
2008	105.0	101.5	97.0	100.6	96.0	108.1	96.0	102.3
RMSE (2001-2008):	**7.63**		**9.10**		**12.18**		**12.79**	

Table 11.8:
Performance of PCR model for July rainfall or the country as a whole for the last 8 years (2001-2008)

YEAR	ACTUAL	FORECAST
2001	95.2	101.6
2002	48.5	84.9
2003	106.5	98.0
2004	81.0	90.3
2005	114.7	103.7
2006	98.0	97.2
2007	97.6	93.6
2008	83.0	93.5
RMSE (2001-2008)		**14.9**

Table 11.9:
Performance of PCR model for August rainfall for the country as a whole for the last 8 years (2001-2008)

YEAR	ACTUAL	FORECAST
2001	80.5	91.83
2002	98.3	97.16
2003	95.5	108.25
2004	95.7	95.25
2005	71.6	91.14
2006	109.2	95.22
2007	98.2	101.23
2008	101.4	98.67
RMSE(2001-2008)		**10.53**

Table 11.10: Details of 6 predictors used for the prediction of monsoon Onset over Kerala

No.	Name of Predictor	Temporal Domain	Geographical Domain	Correlation Coefficient (1975-2000)
1	Zonal Wind at 200hpa over Indonesian Region	16th to 30th April	5S-5N, 90E-120E	0.48
2	OLR Over South China Sea	16th to 30th April	5N-15N, 100E-120E	0.40
3	Pre-Monsoon Rainfall Peak Date	Pre-monsoon April-May	South Peninsula (8N-13N, 74E-78E)	0.48
4	Minimum Surface air Temperature over NW India	1st to 15th May	1. Deesa 2. Rajkot 3. Guna 4. Bikaner 5. Akola 6. Barmer	-0.37
5	Zonal Wind at 925hpa over Equatorial South Indian Ocean	1st -15th May	10S-0, 80E-100E	0.52
6	OLR Over Southwest Pacific	1st to 15th May	30S-20S, 145E-160E	-0.53

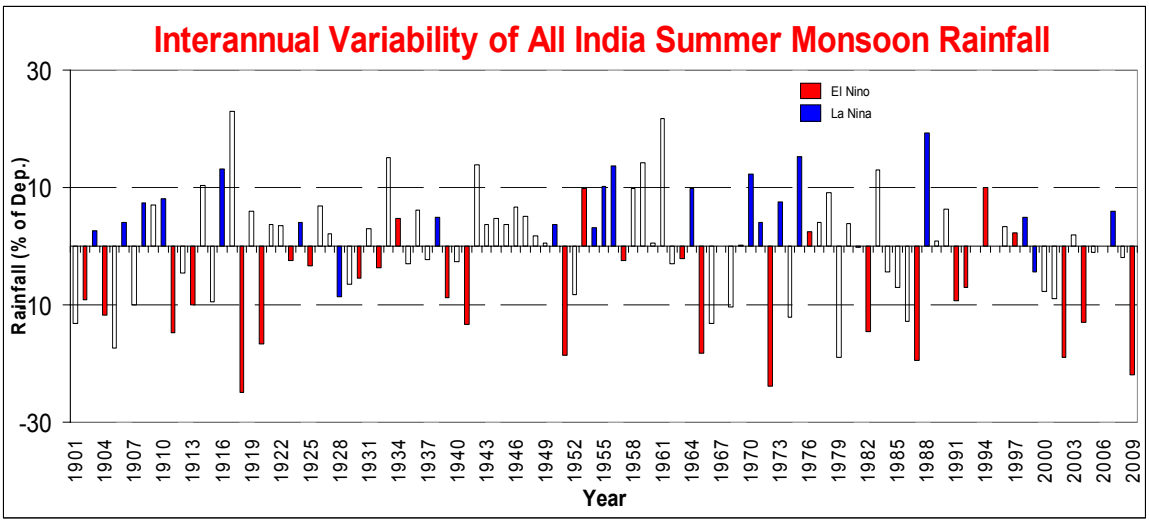

Fig.11.1a: Interannual variability of all India area weighted seasonal monsoon rainfall expressed as the percentage departures from long period average (LPA) for the period 1901-2009. The LPA for the period 1941-90 is 890 mm. The horizontal dashed lines correspond to the ± 10% departure or +/- one standard deviation. The red (blue) bars correspond to El Nino (La Nina) years.

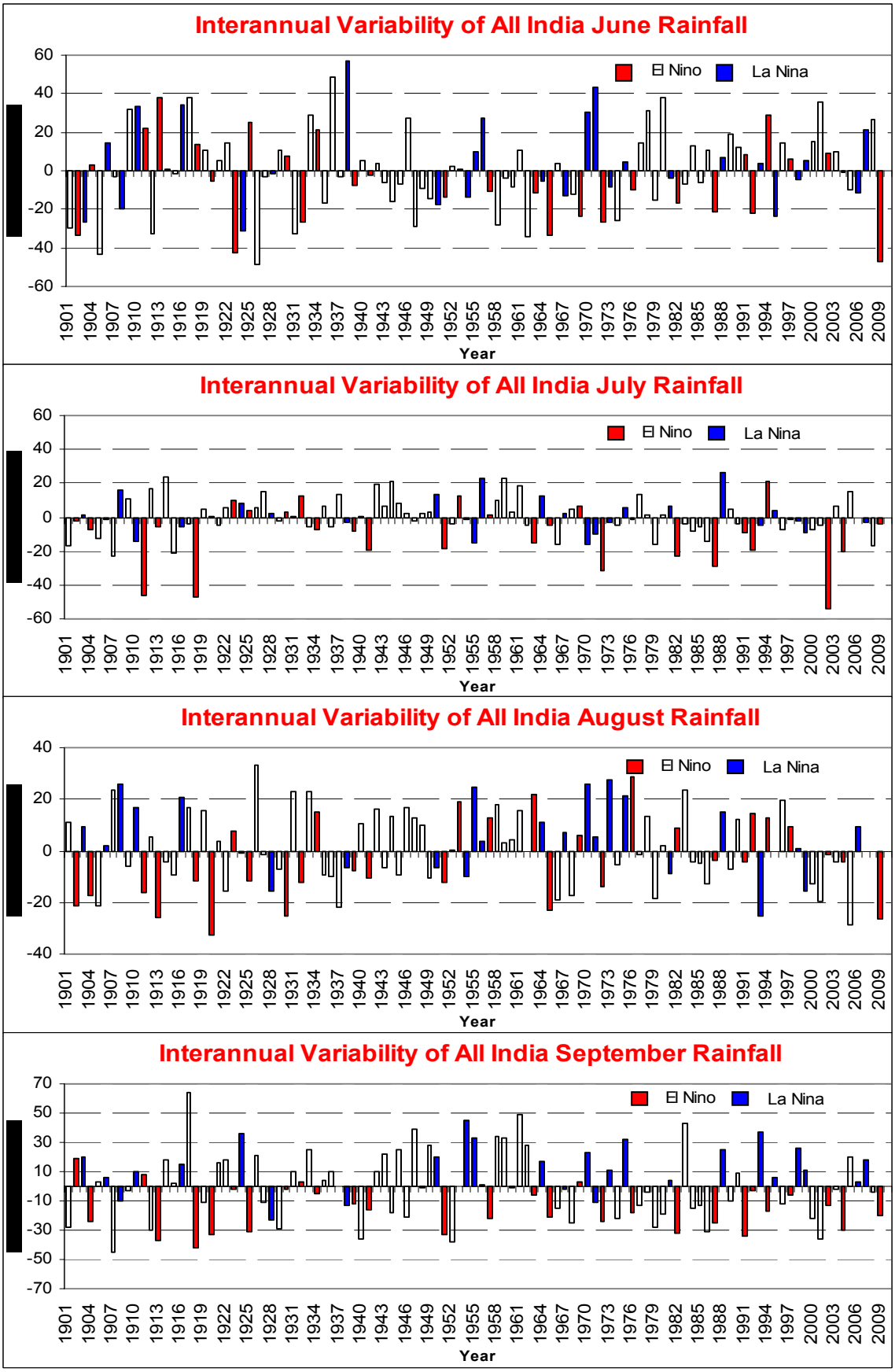

Fig.11.1b: The all India monsoon monthly rainfall percentage departure for the monsoon months (June, July, August and September) for the period 1901-2009.

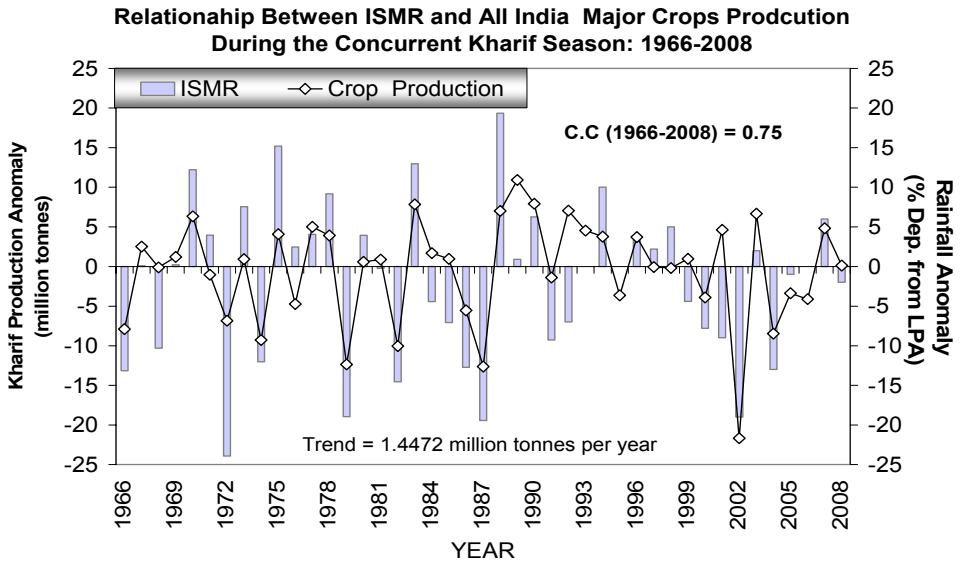

Fig.11.2a: Time series of all India summer monsoon season rainfall (ISMR) expressed in percentage departure and all India detrended production anomaly (in millions of tones) of major crops during the concurrent Kharif Season. .The time series was detrended before anomalies were computed using base period of 1971-2000. The correlations coefficient (C.C.) between the two time series computed for the entire data period (1966-2008) is 0.75.

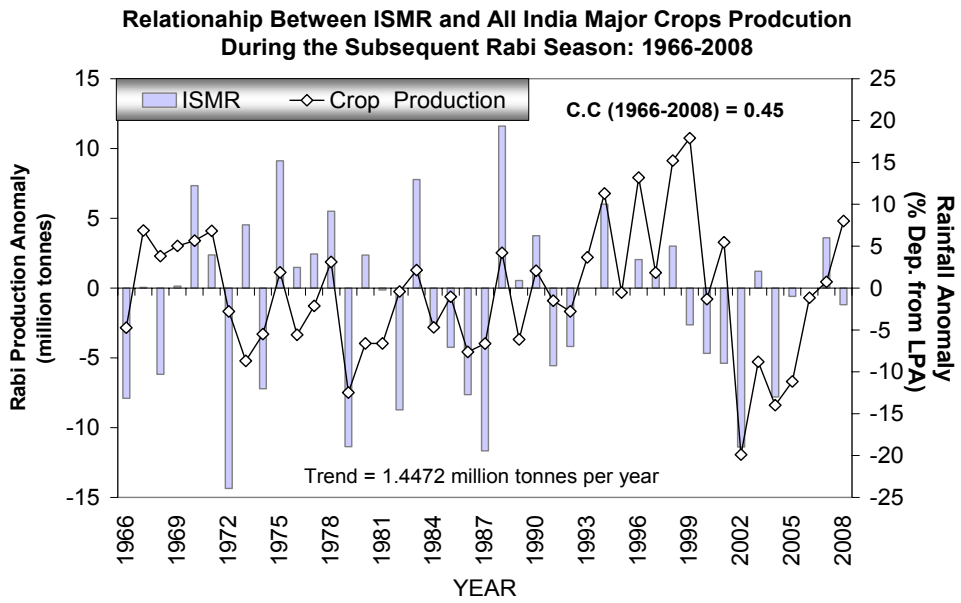

Fig.11.2b: Same as that for Fig.2a but for subsequent Rabi season. The C.C between the time series of ISMR and Rabi crop production anomalies for the period 1966-2008 is 0.45.

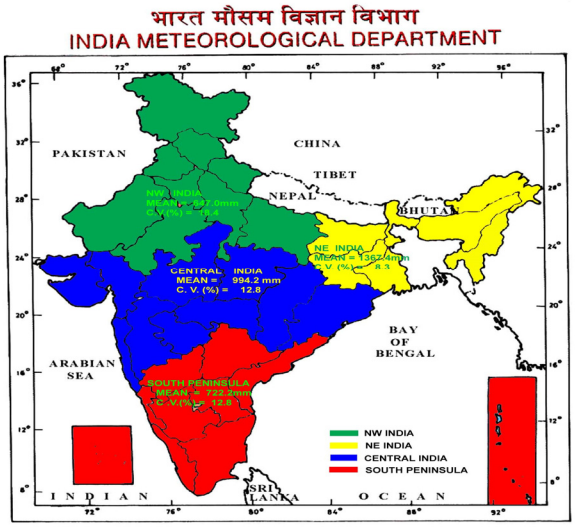

Fig.11.3: The four geographical regions of India.

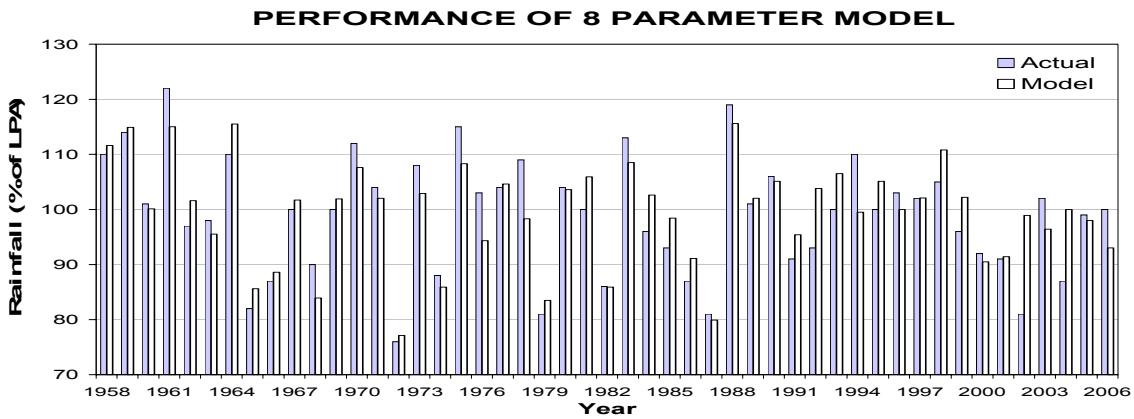

Fig.11.4: Performance of the 8 Parameter PR model for the forecasting of seasonal rainfall over the county as a whole.

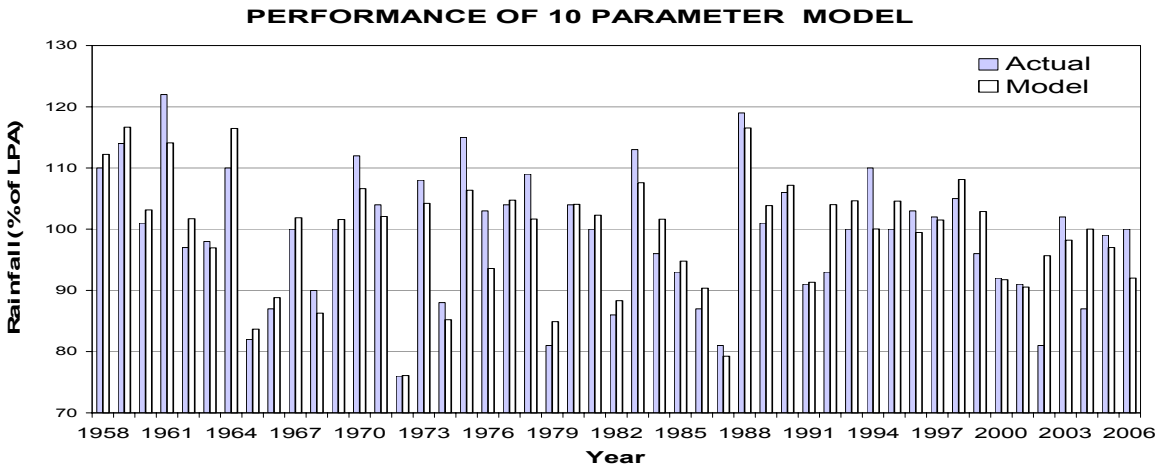

Fig.11.5: Performance of the 8 Parameter PR model for the forecasting of seasonal rainfall over the county as a whole.

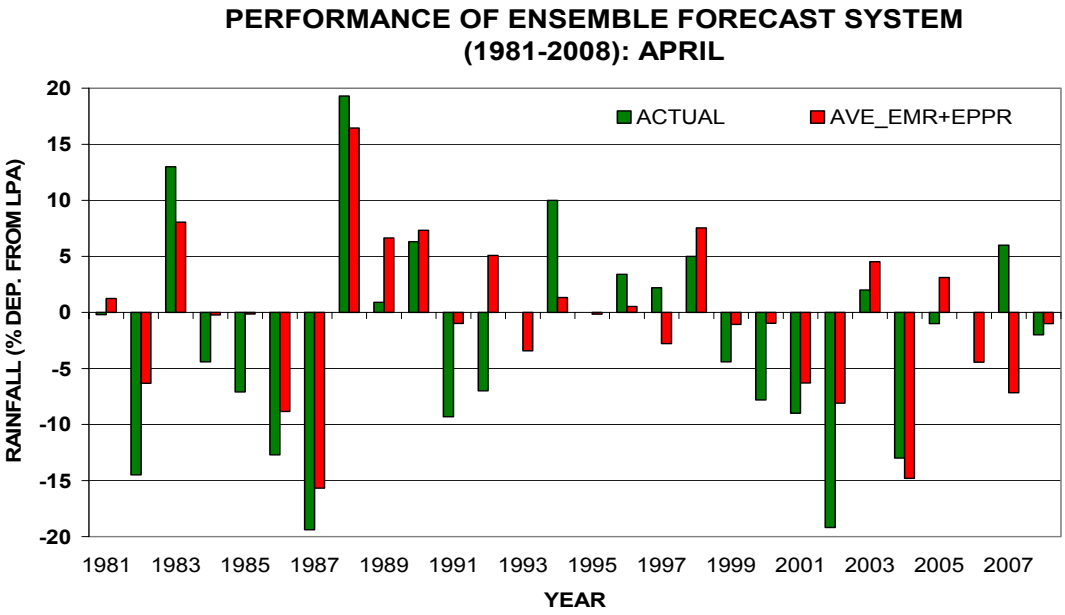

Fig.11.6: Performance of the ensemble forecast system for the April forecast of the seasonal rainfall over the country as a whole.

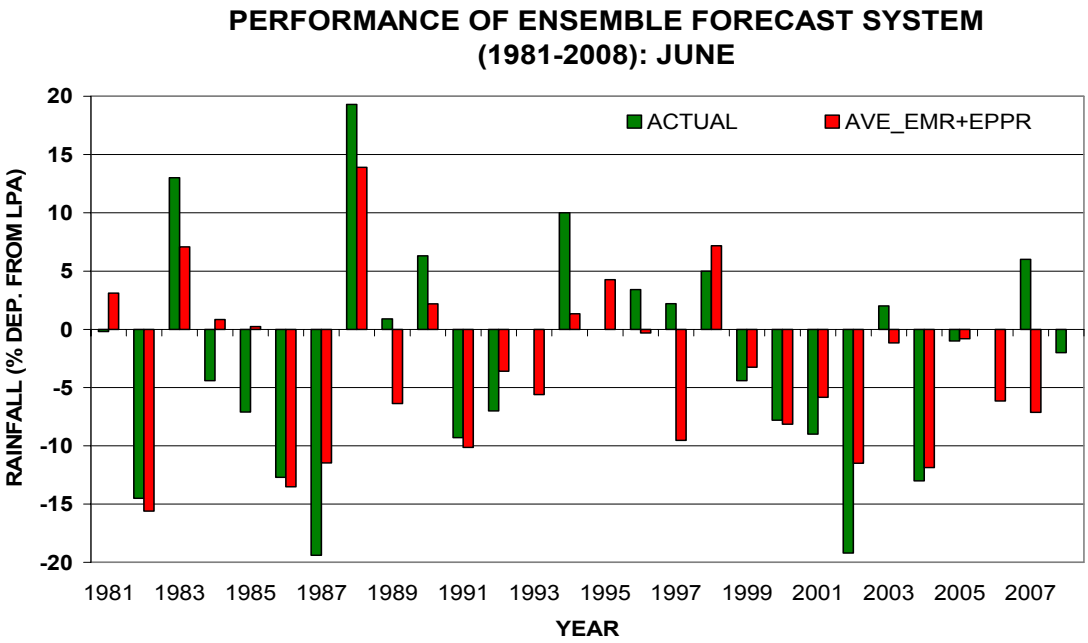

Fig.11.7: Performance of the ensemble forecast system for the June forecast of the seasonal rainfall over the country as a whole.

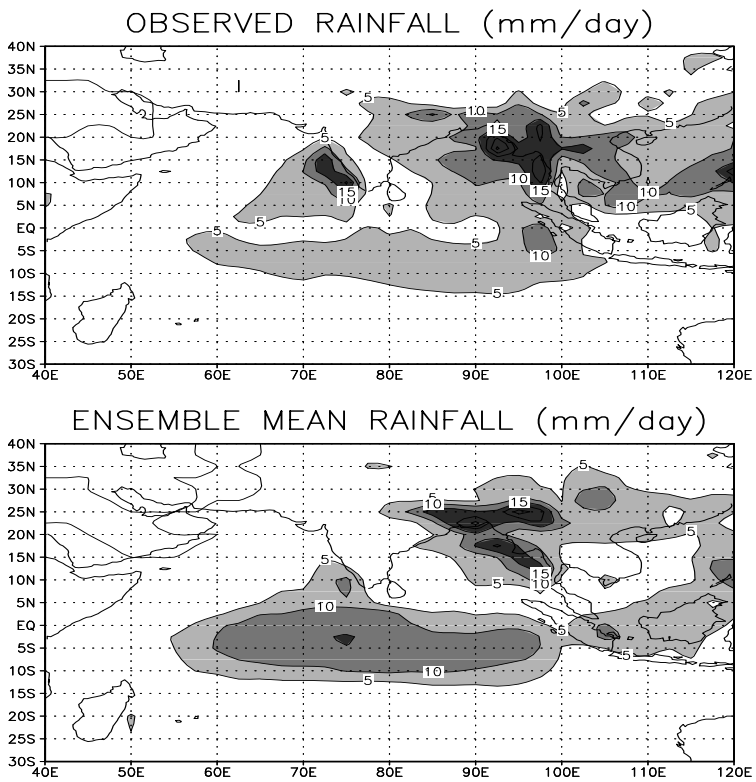

Fig.11.8: Comparison between Observed (ECMWF analysis) and PROVOST ensemble mean forecast of monsoon (JJAS) rainfall. The mean was computed over the period 1979-93. Contour interval is 5mm/day.

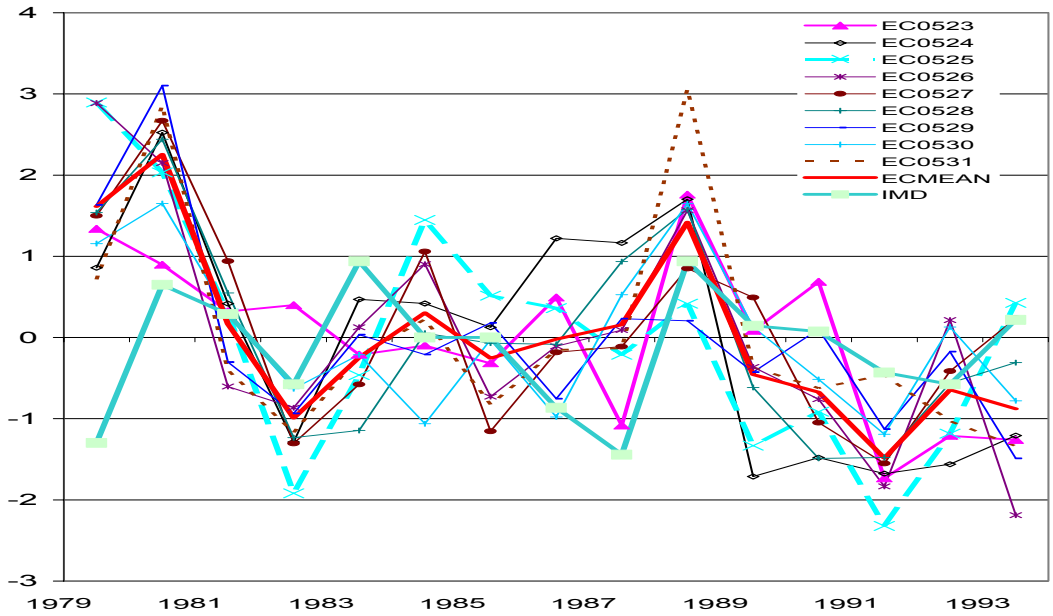

Fig.11.9: Interannual variation of PROVOST ensemble predictions of ISMR anomaly (mm/day) for the period 1979-93. In addition to Individual ensemble member predictions, the ensemble mean and observed (IMD) ISMR anomalies are also shown.

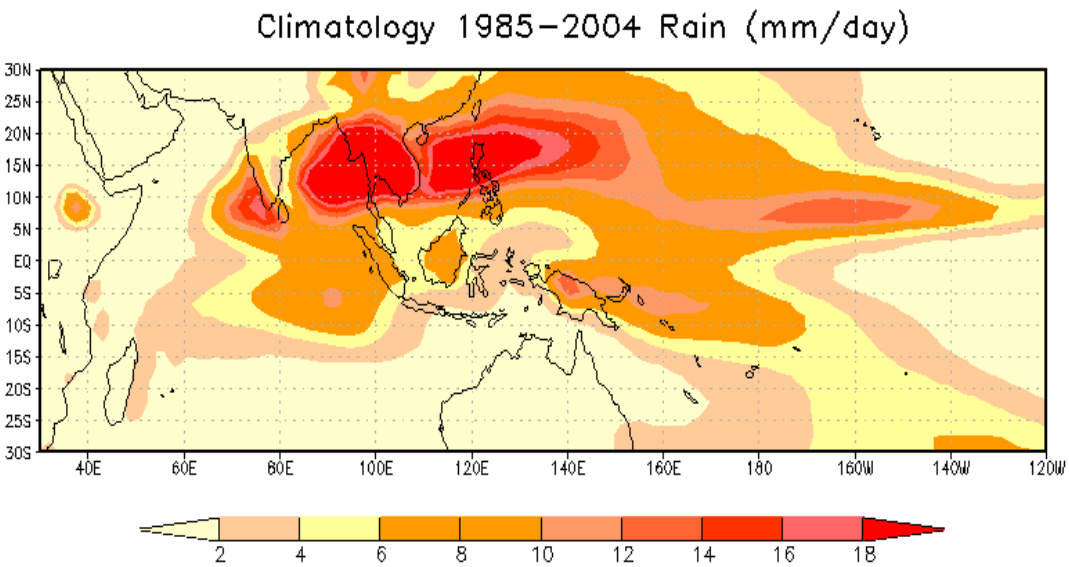

Fig.11.10: Rainfall Climatology (JJAS) of SFM during the hindcast period (1985 – 2004)

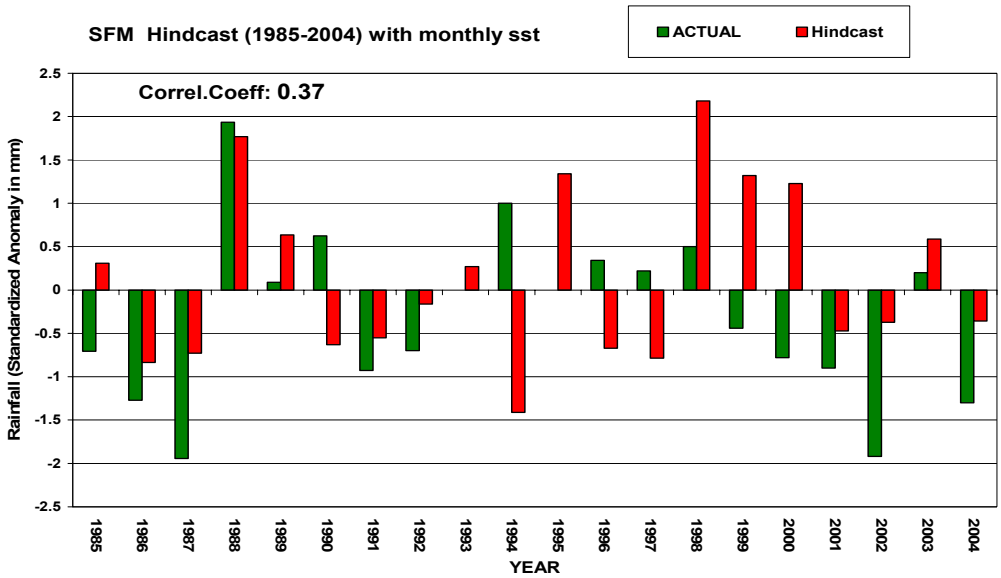

Fig.11.11: Year to year variation of standardized rainfall anomaly over Indian region for the period 1985-2004 derived from SFM global hindcast output.

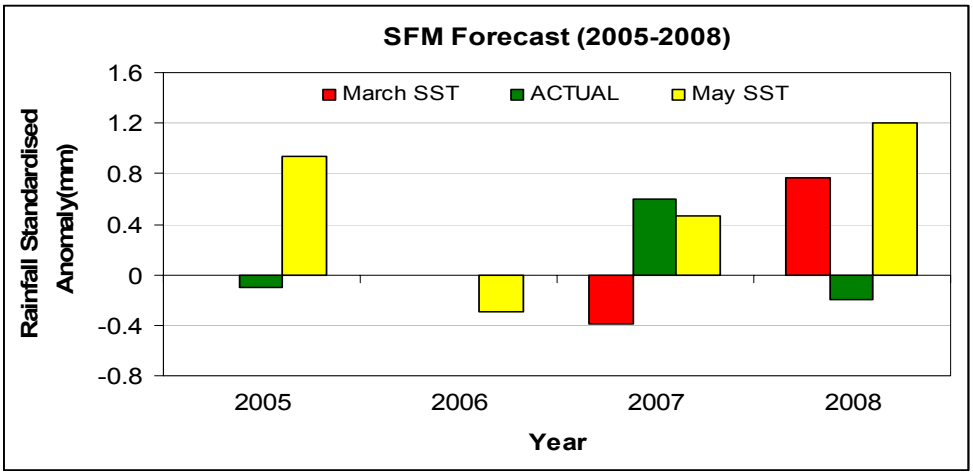

Fig.11.12: Year to year variation of standardized rainfall anomaly over Indian region for the period forecast period of 2005-2009.

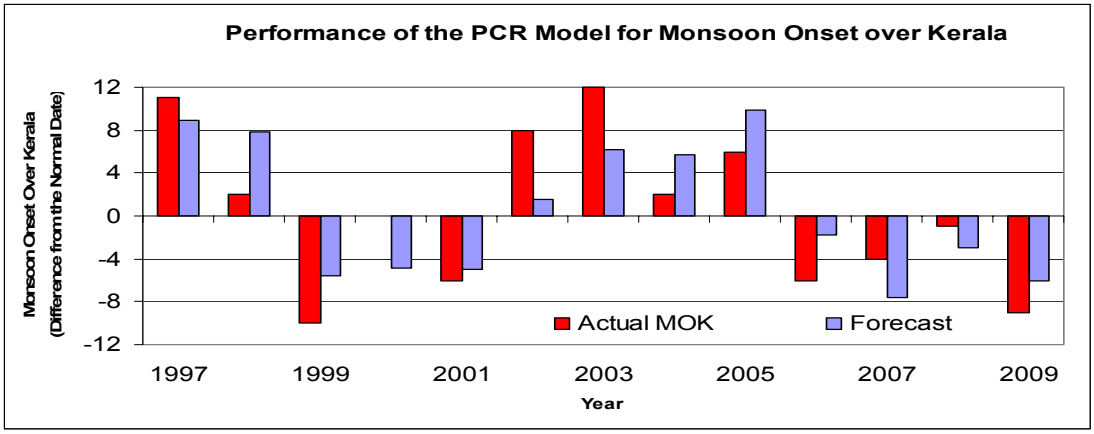

Fig.11.13: Actual dates of monsoon onset over Kerala and their predictions from the PCR model for the period 1997 to 2009.

CHAPTER 12

MONSOON ASPECTS RELATED TO CLIMATE CHANGE

R. H. Kripalani [1] and Ashwini Kulkarni
[1]*Centre for Advanced Training in Earth System Sciences and Climate, Indian Institute of Tropical Meteorology, Pune*

krip@tropmetres.in

12.1. Introduction

The Inter-governmental Panel on Climate Change Fourth Assessment Report (IPCC AR4) has categorically established that global concentrations of CO_2 have increased markedly as a result of human activities since 1750 and now exceed the pre-industrial values. The global increase in CO_2 concentration is due primarily to fossil fuel and land-use change. Global atmospheric CO_2 has increased from pre-industrial value of about 280 ppm to 379 ppm in 2005. Most of the observed increase in globally averaged temperature since mid-20th century is very likely due to observed increase in anthropogenic greenhouse gas concentrations. Thus the warmth of the last half century is unusual in at least the previous 1300 years. The warming of the climate system has been termed "unequivocal" as is evident from observations of increases in global average air and ocean temperatures, widespread melting of snow and ice and rising global average sea level (Solomon et.al. 2007; Meehl et.al. 2007b). Under such a scenario, it becomes imperative to examine the possible impacts of global warming on the Indian summer monsoon and its variability.

In the tropical continents, the largest portion of rainfall during the year is provided by the summer monsoon, occurring as a seasonal reversal of the mean circulation in response to the land-sea thermal contrast. Over South Asia, the summer is dominated by the southwest monsoon which spans 4 months from June through

September. The behavior and changes in monsoon precipitation play a vital role in the agricultural and economic progress of this region. The South Asian region with high human population and monsoon-related economies could be highly vulnerable to changes in monsoon precipitation. Hence the variation in seasonal monsoon rainfall may be considered one of the measures to examine climate change in the context of global warming, even though several indices have been recently reported.

The IPCC AR4 experiments provided outputs of the 25 coupled ocean-atmosphere models to any interested international scientist (Meehl et.al. 2007a). These outputs consisted of the model simulations for the 20th century (designated as 20c3m experiments) for the period 1850-2000. Projections were available for the period 2000-2300 depending on the model. These projections were provided for several scenarios (Nakicenovic et.al. 2000). The future projections of the Indian summer monsoon under the 1% per year CO_2 increase compounded to doubling until year 70 have been reported (Kripalani et.al. 2007a). Such projections of the East Asia summer monsoon are also reported (Kripalani et.al. 2007b). Finally projections of the Indian monsoon for the 21st century under each of the SRES B1, A1B and A2 scenarios for individual models are available in Sabade et.al. (2011). These studies project an increase in precipitation of about 8% over South Asia and 10 % over East Asia. The increase over South Asia could be due to the intensification of heat low dipole snow configuration and increase in atmospheric water vapour, while the increase over East Asia could be due to the intensification of the North Pacific sub-tropical High and Meiyu Changma Baiu front. Here we will present the simulations and projections based on multi-model ensemble (MME) of selected 10 models and average of the 3 mentioned scenarios.

The IPCC AR4 data sets are now designated as WCRP CMIP3 (World Climate Research Program Coupled Model Inter-comparison Project: Phase 3) data sets (Meehl et.al. 2007a). More details on these data sets are available in the above cited publications and in the text to follow.

This Chapter consists of several sections. In section 12.2, details of the data sets used are provided. Section 12.3 describes the observed changes during the 20th century (1901-2000) which have been documented in several recent publications. This covers the observed changes in precipitation, temperature, cyclonic disturbances, active-break spells, intra-seasonal, inter-annual and decadal monsoon variability. Changes in tele-connections are also described. Future projections based on the coupled climate models are covered in section 12.4. This will cover projected changes in seasonal monsoon rainfall, annual cycle and its variability on intra-seasonal to decadal time-scales. Possible physical processes / mechanism responsible for the projected changes are described in Section 12.5. This will cover possible changes in the heat low over northwest India, Eurasian snow cover, ENSO (El Nino Southern Oscillation) - Monsoon connections, changes in Monsoon, Hadley and Walker circulations and finally atmospheric water vapour. Besides greenhouse gases, aerosols could also play a dominant role in future monsoon changes. The impacts of aerosols are discussed in section 12.6. Some important results based on recent publications are discussed in section 12.7. Finally section 12.8 provides a summary of this chapter.

12.2. DATA

(i) The time series of Indian Monsoon Rainfall (IMR: June through September) has been downloaded from the website (www.tropmet.res.in) of the Indian Institute of Tropical Meteorology (IITM) for the 1871-2010 period. This time series has been generated by area-weighting the rainfall at 306 stations well distributed rain-gauges across the country. The original station rainfall data are obtained from the India Meteorological Department. The quality of this data set is very good and it is one of the most reliable long series of data going back to 1871. The mean IMR is 847.7 mm with a standard deviation of 82.6 mm based on data for the period 1871-2010. The variation of this series has been widely studied and can be considered as a measure to represent the intensity of the southwest monsoon.

(ii) The simulated data for the 25 coupled climate models (Table 12.1) available under IPCC AR4 has been downloaded from the website http://www-pcmdi.llnl.gov/ipcc/. Simulations for the 20th century runs (acronym “20c3m”) for the period 1850 to 2000 and

projections for the 21st century under the SRES A1B, A2 and B1 scenarios for the period 2001-2100 have been used. The monthly data for precipitation-flux, sea level pressure, surface vector winds, snowfall-flux, sea surface temperature, velocity potential and atmospheric water vapor are used. The coupled climate models along with a few details are shown in Table 12.1. Each model is identified by an abbreviated acronym. More details on the model characteristics are available in Kripalani et.al. (2007a, b) and in the PCMDI website.

(iii) The model datasets are compared to NCEP-NCAR (National Center for Environmental Prediction-National Center for Atmospheric Research) data (Kalnay et.al. 1996).

(iv) Simulated spatial precipitation patterns are compared with the CMAP (Climate Prediction Center Merged Analysis of Precipitation) data (Xie and Arkin 1997)

(v) Monthly indices for the NINO3.4 (5^0N-5^0S, 170^0W-120^0W) SST anomalies for the 1901-2007 have been downloaded from the site http://badc.nerc.ac.uk/data/hadisst.

Before the above data sets are used to examine the projections, the observed changes during the 20th century, based on recent publications are first presented.

12.3. Observed changes during the Twentieth century

12.3.1. Extremes in precipitation

Goswami et.al. (2006a) have shown significant rising trends in the frequency and the magnitude of extreme rain events and a significant decreasing trend in the frequency of moderate events over central India during the monsoon seasons based on high resolution gridded rainfall data (Rajeevan et.al. 2006) for the period 1951-2000. They further note that the seasonal mean rainfall does not show a significant trend, because the contribution from the increasing heavy events is offset by the decreasing moderate events. They expect a substantial increase in hazards related to heavy rain over central India in the future. However, a study by Nandargi and Dhar (2008) does not support the increasing trend in extreme rainfall events in a warming environment over the Indian region during the recent decades. They note a decadal variability of severe rainstorms of India based on 1891-2006 data, with increasing trend from 1891-1900

through 1961-1970 and thereafter a decreasing trend with minimum during the 2001-2006 periods. They further note that frequencies of such events of heavy rainfall have very rarely been occurring in India during the present times.

While an increasing trend in rainfall is shown over regions with fast industrial growth, a decreasing trend in tropical rainfall is shown over high mountain ranges influenced by intense deforestation (Hingane 1996). Krishnamurthy et.al. (2009) also report statistically significant increasing trends in extremes of rainfall over many parts of India, using the high resolution rainfall data for the 1951-2000 period, consistent with the indications from climate change models and the hypothesis, that the hydrological cycle will intensify as the planet warms. Rajeevan et.al. (2008) using data for 1901-2004 also find increasing trends (after accounting for inter-decadal variations in the extreme events) in both heavy and very heavy rainfall events. They further find that the frequency of extreme rainfall events shows significant inter-annual and inter-decadal variability in addition to a statistically long-term trend of 6% per decade. Their detailed analysis shows that inter-annual, inter-decadal and long-term trends of extreme rainfall events are modulated by the sea surface temperature (SST) variation over the tropical Indian Ocean (IO), supporting the hypotheses that the increasing trend of extreme rainfall events in the last 5 decades could be associated with the increasing trend of SSTs and surface heat flux over the tropical IO. In the global warming scenario, the coherent relationship between IO SST and extreme rainfall events suggests an increase in the risk of major floods over central India. Using data for the period 1901-2003, Guhathakurta and Rajeevan (2008) examined trends in the rainfall patterns over India. While some meteorological sub-divisions showed decreasing trends, some others showed increasing trends.

Alexander et al (2006) examined several precipitation indices and noted a tendency towards wetter conditions throughout the 20th century, but all did not show statistically significant changes. Dash et al (2009) showed that the frequencies of moderate and low rain days have significantly decreased over the entire country in the last half century. On the basis of the duration of rain events they inferred that long spells

show a significant decreasing trend over India as a whole, while short and dry spells indicate significant increasing tendency.

In summary, most of the above studies document an increasing trend in heavy rain events and a decrease in moderate and low rain events during the second half of the 20th century and have been reported in the IPCC AR4 (Trenberth et.al. 2007). Inter-decadal variability in the frequency of extreme rain events has also been reported.

12.3.2. Extremes in temperature

Indian annual mean, maximum and minimum temperatures have shown significant warming trends during 1901-2007. However, accelerated warming has been observed in the recent 1971-2007 period, mainly due to intense warming in the recent decade 1998-2007. After mid-1990s, night time temperatures have started increasing at twice the rate of day time temperatures resulting in 6 of the 10 warmest years on record (Kothawale and Rupa Kumar 2005; Padma Kumari, et.al. 2007; Kothawale et.al. 2010a). Significant influence of ENSO events have also been noted in these trends (Kothawale, et.al. 2010a). Further analysis of data for the period 1970-2005 have shown that the frequency of hot days and hot nights indicate widespread increasing trend, while that of cold days and cold nights a widespread decreasing trend (Kothawale, et.al. 2010b).

Alexander, et.al. (2006) showed a significant decrease in the annual occurrence of cold nights and a significant increase in the annual occurrence of warm nights using data for the 1951-2003 period, implying a positive shift in the distribution of daily minimum temperature throughout the globe. Bawiskar (2009) reported a weakening of the lower troposphere temperature gradient between the Indian landmass and the neighboring oceans. He conjectured that the rate of warming over the oceans is more than that over the land, resulting in a weak temperature gradient and a hindrance to the monsoon performance. Hingane (1996) has shown an increasing trend in surface air temperature over regions where fast industrial growth has been in progress for several

decades. Frequency of severe heat waves and also the duration of heat wave spells have increased during the last decade (Bhadran et.al. 2005).

In summary, temperatures have been increasing over the Indian subcontinent during the recent decades as reported in IPCC AR4 also (Solomon et.al. 2007).

12.3.3. Cyclonic Disturbances

Recent studies document a significant decreasing trend in the cyclonic disturbances over the Bay of Bengal and the north Indian Ocean (Singh 2001; Mandke and Bhide 2003; Dash et.al. 2004; Guhathakurta and Rajeevan 2008; Jadhav and Munot 2009). However, a significant increase in the frequency and duration of low-pressure areas during the monsoon season for the recent decades has been reported (Jadhav and Munot 2009). These may be related with the weakening of monsoon circulation over the Indian sub-continent as discussed subsequently.

12.3.4. Active and Break spells

Rajeevan et.al. (2006, 2010) find that breaks tend to have a longer life-span than the active spells based on data for the period 1951-2007. While almost 80% of the active spells lasted for 3-4 days, only 40% of the break spells lasted for such a short duration. Furthermore, active events occurred every year, not a single break occurred in 26% of the years considered. However, no significant trends in either the days of active or break events were noted (Rajeevan et.al. 2010).

The deterministic and potential predictability of monsoon over the Indian region has been recently examined. While deterministic predictability is based on observed slowly varying bounding condition such as SSTs potential predictability is the extent to which the future state can be reliably predicted by ideal models. Using a nonlinear dynamical technique on gridded rainfall data over India for a 104 year period (1901-2004), Mani et al (2009) have shown that the deterministic predictability of monsoon

weather over central India in the latest quarter has indeed decreased significantly compared to that of the earlier three quarters. However, using the same 104-year data, Neena and Goswami (2010), find that the potential predictability of both active and break spells have undergone a rapid increase during the recent three decades. The potential predictability of active spells has shown an increase from one week to two weeks, while that for the break spells increased from two weeks to three weeks.

12.3.5. Intra-seasonal monsoon variability

The Indian summer monsoon is characterized by rather abrupt onset at the southern tip (Kerala) during June followed by northward progression of the tropical convergence zone and the establishment of monsoon at the northern location. This progression is strongly linked to planning of agricultural activity and water resources management.

Three intra-seasonal oscillations also dominate: around 5-days associated with the oscillation of the monsoon trough over the Indo-Gangetic plains; the 10-20 days westward moving waves associated with the lows and depressions moving inland from the Bay of Bengal; and the northward moving 30-60 days mode associated with the cloud bands moving from the equatorial Indian Ocean region towards the northern parts of India. The northward moving mode is also designated as the 40-day oscillations. These intra-seasonal oscillations play a dominant role in the active-break cycles and as such could modulate the total seasonal summer monsoon rainfall over India (e.g. Kulkarni et.al. 2011 and references therein). In general the faster 10-20 days oscillations are dominant during the excess Indian monsoon, on the other hand the slower 30-60 days mode dominate during the deficient monsoons (e.g. Kripalani et.al. 2004 and references therein). Both these oscillations have weakened amplitudes after the mid-1970s (Kulkarni et.al. 2009). Suhas and Goswami (2010) also note a decreasing trend of significant MJO power during the northern hemisphere winter, besides multi-decadal variations.

Goswami et.al. (2010) have shown that the northward propagation of the first episode of the intra-seasonal oscillation associated with the onset phase of the Indian summer monsoon has slowed down significantly during the past decade compared with the prior decades. Suhas and Goswami (2008) report a regime shift in the Indian summer monsoon climatological intra-seasonal oscillations. They find that while the dominant episode of northward propagation started in the beginning of July pre-1975, in contrast it starts in the beginning of June during post-1979 period. A climate shift has been reported around mid-1970s in several studies.

12.3.6. Inter-annual and decadal monsoon variability

The IMR series has been subjected to simple statistical techniques to investigate the variations on inter-annual and decadal time scales. The lag-1 autocorrelation (-0.09) based on 1871-2010 period is not significant suggesting that the rainfall series is free from the Markovian-type of persistence; however the negative value indicates some element of biennial tendency. The Mann-Kendall test (WMO, 1966) for trend, though negative, depicts no significant trend for the entire 1871-2010 period (trend value = -1.5), but a significant negative trend at 1% level if only the later half (1941-2010) of the period is considered (trend value = -2.58).

Fig.12.1 (green bars) shows the standardized rainfall time series depicting the inter-annual variability. While there appear to be year-to-year random fluctuations on the seasonal to century time scale, the most prominent variations on this time scale are between the so-called good monsoon seasons with above average rainfall and the poor monsoons with deficient rainfall. These can be inferred from Fig. 12.1.

The short-term decadal fluctuations have been examined by applying simple 11-, 21- and 31-year running means of the standardized values. The 21-year running means are super-imposed on the standardized values (Fig. 12.1: red line). The most striking features are the epochs of above and below normal rainfall. The IMR shows major turning points around 1895, 1930 and 1965, with above normal epochs during

1871-1895 and 1930-1965 consistent with earlier studies (e.g. see Kripalani et.al. 2003b and references therein), however the turning point around 1990 suggested by using data until 2001, no longer is discernable if the data for the recent decade (2001-2010) is also included. It is interesting to note that the IMR appears to be in the below normal epoch for the last nearly 5 decades.

Kucharski et.al. (2009) have shown that the increase of greenhouse gases in the 20th century has not significantly contributed to the observed decadal IMR variability, using a selection of control integrations from the WCRP CMIP3 data sets. Thus the decadal IMR variability is not reproduced in coupled ocean-atmosphere models forced with greenhouse gases and may be due to internal coupled variability involving decadal ENSO and AMO (Atlantic Multi-Decadal Oscillation) variability.

Dash et.al. (2007) analyzed rainfall amounts during different seasons over India. Their results indicate a decreasing tendency in the summer monsoon rainfall over the Indian landmass and increasing trend in the rainfall during pre-monsoon and post-monsoon months.

12.3.7. Tele-connections

The link between the Indian Monsoon and ENSO was first suggested by Sir Gilbert Walker more than a hundred years ago. In general, studies have shown that the warm phase (El Nino) is associated with the weakening of the Indian Monsoon with overall reduction in rainfall, while the cold phase (La Nina) is associated with strengthening of the Indian Monsoon with enhancement of rainfall. However, during the last decade several studies have documented a weakening of the ENSO-IMR relationship. Several observational / model simulated factors have been attributed to this weakening:

(a) Modulation by the decadal variability of monsoon rainfall (Kripalani and Kulkarni 1997a,b ; Krishnamurthy and Goswami 2000; Kripalani et.al. 2001)

(b) Chaotic nature of monsoon (Webster and Palmer 1997)

(c) Linkages with the Indian Ocean Dipole Mode (Saji et.al. 1999; Behera et.al. 1999; Webster et.al. 1999,; Ashok et.al. 2001)

(d)Atlantic Circulation (Chang et.al. 2001; Goswami et.al. 2006b) and

(e) Global Warming (Krishna Kumar et.al. 1999; Ashrit et.al. 2001)

While a weakening of the ENSO- Southwest monsoon has been reported, a strengthening relation between ENSO and northeast monsoon over South Asia has been reported (Kumar et.al. 2007).The projections of the ENSO-Monsoon connections will be examined in section 12.5.

12.4. Future Projections: Coupled Climate Model Simulations

Twenty-five modelling groups (Table 12.1) from leading international climate centers participated in the IPCC AR4 program and the model data were collected, archived and made available to the international climate community by the Program for Climate Model Diagnosis and Inter-comparison (PCMDI) at National Livermore Laboratory, USA. The models are forced with concentration of greenhouse gases and other constituents derived from various emission scenarios ranging from non-mitigation scenarios to idealized long-term scenarios (Nakicenovic et.al. 2000; Meehl et.al. 2007a). There are three experiments, also known as storylines B1 (low forcing i.e. CO_2 concentration of about 550 ppm by 2100), A1B (medium forcing, i.e. CO_2 concentration of about 700 ppm by 2100) and A2 (high forcing, i.e. CO_2 concentration about 820 ppm by 2100). Together, they describe divergent future that encompasses a significant portion of the underlying uncertainties in the main driving forces. They cover a wide range of key “future” characteristics such as population growth, economic development and technological change.

The confidence in climate model precipitation projections will depend on how well the models are able to simulate the 20th century (designated as ‘20c3m’ in the IPCC AR4 experiments) monsoon rainfall. Diagnostic studies indicate that the current coupled atmosphere-ocean GCMs capture the gross characteristics of climate over the monsoon region in terms of the mean annual cycle and the dominant modes of

variability. However, there are still significant biases in terms of the spatial patterns of monsoon rainfall over India (Kang et.al. 2002a,b, Kucharski et.al. 2009, Scaife et.al. 2009, Preethi et.al. 2010). Bollasina and Nigam (2009) also note that current models cannot provide durable insights on regional climate feedbacks nor credible projections of regional hydro-climatic variability and change. Notwithstanding, the various limitations of the climate models in realistically portraying the IMR and its variability, a preliminary idea of the possible future monsoon changes can be obtained for different expected concentration of radiatively active constituents of the atmosphere. Currently available model simulations under different socio-economic scenarios are useful tools for this purpose (Rupa Kumar et.al. 2002).

12.4.1. Mean IMR and CV

The performance of the models in simulating the inter-annual monsoon variability is judged with respect to the mean seasonal rainfall and the coefficient of variation (CV). A scatter plot of the mean IMR and the CV for the 25 models is shown in Fig. 12.2. The spread of the models suggests the diverse nature of the model simulations. The mean IMR varies from about 100 mm (models bcc, ips) to about 880 mm (models mim, mih, cnr). However the simulated model CV varies from about 3% (model gir) to nearly 22 % (model csr2). This figure clearly illustrates that one of the major cause of the uncertainties in future projections could be due to this diverse nature of model simulations.

Preethi et.al. (2010) examined hindcasts made by several European climate groups as part of the program called “Development of a European Multi-Model Ensemble System for seasonal-to-inter-annual prediction (DEMETER)”. It was found that the skills of the Indian monsoon rainfall prediction in these hindcasts were generally positive but very modest. In fact the model simulations of the Indian summer monsoon rainfall for the earlier period (1959-1979) were better than the recent period (1980-2001).

We select a set of 10 models (bcr, ccm, ccm2, cnr, ech, eco, inm, mih, mim and ukc) for further analysis. We will present the multi-model ensemble (MME) projections based on the average projections of these 10 selected models and also the average of the 'future' scenarios (B1+A1B+A2) i.e. the projections are based on the net average of all the 10 models plus the 3 scenarios. On the other hand the simulations are based on the average of the 10 models under the 20th century runs (20c3m). Hence in the text 'simulations' would mean the average of the 10 models under the 20c3m experiments, while 'projections' would mean average of the 10 models under the 3 scenarios. The model simulations are available for the 1850-2000 period. As recommended by the AR4 panel, the last 20 years (1981-2000) are used to derive the average characteristics. The projections are available for 100 to 300 years (2001-2300) depending on the model. Here we focus on the 21st century only (2001-2100), in particular during the two time slices, one during the middle of the 21st century or the near-term (2031-2050) and at the end of the 21st century or the long-term (2081-2100). Hence in the description to follow, simulations and projections based on individual models are not considered, but the MME of the models. This will to a certain extent reduce the uncertainty in the future projections.

12.4.2. Annual Cycles

Monthly average rainfall January through December in mm/month averaged over the grid points falling over the Indian land-mass is prepared. These are used to investigate the annual cycles simulated by the models. The CMAP average precipitation for each month depicting the observed annual cycle is shown in Fig.12.3 (black line). Over the course of the annual cycle the precipitation changes from less than 2 mm/day during the January-April period to about 7 mm/day during the peak summer monsoon period June through September. Thus the annual cycle is characterized by a sharp increase from April to June and thereafter a gradual decrease from September through December (3 mm/day). An examination of the model simulated cycle (Fig.12.3 red line) shows that the shape is reasonably well simulated; however the models over-estimate the summer monsoon rainfall and under-estimate the rain pre- and post-monsoon

seasons. The projected annual cycles for the near term (2031-2050; green line) and long-term (2081-2100; purple line) are superimposed on the observed and the simulated annual cycles. Projections reveal a sharp increase of precipitation during the summer monsoon period during the near and long term, in particular during the long-term.

12.4.3. Inter-annual and decadal variability

A time series of the summer monsoon (June through September) rainfall over the same land points falling over the Indian region is prepared for all the available years. Fig. 12.4 depicts the simulated inter-annual variability of the IMR for the 1901-2000 period (green line) and the projected series for the 2001-2100 period (red line). The 21-year running means are superimposed on the inter-annual variability (black line). It is observed that the simulated 20th century series appear to be highly random with no long-term trends, however the time series under climate change scenarios do exhibit significant long-term increasing trend. The rainfall is projected to increase by about 10 % at the end of the century (from approximately 750 mm at the end of the 20th century to approximately 825 mm at the end of the 21st century). The IPCC AR4 also documents that summer precipitation is likely to increase. Furthermore, an increase in the frequency of intense precipitation events in parts of South Asia is very likely (Solomon et.al. 2007; Meehl et.al. 2007; Christensen et.al. 2007).

12.4.4. Spatial patterns

The simulation of the rainfall patterns over the Indian region has been proven to be difficult task due to its extremely complex spatial distribution and large precipitation gradients. This may pose difficulties in replicating the exact pattern with the correct amplitude. The major observed features of IMR are:

(i) primary continental rain belt extending from the Bay of Bengal across the Indo-Gangetic plains corresponding to the monsoon trough and the low pressure systems

(ii) secondary oceanic rain belt near the equatorial regions around 5^0 S

(iii) west coast rainfall maximum due to the western ghats orographic barrier

(iv) maximum rainfall over northeast India associated with the Himalayan orography

(v) low rainfall over northwest India and southeast peninsula.

The observed spatial pattern based on the CMAP data (Fig 12.5: CMAP panel) shows two belts of heavy rainfall, one along the west coast of India and the other over northeast India – Bay of Bengal region. Similarly two regions of low rainfall over northwest India and the southeast peninsula are also observed. A belt of heavy rainfall over the equatorial region can also be inferred. Though the pattern of precipitation is reasonably well captured by the model simulations (Fig 12.5: MME 20c3m panel), the precipitation is under-estimated over regions of heavy rainfall (west coast and the head Bay of Bengal) and over the central and northwestern parts of the country. On the other hand precipitation is over-estimated over regions of low rainfall i.e. southeast peninsula (Fig.12.5: Bias panel).

The failure of the models to simulate finer features i.e. steep gradients in monsoon precipitation with maximum along the west coast of India could be because of the coarse resolution of the models (see Table 12.1). A regional climate model PRECIS (Providing Regional Climates for Impact Studies) at a 50-km resolution have confirmed that significant improvements can be achieved in the representation of regional processes over South Asia (Rupa Kumar et.al. 2006).

The projected patterns during 2031-2050 and 2081-2100 (Fig.12.5: central panels) are similar to the simulated one (Fig 12.5: 20c3m panel). While no appreciable changes are noticed over the Bay of Bengal for the area occupied by heavy rainfall (1000-1200 mm isolines); over the Arabian Sea adjacent to the west coast the 1000 mm isoline expands during 2031-2050 and enlarges further during 2081-2100 (Fig.12.5: central panels), indicating that the models project an expansion of heavy rainfall area over the Arabian Sea and the adjoining areas than over the Bay of Bengal.

The projected changes during the 2031-2050 and 2081-2100 periods are shown in the lower panels in Fig.12.5. While an increase of 40-80 mm during 2031-2050 is

projected over the southern parts of India and the adjoining Arabian Sea, the changes over central parts of India adjoining east coast and Bay of Bengal vary from -20 mm to 20 mm. However increase of precipitation is projected over the entire country during 2081-2100 with maximum of 120-140 mm over the Arabian Sea and northeast India (an increase of 12 to 14 %). Thus regions receiving heavy rainfall (west coast and northeast India) are projected to receive heavier rainfall (rich getter richer mechanism – see section 12.7).

According to IPCC AR4, the precipitation associated with the Asian summer monsoon is projected to increase, as is the inter-annual variability of precipitation accumulated during the monsoon season. The nature of such projections of summer monsoon rainfall is, however, complicated by the uncertain role of aerosols, in particular of carbon aerosols (as will be seen in section 12.6).

12.4.5. Simulated changes in active-break spells and extreme precipitation events

Mandke et.al. (2007) examined the simulations of selected models under IPCC AR4 to study the implication of possible global climate change on the active / break spells of the Indian summer monsoon. The sensitivity to climate change was assessed from two experiments, namely, 1% per year CO_2 increase to doubling (quadrupling). They found that the changes in the daily mean cycle and the standard deviation of precipitation, frequency and duration of active / break spells in future climate are uncertain among the models. However, the break composites of precipitation anomalies strengthen and spread moderately (significantly) in the doubled (quadrupled) CO_2 experiments.

An assessment of possible future climate scenarios associated with greenhouse warming over South Asia for the 2041-2060 period deduced from HadRM2 (Hadley Center Regional Model) was presented by Rupa Kumar et.al.(2005). Their analysis indicates a decrease in the number of rainy days, but with increase in the intensity. Also

the extremes in both the daily maximum and minimum temperatures are expected to increase. PRECIS simulations under scenarios of increasing greenhouse gas concentrations and sulphate aerosols indicate marked increase in both rainfall and temperature towards the end of the 21st century. Extremes in maximum and minimum temperatures are also expected to increase into the future, but the night temperatures are expected to increase faster than the day temperatures.

Extreme precipitation shows substantial increases over a large area, particularly over the west coast of India and west central India (Rupa Kumar et.al. 2006). Krishna Kumar et.al. (2011) also note potential for a modest increase in seasonal mean monsoon rainfall with possible increase in frequency and intensity of heavy rain events. Stowasser et.al. (2009) examined future projections of the mean monsoon and synoptic systems in the GFDL (Geophysical Fluid Dynamic Laboratory) model simulations in which quadrupling of CO_2 concentrations were imposed. In a warmer climate, despite a weakened cross equatorial flow, the time-mean precipitation over peninsula parts of India increases by about 10-15%. They further note that based on the regional model solutions in a CO_2-rich climate an increase in the number of flood days over central India can be expected. Sun et.al. (2007) also analyzed for potential future changes in precipitation characteristics during the 21st century under SRES B1, A1B and A2 scenarios. They find that all the models consistently show a shift toward more intense and extreme precipitation over the globe as a whole and over various regions including South Asia. They indicate more intense and less light precipitation.

Turner and Slingo (2009) examined the impact of doubling CO_2 on IMR. At $2xCO_2$, mean summer rainfall increases slightly, especially over central and northern India. The mean intensity of daily precipitation during the monsoon is found to increase, consistent with fewer wet days and there are increase in heavy rain events. The chance of reaching particular thresholds of heavy rainfall is found to approximately double over northern India, increasing the likelihood of damaging floods on a seasonal basis. Intensification of both active and break events are noted, although there is no suggestion of any change to the duration or likelihood of monsoon breaks.

12.5. Possible mechanisms for increase in precipitation

The land-sea temperature contrast is the basic forcing mechanism of the South Asian summer monsoon. Excessive snowfall during the previous winter and spring can delay the build up of the monsoonal temperature gradient because part of the solar energy will be reflected and part will be utilized in melting snow or in evaporating soil moisture. A relatively small amount of energy will be left to warm the surface and hence the atmosphere. Thus, snow cover tends to create a net radiation deficit, which will weaken the heat low over northern India and the adjoining regions during May resulting in a weak monsoon and significant decrease in rainfall. Pressure in May over the heat low region shows a distinct relationship with seasonal rainfall during the first half of the monsoon season (see Kripalani et. al. 2007a). The above is well supported by the negative relationship between snow cover and monsoon rainfall documented in several publications since the time of Blanford, over a century ago. Besides the role of the Eurasian snow cover, monsoon variability is also influenced by the ENSO phenomenon. These issues are examined in this section.

12.5.1. Heat low over North India

The observed sea level pressure field based on the NCEP-NCAR Reanalysis is presented in Fig.12.6. One of the important features of the monsoon circulation is the establishment of the trough of low pressure along the Indo-Gangetic plains from northwest India to the head Bay of Bengal. Fig.12.6 (NCEP panel) shows that the minimum pressure (~1002 hPa) is located over the northern parts of the country from northwest India (i.e. the heat low region) to the head Bay of Bengal. A visual comparison of the model simulated (Fig. 12.6 MME: 20c3m panel) and observed pattern (Fig. 12.6: NCEP panel) reveals that the models are able to capture the mean sea level pressure (MSL) patterns reasonably well. The differences between the observed and simulated patterns are practically zero over most of the region (Fig.12.6 Bias panel).

The projected patterns during the mid of the 21st century (Fig.126: MME: 2031-2050) and at the end of the 21st century (Fig.12.6: MME: 2081-2100) are similar to the pattern during the end of the 20th century (20c3m panel). The changes in the MSL patterns are examined by computing the differences between the projected patterns and the simulated patterns. It is interesting to note negative pressure anomalies over the northwest region, signifying the intensification of the heat low (Fig.12.6: lower panels). While the magnitude of the change over the heat low region is -0.25 hPa during the mid of the 21st century (2031-2050), it is -0.50 hPa during the end of the 21st century (2081-2100). The projected change in the intensification of the heat low is expected to be twice at the end of the 21st century compared to the middle of the century. Thus, the heat low over northwest India and neighborhood is projected to intensify in the warming world. This feature could be conducive to oceanic moisture convergence from the Arabian Sea towards the northern parts of India, leading to the enhancement of the summer monsoon precipitation. However, over the head Bay of Bengal there is an indication of positive pressure anomalies. Thus, the negative anomalies over northwest India and the positive anomalies over the head Bay of Bengal may imply the intensification of the east-west pressure gradient. This would support moisture convergence from the Bay of Bengal inland. Thus, along with the intensification of the heat low, the east-west pressure gradient is also projected to become stronger. This stronger pressure gradient will also aid oceanic moisture convergence over the Indian landmass from the Bay of Bengal.

12.5.2. Monsoon Circulation

The observed surface wind vector pattern based on NCEP-NCAR reanalysis data during the summer monsoon period (June-September) is shown in Fig.12.7 (NCEP panel). The main components of the well-developed summer monsoon circulation are the cross-equatorial flow from the Southern Hemisphere across the east African coast, southwesterly / westerly flow over the Arabian Sea, Indian peninsula and the Bay of Bengal; westerly flow changing direction over the head Bay of Bengal / Bangladesh with weak easterly flow near the foot of the Himalayas establishing the monsoon trough over

the Indo-Gangetic Plains. A comparison of the first two panels (Fig.12.7: NCEP and 20c3m panels) suggests that the broad-scale features appear to be well captured by the models. However, the strength of the wind vectors is weaker over the east coast of India as evidenced by northerly/northeasterly anomalies (Fig. 12.7: Bias panel). The projected wind vector patterns during the mid (2031-2050) and end (2081-2100) of the 21st century (Fig.12.7 central panels) appear to be similar to the 20th century pattern (20c3m), suggesting that the broad-scale patterns may not change, however the magnitude of the wind vectors could change.

The projected changes in the magnitude of the monsoon circulation are shown in Fig.12.7 (lower 2 panels). Anomalous easterly/northeasterly flow over the Bay of Bengal and to the south and anomalous northeasterly flow over the northern parts of the Arabian Sea suggests weakening of the monsoon circulation (Fig.12.7 lower 2 panels). Such weakening has been reported in several studies. However, the projected anomalous easterly flow over the Bay of Bengal may be conducive to transport oceanic moisture towards the southern parts of India and Sri Lanka. An anomalous anti-cyclonic circulation over the head of the Bay of Bengal is also projected (Fig.12.7 lower 2 panels). During the monsoon season the cyclonic circulation over this region supports the development of low pressure systems and the monsoon depressions. Thus, the projected anomalous anti-cyclonic circulation over the Head of the Bay of Bengal may hinder the formation and further development of these rain bearing systems. Significant decreasing trends in the frequency of these disturbances over the Bay of Bengal have been reported using observed data during the 20th century, as noted in section 12.3.3. Fan et.al. (2010) note that the WCRP CMIP3 simulations capture the observed trend of the weakening of the South Asian summer monsoon circulation over the latter part of the half century.

12.5.3. Eurasian snow cover

The changes in snow cover are presented as the differences between the projected snow patterns and the simulated patterns for the winter season (Fig. 12.8). A cursory glance at the patterns suggests a decrease in snowfall over Eurasia (blue shaded area). It is interesting to note that while the MME project a decrease in snowfall over western Eurasia (blue shaded areas), an increase in snowfall is projected over eastern Eurasia (red shaded areas). Thus, the intensification of the heat low and the pressure gradient could be attributed to the decrease in snowfall in particular over western Eurasia and the Tibetan Plateau.

This dipole configuration of decreased snowfall over western Eurasia and increased snowfall over eastern Eurasia during winter is conducive to the subsequent summer monsoon activity over India (Kripalani and Kulkarni 1999). The low snowfall to the west and high snowfall to the east implies an anomalous anti-cyclonic circulation or a strong ridge over north Asia prior to a strong monsoon. The detailed mechanism on how the ridge would favor a good monsoon can be referred in Meehl (1997) and Kripalani and Kulkarni (1999). Furthermore observed snow depth over eastern Eurasia has increased (Kripalani et.al. 2003b). Thus the projected snowfall decrease over western Eurasia and increase over eastern Eurasia would imply changes in the mid-latitude circulation favorable for summer monsoon precipitation activity over the South Asian sub-continent in the warming world. Kripalani et.al. (2003a) using INSAT satellite data over the western Himalayan region have shown that the spring snow cover area has been declining and snow has been melting faster from winter to spring after the early 1990s.

12.5.4. El Nino Southern Oscillation (ENSO)

Power and Kociuba (2011) examined the impact of global warming on the Southern Oscillation Index (SOI: MSL pressure difference between Tahiti and Darwin). They find that SOI tends to increase during the 21st century. Under global warming

MSLP tends to increase at both Darwin and Tahiti, but tends to rise more at Tahiti than at Darwin. Tahiti lies in the extensive region where MSLP tends to rise in response to global warming. On the other hand, An et.al. (2008) on examination the sensitivity of ENSO to future greenhouse warming predicted by the various IPCC AR4 climate model simulations find it highly model dependent. Thus it may be premature to conclude how ENSO may vary during the global warming. Annamalai et al (2007) find that the strength of the IMR-Nino3.4 SST correlation in the selected IPCC AR4 model runs waxes and wanes to some degree on decadal time scales – similar to observations. They thus conclude that for each of the selected model the ENSO-monsoon correlation in the global warming runs a very similar to that in the 20th century, suggesting that the ENSO-monsoon connection will not weaken as global climate warms. Fan et.al. (2010) find that the WCRP CMIP3 simulations reproduce the observed negative relationship between IMR and ENSO. Coelho and Goddard (2009) find that for the climate change models that reproduce realistic oceanic variability of the ENSO phenomenon, results suggest no robust changes in the strength or frequency of El Nino events. These models exhibit realistic pattern, magnitude and spatial extent of El Nino-induced drought pattern in the 20th century and the tele-connections are not projected to change in the 21st century.

Here, we examine whether global warming due to increases in greenhouse gases could affect the ENSO-Monsoon relationship. SSTs over the NINO3.4 region are used as an index to quantify the ENSO phenomenon. We first examine the ability of the models to simulate the life cycle of ENSO. The life cycle is the composite based on the strong El Nino events (standardized NINO3.4 SST greater than 1.0) simulated by the models. Fig 12.9 shows the life cycle of ENSO simulated by the MME (20c3m: blue line), observed life cycle (red line) and the projected life cycle in the 21st century (green line). SSTs over east equatorial start warming around spring, peak in winter and then start decaying. Thus the life cycle of a typical ENSO event is approximately 2 years. The peak phase of ENSO cycle is reasonably well simulated by the models, though in developing and decaying phase it simulates a warm bias. A comparison of the simulated and projected life cycles indicates a slight increase in SST over NINO3.4

region during the initial and the peak phase, but the projected increase of SST is more during the decaying phase, probably suggesting a longer time to decay.

The relation between the ENSO phenomenon and the monsoon activity is determined by computing 11-year sliding correlation coefficients (CCs) between NINO3.4 SSTs and the IMR (Fig.12.10). The observed CCs (Fig.12.10 upper panel) depict the negative relation throughout the period. However the strength of this relation alternately strengthens and weakens on decadal time scales. The recent ENSO-Monsoon weakening can be clearly seen with positive CCs after the 1990s (Fig.12.10 upper panel). The model simulated relation (Fig.12.10 central panel) and the projected relation (Fig.12.10 lower panel) clearly depicts decadal variability in these connections. Thus the relation waxes and wanes as time progresses as has been noted in some earlier studies. Thus no clear indications of the ENSO-Monsoon connections are projected. The IPCC AR4 also notes that the lack of clarity over changes in ENSO will further contribute to uncertainty.

12.5.5. Changes in Walker, Monsoon and Hadley Circulations

To further explore the possibility of weakening / strengthening of large-scale circulations in a warming climate, we examine the change in zonal (Walker + Monsoon) and meridional (Hadley) circulations in the time slice 2081-2100 only. Fig.12.11a shows the changes (projection minus simulation) in zonal circulations, i.e. differences in 200-hPa velocity potential averaged over 10S-30N during June through September. It is clearly seen that the divergence in the monsoon region (~ 50^0-150^0E) is reduced remarkably, in particular over the Indian region (~50^0-90^0E), consistent with weakened monsoon circulation. A similar weakening is also shown by Ueda et.al. (2006). In addition, the descending branch of the Walker circulation over eastern Pacific becomes weak (170^0W-120^0W). Thus, the tropical east-west circulation including monsoon circulation is weakened along with intensified upward motion over eastern Pacific Ocean in a warming climate.

The differences (projection minus simulation) in global average velocity potential for the time slice 2081-2100 are shown in Fig. 12.11b for 850 hPa (lower panel) and 200 hPa (upper panel), which depicts changes in Hadley circulation. Figure reveals that the difference is positive at lower level (850 hPa) while negative at upper level (200 hPa). Also, the difference is large in the belt 20^0S-20^0N. Beyond 20^0, there is not much difference in the tropics. This implies the weakening of Hadley circulation in the tropical belt 20^0S-20^0N. Tanaka et.al. (2005) have also anticipated the weakening of Hadley circulation by 9% in the twenty-first century.

Vecchi and Soden (2007) note that the strength of the atmospheric overturning circulation decreases as the climate warms in all IPCC AR4 models. The weakening occurs preferentially in the zonally asymmetric (ie Walker) rather that the zonal-mean (ie Hadley) component of the tropical circulation. Evidence suggests that the overall circulation weakens by decreasing the frequency of strong updrafts and increasing the frequency of weak updrafts. Allan and Soden (2007) noted that an emerging signal of rising precipitation trends in the ascending regions and decreasing trends in the descending regimes are detected in the observational datasets. These trends are substantially larger in magnitude, than present-day model simulations and projections into the 21st century. They conjecture that the discrepancy must relate to errors in the satellite data or in the model parameterization. This would have important implications for future projections of global water cycle.

As the climate warms, changes in both the atmospheric and ocean circulation over the tropical Pacific Ocean resemble “El Nino Like” conditions. The character of the Indian Ocean response to global warming resembles of the Indian Ocean Dipole Mode events. Despite the large changes in the tropical Pacific mean state, the changes in ENSO amplitude are highly model dependent (Yeh and Kirtman 2007). Using IPCC AR4 data sets Ye and Hsieh (2008) also report that in the tropical Pacific, the warming in the mean SST was found to have an El Nino-like pattern, with both the equatorial zonal circulation and the meridional overturning circulation weakened under increased greenhouse forcing. According to McPhaden and Zhang (2002), there appeared to be a

strong decadal variability superimposed on a linear weakening trend during the period 1953-2001. Merryfield (2006) found that anthropogenic forcing may have contributed to the observed slowdown of the meridional overturning circulation. The zonal Walker circulation driven by the convection in the western equatorial Pacific and subsidence in the east shows a weakening trend since the mid-nineteenth century due to anthropogenic forcing (Vecchi et.al. 2006). There is much uncertainty in how ENSO will change its characteristics (e.g. amplitude and frequency) under increased greenhouse gases in the coupled models. The IPCC AR4 also reports that monsoonal flows and the tropical large-scale circulation are likely to be weakened.

Thus, the weakening in Walker and Hadley circulation could result in the substantial weakening of monsoonal circulation over the South Asian domain.

12.5.6. Indian Ocean Dipole Mode

Long-term variability in the Indian Ocean Dipole Mode (IODM) clearly reveals an increasing trend (Kripalani and Kumar 2004). With the dominance of the negative phase during earlier decades (1880 – 1970) and positive phase during thr\e recent decades (1960 – 2000). Zheng et.al. (2010) examined the IODM response to global warming, one under constant climate forcing and one forced by increasing greenhouse gas concentration. In the unforced simulation, there is significant decadal and multi-decadal modulation of the IODM variance. Little change under global warming in IODM variance in the model suggests that the apparent intensification of IODM activity during recent decades is likely part of natural chaotic modulation of the ocean-atmosphere system or the response to non greenhouse gas radiative changes.

A recent study by Kulkarni et.al. (2007) suggests that the summer monsoon rainfall over India has more influence on the autumn dipole mode than vice versa. Since little change under global warming is suggested, no projections on IODM-Monsoon connections are attempted.

12.5.7. Atmospheric Water Vapour

Troposphere warming (e.g. due to increased greenhouse gases) leads to exponential increases in the water-holding capacity of the atmosphere by ~ 7% / ^{0}K, which is largely governed by the Clausius-Clapeyron equation (Trenberth 1998). Trenberth et.al. (2003) argued that in a warmer climate, heavy precipitation intensity should increase at the same rate as for atmosphere moisture (i.e.~7% / ^{0}K). Since the change in the overall intensity of the global hydrological cycle (global evaporation and precipitation) is controlled by the availability of energy at the surface, not the availability of moisture, climate models predict that the intensity of global hydrological cycle increases by about 1 – 2% / ^{0}K.

Both the oceans and the atmosphere are warming as greenhouse gases build up in the atmosphere. Warmer tropical SSTs with increased greenhouse gases produce relatively large increases in water vapor due to increased evaporation and consequently a general increase in tropical precipitation. Most of the studies attribute the increase in mean rainfall due to an increase in moisture convergence to an increase in water content in a warmer climate (see references in Kripalani et.al. 2007a, b; Meehl 2007b). General increase in water vapor, associated with positive SST anomalies in the warmer climate, is responsible for the increased precipitation intensity over most land areas in the tropics. To investigate this issue we determined the percent increase in precipitable water (atmospheric water vapor content vertically integrated through the atmospheric column) in the 21st century (Fig.12.12). An increase of 8-12 % over the Indian landmass during the mid of the 21st century (2031-2050) and 20-25 % during the end of the 21st century (2081-2100) is projected. However, a maximum increase of 25-30 % is projected over the Arabian Peninsula, adjoining regions of Pakistan, northwest India, over the foothills of the Himalayas and over the Nepal region. The maximum increase of precipitable water over these regions may be related to the larger moisture flux convergence due to the intensification of heat low over northwest India and the adjoining regions.

Thus, a major cause for increase in precipitation may be due to the increase in atmospheric water vapor over the land area advected from the adjacent Bay of Bengal and the Arabian Sea.

12.6. Impact of Aerosols

One of the major human contributors to climate change could be the greenhouse gases such as carbon dioxide, methane, nitrous oxide, and halocarbons. Greenhouse gases are globally mixed pollutants with long residence times in the atmosphere. Their impact is not therefore determined by the source from which they are emitted. Particulate emissions could also contribute to climate change because they do not disperse as quickly and their impacts on the climate are mainly felt in their region of origin. Thus the climatic impacts of South Asian particulate emissions could be felt mainly in South Asia.

Aerosols absorb and scatter solar radiation. The absorption together with the scattering leads to a large reduction of solar radiation at the surface. In addition aerosols nucleate more cloud drops that enhance scattering of solar radiation and contributes to additional reduction. The nucleation of clouds by aerosols also reduces the precipitation efficiency of clouds. Thus aerosol radiation forcing can reduce rainfall through several mechanisms (details and more references in Ramanathan et.al. 2005).

One of the areas of the world with higher aerosol concentration is South Asia, a result of recent rapid urbanization and population growth, a 3-km thick brownish haze layer (brown cloud). As noted above, aerosols play an important role in both the global and regional climate balance. They are recognized as a significant climate forcing, a factor that alters earths radiation balance and thus possibly affecting climate (Ji et.al. 2011). India ranks second in Asia for the emission of anthropogenic aerosols (Ohara et al 2007). This could have impact on the climate over India. Ji et. al. (2011) have shown that pre-monsoon season aerosols result in surface air temperature decreasing by 0.1 – 0.5^{0}C over northeast India and Myanmar. Meanwhile the precipitation increases by 5-

25% in these regions. These changes are more consistent with monsoon onset variety. In the areas of increasing precipitation, monsoon breaks out earlier and vice versa. In the monsoon season, the surface air temperature cools by 0.1 – 0.5^{0}C in northwest and northeast Indian sub-continent and accompanies with increasing precipitation by 5-25 %.

Bollasina et.al. (2008) note that anomalous loading in late spring leads to remarkable and large-scale variation in the monsoon evolution. Excessive aerosols in May lead to reduced cloud amount and precipitation, increased surface shortwave radiation, and land surface warming. The June-July monsoon anomaly associated with excessive May aerosols is of opposite sign over much of the sub-continent. The monsoon strengthens in June-July.

The inclusion of aerosols / soil dust, black and organic carbons, sulfate and sea salts, results in drops in surface temperature and increases in precipitation over central India during the pre-monsoon months of March through May. This cooling during the pre-monsoon months will weaken the near-surface cyclonic circulation and consequently, has a negative feedback on precipitation during the active monsoon months of June-July (Collier and Zhang 2009).

A seminal role played by the absorbing aerosols in the transition from break to active spells has been shown by Manoj et.al. (2011). Aerosols could modify the north-south temperature gradient at lower levels. The meridional gradient of temperature at low level between aerosol-rich central India and pristine equatorial Indian Ocean is large (> 6 deg C) and sustains for long time (> 10 days) during breaks following active spells leading to significant moisture convergence to central India. During breaks not followed by active spells, the temperature gradient is weaker and could not sustain required moisture convergence and failed to lead to a sustained active spell. Results highlight the need for proper inclusion of absorbing aerosols in dynamical models for simulation of the observed variability of the intra-seasonal oscillations and their extended range prediction.

Kim et.al. (2008) suggest the climatic importance of the volcanic forcing in the global monsoon precipitation variability. They conclude that from about one-fourth to one-third of the drying trend in the northern hemisphere land monsoon precipitation over the latter half of the twentieth century was likely forced by the volcanic aerosols. Lambert et.al. (2004) argued that variation in terrestrial precipitation is controlled more by the natural short-wave forcing of volcanic aerosols than the long-wave forcing of greenhouse gases. Their results lend support to and confirm essential role of natural volcanic forcing in replicating multi-decadal variation of the large-scale land precipitation. Shiogama et.al. (2010) also note that precipitation is more sensitive to carbon aerosols than well mixed greenhouse gases. They further note that surface dimming due to the direct and indirect effects of carbon aerosols effectively decreases evaporation and precipitation, which enhances the precipitation sensitivity in the carbon aerosol runs. Thus from the above cited literature it is apparent that besides greenhouse gases, aerosols will also play an important role in future projections.

12.7. Discussion

This discussion is based on the recent publications on impacts of global warming on climate. Cherchi et.al. (2011) note that increased atmospheric carbon dioxide provided warmer atmospheric temperature and higher atmospheric water vapor content, but not necessarily more precipitation. They further note that monsoon precipitation responses to CO2 forcing are largest if extreme concentration of CO_2 are used, but they are not necessarily proportional to the forcing applied.

Model results including climate future scenarios show that the rainfall tends to increase in convergence zones with large climatological precipitation and to decrease in subsidence regions (“Rich-get-Richer” mechanism; Chou and Neelan (2004), Held and Soden 2006; Sun et.al. 2007, Chou et.al. 2009). However, a recent high-resolution regional model study demonstrated a reduction of IMR associated with anthropogenic increase in greenhouse gas concentration (Ashfag et.al. 2009), thus suggesting that there are still great uncertainties for projecting the South Asian monsoon precipitation.

For the Asian summer monsoon, increased monsoon rainfall despite weakened monsoon winds ("Precipitation-Wind Paradox", Ueda et.al. 2006) has been ascribed to larger moisture transport from a warmer Indian Ocean towards the Indian subcontinent. Furthermore, over the monsoon region, the precipitation rate increase is weaker than the associated atmospheric vertically integrated moisture content rise in agreement with the so-called "Suppressed Effect of CO2" (Allen and Ingram 2002, Held and Soden 2006, Ueda et.al. 2006, Vecchi and Soden 2007).

May (2011) noted marked changes in the Indian summer monsoon associated with a global warming of 2^0C with respect to pre-industrial conditions, namely an intensification of the summer monsoon precipitation despite a weakening of the large-scale monsoon circulation. The increase in monsoon rainfall is related to a variety of different mechanisms, with the intensification of the atmospheric moisture transport into the India region as the most important one. The weakening of the large-scale monsoon circulation is mainly caused by changes in the Walker circulation with large-scale divergence in the lower troposphere and convergence in the upper troposphere over the Indian Ocean in response to enhanced convective activity over the Indian Ocean and the central and eastern Pacific and reduced convective activity over the western tropical Pacific Ocean.

Krishna Kumar et.al. (2011) state that the projected anthropogenic climate changes are likely to have large impacts on key socio-economic sectors – agriculture and public health, which could have pervasive negative effect throughout the entire economy barring appreciable mitigation efforts. Recent studies show that the annual total all-India production of the major crops shows a strong relationship with all-India monsoon rainfall. Furthermore, majority of the kharif (ie during summer, autumn) crops are strongly associated with the ENSO conditions; however, none of the rabi (i.e. winter, spring) crops show this relationship (Krishna Kumar et.al. 2004). Revedekar and Preethi (2011) also show that a large part of the country exhibits a significant positive relationship between kharif food grain yield and the indices of extreme precipitation.

They further note that the extent and strength of the positive relationship decreases with an increase in threshold values indicating that very heavy daily rainfall is less useful than moderate daily rainfall. Thus, very heavy daily rainfall has an adverse effect on crop.

Characterizing and quantifying uncertainty in climate change projections is of fundamental importance not only for purposes of detection and attribution, but also for strategic approaches to adaptation and mitigation. Uncertainties in future climate change derive from three main reasons: forcing, model response and internal variability. Internal variability (also termed as “climate noise”) is the natural variability of the climate system that occurs in the absence of external forcing, and includes processes intrinsic to the atmosphere, the ocean and the coupled ocean-atmosphere system (Deser et.al. 2011).

Most regional climate-change information has been based on the use of coupled Atmosphere-Ocean General Circulation models. The coarse resolution precludes models from providing an accurate description of extreme events at regional levels. Recognizing this, WCRP has initiated a framework called the Coordinated Regional Climate Downscaling Experiment (CORDEX). Once the outputs under this initiative are made available to the international scientific community, it will go a long way in providing useful information on smaller regional scales (Giorgi et.al. 2009).

12.8. Summary

This Chapter examined the observed, the model simulated and the model projections of the Indian summer monsoon in the global warming scenario. Based on several recent studies, observed changes during the 20th century are noted. Changes in extremes of precipitation, extremes in temperature, intra-seasonal and inter-annual monsoon variability are noted.

Majority of the studies cited here report an increase in heavy rainfall events and a decrease in moderate and low rain events in particular during the second half of the

20th century. These extreme rain events suggest an increase in the risk of major floods in particular over the central parts of India. Temperatures have been increasing over the Indian sub-continent during recent decades. Studies report that night time temperatures have started increasing at twice the rate of day time temperatures. Widespread increasing trends in temperatures are reported, with possibility of increase in severe heat waves.

Some changes in the intra-seasonal behavior of monsoon rainfall have been reported; in particular the northward propagating mode from the equatorial Indian Ocean has slowed down. Inter-annual IMR depicts random fluctuations; however the decadal variability shows alternate epochs of above and below normal rainfall. The IMR appears to be in the below normal epoch during the last 4-5 decades.

Projections in several facets of Indian monsoon are examined from the set of IPCC AR4 models. Increase in overall summer monsoon rainfall over India is projected, in particular over the Arabian Sea, west coast and northeast India i.e. regions with heavy rainfall will continue to get heavier rainfall. The increase in rainfall could be due to projected intensification of the heat low over northwest India, in spite of projected weakening of the monsoon, Hadley and Walker circulations. A dipole snow configuration with decrease over western Eurasia and increase over eastern Eurasia is projected. This dipole snow configuration suggests changes in northern hemisphere mid-latitude circulation conducive for the summer monsoon over India. No clear indications of the ENSO-Monsoon connections are projected. A major cause for the increase in precipitation may be due to increase in atmospheric water vapor over the land areas advected from the warmer Bay of Bengal and the Arabian Sea.

There could be lot of uncertainties in these projections. The three climate change experiments considered here together describe divergent futures of the underlying uncertainties in the main driving forces. They cover a wide range of key “future” characteristics such as population, economic development and technological change. The rate of population growth as well as the economic and technological development is

simply astonishing in today's world. Hence, it is very important to study future climate projections under these scenarios, especially in the densely populated region of the world like South Asia. There is a lot of diversity among the various models in these projections. Besides the greenhouse gases, aerosols are also expected to play an important role in the future projections. How the greenhouse gases and aerosols will behave in the future is also debatable. More research in all these aspects need to be undertaken so that we can link climate science with society and to analyze opportunities for monsoon science to benefit society in several sectors such as natural hazards management, agriculture, public health and water management (Ray et.al. 2007).

References

Alexander, L.V., Zhang, X., Peterson, T. C., Caesar, J., Gleason, B., Klein Tank, A.M.G., Haylock, M., Collins, D., Trewin, B., Rahimzadeh, F., Tagipour, A., Rupa Kumar, K., Revadekar, J., Griffiths, G., Vincent, L., Stephenson, D.B., Burn, J., Aguilar, E., Brunet, M., Taylor, M., New, M., Zhai, P., Rusticucci M. and Vazquez-Aguirre, L., 2006, "Global observed changes in daily climate extremes of temperature and precipitation", *J. Geophy Res.,* Vol III, D05109, doi: 10.1029/2005JD006290.

Allan, R. P. and Soden, B. J., 2007, "Large discrepancy between observed and simulated precipitation trends in the ascending branches of all tropical circulation", *Geophy. Res. Lett.*, 34, L18705, doi: 10.1029/2007GL031460.

An, S. I., Kug, J. S., Ham, Y.G., and Kang, I.S., 2008, "Successive modulation of ENSO to future greenhouse warming", *J. Clim*, 21, 3-21.

Annamalai, H., Hamilton, K., and Sperber, K.R., 2007, "The South Asian summer monsoon and its relationship with ENSO in the IPCC AR4 simulations", *J. Clim.,* 20, 1071-1092.

Ashok, K., Guan, Z. and Yamagata, T., 2001, "Impact of the Indian Ocean Dipole between Indian Monsoon Rainfall and ENSO", *Geophy. Res. Lett.*, 28, 4499-4502.

Ashrit, R.G., Rupa Kumar, K. and Krishna Kumar, K., 2001, "ENSO-Monsoon relationship in a greenhouse warming scenario", *Geophy. Res. Lett.*, 28, 1727-1730.

Allen, M. R. and Ingram, W.J., 2002, "Constraints on future changes in climate and hydrological cycle",. *Nature,* 419, 224-232.

Ashfaq, M., Shi, Y., Tung, W.W., Trapp, R.J., Gao, X.J., Pal, J.S. and Diffenbaugh, N.S., 2009, "Suppression of the South Asian summer precipitation in the 21st century", *Geophy. Res. Lett.,* 36, L01704, doi 10.1029/2008GL036500.

Bawiskar, S. M., 2009, "Weakening of lower tropospheric temperature gradient between Indian landmass and neighboring oceans and its impact on Indian monsoon", *J. Earth Syst Sci.,* 118, 273-280.

Behera, S. K., Krishnan, R. and Yamagata, T., 1999, "Unusual ocean-atmosphere conditions in the tropical Indian Ocean during 1994", *Geophy. Res. Lett.,* 26, 3001-3004.

Bhadran, C.V.V., Amatya, B.V.S. and Pant, G.B., 2005, "Heat waves over Andhra Pradesh: A case study of summer 2003", *Mausam,* 56, 385-394.

Bollasina, M. and Nigam, S., 2009, "Indian Ocean SST, evaporation and precipitation during the south Asian summer monsoon in IPCC AR4 coupled simulations", *Clim. Dyn.*, 33, 1017-1032.

Bollasina, M., Nigam, S. and Lau, K.M., 2008, "Absorbing aerosols and summer evolution over South Asia: An observational portrayal", *J. Clim.,* 21, 3221-3239.

Chang, C. P., Harr, P. and Ju, J., 2001, "Possible roles of Atlantic circulations on the weakening Indian monsoon rainfall-ENSO relationship", *J. Clim.,* 14, 2376-2380.

Cherchi, A., Alessandri, A., Masina, S., and Navarra, N., 2011, "Effects of increased CO_2 levels on monsoons", *Clim. Dyn.*, online DOI 10.1007/s00382-010-0801-7.

Christensen, J.H., Hewitson, B., Busuioc, A., Chen, A., Gao, X., Held, I., Jones, R., Kolli, R.K., Kwon, W.T., Laprise, R., Magana Rueda, V., Mearns, L., Menendez, C.G., Raisanen, J., Rinke, A., Sarr, A. and Whetton, P., 2007, "Regional Climate Projections. In: Climate Change 2007: The Physical Science Basis. Contribution of Working Group I to the Fourth Assessment Report of the Intergovernmental Panel on Climate Change" [Solomon S, D Qin, M Manning, Z Chen, M Marquis, KB Averyt, M Tignor and HL Miller (eds), Cambridge University Press, Cambridge, United Kingdom and New York, NY, USA.

Chou, C., Neelin, J.D., Chen, C.A., Tu, J.Y., 2009, "Evaluating the "Rich-getting-Richer" mechanism in tropical precipitation change under global warming", *J. Clim.,* 22, 1982-2005.

Coelho, C.A. and Goddard, L., 2009, "El Nino-induced tropical droughts in climate change projections", *J. Clim.*, 22, 6456-6476.

Collier, J.C. and Zhang, G.J., 2009, "Aerosol direct forcing of the summer Indian monsoon as simulated by the NCAR CAM3" *Clim. Dyn.*, 32, 313-332.

Dash, S.K., Jenamani, R.K., Kalsi, S.R. and Panda, S.K., 2007, "Some evidence of climate change in 20th century India", *Climatic Change* DOI:10.1007/s10584-007-9305-9.

Dash, S.K., Jenamani, R.K. and Shekhar, S., 2004, "On the decreasing frequency of monsoon depression over the Indian region", *Curr. Sci.,* 86, 1406-1411.

Dash, S.K., Kulkarni, M.A., Mohanty, U.C. and Prasad, K., 2009, "Changes in the characteristics of rain events in India",*J. Geophy. Res.*, 114, D10109, doi:10.1029/2008JD010572.

Deser, C., Phillips, A., Bourdette, V. and Teng, H., 2011, "Uncertainty in climate change projection: the role of interannual variability", *Clim. Dyn.*, DOI 10.1007/s00382-010-0977-x.

Fan, F., Mann, M.E., Lee, S. and Evans, J.L., 2010, "Observed and modeled changes in the South Asian summer monsoon over the historical period", *J. Clim.,* 23, 5193-5205.

Giorgi, F., Jones, C. and Asrar, G.A., 2009, "Addressing climate information needs at regional level: the CORDEX framework", *WMO Bulletin,* 58(3), 175-183.

Goswami, B. N., Kulkarni, J. R., Mujumdar, V.R. and Chattopadhyay, R., 2010,"On factors responsible for recent secular trend in the onset phase of monsoon intraseasonal oscillations", *Int. J. Climatol*, 30, 2240-2246.

Goswami, B.N., Venugopal, V., Sengupta, D., Madhusoodanan, M.S. and Xavier, P.K., 2006a, "Increasing trend of extreme rain events over India in a warming environment", *Science,* 314, 1142-1145.

Goswami, B.N., Madhusoodanan, M.S.,. Neema, C.P. and Sengupta, D., 2006b, "A physical mechanism for North Atlantic SST influence on the Indian summer monsoon", *Geophy. Res. Lett.,* 33, L02706, doi: 10.1029/2005GL024803.

Guthakurta, P. and Rajeevan, M., 2008, "Trends in the rainfall pattern over India", *Int. J. Climatol*, 28, 1453-1469.

Held, I.M. and Soden, B.J., 2006, "Robust responses of the hydrological cycle to global warming", *J. Clim.,* 19, 5686-5699.

Hingane, L.S., 1996, “Is a signature of socio-economic impact written on the climate?”, *Climatic Change*, 32, 91-102.

Jadhav, S.K. and Munot, A.A., 2009, “Warming SST of Bay of Bengal and decrease in formation of cyclonic disturbances over Indian region during the southwest monsoon season”, *Theo. Appl. Climatol,* 96, 327-336.

Ji, Z., Kang, S., Zhang, D., Zhu, C., Wu, J. and Xu, Y., 2011, “Simulation of the anthropogenic aerosols over South Asia and their effects on Indian summer monsoon”, *Clim. Dyn.,* DOI: 10.1007/s00382-010-0982-0.

Kalnay, E., Kanamitsu, M., Kistler, R., Collins, W., Deaven, D., Gandin, L., Iredell, M., Saha, S., White, G., Woollen, J., Zhu, Y., Leetmaa, A., Reynolds, B., Chelliah, M., Ebisuzaki, W., Higgins, W., Janowiak, J., Mo, K.C., Ropelewski, C., wang, J., Jenne, R., and Joseph, D., 1996, “The NCEP-NCAR 40-year reanalysis project”, *Bull Amer Met. Soc.,* 77: 437-471.

Kang, I. S., Jin, K., Wang, B., Lau, K.M., Shukla, J., Krishnamurthy, V., Schubert, S.D., Waliser, D.E., Stern, W.F., Kitoh, A., Meehl, G.A., Kanamitsu, M., Galin, V.Ya., Satyan, V., Park, C.K., and Liu, Y., 2002a, “Inter-comparison of the climatological variation of Asian summer monsoon precipitation simulated by 10 GCMs”, *Clim. Dyn.,* 19, 383-395.

Kang, I.S., Jin, K., Lau, K.M., Shukla, J., Krishnamurthy, V., Schubert, S.D., Waliser, D.E., Stern, W.F., Satyan, V., Kitoh, G.A., Meehl, G.A., Kanamitsu, M., Galin, V.Ya., Sumi, A., Wu, G., Liu, Y., and Kim, J.K., 2002b, “Inter-comparison of atmospheric GCM simulated anomalies associated with the 1997/98 El Nino”, *J. Clim.*, 15, 2791-2805.

Kim, H. J., Wang, B. and Ding, Q., 2008, “The global monsoon variability simulated by CMIP3 coupled climate models”, *J. Clim.,* 21, 5271-5294.

Kothawale, D.R., Munot, A.A., Krishna Kumar, K., 2010a, “Surface air temperature variability over India during 1901-2007 and its association with ENSO”, *Clim. Res.,* 42, 89-104.

Kothawale, D.R., Revadekar, J.V. and Rupa Kumar, K., 2010b, “Recent trends in pre-monsoon daily temperature extremes over India”, *J. Earth Syst. Sci.*,119, 51-65.

Kothawale, D.R. and Rupa Kumar, K., 2005, “On the recent changes in surface temperature trends over India”, *Geophy. Res. Lett.,* 32, L18714, doi:10.1029/2005GL023528.

Kripalani, R.H. and Kulkarni, A., 1997a, “Climatic impact of El Nino / La Nina on the Indian Monsoon”, *Weather,* 52, 39-46.

Kripalani, R.H. and Kulkarni, A., 1997b, “Rainfall variability over southeast Asia-connections with Indian Monsoon and ENSO extremes: new perspectives”, *Int. J. Climatol*, 17, 1155-1168.

Kripalani, R.H. and Kulkarni, A., 1999, “Climatology and variability of historical Soviet snow depth: some new perspectives in snow-Indian monsoon tele-connections”, *Clim. Dyn.,* 15, 475-489.

Kripalani, R.H. and Kulkarni, A., 2001, “Monsoon rainfall variations and tele-connections over South and East Asia”, *Int. J. Climatol*, 21, 603-616.

Kripalani, R.H. and Kumar, P., 2004, “Northeast monsoon rainfall variability over south peninsular India vis-à-vis the Indian Ocean Dipole Mode”, *Int. J. Climatol*, 24, 1267-1282.

Kripalani, R,H., Kulkarni, A. and Sabade, S.S., 2003a, “Western Himalayan snow cover and Indian monsoon rainfall: a re-examination with INSAT and NCEP/NCAR data”, *Theo. Appl. Climatol,* 74, 1-18.

Kripalani, R.H., Kulkarni, A., Sabade, S.S. and Khandekar, M.L., 2003b, “Indian monsoon variability in a global warming scenario”, *Natural Hazards* 29: 189-206.

Kripalani, R.H., Oh, J.H., Kulkarni, A., Sabade S.S., and Chaudhari, H.S., 2007a, “South Asian summer monsoon precipitation variability: Coupled climate model simulations and projections under IPCC AR4”, *Theor. Appl. Climatol,* 90: 133-159.

Kripalani, R.H., Oh, J.H. and Chaudhari, H.S., 2007b, “Response of the East Asian summer monsoon to doubled atmospheric CO2: Coupled climate model simulations and projections under IPCC AR4”, *Theor. Appl. Climatol,* 87, 1-28.

Kripalani, R.H., Kulkarni, A., Sabade, S.S., Revadekar, J.V., Patwardhan, S.K. and Kulkarni, J.R., 2004, “Intra-seasonal oscillations during monsoon 2002 and 2003”, *Curr. Sci.,* 87, 325-331.

Krishna Kumar K., Rajagopalan, B. and Cane, A., 1999, “On the weakening relationship between the Indian monsoon and ENSO”, *Science,* 284, 2156-2159.

Krishna Kumar K, Kamala, K., Rajagopalan, B., Hoerling, P., Eischeid, J.K., Patwardhan, S.K., Stinivasan, G., Goswami, B.N. and Nemani, R., 2011, “The once and future pulse of Indian monsoonal climate”, *Clim. Dyn.,* DOI 10.1007/s00382-010-0974-0.

Krishna Kumar K, Rupa Kumar, K., Ashrit, R.G., Deshpande, N.R. and Hansen, J.W., 2004, “Climate impacts on Indian Agriculture”, *Int. J. Climatol*, 24, 1375-1393.

Krishnamurthy, C.K.B., Lall, U. and Kwon, H.H., 2009, “Changing frequency and intensity of rainfall extremes over India from 1951-2003”, *J. Clim.,* 22, 4737-4746.

Krishnamurthy, V. and Goswami, B.N., 2000, “Indian-Monsoon ENSO relationship on inter-decadal timescale”, *J. Clim.,* 13, 579-595.

Kucharski, F., Scaife, A.A., Yoo, J.H., Folland, C.K., Kinter, J., Knight, J., Fereday, D., Fisher, A.M., Jin, E.K., Kroger, J., Lau, N.C., Nakaegawa, T., Nath, M.J., Pegion, P., Rozanov, E., Schubert, S., Sporyshev, P.V., Syktus, J., Voldoire, A., Yoon, J.H., Zeng, N., Zhou, T., 2009, “The CLIVAR C20C project: skill of simulating Indian monsoon rainfall on interannual to decadal time scales. Does GHG forcing play a role?”, *Clim. Dyn.,* 33, 615-627.

Kulkarni, A., Kripalani, R.H., Sabade, S.S. and Rajeevan, M., 2011, “Role of intra-seasonal oscillations in modulating Indian summer monsoon rainfall”, *Clim. Dyn.*, 36, 1005-1021.

Kulkarni, A., Sabade, S.S., and Kripalani, R.H., 2009, “Spatial variability of the Intra-seasonal oscillations during extreme Indian monsoon” *Int. J. Climatol*, 29, 1945-1955.

Kulkarni, A., Sabade, S.S., and Kripalani, R.H., 2007, “Association between the extreme monsoons and the dipole mode over the Indian subcontinent”, *Met. Atmos. Phys.*, 95, 255-268.

Kumar, P., Rupa Kumar, K., Rajeevan, M and Sahai, A.K., 2007,“On the recent strengthening of the relationship between ENSO and Northeast Monsoon rainfall over South Asia”, *Clim. Dyn.*, 28, 649-660.

Lambert, F.H., Stott, P.A., Allen, M.R. and Palmer, M.A., 2004, "Detection and Attribution of Changes in the 20th century land precipitation", *Geophy. Res. Lett.,* 31, L10203, doi 10.1029/2004GL019545.

Mandke, S.K. and Bhide, U.V., 2003, "A study of decreasing storm frequency over the Bay of Bengal", *J. Ind. Geophy. Union*, 7, 53-58.

Mandke, S.K., Sahai, A.K., Shinde, M.A., Joseph, S. and Chattopadhyay, R., 2007, "Simulated changes in active/break spells during the Indian summer monsoon due to enhanced CO_2 concentration: assessment from selected coupled atmosphere-ocean global models", *Int. J. Climatol,* 27, 837-859.

Mani, N.J., Suhas, E. and Goswami, B.N., 2009, "Can global warming make Indian Monsoon weather less predictable?", *Geophy. Res. Lett.,* 36, L08811, doi:10.1029/2009GL037989.

Manoj, M.G., Devara, P.C.S., Safai, P.D. and Goswami, B.N., 2011, "Absorbing aerosols facilitate transition of Indian monsoon breaks to active spells", *Clim. Dyn.*, DOI 10.1007/s00382-010-0971-3.

May, M., 2011, "The sensitivity of the Indian summer monsoon to a global warming of 2^0C with respect to pre-industrial times", *Clim. Dyn.,* DOI 10.1007/s00382-010-0942-8.

McPhaden, M.J. and Zhang, D., 2002, "Slowdown of the meridional overturning circulation in the upper Pacific Ocean", *Nature,* 415, 606-608.

Meehl, 1997, "The south Asian monsoon and the tropospheric biennial oscillation", *J. Clim.,* 10, 1921-1943.

Meehl, G.A., Covey, C., Delworth, T., Latif, M., McAvaney, B., Mitchell, J.F.B., Stouffer, R.J. and Taylor, K,E., 2007a, "The WCRP CMIP3 multi-model data set. A new era in climate change research", *Bull Amer Met Soc*, 88: 1383-1394.

Meehl, G.A., Stocker, T.F., Collins, W.D., Friedlingstein, P., Gaye, A.T., Gregory, J.M., Kitoh, A., Knutti, R., Murphy, J.M., Noda, A., Raper, S.C.B., Watterson, I.G., Weaver, A.J. and Zhao, Z.C., 2007b, "Global Climate Projections. In: Climate Change 2007: The Physical Science Basis. Contribution of Working Group I to the Fourth Assessment Report of the Intergovernmental Panel on Climate Change", [Solomon S, D Qin, M Manning, Z Chen, M Marquis, KB Averyt, M Tignor and HL Miller (eds), Cambridge University Press, Cambridge, United Kingdom and New York, NY, USA.

Merryfield, W.J., 2006, "Changes to ENSO under CO_2 doubling in Multi-model ensemble", *J. Clim.,* 19, 4009-4027.

Nakicenovic, N., Alcamo, J. Davis, G. Vries, B. de., Fenhann, J., Gaffin, S.,. Gregory, K., Grubler, A. et.al. 2000, "*Special Report on Emissions Scenarios*. Working Group III, Inter-governmental Panel on Climate Change (IPCC)", Cambridge University Press, Cambridge, UK, 595 pp.

Nandargi, S. and Dhar, O.N., 2008, "Have extreme rainform events or the frequency of tropical disturbances experienced an increasing trend in recent decades over India?", *Int. J. Climatol,* 33, 49-52.

Neena, J.M. and Goswami, B.N., 2010, "Extension of potential predictability of Indian summer monsoon dry and wet spells in recent decades" *Q. J. R. Met. Soc.,* 136, 583-592.

Ohara, T. et.al. 2007, "An Asian emission inventory of anthropogenic emission sources for the period 1980-2020", *Atmos. Chem. Phys,* 7, 4419-4444.

Padma Kumari, B., Londhe, A.L., Daniel, S. and Jadhav, D.B., 2007, "Observational evidence of solar dimming: offsetting surface temperature warming over India", *Geophy. Res. Lett.,* 34: L21810 doi 10.1029/2007GL031133.

Power, S.B. and Kociuba, G., 2011, "The impact of global warming on the SOI", *Clim. Dyn.,* DOI 10.1007/s00382-010-0951-7.

Preethi, B., Kripalani, R.H. and Krishna Kumar, K., 2010, "Indian summer monsoon rainfall variability in global coupled ocean-atmospheric models", *Clim. Dyn.,* 35, 1521-1539.

Rajeevan, M., Bhate, J. and Jaswal, A., 2008, "Analysis of variability and trends of extreme rainfall events over India using 104 years of gridded daily rainfall data", *Geophy. Res. Lett.,* 35, L18707 doi 10.1029/2008GL035143.

Rajeevan, M., Bhate, J., Kale, K.D. and Lal, B., 2006, "High resolution daily gridded rainfall data for the Indian region. Analysis of break and active monsoon spells" *Curr. Sci.,* 91, 296-306.

Rajeevan, M., Gadgil, S. and Bhate, J., 2010, "Active and break spells of the Indian summer Monsoon", *J. Earth Syst. Sci.,* 119, 229-247.

Ramanathan, V,, Chung, C. Kim, D., Bettge, T., Buja, L., Kiehl, J.T., Washington, W.M., Fu, Q., Sikka, D.R. and wild, M., 2005, "Atmospheric brown clouds: Impacts on South Asia Climate and hydrological cycle", *Proc. Nat. Acad. Sc.,* USA, 102, 5326-5333.

Ray, A.J., Garfin, G.M., Wilder, M., Vasquez-Leon, M., Lenart, M. and Comrie, A.C., 2007, "Application of Monsoon Research: Opportunities to information decision making and reduce regional vulnerability", *J. Clim.,* 20, 1608-1627.

Revadekar, J.V. and Preethi, B., 2011, "Statistical analysis of the relationship between summer monsoon precipitation extremes and foodgrain yield over India", *Int. J. Climatol*, DOI:10.1002/joc.2282.

Rupa Kumar, K., Ashrit, R.G. and Pant, G.B., 2002, "The Indian summer monsoon: past, present and future", *Science and Culture*, 68, 217-224.

Rupa Kumar, K., Krishna Kumar, K., Patwardhan, S.K., Deshpande, N.R., Sharma, C., and Mitra, A.P., 2005, "Future climate scenarios for the South Asian region as simulated by the regional climate model HADRM2", *Science and Culture*, 71, 214-224.

Rupa Kumar, K., Sahai, A.K., Krishna Kumar, K. Patwardhan, S.K., Mishra, P.K., Revadekar, J.V., Kamala, K. and Pant, G.B., 2006, "High-resolution climate change scenarios for India for the 21st century", *Curr. Sc.,* 90, 334-345.

Sabade, S.S., Kulkarni, A. and Kripalani, R.H., 2011, "Projected changes in South Asian summer monsoon by multi-model global warming experiments", *Theor. Appl. Climatol*, 103, 543-568.

Saji, N.H., Goswami, B.N., Vinayachandran, P.N. and Yamagata, T., 1999, "A dipole mode in the tropical Indian Ocean"*Nature,* 401, 360-363.

Scaife, A.A., Kucharski, Folland, C.K., Kinter, J., Bronnimann, S., Fereday, D., Fischer, A.M., Grainger, S., Jin, E.K., Kang, I. S., Knight, J.R., Kusunoki, S., Lau, N.C., Nath, M.J., Nakaegawa, T., Region, P., Schubert, S., Sporyshev, P., Syktus, J., Yoon, J.H., Zeng, N. and Zhou, T., 2009, "The CLIVAR C20C project: selected 20th century climate events", *Clim Dyn*, 33, 603-614.

Singh, O.P., 2001, "Long-term trends in the frequency of monsoonal cyclonic disturbances over the north Indian Ocean", *Mausam*, 52, 655-658.

Shiogama, H., Emori, S., Takahashi, K., Nagashima, T., Ogura, T., Nozawa, T. and Takemura, T., 2010, "Emission scenario dependency of precipitation on global warming in the MIROC3.2 Model", *J. Clim.,* 23, 2404-2417.

Solomon, S., Qin, D., Manning, M., Chen, Z., Marquis, M., Averyt, K.B., Tignor, M. and Miller, H.L. (eds) 2007, "Climate Change 2007 – The Physical Science Basis. Contribution of Working Group I to the Fourth Assessment Report of the Intergovernmental Panel on Climate Change", Cambridge University Press, Cambridge, United Kingdom and New York, NY, USA.

Stowasser, M., Annamalai, H. and Hafner, J., 2009, "Response of the South Asian summer monsoon to Global Warming: Mean and Synoptic Systems", *J. Clim.,* 22, 1014-1036.

Suhas, E. and Goswami, B.N., 2008, "Regime shift in Indian summer monsoon climatological intra-seasonal oscillation", *Geophy. Res. Lett.,* 35, L20703, doi:10.1029/2008GL035511.

Suhas, E. and Goswami, B.N ., 2010, "Loss of significance and multi-decadal variability of the Madden-Julian Oscillations", *J. Clim.,* 23, 3739-3751.

Sun, Y., Solomon, S., Dai, A. and Portmann, R.W., 2007, "How often will it rain?", *J. Clim.,* 20, 4801-4818.

Tanaka, H.L., Ishizaki, N. and Nohara, D., 2005, “Inter-comparison of the intensities and trends of Hadley, Walker and Monsoon circulation in the global warming projections”, *Scientific Online Letters in Atmosphere (SOLA),* 1, 77-80.

Trenberth, K.E .,1998, “Atmospheric moisture residence times and cycling: Implication for rainfall rates with climate change”, *Climatic Change*, 39, 667-694.

Trenberth, K,E,, Dai, A., Rasmussen, R,M, and Parsons, D.B., 2003, “The changing character of precipitation”, *Bull Amer Meteorol Soc.,* 84, 1205-1217.

Trenberth, K.E., Jones, P.D., Ambenje, P., Bojariu, R., Easterling, D., Klein Tank, A., Parker, D., Rahimzadeh, F., Renwick, J.A., Rusticucci, M., Soden, B. and Zhai, P., 2007, “Observations: Surface and Atmospheric Climate Change. In: Climate Change 2007: The Physical Science Basis. Contribution of Working Group I to the Fourth Assessment Report of the Intergovernmental Panel on Climate Change”, [Solomon S, D Qin, M Manning, Z Chen, M Marquis, KB Averyt, M Tignor and HL Miller (eds), Cambridge University Press, Cambridge, United Kingdom and New York, NY, USA.

Turner, A.G. and Slingo, J.M., 2009, “Subseasonal extremes of precipitation and active-break cycles of the Indian summer monsoon in a climate-change scenario” *Q. J. R. Met. Soc.,* DOI:10.1002/qj.401.

Ueda, H., Iwai, A., Kuwako K. and Hori, M.E., 2006, “Impact of anthropogenic forcing on the Asian summer monsoon as simulated by 8 GCMs”, *Geophy. Res. Lett.*, 33: L06703 doi 10.1029/2005GL025336.

Vecchi, G.A. and Soden, B.J., 2007, “Global warming and weakening of the tropical of the tropical circulation”, *J Clim,* 20: 4316-4340.

Vecchi, G.A., Soden, B.J., Wittenberg, A.T., Held, I.M., Leetma, A, and Harrison, M.J. 2006, “Weakening of tropical Pacific atmospheric circulation due to anthropogenic forcing”, *Nature*, 441, 73-76.

Webster, P.J. and Palmer, T.N., 1997, “The past and future of El Nino”, *Nature,* 390, 562-564.

Webster, P.J., Moore, A.M., Loschning, J.P. and Leben, R.R., 1999, “Coupled ocean-atmosphere dynamics in the Indian Ocean during 1997-1998”, *Nature*, 401, 356-360.

WMO 1966: Climatic Change*, WMO Technical Note No. 79, WMO No. 195-TP-100,* World Meteorological Organization, Geneva.

Xie, P. and Arkin, P.A., 1997, “Global precipitation: a 17-year monthly analysis based on gauge observations, satellite estimates and numerical model outputs”, *Bull Amer Met. Soc.,* 78: 2539-2558.

Ye, Z. and Hsieh, W.W., 2008, “Changes in ENSO and associated overturning circulation from enhanced greenhouse gases by the end of the 20th century”, *J. Clim.*, 21, 5745-5763.

Yeh, S.W. and Kirtman, B.P., 2007, “ENSO amplitude changes due to climate change projections in different coupled models”, *J. Clim.*, 20, 203-217.

Zheng, X.T., Xie, S.P., Vecchi, G.A., Liu, Q., Hafner, J., 2010, “Indian Ocean Dipole response to global warming: Analysis of ocean-atmospheric feedbacks in a coupled model”, *J. Clim.,* 23, 1240-1253.

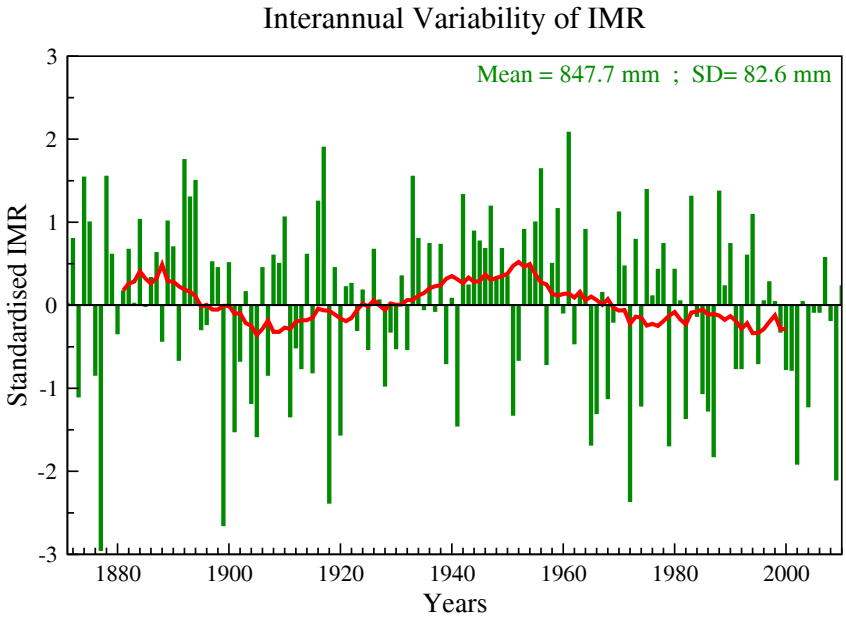

Fig. 12.1: Observed year-to-year standardized IMR (green bars) depicting inter-annual variability for

.

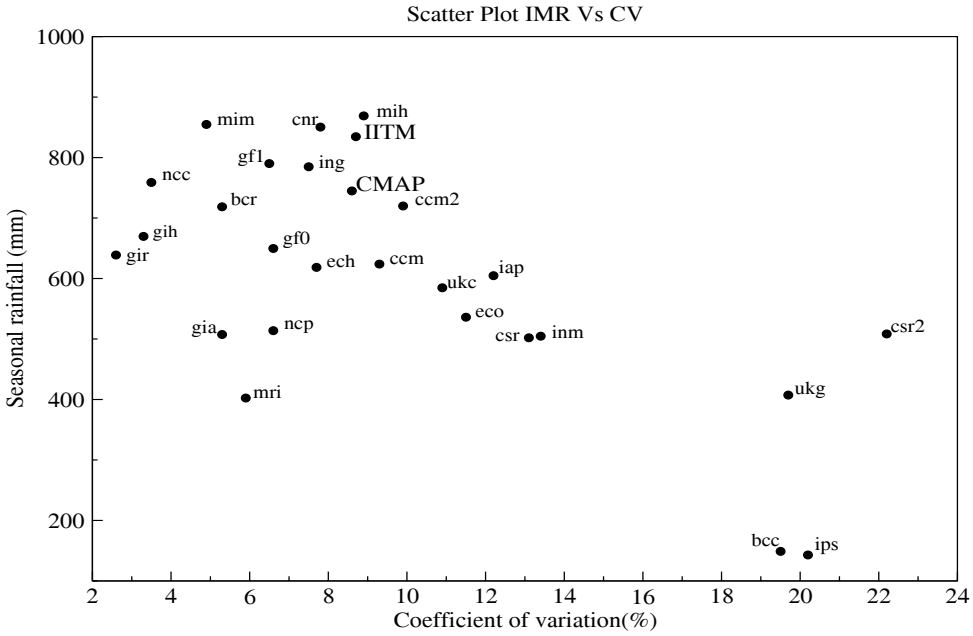

Fig. 12.2: Scatter plot of the mean seasonal (JJAS) rainfall in mm and CV in % for the 25 coupled models. Each dot represents the corresponding values for each model, identified by the acronyms. Observed values are shown as IITM and CMAP.

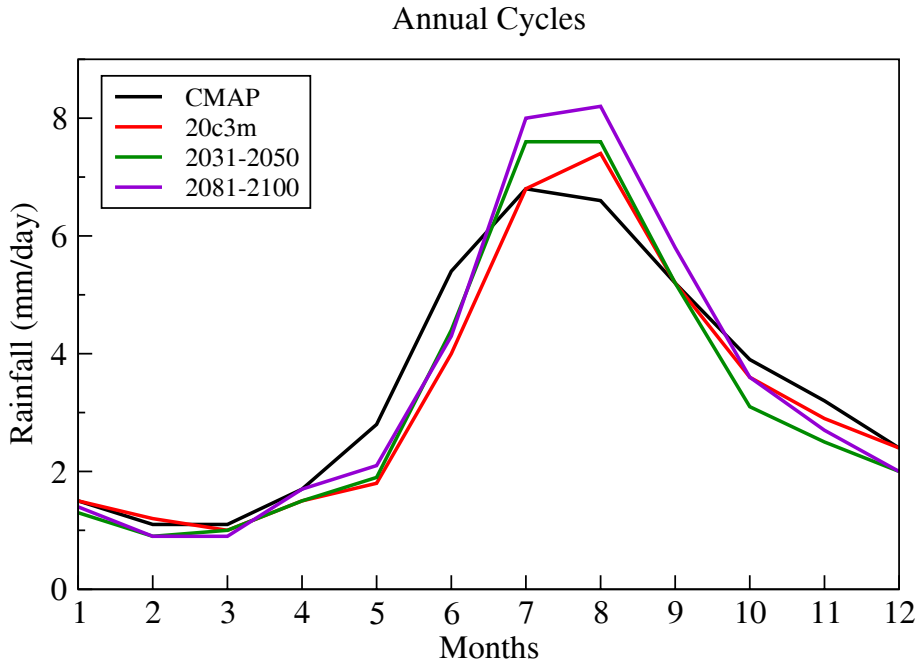

Fig. 12.3: Average monthly rainfall in mm/month for the observed (CMAP), MME simulated (20c3m: red line) and projections under two time slices 2031-2050 (green line) and 2081-2100 (purple line).

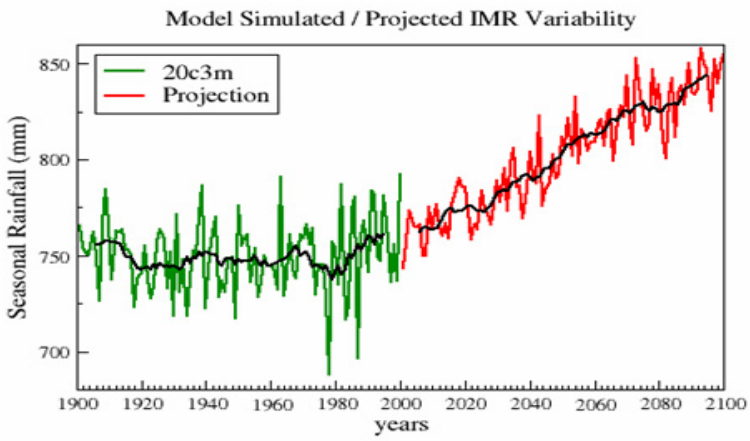

Fig.12.4: Simulated (1901-2000: green line) and projected (2100-2100:red line) inter-annual IMR variability. The 21-year running means (black line) are superimposed on the inter-annual variability.

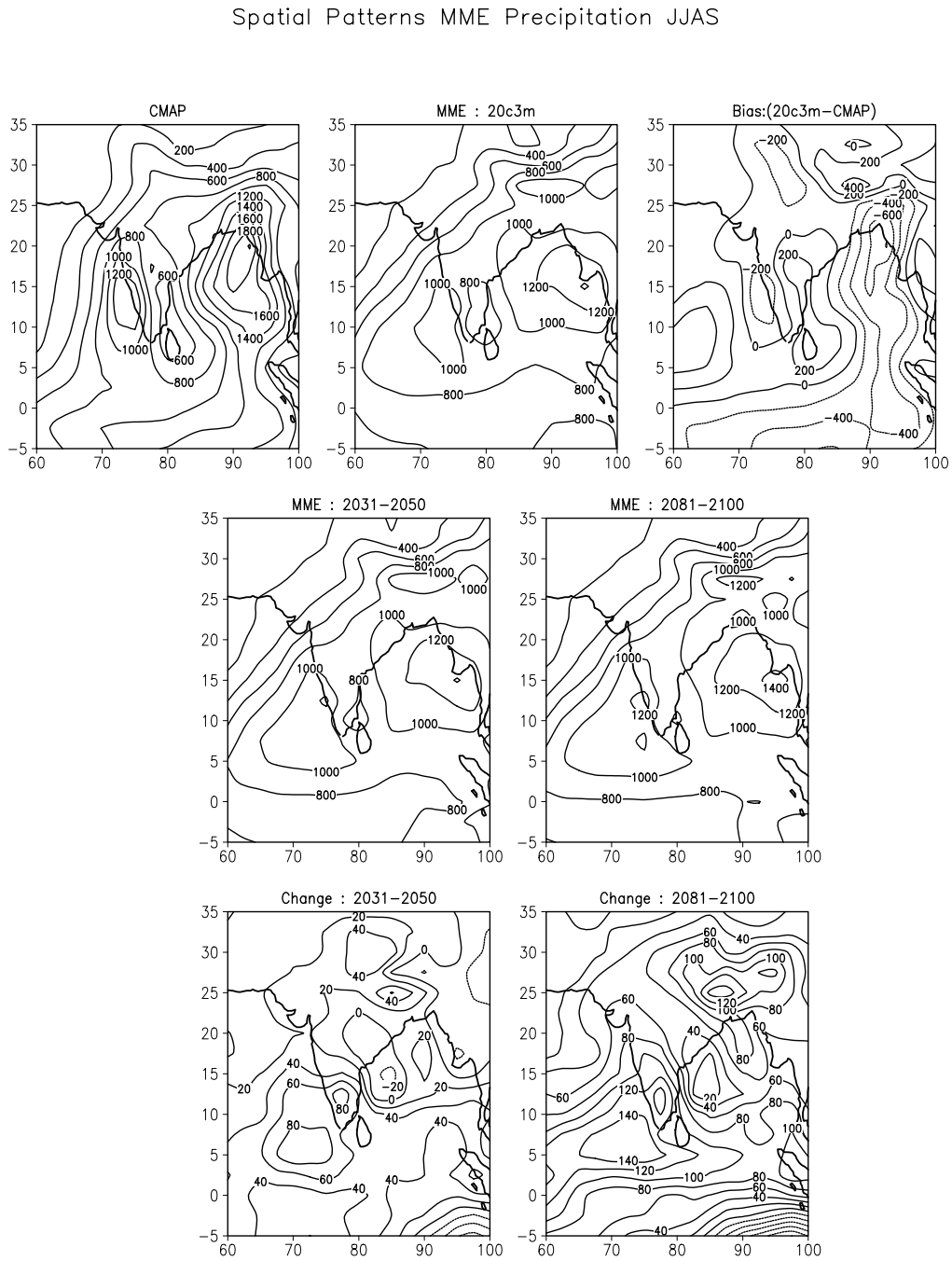

Fig.12.5: Spatial patterns of the summer monsoon rainfall over the Indian region: observed based on the CMAP data; model simulated MME pattern (20c3m); difference between the observed and simulated indicated as Bias (top 3 panels); projected patterns for the 2031-2050 time slice and for the 2081-2100 time slice (central panels); projected difference for the 2031-2050 time slice and for the 2081-2100 time slice (lower two panels).

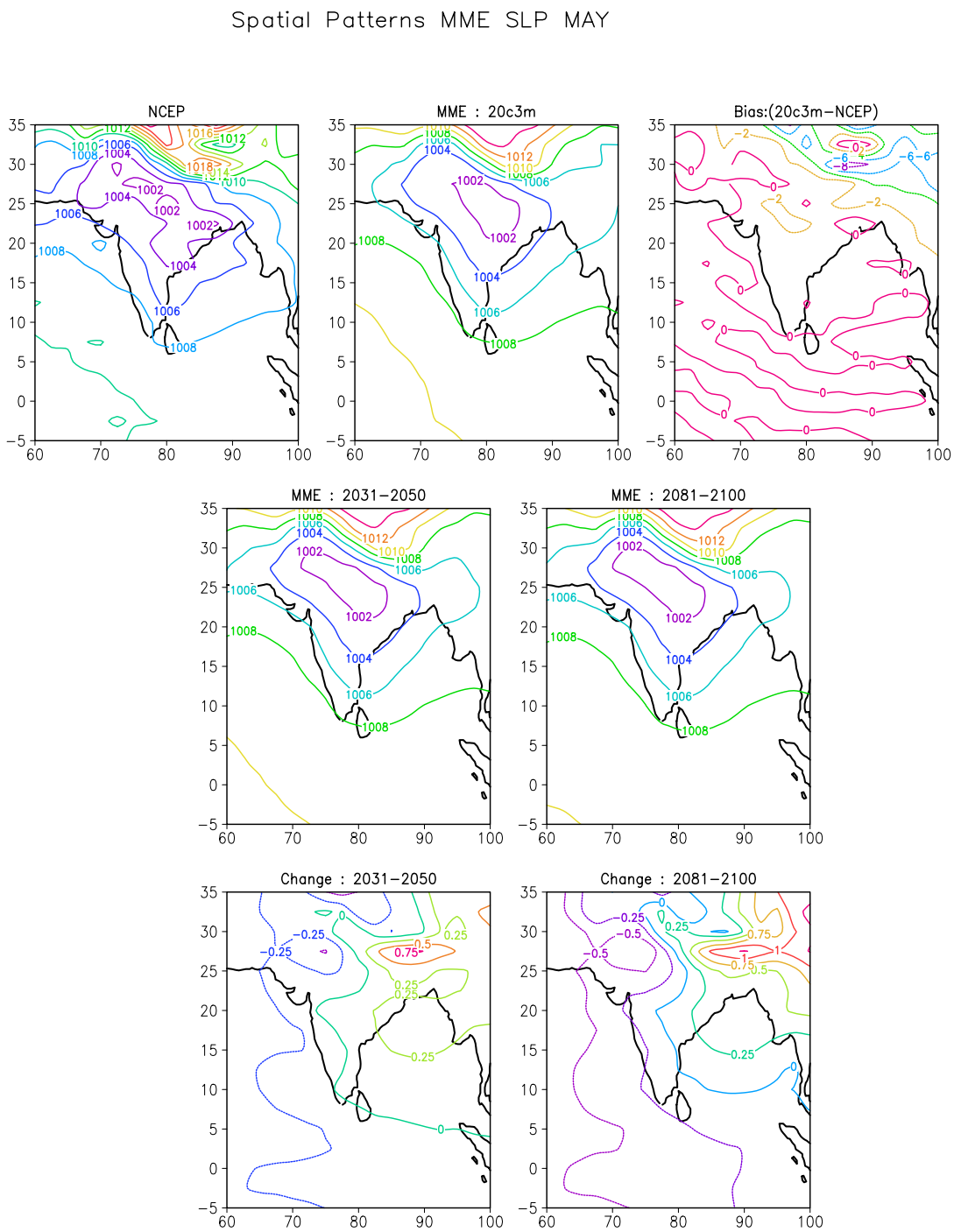

Fig. 12.6: Same as Fig. 5 but for the May MSL Pressure.

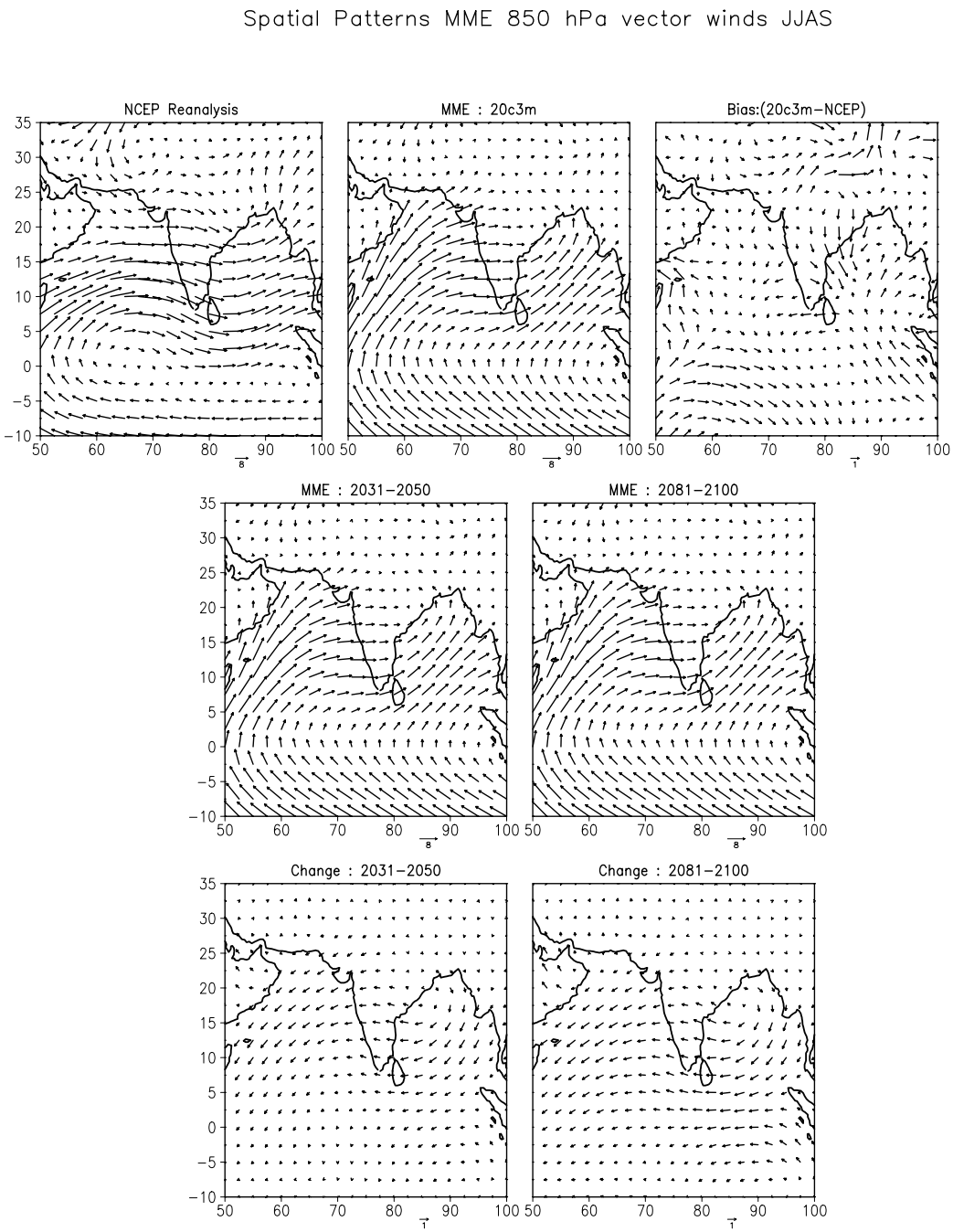

Fig.12.7: Same as Fig 12.5 but for the lower troposphere vector winds at 850 hPa

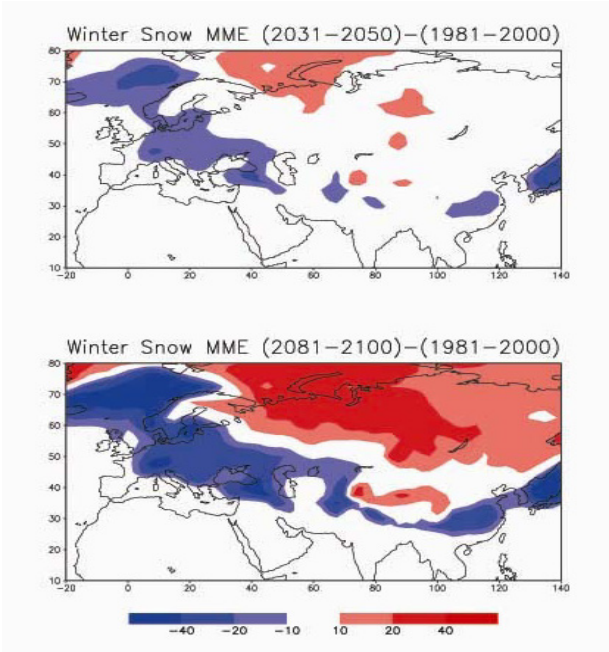

Fig.12.8: Differences between projected and simulated winter snowfall for the two periods 2031-2050 and 2081-2100 depicting projected changes in snow over the northern hemisphere. Blue (red) shaded areas indicate negative (positive) snow anomalies.

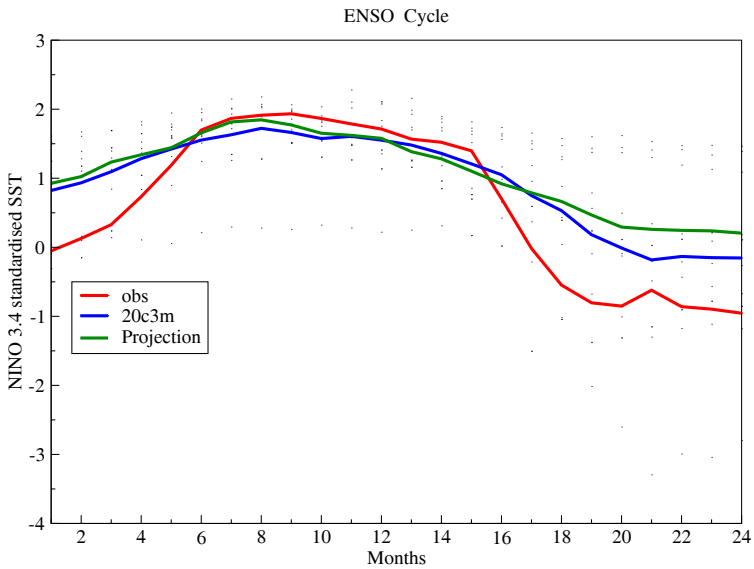

Fig.12.9: Monthly temporal evolution of composite standardized SSTs over the NINO3.4 region based on observed SST data (red line), MME simulated (blue line) and projections (green line). The composites are based on strong El Nino events (standardized SST > +1.0 over NINO3.4).

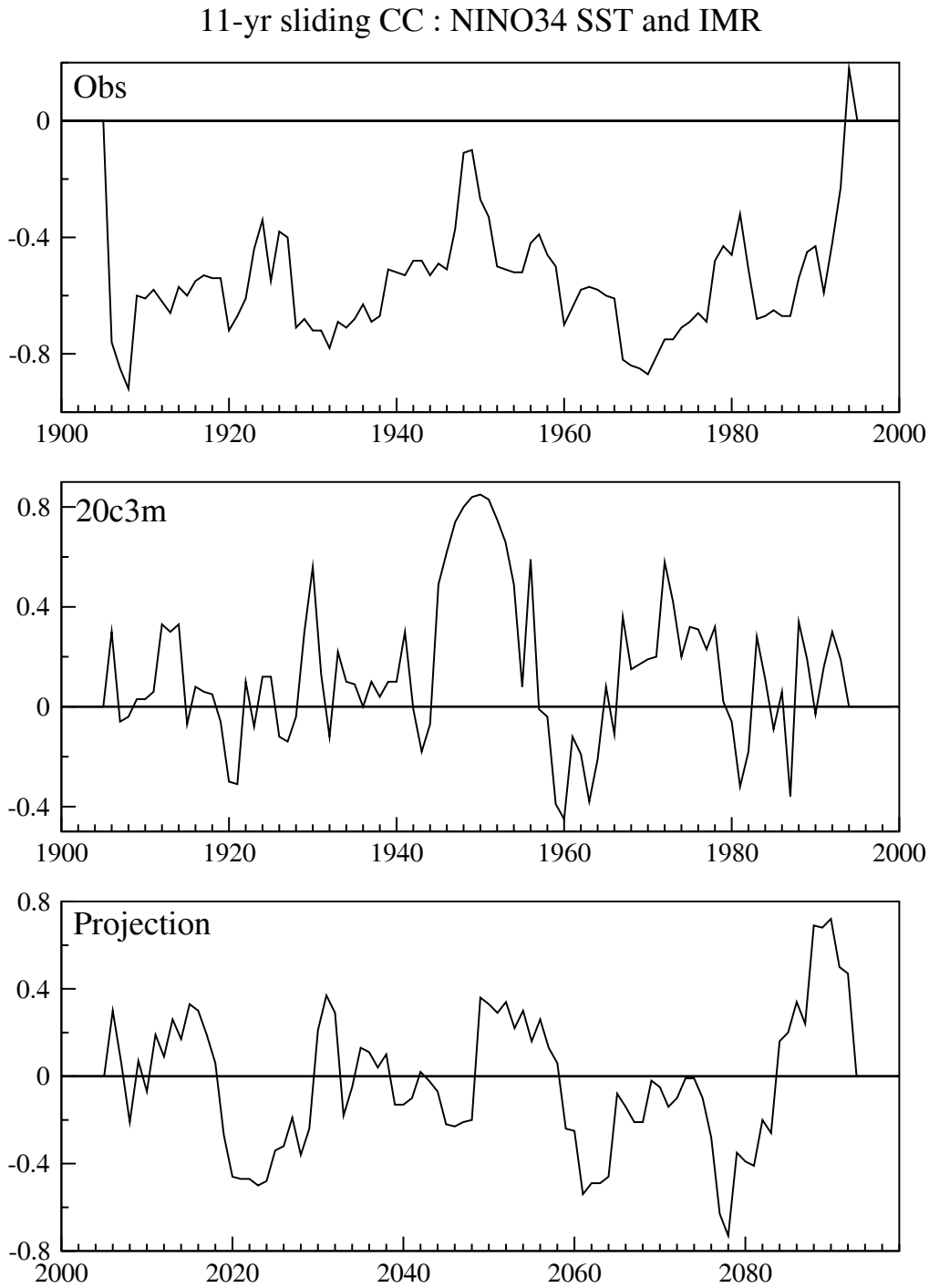

Fig.12.10: ENSO-Monsoon relationship. Eleven year running correlation coefficients between IMR and SST over NINO 3.4 region: observed (upper panel); model simulated (central panel) and projected (lower panel).

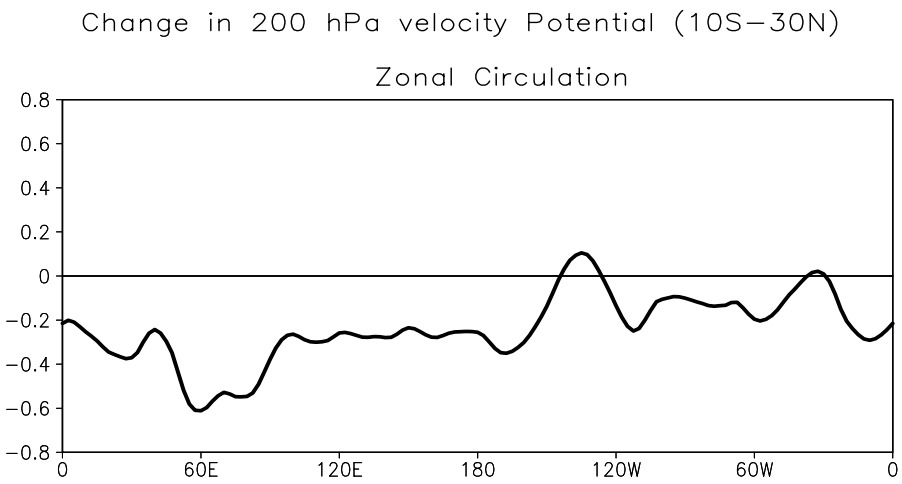

Fig.12.11 (a): Difference in the 200-hPa velocity potential for the latitudinal belt of 10S-30N during June through September between 2081-2100 (projected) and 1981-2000 (simulated) period signifying the projected change in Walker+Monsoon (Zonal) circulation. X-axis denotes the longitudes

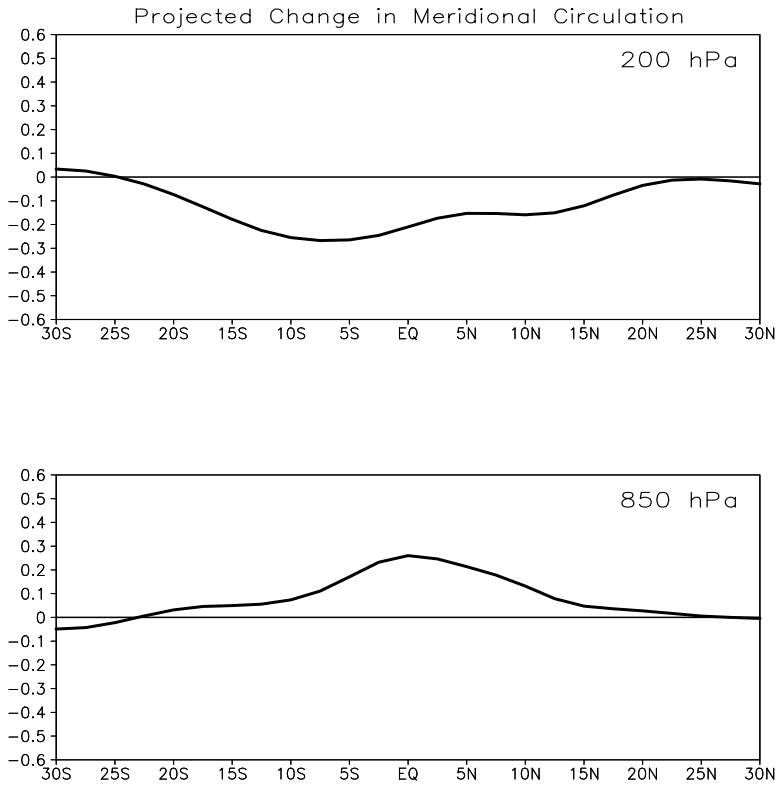

Fig. 12.11 (b): Global zonal velocity potential average depicting the projected changes in Hadley (meridional) circulation for 200 hPa (upper panel) and 850 hPa (lower panel).

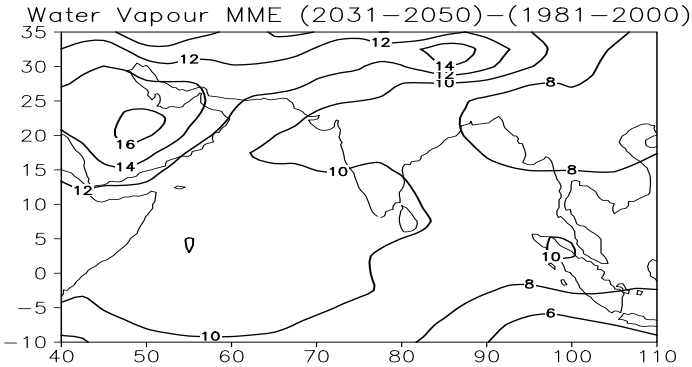

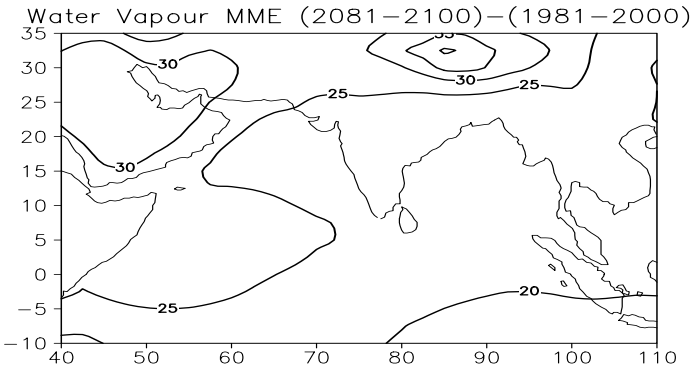

Fig. 12.12: Spatial patterns of percent increase in precipitable water for the two time slices 2031-2050 and 2081-2100.

Table 12.1: Climate models which participated in the IPCC AR4 experiments. Abbreviated acronyms are used in text to identify the respective models. Out of these, 10 models (bcr,ccm,ccm2, cnr, ech, eco, inm, mih, mim and ukc) are used for the MME.

No	Originating Group(s)	Country	IPCC I.D.	Approx Resolution
1	Beijing Climate Center	China	BCC-CM1 (bcc)	1.9 x 1.9
2	Bjerknes Centre for Climate Research	Norway	BCCR-BCM2.0 (bcr)	2.8 x 2.8
3	National Center for Atmospheric Research	USA	CCSM3 (ncc)	1.4 x 1.4
4	Canadian Centre for Climate Modelling & Analysis	Canada	CGCM3.1(T47) (ccm)	3.7 x 3.7
5	Canadian Centre for Climate Modelling & Analysis	Canada	CGCM3.1(T63) (ccm2)	2.8 x 2.8
6	Météo-France / Centre National de Recherches Météorologiques	France	CNRM-CM3 (cnr)	2.8 x 2.8
7	CSIRO Atmospheric Research	Australia	CSIRO-Mk3.0 (csr)	1.9 x 1.9
8	CSIRO Atmospheric Research	Australia	CSIRO-Mk3.5 (csr2)	
9	Max Planck Institute for Meteorology	Germany	ECHAM5/MPI-OM (ech)	1.9 x 1.9
10	Meteorological Institute of the University of Bonn, Meteorological Research Institute of KMA, and Model and Data group.	Germany / Korea	ECHO-G (eco)	3.7 x 3.7
11	LASG / Institute of Atmospheric Physics	China	FGOALS-g1.0 (iap)	2.8 x 3.0
12	US Dept. of Commerce / NOAA / Geophysical Fluid Dynamics Laboratory	USA	GFDL-CM2.0 (gf0)	2.5 x 2.0
13	US Dept. of Commerce / NOAA / Geophysical Fluid Dynamics Laboratory	USA	GFDL-CM2.1 (gf1)	2.5 x 2.0
14	NASA / Goddard Institute for Space Studies	USA	GISS-AOM (gia)	4.0 x 3.0
15	NASA / Goddard Institute for Space Studies	USA	GISS-EH (gih)	5.0 x 4.0
16	NASA / Goddard Institute for Space Studies	USA	GISS-ER (gir)	5.0 x 4.0
17	Instituto Nazionale di Geofisica e Vulcanologia	Italy	INGV-SXG (ing)	1.1 x 1.1
18	Institute for Numerical Mathematics	Russia	INM-CM3.0 (inm)	5.0 x 4.0
19	Institut Pierre Simon Laplace	France	IPSL-CM4 (ips)	3.7 x 2.5
20	Center for Climate System Research (The University of Tokyo), National Institute for Environmental Studies, and Frontier Research Center for Global Change (JAMSTEC)	Japan	MIROC3.2(hires (mih)	1.1 x 1.1
21	Center for Climate System Research (The University of Tokyo), National Institute for Environmental Studies, and Frontier Research Center for Global Change (JAMSTEC)	Japan	MIROC3.2(medres) (mim)	2.8 x 2.8
22	Meteorological Research Institute	Japan	MRI-CGCM2.3.2 (mri)	2.8 x 2.8
23	National Center for Atmospheric Research	USA	PCM(ncp)	2.8 x 2.8
24	Hadley Centre for Climate Prediction and Research / Met Office	UK	UKMO-HadCM3 (ukc)	3.7 x 2.5
25	Hadley Centre for Climate Prediction and Research / Met Office	UK	UKMO-HadGEM1 (ukg)	1.9 x 1.2

Monsoon Monograph Volume II

C O N T E N T S

Preface

Chapter	*Topic*	*Pages No.*
Chapter - 1	Synoptic Systems during Monsoon season - ***P. V. Joseph***	1-34
Chapter - 2	Indian Monsoon variability - ***D. R. Pattanaik***	35-77
Chapter - 3	Tele-connections of Monsoon - ***M. Rajeevan***	78-128
Chapter - 4	Monsoon Oceanic aspects - ***Sulochana Gadgil and P. A. Francis***	129-188
Chapter - 5	Monsoon Simulation - ***R. Krishnan, Ayantika Dey Choudhury, Rajib Chattopadhyay, and M. Mujumdar***	189-232
Chapter- 6	Modeling of forecast sensitivity of the march of the monsoon isochrones from Kerala to New Delhi during the first 25 days. - ***T. N. Krishnamurti, Anu Simo, Aupe Thomas, Akhilesh Mishra, Dev Sikka, Dev Niyogi, Aridam Chakraborty and Li Li***	233-265
Chapter - 7	Predictability of the Indian monsoon in coupled general circulation models - ***V. Krishnamurty and J. Shukla***	266-306
Chapter - 8	Short Range Forecasting of Monsoons - ***S. K. Roy Bhowmick***	307-358
Chapter - 9	Medium Range Forecasting of Monsoons - ***A. K. Bohra and L. Harenduprakash***	359-412
Chapter - 10	Extended Range forecasting of Monsoon - ***U. C. Mohanty, P. Sinha, M. A. Kulkarni, N. Acharya, A. Singh, A. Nair and M. M. N. Rao***	413-467
Chapter - 11	Long Range Forecasting of Monsoon - ***D. S. Pai***	468-504
Chapter - 12	Monsoon Aspects related to Climate change - ***R. H. Kriplani and Ashwini Kulkarni***	505-559

DESIGNED & PRINTED AT
CENTRAL PRINTING UNIT,
OFFICE OF THE
ADDITIONAL DIRECTOR GENERAL
OF METEOROLOGY (RESEARCH),PUNE